U.S. Department of
Transportation

**Federal Railroad
Administration**

Experimental Determination of Release Fields in Cut Railroad Car Wheels

Office of Research
and Development
Washington, DC 20590

Research and Special Programs Administration
John A. Volpe National Transportation Systems Center
Cambridge, MA 02142-1093

DOT/FRA/ORD-97/06
DOT-VNTSC-FRA-96-13

Final Report
February 1999

NOTICE

This document is disseminated under the sponsorship of the Department of Transportation in the interest of information exchange. The United States Government assumes no liability for its contents or use thereof.

NOTICE

The United States Government does not endorse products or manufacturers. Trade or manufacturers' names appear herein solely because they are considered essential to the objective of this report.

REPORT DOCUMENTATION PAGE

Form Approved
OMB No. 0704-0188

1. A  PB99-140121	2. REPORT DATE February 1999	3. REPORT TYPE & DATES COVERED Final Report July 1993-November 1995

4. TITLE AND SUBTITLE
Experimental Determination of Release Fields in Cut Railroad Car Wheels

5. FUNDING NUMBERS
R-9050/RR-928

6. AUTHOR(S)
Robert Czarnek, PH.D.

7. PERFORMING ORGANIZATION NAME(S) AND ADDRESS(ES)
Concurrent Technologies Corporation*
1450 Scalp Avenue
Johnstown, PA 15904

8. PERFORMING ORGANIZATION REPORT NUMBER
DOT-VNTSC-FRA-96-13

9. SPONSORING/MONITORING AGENCY NAME(S) AND ADDRESS(ES)
U.S. Department of Transportation
Federal Railroad Administration
Office of Research and Development
400 7th Street, SW
Washington, D.C. 20590

10. SPONSORING OR MONITORING AGENCY REPORT NUMBER
DOT/FRA/ORD-97/06

11. SUPPLEMENTARY NOTES
*Under Contract to: U.S. Department of Transportation
Research and Special Programs Administration
John A. Volpe National Transportation Systems Center
Cambridge, MA 02142-1093

12a. DISTRIBUTION/AVAILABILITY
This document is available to the public through the National Technical Information Service, Springfield, VA 22161

12b. DISTRIBUTION CODE

13. ABSTRACT (Maximum 200 words)

A new approach to the measurement of residual stresses in railroad wheels is investigated using a saw cut method of releasing stresses in the structure. High-sensitivity moiré interferometry combined with Michelson interferometry provides full-field information about the distribution of displacements around a saw cut notch on both flat surfaces of the rim of a wheel. The precision of the measurements is better than 100nm. Additional discrete gages provide information about the absolute displacements of the points on the rim with respect to the center of the wheel and strains in selected locations.

14. SUBJECT TERMS
Railroad wheels; Residual stress, Moiré interferometry

15. NUMBER OF PAGES
400

16. PRICE CODE

17. SECURITY CLASSIFICATION OF REPORT	18. SECURITY CLASSIFICATION OF THIS PAGE	19. SECURITY CLASSIFICATION OF ABSTRACT	20. LIMITATION OF ABSTRACT
Unclassified	Unclassified	Unclassified	Unlimited

Page Intentionally Left Blank

PREFACE

This report is the ninth in a series on the effects of service loads on railroad vehicle wheels. The study began in 1991 when wheels on three similar fleets of multiple unit (MU) power cars used in commuter service were found to have unusually high rates of cracking. The Federal Railroad Administration (FRA) Office of Safety requested technical support from the FRA Office of Research and Development in monitoring the affected fleets. At the same time, the FRA Office of Research and Development undertook a wheel performance research project to identify and evaluate options for long-term solutions.

The first eight reports cover the work performed to evaluate the immediate actions that were taken to assure continued operational safety and to assess the effects of modifications made to the braking system on one of the affected fleets. The reports in the series are listed at the end of the document, before the appendices. The second phase, now underway, focuses on wheel performance research, where the goal is to develop a method of analysis that can be proactively applied to estimate the point at which the service demands placed upon wheels could lead to adverse residual stresses in the outer rim. Numerical analyses using conventional and specially developed software have been used to make estimates of these stresses.

This report documents a series of destructive experiments designed to gather information about wheel rim residual stresses for the purposes of verifying the integrity of the numerical estimates. A new approach to the measurement of these stresses, which uses a saw cut to release the stresses in the wheel, is employed. A combination of high-sensitivity moiré interferometry and Michelson interferometry is applied to provide full-field information about the distribution of displacements around a saw cut notch on both flat surfaces of the wheel rim. The technique is applied to eight railroad wheels (four passenger wheels and four freight wheels). Results in the form of contour plots of displacements in the vicinity of the notch are presented for the eight specimens in the eight appendices.

METRIC/ENGLISH CONVERSION FACTORS

ENGLISH TO METRIC

LENGTH (APPROXIMATE)

1 inch (in) = 2.5 centimeters (cm)
1 foot (ft) = 30 centimeters (cm)
1 yard (yd) = 0.9 meter (m)
1 mile (mi) = 1.6 kilometers (km)

AREA (APPROXIMATE)

1 square inch (sq in, in^2) = 6.5 square centimeters (cm^2)
1 square foot (sq ft, ft^2) = 0.09 square meter (m^2)
1 square yard (sq yd, yd^2) = 0.8 square meter (m^2)
1 square mile (sq mi, mi^2) = 2.6 square kilometers (km^2)
1 acre = 0.4 hectare (ha) = 4,000 square meters (m^2)

MASS - WEIGHT (APPROXIMATE)

1 ounce (oz) = 28 grams (gm)
1 pound (lb) = .45 kilogram (kg)
1 short ton = 2,000 pounds (lb) = 0.9 tonne (t)

VOLUME (APPROXIMATE)

1 teaspoon (tsp) = 5 milliliters (ml)
1 tablespoon (tbsp) = 15 milliliters (ml)
1 fluid ounce (fl oz) = 30 milliliters (ml)
1 cup (c) = 0.24 liter (l)
1 pint (pt) = 0.47 liter (l)
1 quart (qt) = 0.96 liter (l)
1 gallon (gal) = 3.8 liters (l)
1 cubic foot (cu ft, ft^3) = 0.03 cubic meter (m^3)
1 cubic yard (cu yd, yd^3) = 0.76 cubic meter (m^3)

TEMPERATURE (EXACT)

$°C=5/9(°F - 32)$

METRIC TO ENGLISH

LENGTH (APPROXIMATE)

1 millimeter (mm) = 0.04 inch (in)
1 centimeter (cm) = 0.4 inch (in)
1 meter (m) = 3.3 feet (ft)
1 meter (m) = 1.1 yards (yd)
1 kilometer (km) = 0.6 mile (mi)

AREA (APPROXIMATE)

1 square centimeter (cm^2) = 0.16 square inch (sq in, in^2)
1 square meter (m^2) = 1.2 square yards (sq yd, yd^2)
1 square kilometer (km^2) = 0.4 square mile (sq mi, mi^2)
10,000 square meters (m^2) = 1 hectare (ha) = 2.5 acres

MASS - WEIGHT (APPROXIMATE)

1 gram (gm) = 0.036 ounce (oz)
1 kilogram (kg) = 2.2 pounds (lb)
1 tonne (t) = 1,000 kilograms (kg) = 1.1 short tons

VOLUME (APPROXIMATE)

1 milliliter (ml) = 0.03 fluid ounce (fl oz)
1 liter (l) = 2.1 pints (pt)
1 liter (l) = 1.06 quarts (qt)
1 liter (l) = 0.26 gallon (gal)
1 cubic meter (m^3) = 36 cubic feet (cu ft, ft^3)
1 cubic meter (m^3) = 1.3 cubic yards (cu yd, yd^3)

TEMPERATURE (EXACT)

$°F=9/5(°C) + 32$

QUICK INCH-CENTIMETER LENGTH CONVERSION

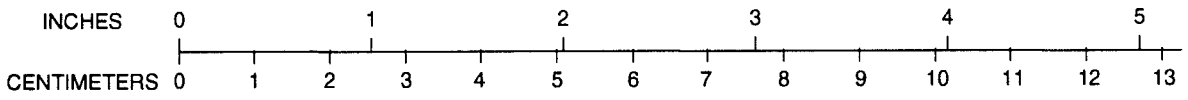

QUICK FAHRENHEIT-CELSIUS TEMPERATURE CONVERSION

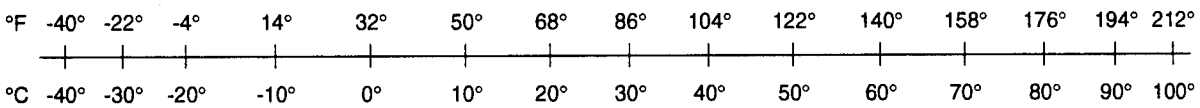

For more exact and or other conversion factors, see NIST Miscellaneous Publication 286, Units of Weights and Measures. Price $2.50. SD Catalog No. C13 10286.

Updated 8/1/96

TABLE OF CONTENTS

LIST OF FIGURES

LIST OF TABLES

INTRODUCTION

Railroad car wheels during normal service, with time, develop large residual stresses that can lead to premature, and in some instances, catastrophic failure. These stresses are caused by thermal cycles combined with contact stresses. A good understanding of this stress distribution and its variation over time in service can help in developing a better wheel design that would minimize the magnitude of maximum stresses and the danger of catastrophic failure of a wheel. A knowledge of this distribution can also help in improving the techniques used for routine inspection of wheels and the detection of potentially dangerous stress distribution.

In past years, a significant effort has been made to develop experimental techniques for testing railroad car wheels. The most accepted and commonly used destructive technique has been measurement, using an extensometer, of the closing or opening of a gap introduced by saw cutting along the radius of a wheel from the flange tip to some distance into the rim or plate of the wheel. This standard procedure provides a qualitative evaluation of the average conditions in the rim, namely, the magnitude of the net force, and the overall character of the stress distribution (tensile or compressive). Unfortunately, it only provides information at one point. In addition, measurement errors result from the harsh cutting conditions. Some improvement can be realized by the application of resistance strain gages, but strain gage limitations and the limited number of data points provide only a partial view of the total stress pattern in the wheel. Although this procedure is well suited for its original surveying purpose, recent experiments and calculations have shown that the procedure must be refined to provide the research-quality data required for the present studies.

A new approach to generating the deformation data in wheel cutting tests was introduced by R. Czarnek in 1992 [1], [2]. High-sensitivity moiré interferometry was used to measure the displacement distribution along a cut [3], [4]. Full-field information provided by the recorded interferograms allowed the determination of radial and hoop displacement distribution in the vicinity of the cuts, as well as the detection of plastic deformation along the edges of the cuts. A new, portable moiré interferometer allowed the application of this technique in a machine shop rather than in a holographic laboratory [5], [6].

In support of the Federal Railroad Administration (FRA) Office of Research and Development, the Volpe Center is conducting studies of factors related to the development of cracks in railroad car wheels. These studies require the collection of experimental data for use in various ways to estimate the actual residual stresses present in a wheel, either as-manufactured or incurred during service.

Presented below are the results of an experiment performed using a revised procedure in which high-resolution, full-field data were produced by high-sensitivity moiré interferometry and Michelson interferometry on both flat surfaces of the rim of a wheel. Since interferometric measurements are made from the flat surfaces of the wheel rim, this technique may be applied to any wheel design (that is, straight-, curved-, or parabolic-plate passenger or freight wheels). The secondary data, related to the absolute reference for the released radial displacement field, were produced using dial indicators mounted on a reference plate attached to the hub of the wheel. In the locations having a large surface curvature, additional data were collected at selected discrete points using resistance strain gages.

EXPERIMENTAL METHODS

High-Sensitivity Moiré Interferometry

High-sensitivity moiré interferometry is a method of precisely measuring the deformation of solid bodies under various loading conditions. As opposed to strain gages and extensometers, which provide information about the state of deformation at a point and are averaged over the sensor area, this method is a full-field technique. The resulting fringe patterns are contour maps of the measured displacements. With the help of computers, these patterns can be converted to contour maps of strains and, if material properties are known, stresses. Moiré interferometry can be classified as a combination of holography and the traditional moiré method. It maintains all the sensitivity of holography, (i.e., a fraction of a micrometer) and at the same time offers easy interpretation of interferograms that are typical for moiré methods. The fringes are simply contour lines of a measured component of an in-plane displacement. Furthermore, the contrast of the patterns is usually better than in either one of the parent techniques. If properly implemented, the recorded fringes have full contrast, even for very large deformations. Under the same conditions, interferograms produced by holography would be hardly readable. At present, moiré interferometry is routinely used on flat surfaces only. Applications to cylindrical surfaces have been tried, but the amount of effort required and the questionable quality of the results made them hard to justify as anything other than an interesting academic exercise.

Moiré interferometry is an optical measuring technique based on two-beam interference. Figure 1 illustrates the basic principle of a moiré interferometry system. Two collimated and mutually coherent beams of light illuminate a diffraction grating produced through a replication process on a flat surface of a specimen. This specimen grating follows the deformation of the specimen surface and modulates the shape of the wave fronts of the diffracted beams. The first diffraction order of one and the negative first diffraction order of the other interfere, producing an interference fringe pattern recorded on the camera.

If the interferometer is tuned properly at the initial no-load configuration, the two diffracted beams emerge along the normal to the specimen surface and produce a uniform intensity field called a null field. After the load is applied, the specimen deforms and a new contour map of the phase difference of the two interfering beams is formed. Each fringe is assigned a number called a fringe-order, defined by equation (1):

$$N = \frac{S}{\lambda} + C \qquad (1)$$

where
- N is the fringe order
- S is the phase difference
- λ is the wavelength of light
- C is a constant corresponding to rigid body motion of the origin of the coordinate system.

Fringe orders are directly proportional to the in-plane displacements of the points on the specimen surface, in the direction perpendicular to the grating lines. Equation (2) defines the

relationship between the fringe order and the displacement it represents for the case presented above:

$$U = \frac{N}{2 f_s} \tag{2}$$

where U is the displacement
f_s is the frequency of the diffraction grating replicated on the specimen.

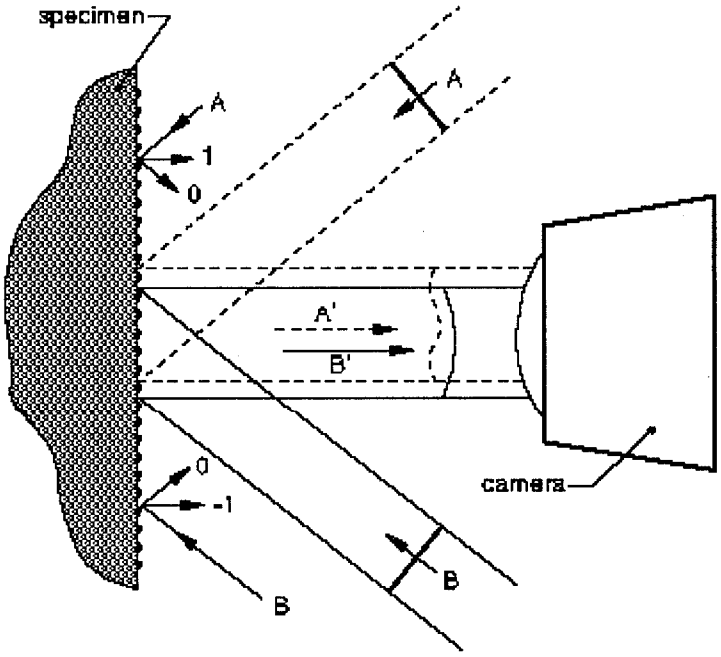

Figure 1. Basic Moiré Interferometry System

Michelson Interferometry

The Michelson interferometer produces an interference pattern by combining a beam of light reflected from the surface of the specimen with a beam reflected from a flat reference surface. The interference fringes are the contour lines representing the topography of the specimen surface. The contour interval is equal to half of the wavelength of light used in the experiment. A schematic diagram of a Michelson interferometer is illustrated in Figure 2.

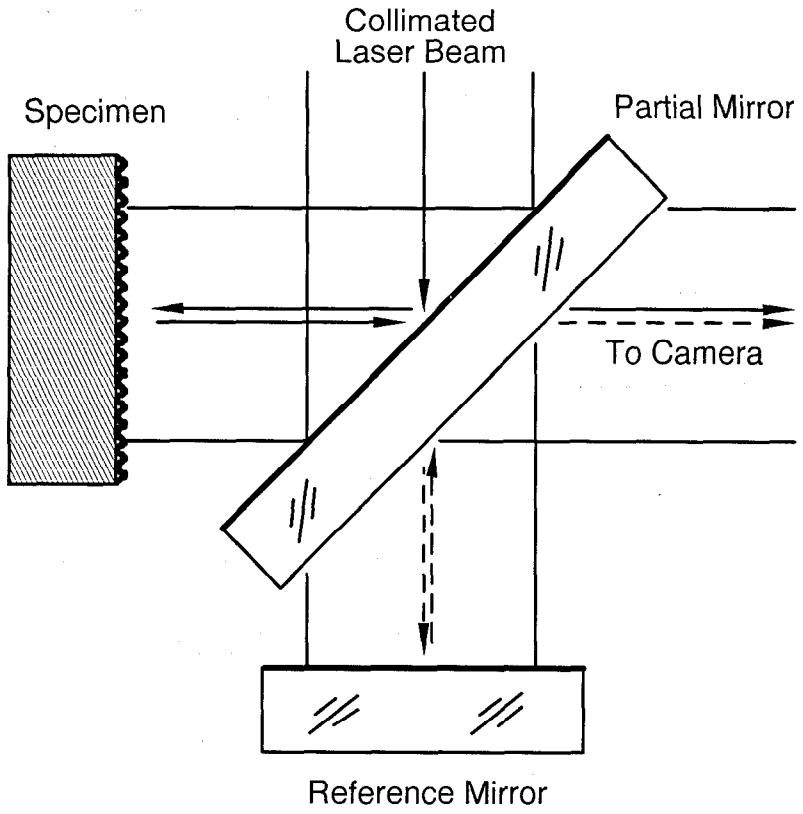

Figure 2. Schematic Diagram of the Michelson Interferometer

EXPERIMENTAL PROCEDURE

Handling Fixture

Since the railroad car wheels are heavy (about 400 kg) and access to both sides is needed, it is important to be able to handle these wheels without risking injury to people or damage to the instrumentation. A simple but effective device was developed for this purpose consisting of a fork-shaped frame and a shaft mounted in a sleeve bearing attached to a fork of a standard industrial fork-lift. The recommended configuration is illustrated in Figure 3. A wheel remains attached to this device throughout the duration of a test. This fixturing also makes it easier to clamp the wheel to the table of a band saw.

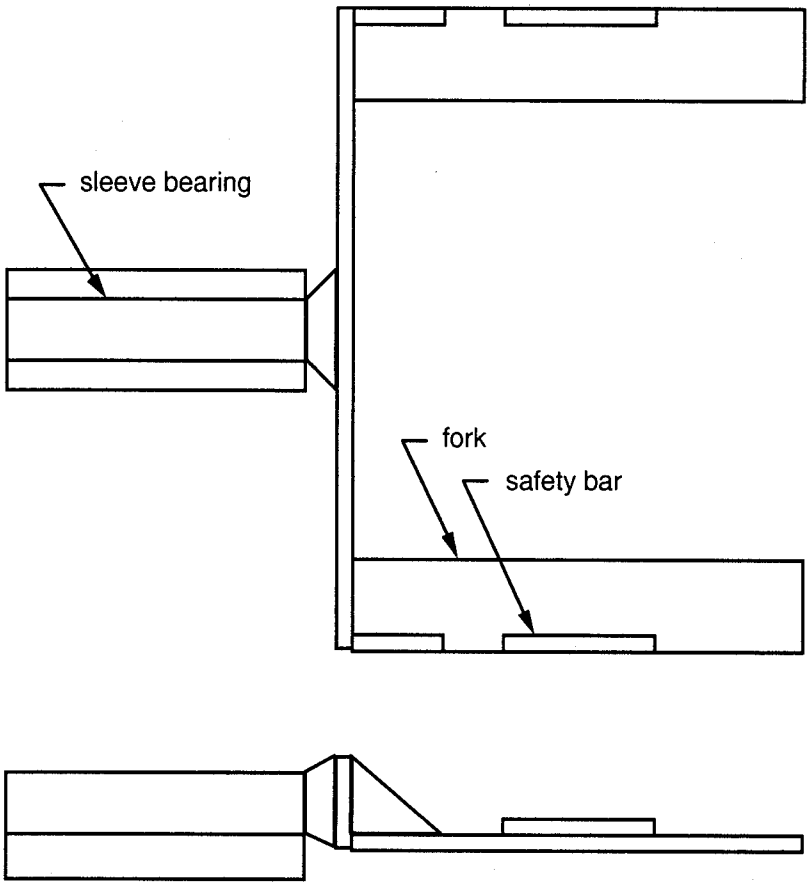

Figure 3. A Wheel Handling Fixture

Specimen Preparation

The specimen is prepared by the application of diffraction gratings for full-field interferometric measurements, and deformation and temperature sensors for point monitoring at discrete locations. Two diffraction gratings are applied to the surfaces of interest. It is important that the two gratings be positioned exactly along the same radial plane. The replication procedure is described in detail in reference [4]. The surface of the wheel is prepared for the replication using a portable hand-held grinder. The surface should be free of rust, contaminations, and major deviations from flatness. An area about 100 by 100 millimeters is cleaned and degreased. The replicating procedure is illustrated in Figure 4. The mold is a phase diffraction grating treated with a parting substance and coated with a thin metallic layer by physical vapor deposition. The mold is cemented to the specimen surface with a two-component adhesive and pulled away after the adhesive is cured. The thin metallic layer remains on the surface of the specimen providing high diffraction efficiency for the grating. Since the mold is made of a flat piece of glass, the formed grating is flat enough to serve as a mirror surface in a Michelson interferometer.

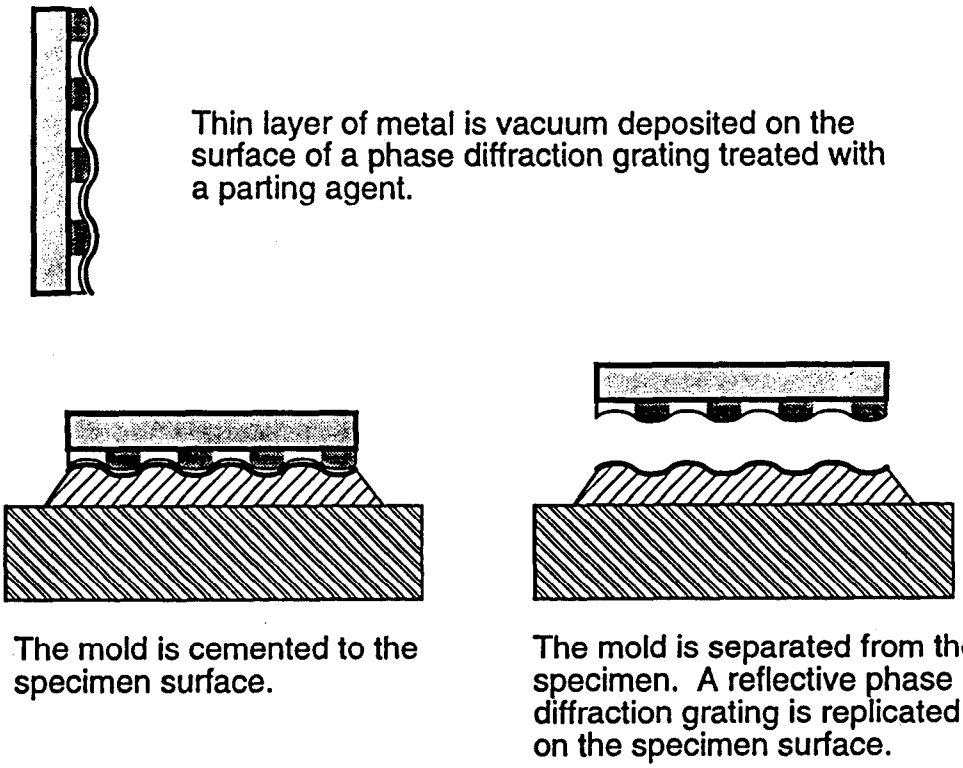

Figure 4. Preparation of a Specimen Grating Using Replication Process

In addition, five to seven strain gauges and at least two thermocouples are applied to the tread surface of the wheel. A disposable mount, illustrated in Figure 5, is spot-welded to the tip of the flange for the attachment of an extensometer.

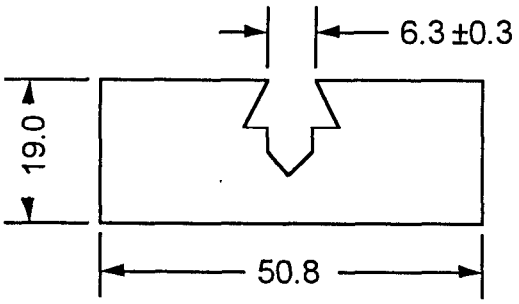

Figure 5. Disposable Extensometer Mount (Dimensions in Millimeters)

A special reference plate was manufactured for taking measurements of absolute displacements of points on the rim. This plate was reinforced with stiffeners to minimize deflections and was bolted to the wheel using two nuts spot-welded to the hub. Three precision displacement sensors were mounted to this plate in the vicinity of the cut. The exact position of all the sensors is indicated in Figures 6 and 7. In the first experiment, the three displacement sensors were high-precision mechanical dial gauges. In subsequent experiments, these were replaced by strain-gauge instrumented beams and capacitive probes, improving the accuracy of measurements by two orders of magnitude.

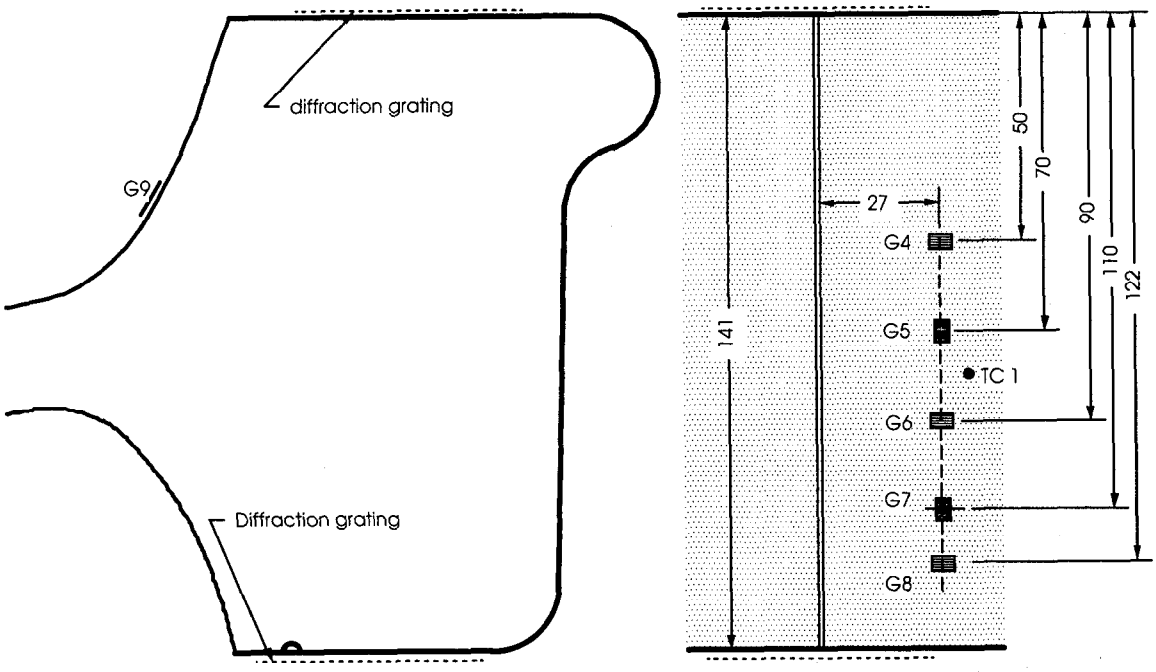

Figure 6. Location of Strain Gages, Thermocouples, and Gratings around the Cut (Dimensions in Millimeters)

Cutting and Data Recording

Before the first cut, all the strain gages and the extensometer are connected to a multichannel indicator and balanced to zero. The initial patterns are photographed and the wheel is positioned on the band saw. After all the dial indicators and the extensometer are attached, the initial readings are recorded.

The first cut is made to the depth of 28 mm, corresponding to the radial distance from the tip of the flange to the point at the center of the tread. After this first increment, all the gage and thermocouple readings are recorded. During the cutting, the blade is continuously lubricated using a cutting oil harmless to the coating of the diffraction grating.

The second cut increment is introduced to a predetermined depth. Again the readings are recorded and the wheel is moved off the table for interferometric measurements.

After the temperature of the wheel reaches an acceptable uniformity, the moiré interferometer is positioned on the wheel. The instrument is tuned to the mold used in the replication of the grating under investigation. Both in-plane displacement fields are recorded. The moiré interferometer is removed and replaced with the Michelson interferometer. The out-of-plane displacement pattern is recorded. All the interferograms are photographed with and without a carrier pattern. Those with a carrier pattern are used for the determination of the sign of the gradients of the measured displacements.

The measurements are performed on both sides of the wheel. Once the interferograms are developed, the wheel is repositioned on the table of the saw and the cycle is repeated. In the interest of timely completion of the experiments, the number of cuts at which the interferometric measurements were performed under this program was limited to three, with the exception of wheel #2, in which five interferometric measurements were made. After that, the cut is extended in 10 mm increments to a total depth of at least 150 mm or until the cut closed. The data are recorded using discrete sensors.

All the data from the discrete sensors are tabulated and the deformation parameters are calculated for each cut increment. Since the displacement sensors and the extensometers must be removed at each increment, the absolute displacements are calculated as the sum of the measured increments.

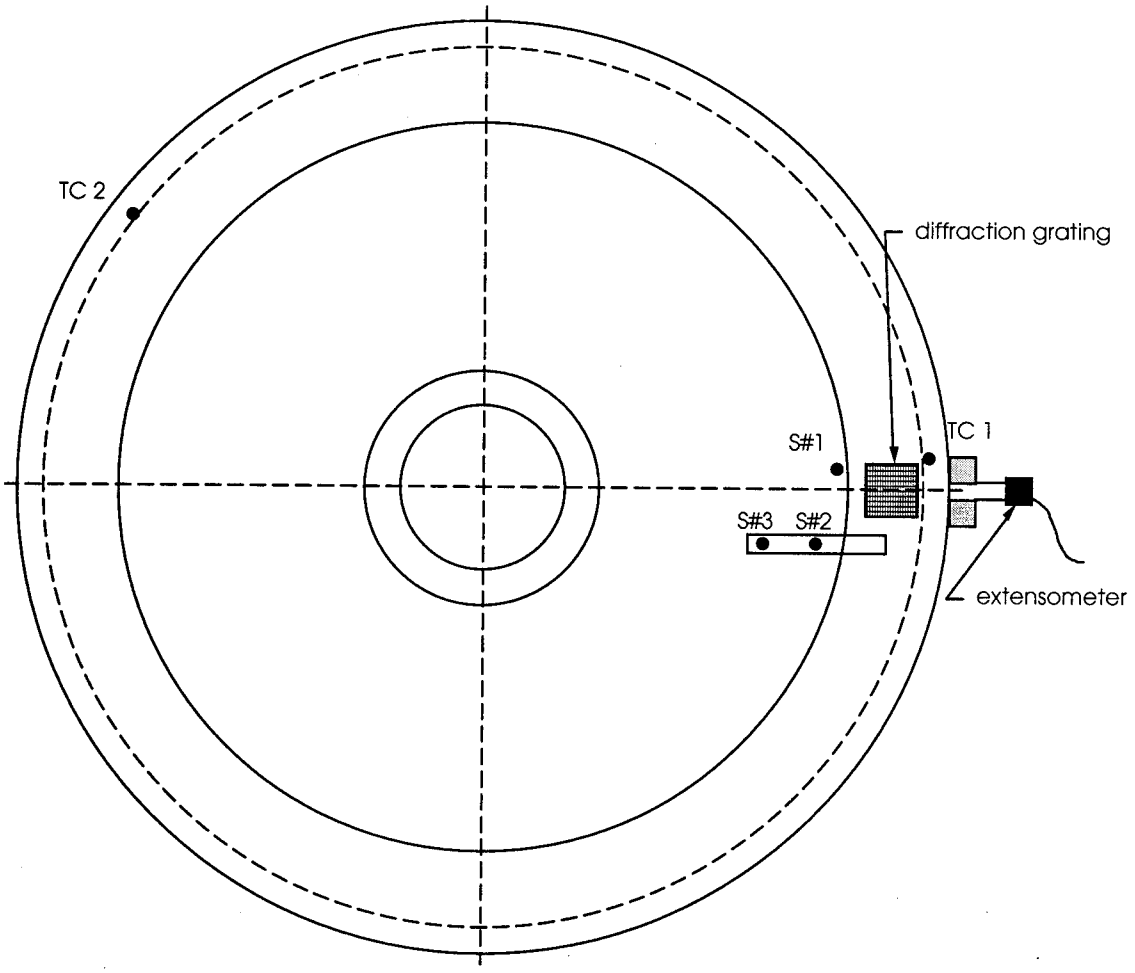

Figure 7. Location of Thermocouples, Gratings, and Displacement Sensors on the Wheel (Sensor S#1 measures the radial displacement. Sensors S#2 and S#3 measure displacements along the axis of the wheel.)

Data Analysis and Experimental Results

The data recorded using the extensometer indicates that the gap measured at the tip of the flange was closing as the depth increased. The displacement curve representing this motion is illustrated in Figure 8.

The interferograms were recorded at approximately every 10 millimeters of cut depth measured from the tread surface. An example of such a pattern is illustrated in Figure 9. Both gratings survived the cutting process with a minimum amount of damage, and the data could be collected to within 1 mm of the edge of the cut.

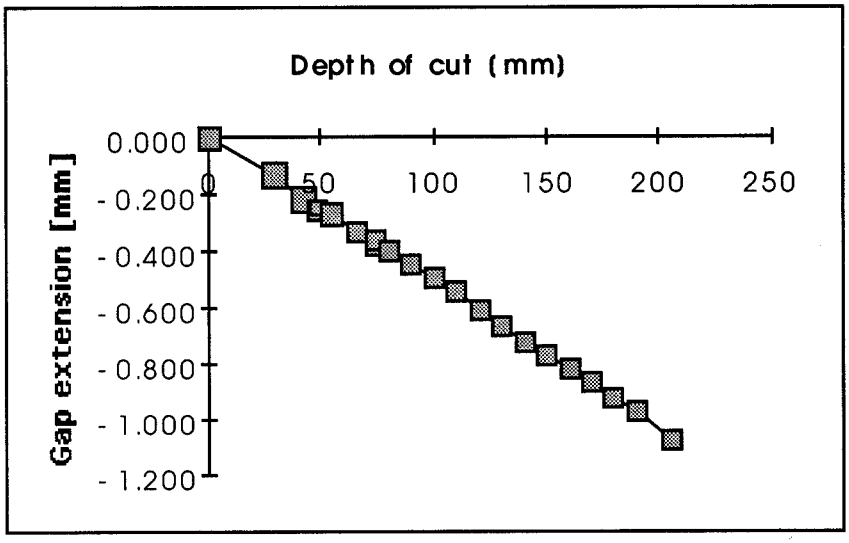

Figure 8. Gap Extension as a Function of the Cut Depth Measured Using an Extensometer

The data were collected from the interferograms using a digitizing tablet connected to a personal computer. The two in-plane components of the displacement field were combined numerically using the hybrid analysis package developed by Czarnek, Lee, and Lin [7], [8], [9]. As a result, six contour maps per grating were produced for each cut increment. These maps represent the three orthogonal components of displacement and the three in-plane components of strain. The displacement maps are presented in Figure 10 and strains in Figure 11. In addition, the hybrid analysis program produced a set of numerical data for further numerical analysis. The data can be provided at the nodal points of the mesh generated by a finite element package, or at the nodal points of the mesh generated by the hybrid analysis package. The overall accuracy of the interferometric measurements was approximately 100 nm.

The interferometric measurements of all three components of the displacement field were fully successful. The two interferometers offered high mechanical stability, allowing quality measurements to be made in a shop environment.

It was noticed that due to the mode hopping in one of the lasers there was the possibility of introducing an artificial pattern of uniform strain. To avoid this possibility, it is recommended

that in future experiments temperature-stabilized lasers be used or a strain gage rosette be applied in the vicinity of the grating.

The dial gage measurements indicate that the absolute displacement measurements require a set of dedicated, high-sensitivity sensors. The measured displacements are too small to allow the grid method to be reliable enough in this application. The displacements measured in the radial and axial directions were on the order of 100 micrometers at a cut depth of 74 mm. It is recommended that small contact sensors based on strain gages be used in at least two points, one for each direction. As an alternative, capacitive non-contact probes could be used.

The displacements measured by the extensometer are relatively large, making it feasible to use the grid method for cut opening along the cut line through the tread surface. However, strain levels below 1000 μm/m are too small to be measured using the grid technique.

The application of thermocouples proved to be very useful. In comparison with a contact thermometer used in earlier work, the response time and the accuracy of measurements were much better. The collected data indicate that the amount of generated heat strongly depends on the blade used and the lubrication applied. The maximum temperature change measured during this experiment for all but one cut did not exceed 3 degrees Celsius during any one of the cuts. The thermocouple closest to the cut was located 27 mm from the blade.

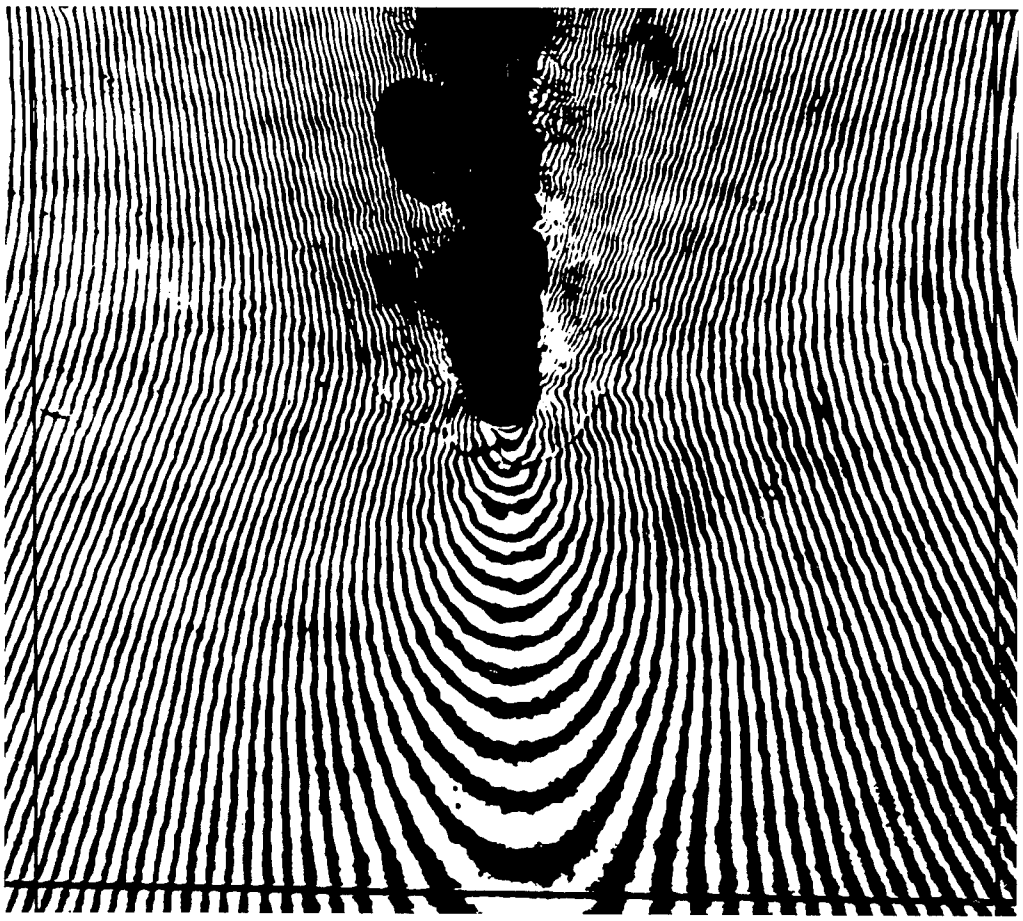

Figure 9. A Fragment of a Radial Displacement Pattern at the Second Increment of the Cut on the Back Rim Face (Fringe interval is 417 nm)

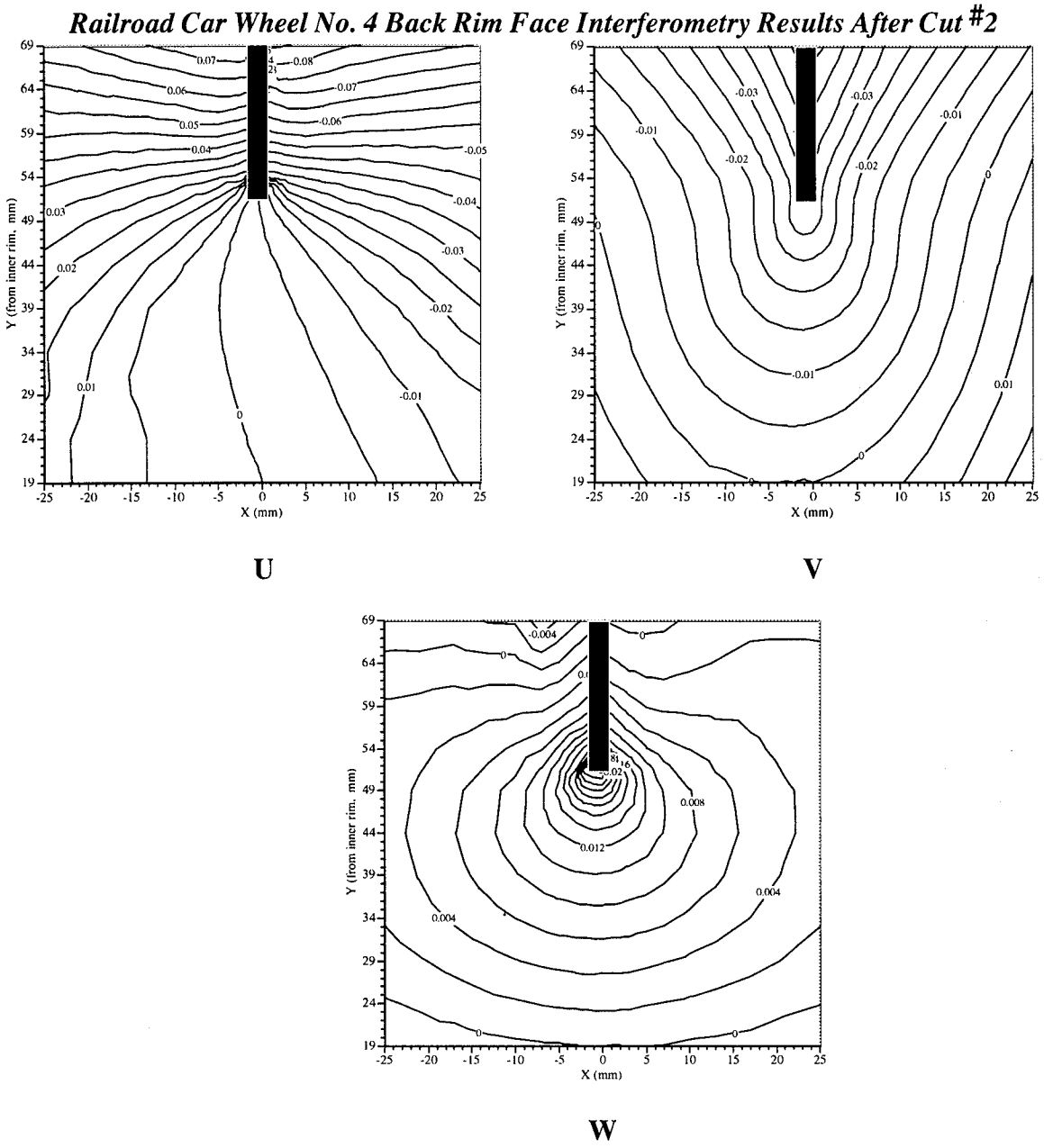

Figure 10. Computer Generated Contour Maps of the Three Components of the Displacement Field Representing the Data Collected from the Interferograms Recorded at the Second Cut Increment (Dimensions and displacements are in millimeters)

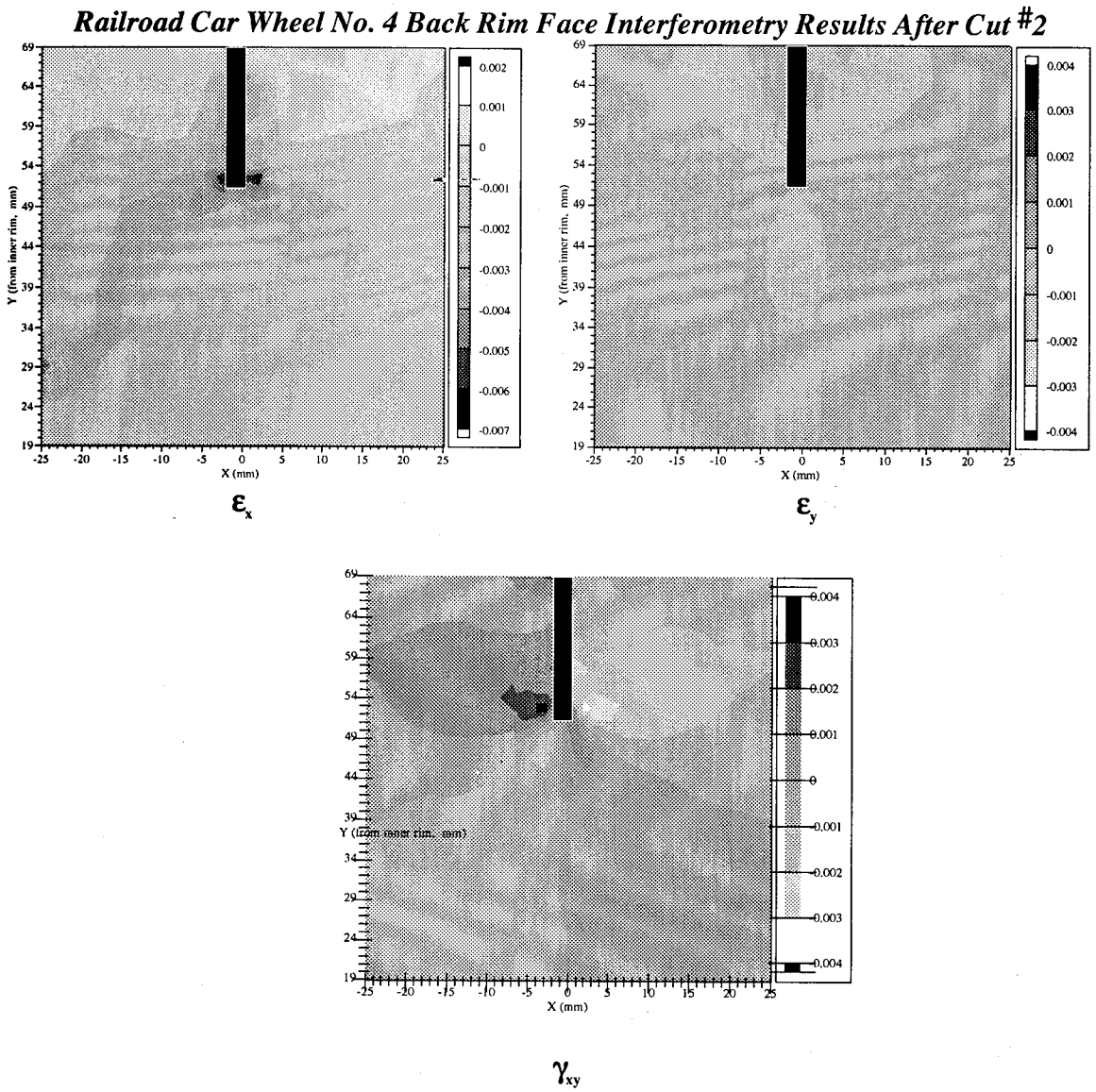

Figure 11. Computer Generated Contour Maps of the Three Components of the In-Plane Strain Calculated from the Displacement Fields Presented in Figure 10 (Dimensions are in millimeters)

SUMMARY AND CONCLUSIONS

This report documents the experimental procedure and the data resulting from the saw-cut tests. The data collected during each of the eight experiments appear in the following appendices. Table 1, below, is a guide for identification of the subject wheel in each of the experiments.

Table 1. Wheel Identification from Moiré Experiments

Experiment #	Wheel Identification	New/Used?	Passenger/Freight?
1	FRA 1530 142 T	New	Passenger
2	322-1480 142 T	Used	Passenger
3	36524-46 146	Used	Passenger
4	44543-46 146	New	Passenger
5	26526 242	Used	Freight
6	26508 242	New	Freight
7	26524	Used	Freight
8	26512	New	Freight

Generally, the data are consistent with findings of previous saw-cut tests on freight wheels in that cuts into new wheels tend to close (net compressive rim stress) as the saw progresses into the rim and used wheels exhibit cut opening behavior (net rim tension) [10]. The tendency of a saw-cut to open or close is related to the state of residual stress in the wheel rim. Residual stresses are imparted to wheels from three primary contributors:

- initial residual stresses resulting from the wheel manufacturing process,
- mechanical contact stresses from wheel-on-rail contact loads, and
- thermal stresses due to on-tread friction braking.

During manufacture, wheels are heat-treated (quenched) to induce residual compression in the rim. Such compression near the wheel-rail contact surface has the beneficial effect of retarding the formation and growth of fatigue cracks, which may form due to service loads. It is well known that severe service environments can result in negation of the beneficial residual surface compression, leaving this region in a state of tension, which may promote the development of fatigue cracking.

This phenomenon, known as rim stress reversal, is the result of flash-heating of a shallow layer of material near the wheel tread during on-tread braking when wheels are put to use. The frictional heat generated at the brake shoe causes a shallow layer of the material near the tread surface to expand. The expansion is resisted by the unheated bulk of the wheel rim. If the thermal load is sufficient, the material near the tread surface yields (undergoes plastic deformation) and upon cooling, the as-manufactured compressive condition at the tread is reversed to tension.

Quantification of the degree of rim stress reversal as a function of the service conditions to which the wheels are exposed is the subject of the wheel performance research described previously. Following initial investigations of the cracking observed in the affected fleets by the FRA and the Volpe Center, a plan that lays out a strategy for this study was developed. The major components of the plan are identified in Figure 12.

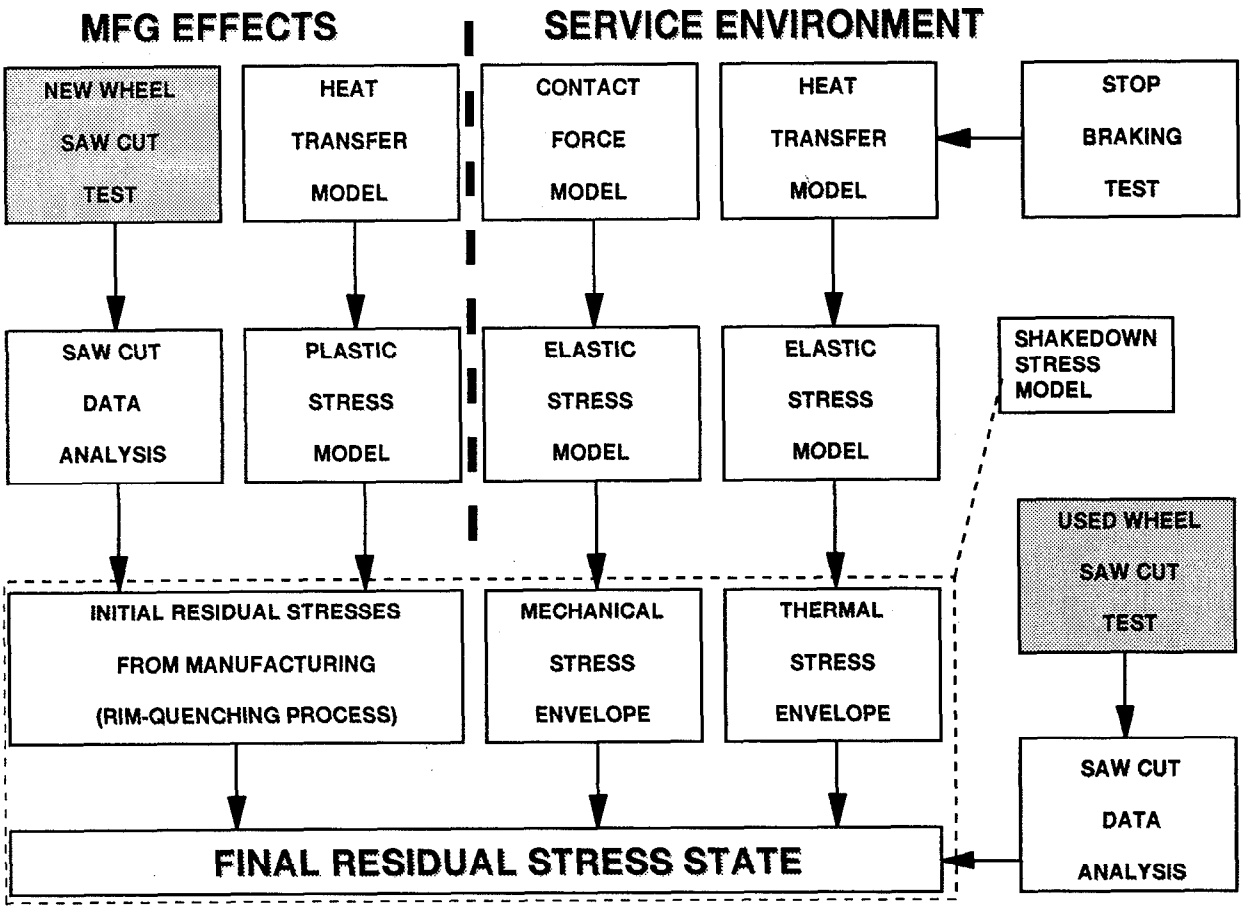

Figure 12. Master Plan for Investigating the Effects of Service Variables on Wheel Residual Stresses

The dashed box in Figure 12 represents the target of the wheel research program, which involves development of a set of analytical tools to be used to provide estimates of the final residual stress state in railroad wheels from the three contributors identified above. To assess the validity of the analytical scheme, experimental corroboration of model predictions is required. The shaded portions of Figure 12 identify those aspects of the program that have been accomplished through this series of experiments.

The collected data will be used by the Volpe Center to develop estimates of the relieved stresses, which correspond to the relieved strains measured in these experiments. Reconstruction of these stresses (the "saw-cut data analysis" portions of Figure 12) is a formidable task as the amount of data collected per wheel is significant. In order to accomplish this task, the Volpe Center is working with researchers from the Cracow University of Technology, under a joint research

research program, in the development of a hybrid technique capable of reconstructing the relieved residual stresses from the measurements described herein. This work is underway, and limited preliminary results indicate that reasonable estimates of the residual stress field can be obtained. Details of the reconstruction procedure and the results of its application will be the subject of a future report.

This experiment demonstrated that interferometric techniques can be successfully used in testing the deformation of railroad wheels in a machine shop environment. The results indicate that the experimental procedure is practical, however, some modifications would be beneficial. Two major changes would be the addition of grid measurements to the tread area and the use of small discrete sensors for point measurements of absolute displacements. Numerical analysis of the data produced will determine whether other modifications are needed.

REFERENCES

[1] Czarnek, R. 1992. *Interferometric Measurements of Cut Opening in Railroad Car Wheel Saw Cut Test.* Final Report submitted to ENSCO, Inc., on March 25, 1992.

[2] Stuart, C. 1994. *Experimental Residual Stress Measurement of New and Used Commuter Rail Wheels.* ENSCO, Inc., Final Report. FRA/ORD-94/12 (January 1994).

[3] Guild, J. 1956. *The Interference Systems of Crossed Diffraction Gratings; Theory of Moiré Fringes.* Oxford at the Clardendon Press.

[4] Czarnek, R. 1993. Moiré Interferometry. Chapter 11.2 in *Structural Testing: A Monograph for the Society for Experimental Mechanics*, edited by R. T. Reese and W. A. Kawahara.

[5] Czarnek, R. 1984. New Methods in Moiré Interferometry. Ph.D. Dissertation, Virginia Polytechnic Institute and State University.

[6] Czarnek, R. 1990. High-Sensitivity Moiré Interferometry with a Compact Achromatic Interferometer. In *Optics and Lasers in Engineering* 13, no. 2:99-115.

[7] Czarnek, R., J. Lee, and T. Rantis. 1990. Moiré Interferometry with Enhanced Resolution. In *Experimental Techniques* 14, no. 4:24-28 (July/August).

[8] Lin, S. Y., J. Lee, and R. Czarnek. 1991. Integration and Processing of High-Resolution Moiré-Interferometry Data. In *Proceedings of the 1991 Society for Experimental Mechanics Spring Conference on Experimental Mechanics*, at Milwaukee, Wisconsin (June).

[9] Lin, S-Y., M. Y. Tsai, D. Peters, R. Czarnek, and J. Morton. 1992. Hybrid Analysis of Deformation Using Interferometric Measurements. In *Proceedings of the VII International Congress on Experimental Mechanics*, at Las Vegas, Nevada (June).

REPORTS IN THIS SERIES

1. Orringer O., D. E. Gray, and R. J. McCown. 1993. *Evaluation of Immediate Actions Taken to Deal with Cracking Problems Observed in Wheels of Rail Commuter Cars.* Volpe National Transportation Systems Center, Cambridge, MA, and Federal Railroad Administration, Washington, DC. Report No. DOT/FRA/ORD-93/15 (July).

2. Stuart, C. and S. Yu. 1993. *Thermal Measurements of Commuter Rail Wheels under Revenue Service Conditions.* ENSCO, Inc., Springfield, VA. Report No. DOT/FRA/ORD-93/19 (September).

3. Tang, Y. H., J. E. Gordon, A. B. Perlman, and O. Orringer. 1993. *Finite Element Models, Validation and Results for Wheel Temperature and Elastic Thermal Stress Distributions.* Volpe National Transportation Systems Center, Cambridge, MA. Report No. DOT/FRA/ORD-93/17 (September).

4. Tang, Y. H., J. E. Gordon, O. Orringer, and A. B. Perlman. 1993. *Stress Reconstruction Analysis Of Wheel Saw Cut Tests And Evaluation Of Reconstruction Procedure.* Volpe National Transportation Systems Center, Cambridge, MA. Report No. DOT/FRA/ORD-93/18 (September).

5. Pelloux, R. M. and D. C. Grundy. 1994. *Thermomechanical Testing and Microstructural Development of Class L Steel Wheel Alloy.* Department of Materials Science and Engineering, MIT, Cambridge, MA. Report No. DOT/FRA/ORD-94/01 (March).

6. Gordon, J. E. and O. Orringer. 1996. *Investigation of the Effects of Braking System Configurations on Thermal Input to Commuter Car Wheels.* Volpe National Transportation Systems Center, Cambridge, MA. Report No. DOT/FRA/ORD-96/01 (March).

7. Holowinski, M. and E. S. Bobrov. 1996. *Estimation of Actual Residual Stresses Due to Braking and Contact Loading of Rail Vehicle Wheels.* Francis Bitter National Magnet Laboratory, MIT, Cambridge, MA. Report No. DOT/FRA/ORD-96/02 (March).

8. Crowe, K. E. and P. K. Raj. 1995. *Analyses of Rail Chill Effect.* Technology and Management Systems, Inc., Burlington, MA. (in review/press).

Page Intentionally Left Blank

Appendix 1. Wheel #1 Experimental Results

This appendix contains the results from the test on both sides (front and back rim faces) of the first wheel. All the data are in a local coordinate system that is located at the intersection of the inner edge of the rim and the cutting line; the vertical axis points away from the center of the wheel.

The attached figures show the location of all the sensors. At three points on the wheel, thermocouples (TC) measure the temperature difference (which never exceeded 3.1°C) immediately after each cut. The temperature at TC3, the one farthest from the cut, was equal to the ambient temperature. The strain measurements were taken after the difference decreased to about 1°C or less at an ambient temperature in the range of 25°C to 29°C.

The extensometer, strain gage, and displacement sensor data are provided in tabular form. The interferometric data is provided in the form of contour maps and as data files in ASCII format for three specific cutting stages. The corresponding cut depths are 43 mm, 54 mm, and 74 mm.

The wheel was identified by the following markings:

FRA 1530
142 T

Location of strain gages, thermocouples and gratings on the wheel #1

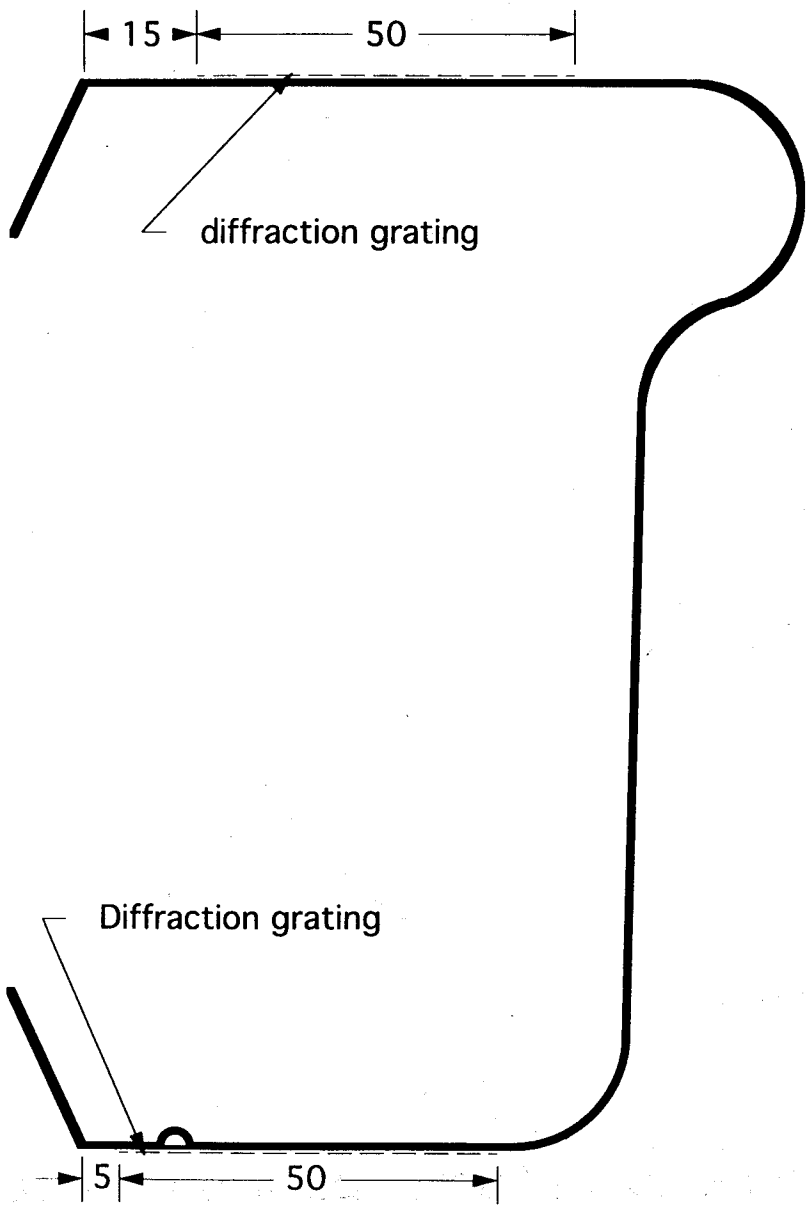

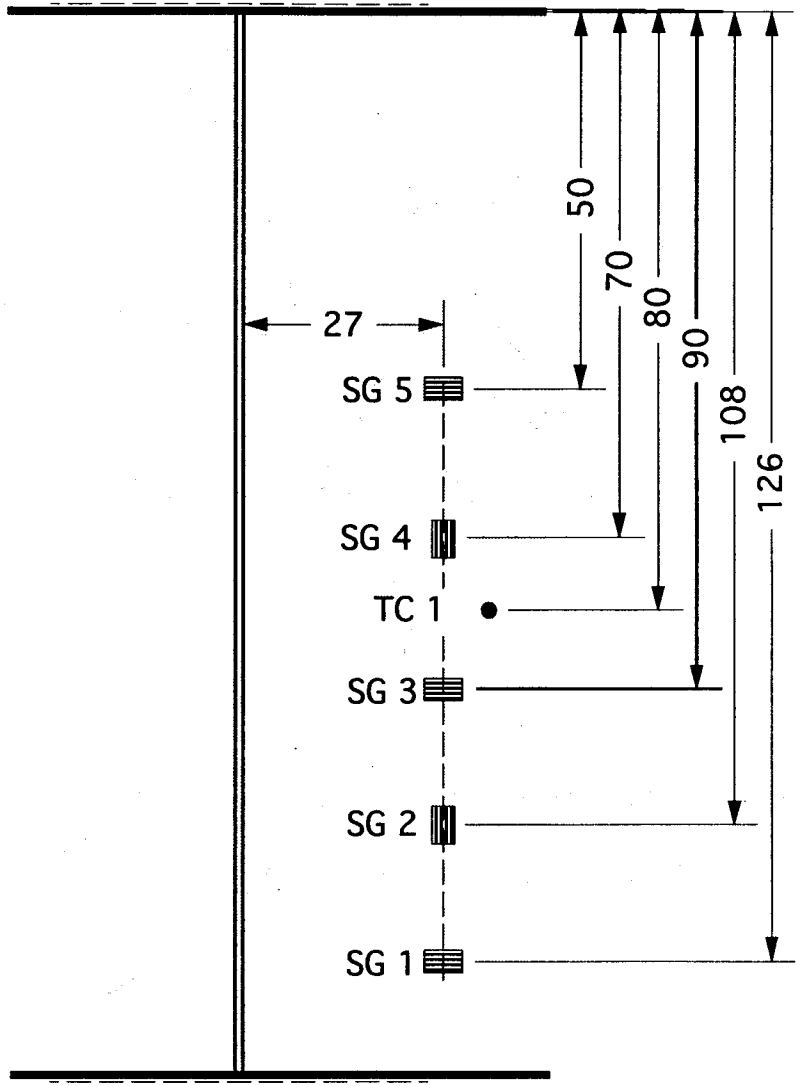

Location of dial indicators, thermocouples and gratings on the wheel #1

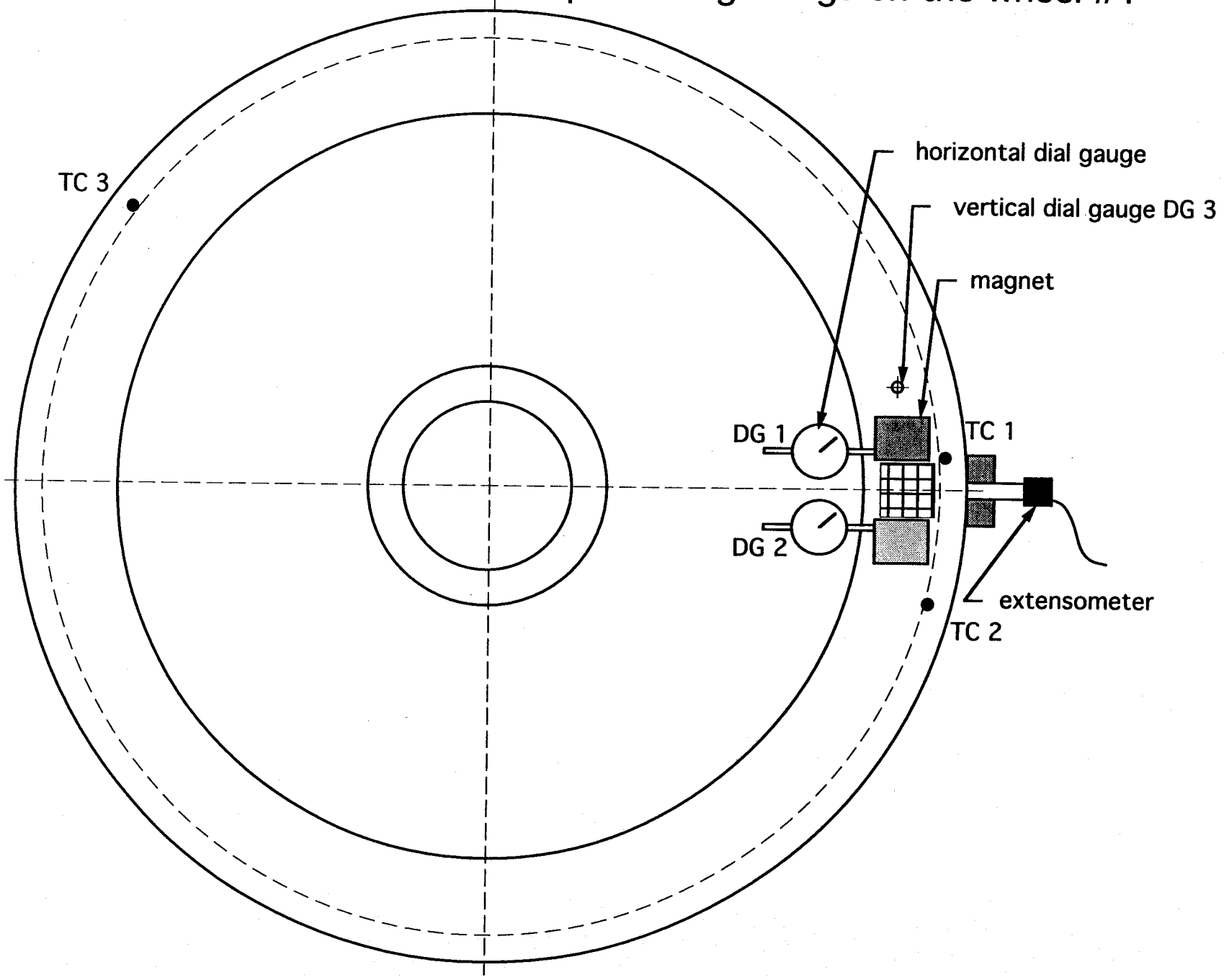

WHEEL #1 TEST DATA

TESTING OF DOT RAILROAD CAR WHEEL #1						142T			FRA 1530			
DATE:	Aug-94											
	mm/mm					Dial Gages (mm)			mm	(°C)	(°C)	(°C)
Cut Depth (mm)	Gage1	Gage2	Gage3	Gage4	Gage5	1	2	3	Opening Displacement	TC 1	TC2	TC 3
0	0	0	0	0	0	.0000	.0000	.0000	.000	26.4	25.8	25.9
29	-8	10	-35	28	-85	-.0037	-.0020	.0003	-.013	26.8	25.9	25.8
43	341	-6	344	29	376	-.0029	-.0007	.0009	-.218	29.2	26.2	26.1
48	480	-17	442	39	457	-.0031	-.0008	.0013	-.259	NA	NA	NA
54	614	-31	540	34	536	-.0022	-.0004	.0016	-.267	27.0	25.5	25.4
66	779	-43	631	34	605	-.0013	removed	.0023	-.327	28.1	26.9	27.0
74	806	-43	658	39	617	-.0007	removed	.0028	-.365	30.1	27.9	27.5
80	994	113	831	199	789	.0001	removed	.0034	-.397	29.8	29.0	28.9
90	988	98	831	178	785	.0010	removed	.0042	-.447	30.7	29.4	28.8
100	972	81	817	153	785	.0024	removed	.0057	-.495	31.1	30.1	28.9
110	942	81	802	132	762	.0035	removed	.0073	-.543	30.9	29.9	28.9
120	961	108	805	161	761	.0045	removed	.0090	-.605	31.0	30.0	29.0
130	926	56	769	117	749	.0060	removed	.0106	-.664	31.1	30.0	28.9
140	917	73	791	117	736	.0068	removed	.0118	-.723	30.9	30.3	28.8
150	887	51	760	104	729	.0077	removed	.0129	-.771	30.8	30.1	28.9
160	886	66	780	130	750	.0083	removed	.0138	-.820	30.8	30.1	28.9
170	891	79	786	140	742	removed	removed	.0145	-.867	30.8	30.1	28.9
180	891	58	750	138	747	removed	removed	.0154	-.916	30.6	30.0	28.9
190	910	58	774	122	739	removed	removed	.0164	-.969	30.4	29.9	28.9
206	914	69	771	124	741	removed	removed	.0179	-1.072	30.3	30.0	28.9
208	811	-147	732	-47	561	removed	removed	.5316	-1.234	22.2	22.4	22.4
END												

Railroad Wheel No. 1 Test
Displacement vs. Cut Depth

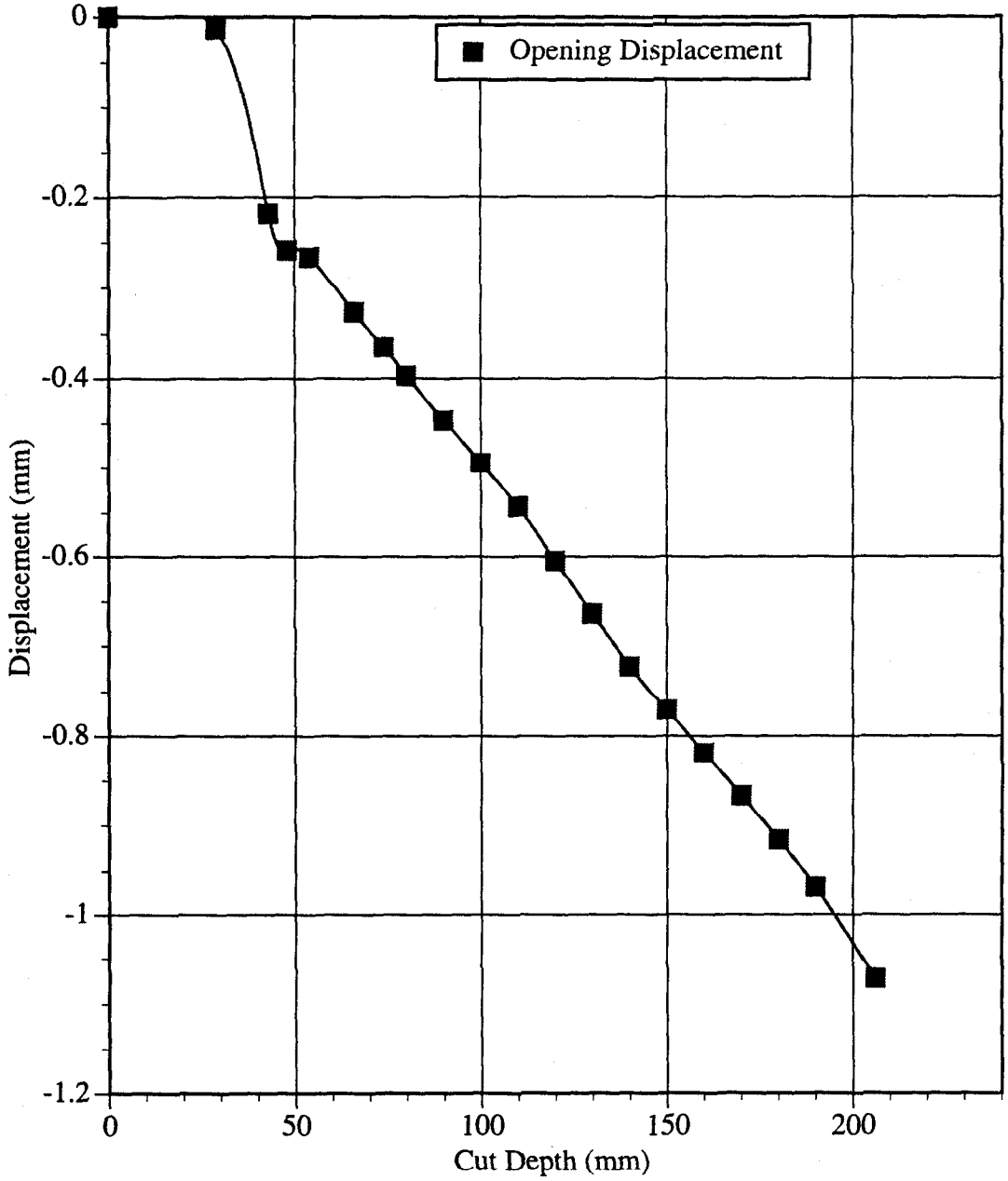

Railroad Wheel No. 1 Test
Strain Gage Readings vs. Cut Depth

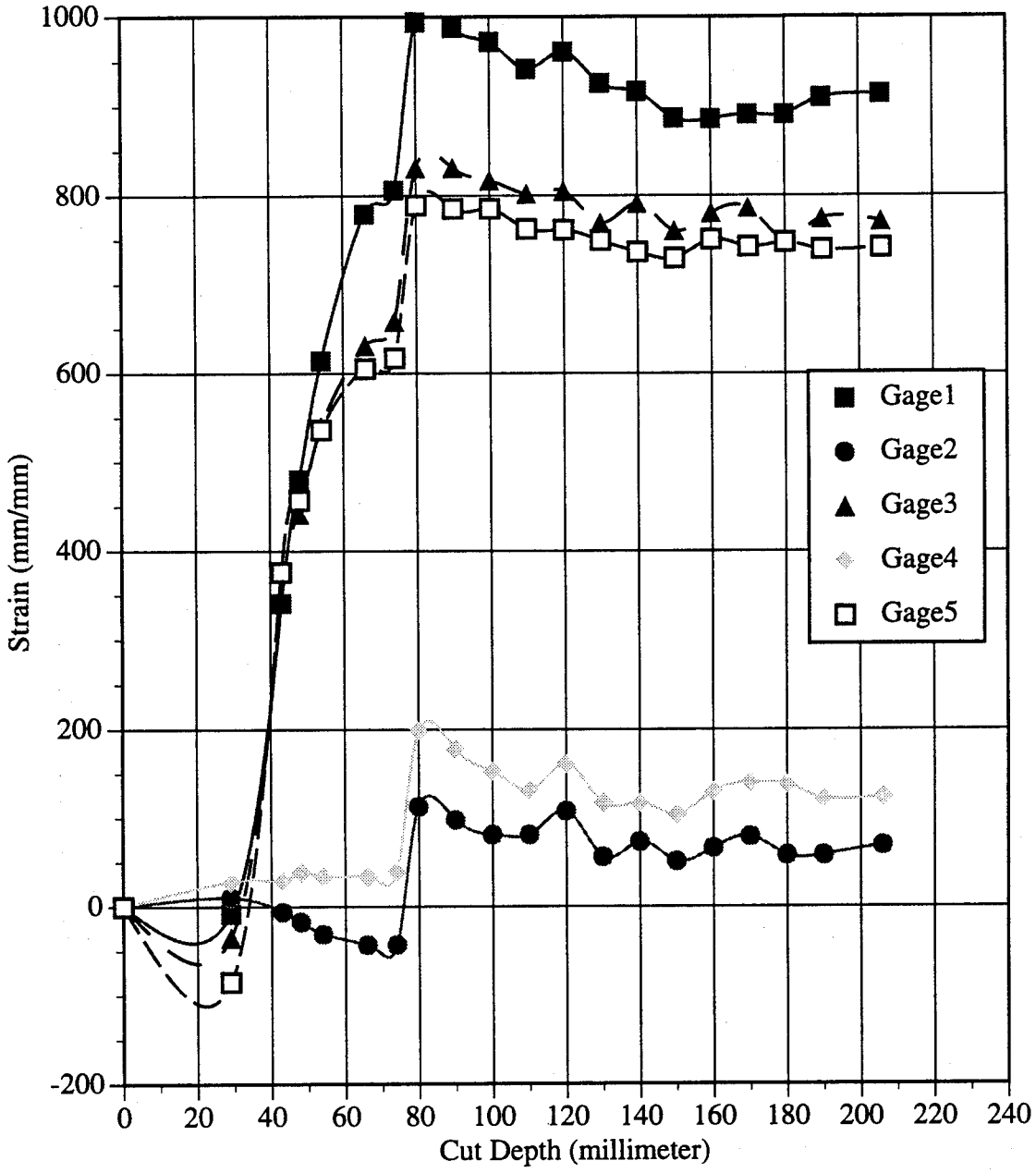

Railroad Wheel No. 1 Test
Dial Gage Reading vs. Cut Depth

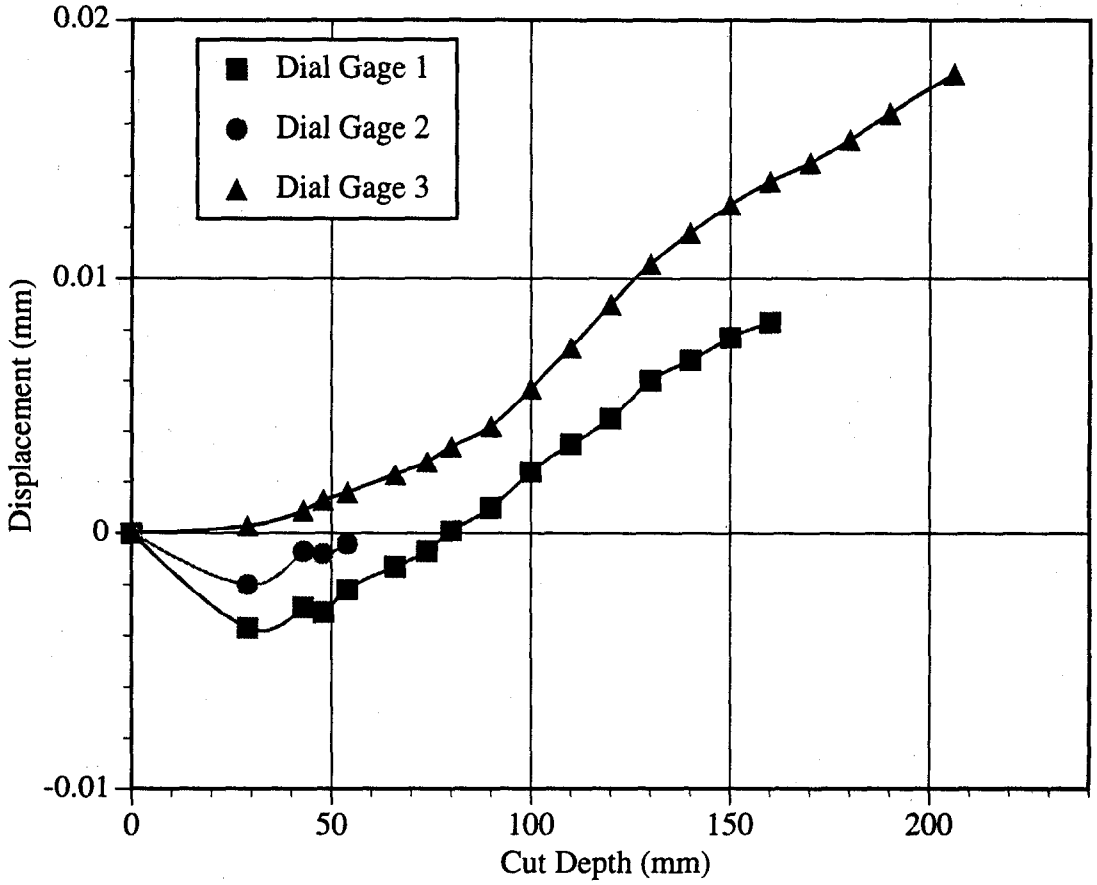

Railroad Car Wheel No. 1 Flange Side Interferometry Results
Horizontal Displacement Field After Cut No. 1 (in mm)

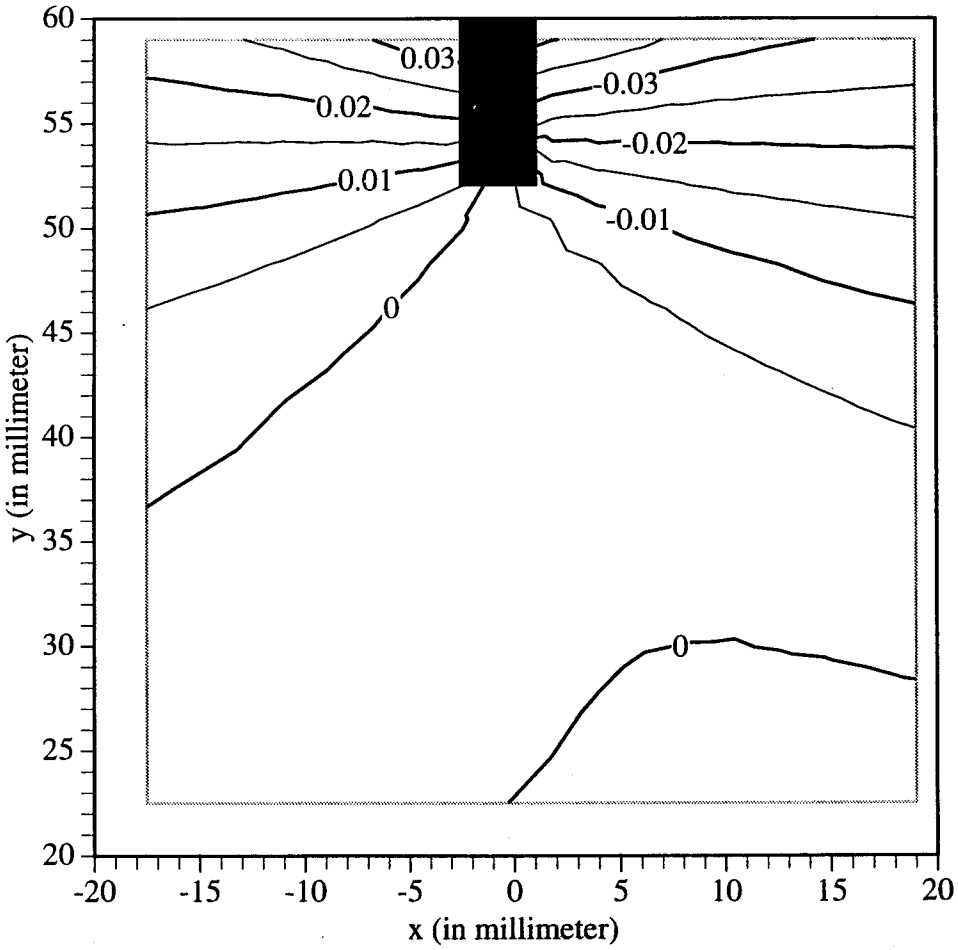

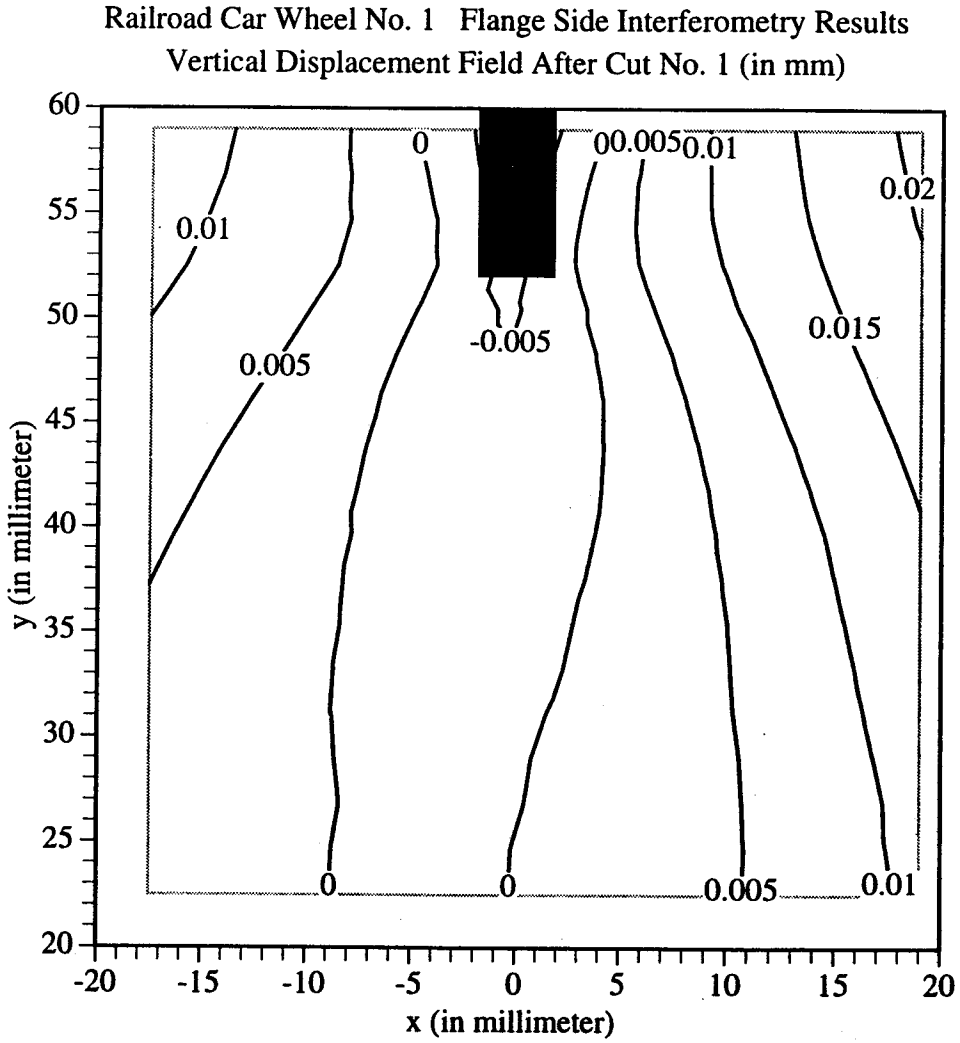
Railroad Car Wheel No. 1 Flange Side Interferometry Results
Vertical Displacement Field After Cut No. 1 (in mm)
y (in millimeter)
x (in millimeter)
60
55
50
45
40
35
30
25
20
-20
-15
-10
-5
0
5
10
15
20
0.01
0.005
0
-0.005
00.005
0.01
0.02
0.015
0
0
0.005
0.01

Railroad Car Wheel No. 1 Flange Side Interferometry Results
Out-of-plane Displacement Field After Cut No. 1 (in mm)

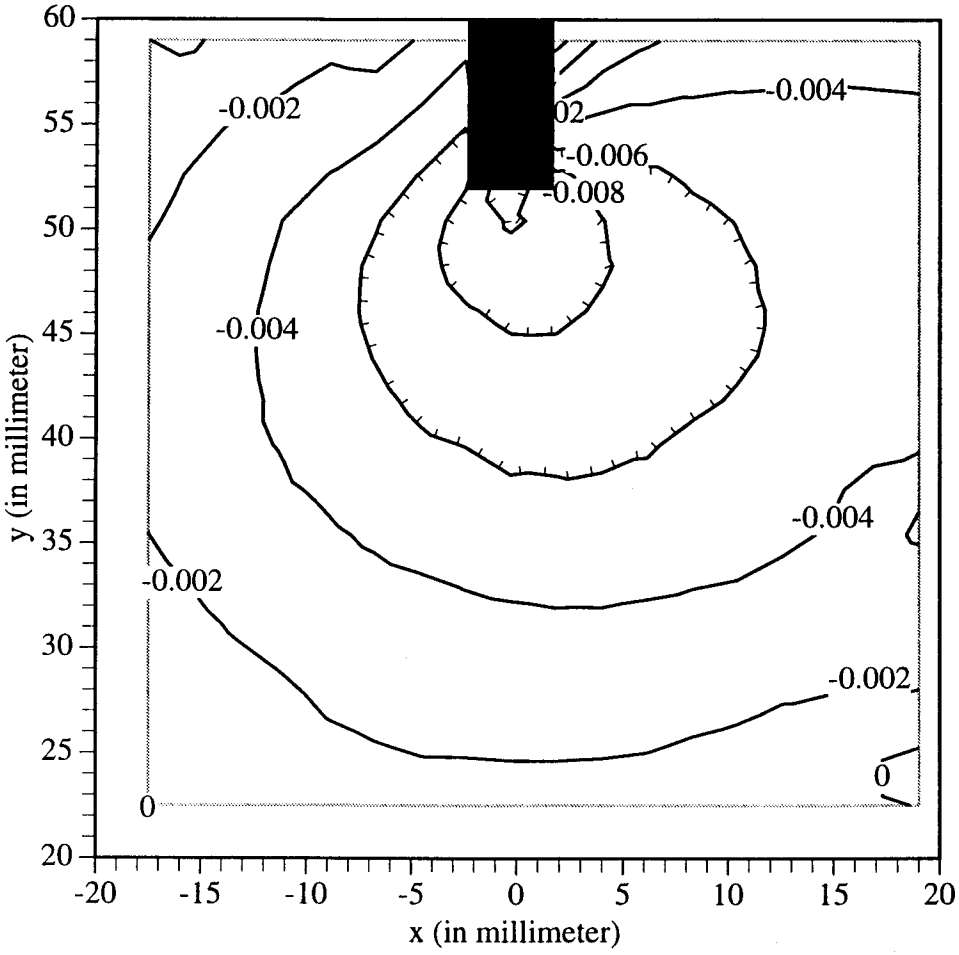

Railroad Car Wheel No. 1 Flange Side Interferometry Results
Horizontal Strain Field After Cut No. 1 (in mm/mm)

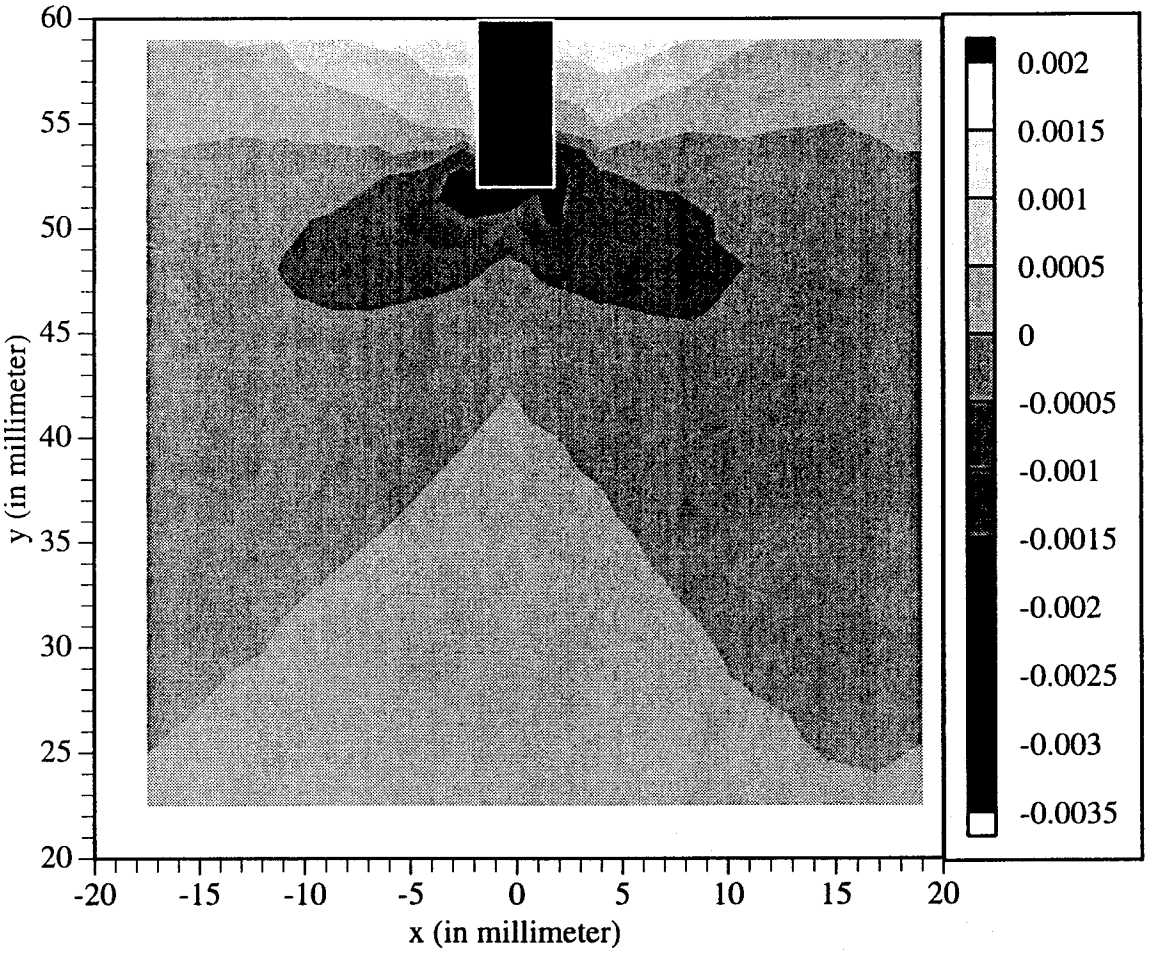

Railroad Car Wheel No. 1 Flange Side Interferometry Results
Vertical Strain Field After Cut No. 1 (in mm/mm)

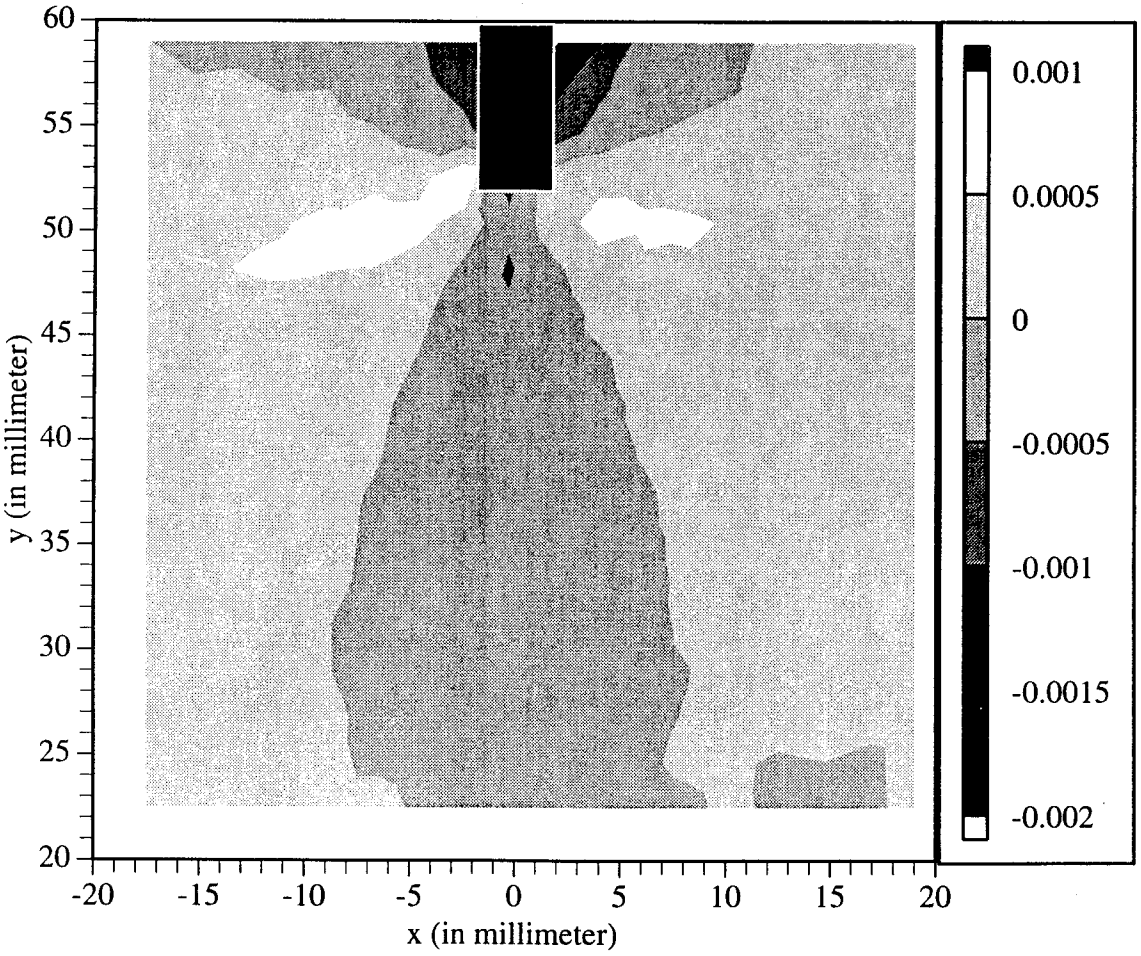

Railroad Car Wheel No. 1 Flange Side Interferometry Results
Shear Strain Field After Cut No. 1 (in mm/mm)

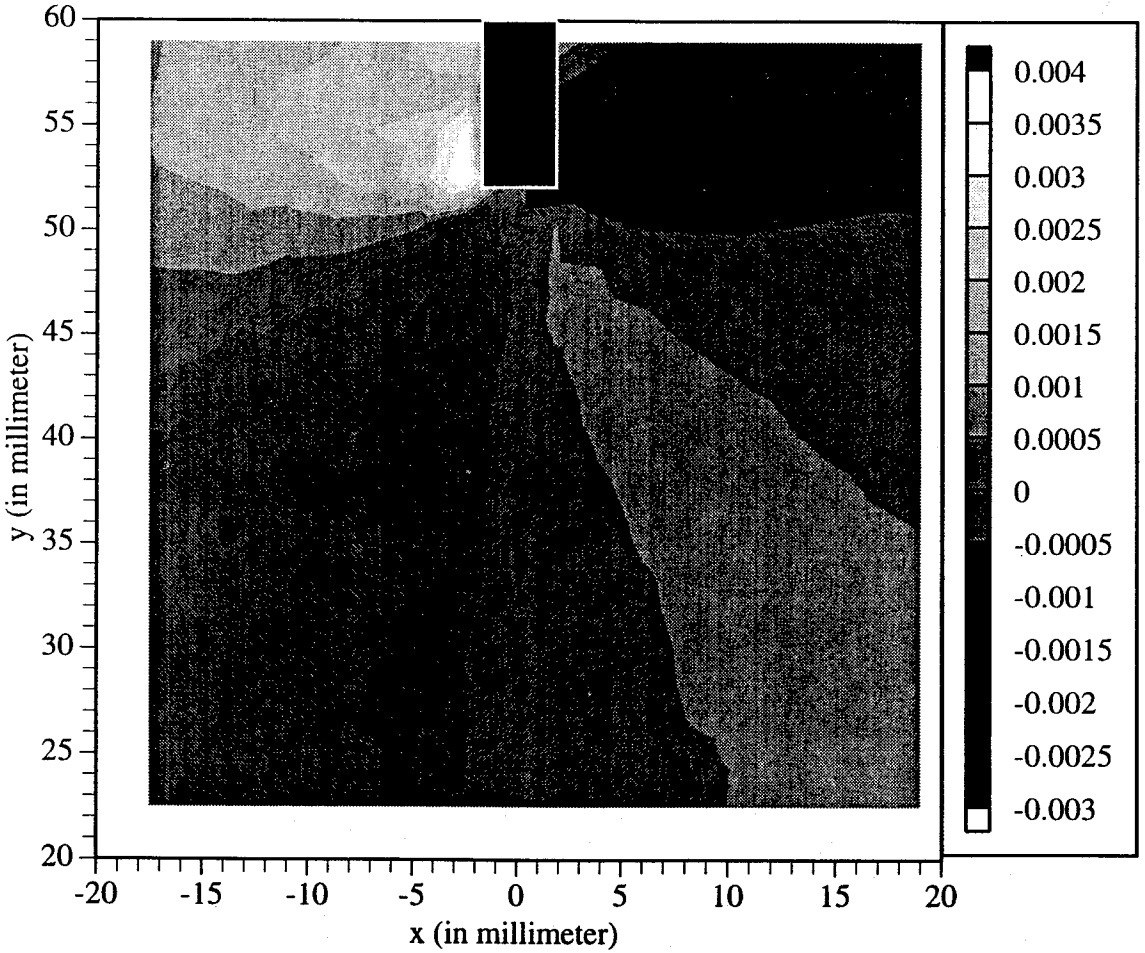

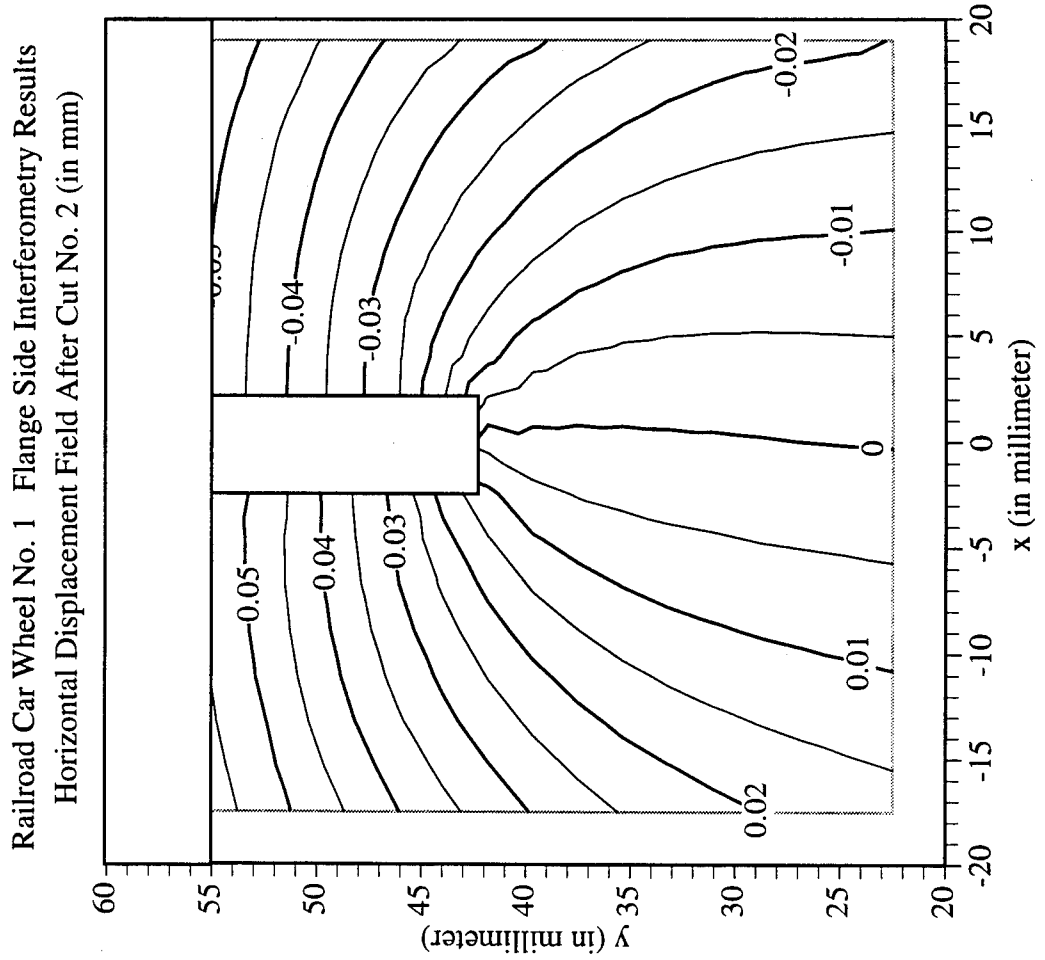
Railroad Car Wheel No. 1 Flange Side Interferometry Results
Horizontal Displacement Field After Cut No. 2 (in mm)
y (in millimeter)
x (in millimeter)
60
55
50
45
40
35
30
25
20
-20
-15
-10
-5
0
5
10
15
20
0.05
0.04
0.03
0.02
0.01
0
-0.01
-0.02
-0.03
-0.04

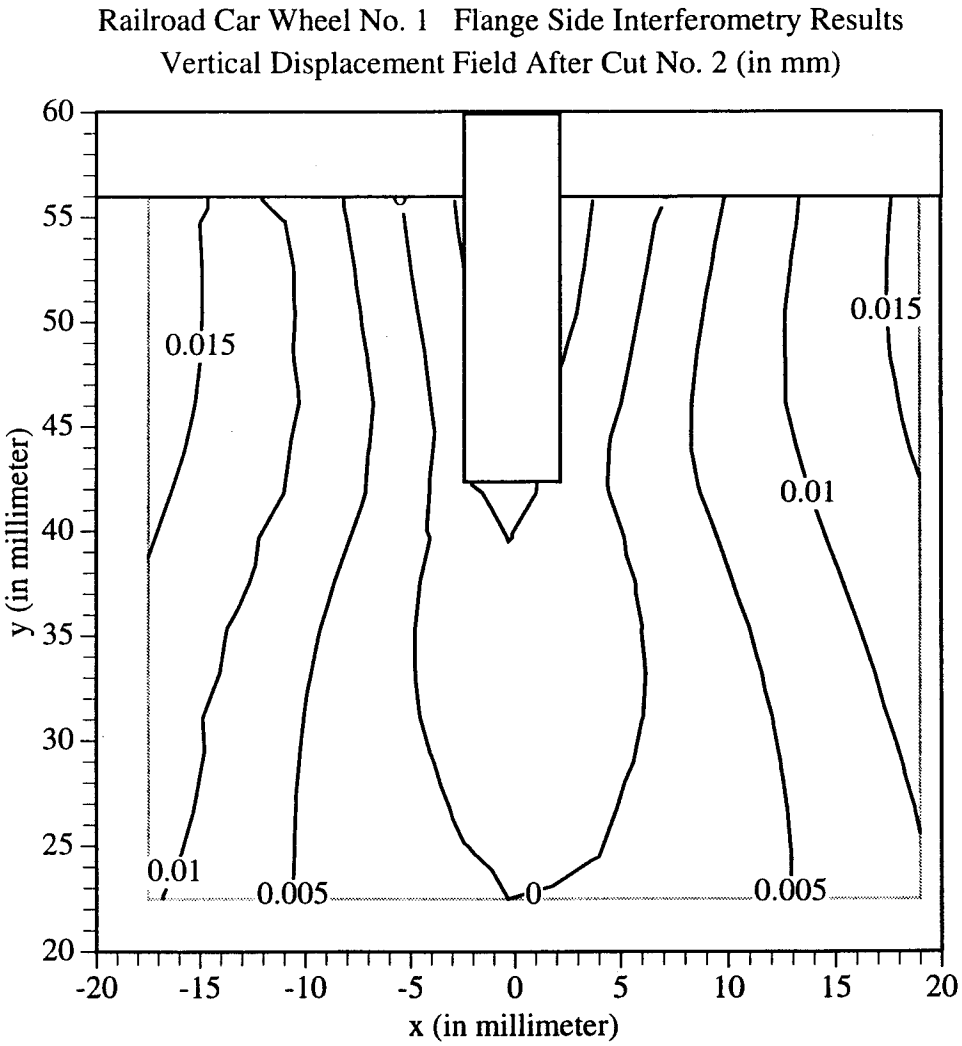
Railroad Car Wheel No. 1 Flange Side Interferometry Results
Vertical Displacement Field After Cut No. 2 (in mm)
y (in millimeter)
x (in millimeter)
60
55
50
45
40
35
30
25
20
-20
-15
-10
-5
0
5
10
15
20
0.015
0.015
0.01
0.01
0.005
0
0.005

Railroad Car Wheel No. 1 Flange Side Interferometry Results
Out-of-plane Displacement Field After Cut No. 2 (in mm)

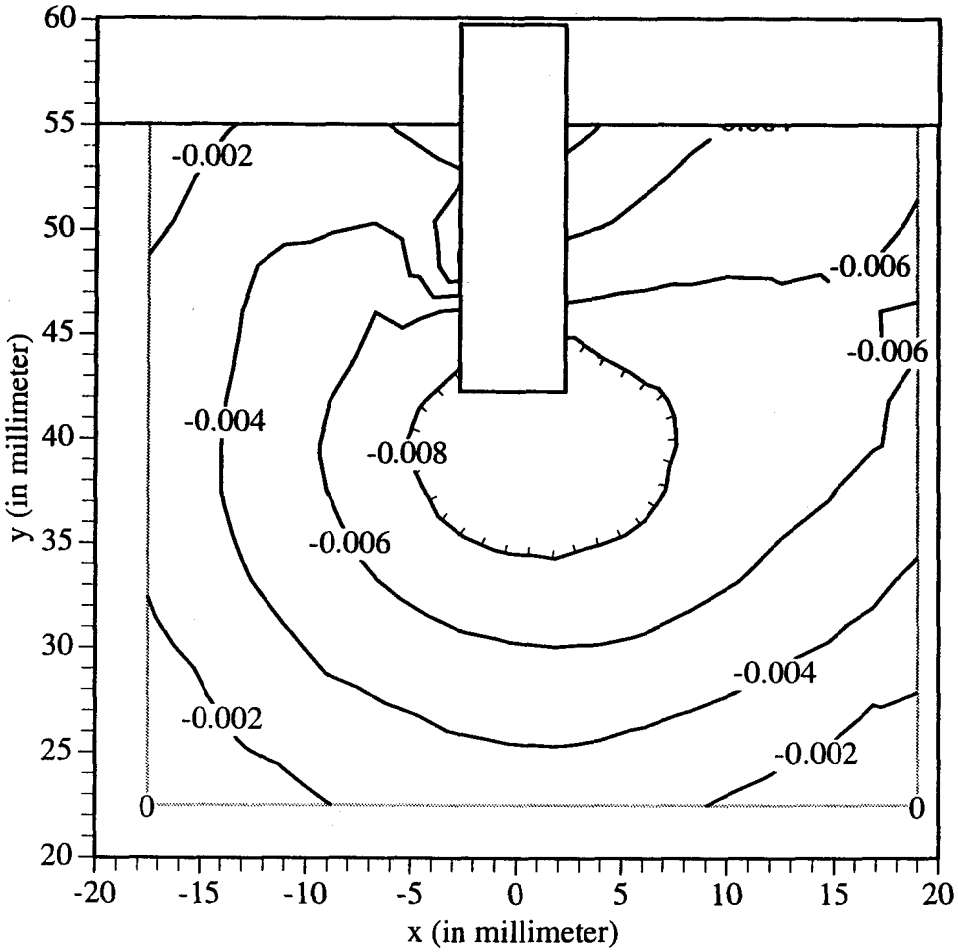

Railroad Car Wheel No. 1 Flange Side Interferometry Results
Horizontal Strain Field After Cut No. 2 (in mm/mm)

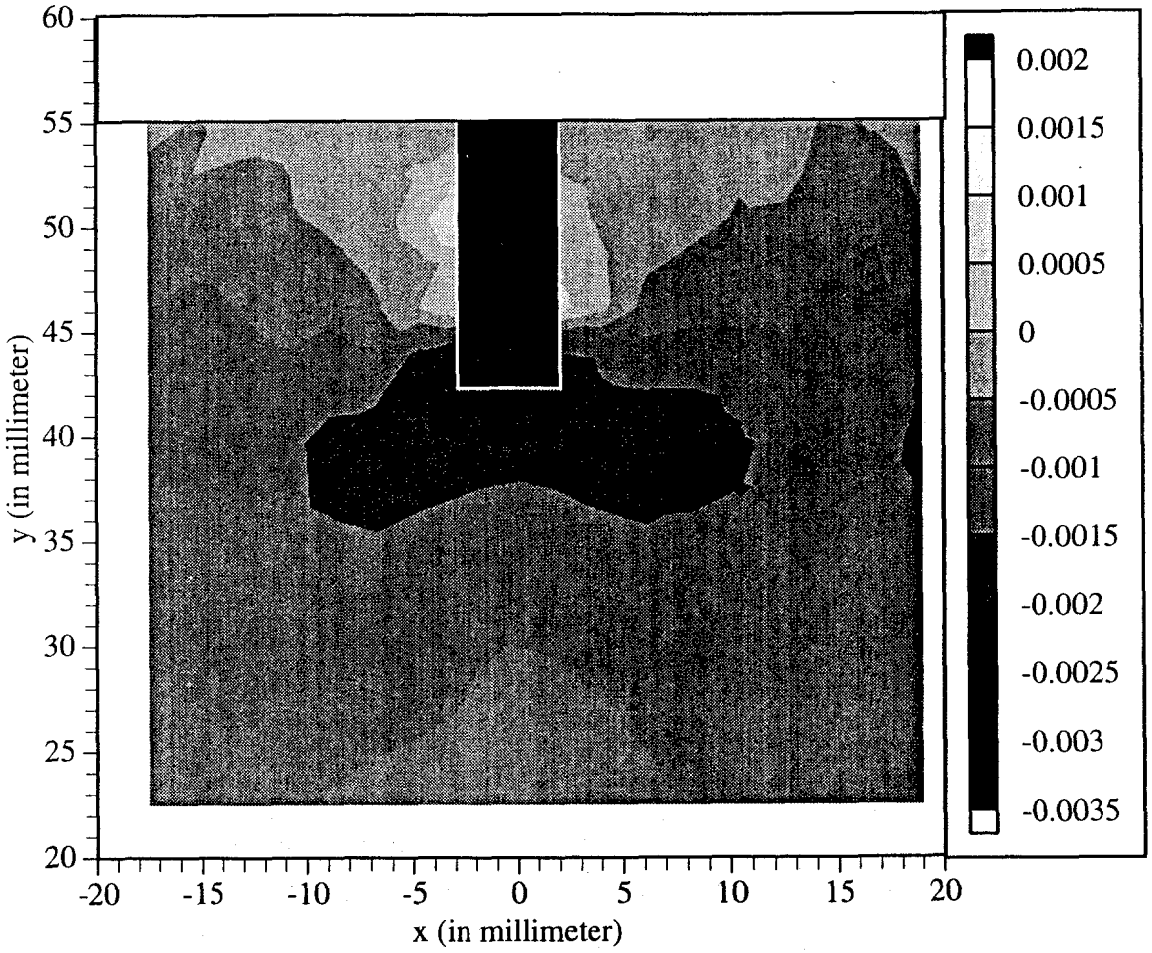

Railroad Car Wheel No. 1 Flange Side Interferometry Results
Vertical Strain Field After Cut No. 2(in mm/mm)

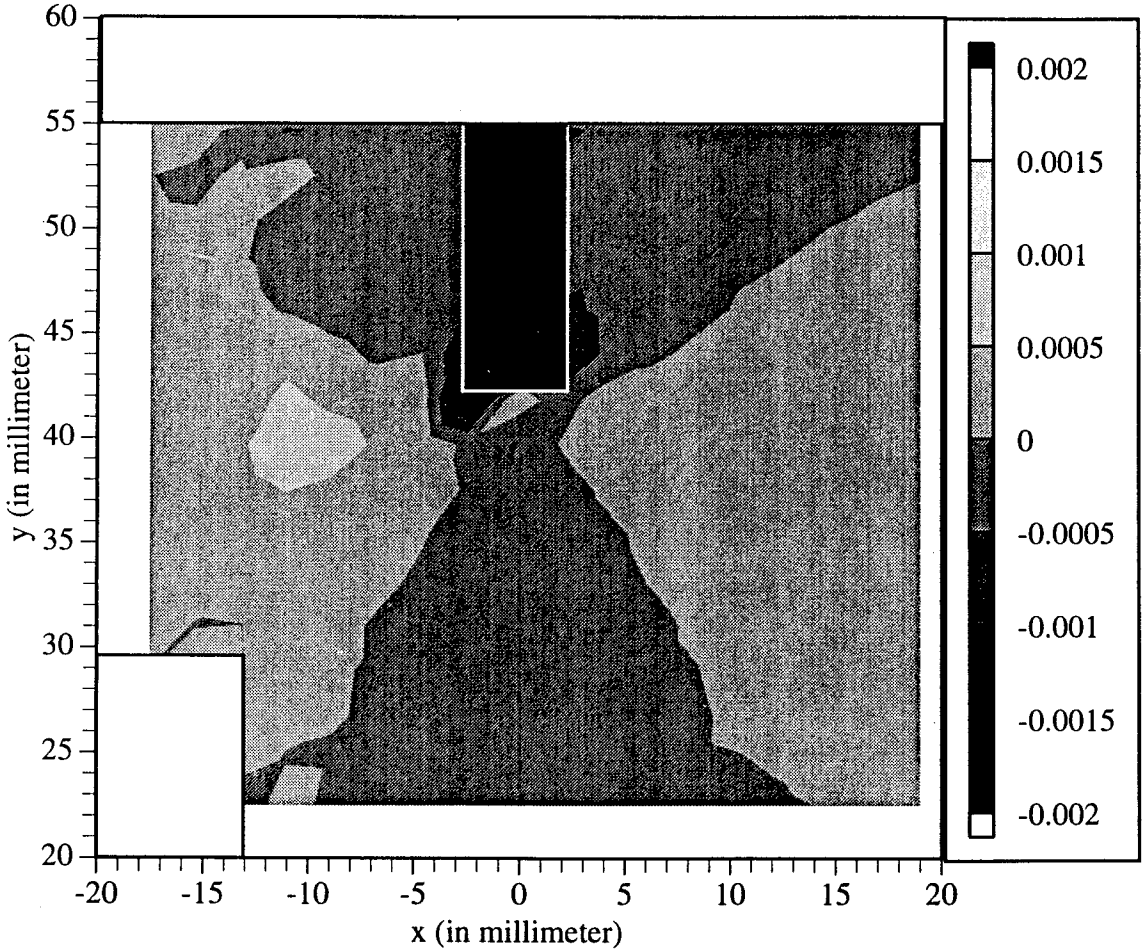

Railroad Car Wheel No. 1 Flange Side Interferometry Results
Shear Strain Field After Cut No. 2 (in mm/mm)

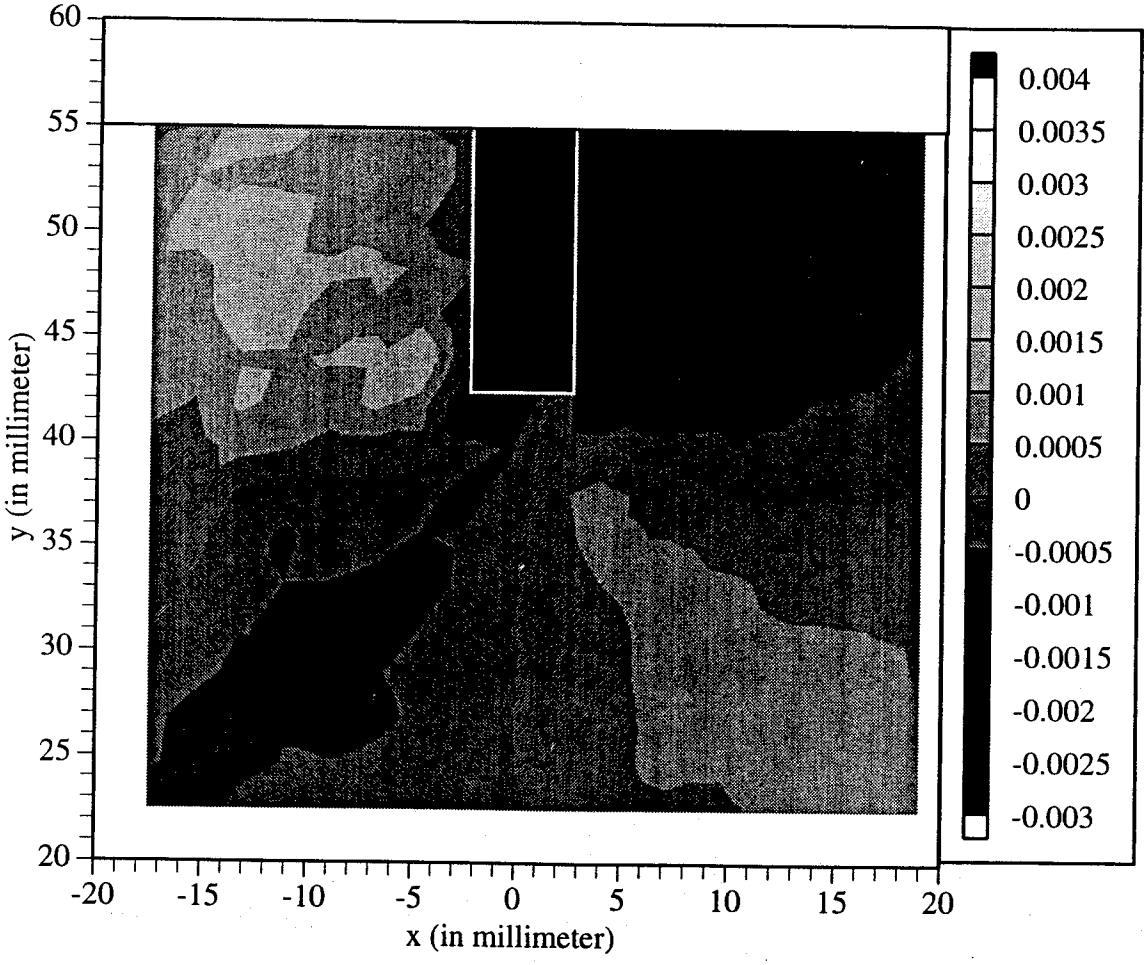

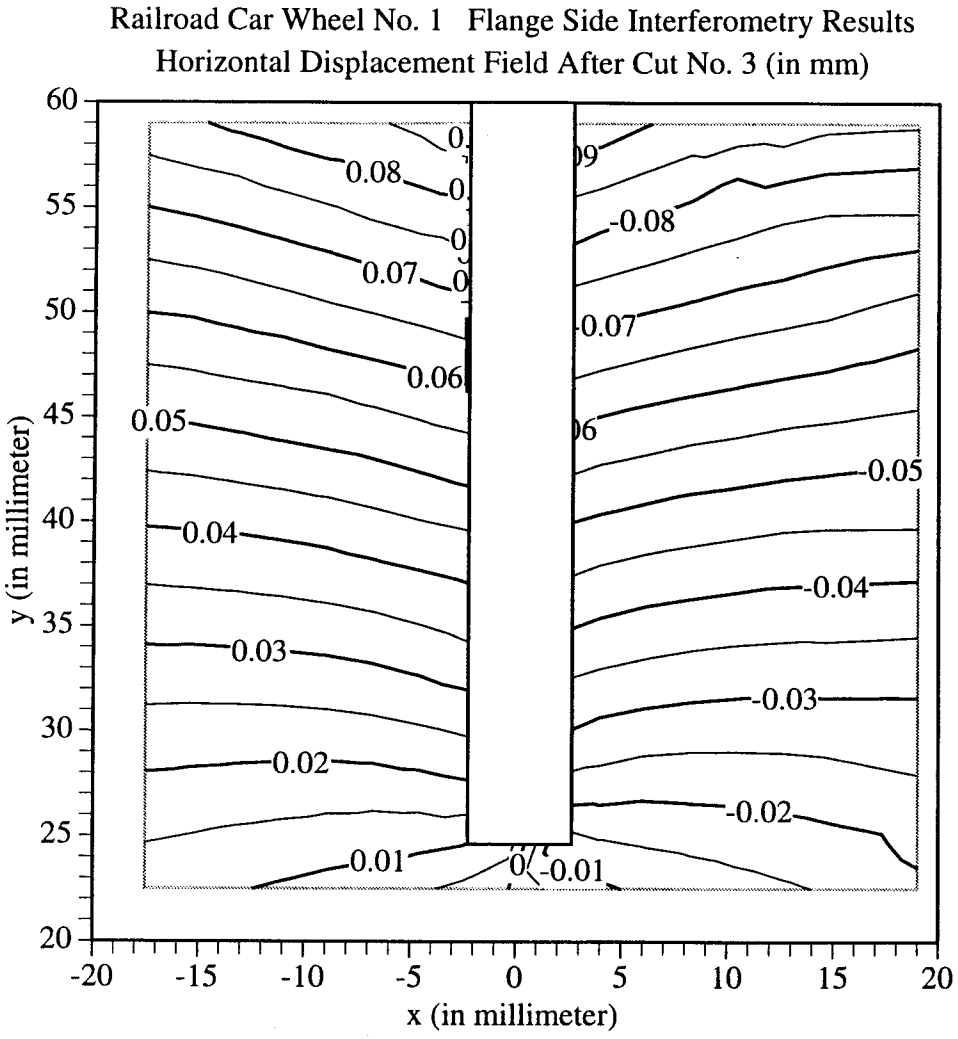
Railroad Car Wheel No. 1 Flange Side Interferometry Results
Horizontal Displacement Field After Cut No. 3 (in mm)
y (in millimeter)
x (in millimeter)
60
55
50
45
40
35
30
25
20
-20
-15
-10
-5
0
5
10
15
20
0.08
0.07
0.06
0.05
0.04
0.03
0.02
0.01
0
-0.01
-0.08
-0.07
-0.05
-0.04
-0.03
-0.02

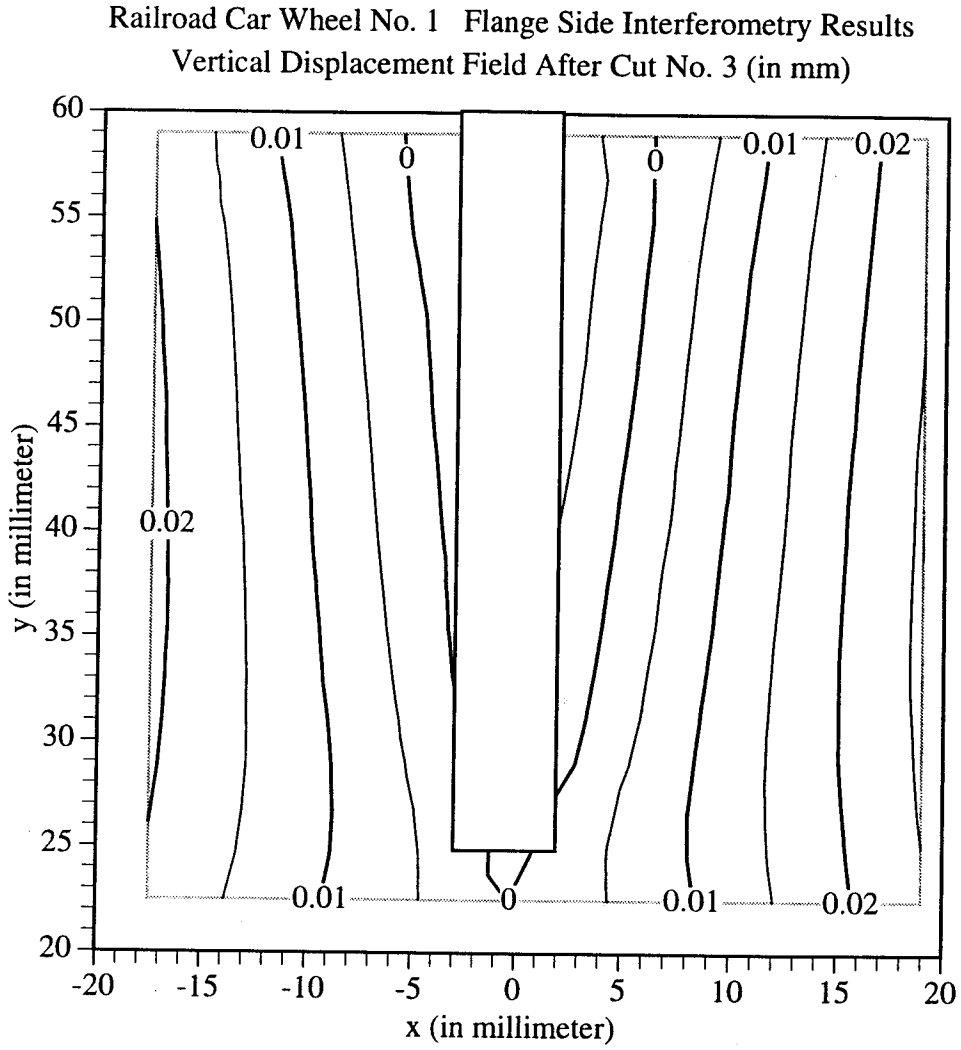
Railroad Car Wheel No. 1 Flange Side Interferometry Results
Vertical Displacement Field After Cut No. 3 (in mm)
0.01
0
0
0.01
0.02
0.02
0.01
0
0.01
0.02
y (in millimeter)
x (in millimeter)
60
55
50
45
40
35
30
25
20
-20
-15
-10
-5
0
5
10
15
20

Railroad Car Wheel No. 1 Flange Side Interferometry Results
Out-of-plane Displacement Field After Cut No. 3 (in mm)

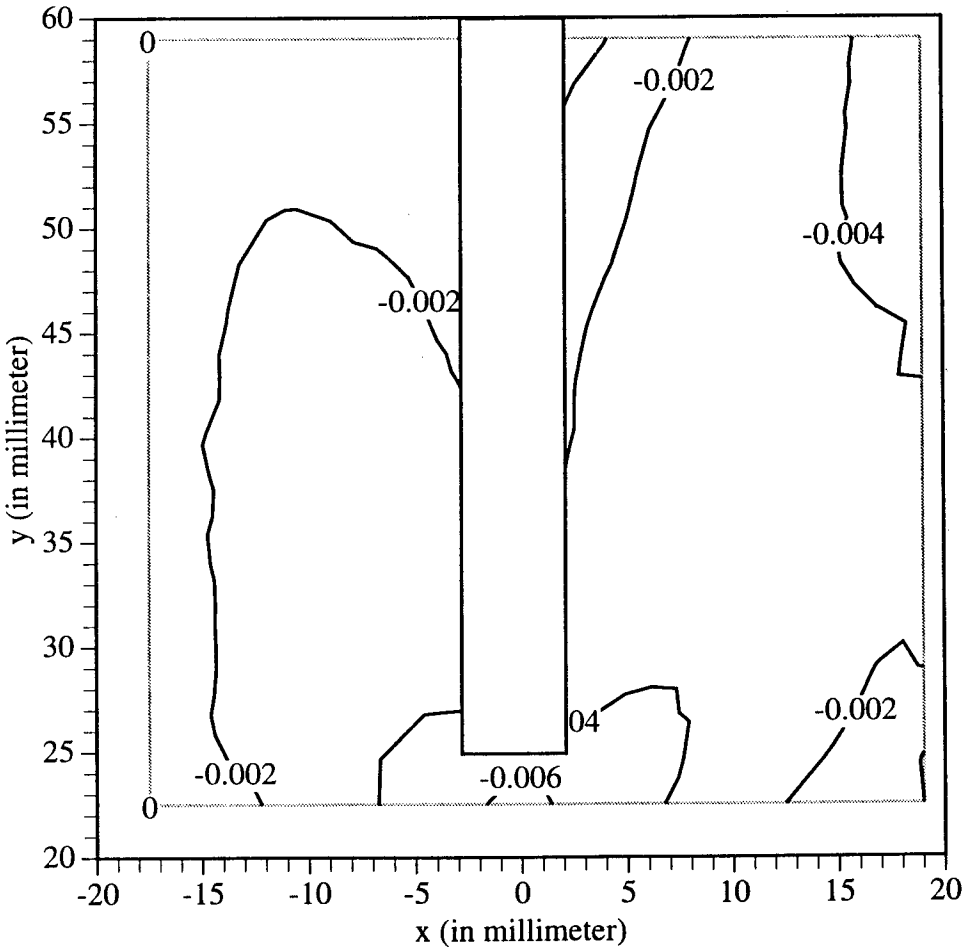

Railroad Car Wheel No. 1 Flange Side Interferometry Results
Horizontal Strain Field After Cut No. 3 (in mm/mm)

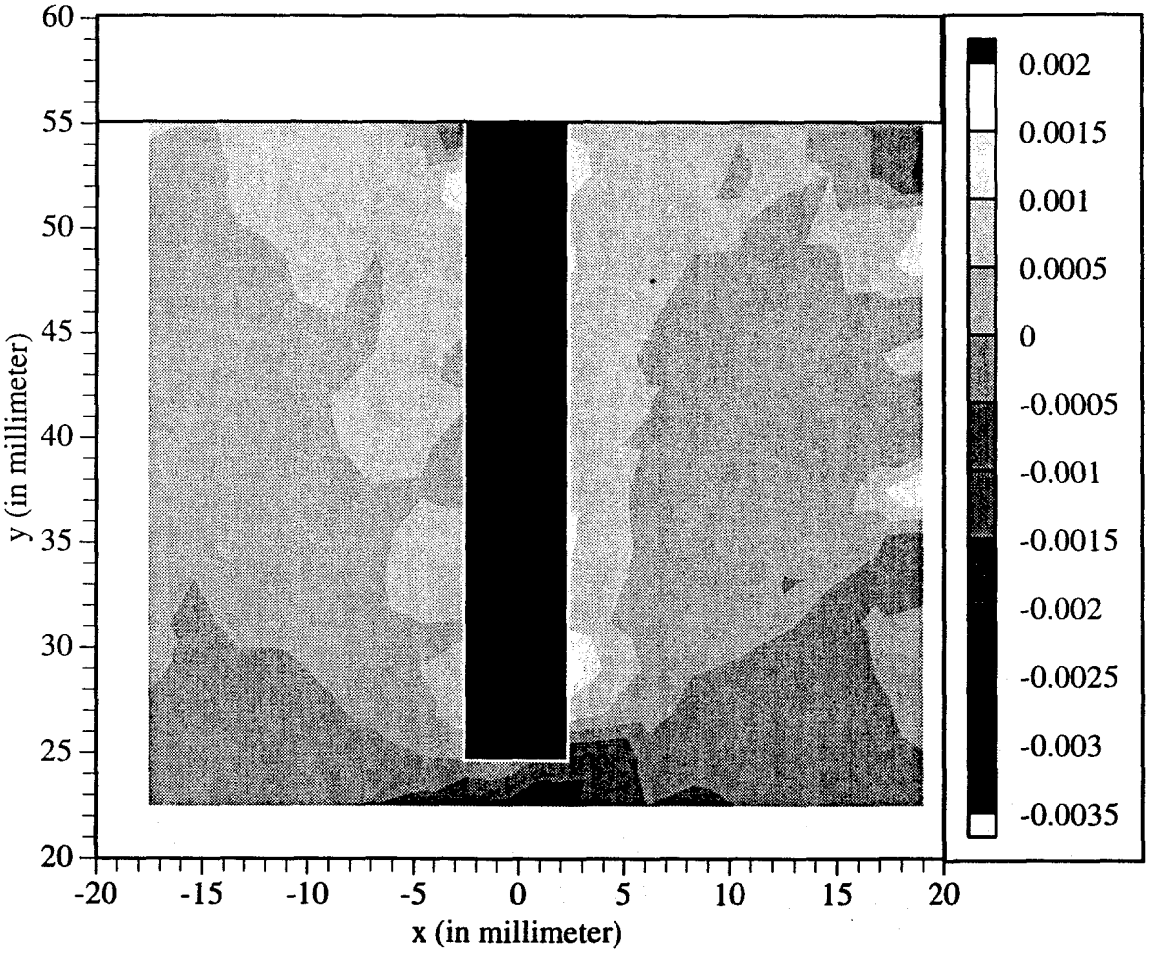

Railroad Car Wheel No. 1 Flange Side Interferometry Results
Vertical Strain Field After Cut No. 3 (in mm/mm)

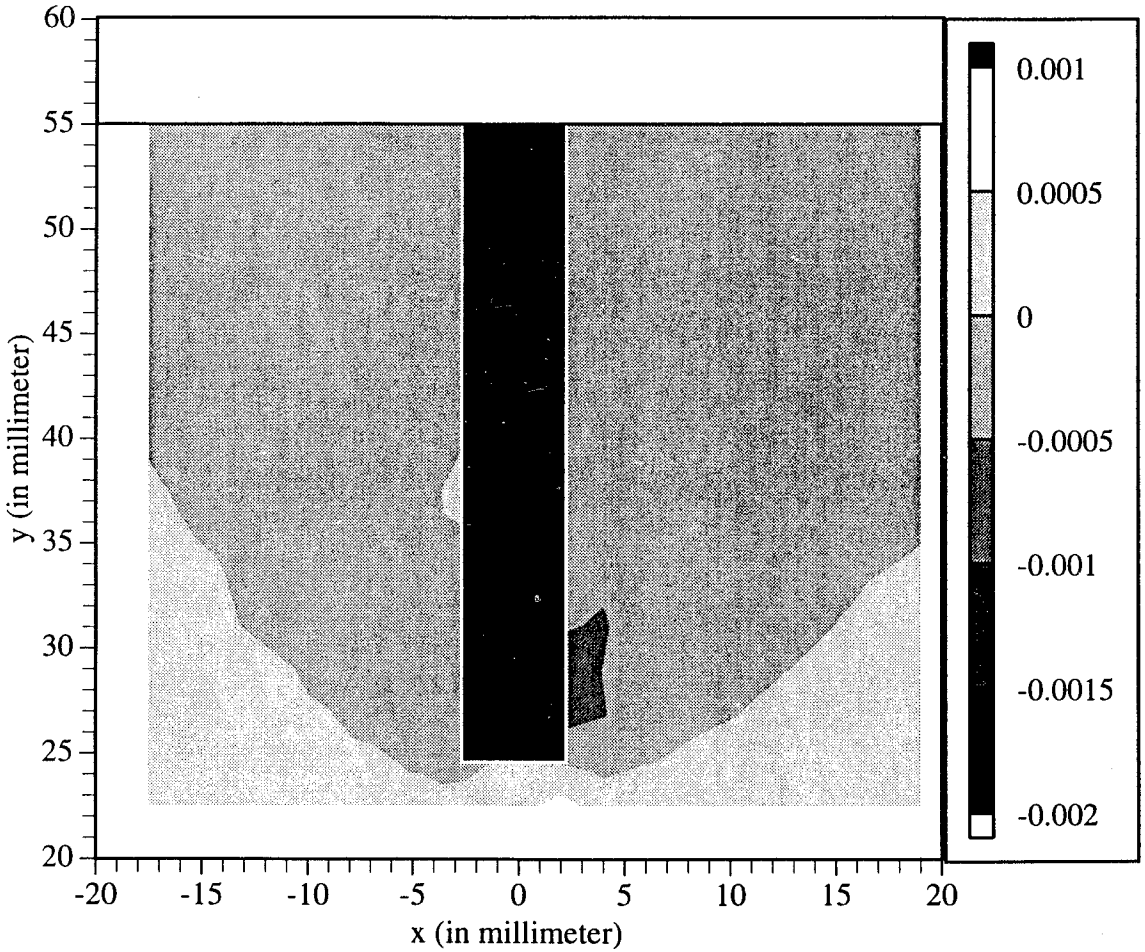

Railroad Car Wheel No. 1 Flange Side Interferometry Results
Shear Strain Field After Cut No. 3 (in mm/mm)

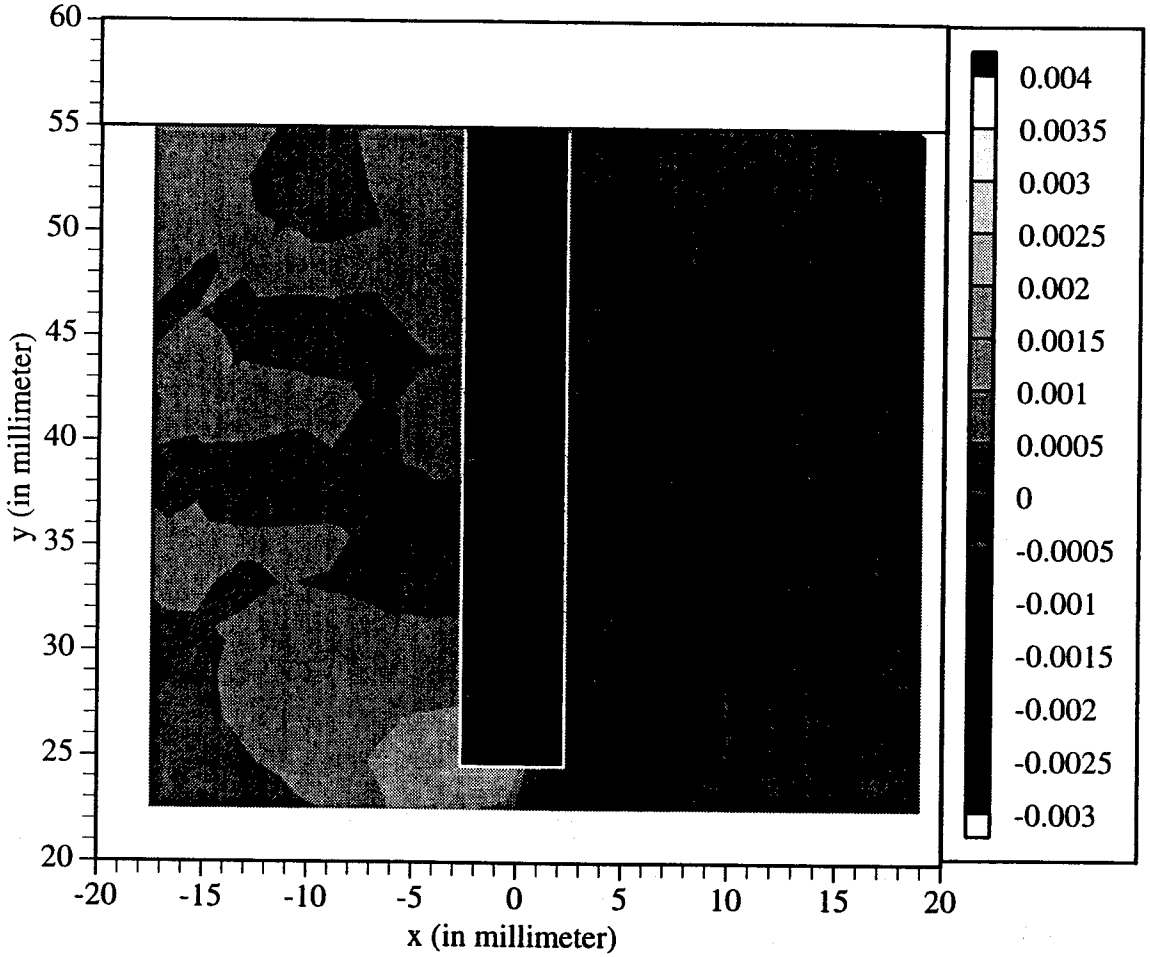

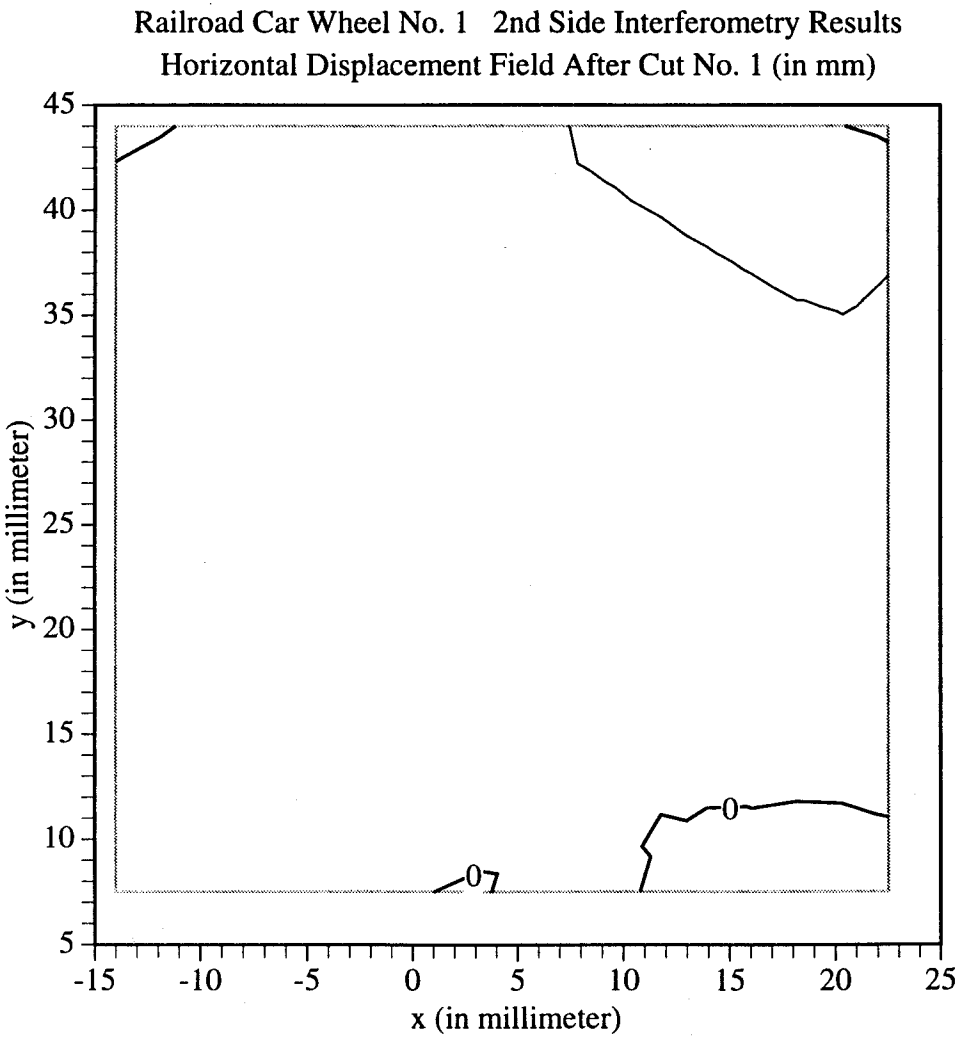
Railroad Car Wheel No. 1 2nd Side Interferometry Results
Horizontal Displacement Field After Cut No. 1 (in mm)
45
40
35
30
25
20
15
10
5
y (in millimeter)
-15
-10
-5
0
5
10
15
20
25
x (in millimeter)
0
0

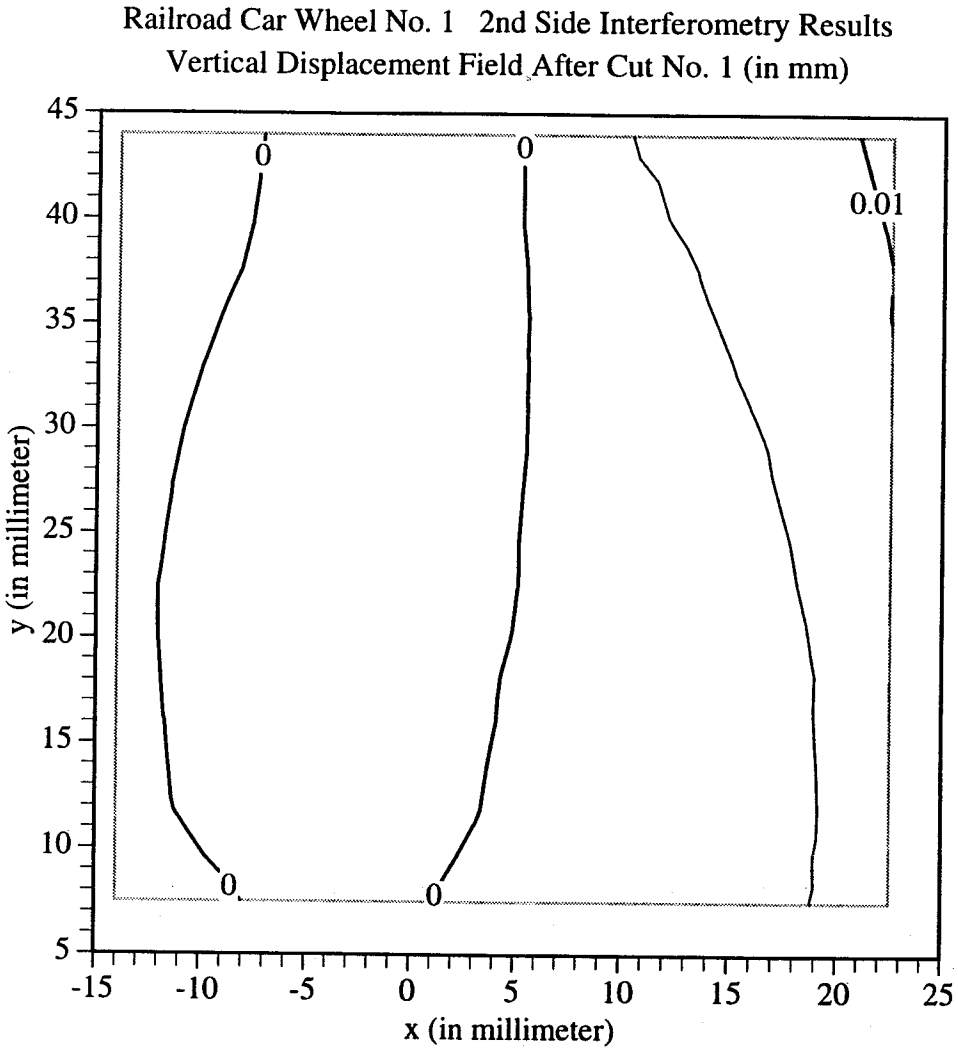
Railroad Car Wheel No. 1 2nd Side Interferometry Results
Vertical Displacement Field After Cut No. 1 (in mm)
0
0
0.01
0
0
y (in millimeter)
x (in millimeter)
45
40
35
30
25
20
15
10
5
-15
-10
-5
0
5
10
15
20
25

Railroad Car Wheel No. 1 2nd Side Interferometry Results
Out-of-plane Displacement Field After Cut No. 1 (in mm)

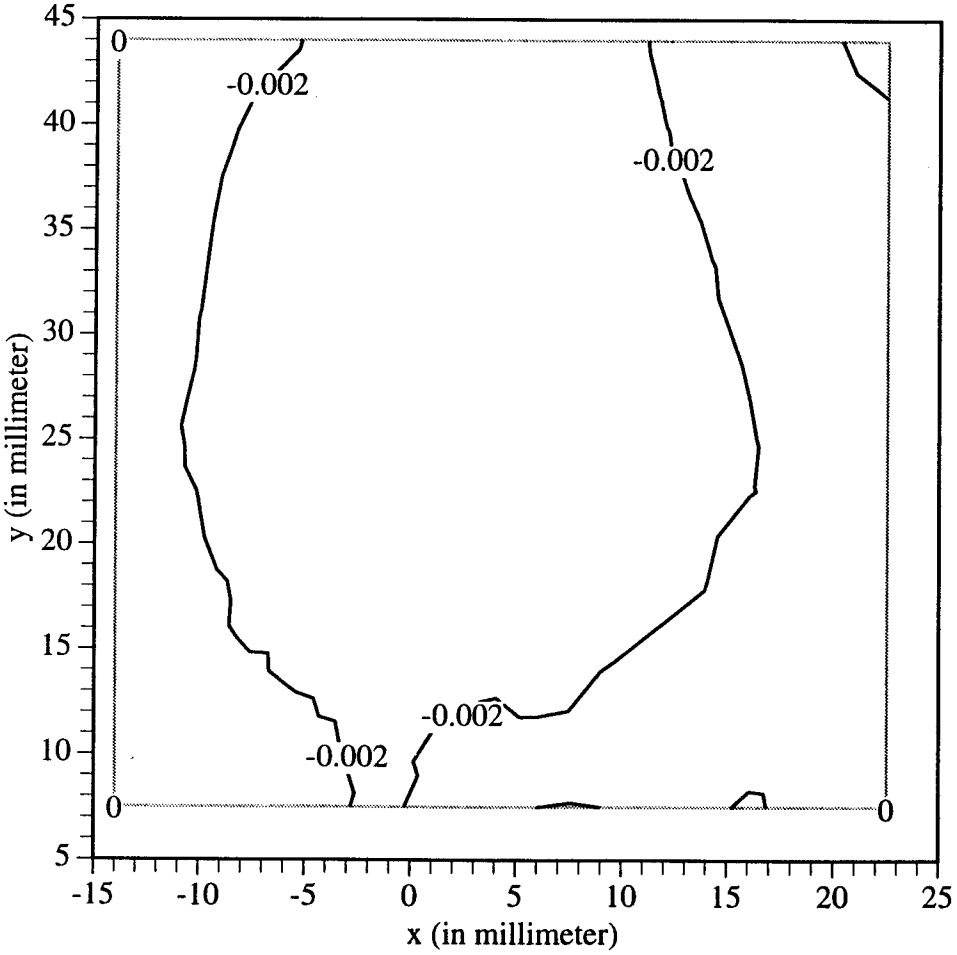

Railroad Car Wheel No. 1 2nd Side Interferometry Results
Horizontal Strain Field After Cut No. 1 (in mm/mm)

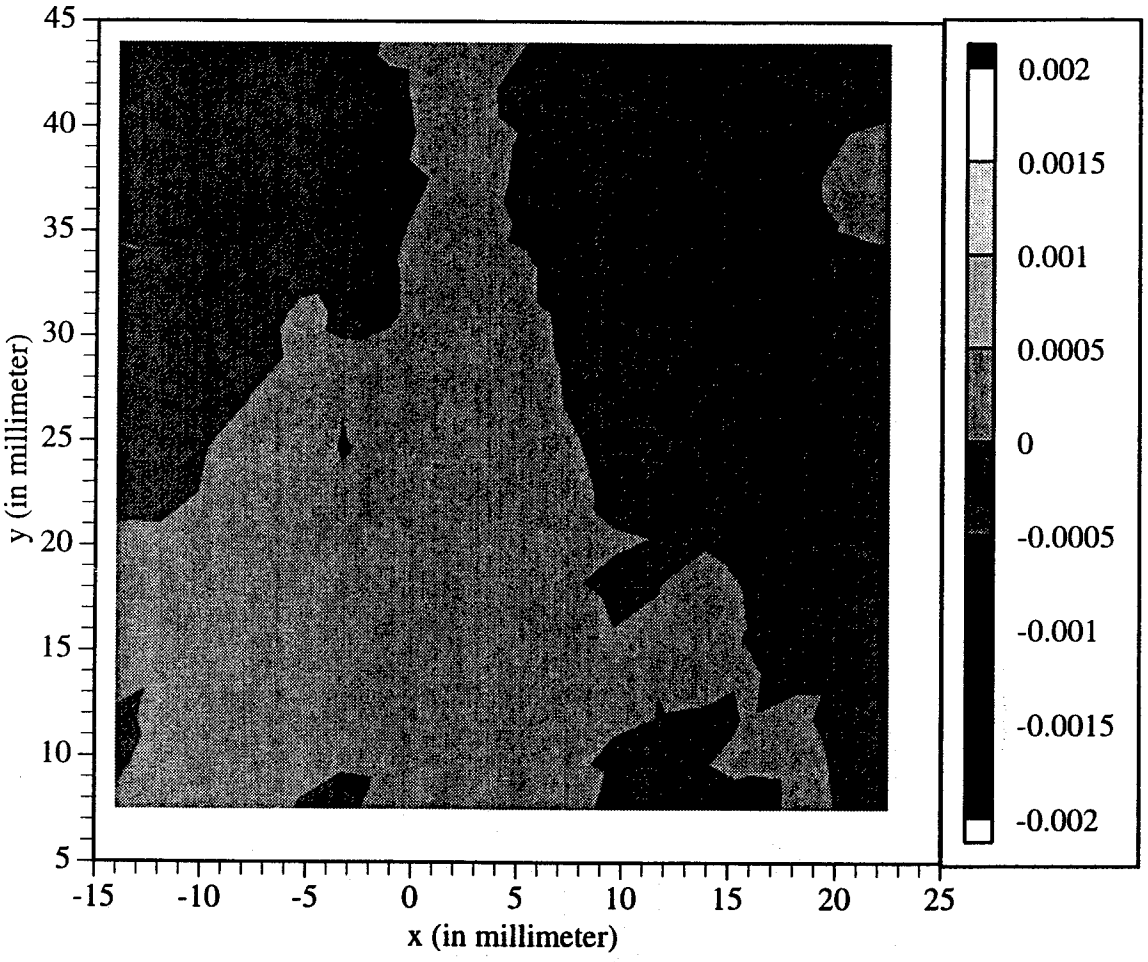

Railroad Car Wheel No. 1 2nd Side Interferometry Results
Vertical Strain Field After Cut No. 1 (in mm/mm)

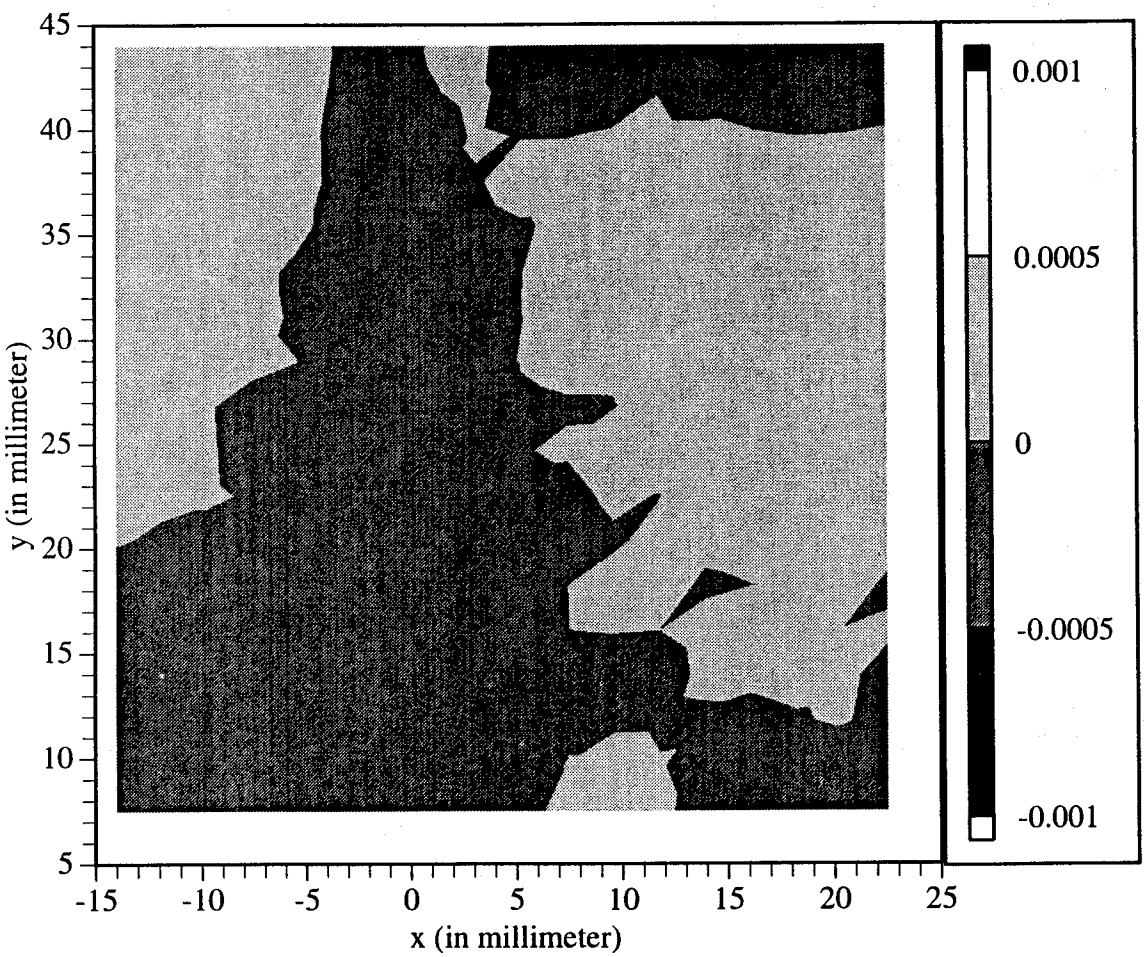

Railroad Car Wheel No. 1 2nd Side Interferometry Results
Shear Strain Field After Cut No. 1 (in mm/mm)

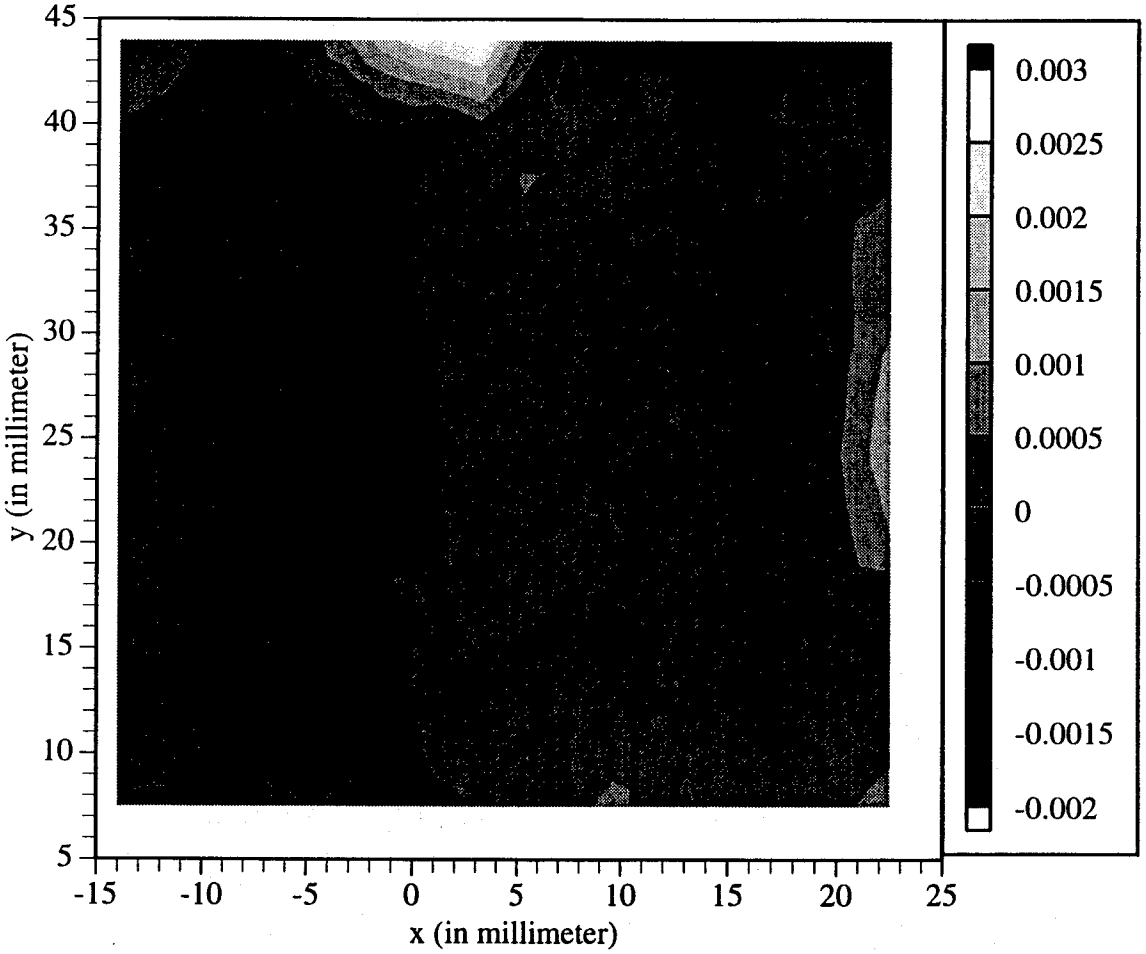

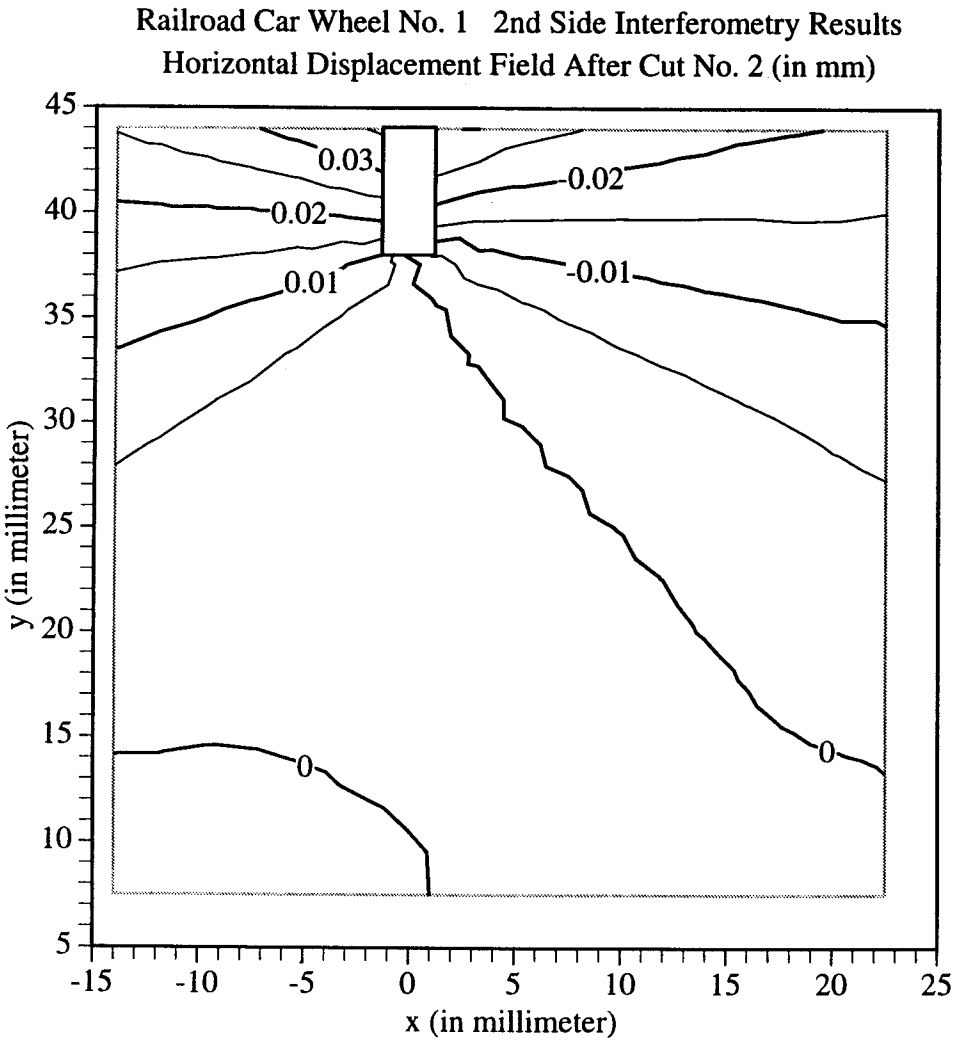
Railroad Car Wheel No. 1 2nd Side Interferometry Results
Horizontal Displacement Field After Cut No. 2 (in mm)
0.03
0.02
0.02
0.01
-0.01
0
0
y (in millimeter)
x (in millimeter)
45
40
35
30
25
20
15
10
5
-15
-10
-5
0
5
10
15
20
25

Railroad Car Wheel No. 1 2nd Side Interferometry Results
Vertical Displacement Field After Cut No. 2 (in mm)

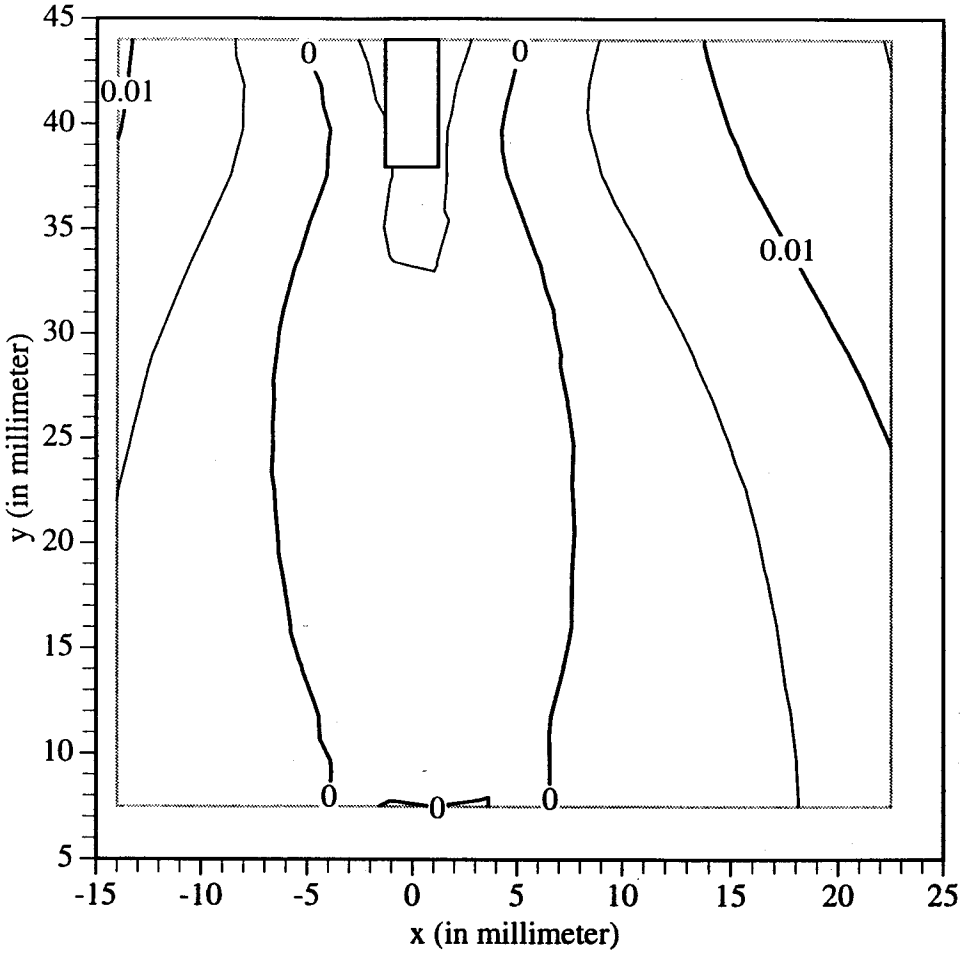

Railroad Car Wheel No. 1 2nd Side Interferometry Results
Out-of-plane Displacement Field After Cut No. 2 (in mm)

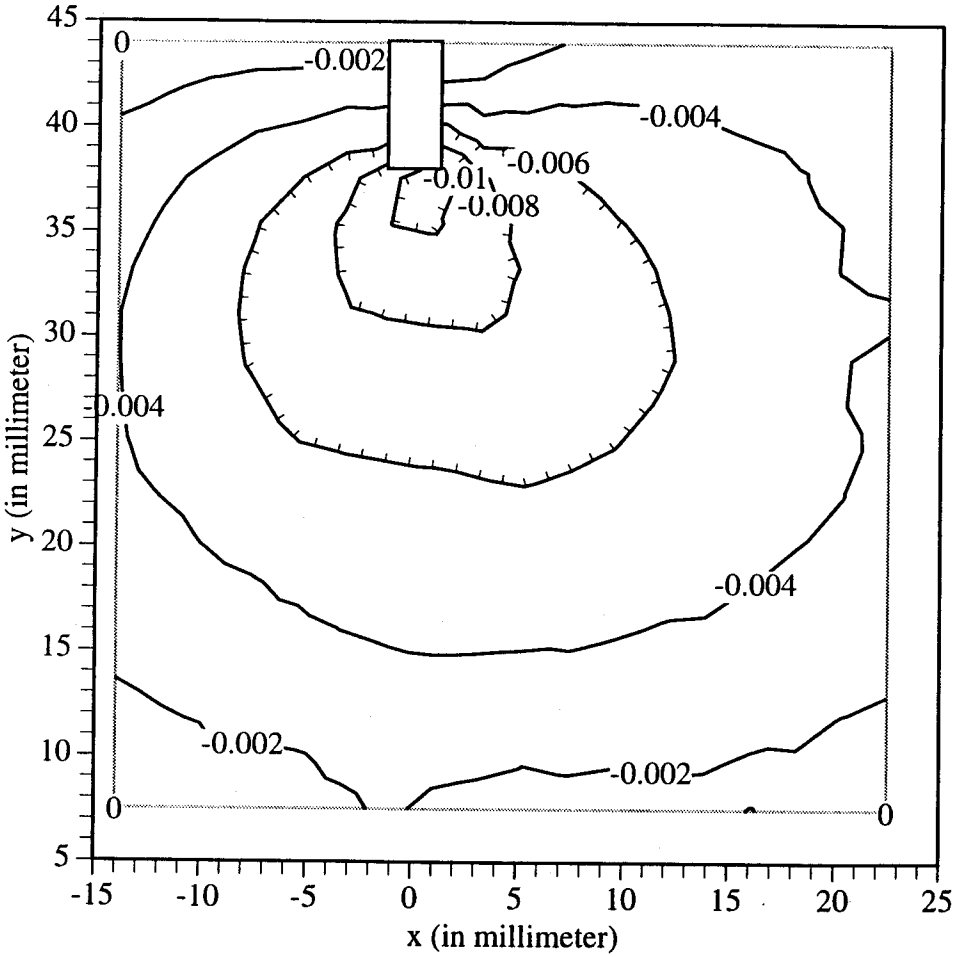

Railroad Car Wheel No. 1 2nd Side Interferometry Results
Horizontal Strain Field After Cut No. 2 (in mm/mm)

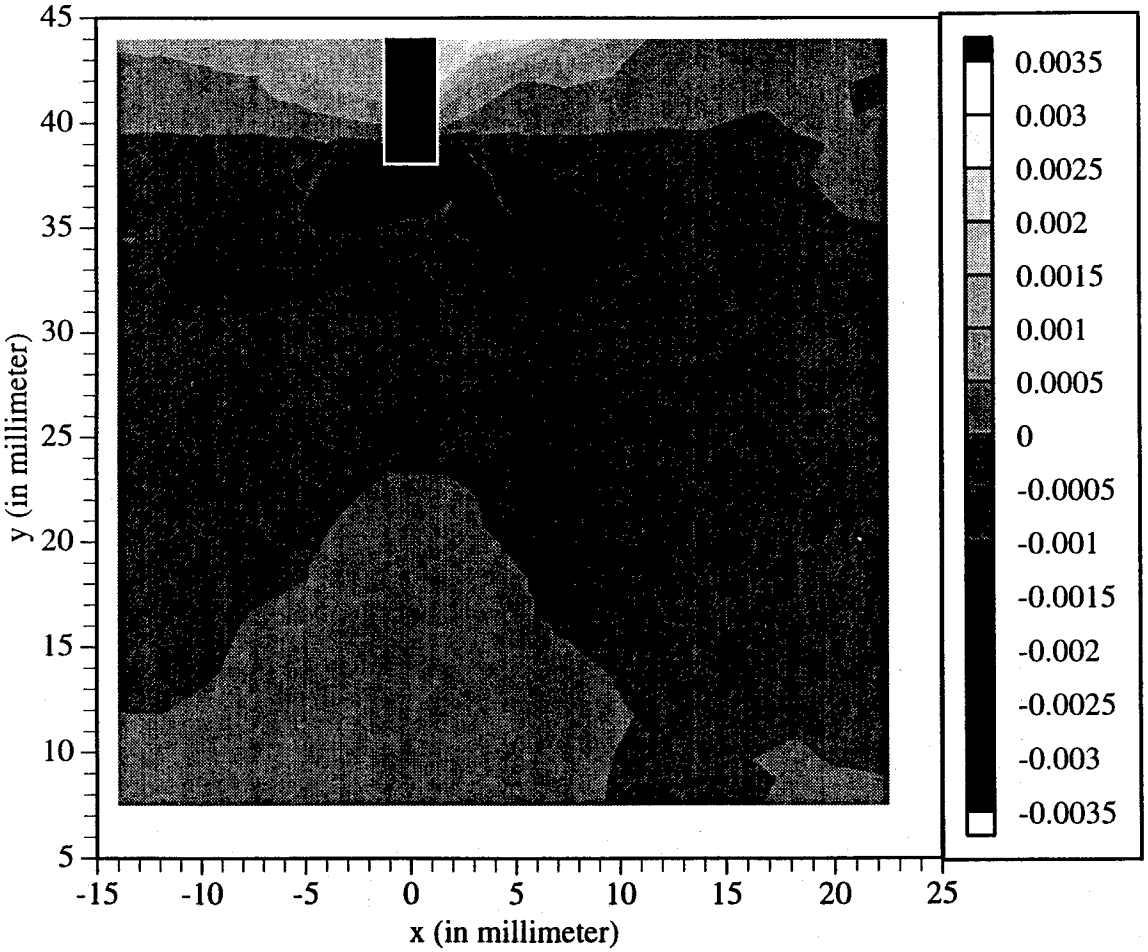

Railroad Car Wheel No. 1 2nd Side Interferometry Results
Vertical Strain Field After Cut No. 2 (in mm/mm)

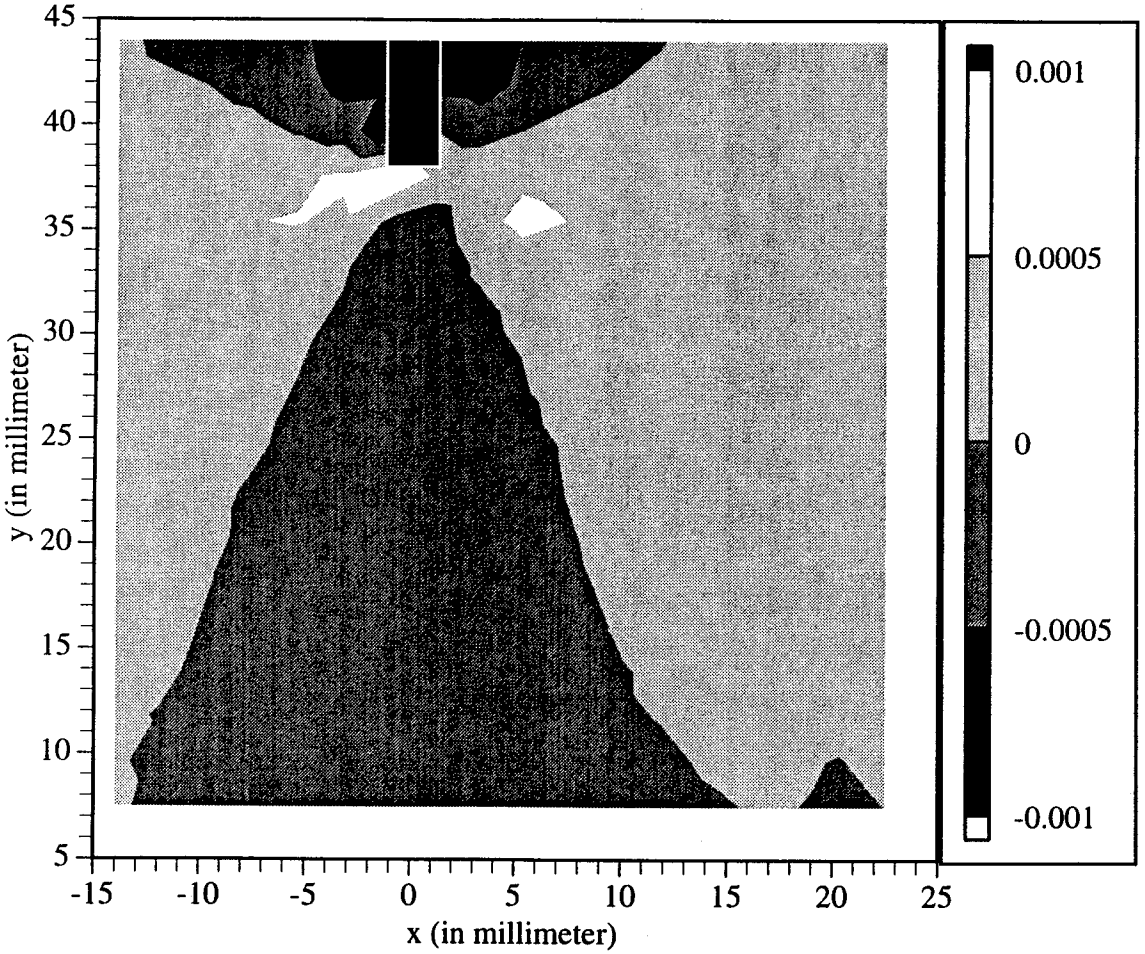

Railroad Car Wheel No. 1 2nd Side Interferometry Results
Shear Strain Field After Cut No. 2 (in mm/mm)

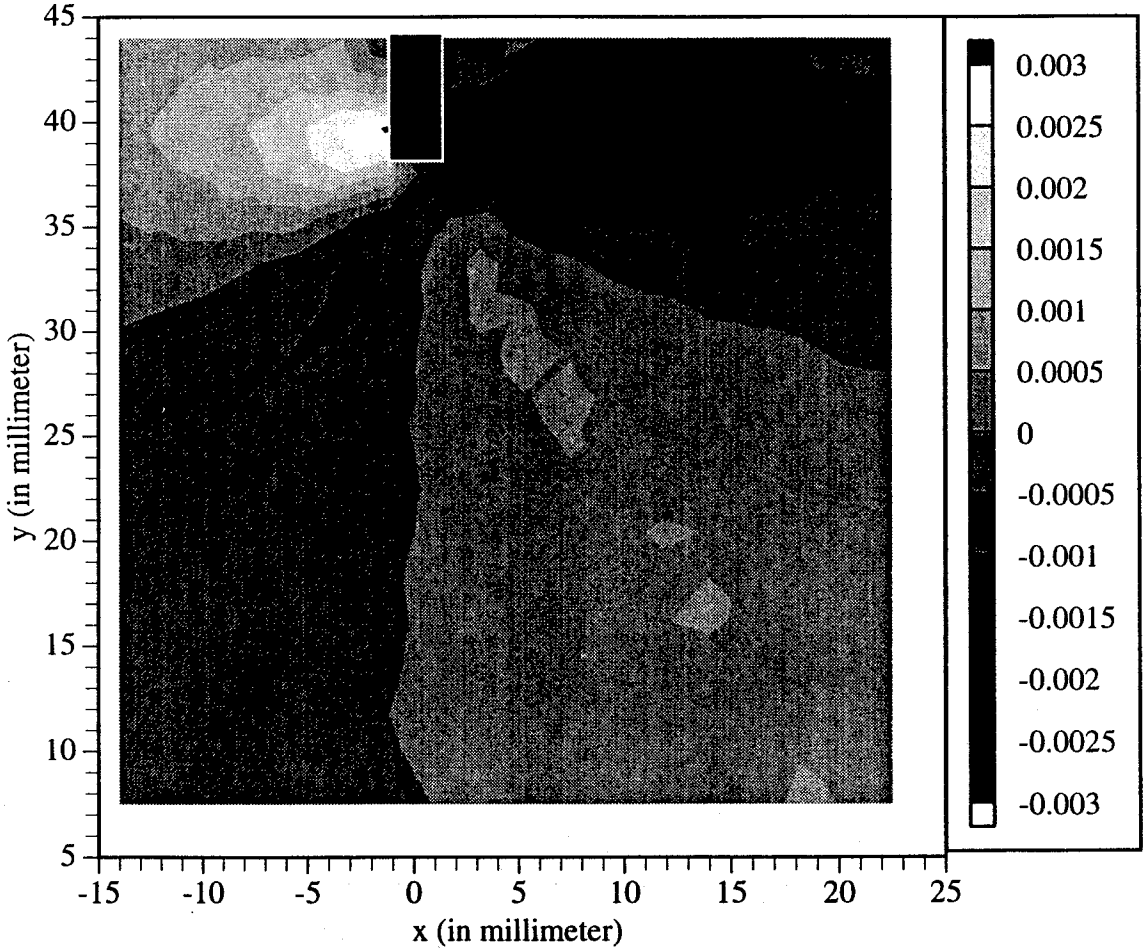

Railroad Car Wheel No. 1 2nd Side Interferometry Results
Horizontal Displacement Field After Cut No. 3 (in mm)

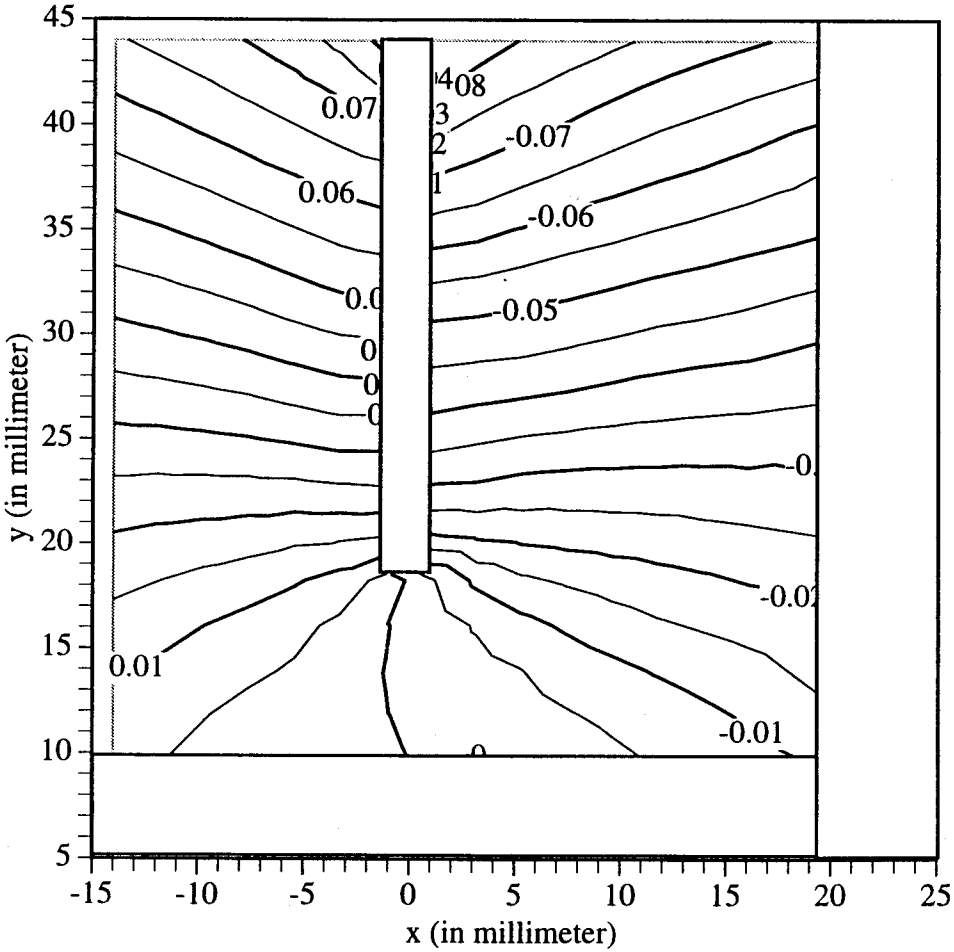

Railroad Car Wheel No. 1 2nd Side Interferometry Results
Vertical Displacement Field After Cut No. 3 (in mm)

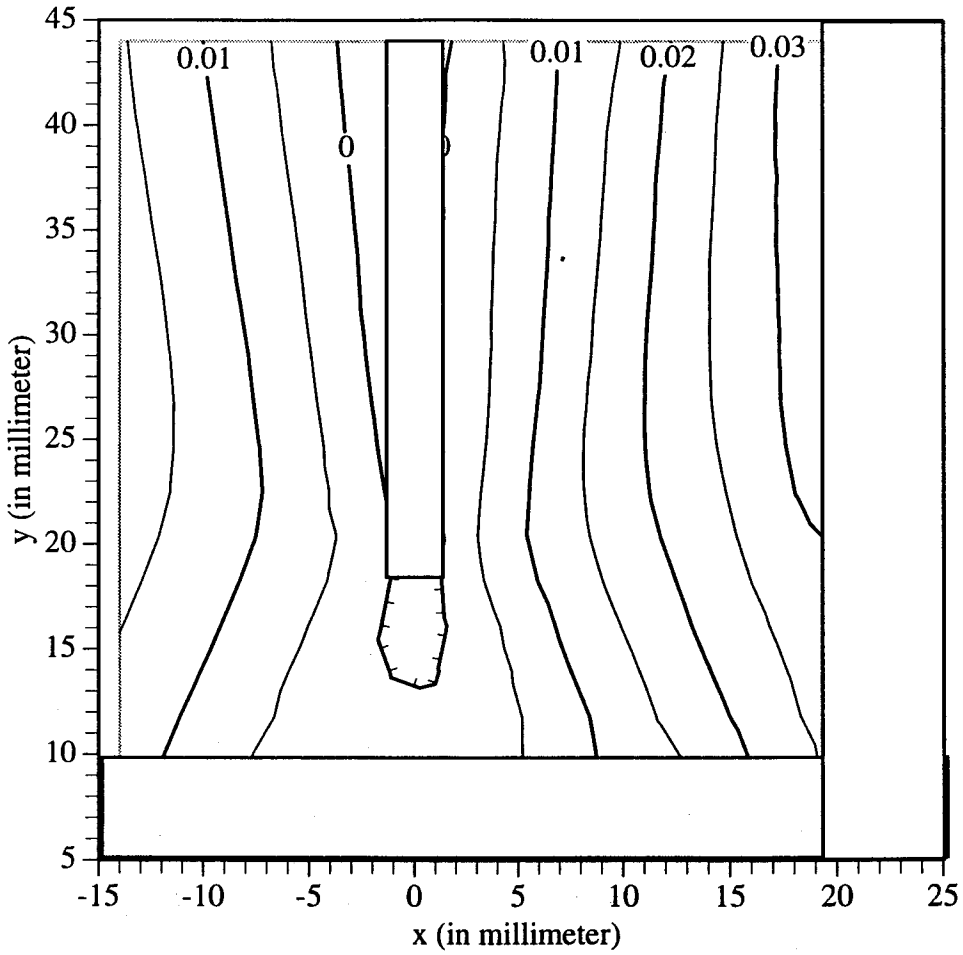

Railroad Car Wheel No. 1 2nd Side Interferometry Results
Out-of-plane Displacement Field After Cut No. 3 (in mm)

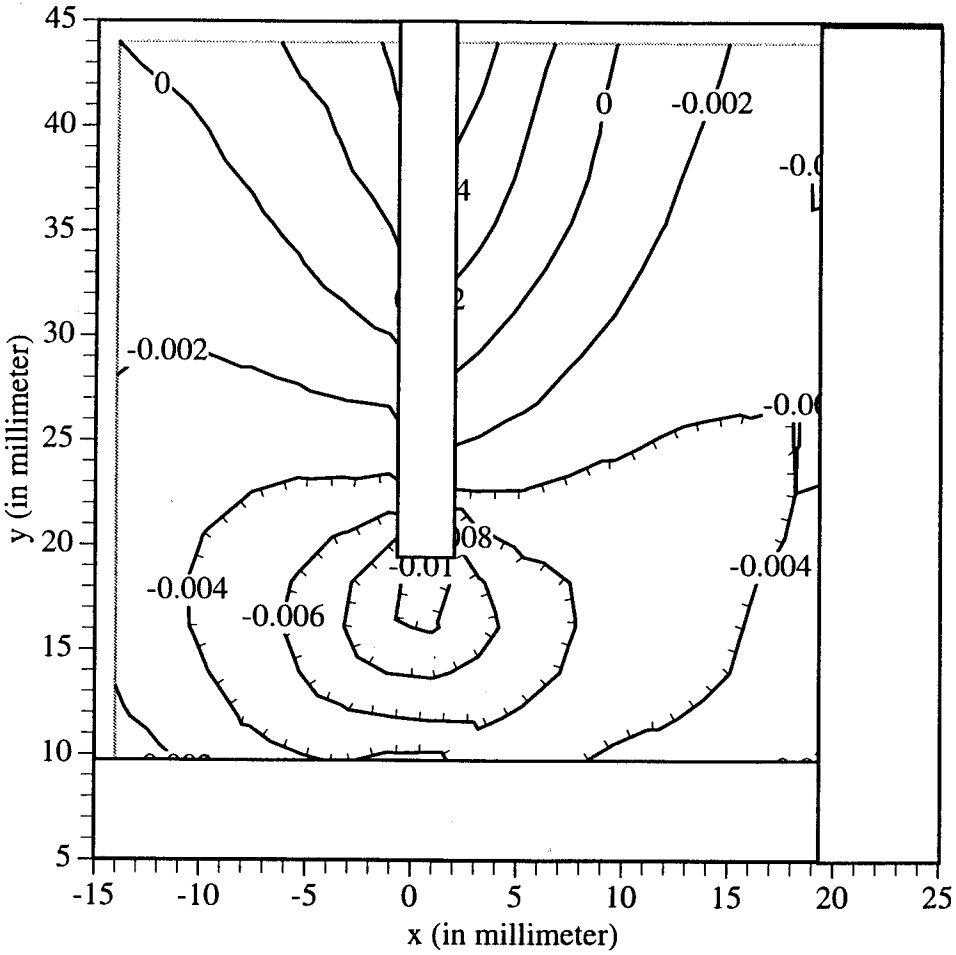

Railroad Car Wheel No. 1 2nd Side Interferometry Results
Horizontal Strain Field After Cut No. 3 (in mm/mm)

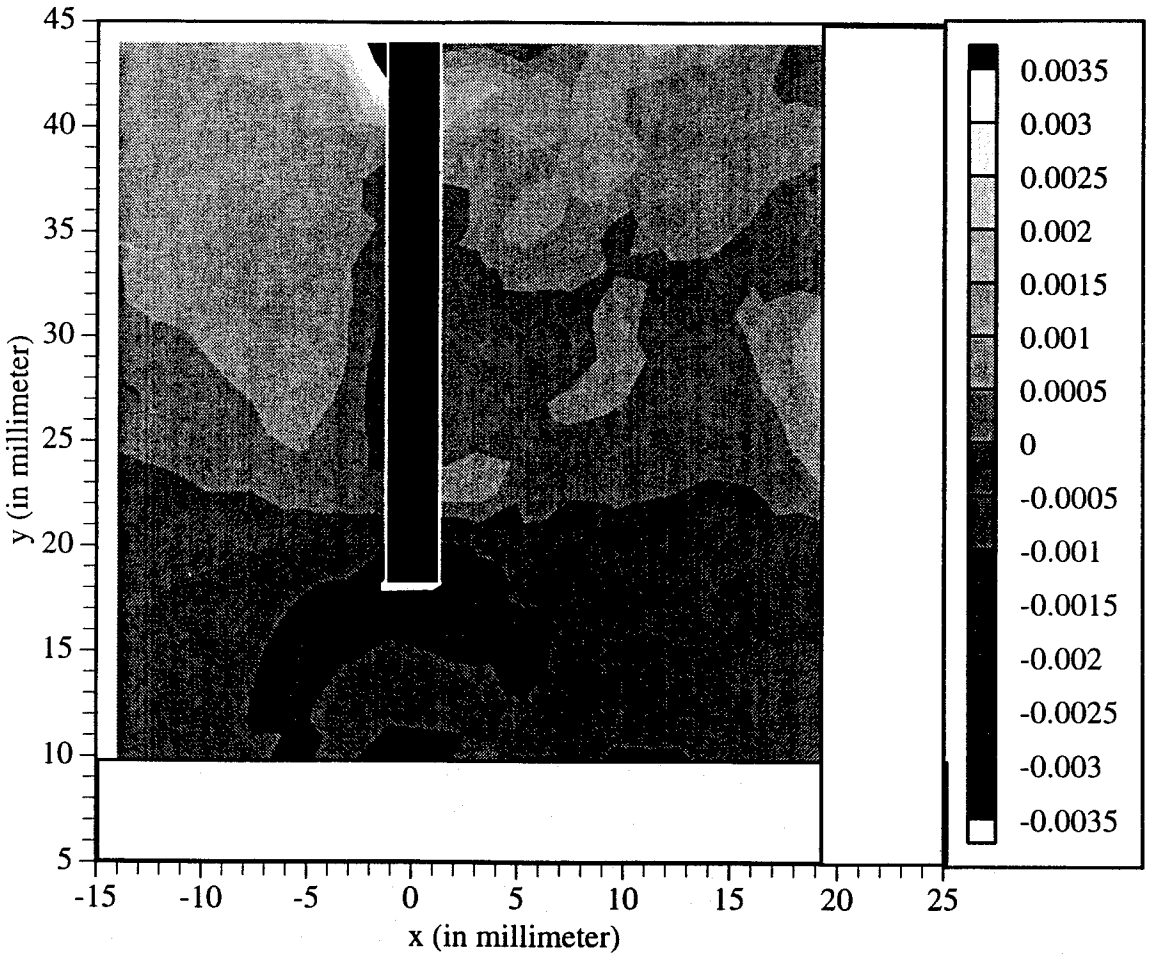

Railroad Car Wheel No. 1 2nd Side Interferometry Results
Vertical Strain Field After Cut No. 3 (in mm/mm)

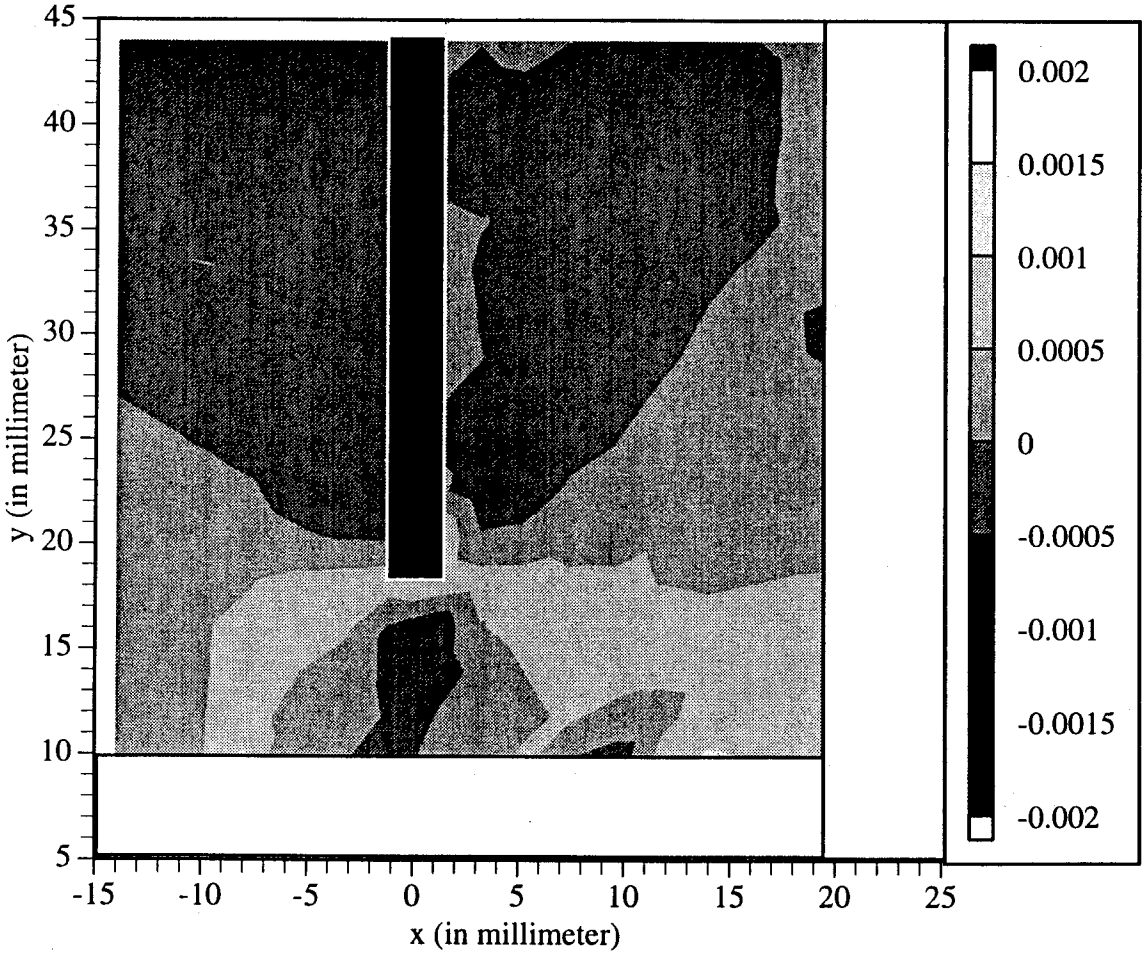

Railroad Car Wheel No. 1 2nd Side Interferometry Results
Shear Strain Field After Cut No. 3 (in mm/mm)

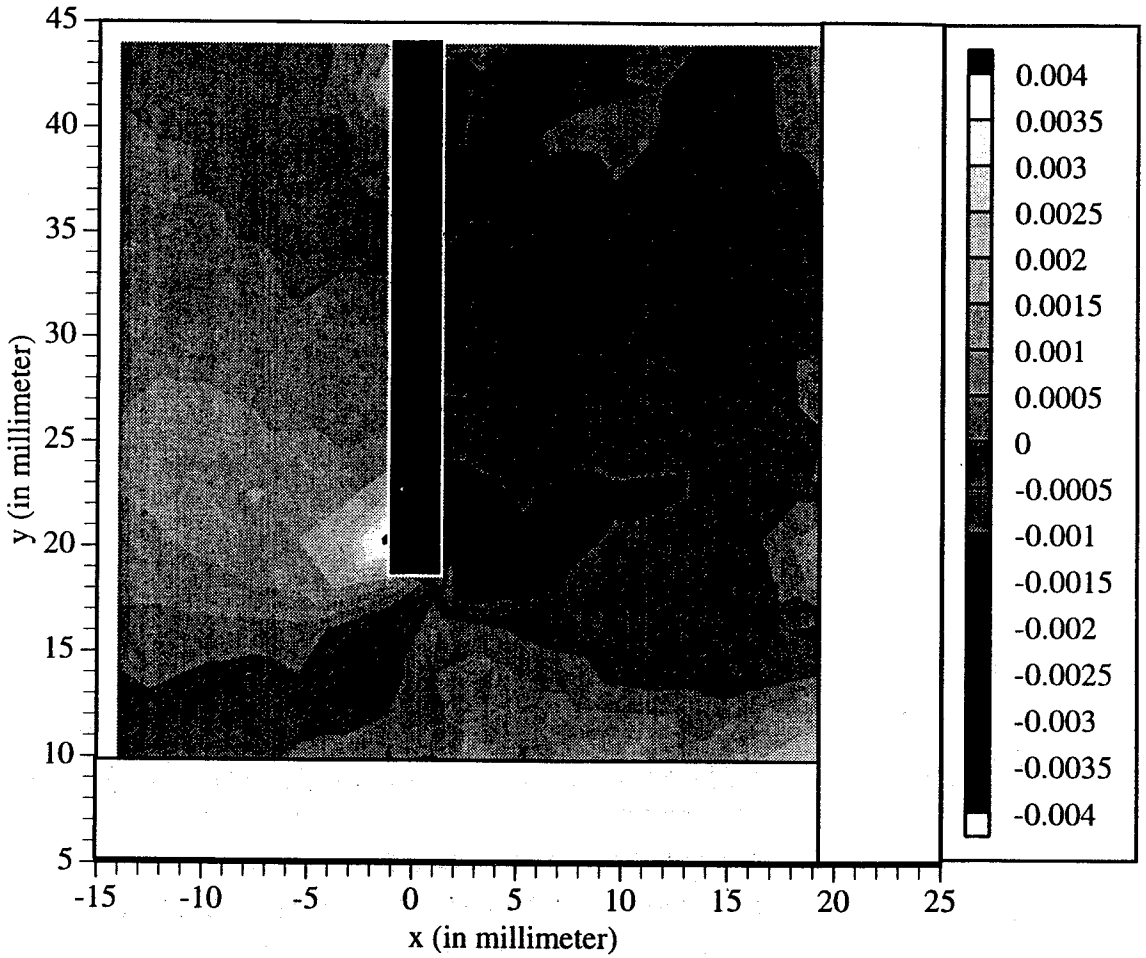

Page Intentionally Left Blank

Appendix 2. Wheel #2 Experimental Results

This appendix contains the results from the test on both sides (front and back rim faces) of the second wheel. All the data are in a local coordinate system that is located at the intersection of the inner edge of the rim and the cutting line; the vertical axis points away from the center of the wheel.

The attached figures show the location of all the sensors. At two points on the wheel, thermocouples (TC) measure the temperature difference (which never exceeded 1.9°C) immediately after each cut. The temperature at TC2, the one farther from the cut, was equal to the ambient temperature. The strain measurements were taken after the difference decreased to about 1°C or less at an ambient temperature in the range of 22°C to 26°C.

The extensometer, strain gage, and displacement sensor data are provided in tabular form. The interferometric data is provided in the form of contour maps and as data files in ASCII format for five specific cutting stages. The corresponding cut depths are 33 mm, 39 mm, 45 mm, 59 mm, and 74 mm.

The wheel was identified by the following markings:

322-1480
142 T

Location of strain gauges, thermocouples and gratings on wheel #2

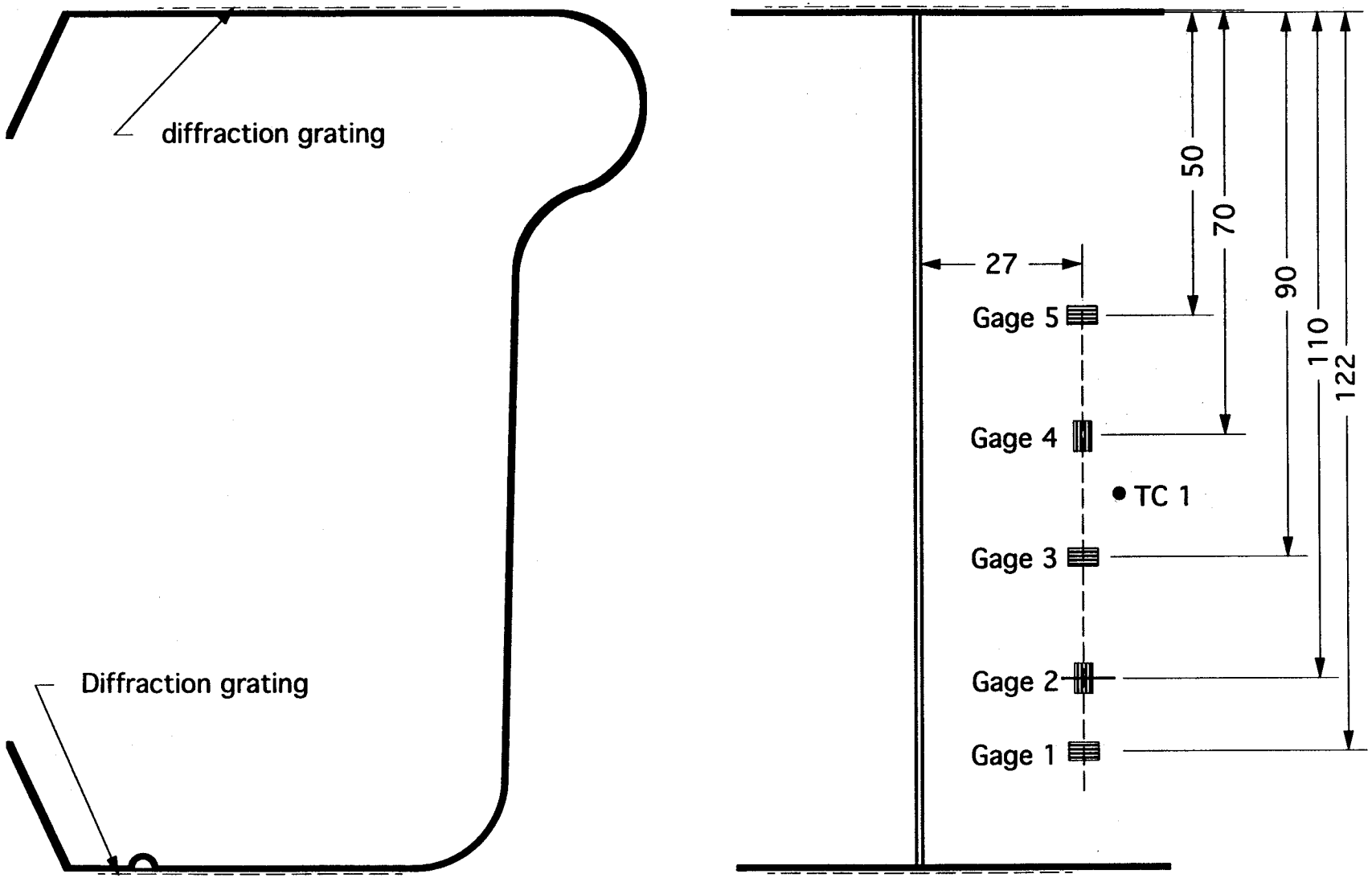

Location of dial indicators, thermocouples and gratings on wheel #2

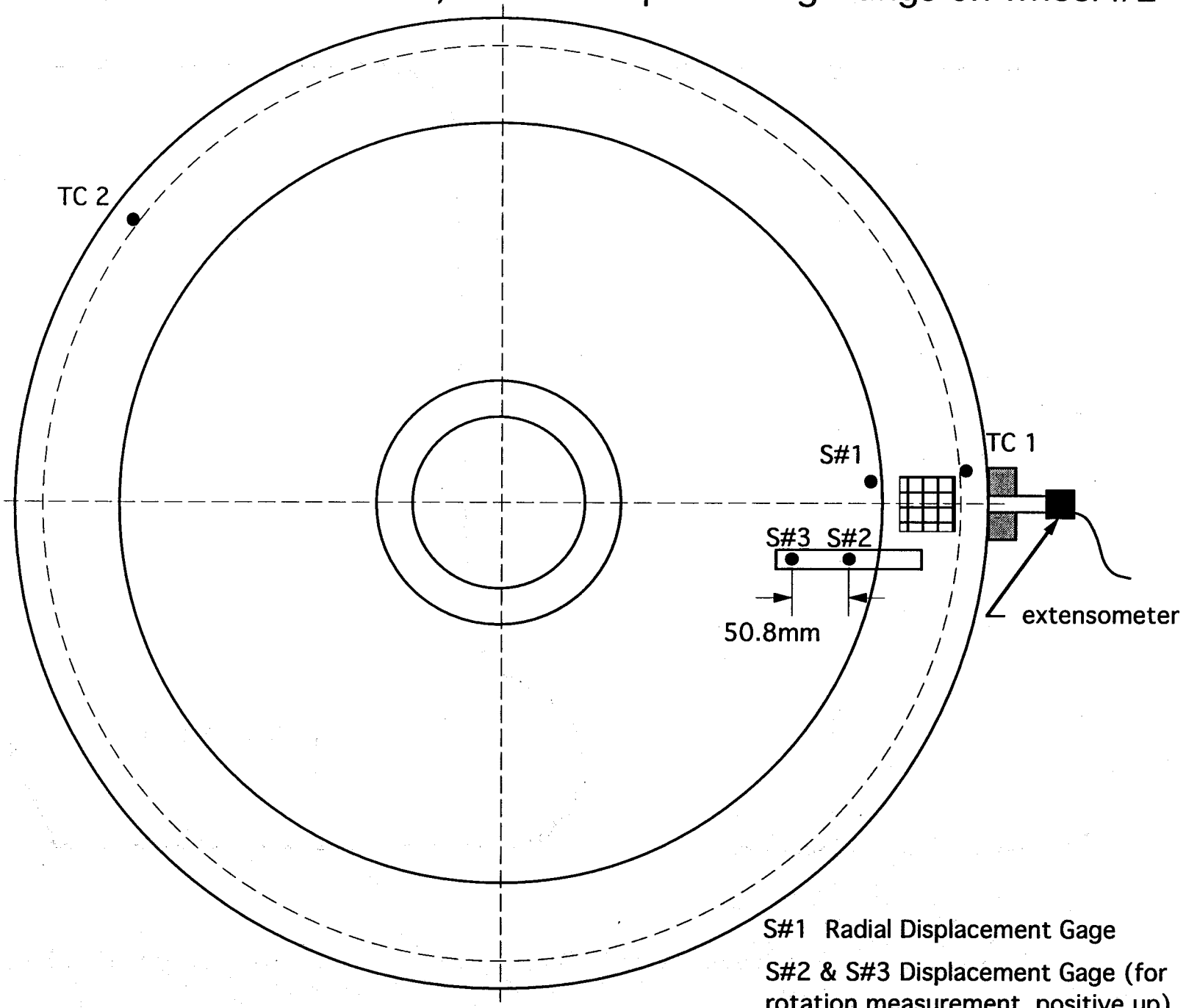

S#1 Radial Displacement Gage

S#2 & S#3 Displacement Gage (for rotation measurement, positive up)

TESTING OF DOT RAILROAD CAR WHEEL #2						322-1408	142T			
DATE:	AUGUST 18 1994									
	mm/mm					mm	mm	rad	(°C)	(°C)
Cut Depth (mm)	Gage1	Gage2	Gage3	Gage4	Gage5	Radial Displacement	Opening Displacement	Rotation	TC 1	TC 2
0	0	0	0	0	0	.000	.000	0.00E+00	24.4	24.4
28	-13	8	33	24	-72	.013	.087	-4.63E-05	24.8	24.4
33	22	11	37	32	54	.018	.112	-6.35E-05	25.3	24.4
39	122	-14	253	30	250	.028	.140	-3.61E-05	26.8	24.5
45	425	-47	496	30	426	.040	.173	-9.51E-06	27.0	25.1
59	776	-101	713	29	554	.070	.237	-1.25E-04	25.6	23.3
74	852	-132	760	14	575	.109	.312	-1.65E-04	26.3	24.1
85	867	-147	769	9	577	.140	.363	-1.81E-04	26.0	25.1
95	868	-157	776	-20	578	.173	.422	-1.45E-04	26.5	25.0
105	846	-153	766	-42	581	.222	.473	1.66E-04	26.6	25.1
115	834	-147	751	-45	578	.278	.553	2.35E-04	26.6	25.1
125	821	-156	743	-52	567	.319	.629	2.52E-04	26.2	25.1
135	816	-151	739	-49	565	.354	.761	2.18E-04	26.2	25.1
145	814	-150	735	-48	563	.375	.816	1.89E-04	22.1	22.1
155	813	-150	735	-47	564	.399	.868	2.09E-04	22.1	22.1
165	812	-150	734	-47	562	.417	.919	1.94E-02	22.1	22.1
175	812	-150	734	-47	562	.440	.973	1.02E-04	22.1	22.1
185	811	-149	733	-47	561	.462	1.039	8.32E-05	22.3	22.1
195	811	-148	733	-47	561	.488	1.106	2.17E-06	22.2	22.1
205	810	-148	732	-47	560	.520	1.202	-1.05E-04	22.3	22.2
208	811	-147	732	-47	561	.532	1.234	-1.62E-04	22.2	22.4
END								Estimated		

Railroad Wheel No. 2 Test
Displacement vs. Cut Depth

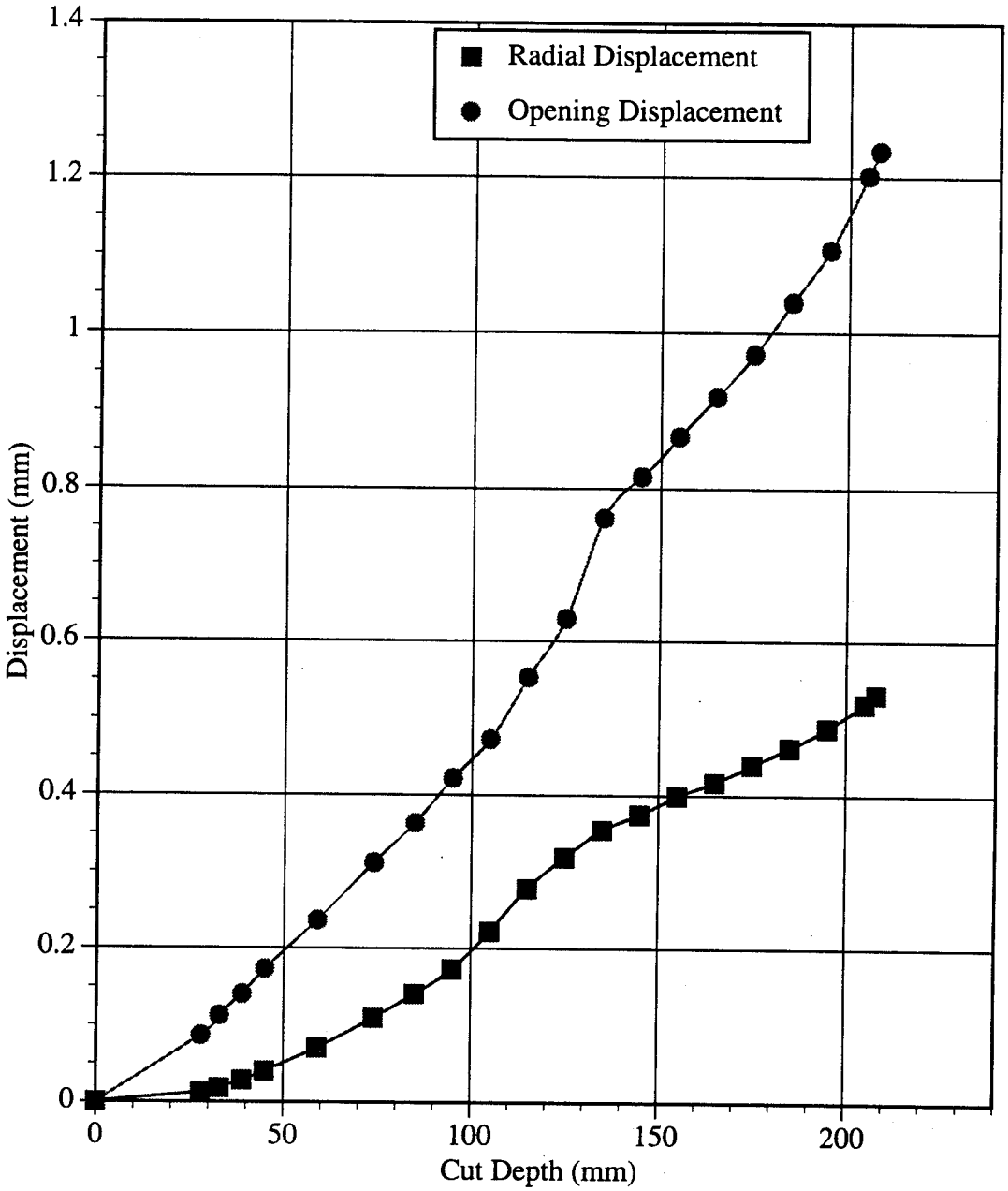

Railroad Wheel No. 2 Test
Strain Gage Readings vs. Cut Depth

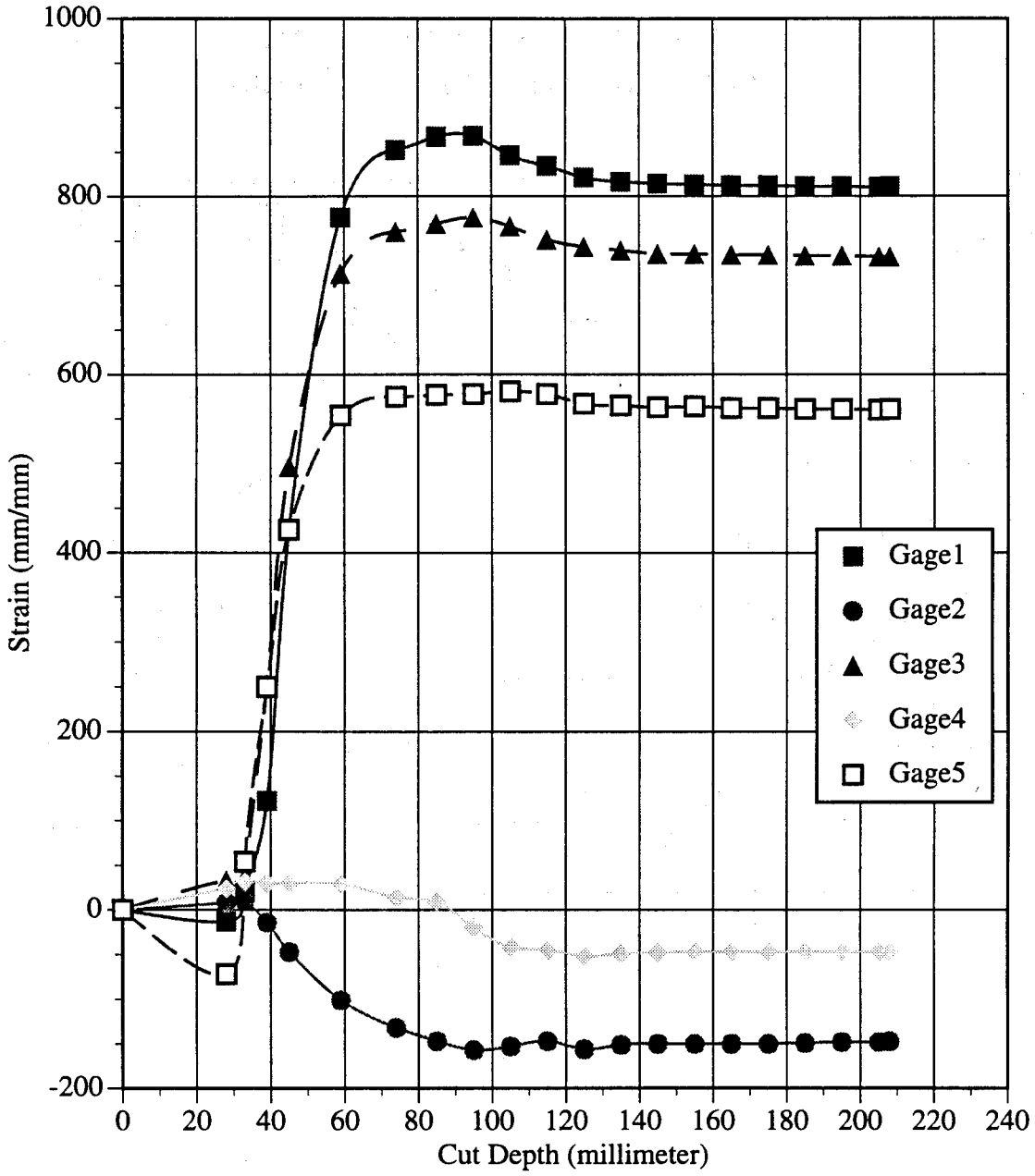

Railroad Wheel No. 2 Test
Wheel Rotation vs. Cut Depth

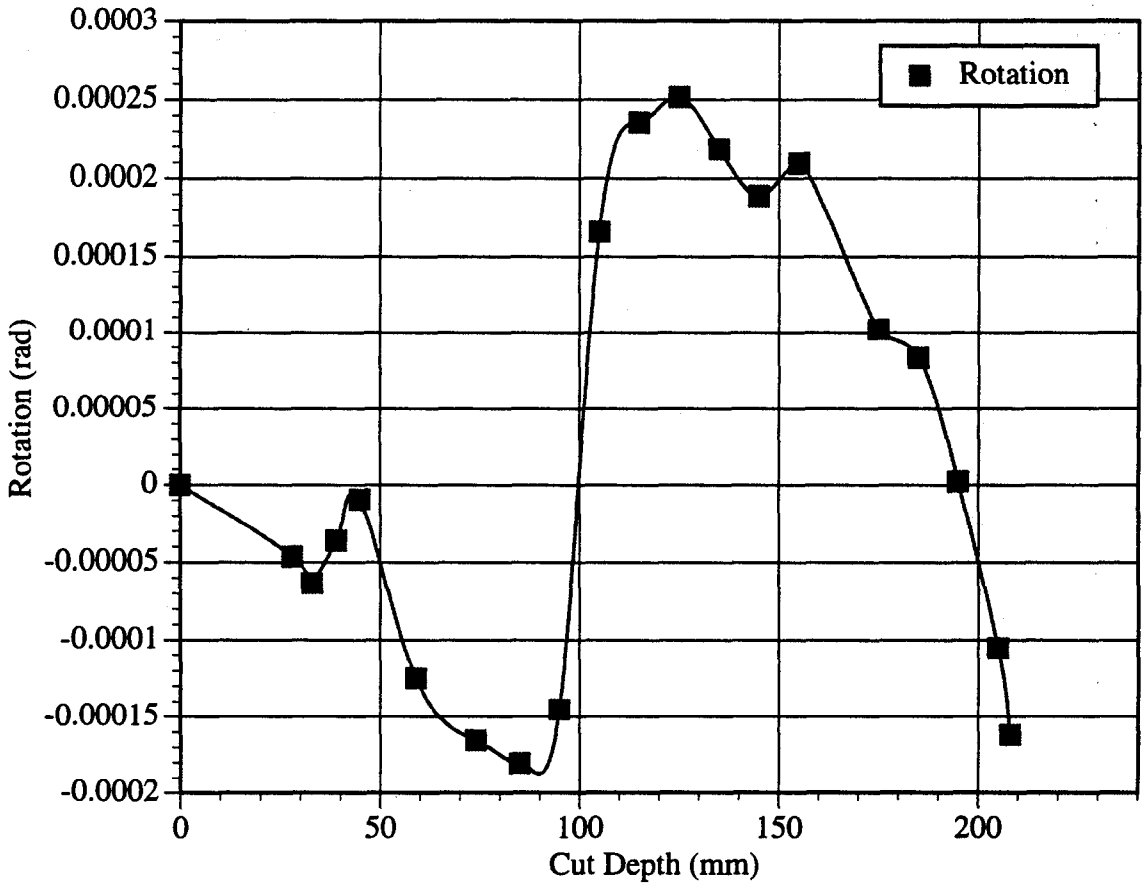

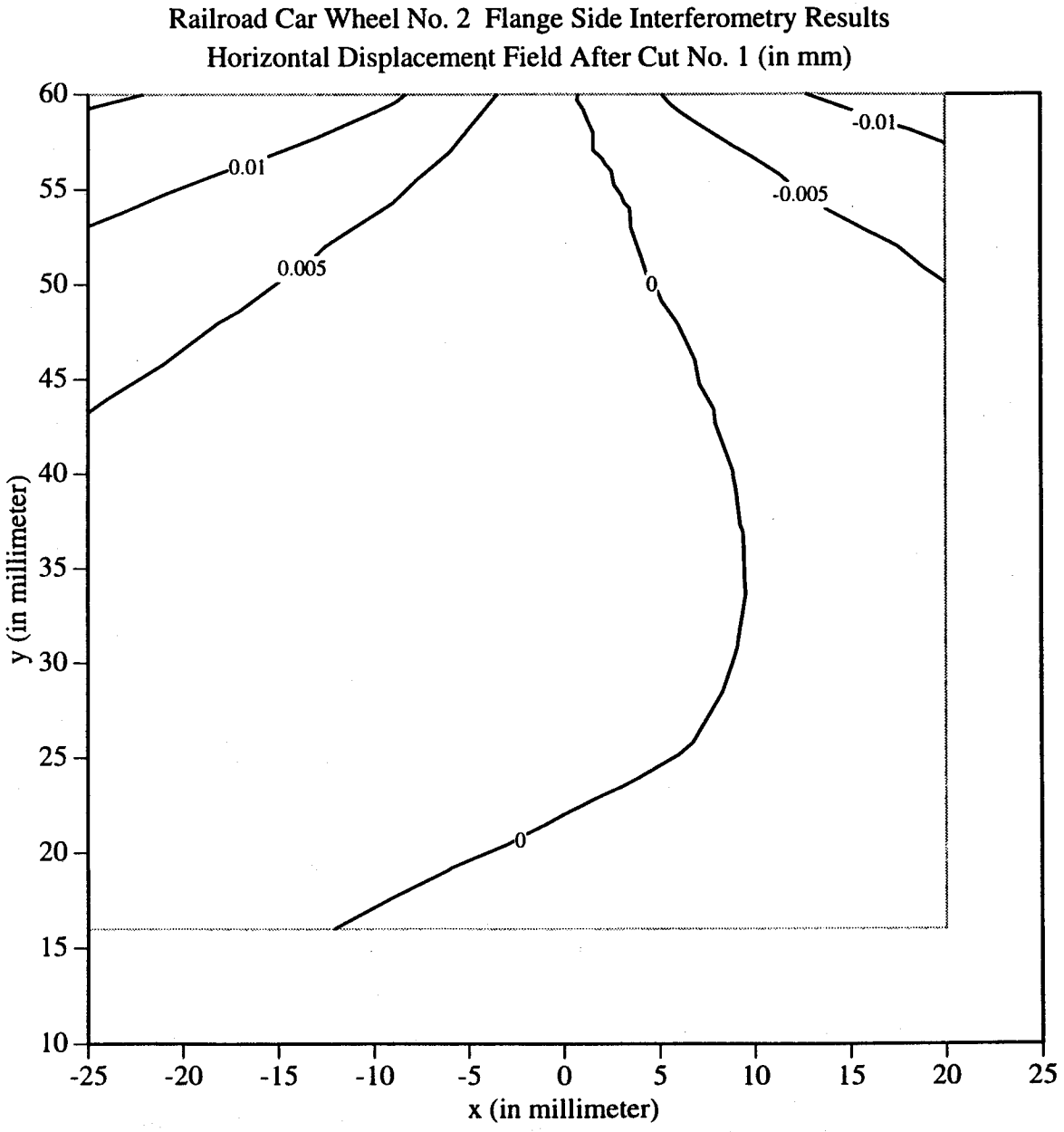
Railroad Car Wheel No. 2 Flange Side Interferometry Results
Horizontal Displacement Field After Cut No. 1 (in mm)
0.01
0.005
0
-0.005
-0.01
y (in millimeter)
x (in millimeter)
60
55
50
45
40
35
30
25
20
15
10
-25
-20
-15
-10
-5
0
5
10
15
20
25

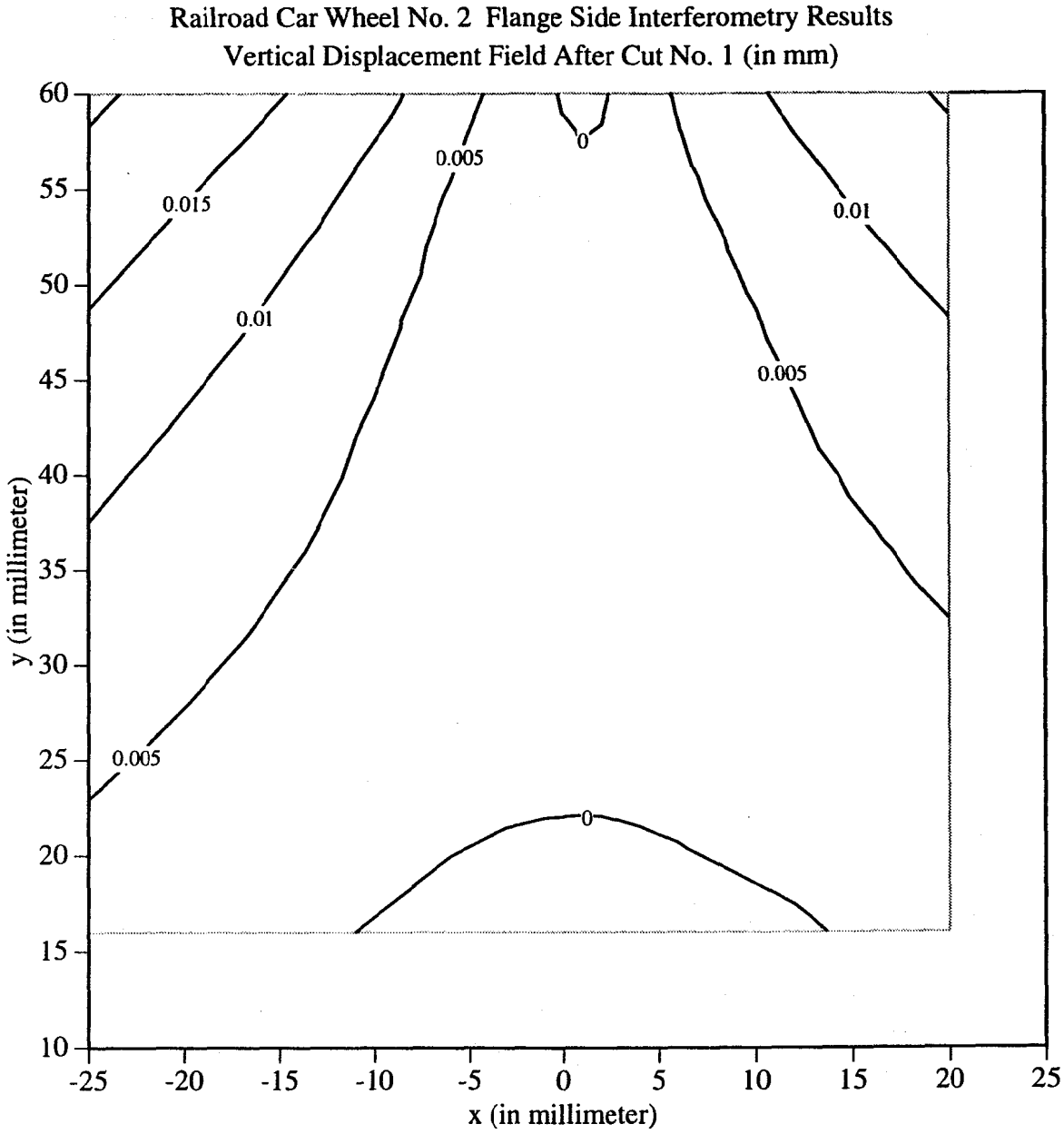
Railroad Car Wheel No. 2 Flange Side Interferometry Results
Vertical Displacement Field After Cut No. 1 (in mm)
y (in millimeter)
x (in millimeter)
60
55
50
45
40
35
30
25
20
15
10
-25
-20
-15
-10
-5
0
5
10
15
20
25
0.015
0.01
0.005
0
0.005
0.01
0.01
0.005
0

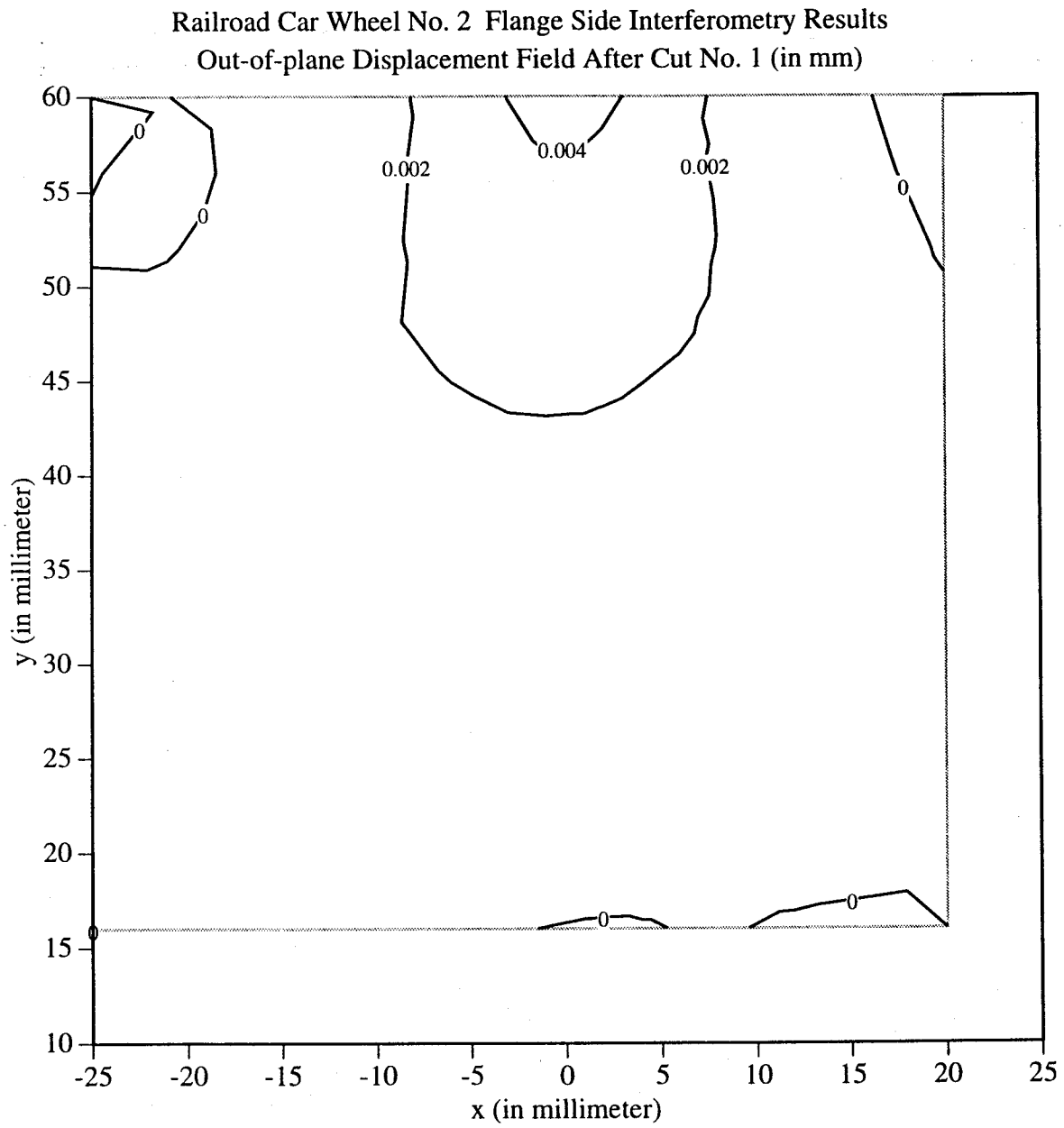
Railroad Car Wheel No. 2 Flange Side Interferometry Results
Out-of-plane Displacement Field After Cut No. 1 (in mm)
0
0
0.002
0.004
0.002
0
0
0
0
y (in millimeter)
60
55
50
45
40
35
30
25
20
15
10
-25
-20
-15
-10
-5
0
5
10
15
20
25
x (in millimeter)

Railroad Car Wheel No. 2 Flange Side Interferometry Results
Horizontal Strain Field After Cut No. 1

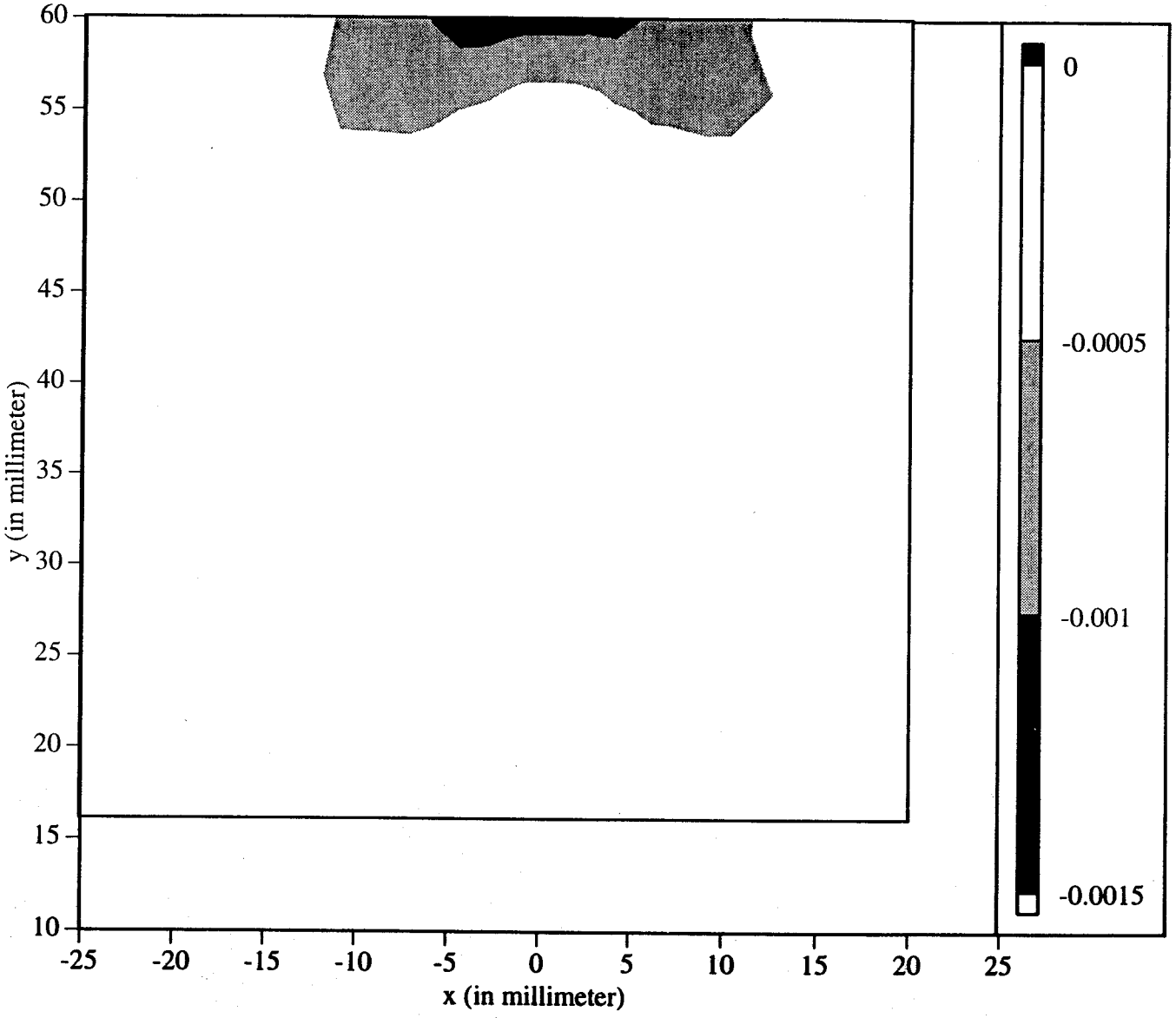

Railroad Car Wheel No. 2 Flange Side Interferometry Results
Vertical Strain Field After Cut No. 1

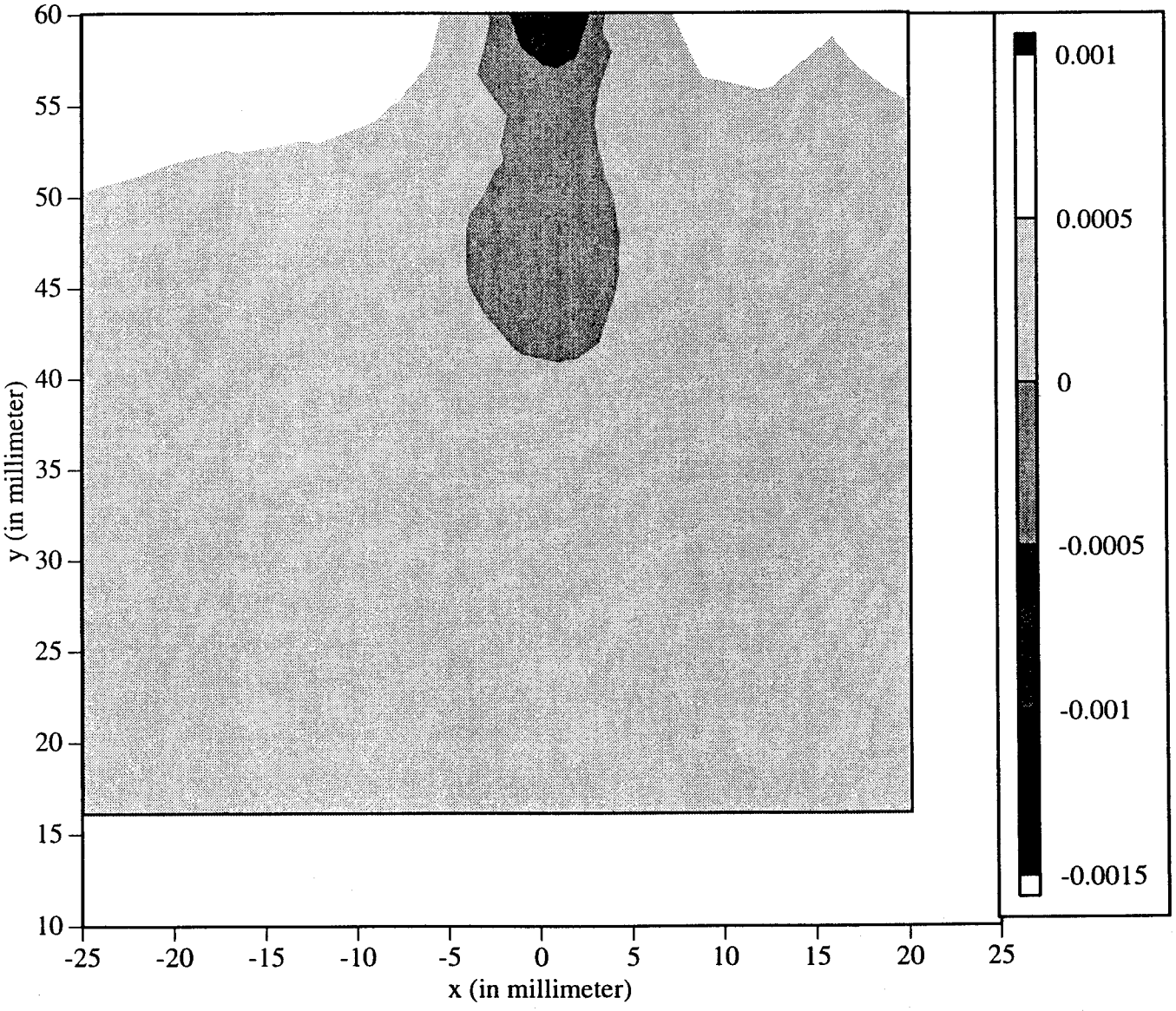

Railroad Car Wheel No. 2 Flange Side Interferometry Results
Shear Strain Field After Cut No. 1

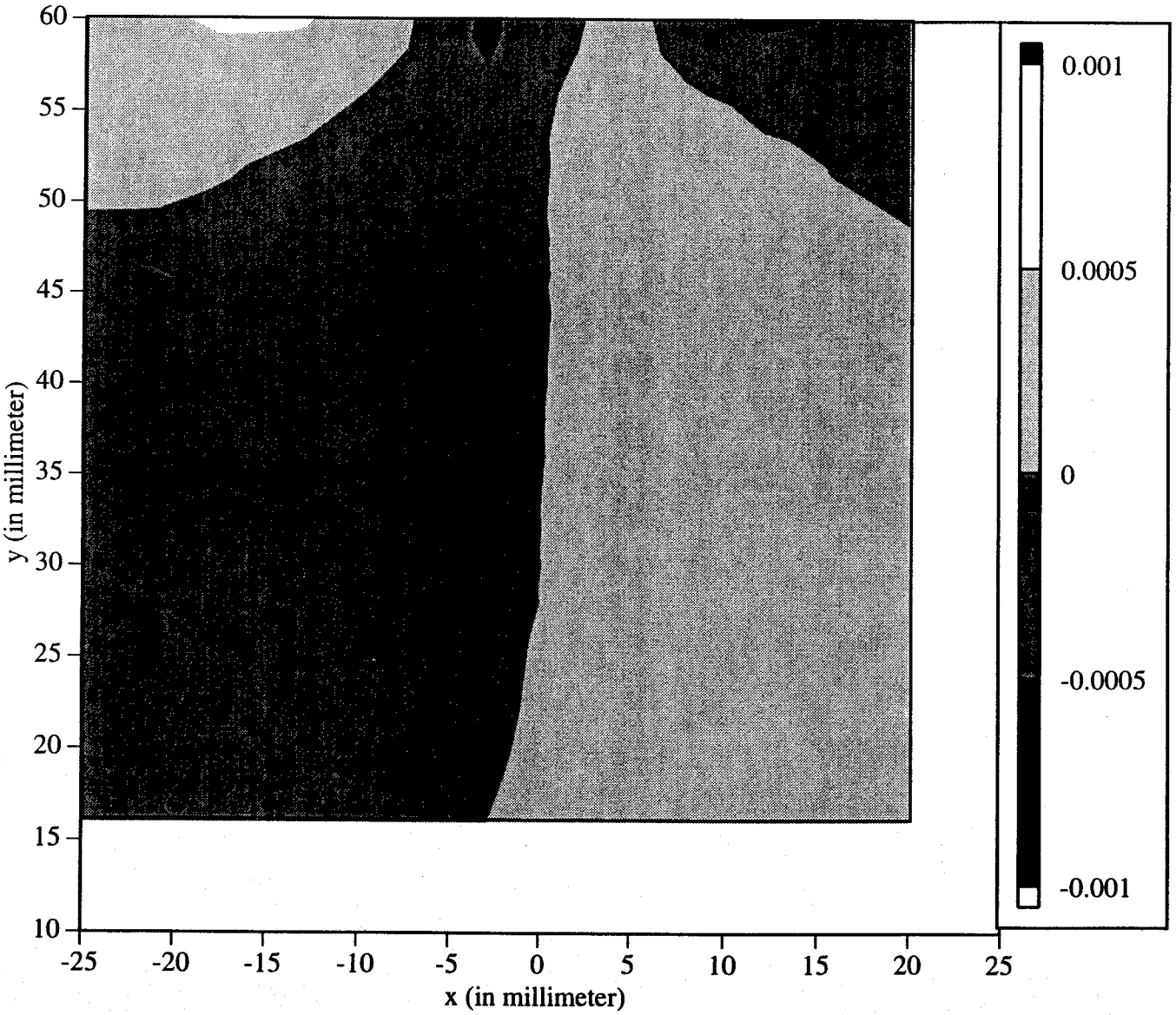

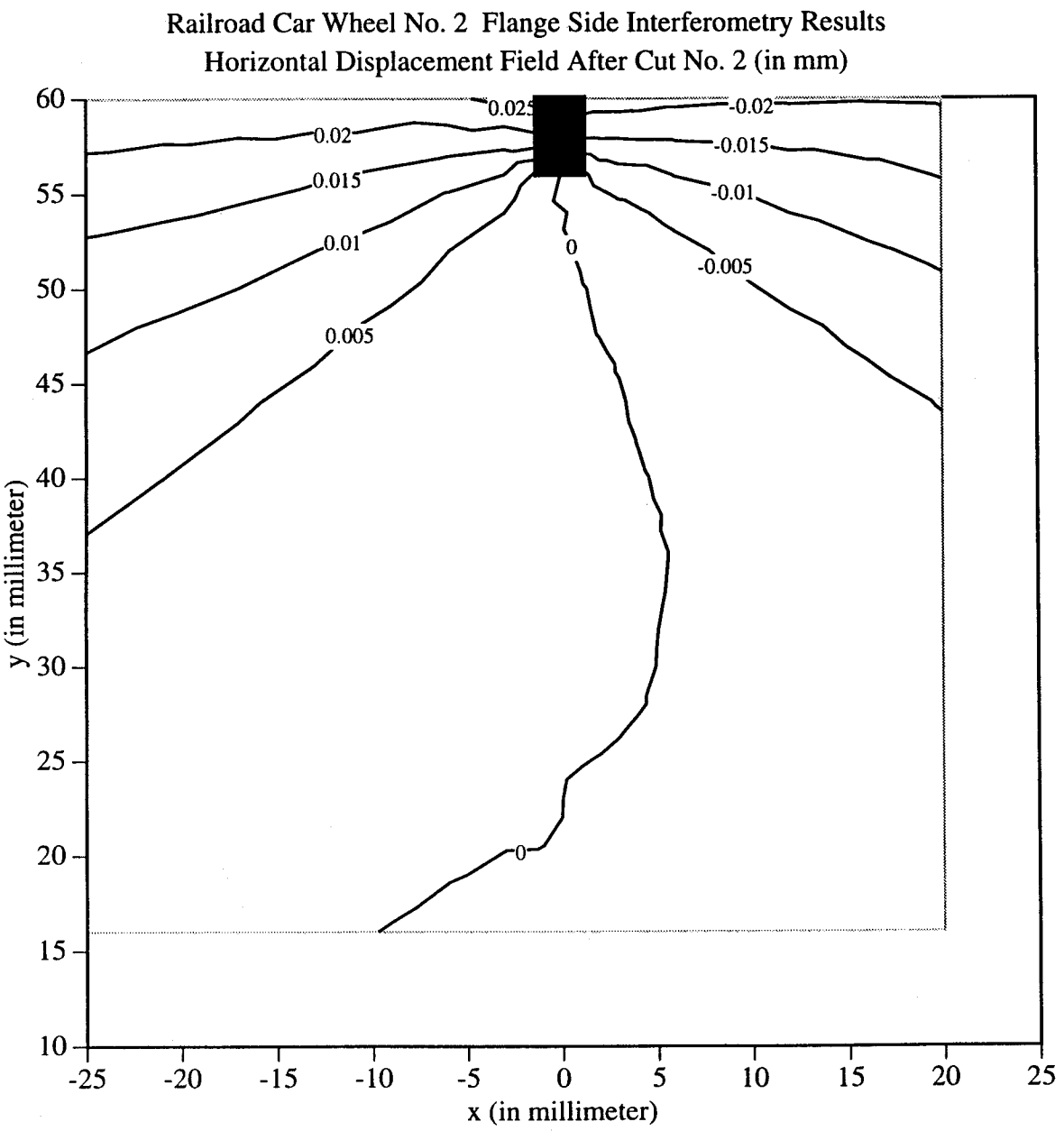
Railroad Car Wheel No. 2 Flange Side Interferometry Results
Horizontal Displacement Field After Cut No. 2 (in mm)
0.025
0.02
0.015
0.01
0.005
0
-0.02
-0.015
-0.01
-0.005
0
y (in millimeter)
x (in millimeter)
60
55
50
45
40
35
30
25
20
15
10
-25
-20
-15
-10
-5
0
5
10
15
20
25

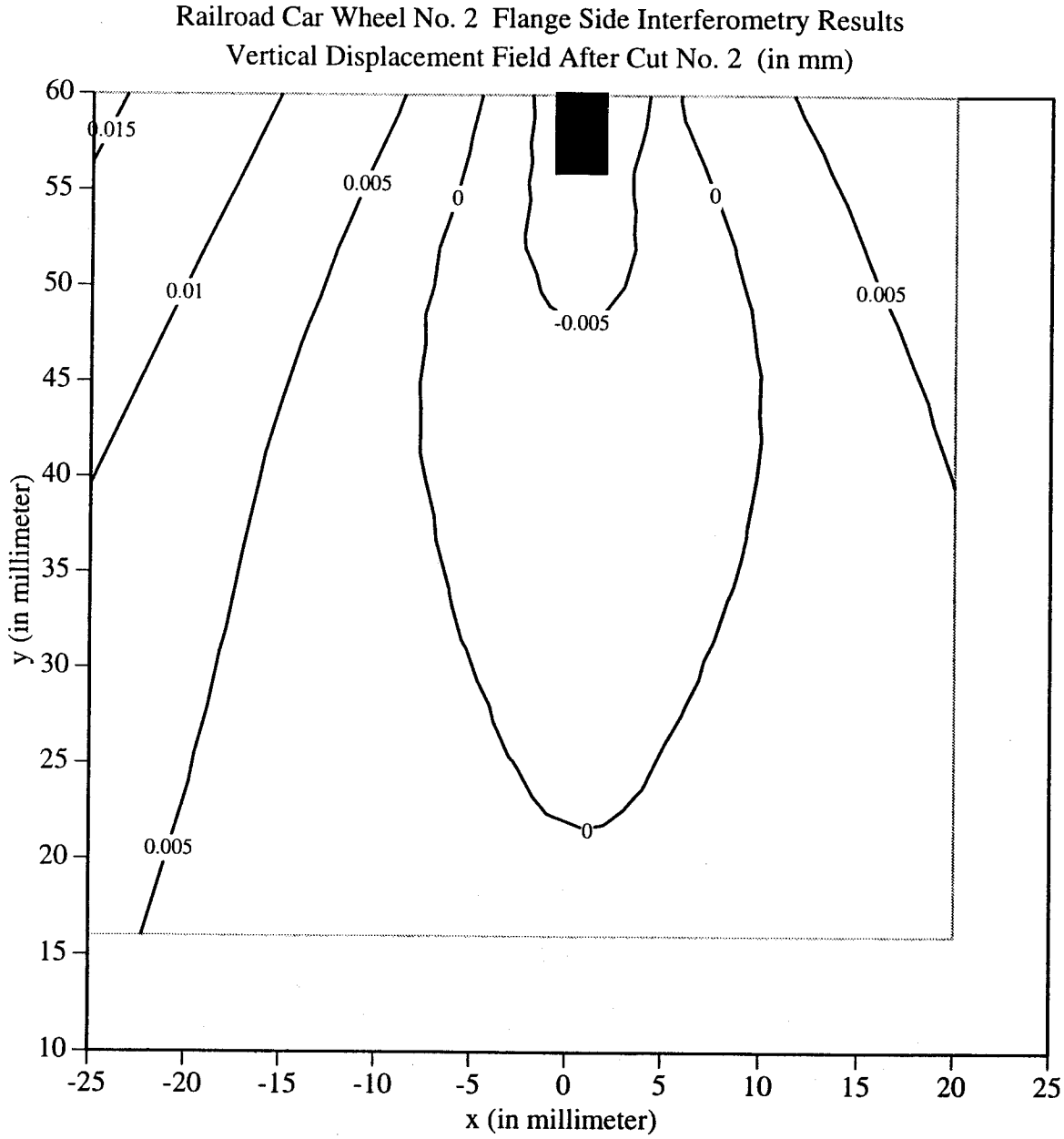
Railroad Car Wheel No. 2 Flange Side Interferometry Results
Vertical Displacement Field After Cut No. 2 (in mm)
0.015
0.01
0.005
0.005
0
-0.005
0
0.005
0
y (in millimeter)
x (in millimeter)
60
55
50
45
40
35
30
25
20
15
10
-25
-20
-15
-10
-5
0
5
10
15
20
25

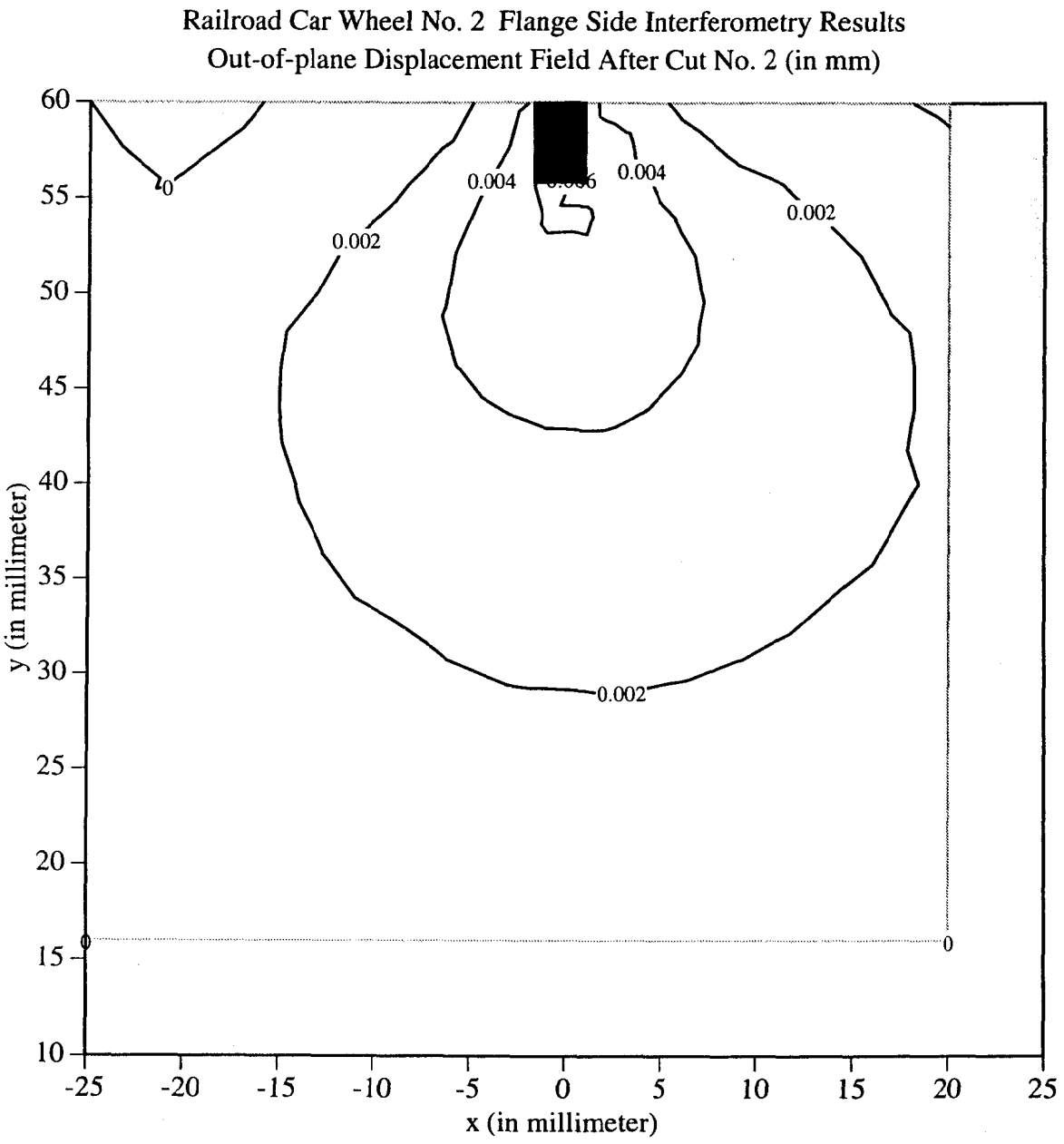
Railroad Car Wheel No. 2 Flange Side Interferometry Results
Out-of-plane Displacement Field After Cut No. 2 (in mm)
y (in millimeter)
x (in millimeter)
60
55
50
45
40
35
30
25
20
15
10
-25
-20
-15
-10
-5
0
5
10
15
20
25
0
0.002
0.004
0.004
0.002
0.002
0
0

Railroad Car Wheel No. 2 Flange Side Interferometry Results
Horizontal Strain Field After Cut No. 2

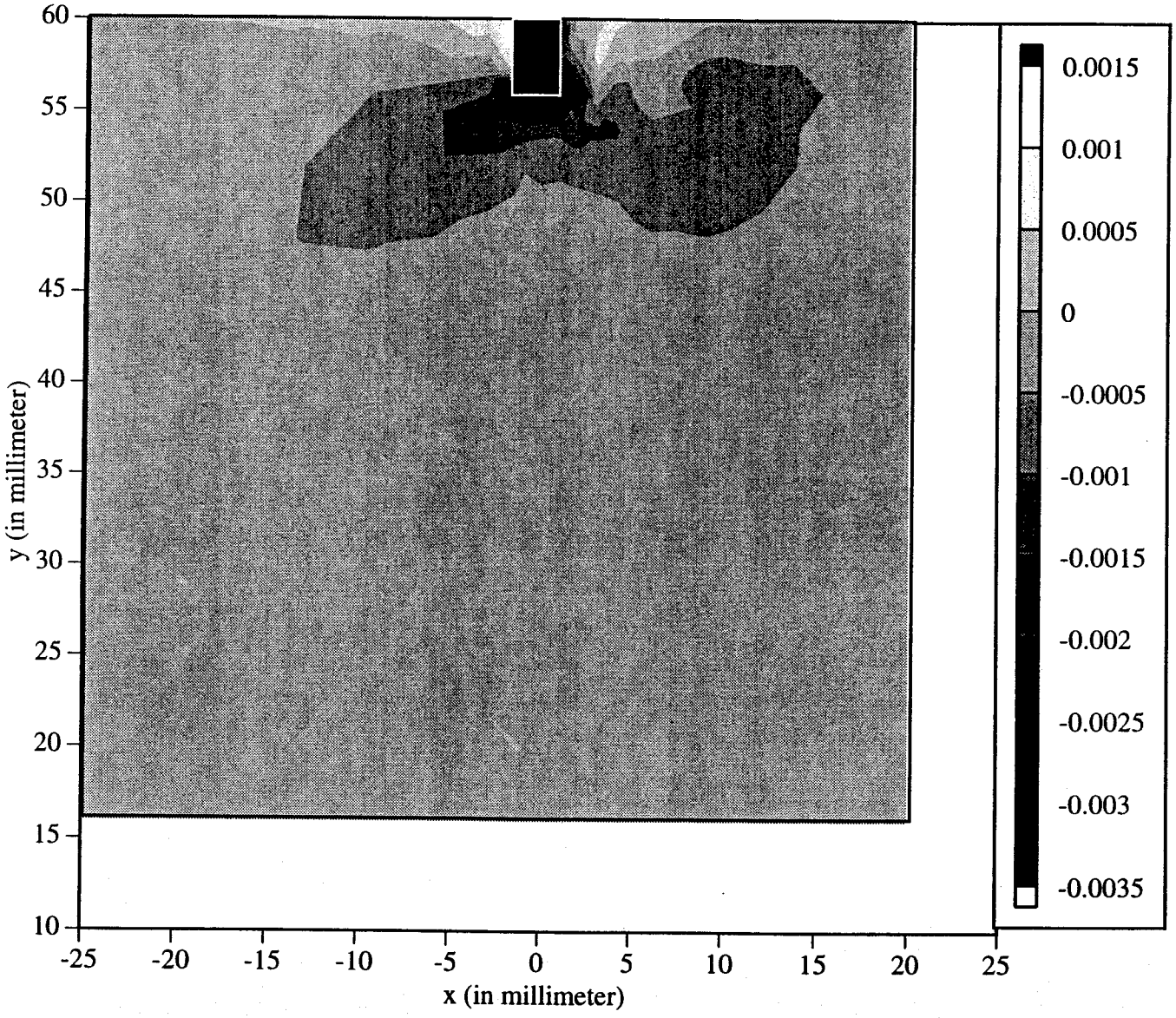

Railroad Car Wheel No. 2 Flange Side Interferometry Results
Vertical Strain Field After Cut No. 2

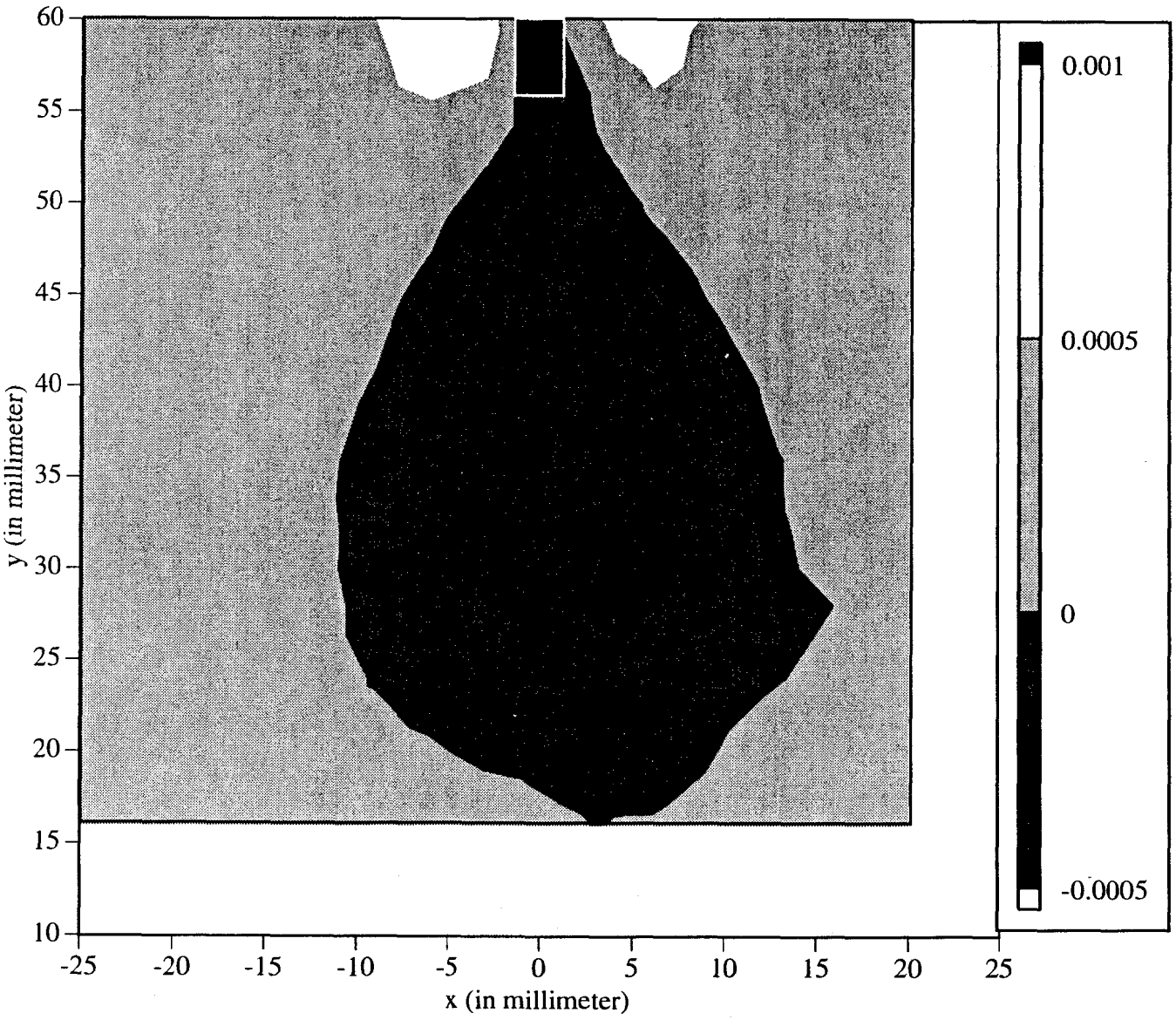

Railroad Car Wheel No. 2 Flange Side Interferometry Results
Shear Strain Field After Cut No. 2

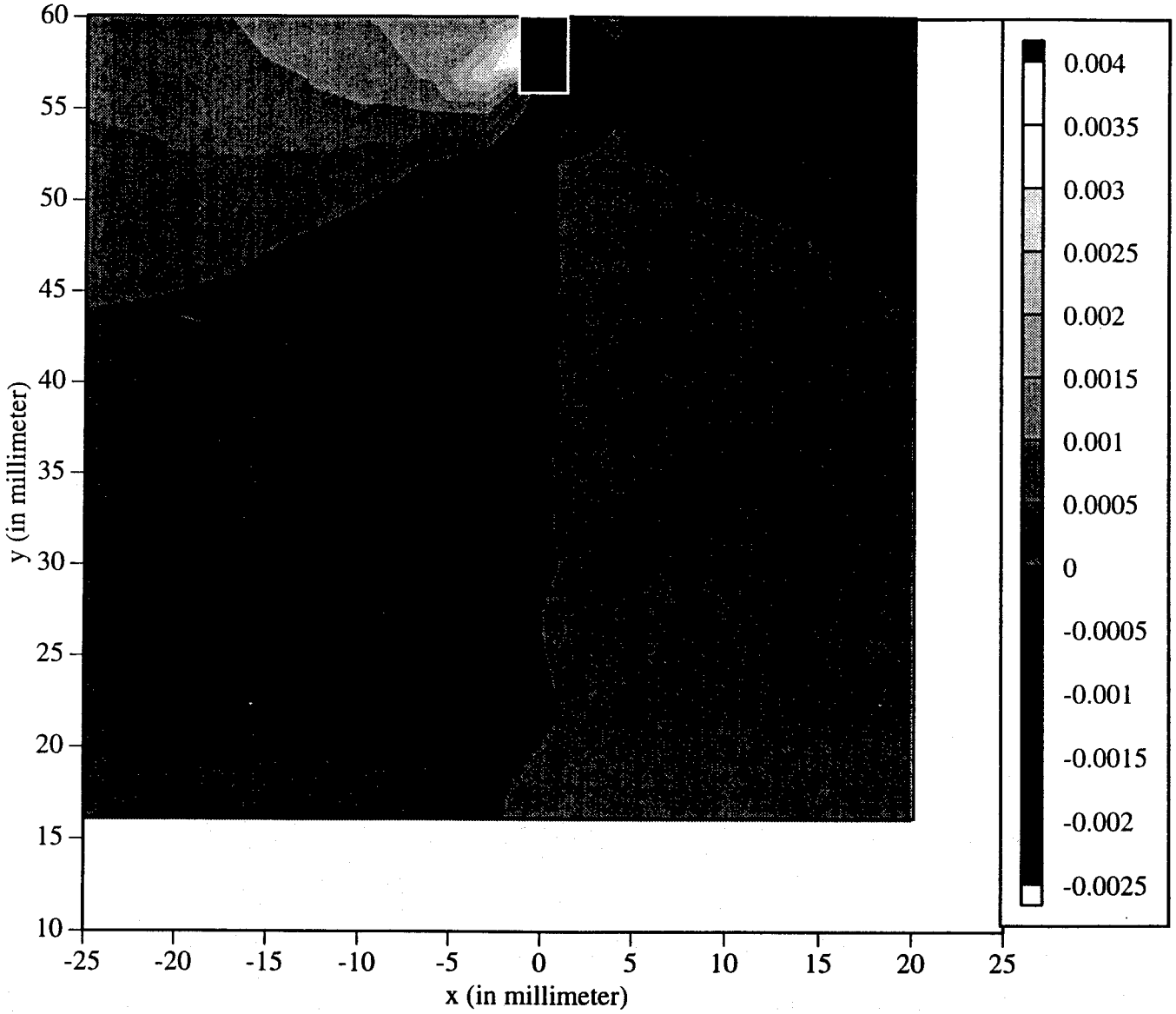

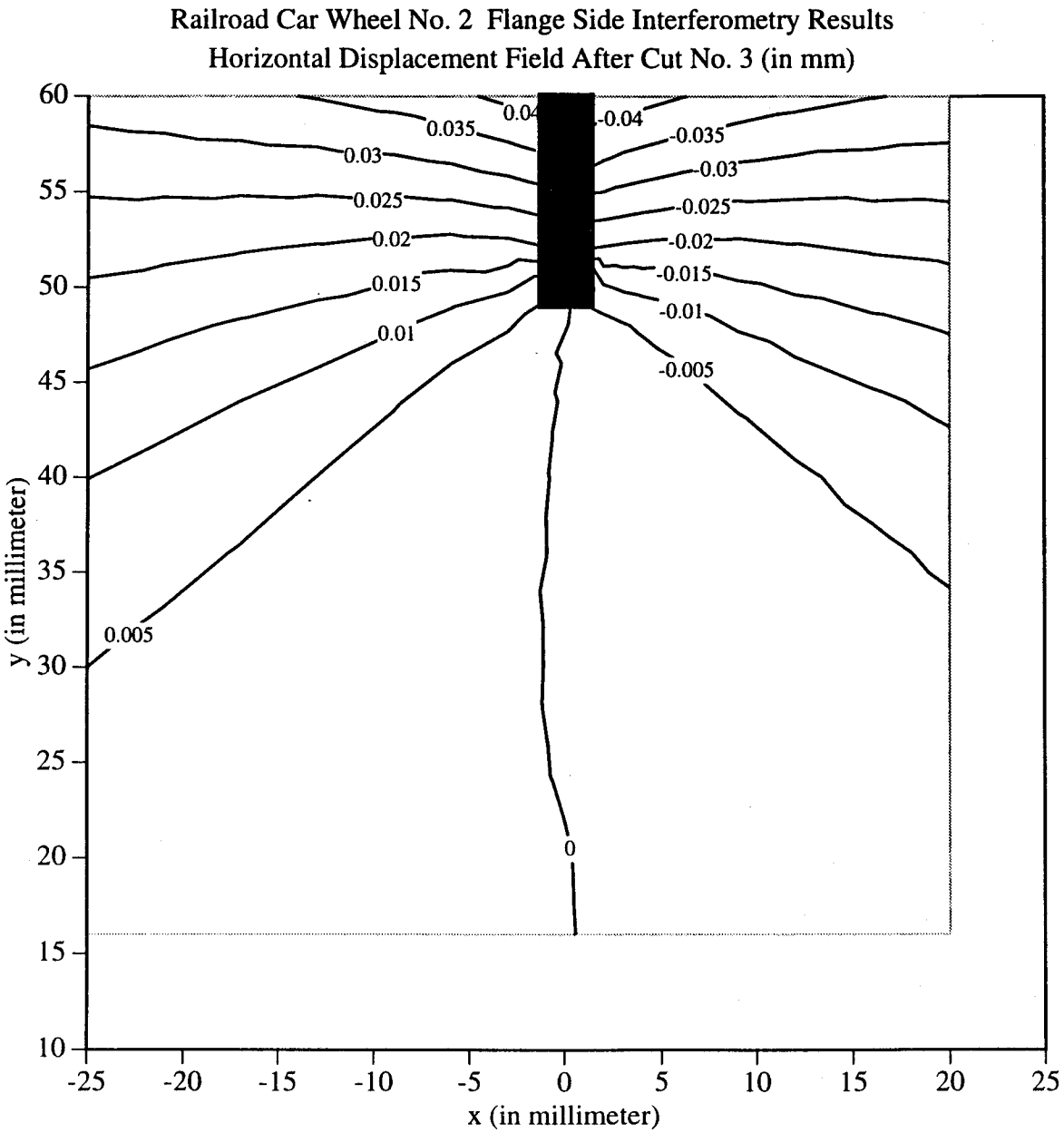
Railroad Car Wheel No. 2 Flange Side Interferometry Results
Horizontal Displacement Field After Cut No. 3 (in mm)
0.04
0.035
0.03
0.025
0.02
0.015
0.01
0.005
0
-0.04
-0.035
-0.03
-0.025
-0.02
-0.015
-0.01
-0.005
y (in millimeter)
x (in millimeter)
60
55
50
45
40
35
30
25
20
15
10
-25
-20
-15
-10
-5
0
5
10
15
20
25

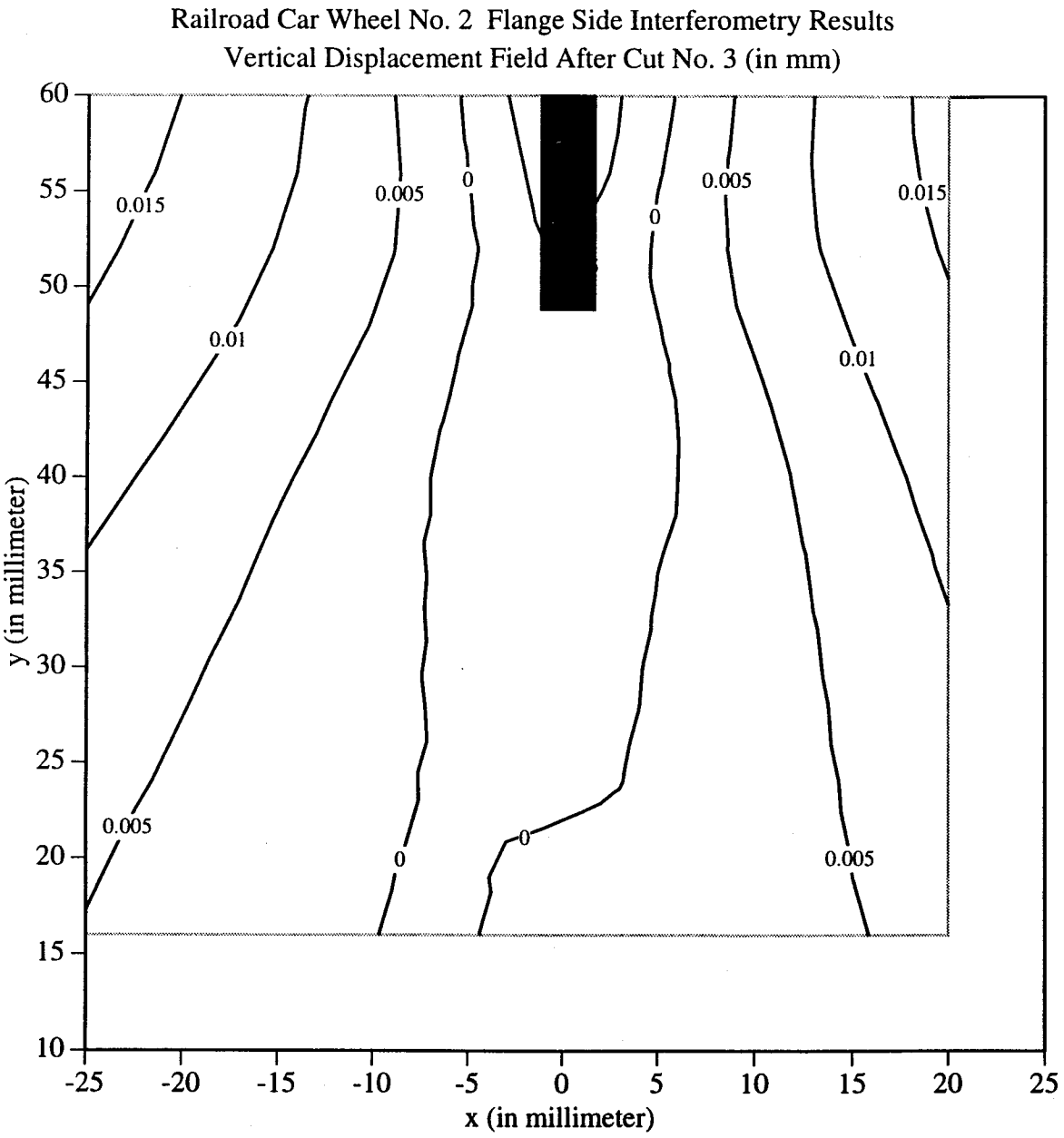
Railroad Car Wheel No. 2 Flange Side Interferometry Results
Vertical Displacement Field After Cut No. 3 (in mm)
y (in millimeter)
x (in millimeter)
60
55
50
45
40
35
30
25
20
15
10
-25
-20
-15
-10
-5
0
5
10
15
20
25
0.015
0.005
0
0.005
0
0.015
0.01
0.01
0.005
0
0
0.005

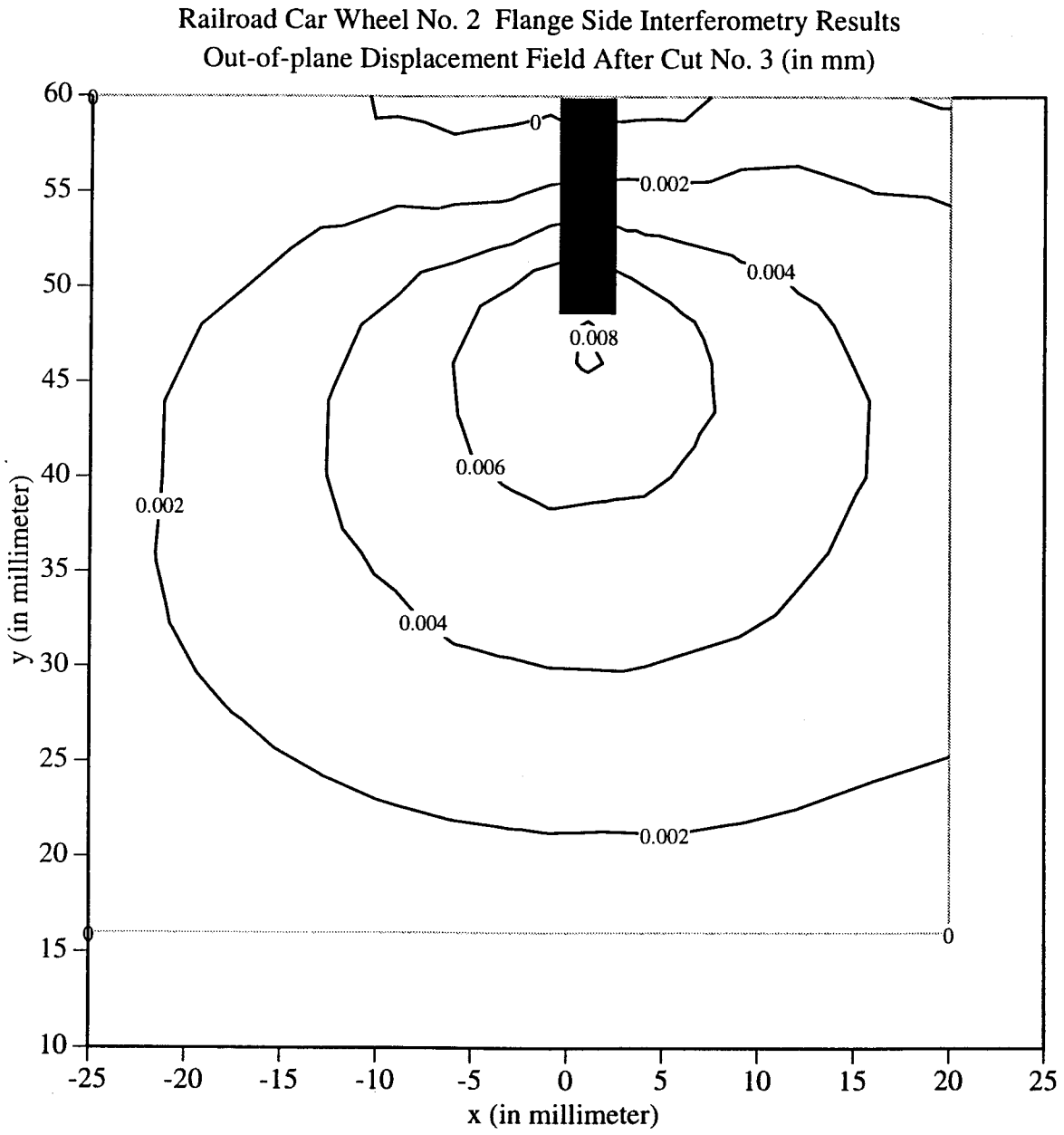
Railroad Car Wheel No. 2 Flange Side Interferometry Results
Out-of-plane Displacement Field After Cut No. 3 (in mm)
0
0.002
0.004
0.008
0.006
0.002
0.004
0.002
0
0
y (in millimeter)
x (in millimeter)
60
55
50
45
40
35
30
25
20
15
10
-25
-20
-15
-10
-5
0
5
10
15
20
25

Railroad Car Wheel No. 2 Flange Side Interferometry Results
Horizontal Strain Field After Cut No. 3

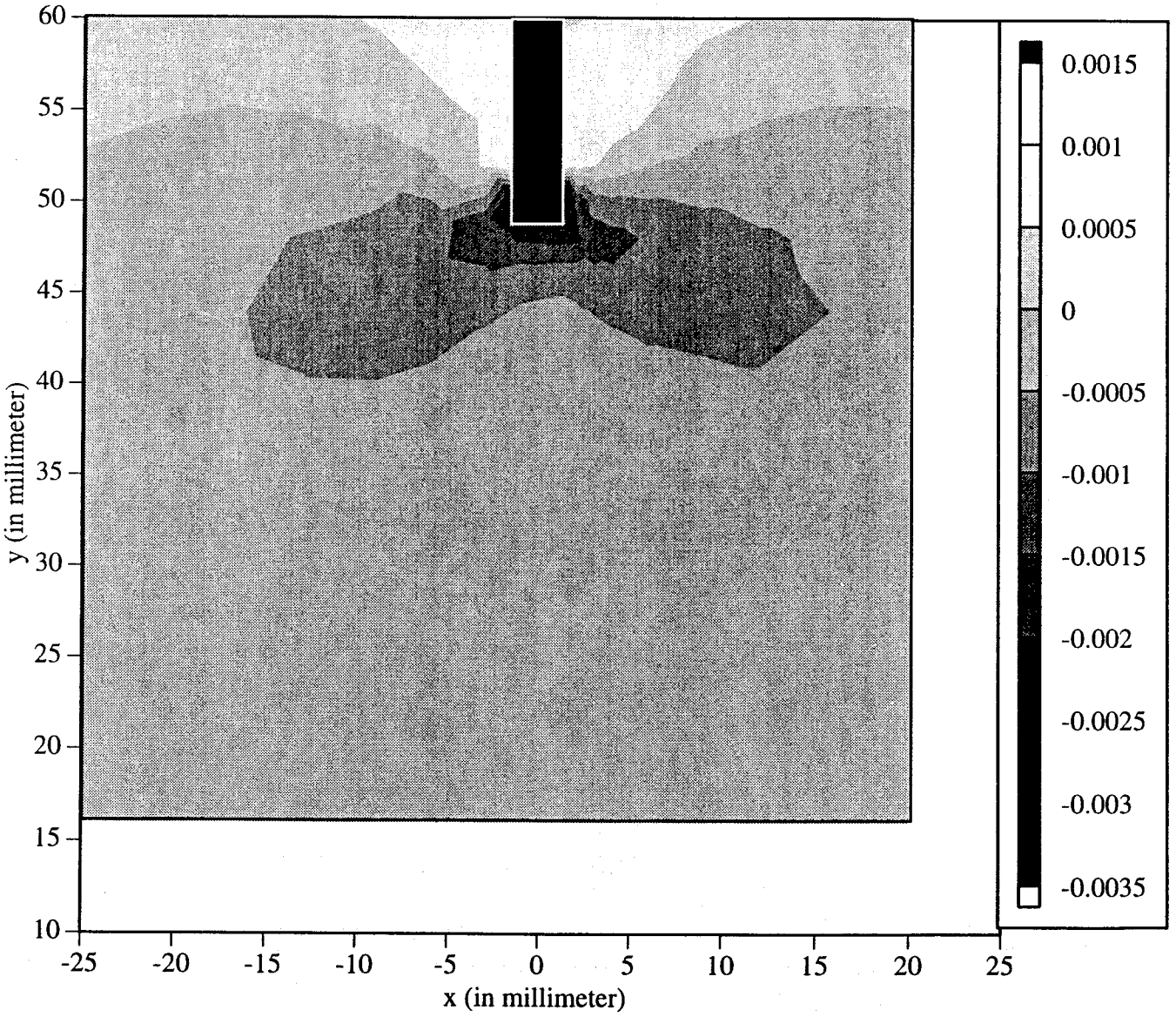

Railroad Car Wheel No. 2 Flange Side Interferometry Results
Vertical Strain Field After Cut No. 3

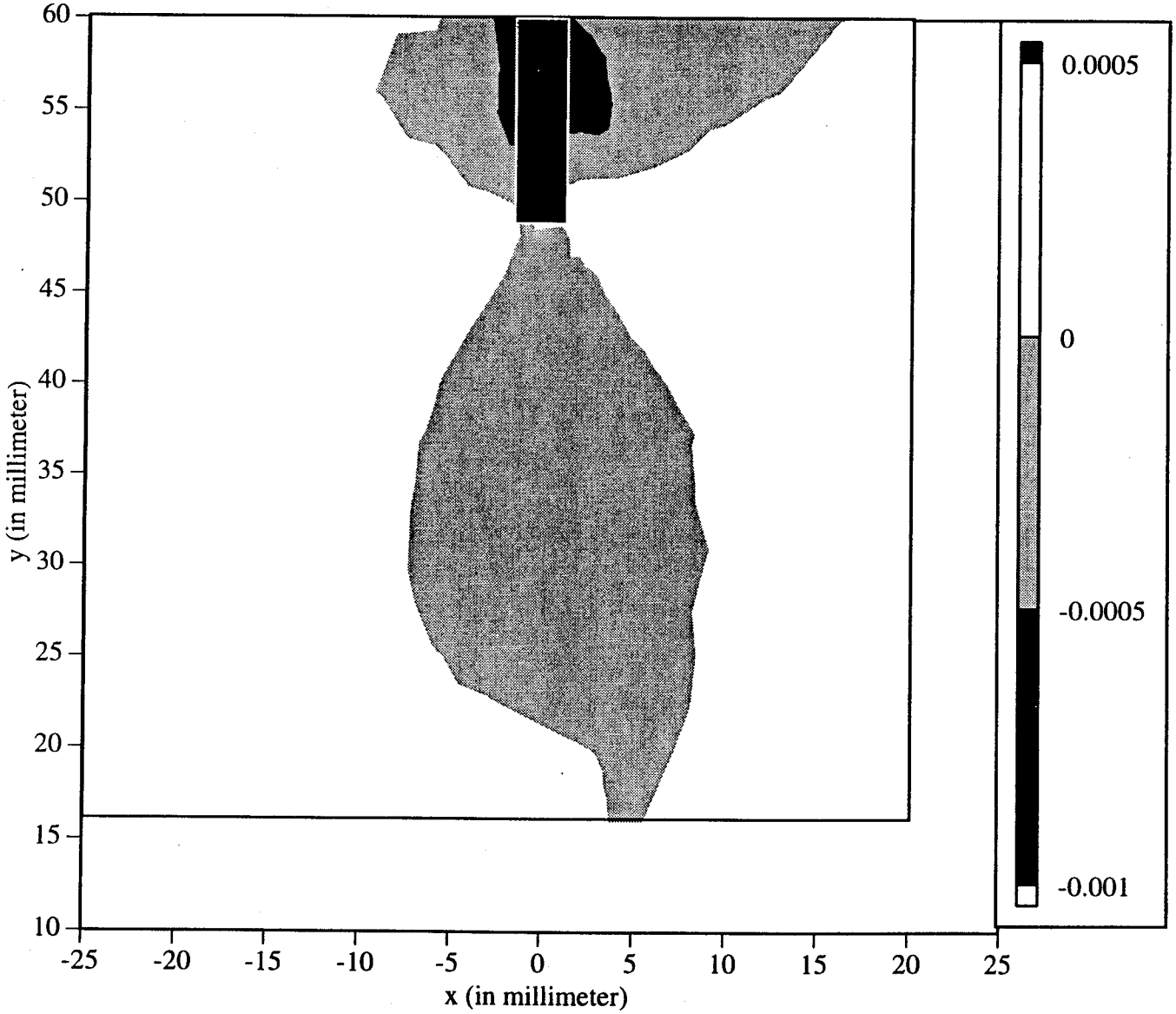

Railroad Car Wheel No. 2 Flange Side Interferometry Results
Shear Strain Field After Cut No. 3

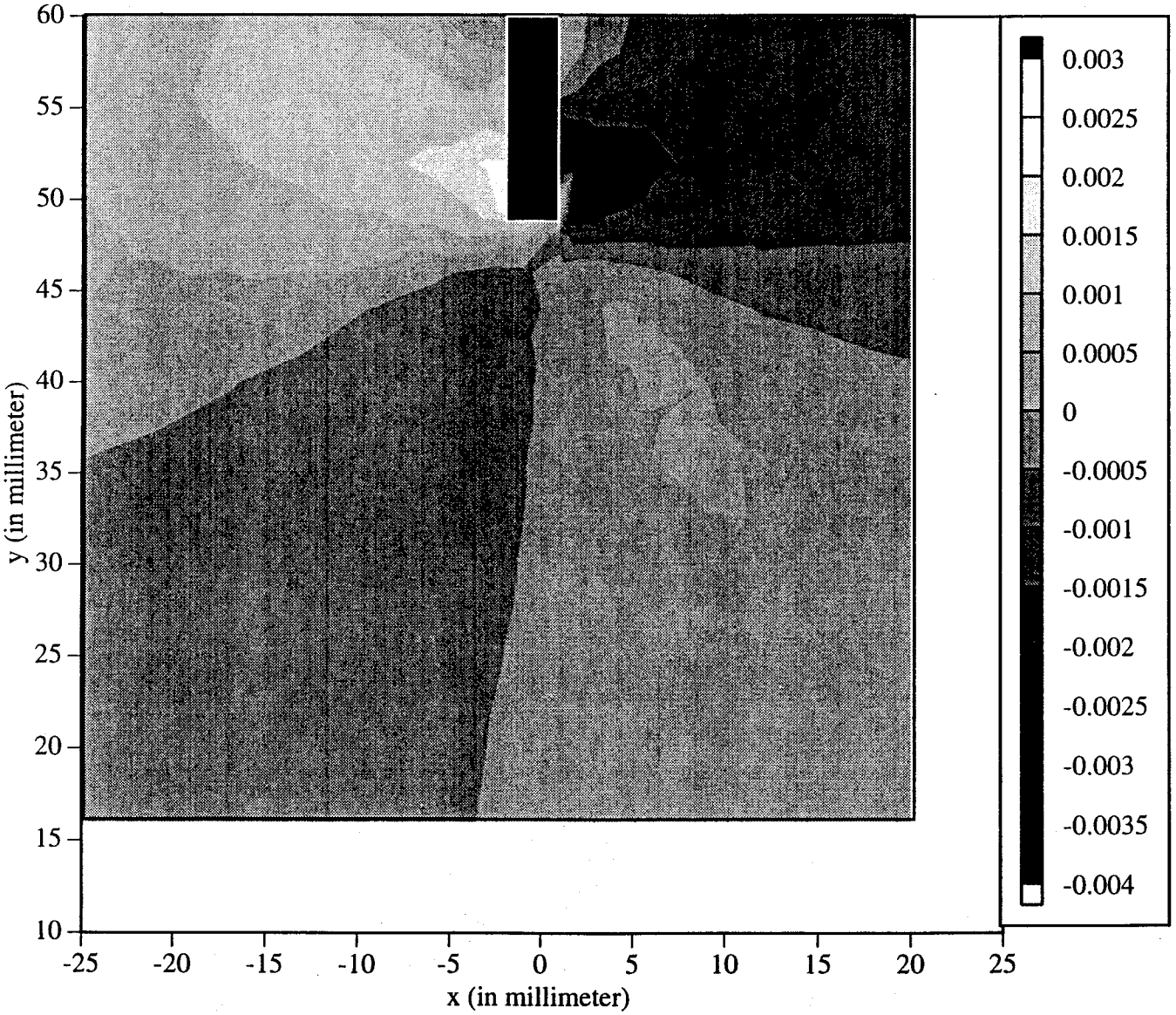

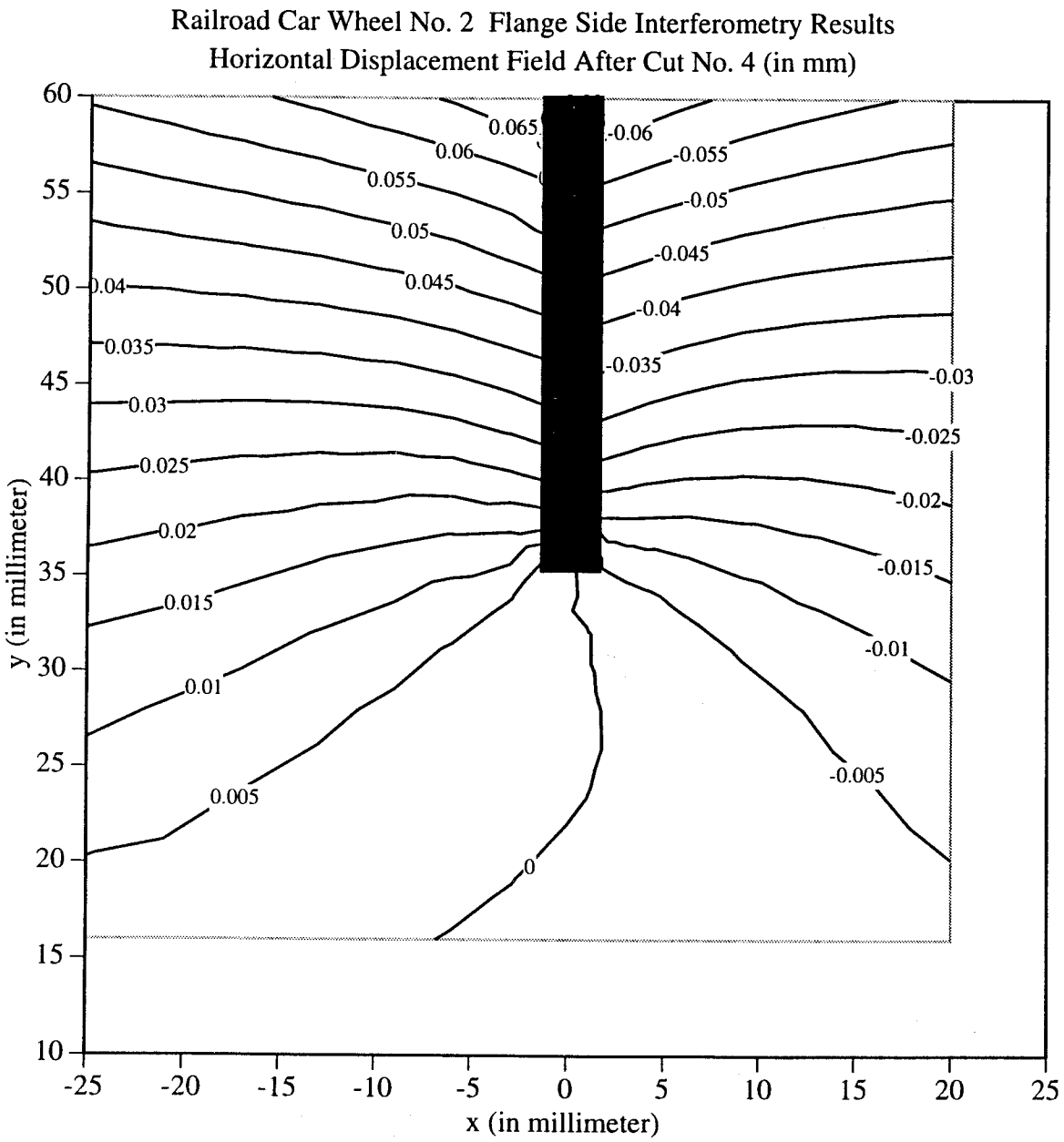
Railroad Car Wheel No. 2 Flange Side Interferometry Results
Horizontal Displacement Field After Cut No. 4 (in mm)
y (in millimeter)
x (in millimeter)
60
55
50
45
40
35
30
25
20
15
10
-25
-20
-15
-10
-5
0
5
10
15
20
25
0.065
0.06
0.055
0.05
0.045
0.04
0.035
0.03
0.025
0.02
0.015
0.01
0.005
0
-0.06
-0.055
-0.05
-0.045
-0.04
-0.035
-0.03
-0.025
-0.02
-0.015
-0.01
-0.005

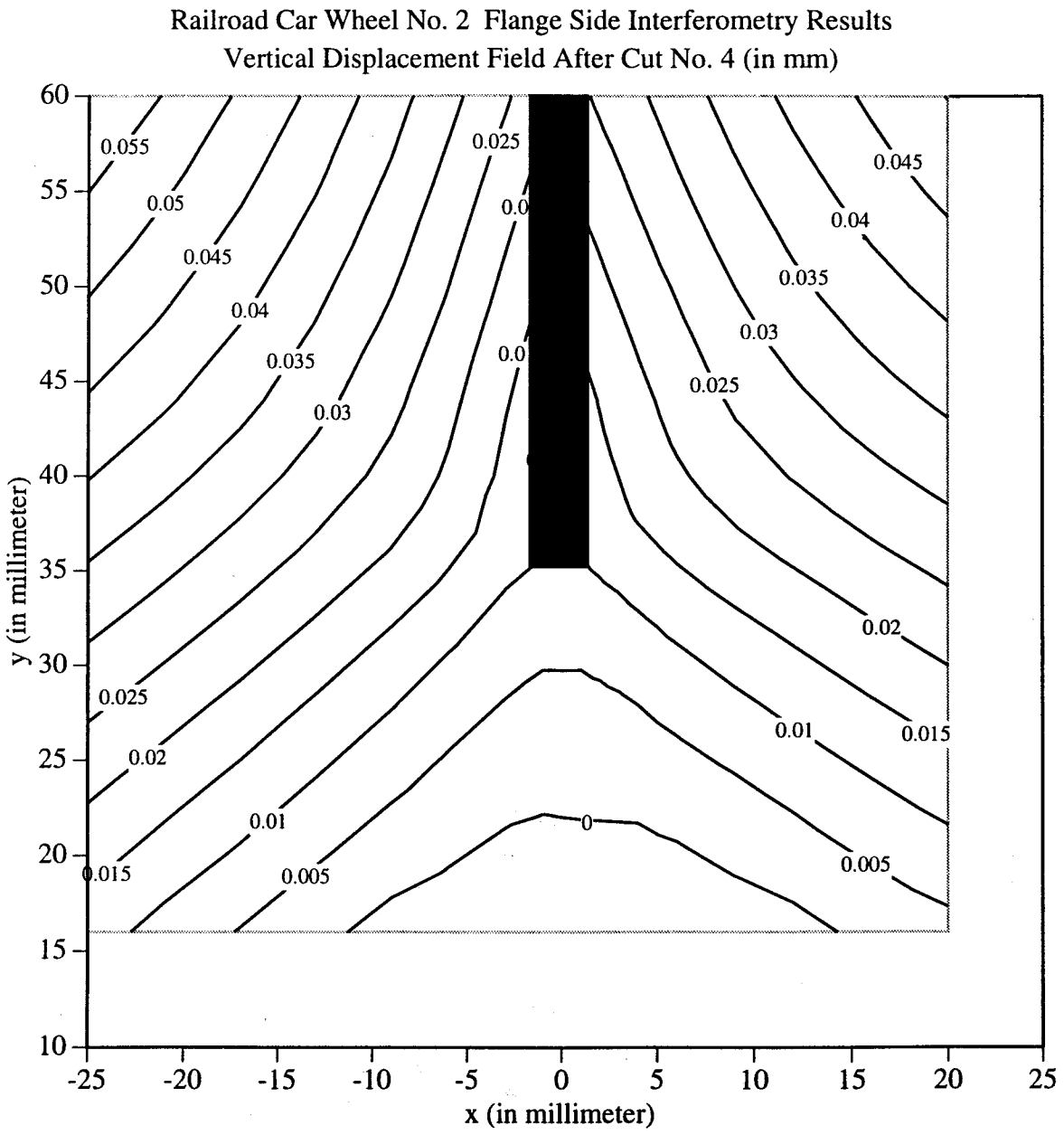
Railroad Car Wheel No. 2 Flange Side Interferometry Results
Vertical Displacement Field After Cut No. 4 (in mm)
y (in millimeter)
x (in millimeter)
60
55
50
45
40
35
30
25
20
15
10
-25
-20
-15
-10
-5
0
5
10
15
20
25
0.055
0.05
0.045
0.04
0.035
0.03
0.025
0.02
0.015
0.01
0.005
0

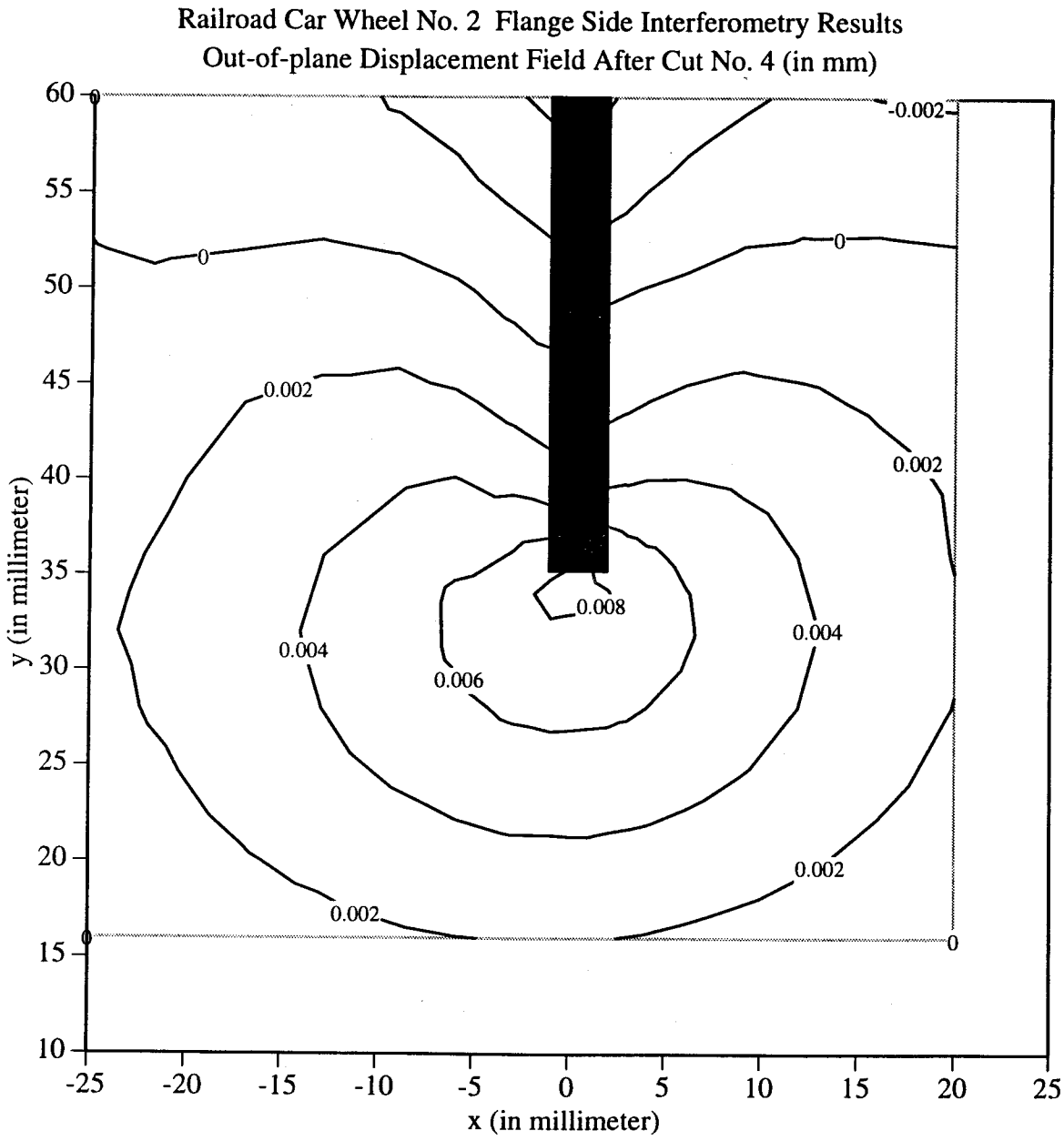
Railroad Car Wheel No. 2 Flange Side Interferometry Results
Out-of-plane Displacement Field After Cut No. 4 (in mm)
y (in millimeter)
x (in millimeter)
60
55
50
45
40
35
30
25
20
15
10
-25
-20
-15
-10
-5
0
5
10
15
20
25
-0.002
0
0.002
0.004
0.006
0.008

Railroad Car Wheel No. 2 Flange Side Interferometry Results
Horizontal Strain Field After Cut No. 4

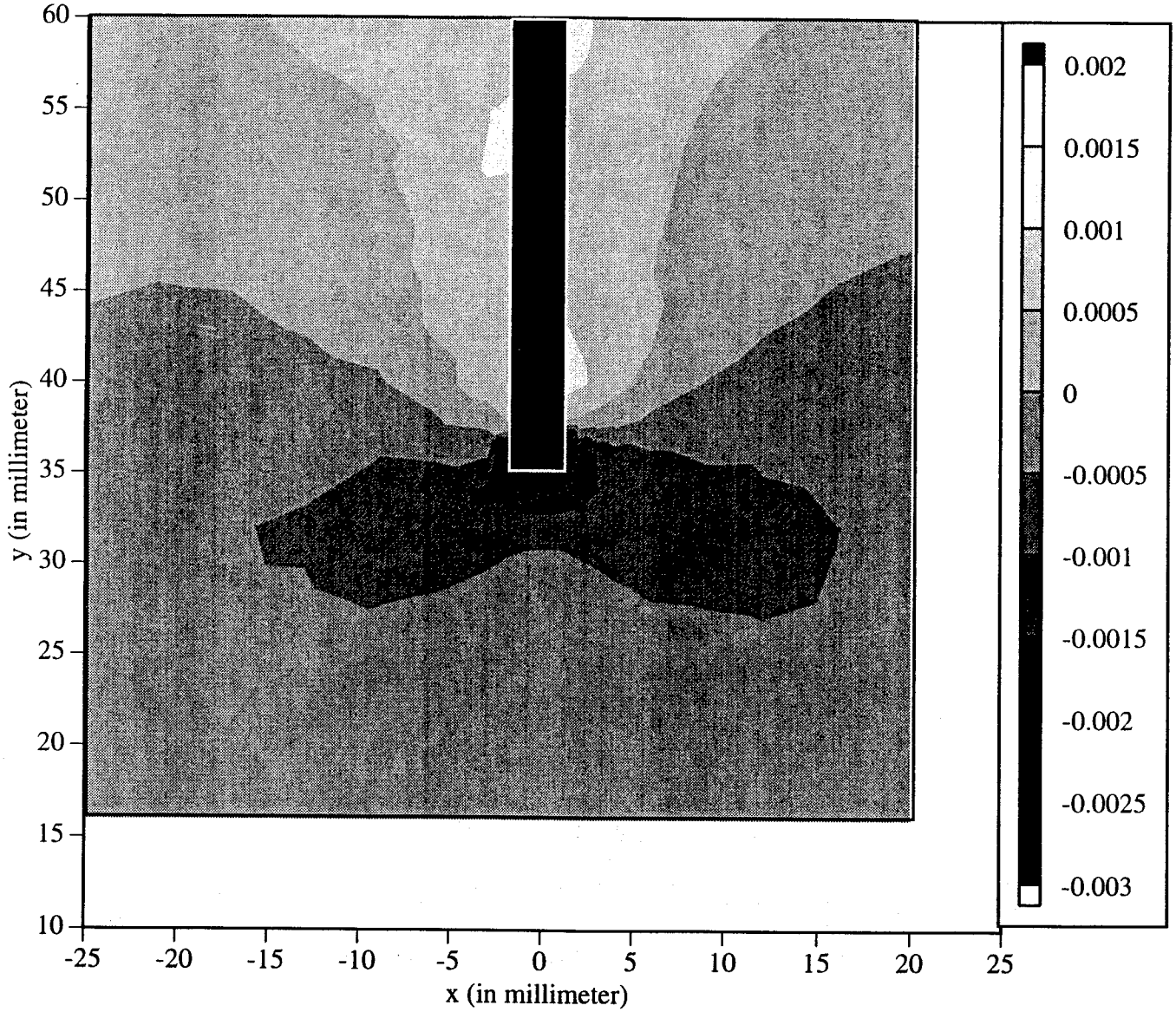

Railroad Car Wheel No. 2 Flange Side Interferometry Results
Vertical Strain Field After Cut No. 4

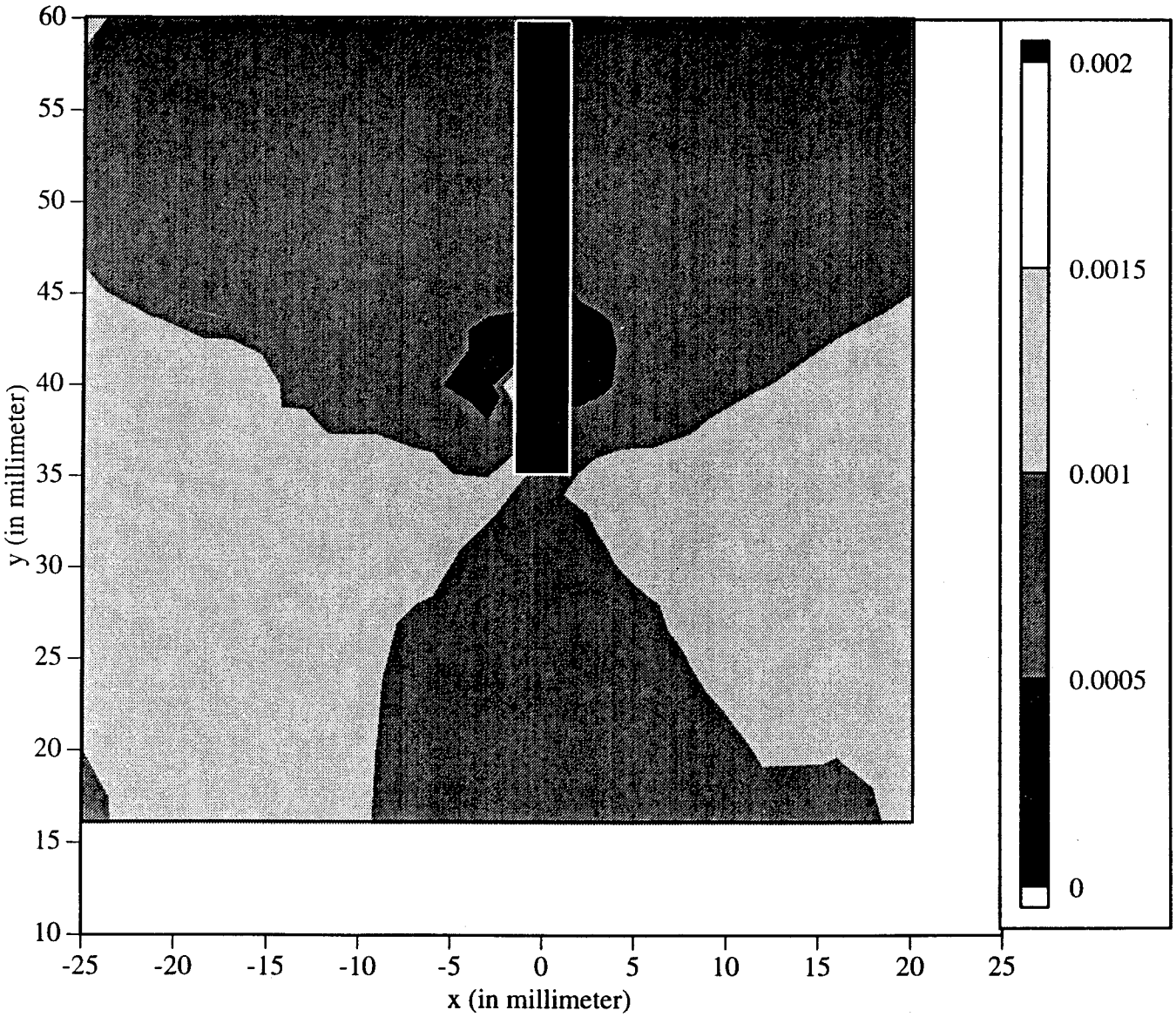

Railroad Car Wheel No. 2 Flange Side Interferometry Results
Shear Strain Field After Cut No. 4

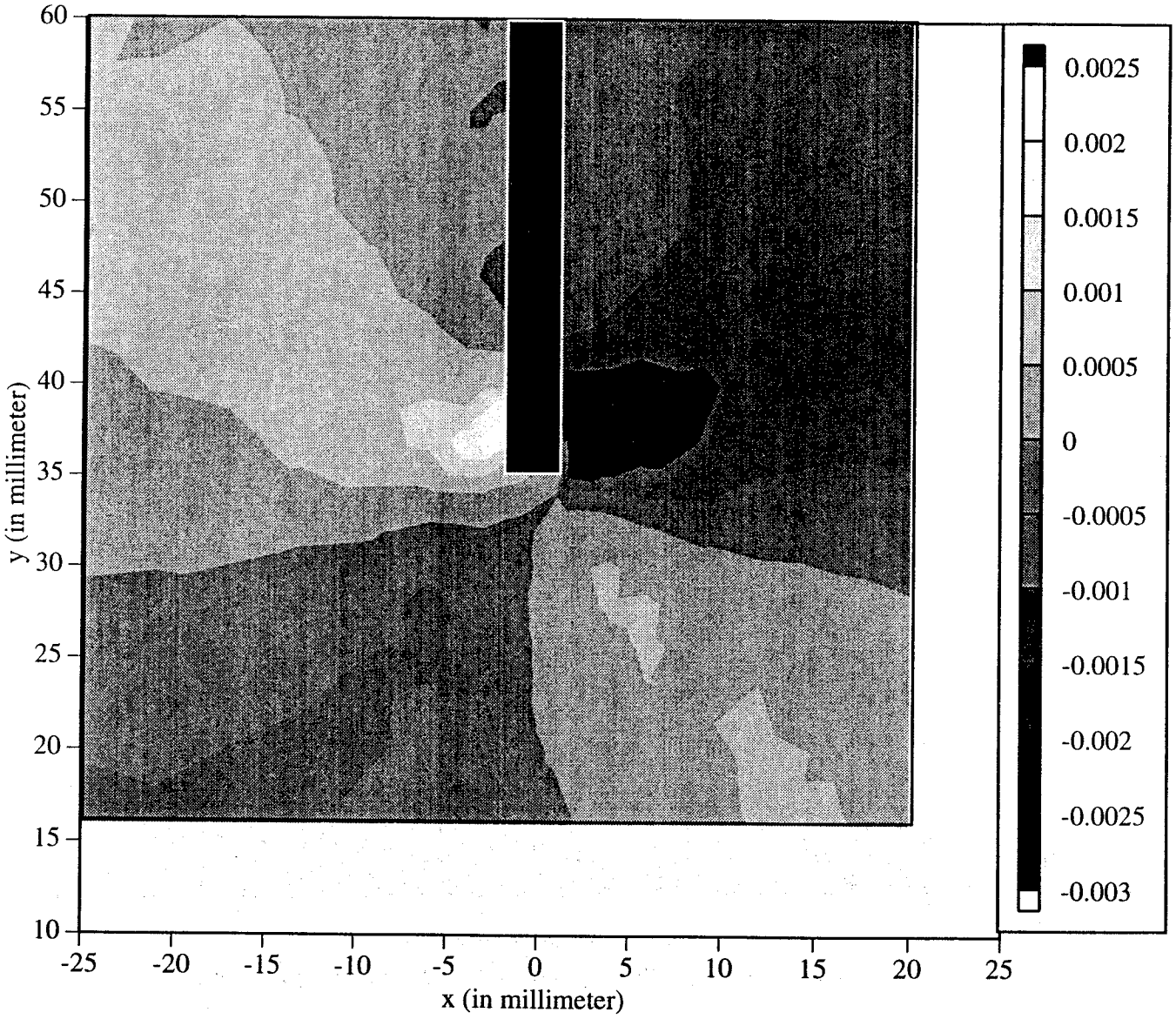

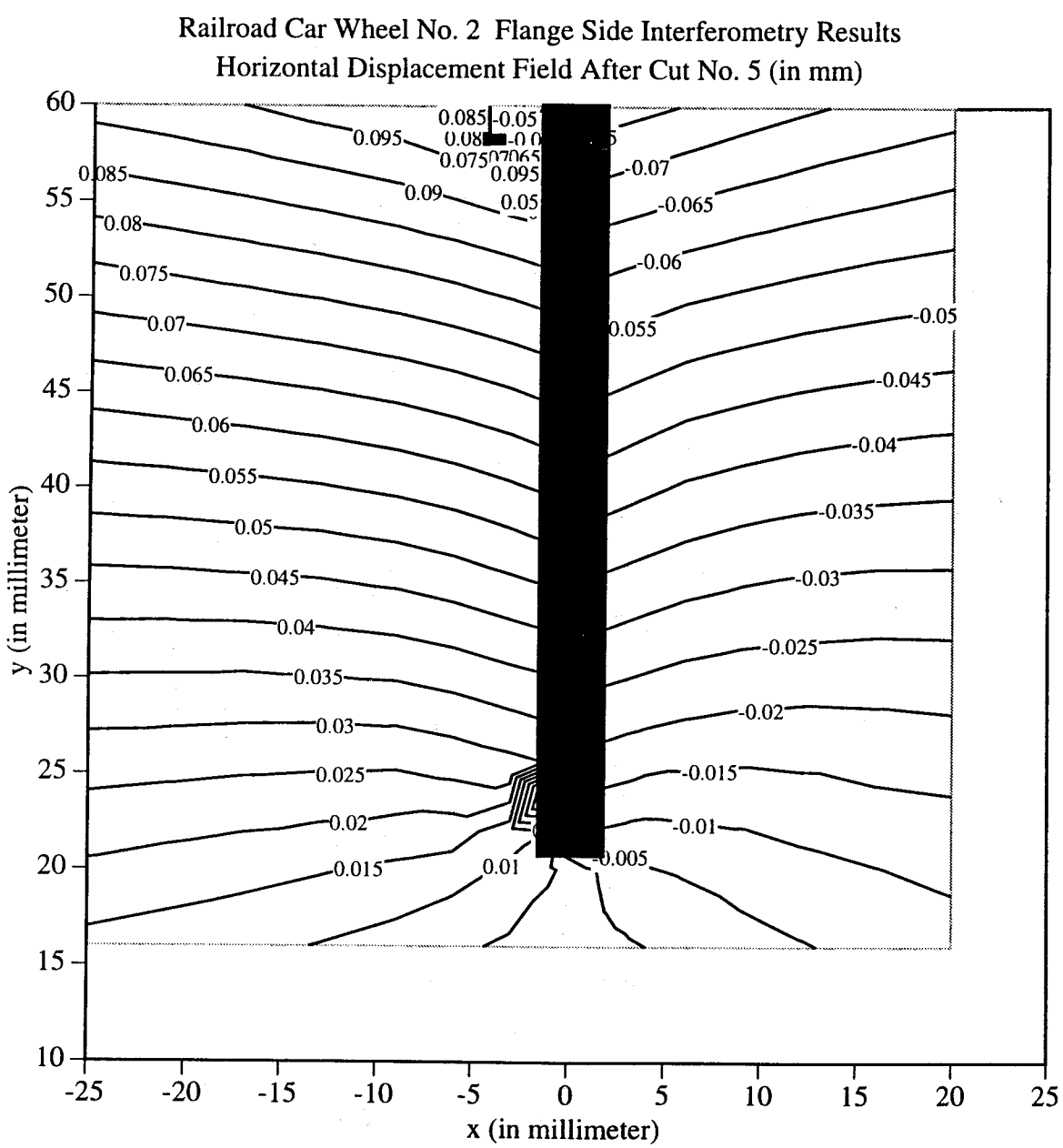
Railroad Car Wheel No. 2 Flange Side Interferometry Results
Horizontal Displacement Field After Cut No. 5 (in mm)
y (in millimeter)
x (in millimeter)
60
55
50
45
40
35
30
25
20
15
10
-25
-20
-15
-10
-5
0
5
10
15
20
25
0.095
0.085
0.09
0.08
0.075
0.07
0.065
0.06
0.055
0.05
0.045
0.04
0.035
0.03
0.025
0.02
0.015
0.01
-0.07
-0.065
-0.06
-0.05
-0.045
-0.04
-0.035
-0.03
-0.025
-0.02
-0.015
-0.01
-0.005

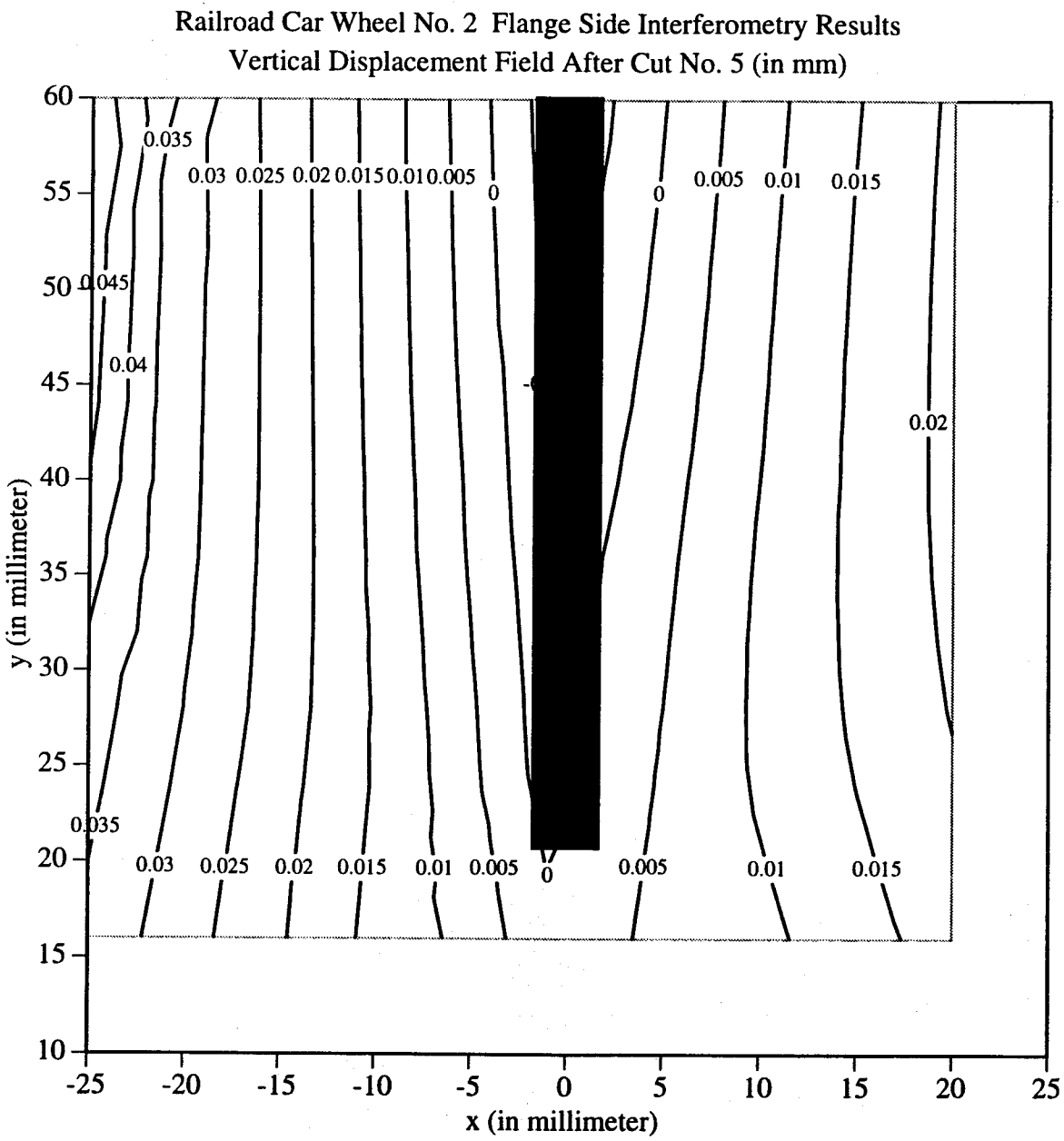
Railroad Car Wheel No. 2 Flange Side Interferometry Results
Vertical Displacement Field After Cut No. 5 (in mm)
y (in millimeter)
x (in millimeter)
60
55
50
45
40
35
30
25
20
15
10
-25
-20
-15
-10
-5
0
5
10
15
20
25
0.035
0.03
0.025
0.02
0.015
0.01
0.005
0
0.005
0.01
0.015
0.045
0.04
0.02
0.035
0.03
0.025
0.02
0.015
0.01
0.005
0
0.005
0.01
0.015

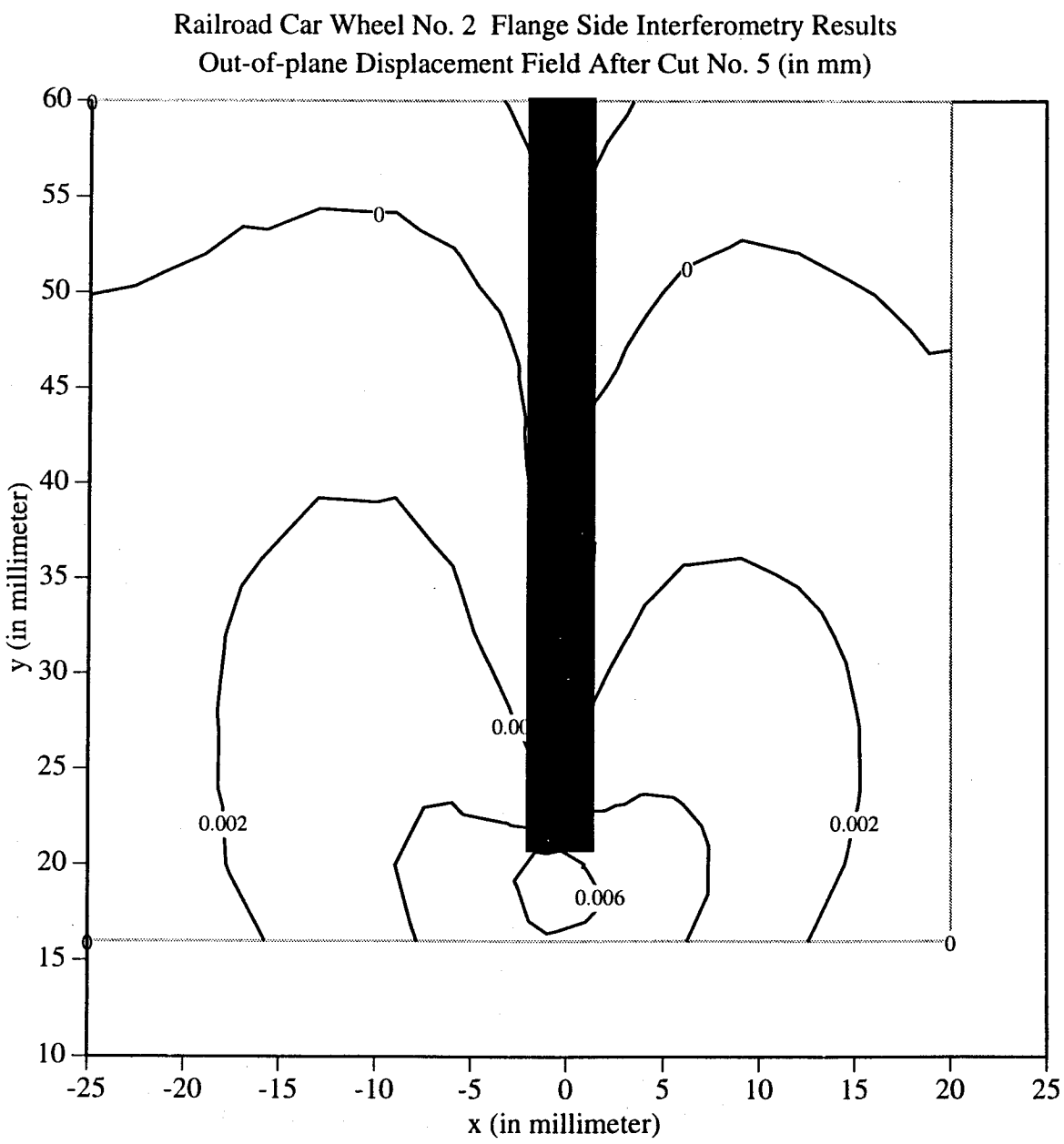
Railroad Car Wheel No. 2 Flange Side Interferometry Results
Out-of-plane Displacement Field After Cut No. 5 (in mm)
y (in millimeter)
x (in millimeter)
60
55
50
45
40
35
30
25
20
15
10
-25
-20
-15
-10
-5
0
5
10
15
20
25
0
0
0
0
0.002
0.002
0.006
0

Railroad Car Wheel No. 2 Flange Side Interferometry Results
Horizontal Strain Field After Cut No. 5

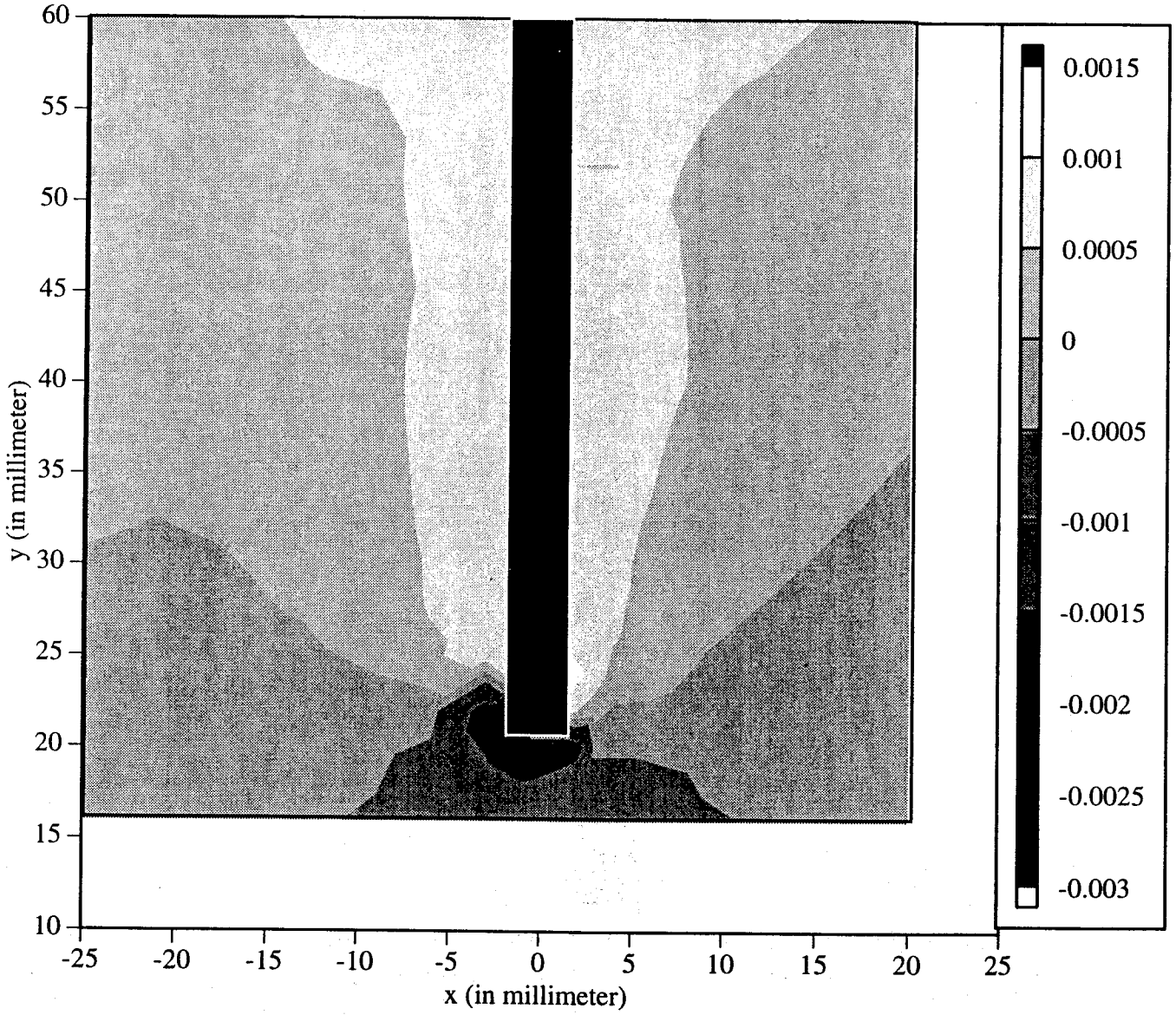

Railroad Car Wheel No. 2 Flange Side Interferometry Results
Vertical Strain Field After Cut No. 5

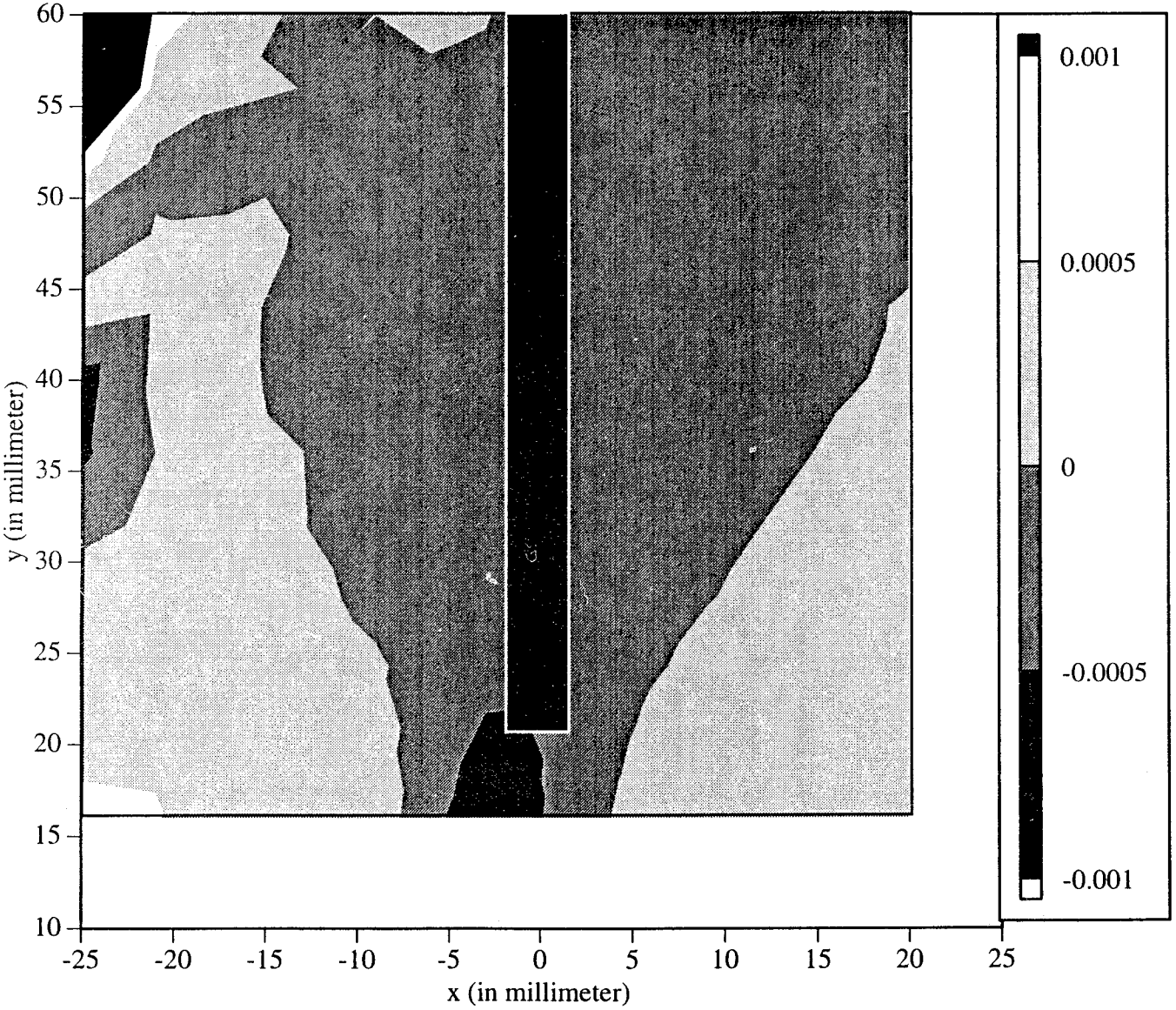

Railroad Car Wheel No. 2 Flange Side Interferometry Results
Shear Strain Field After Cut No. 5

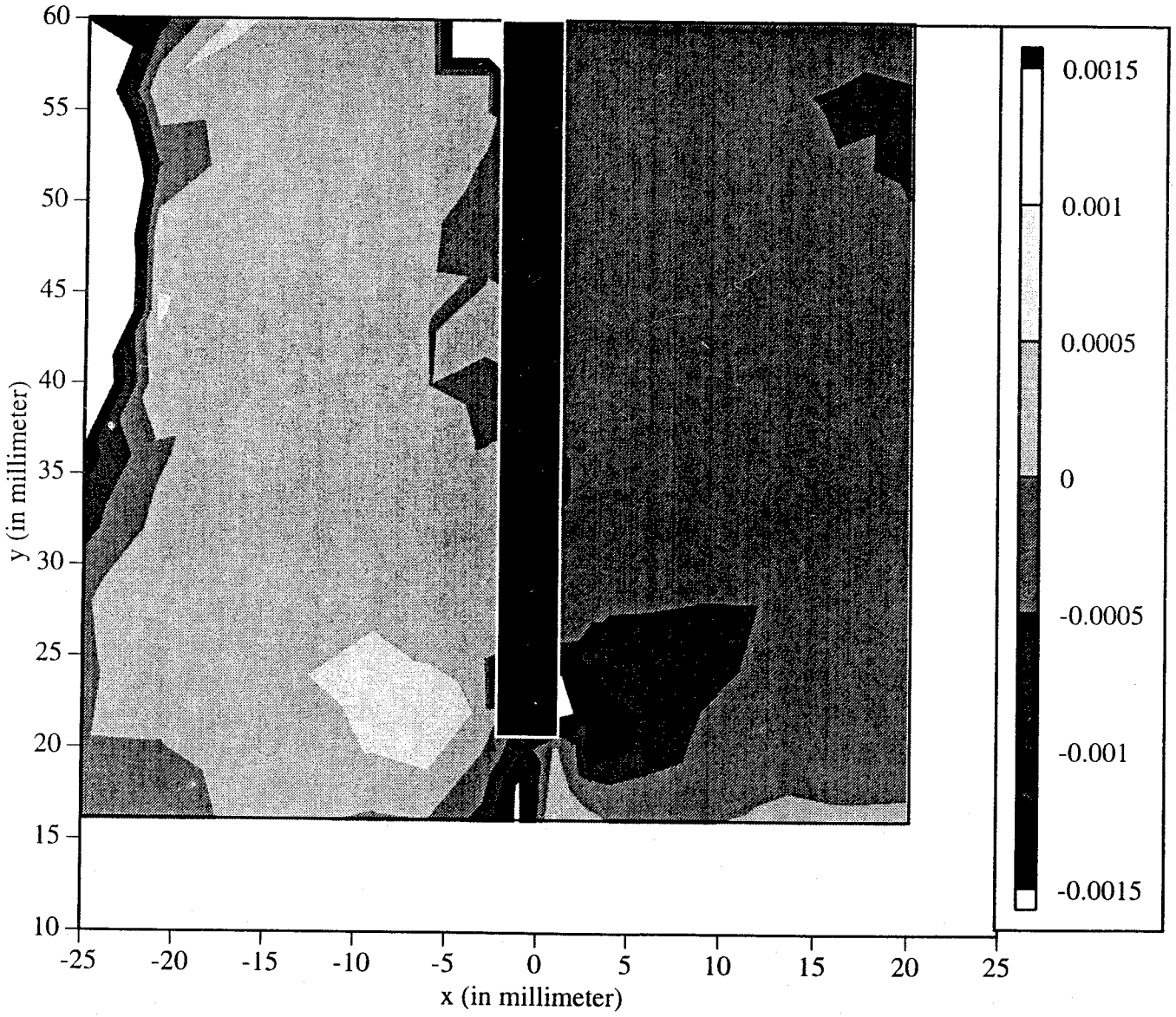

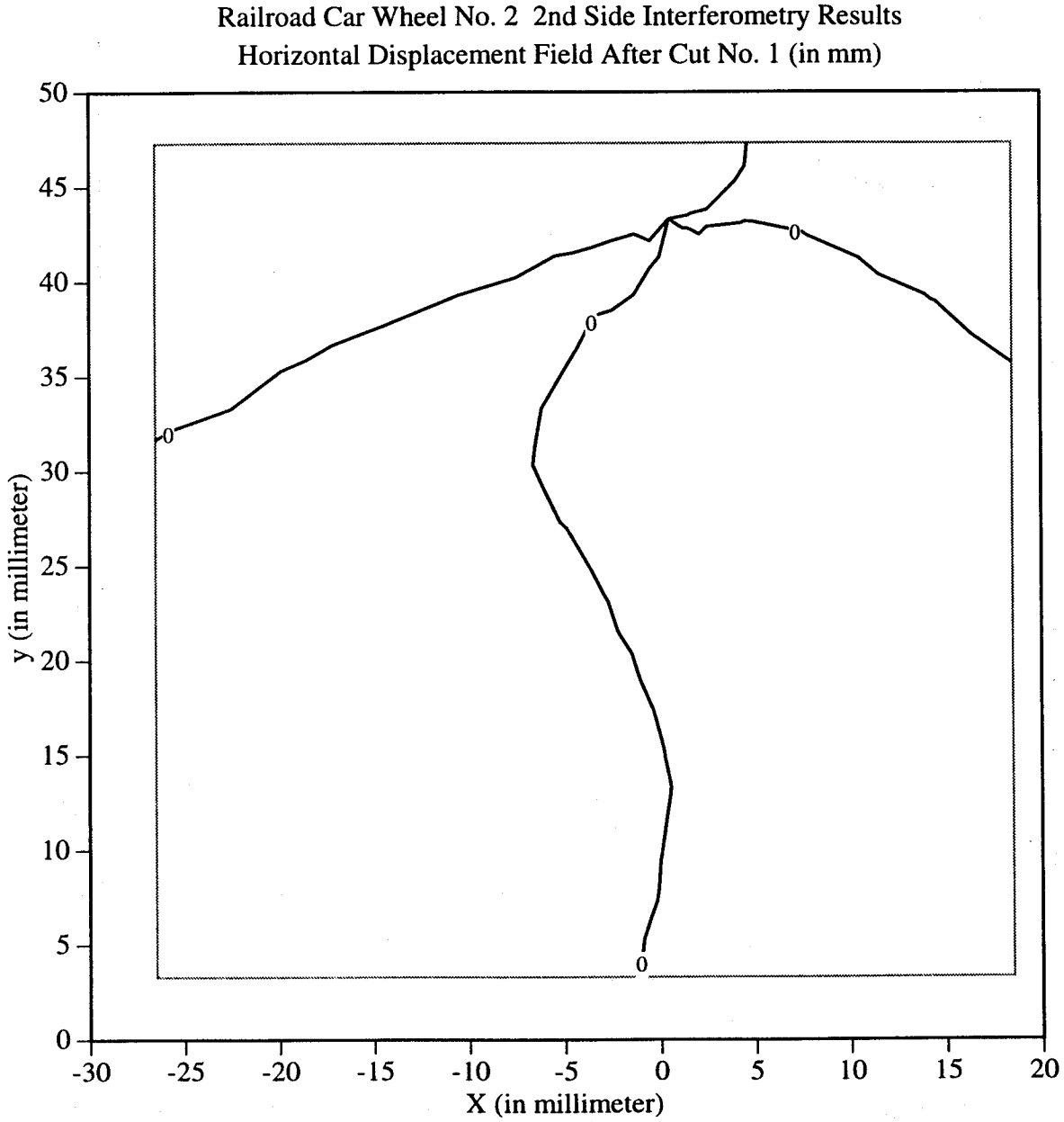
Railroad Car Wheel No. 2 2nd Side Interferometry Results
Horizontal Displacement Field After Cut No. 1 (in mm)
y (in millimeter)
X (in millimeter)
50
45
40
35
30
25
20
15
10
5
0
-30
-25
-20
-15
-10
-5
0
5
10
15
20
0
0
0
0

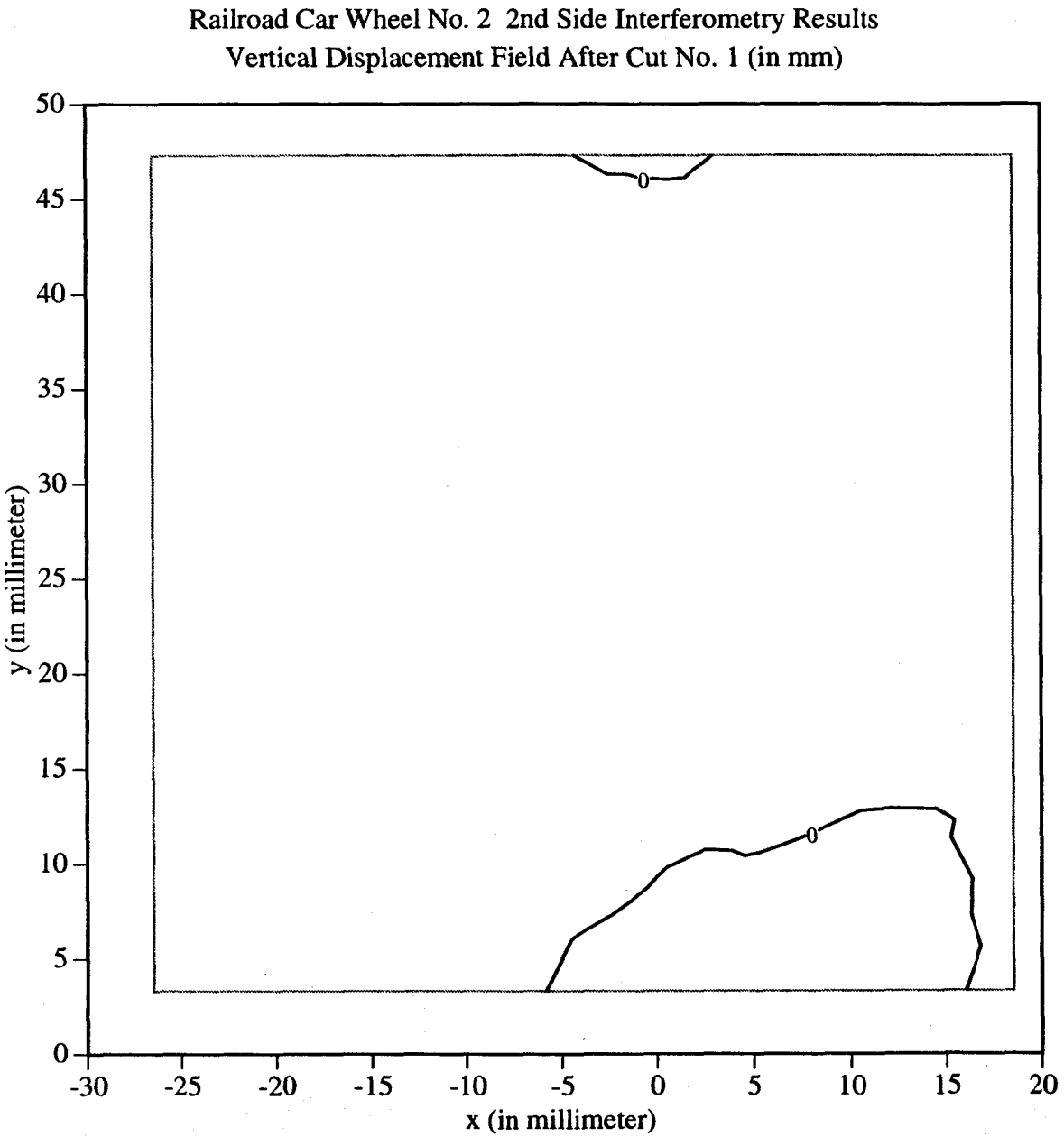
Railroad Car Wheel No. 2 2nd Side Interferometry Results
Vertical Displacement Field After Cut No. 1 (in mm)
y (in millimeter)
x (in millimeter)
50
45
40
35
30
25
20
15
10
5
0
-30
-25
-20
-15
-10
-5
0
5
10
15
20
0
0

Railroad Car Wheel No. 2 2nd Side Interferometry Results
Out-of-plane Displacement Field After Cut No. 1 (in mm)

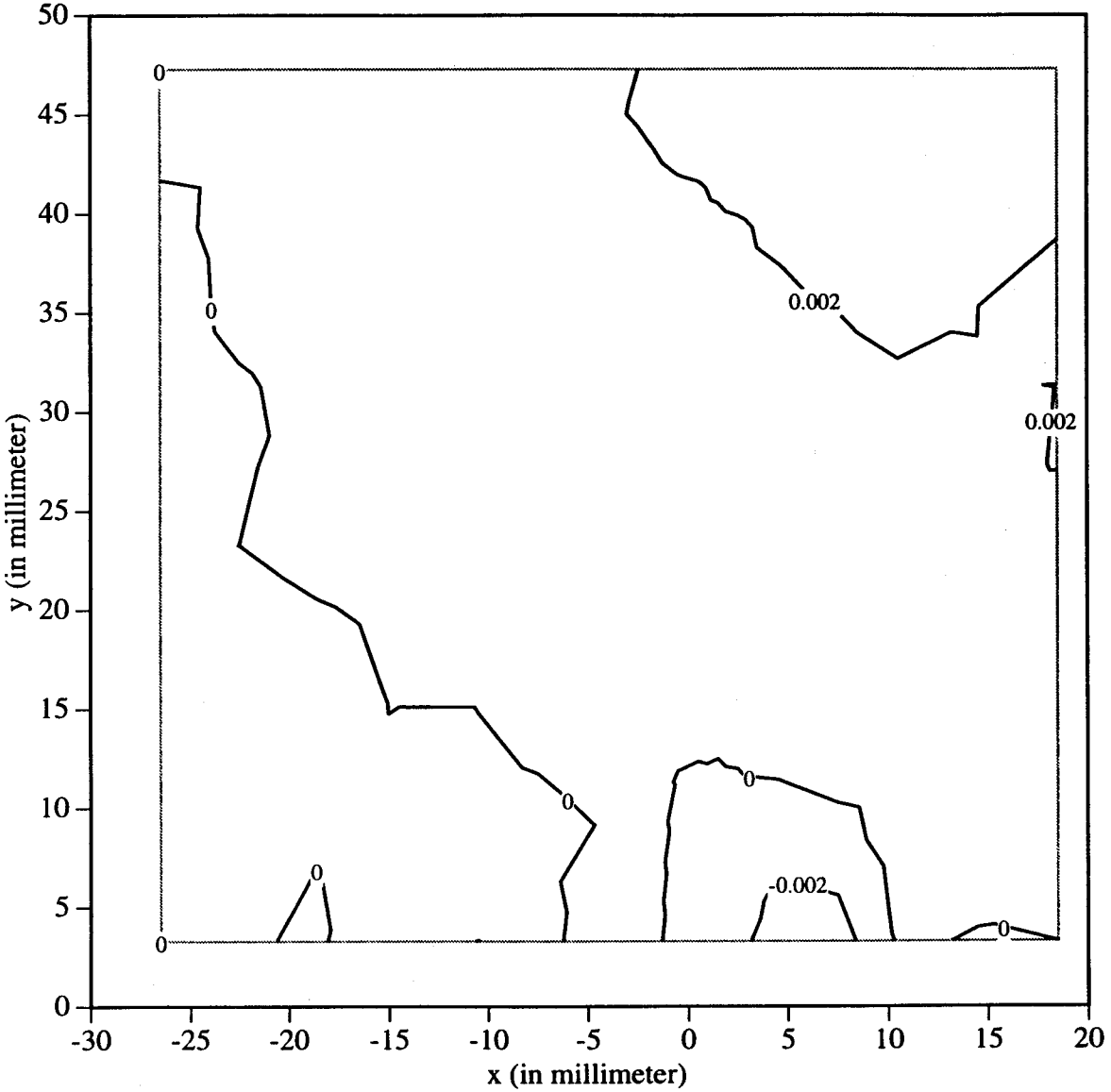

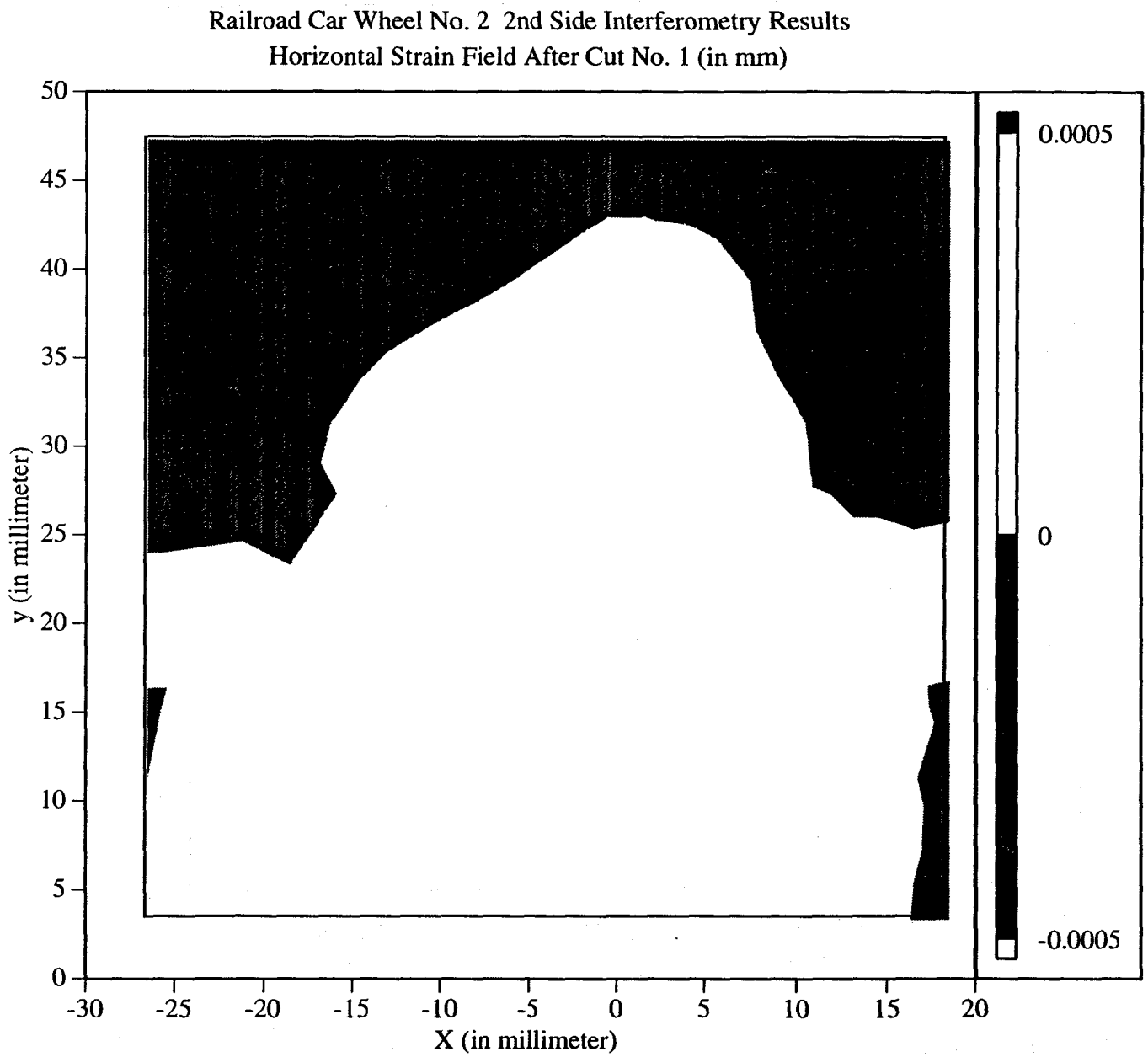
Railroad Car Wheel No. 2 2nd Side Interferometry Results
Horizontal Strain Field After Cut No. 1 (in mm)
y (in millimeter)
X (in millimeter)
50
45
40
35
30
25
20
15
10
5
0
-30
-25
-20
-15
-10
-5
0
5
10
15
20
0.0005
0
-0.0005

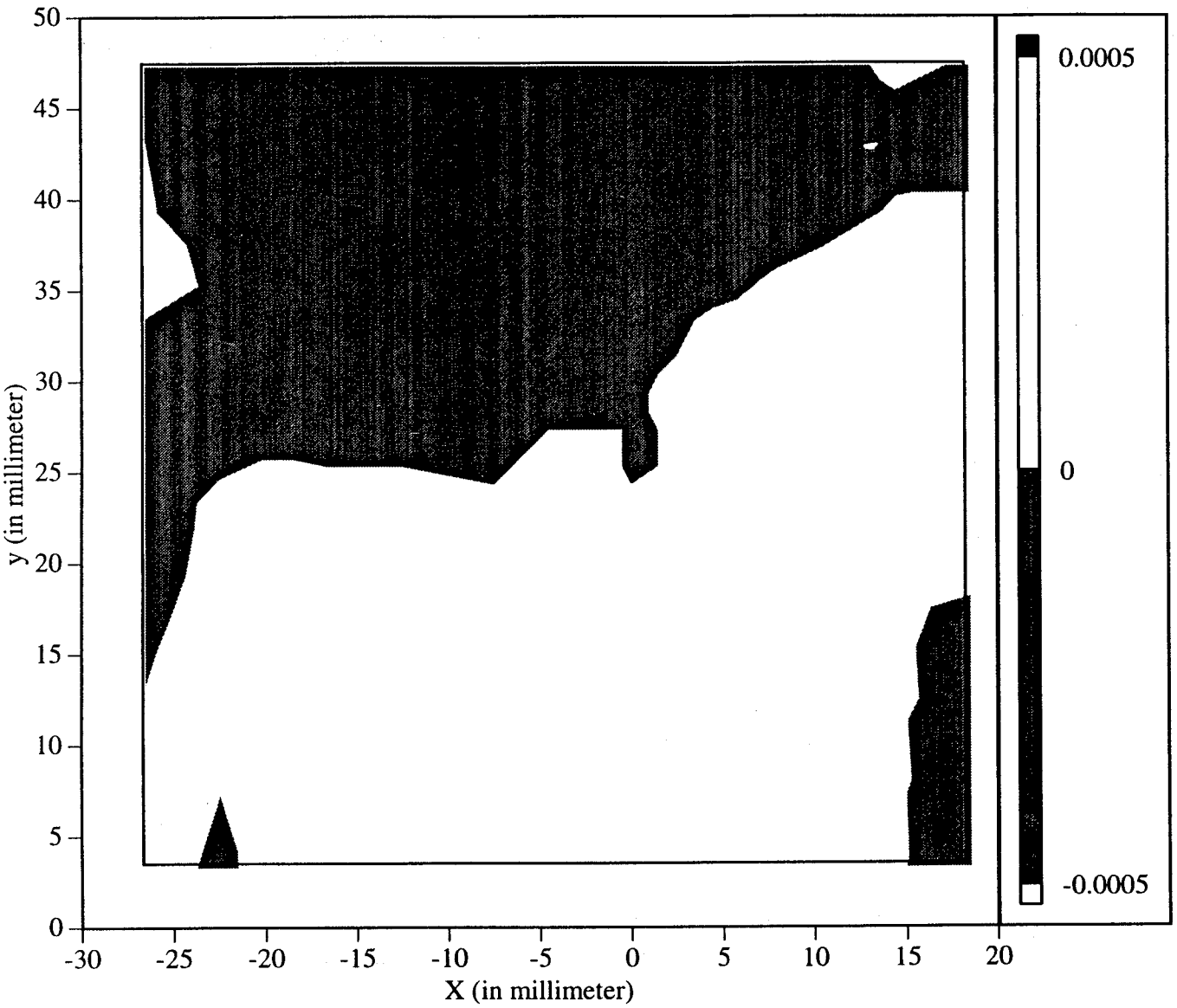
Railroad Car Wheel No. 2 2nd Side Interferometry Results
Vertical Strain Field After Cut No. 1 (in mm)
y (in millimeter)
X (in millimeter)
50
45
40
35
30
25
20
15
10
5
0
-30
-25
-20
-15
-10
-5
0
5
10
15
20
0.0005
0
-0.0005

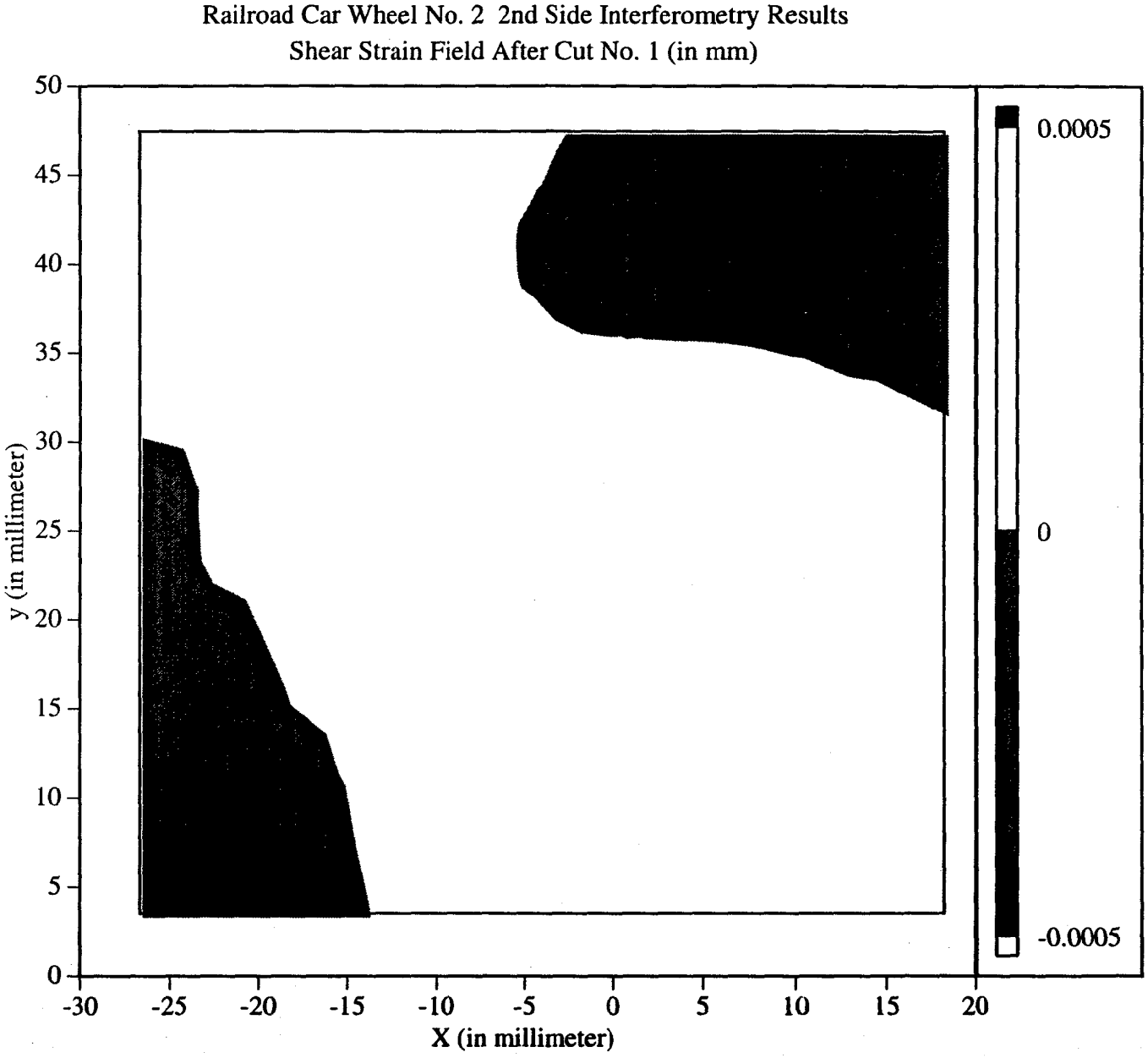
Railroad Car Wheel No. 2 2nd Side Interferometry Results
Shear Strain Field After Cut No. 1 (in mm)
y (in millimeter)
X (in millimeter)
50
45
40
35
30
25
20
15
10
5
0
-30
-25
-20
-15
-10
-5
0
5
10
15
20
0.0005
0
-0.0005

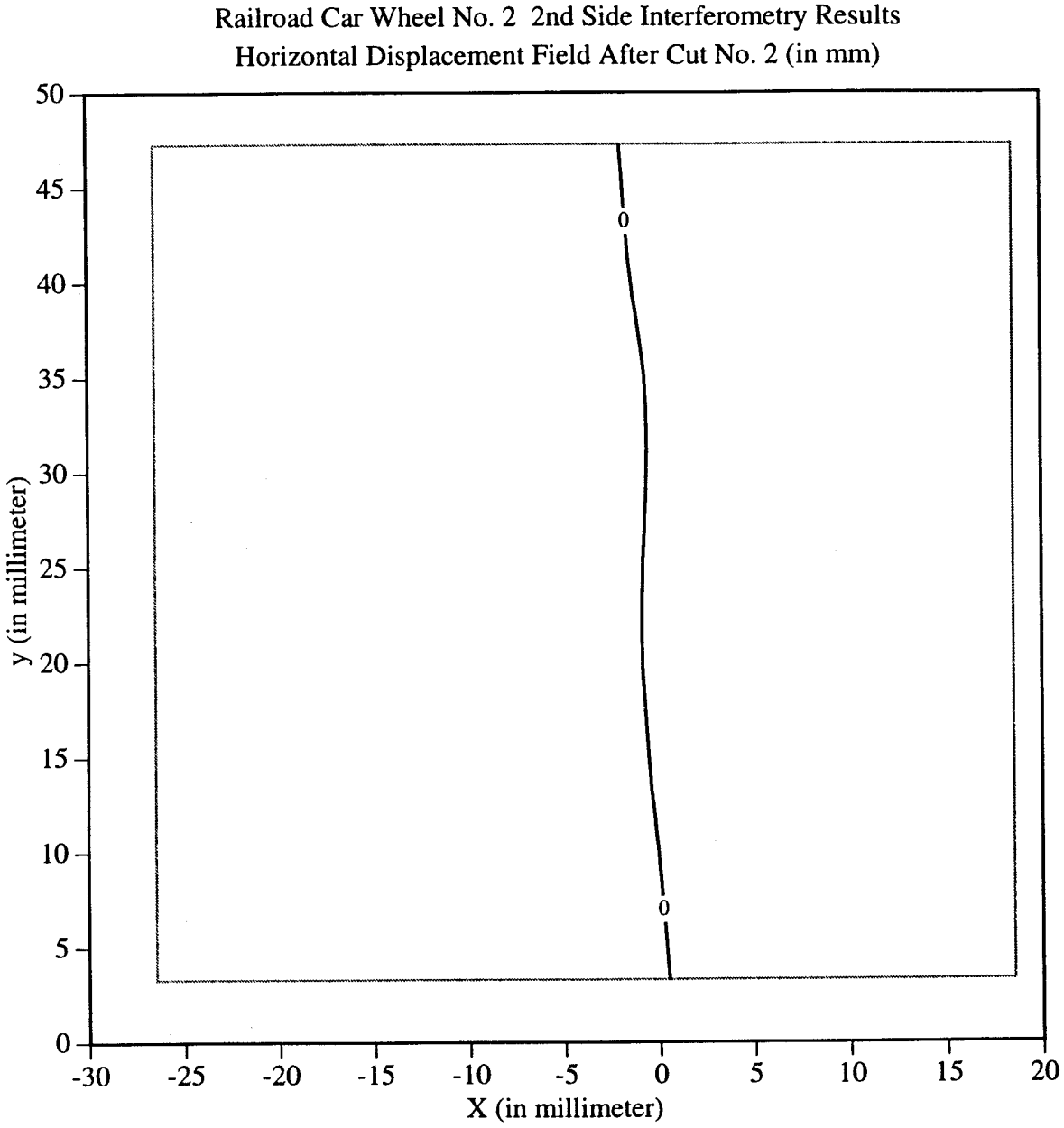
Railroad Car Wheel No. 2 2nd Side Interferometry Results
Horizontal Displacement Field After Cut No. 2 (in mm)
50
45
40
35
30
25
20
15
10
5
0
y (in millimeter)
0
0
-30
-25
-20
-15
-10
-5
0
5
10
15
20
X (in millimeter)

Railroad Car Wheel No. 2 2nd Side Interferometry Results
Vertical Displacement Field After Cut No. 2 (in mm)

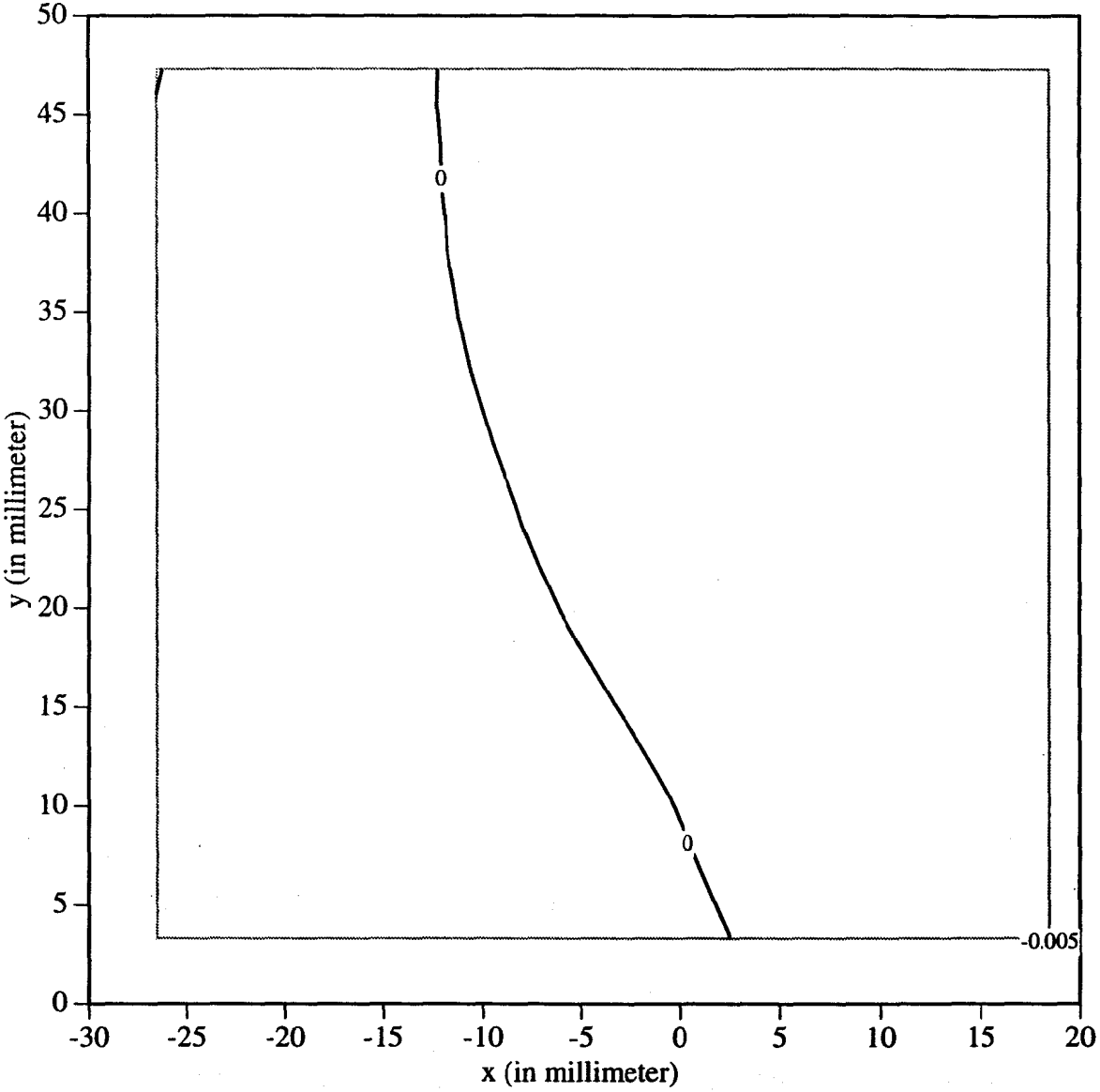

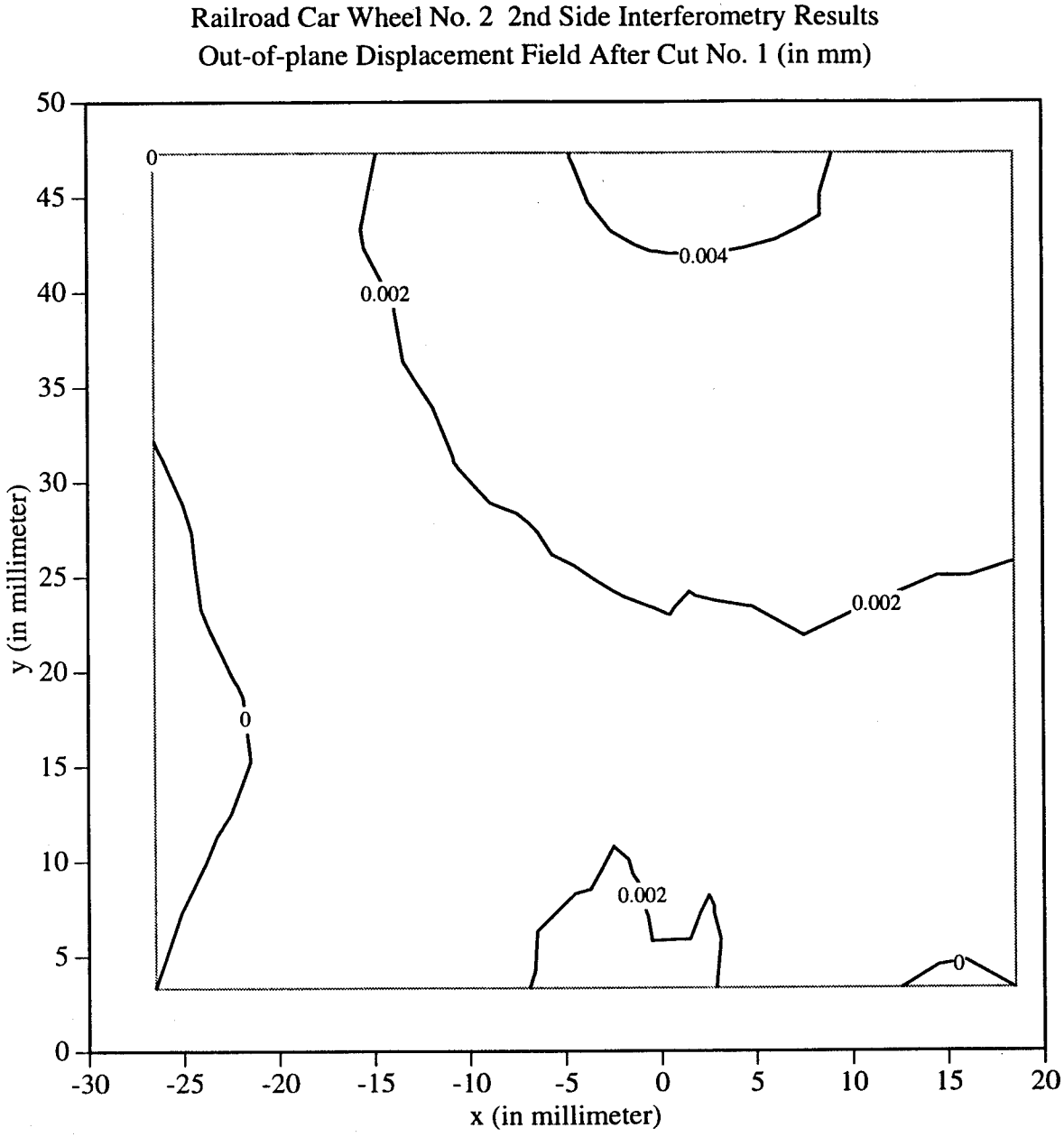
Railroad Car Wheel No. 2 2nd Side Interferometry Results
Out-of-plane Displacement Field After Cut No. 1 (in mm)
0
0.004
0.002
0.002
0
0.002
0
y (in millimeter)
x (in millimeter)
50
45
40
35
30
25
20
15
10
5
0
-30
-25
-20
-15
-10
-5
0
5
10
15
20

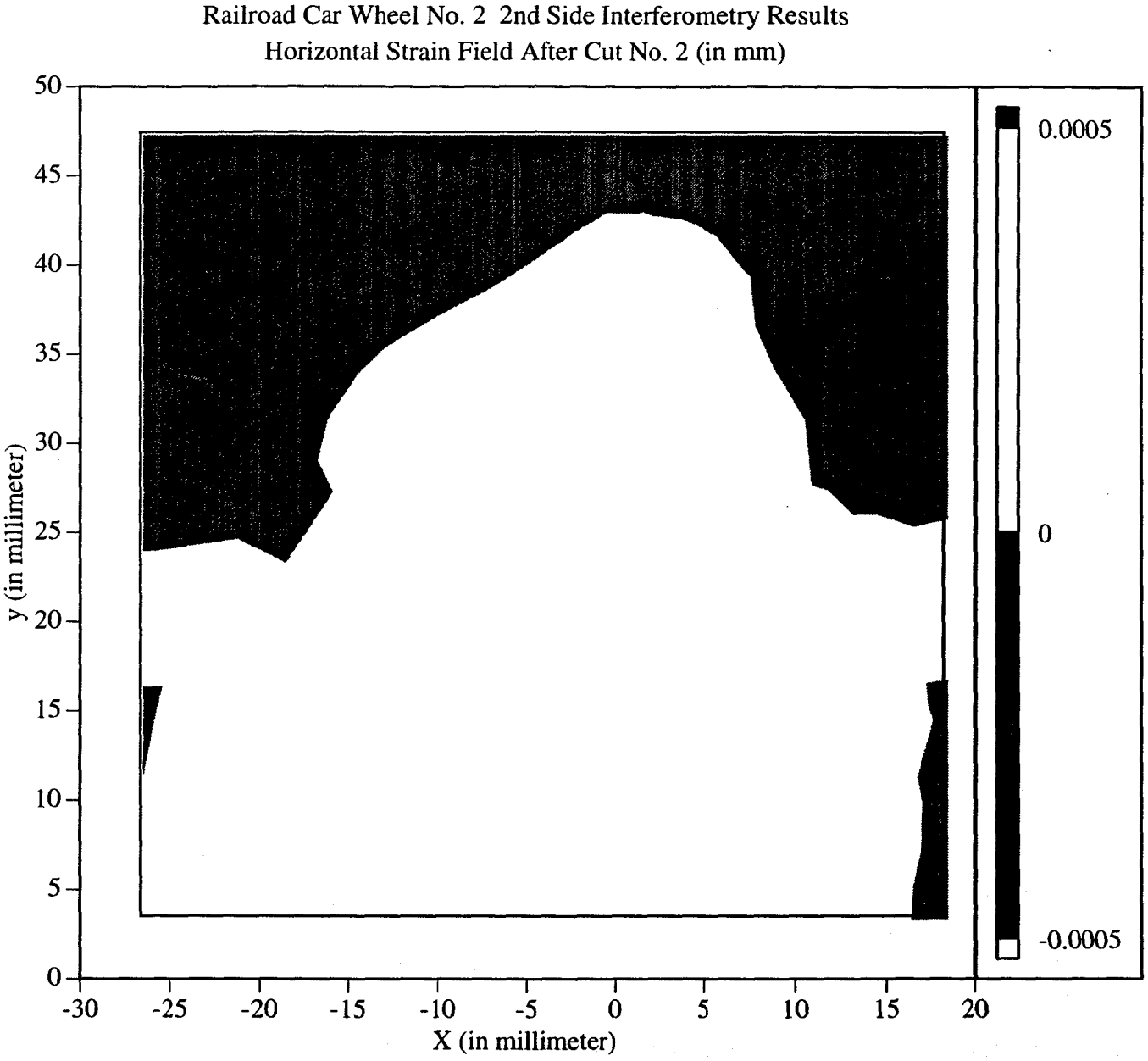
Railroad Car Wheel No. 2 2nd Side Interferometry Results
Horizontal Strain Field After Cut No. 2 (in mm)
y (in millimeter)
X (in millimeter)
50
45
40
35
30
25
20
15
10
5
0
-30
-25
-20
-15
-10
-5
0
5
10
15
20
0.0005
0
-0.0005

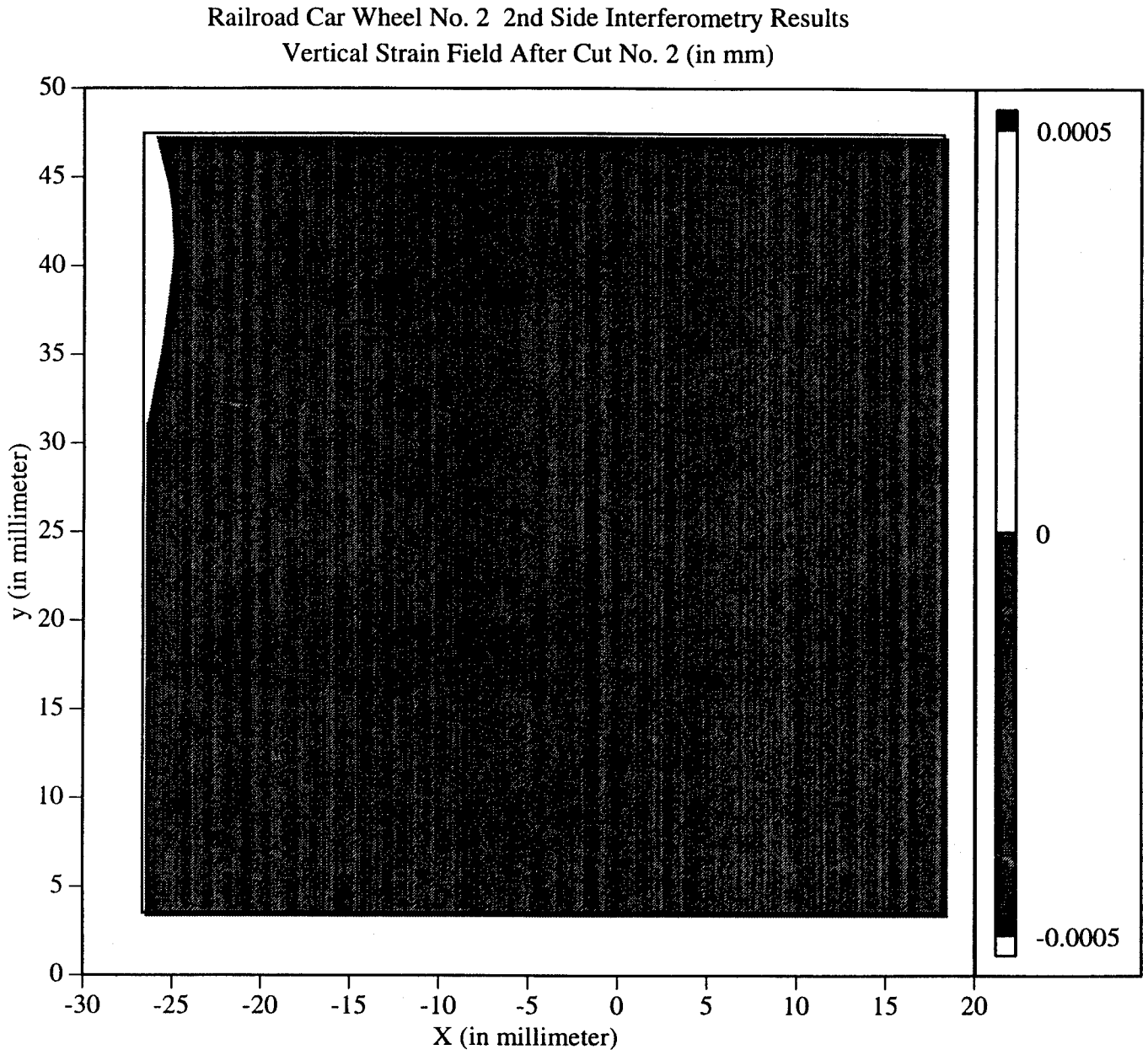
Railroad Car Wheel No. 2 2nd Side Interferometry Results
Vertical Strain Field After Cut No. 2 (in mm)
y (in millimeter)
X (in millimeter)
50
45
40
35
30
25
20
15
10
5
0
-30
-25
-20
-15
-10
-5
0
5
10
15
20
0.0005
0
-0.0005

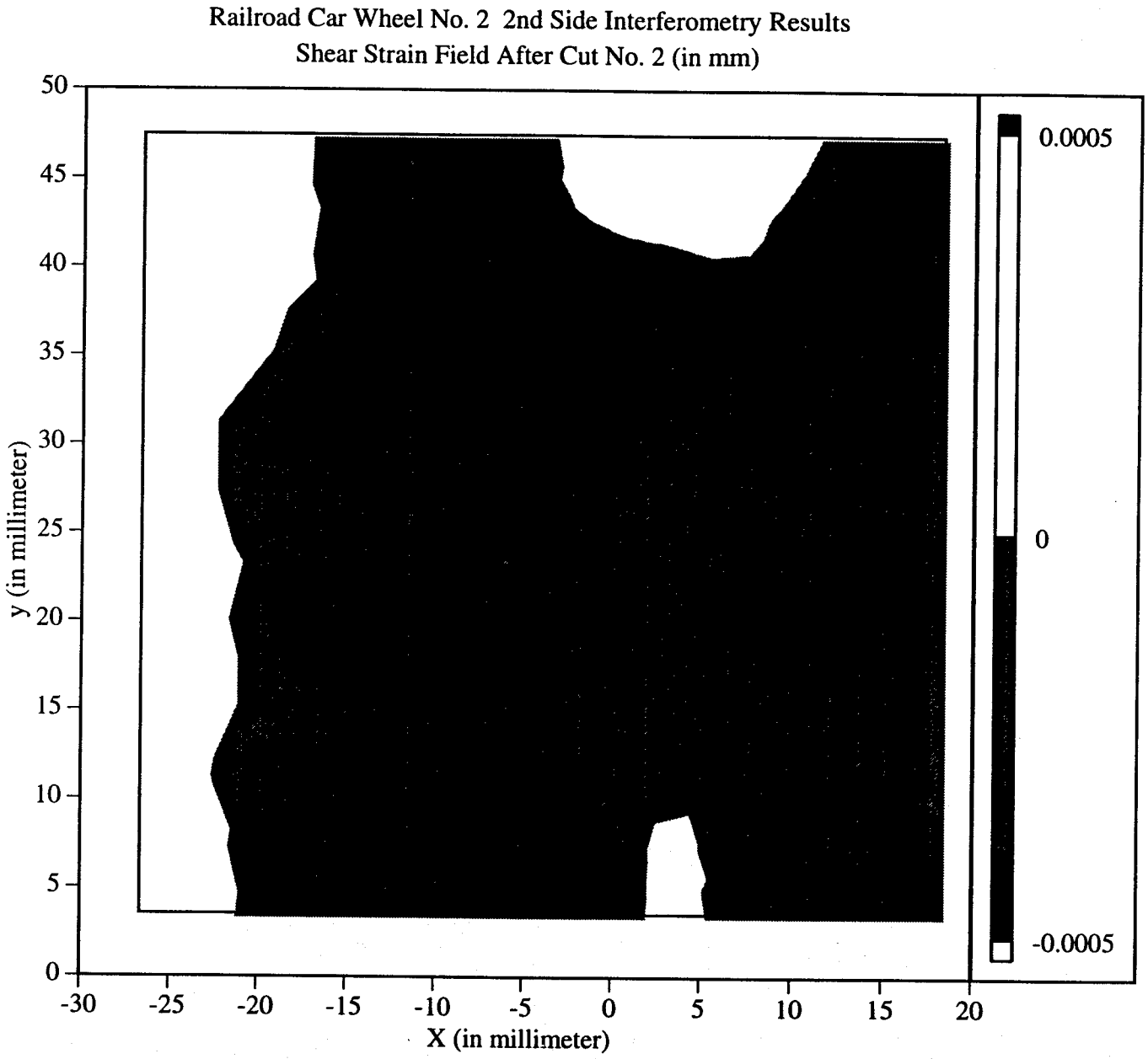
Railroad Car Wheel No. 2 2nd Side Interferometry Results
Shear Strain Field After Cut No. 2 (in mm)
y (in millimeter)
X (in millimeter)
50
45
40
35
30
25
20
15
10
5
0
-30
-25
-20
-15
-10
-5
0
5
10
15
20
0.0005
0
-0.0005

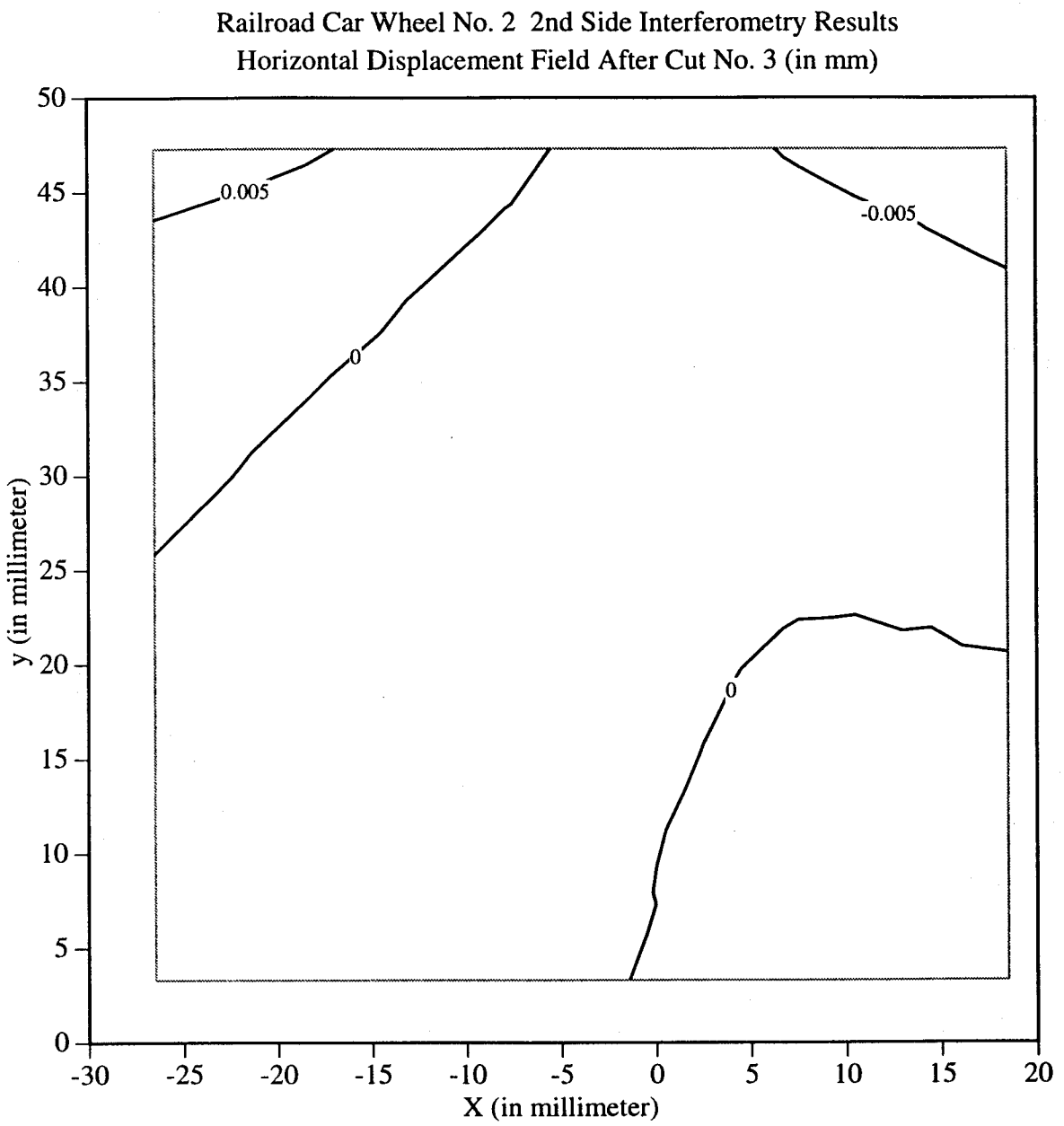
Railroad Car Wheel No. 2 2nd Side Interferometry Results
Horizontal Displacement Field After Cut No. 3 (in mm)
0.005
-0.005
0
0
y (in millimeter)
X (in millimeter)
50
45
40
35
30
25
20
15
10
5
0
-30
-25
-20
-15
-10
-5
0
5
10
15
20

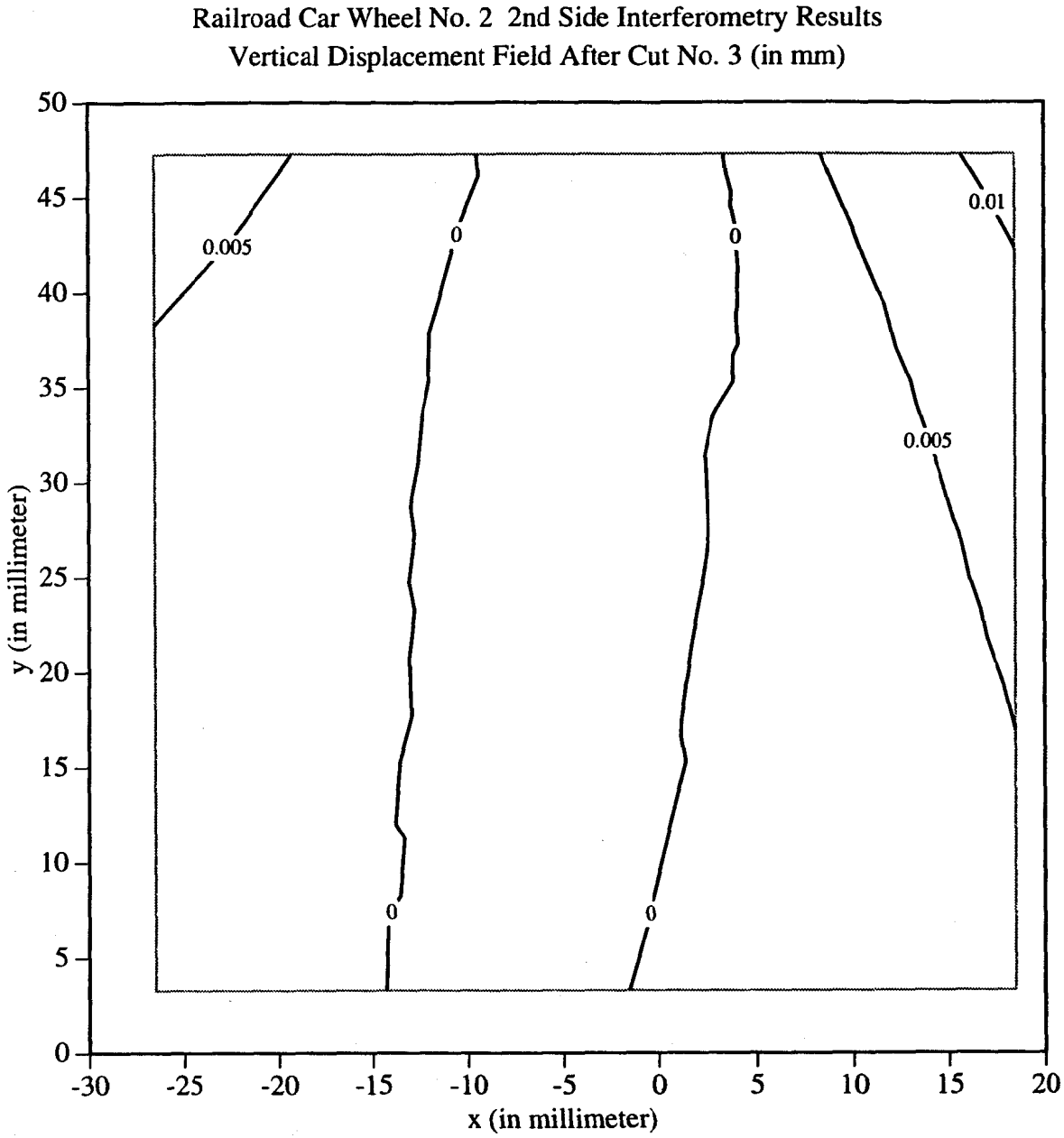
Railroad Car Wheel No. 2 2nd Side Interferometry Results
Vertical Displacement Field After Cut No. 3 (in mm)
y (in millimeter)
x (in millimeter)
0.005
0
0
0.01
0.005
0
0
50
45
40
35
30
25
20
15
10
5
0
-30
-25
-20
-15
-10
-5
0
5
10
15
20

Railroad Car Wheel No. 2 2nd Side Interferometry Results
Out-of-plane Displacement Field After Cut No. 3 (in mm)

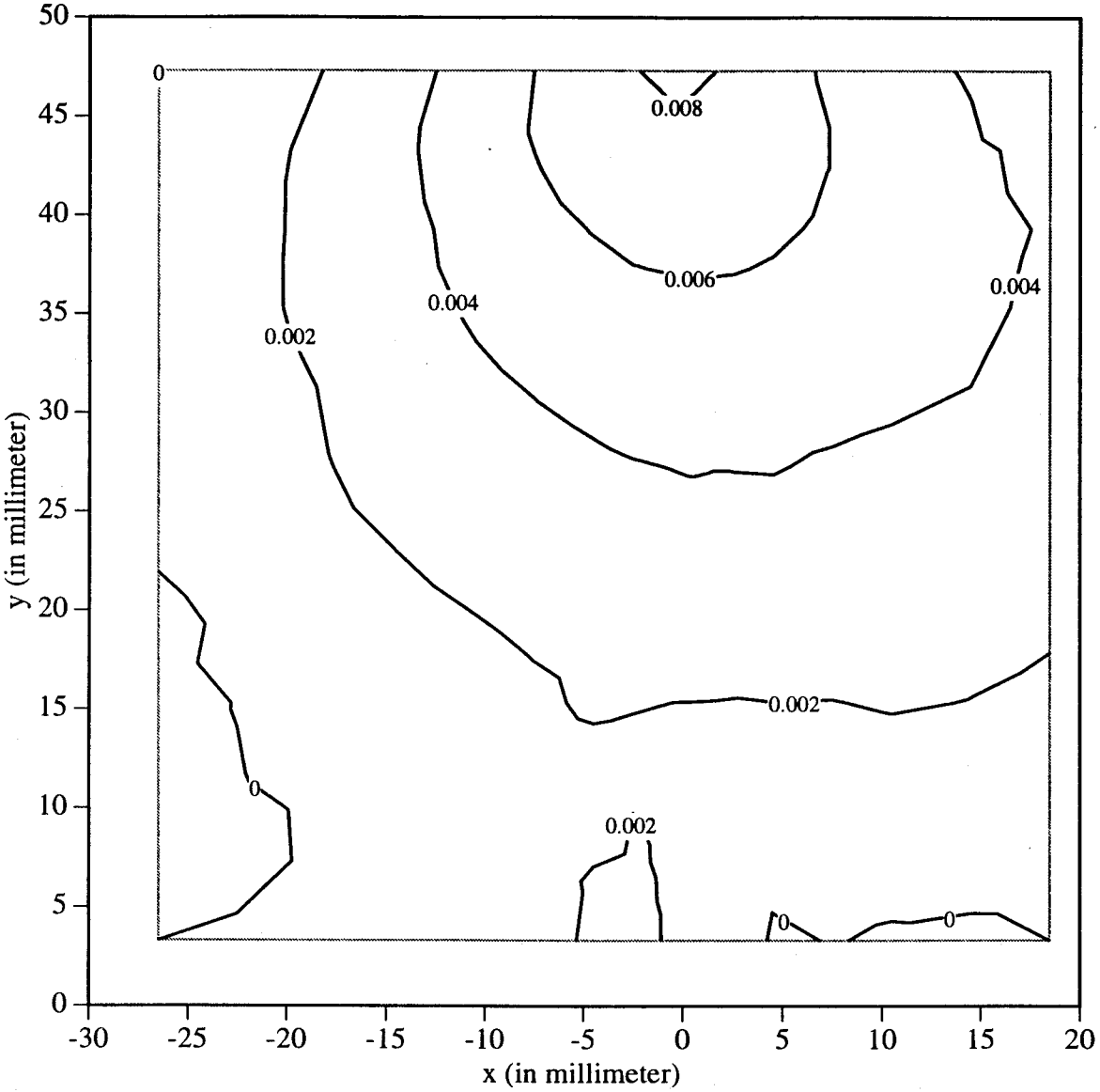

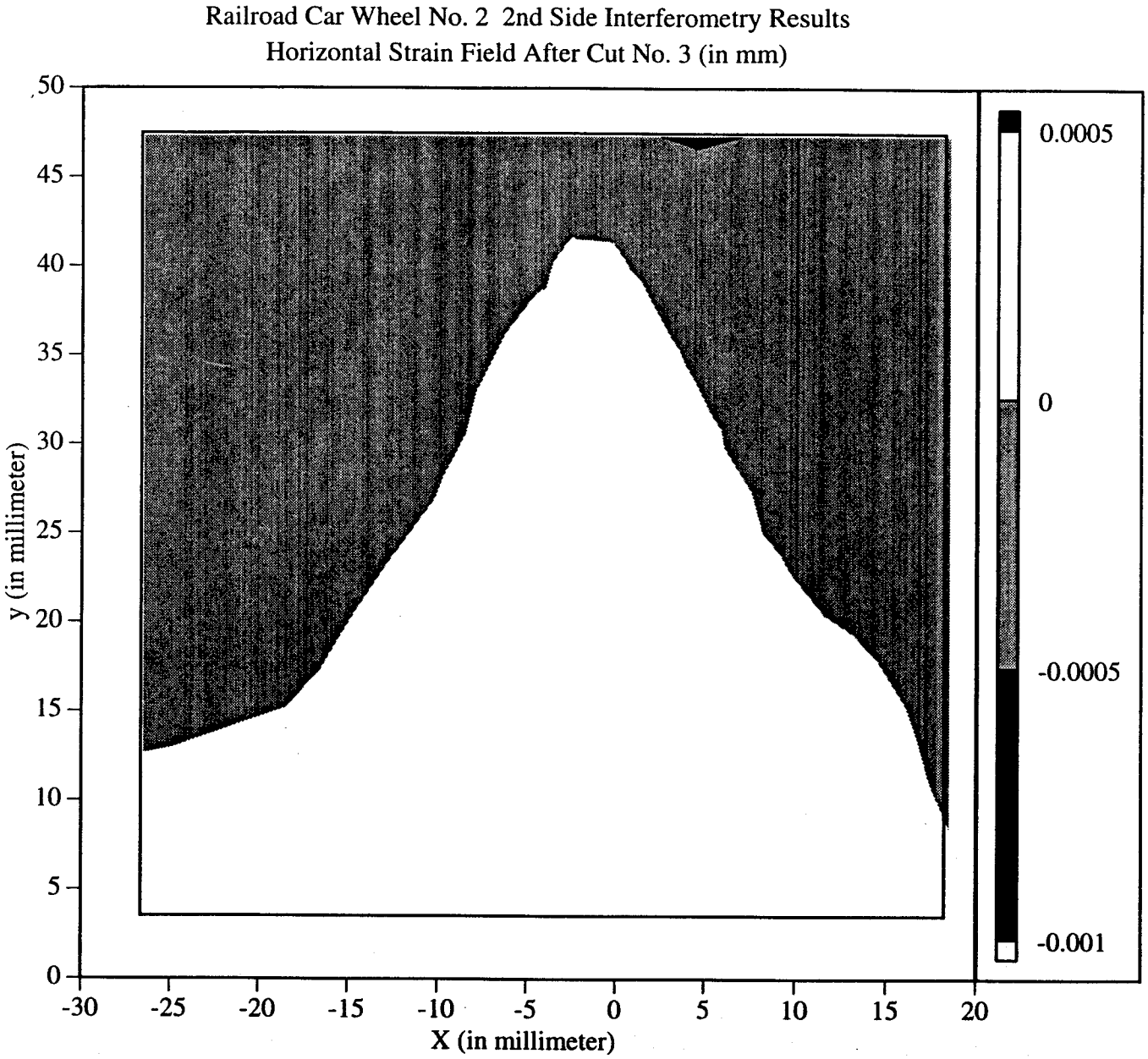
Railroad Car Wheel No. 2 2nd Side Interferometry Results
Horizontal Strain Field After Cut No. 3 (in mm)
y (in millimeter)
X (in millimeter)
0.0005
0
-0.0005
-0.001
50
45
40
35
30
25
20
15
10
5
0
-30
-25
-20
-15
-10
-5
0
5
10
15
20

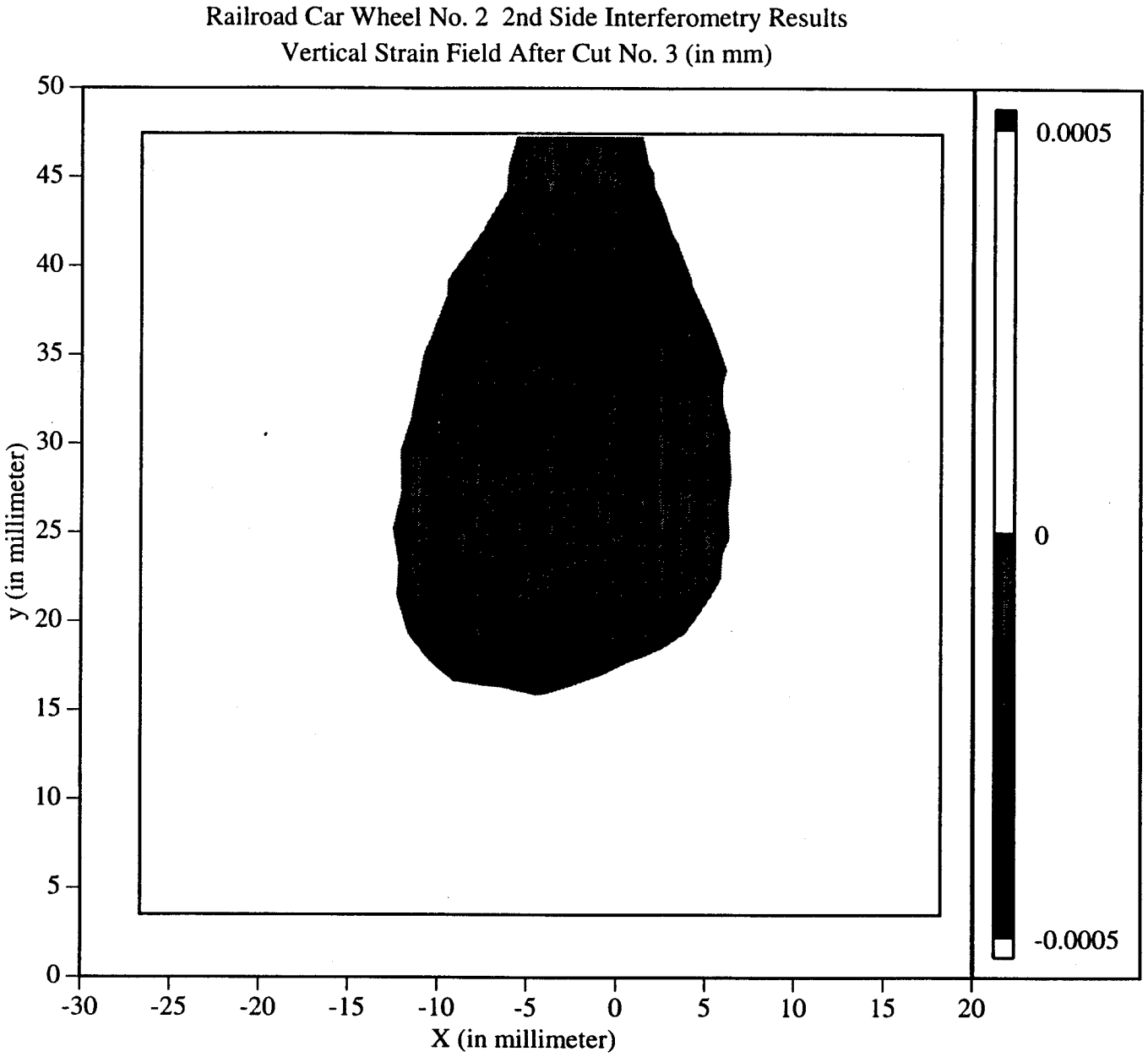
Railroad Car Wheel No. 2 2nd Side Interferometry Results
Vertical Strain Field After Cut No. 3 (in mm)
y (in millimeter)
50
45
40
35
30
25
20
15
10
5
0
-30
-25
-20
-15
-10
-5
0
5
10
15
20
X (in millimeter)
0.0005
0
-0.0005

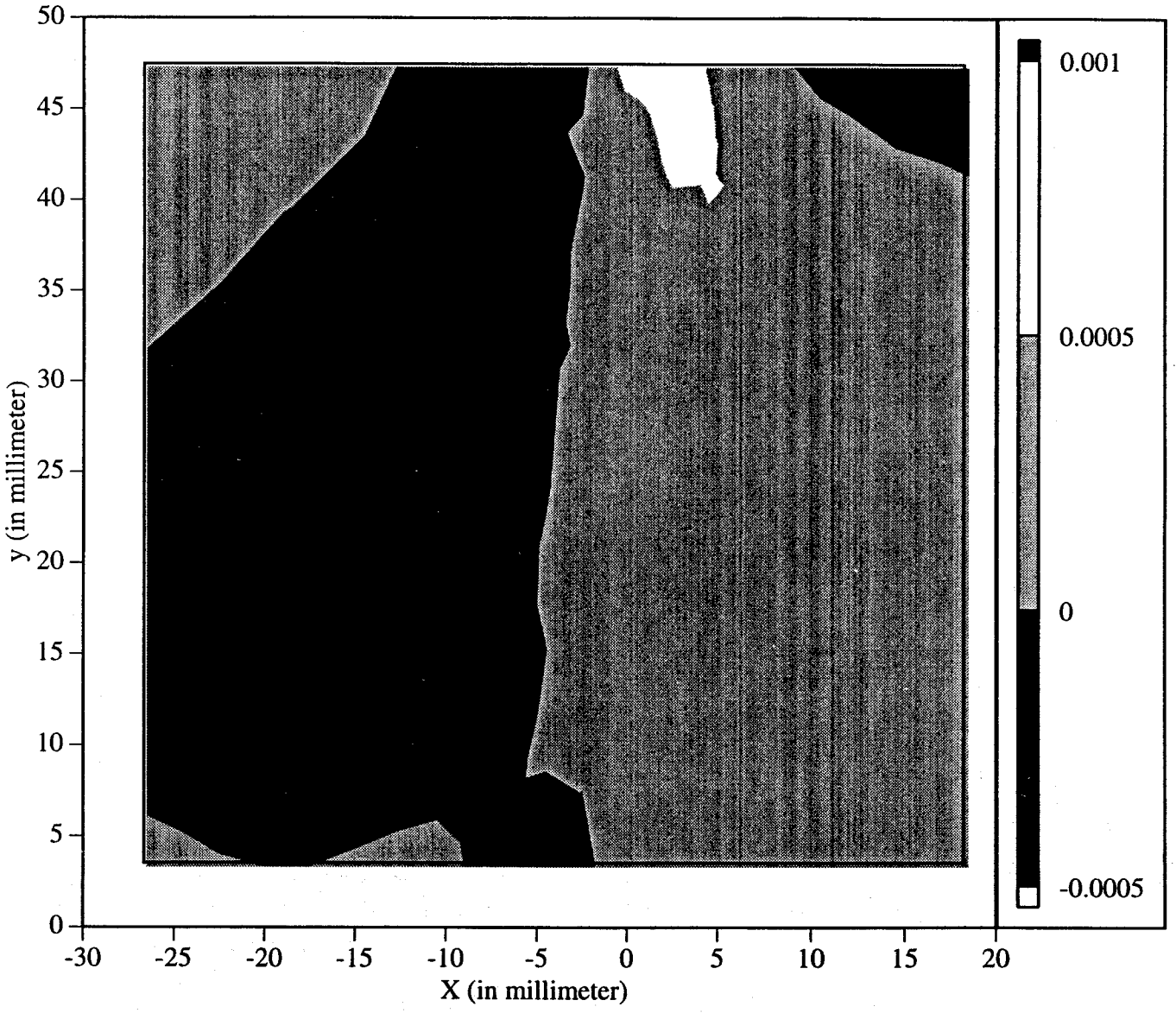
Railroad Car Wheel No. 2 2nd Side Interferometry Results
Shear Strain Field After Cut No. 3 (in mm)
y (in millimeter)
X (in millimeter)
50
45
40
35
30
25
20
15
10
5
0
-30
-25
-20
-15
-10
-5
0
5
10
15
20
0.001
0.0005
0
-0.0005

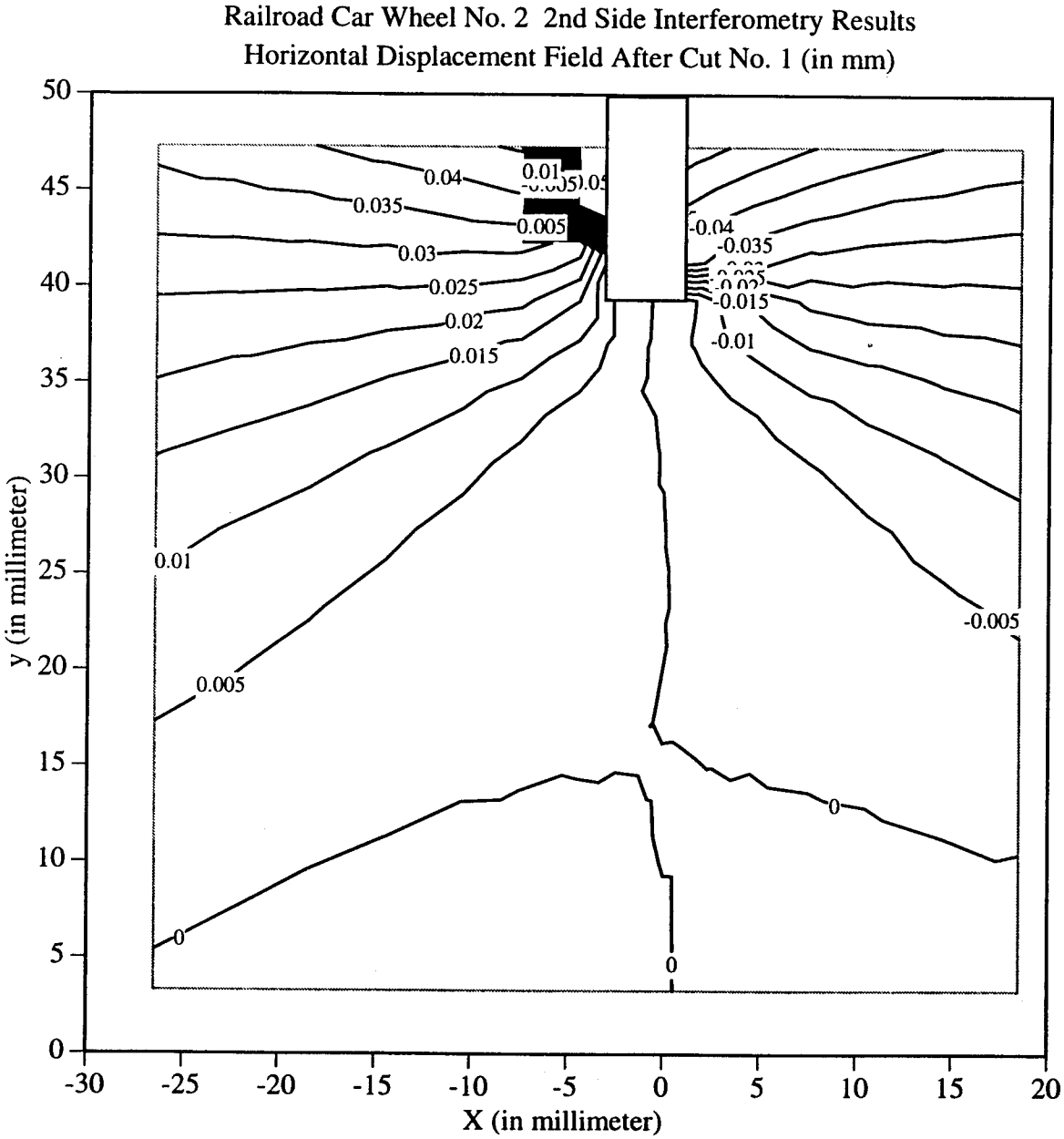
Railroad Car Wheel No. 2 2nd Side Interferometry Results
Horizontal Displacement Field After Cut No. 1 (in mm)
y (in millimeter)
X (in millimeter)
50
45
40
35
30
25
20
15
10
5
0
-30
-25
-20
-15
-10
-5
0
5
10
15
20
0.04
0.035
0.03
0.025
0.02
0.015
0.01
0.005
0
-0.04
-0.035
-0.015
-0.01
-0.005

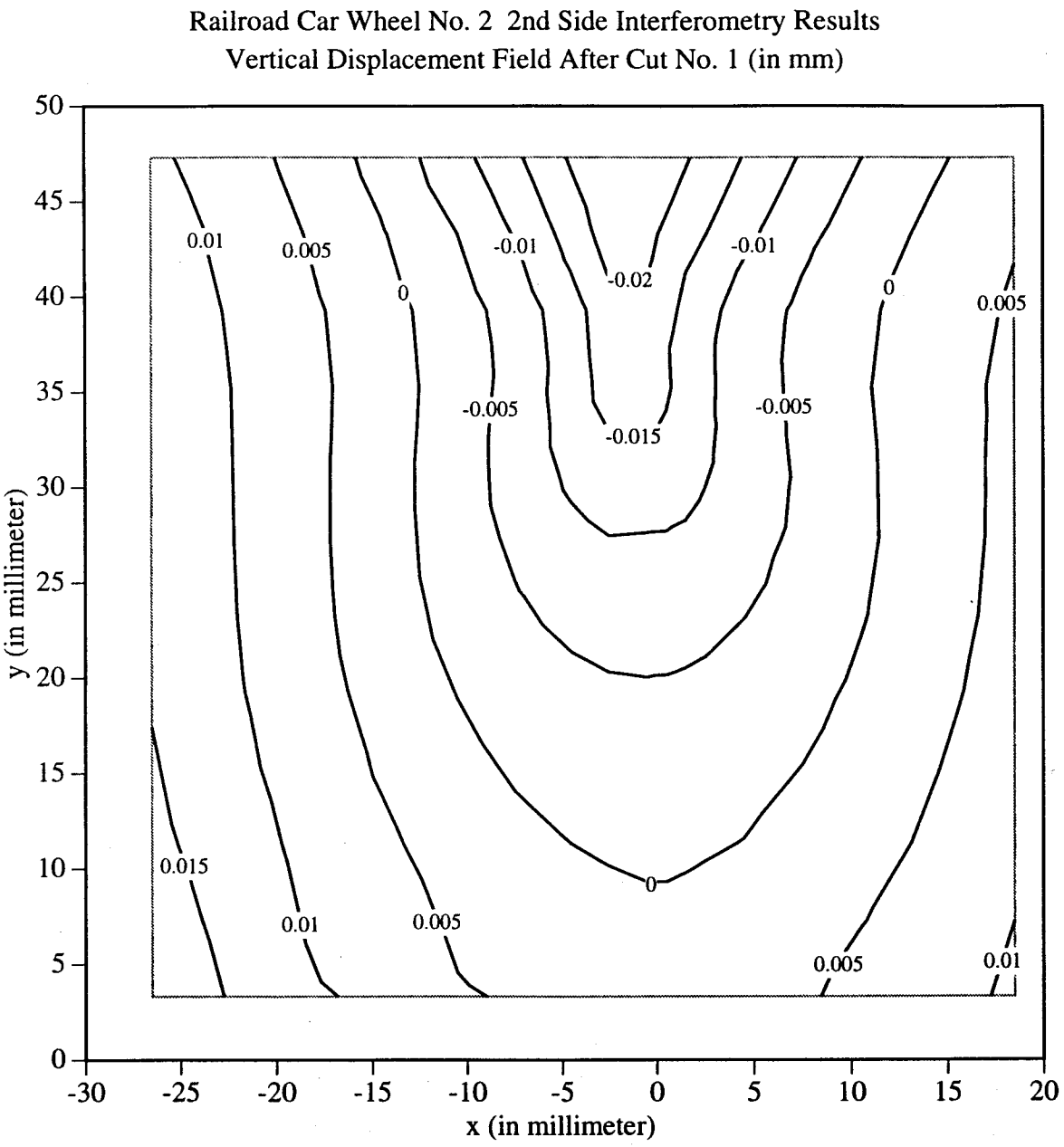
Railroad Car Wheel No. 2 2nd Side Interferometry Results
Vertical Displacement Field After Cut No. 1 (in mm)
y (in millimeter)
x (in millimeter)
50
45
40
35
30
25
20
15
10
5
0
-30
-25
-20
-15
-10
-5
0
5
10
15
20
0.01
0.005
0
-0.01
-0.02
-0.01
0
0.005
-0.005
-0.015
-0.005
0.015
0.01
0.005
0
0.005
0.01

Railroad Car Wheel No. 2 2nd Side Interferometry Results
Out-of-plane Displacement Field After Cut No. 3 (in mm)

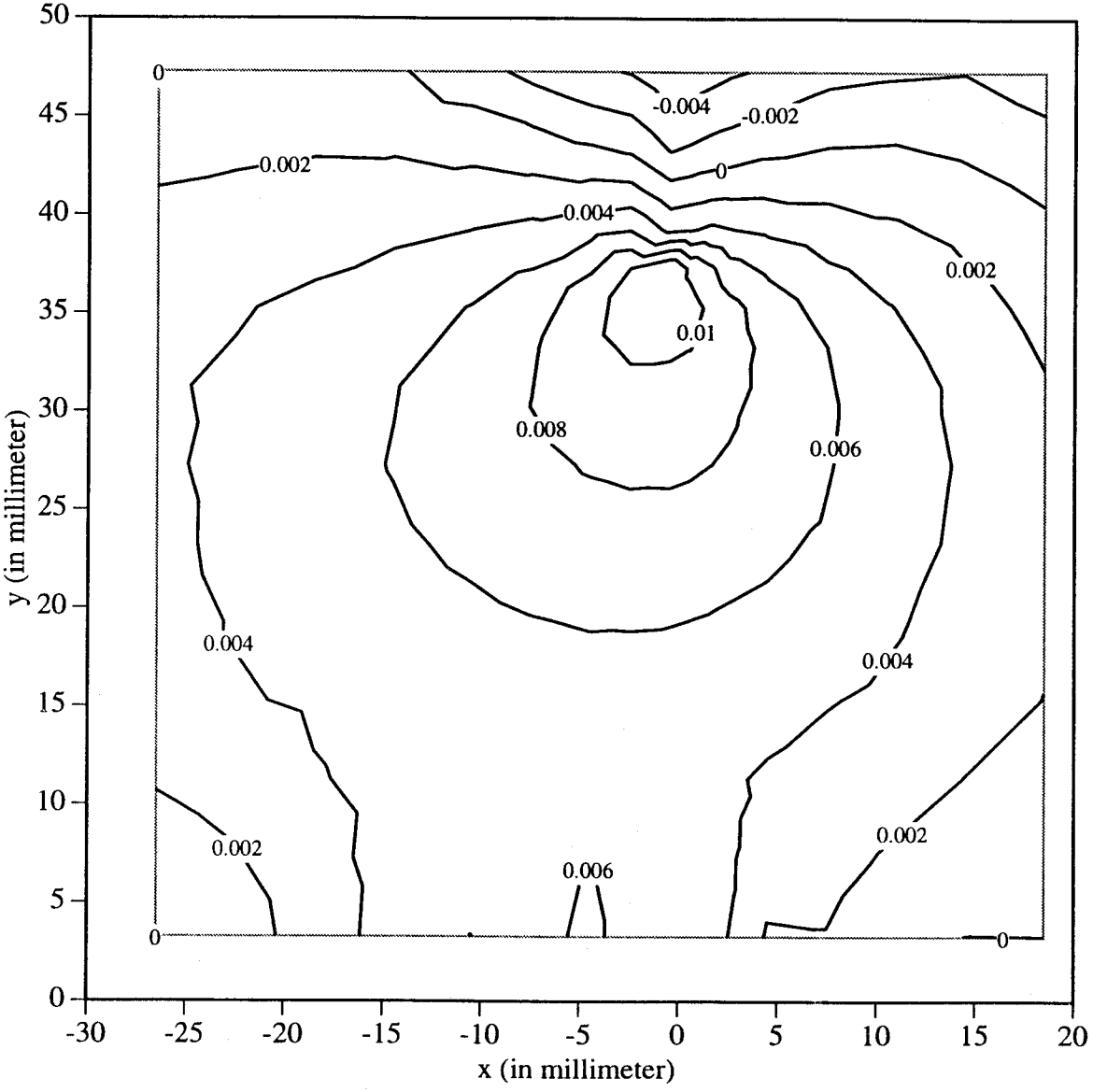

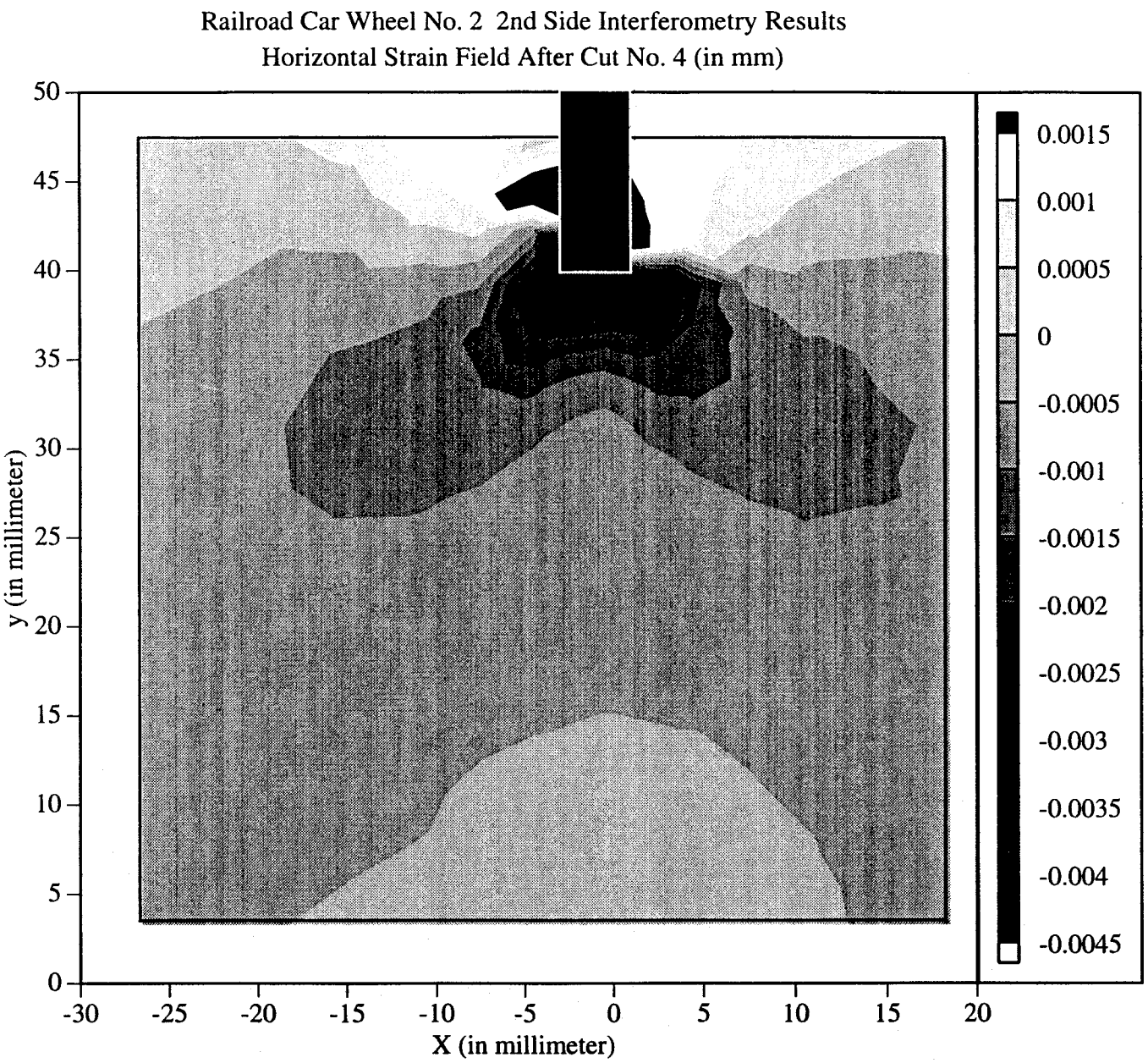
Railroad Car Wheel No. 2 2nd Side Interferometry Results
Horizontal Strain Field After Cut No. 4 (in mm)
y (in millimeter)
X (in millimeter)
50
45
40
35
30
25
20
15
10
5
0
-30
-25
-20
-15
-10
-5
0
5
10
15
20
0.0015
0.001
0.0005
0
-0.0005
-0.001
-0.0015
-0.002
-0.0025
-0.003
-0.0035
-0.004
-0.0045

Railroad Car Wheel No. 2 2nd Side Interferometry Results
Vertical Strain Field After Cut No. 4 (in mm)

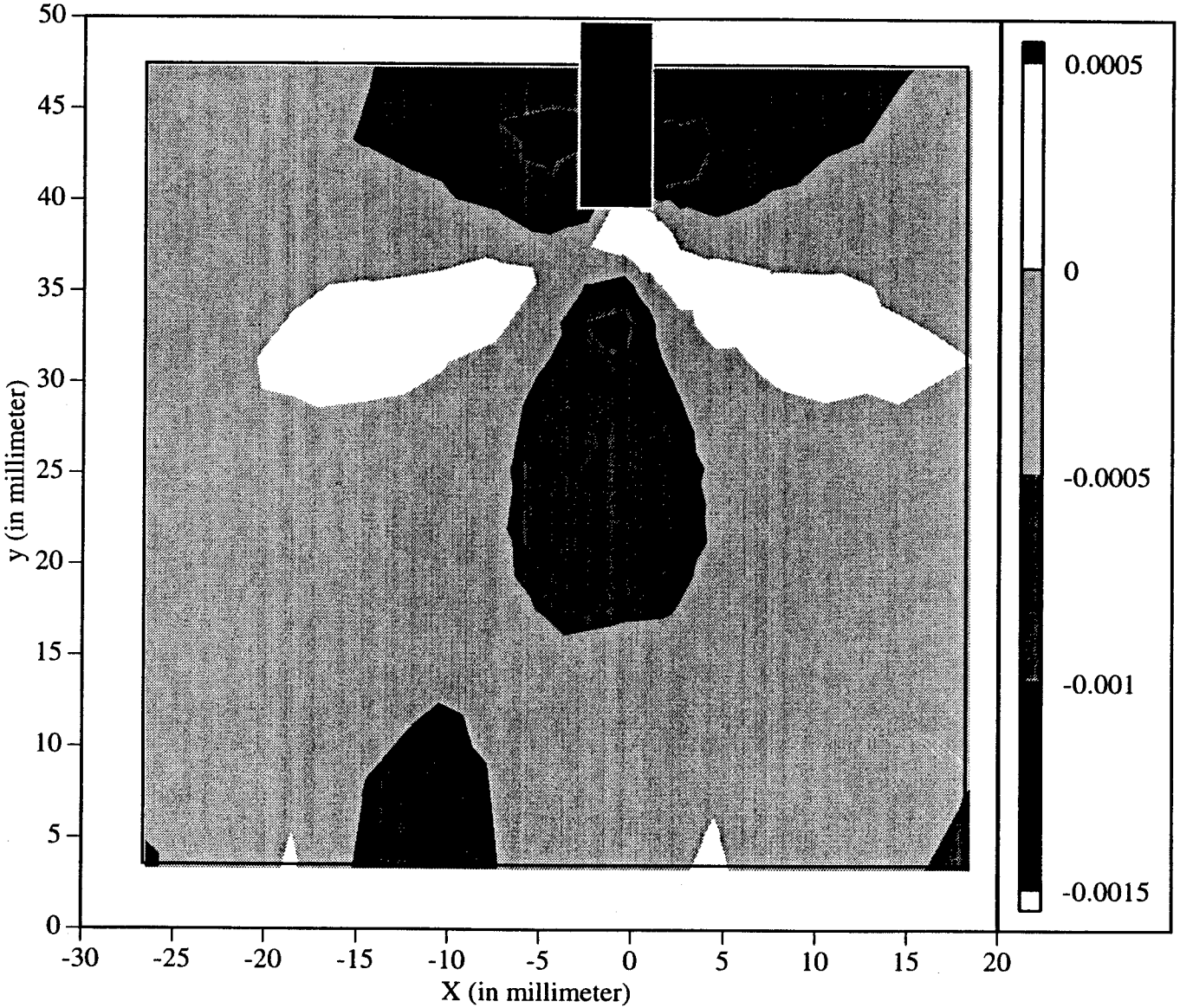

Railroad Car Wheel No. 2 2nd Side Interferometry Results
Shear Strain Field After Cut No. 4 (in mm)

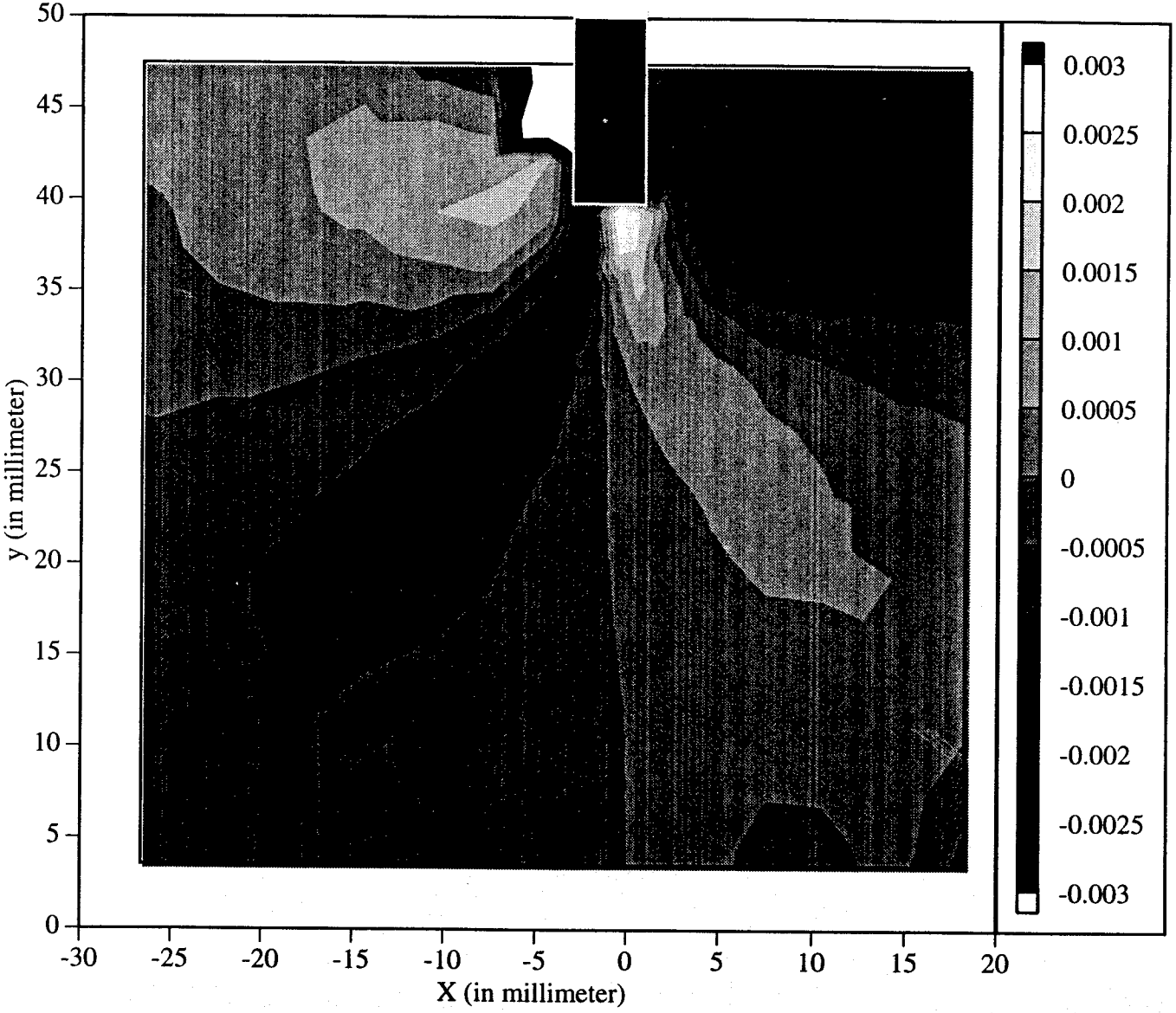

Railroad Car Wheel No. 2 2nd Side Interferometry Results
Horizontal Displacement Field After Cut No. 5 (in mm)

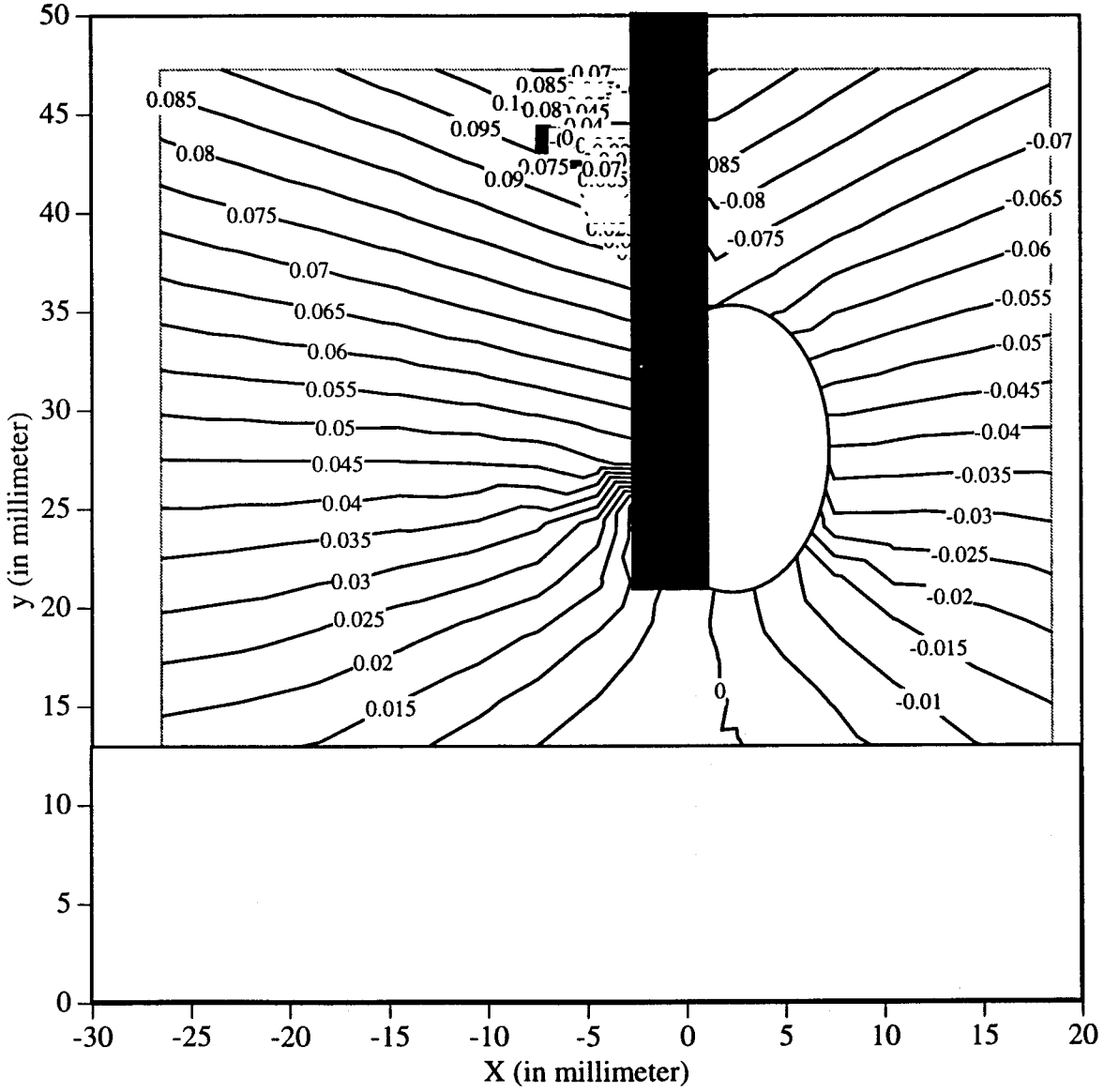

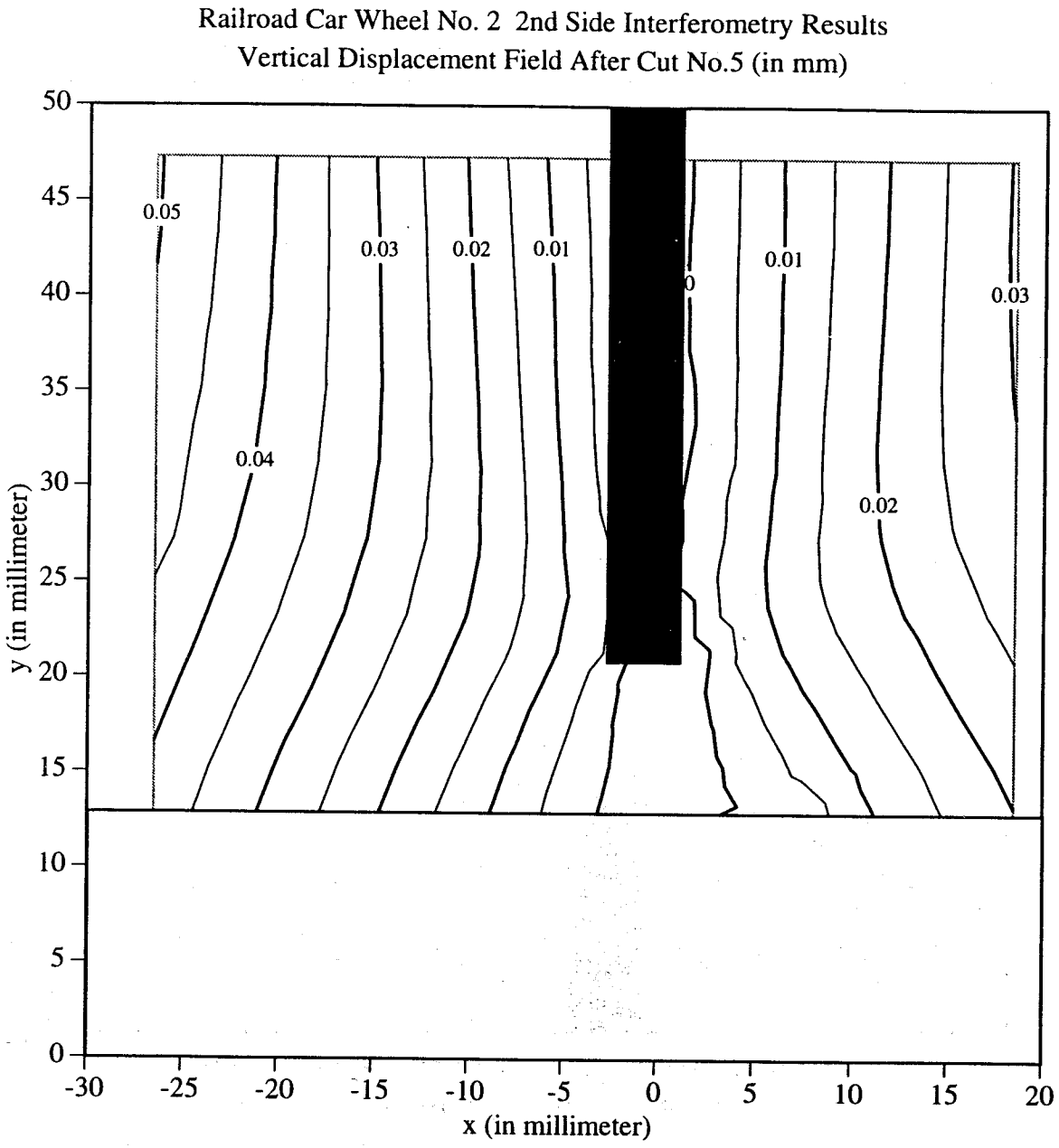
Railroad Car Wheel No. 2 2nd Side Interferometry Results
Vertical Displacement Field After Cut No.5 (in mm)
0.05
0.04
0.03
0.02
0.01
0
0.01
0.02
0.03
y (in millimeter)
x (in millimeter)
50
45
40
35
30
25
20
15
10
5
0
-30
-25
-20
-15
-10
-5
0
5
10
15
20

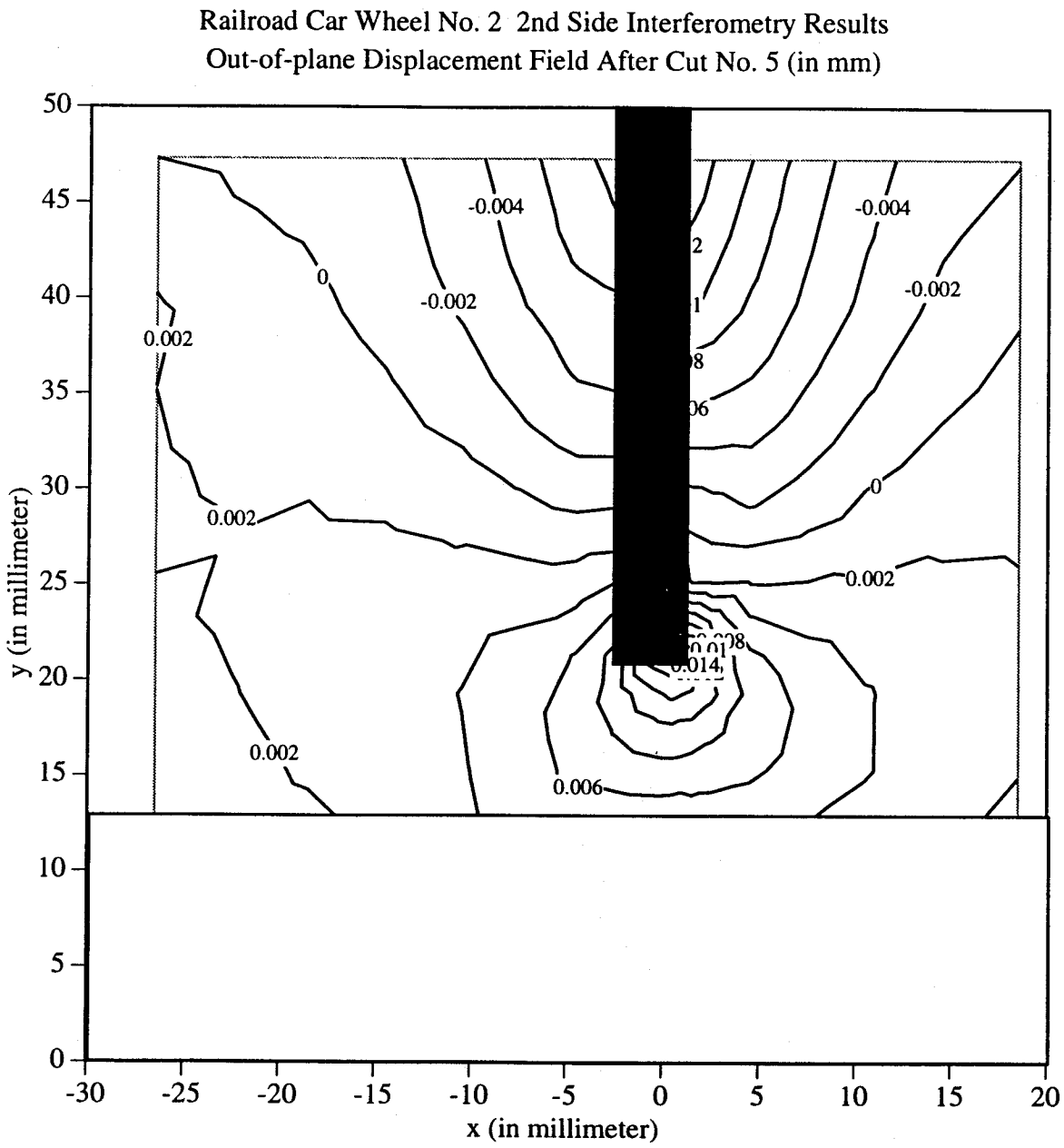
Railroad Car Wheel No. 2 2nd Side Interferometry Results
Out-of-plane Displacement Field After Cut No. 5 (in mm)
y (in millimeter)
x (in millimeter)
50
45
40
35
30
25
20
15
10
5
0
-30
-25
-20
-15
-10
-5
0
5
10
15
20
-0.004
-0.004
-0.002
-0.002
0
0
0.002
0.002
0.002
0.002
0.002
0.006

Railroad Car Wheel No. 2 2nd Side Interferometry Results
Horizontal Strain Field After Cut No. 5 (in mm)

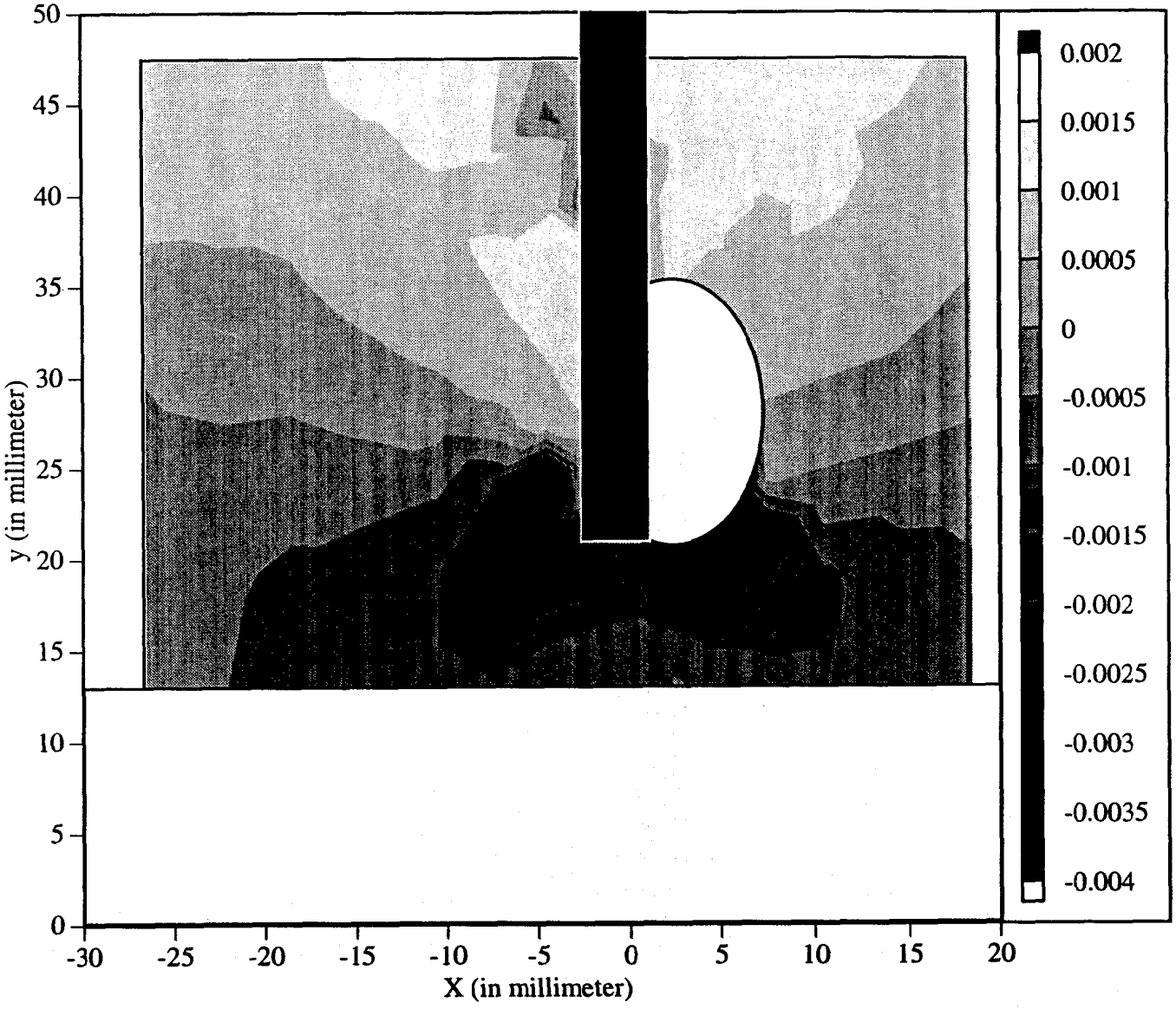

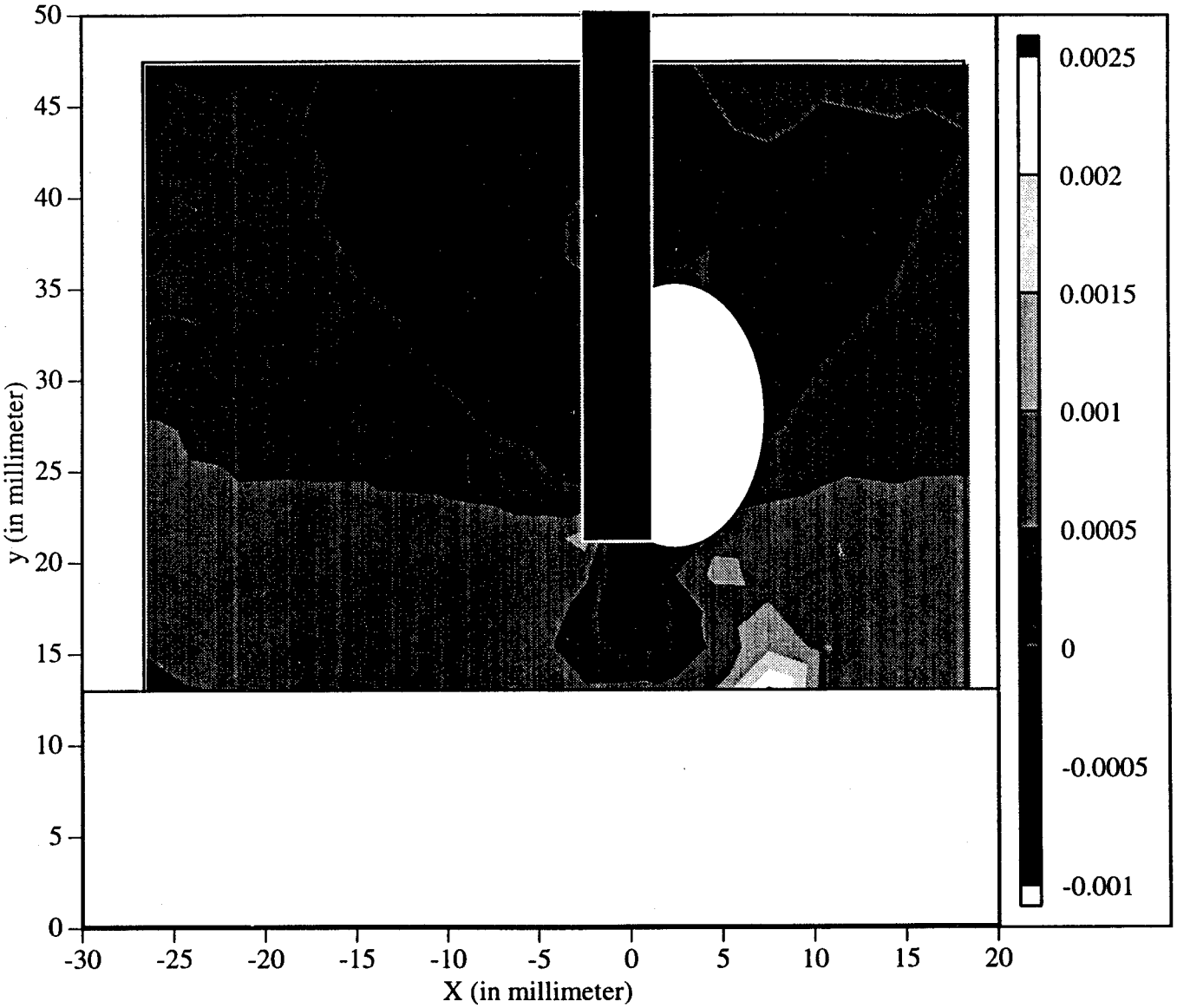
Railroad Car Wheel No. 2 2nd Side Interferometry Results
Vertical Strain Field After Cut No. 5 (in mm)
y (in millimeter)
X (in millimeter)
50
45
40
35
30
25
20
15
10
5
0
-30
-25
-20
-15
-10
-5
0
5
10
15
20
0.0025
0.002
0.0015
0.001
0.0005
0
-0.0005
-0.001

Railroad Car Wheel No. 2 2nd Side Interferometry Results
Shear Strain Field After Cut No. 5 (in mm)

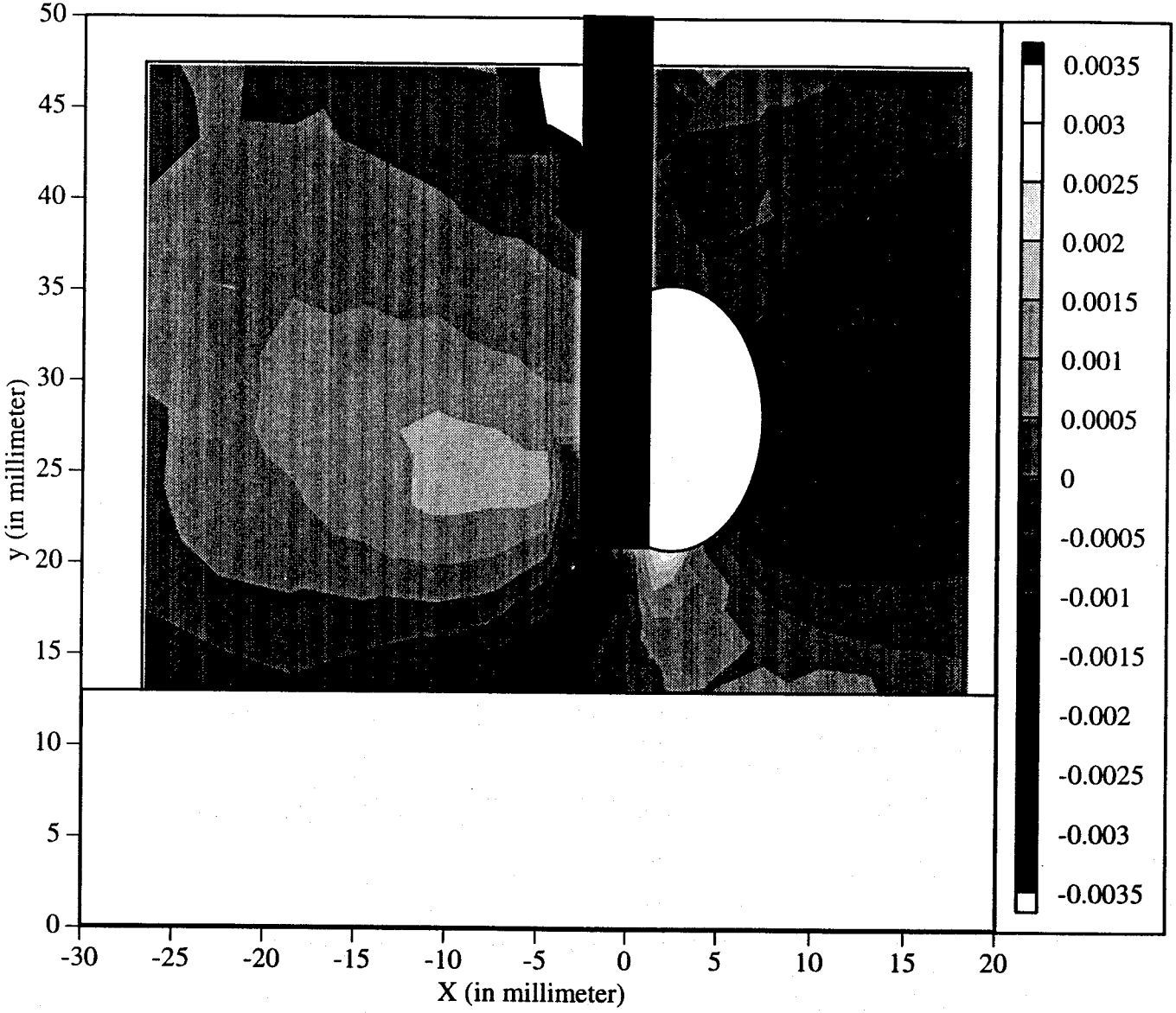

Page Intentionally Left Blank

Appendix 3. Wheel #3 Experimental Results

This appendix contains the results from the test on both sides (front and back rim faces) of the third wheel. All the data are in a local coordinate system that is located at the intersection of the inner edge of the rim and the cutting line; the vertical axis points away from the center of the wheel.

The attached figures show the location of all the sensors. At two points on the wheel, thermocouples (TC) measure the temperature difference (which never exceeded 6°C) immediately after each cut. The temperature at TC2, the one farther from the cut, was equal to the ambient temperature. The strain measurements were taken after the difference decreased to about 1°C or less at an ambient temperature in the range of 18°C to 22°C.

The extensometer, strain gage, and displacement sensor data are provided in tabular form. The interferometric data is provided in the form of contour maps and as data files in ASCII format for three specific cutting stages. The corresponding cut depths are 35 mm, 48 mm, and 63 mm.

The wheel was identified by the following markings:

36524-46
146

Location of strain gauges, thermocouples and gratings on wheel #3

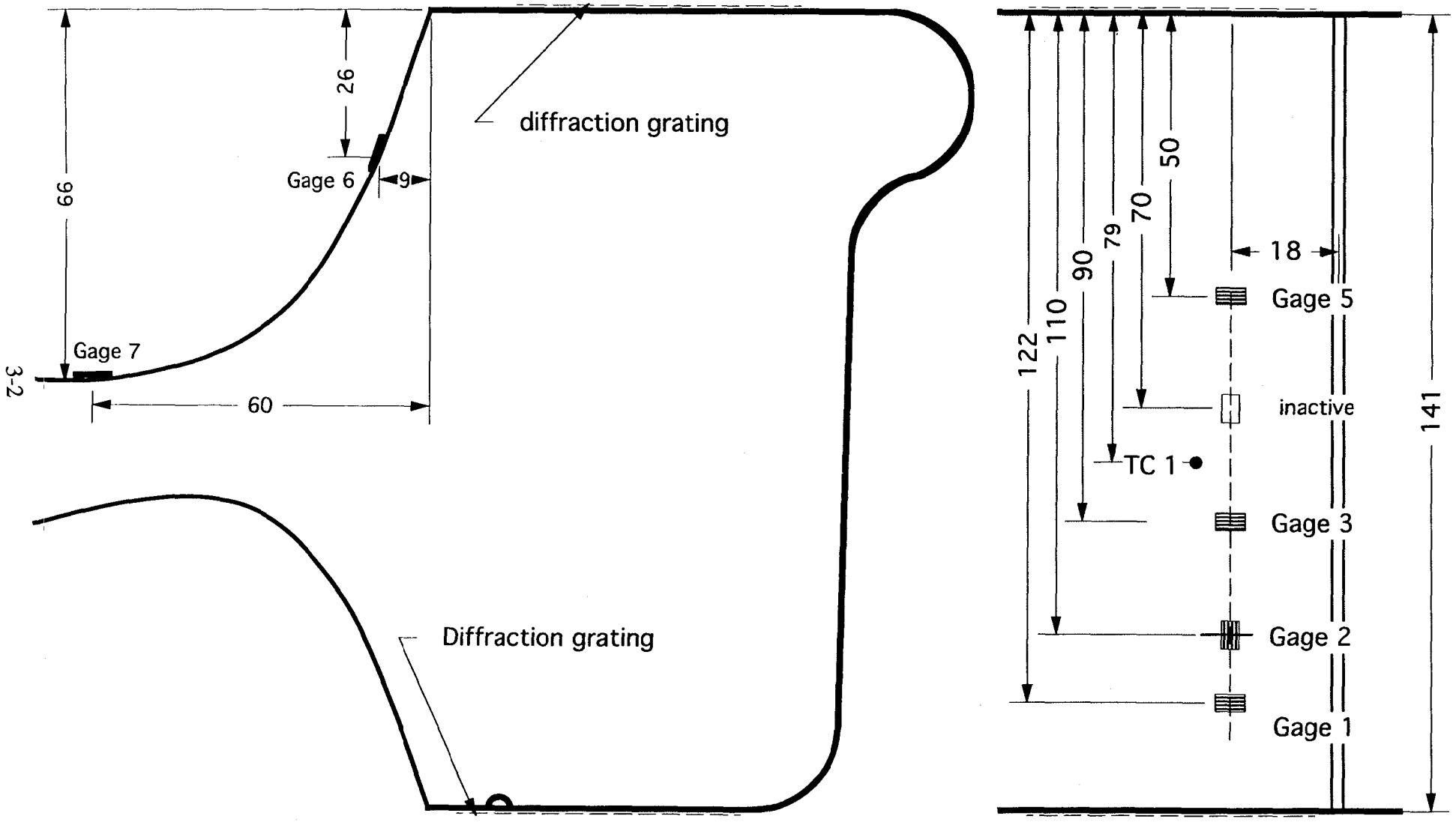

Gage 6 & 7 were located 20mm from the plane of the cut.

Location of displacement sensors thermocouples and gratings on wheel #3

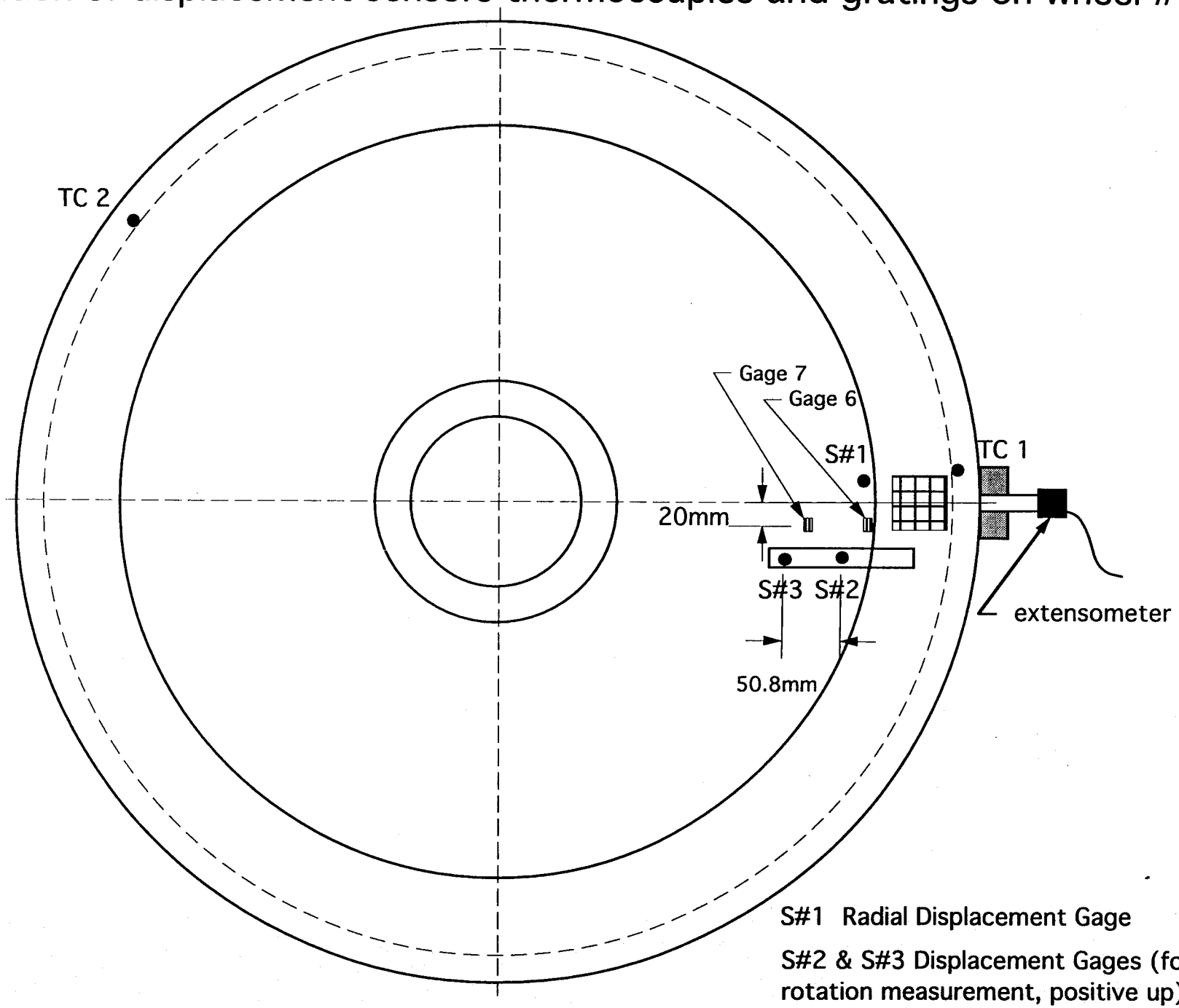

S#1 Radial Displacement Gage

S#2 & S#3 Displacement Gages (for rotation measurement, positive up)

WHEEL #3 TEST DATA

TESTING OF DOT RAILROAD CAR WHEEL #3							36524-46	146			
DATE:	December 12 1994										
	mm/mm						mm	mm	rad	(°C)	(°C)
Cut Depth (mm)	Gage1	Gage2	Gage3	Gage5	Gage6	Gage7	Radial Displacement	Opening Displacement	Rotation	TC 1	TC 2
0	0	0	0	0	0	0	.000	.000	0.00E+00	18.6	18.6
28	-15	10	-47	-110	24	16	-.017	.130	6.00E-05	18.6	23.5
35	124	13	247	409	35	30	-.033	-1.409	8.00E-05	18.6	24.6
48	852	-26	1011	1146	73	106	-.081	-1.288	1.20E-04	20.3	23.5
55	1016	-62	1130	1225	73	166	-.119	-1.205	4.00E-05	20.0	22.3
63	1056	-91	1160	1236	44	221	-.158	-1.129	-2.00E-05	20.0	22.9
70	1057	-118	1162	1236	-41	276	-.201	-1.054	-1.60E-04	21.5	22.9
80	1044	-148	1162	1225	-278	341	-.261	-.941	-2.80E-04	21.6	23.4
90	1033	-172	1161	1223	-666	378	-.320	-.833	-3.20E-04	21.5	23.6
100	1022	-200	1164	1221	-917	411	-.393	-.709	-3.00E-04	21.6	24.0
110	1022	-200	1164	1221	-917	411	-.489	-.612	-9.50E-04	21.6	24.4
END											

Railroad Wheel No. 3 Test
Displacement vs. Cut Depth

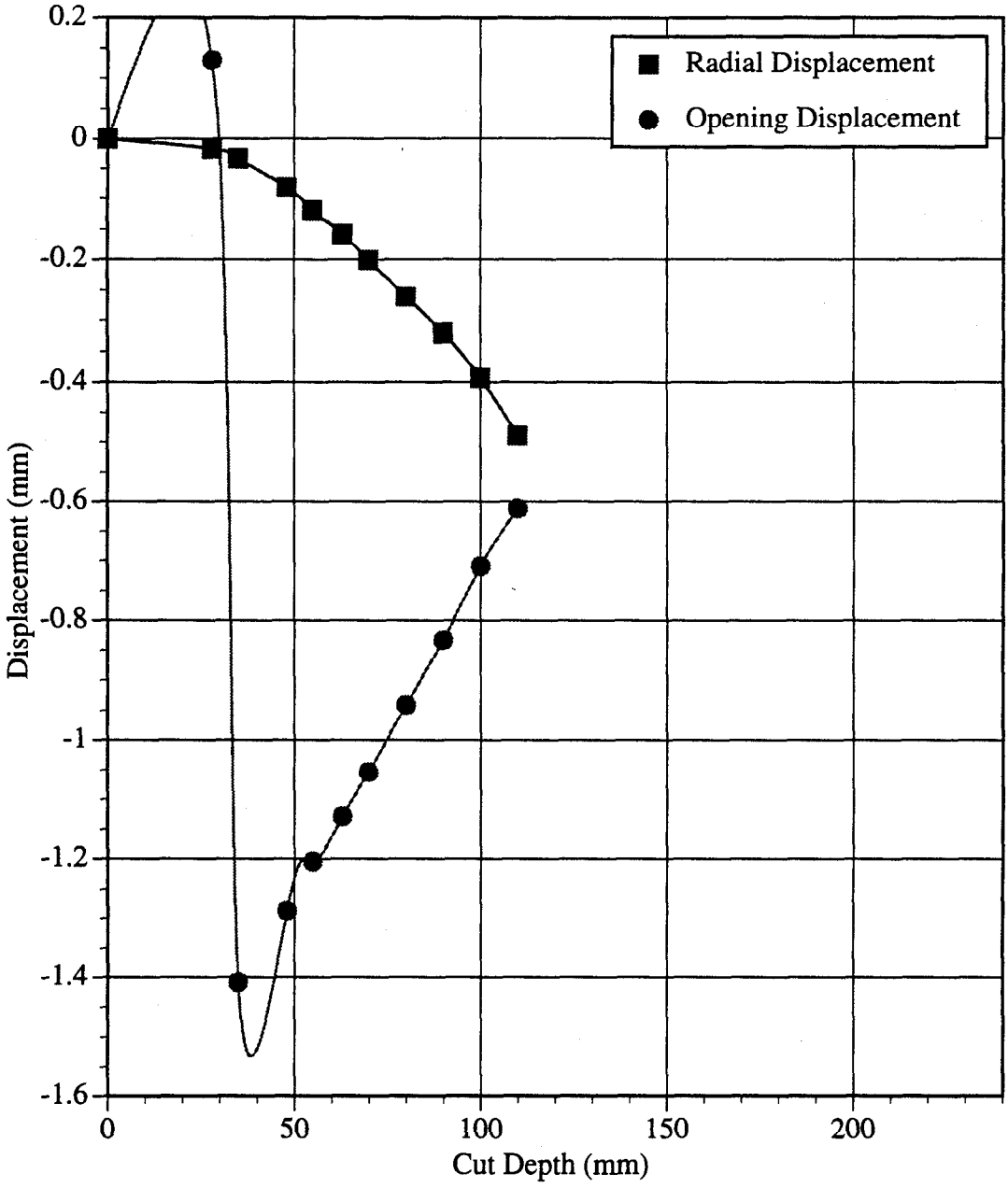

Railroad Wheel No. 3 Test
Strain Gage Readings vs. Cut Depth

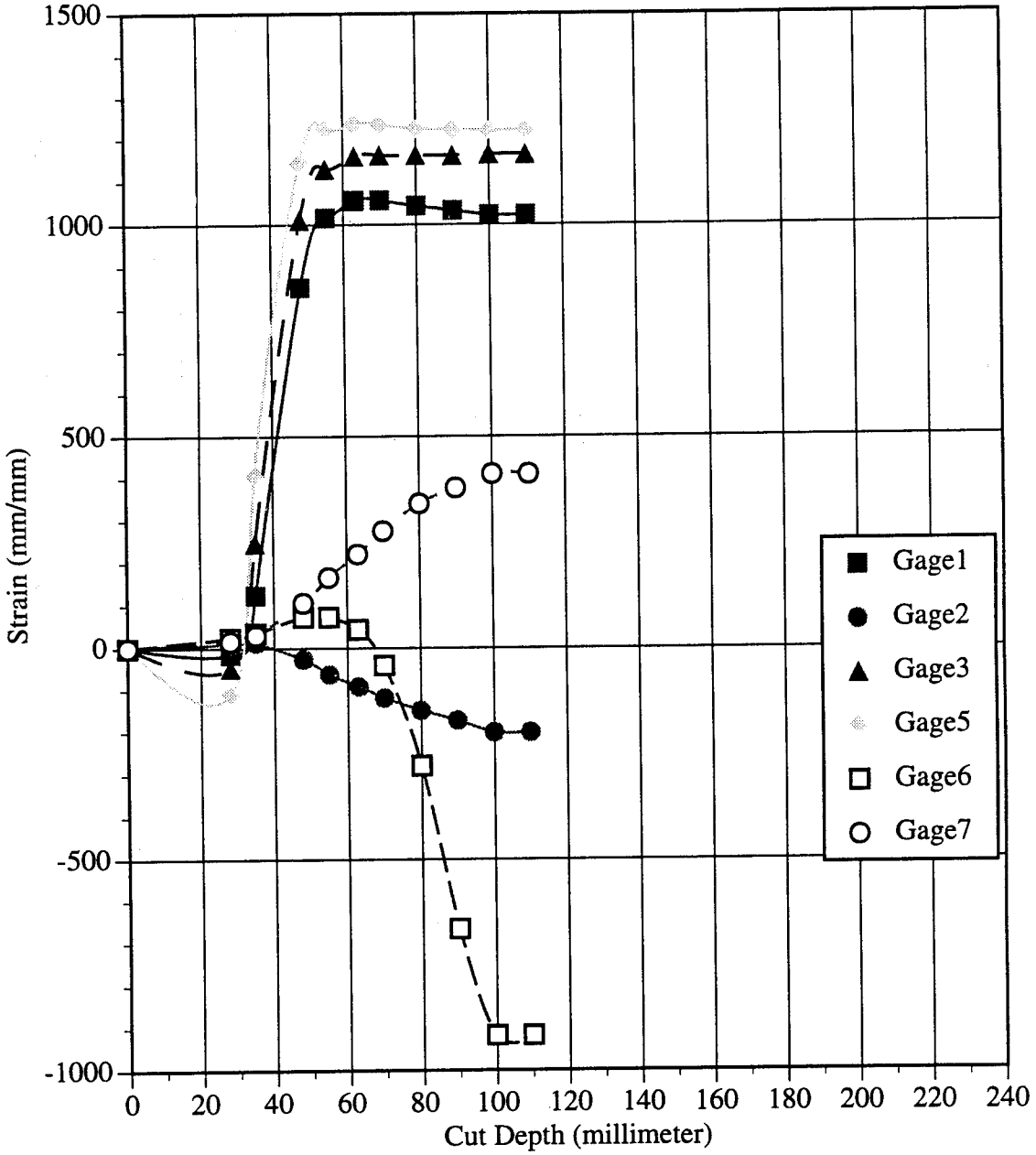

Railroad Wheel No. 3 Test
Wheel Rotation vs. Cut Depth

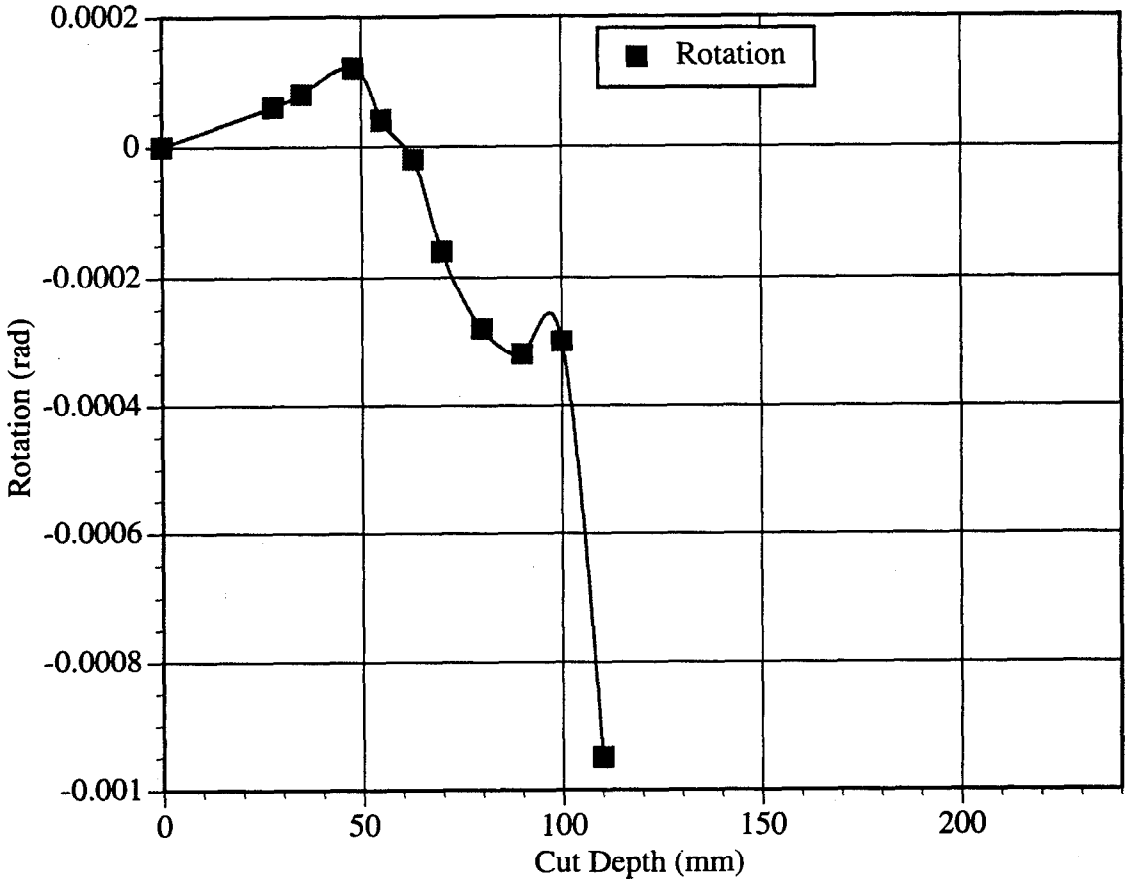

Railroad Car Wheel No. 3 Flange Side Interferometry Results
Horizontal Displacement Field After Cut No. 1 (in mm)

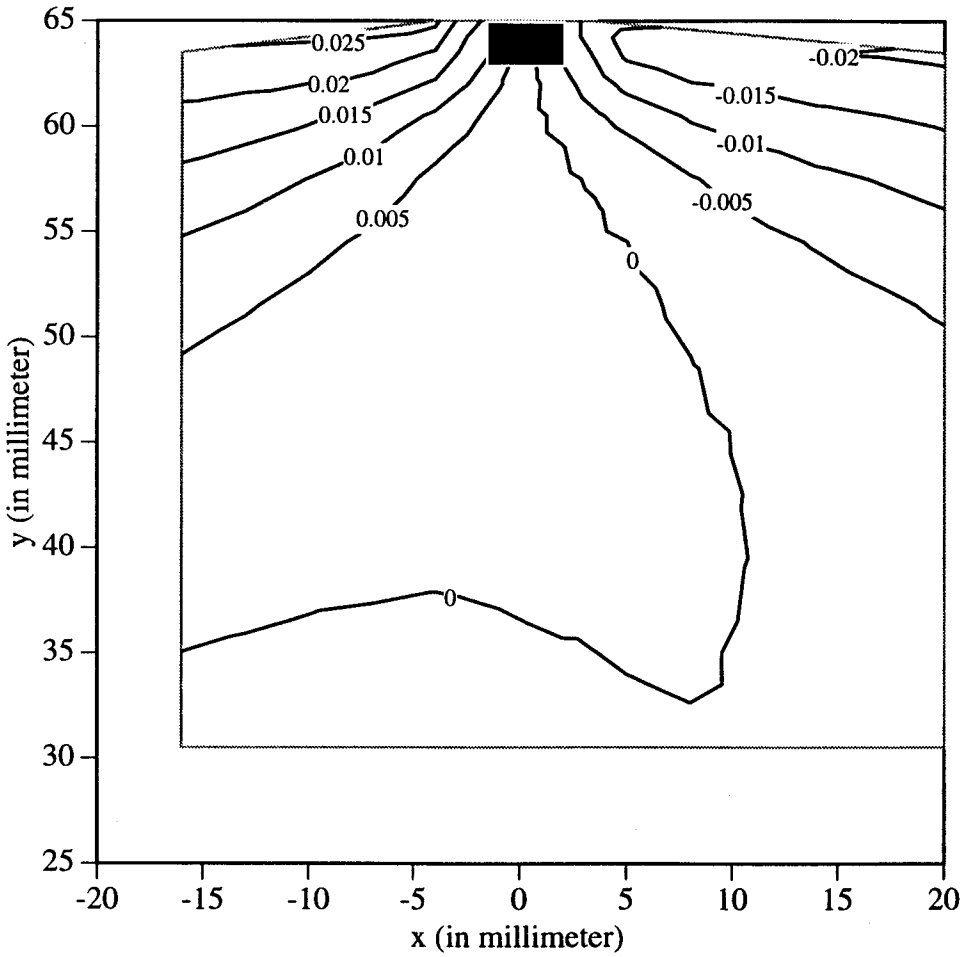

Railroad Car Wheel No. 3 Flange Side Interferometry Results
Vertical Displacement Field After Cut No. 1 (in mm)

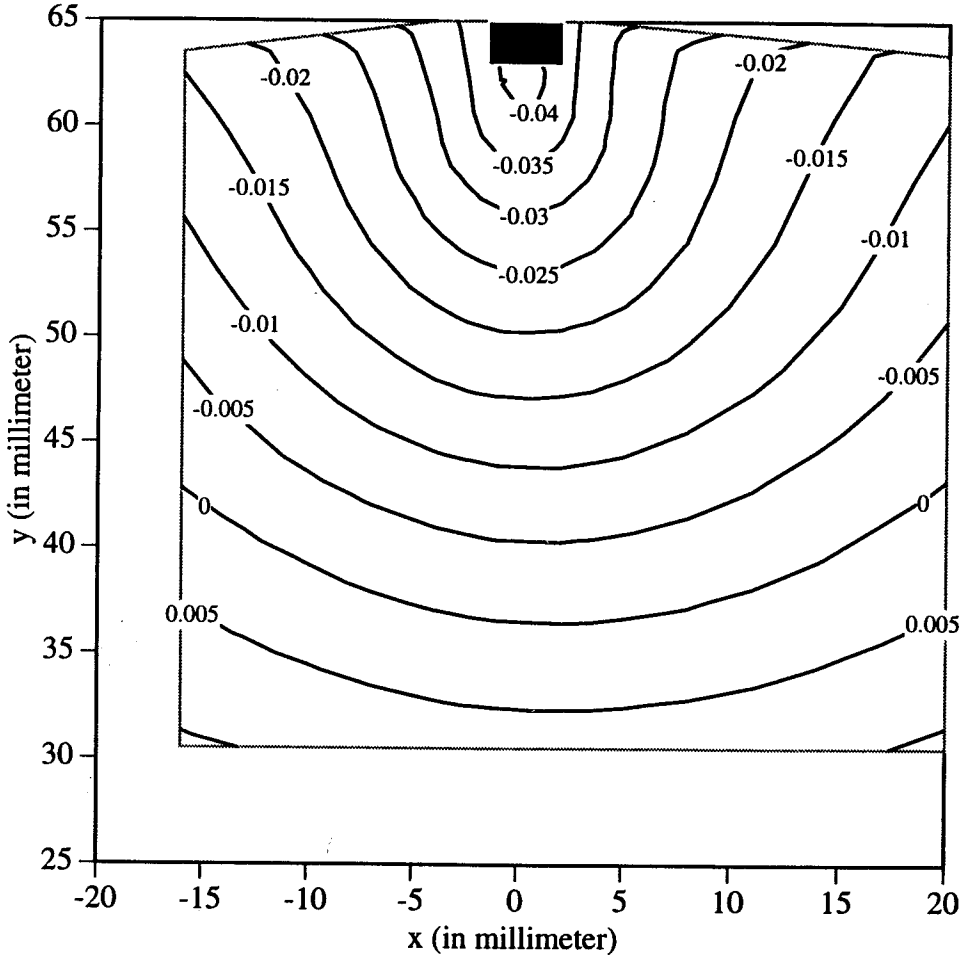

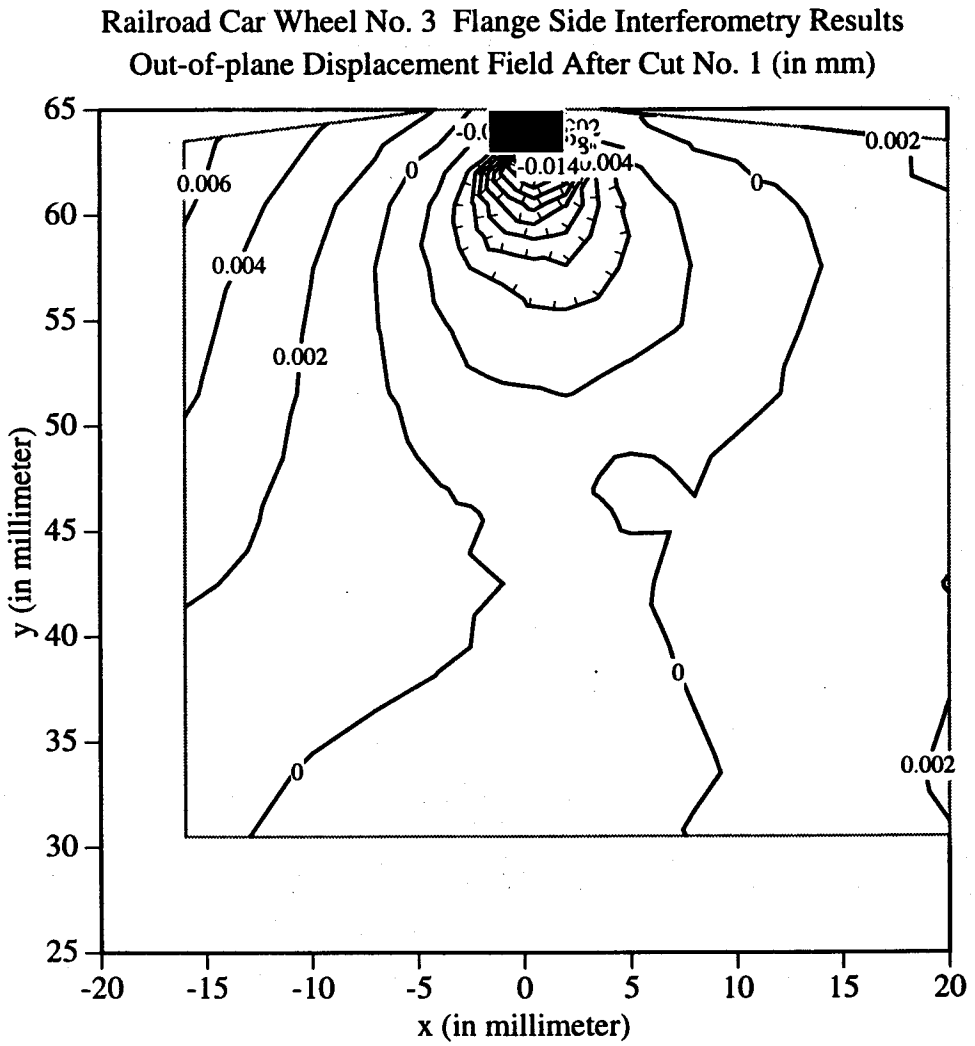
Railroad Car Wheel No. 3 Flange Side Interferometry Results
Out-of-plane Displacement Field After Cut No. 1 (in mm)
0.006
0.004
0.002
0
-0.014
0.004
0.002
0
0
0
0.002
0.002
y (in millimeter)
65
60
55
50
45
40
35
30
25
-20
-15
-10
-5
0
5
10
15
20
x (in millimeter)

Railroad Car Wheel No. 3 Flange Side Interferometry Results
Horizontal Strain Field After Cut No. 1

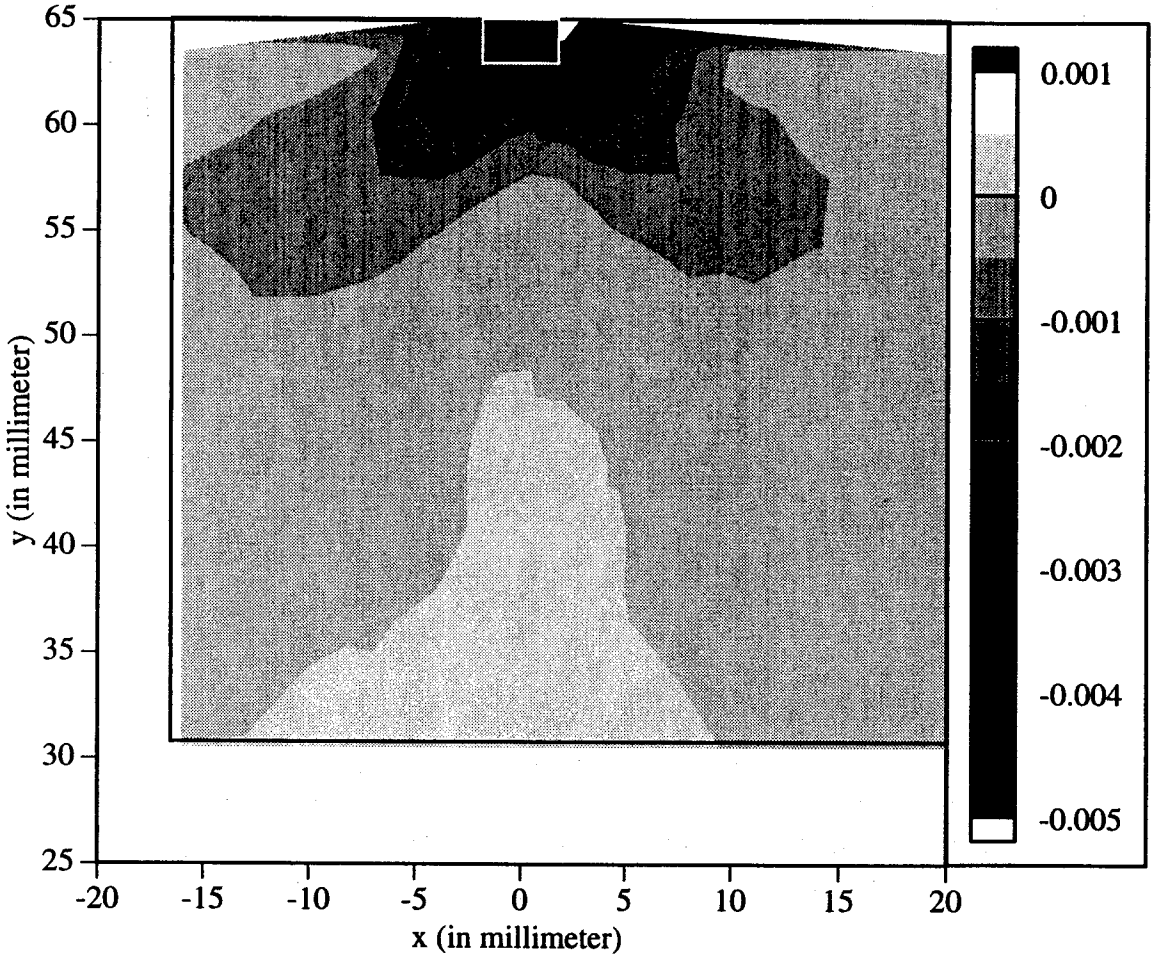

Railroad Car Wheel No.3 Flange Side Interferometry Results
Vertical Strain Field After Cut No. 1

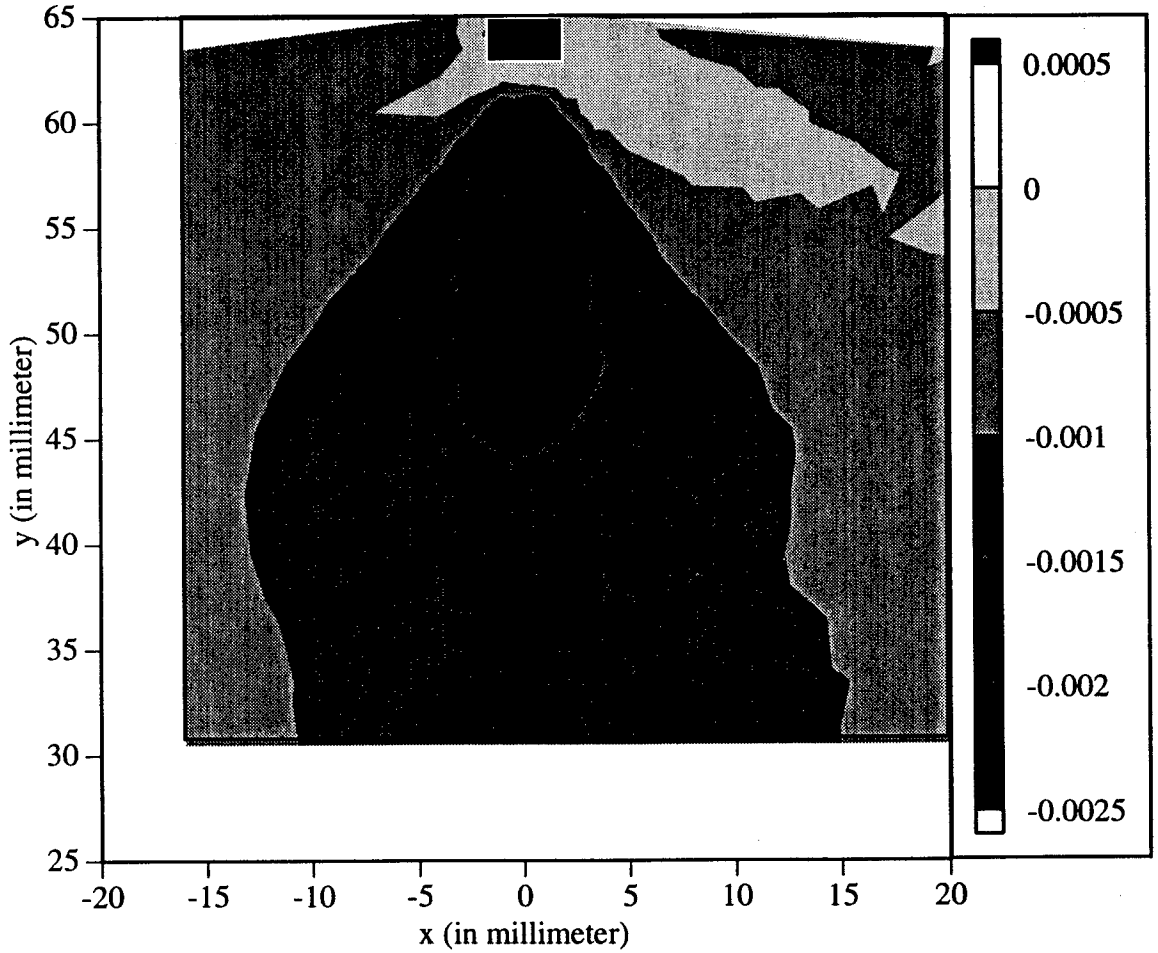

Railroad Car Wheel No. 3 Flange Side Interferometry Results
Shear Strain Field After Cut No. 1

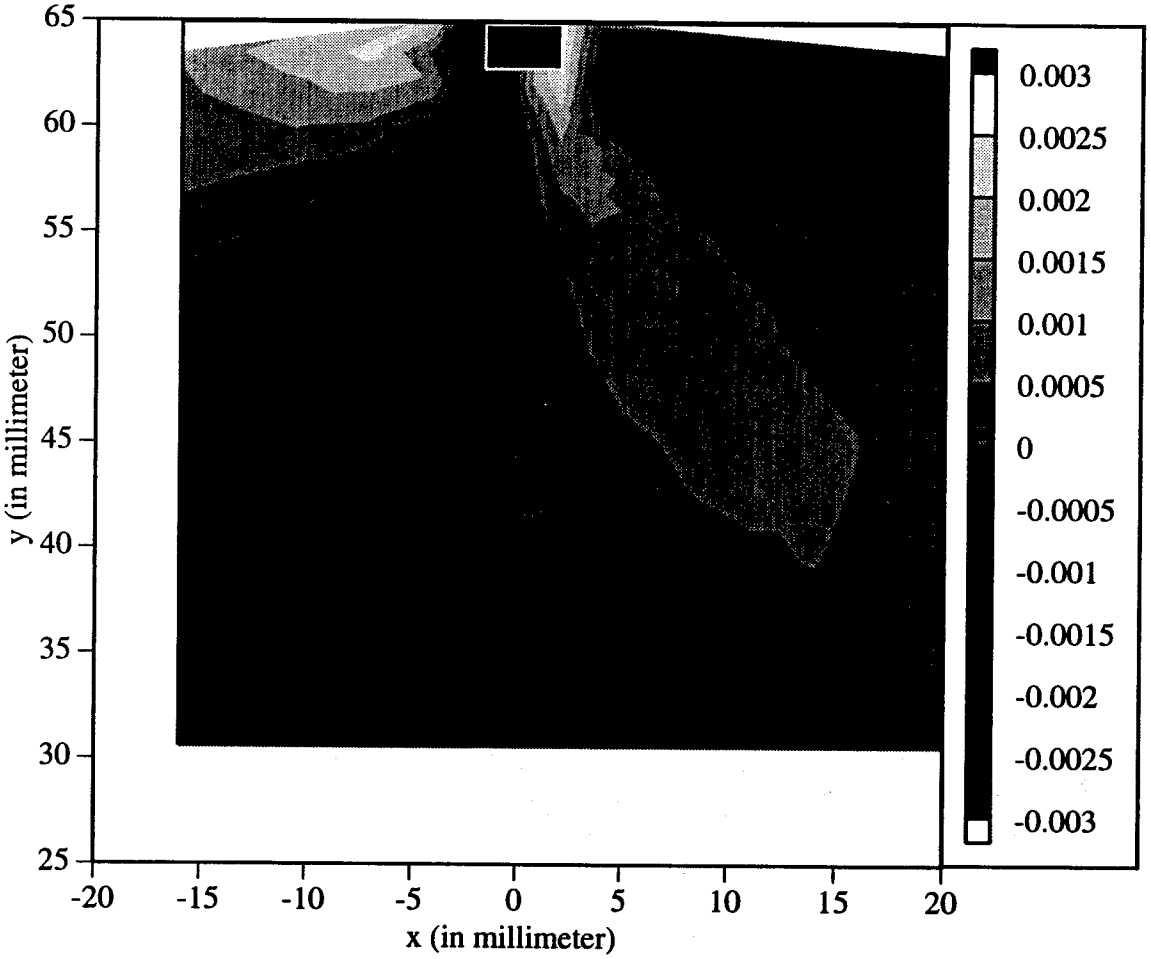

Railroad Car Wheel No. 3 Flange Side Interferometry Results
Horizontal Displacement Field After Cut No. 2 (in mm)

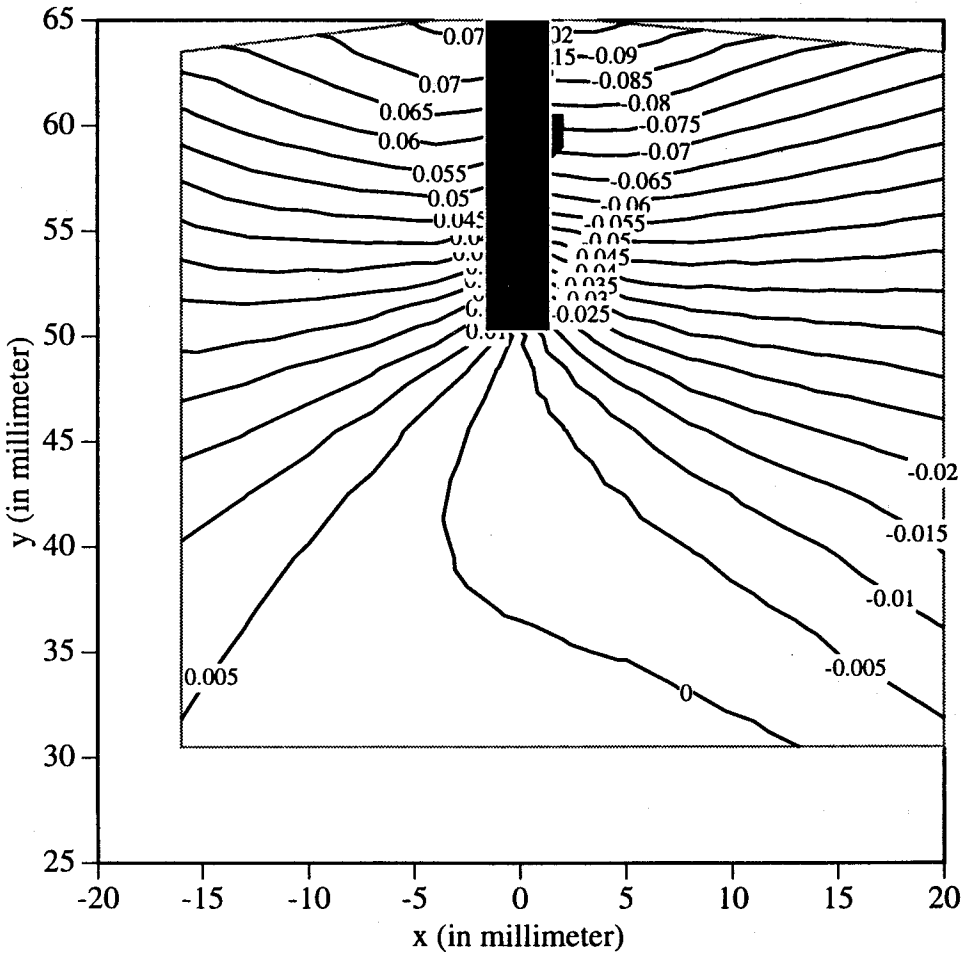

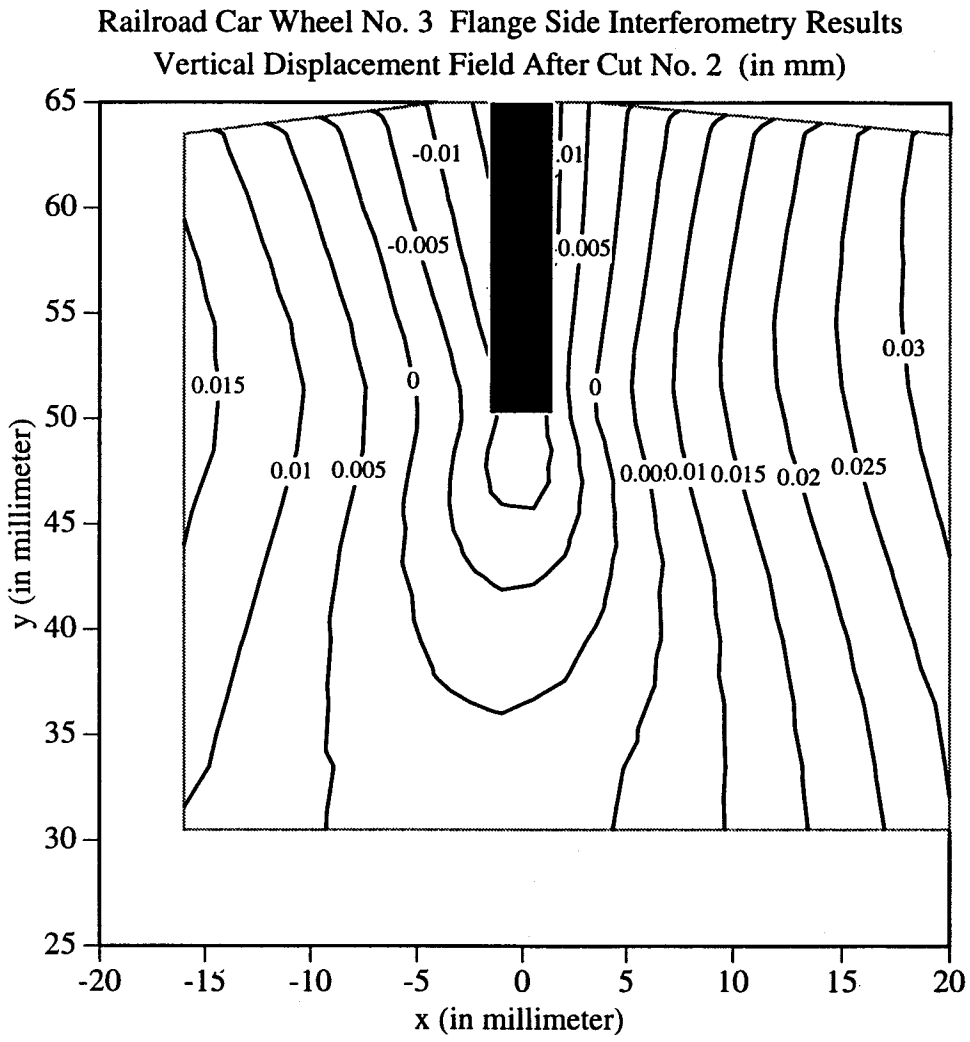
Railroad Car Wheel No. 3 Flange Side Interferometry Results
Vertical Displacement Field After Cut No. 2 (in mm)
-0.01
.01
-0.005
0.005
0.015
0
0
0.03
0.01
0.005
0.00
0.01
0.015
0.02
0.025
y (in millimeter)
65
60
55
50
45
40
35
30
25
-20
-15
-10
-5
0
5
10
15
20
x (in millimeter)

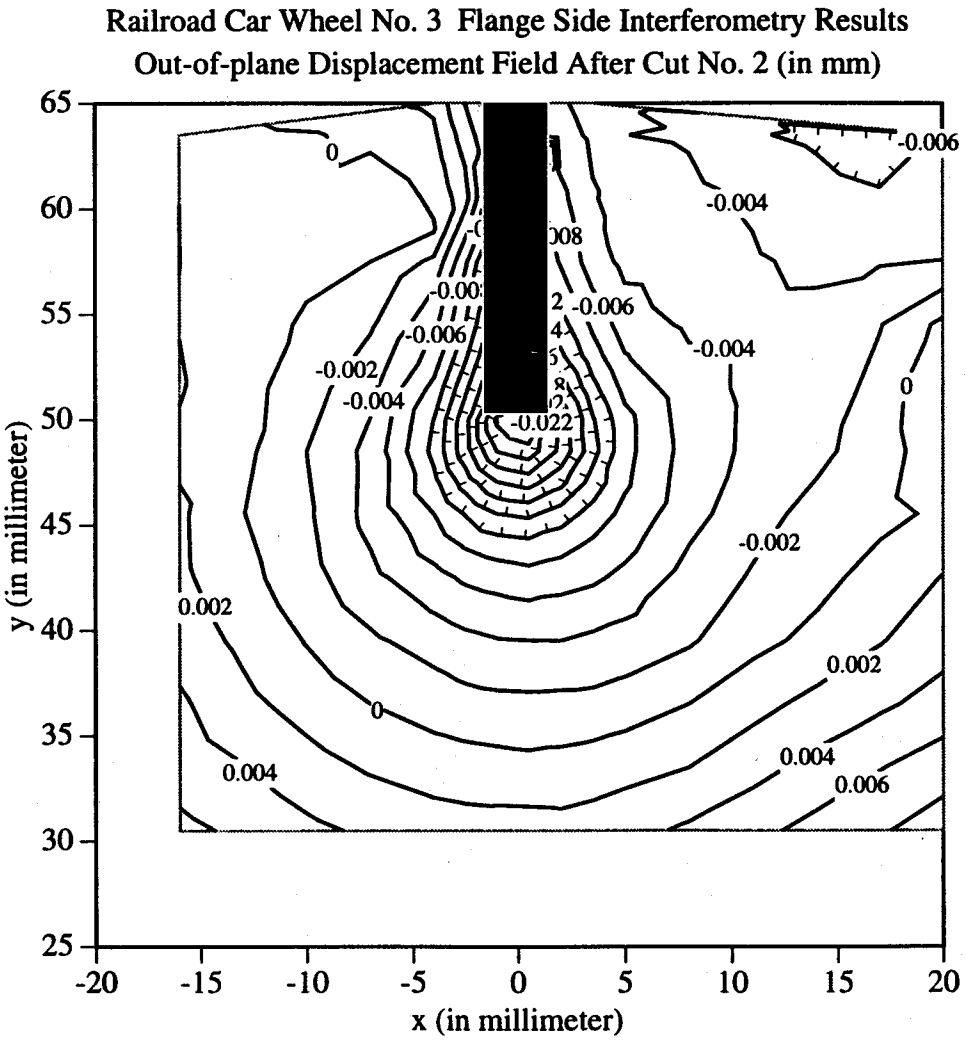
Railroad Car Wheel No. 3 Flange Side Interferometry Results
Out-of-plane Displacement Field After Cut No. 2 (in mm)
y (in millimeter)
x (in millimeter)
65
60
55
50
45
40
35
30
25
-20
-15
-10
-5
0
5
10
15
20
0
-0.006
-0.004
-0.006
-0.002
-0.004
-0.022
0
-0.002
0.002
0
0.004
0.002
0.004
0.006

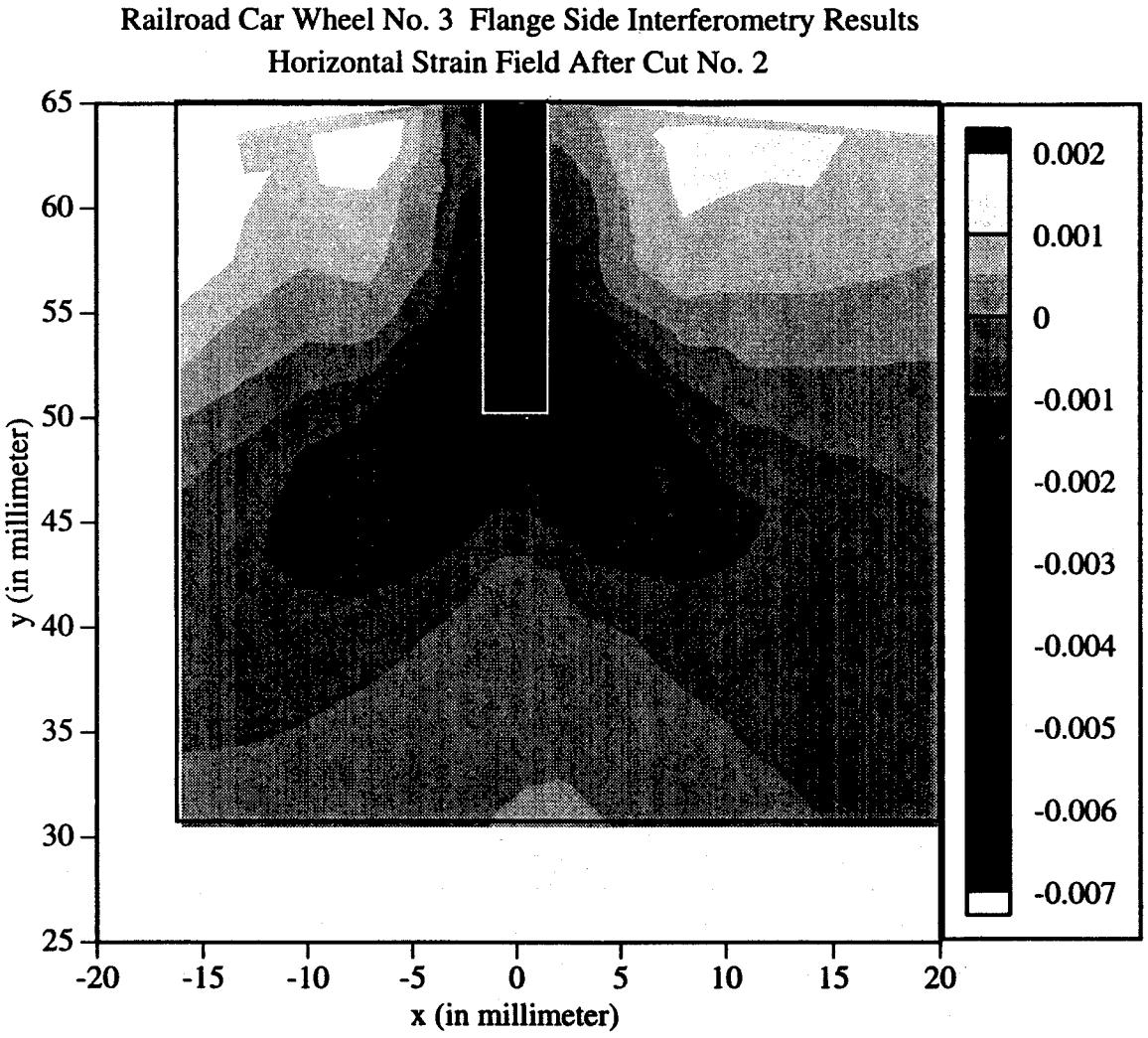
Railroad Car Wheel No. 3 Flange Side Interferometry Results
Horizontal Strain Field After Cut No. 2
y (in millimeter)
65
60
55
50
45
40
35
30
25
-20
-15
-10
-5
0
5
10
15
20
x (in millimeter)
0.002
0.001
0
-0.001
-0.002
-0.003
-0.004
-0.005
-0.006
-0.007

Railroad Car Wheel No. 3 Flange Side Interferometry Results
Vertical Strain Field After Cut No. 2

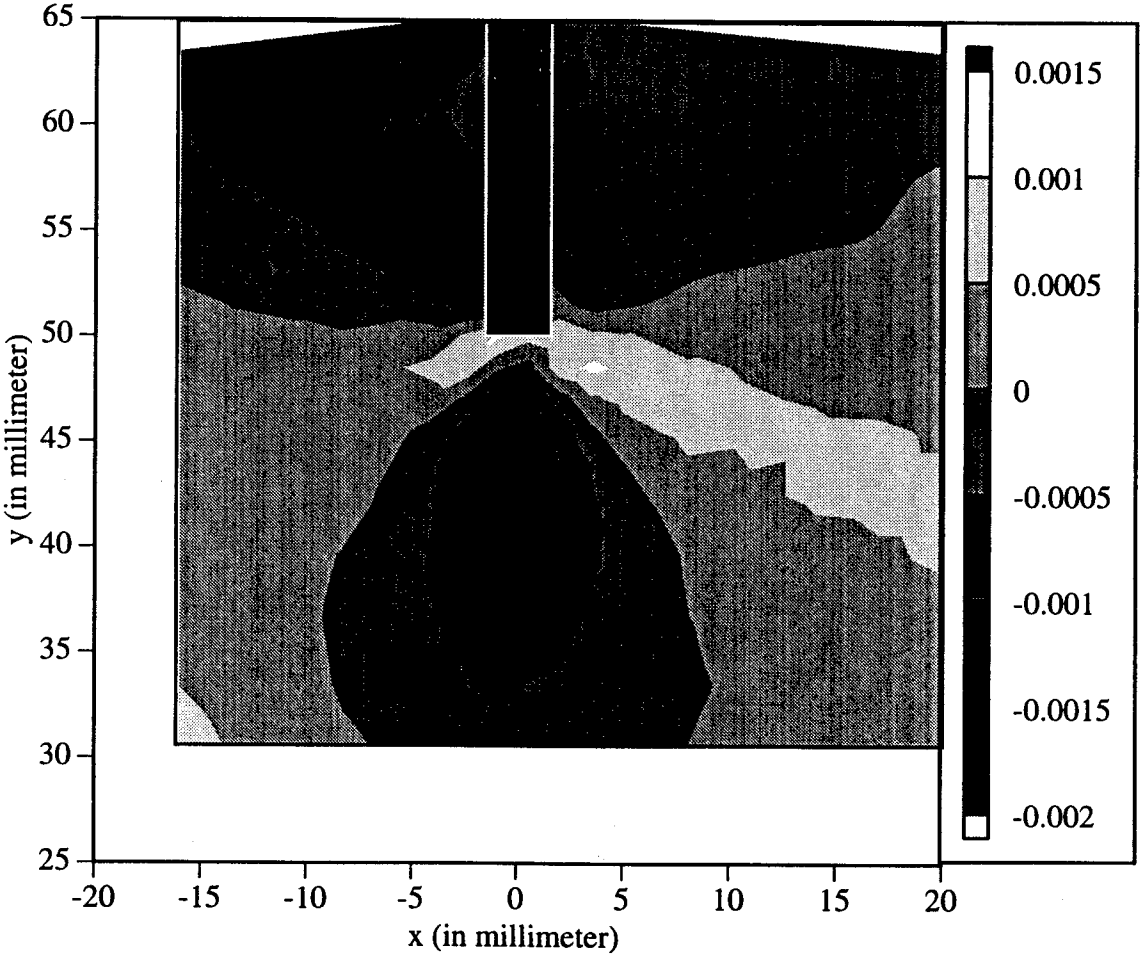

Railroad Car Wheel No. 3 Flange Side Interferometry Results
Shear Strain Field After Cut No. 2

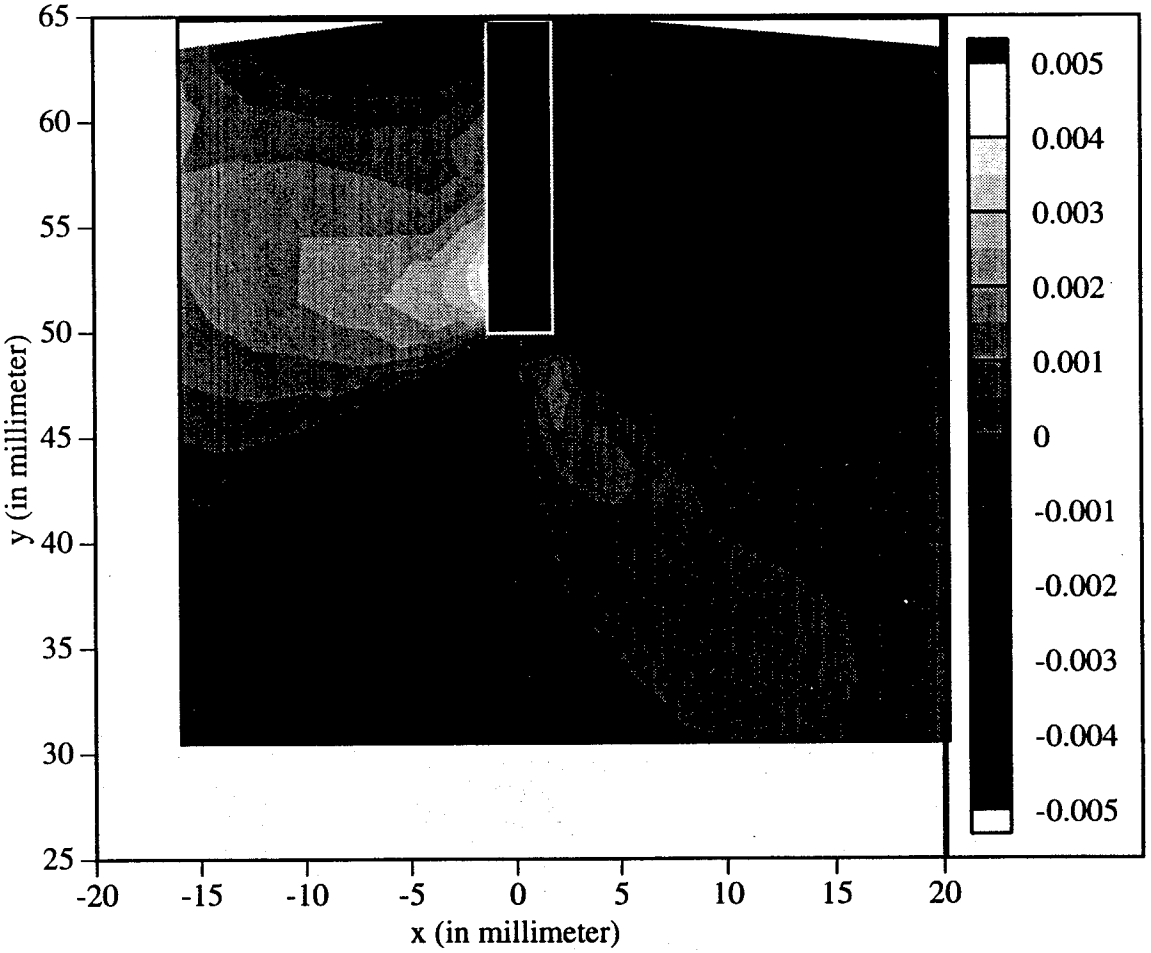

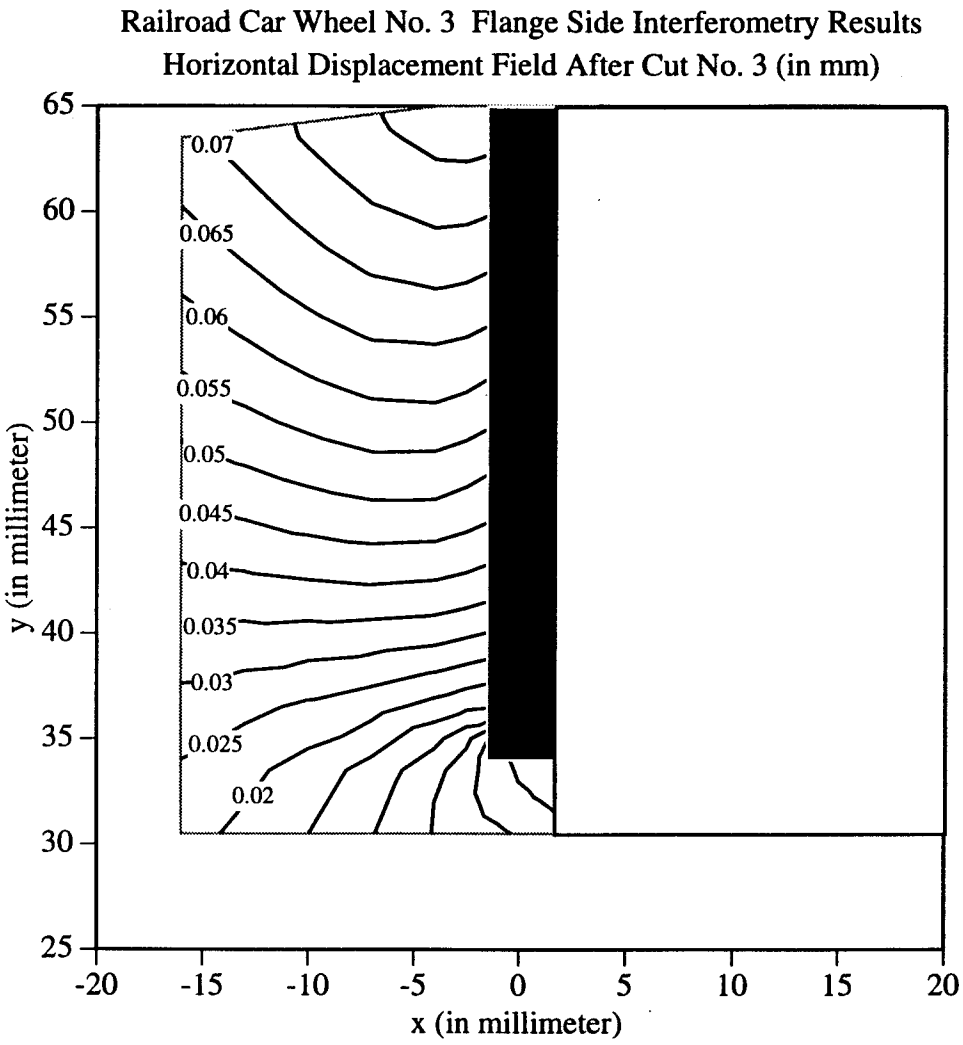
Railroad Car Wheel No. 3 Flange Side Interferometry Results
Horizontal Displacement Field After Cut No. 3 (in mm)
0.07
0.065
0.06
0.055
0.05
0.045
0.04
0.035
0.03
0.025
0.02
65
60
55
50
45
40
35
30
25
-20
-15
-10
-5
0
5
10
15
20
y (in millimeter)
x (in millimeter)

Railroad Car Wheel No. 3 Flange Side Interferometry Results
Vertical Displacement Field After Cut No. 3 (in mm)

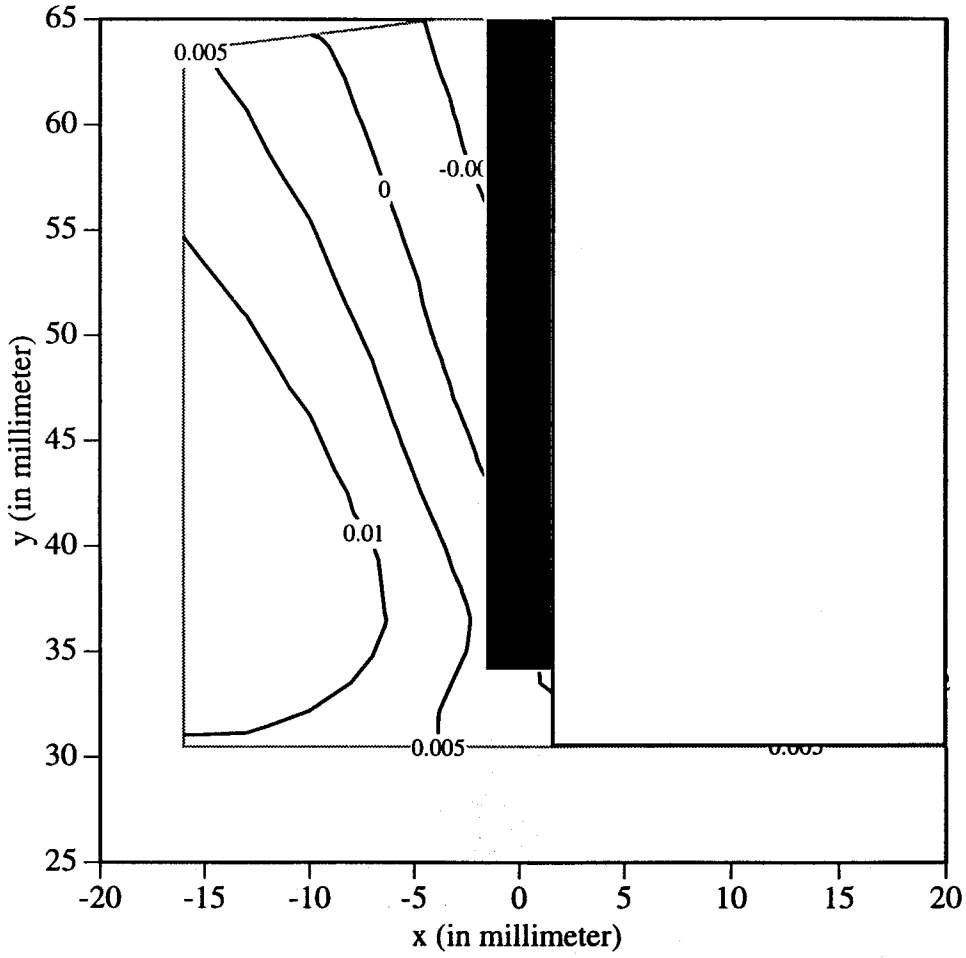

Railroad Car Wheel No. 3 Flange Side Interferometry Results
Out-of-plane Displacement Field After Cut No. 3 (in mm)

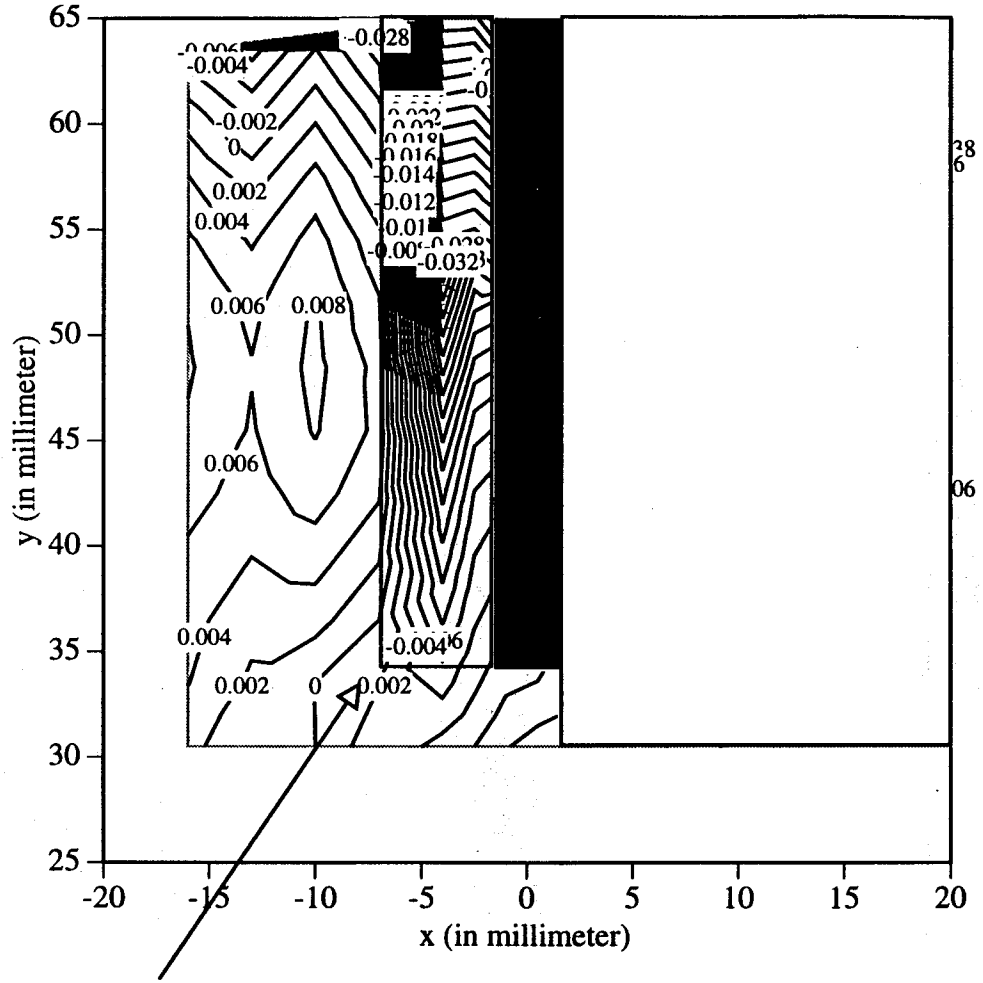

Dense Fringe Pattern, Poor Picture Quality, and
Severe Surface Distortion Causes Poor Data

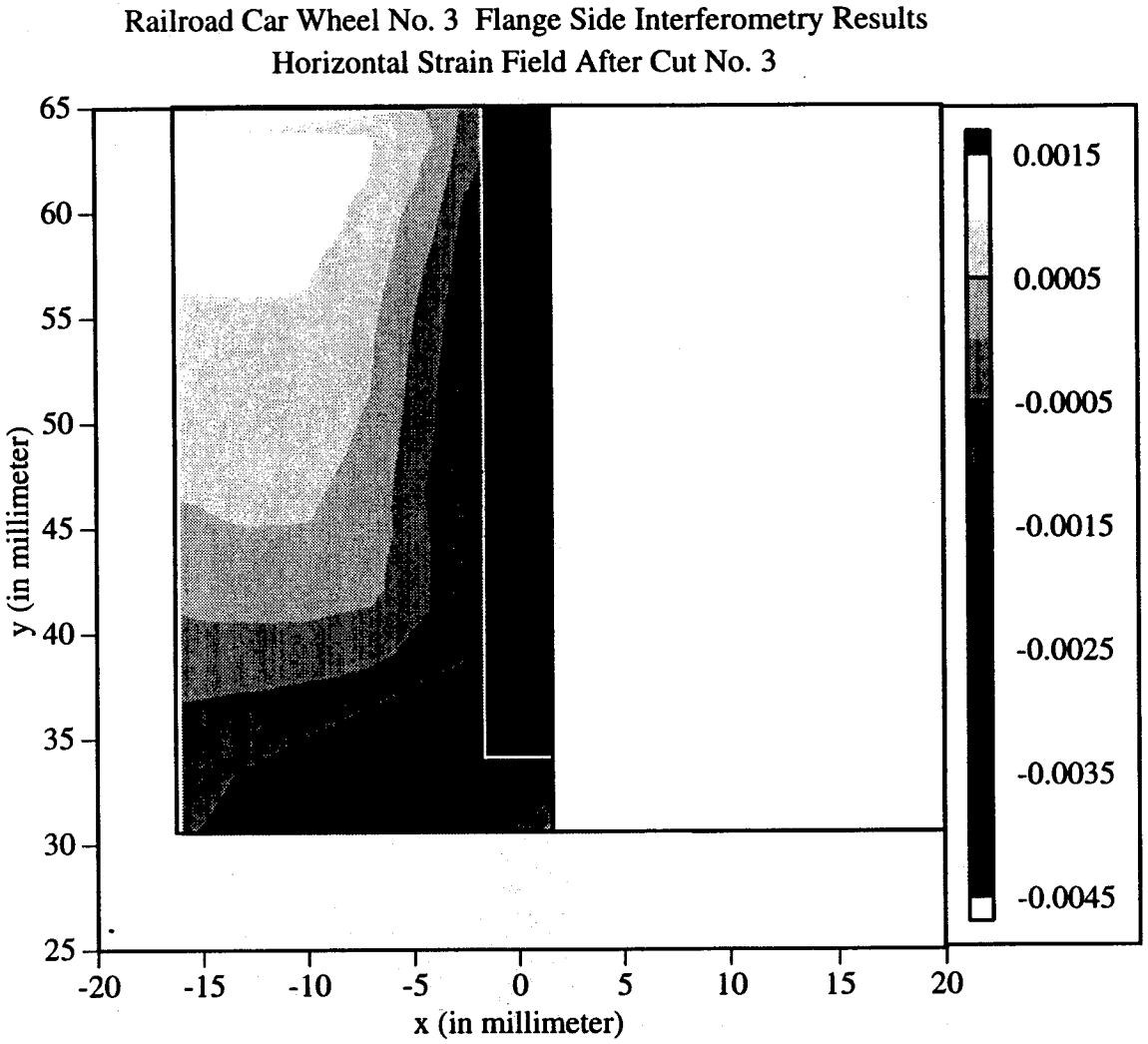
Railroad Car Wheel No. 3 Flange Side Interferometry Results
Horizontal Strain Field After Cut No. 3
65
60
55
50
45
40
35
30
25
y (in millimeter)
-20
-15
-10
-5
0
5
10
15
20
x (in millimeter)
0.0015
0.0005
-0.0005
-0.0015
-0.0025
-0.0035
-0.0045

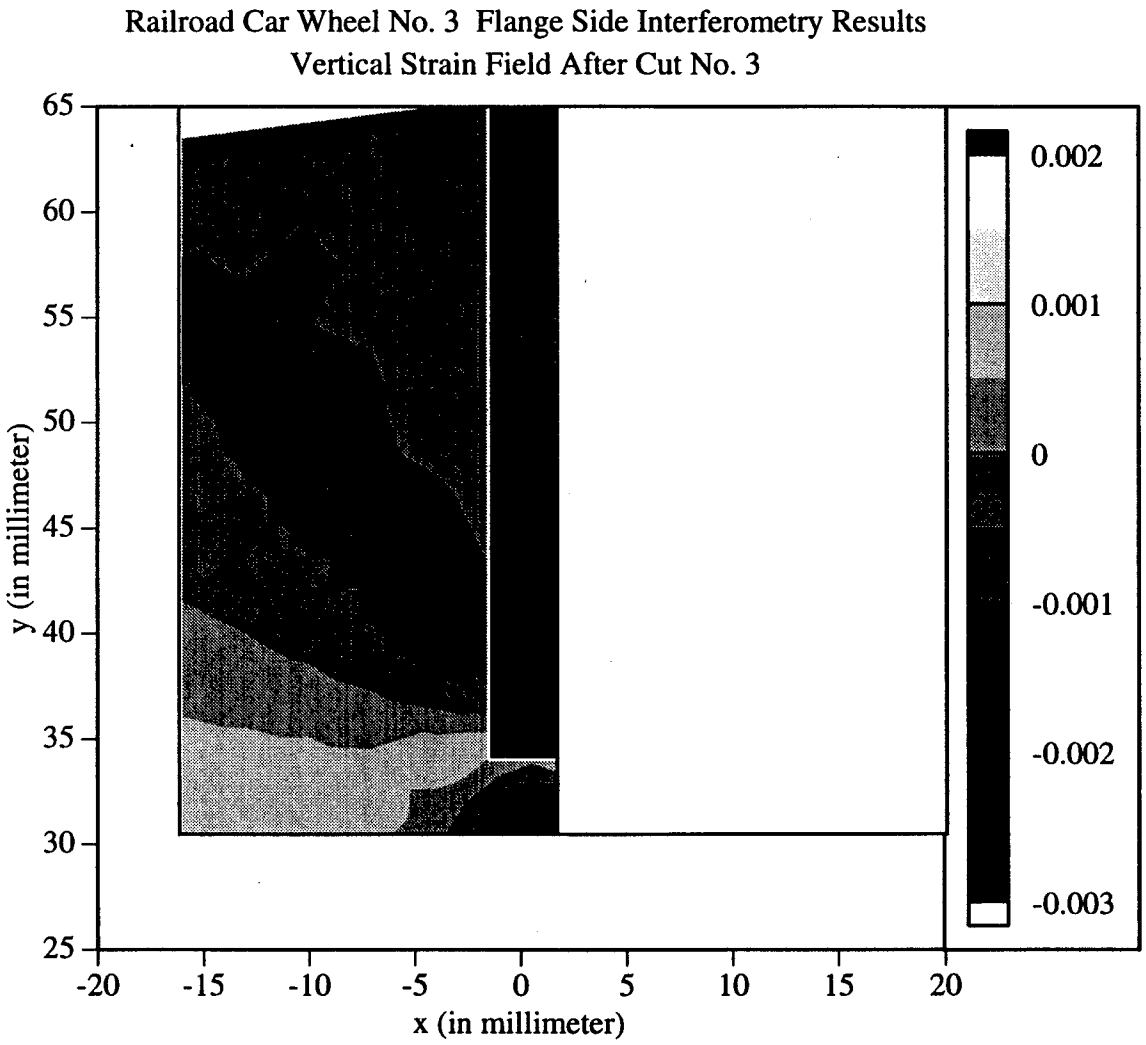
Railroad Car Wheel No. 3 Flange Side Interferometry Results
Vertical Strain Field After Cut No. 3
y (in millimeter)
65
60
55
50
45
40
35
30
25
-20
-15
-10
-5
0
5
10
15
20
x (in millimeter)
0.002
0.001
0
-0.001
-0.002
-0.003

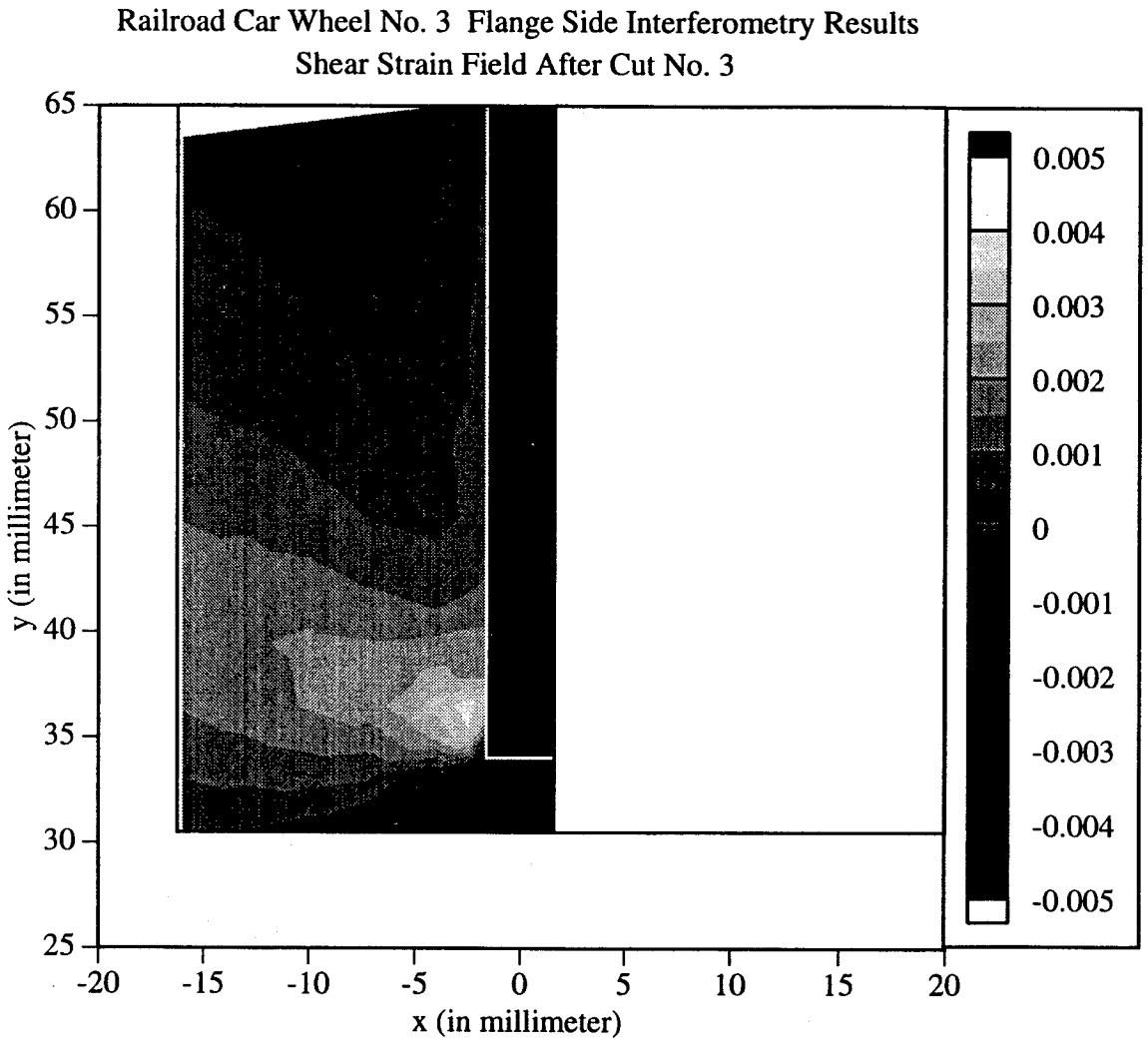
Railroad Car Wheel No. 3 Flange Side Interferometry Results
Shear Strain Field After Cut No. 3
y (in millimeter)
65
60
55
50
45
40
35
30
25
-20
-15
-10
-5
0
5
10
15
20
x (in millimeter)
0.005
0.004
0.003
0.002
0.001
0
-0.001
-0.002
-0.003
-0.004
-0.005

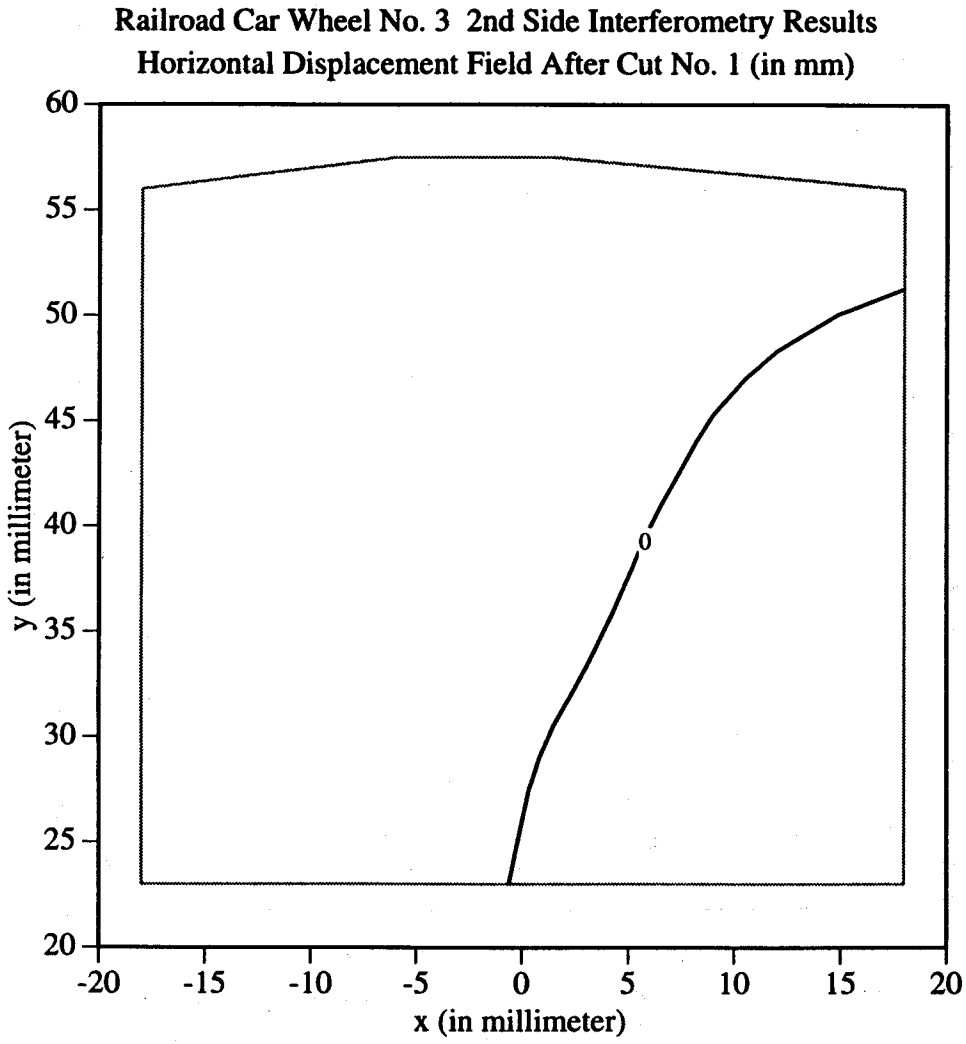
Railroad Car Wheel No. 3 2nd Side Interferometry Results
Horizontal Displacement Field After Cut No. 1 (in mm)
60
55
50
45
40
35
30
25
20
y (in millimeter)
0
-20
-15
-10
-5
0
5
10
15
20
x (in millimeter)

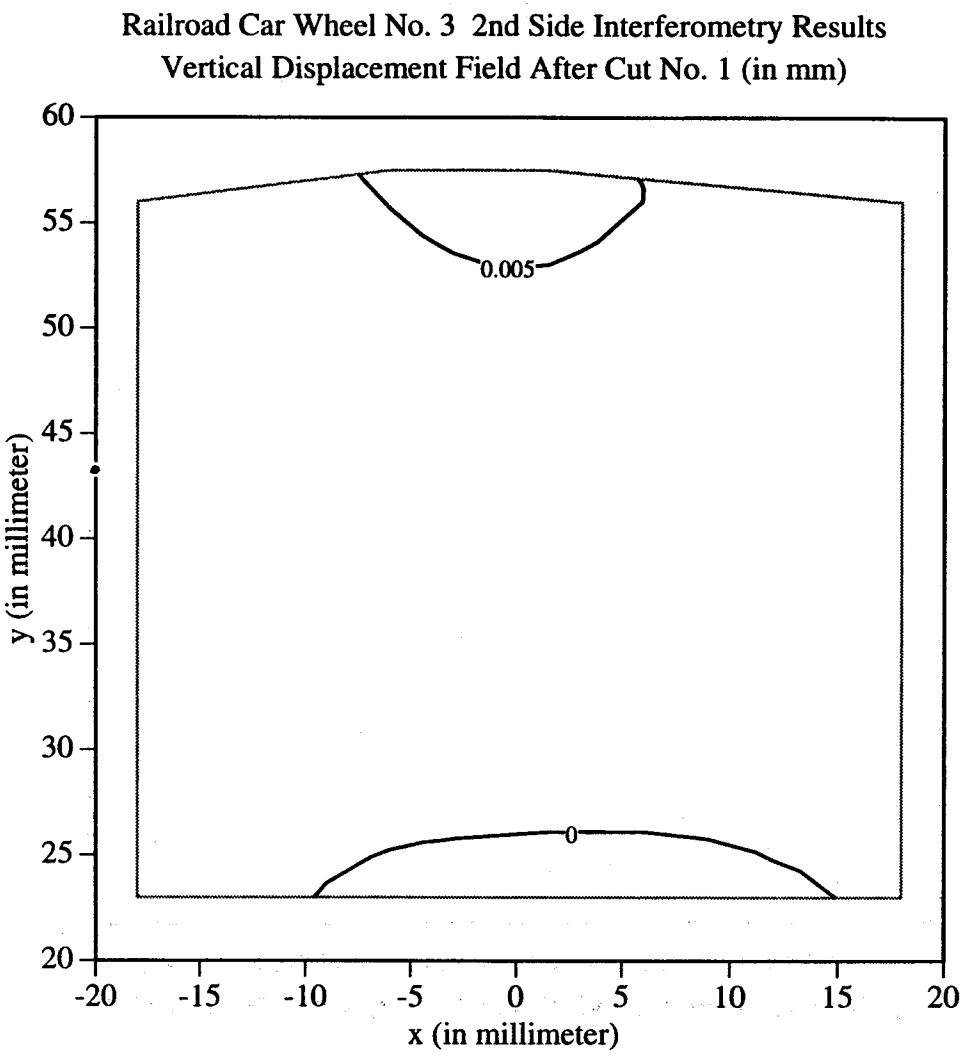
Railroad Car Wheel No. 3 2nd Side Interferometry Results
Vertical Displacement Field After Cut No. 1 (in mm)
60
55
50
45
40
35
30
25
20
y (in millimeter)
0.005
0
-20
-15
-10
-5
0
5
10
15
20
x (in millimeter)

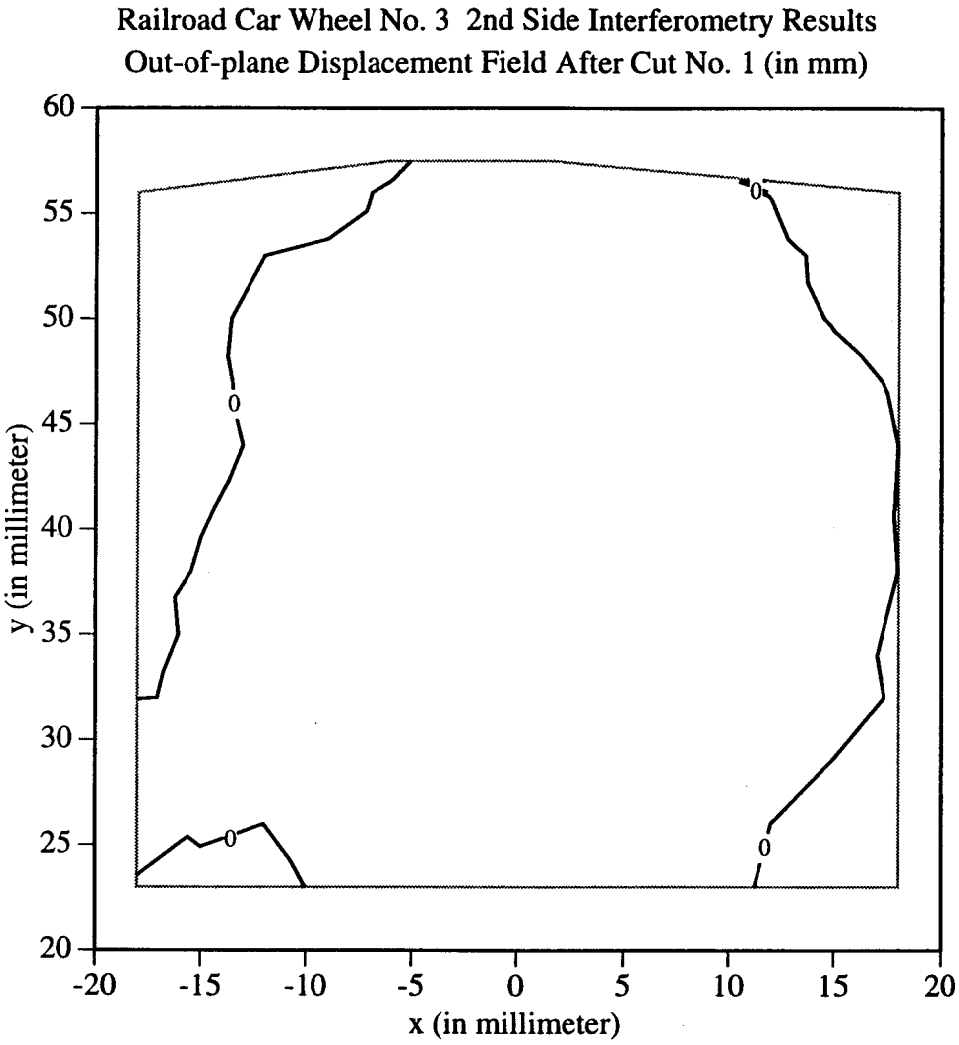
Railroad Car Wheel No. 3 2nd Side Interferometry Results
Out-of-plane Displacement Field After Cut No. 1 (in mm)
60
55
50
45
40
35
30
25
20
y (in millimeter)
-20
-15
-10
-5
0
5
10
15
20
x (in millimeter)
0
0
0
0

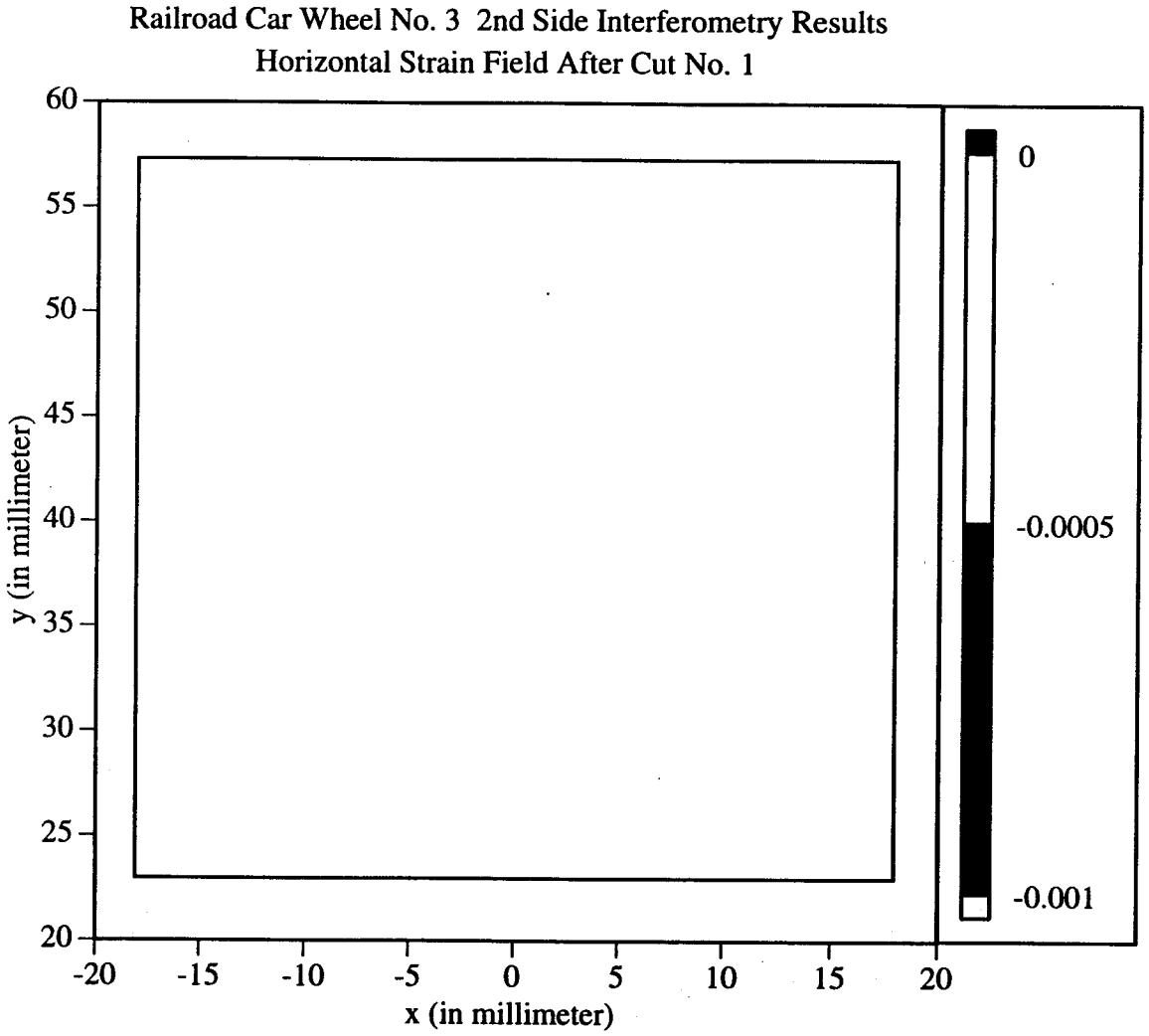
Railroad Car Wheel No. 3 2nd Side Interferometry Results
Horizontal Strain Field After Cut No. 1
60
55
50
45
40
35
30
25
20
y (in millimeter)
-20
-15
-10
-5
0
5
10
15
20
x (in millimeter)
0
-0.0005
-0.001

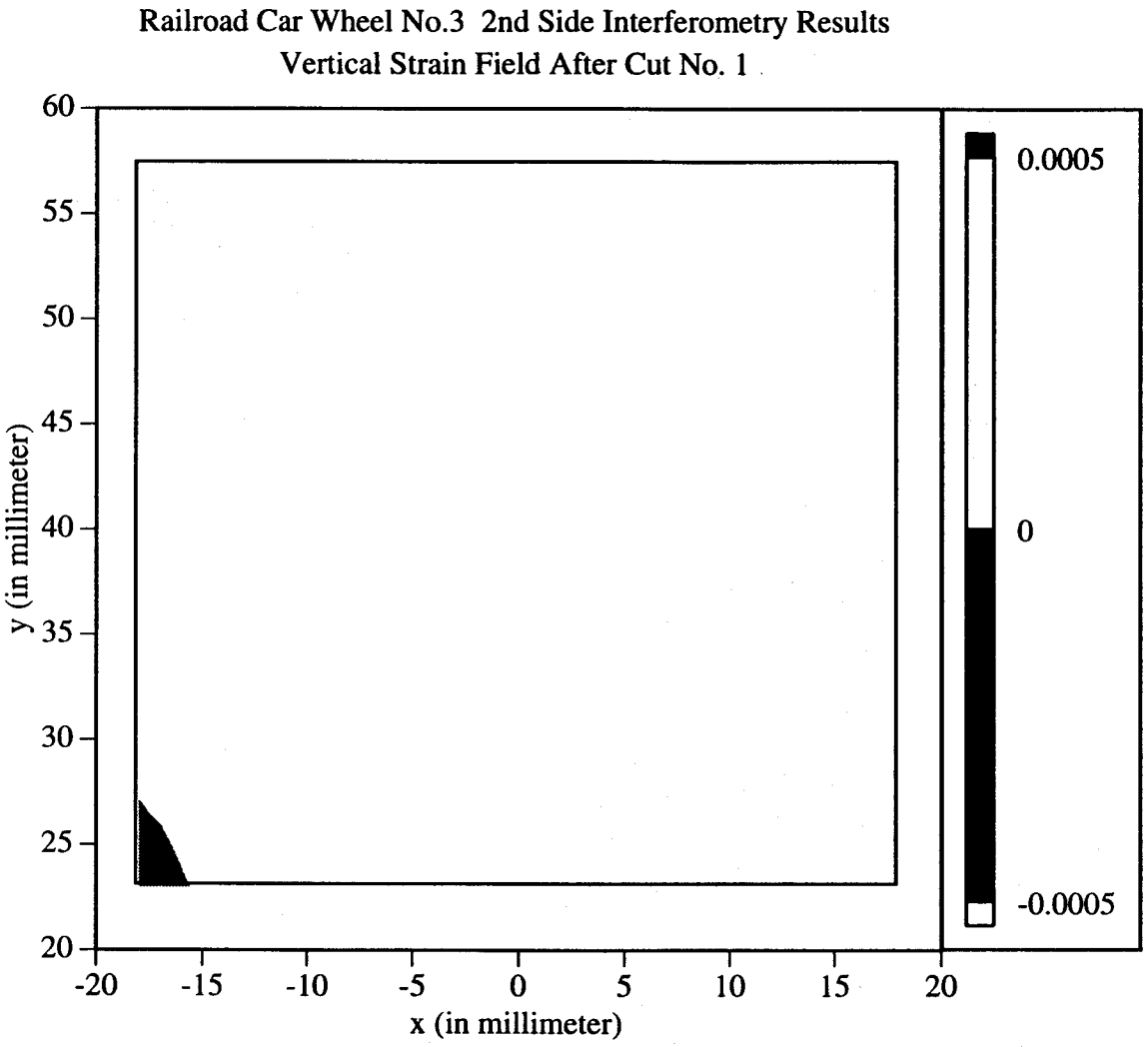
Railroad Car Wheel No.3 2nd Side Interferometry Results
Vertical Strain Field After Cut No. 1
60
55
50
45
40
35
30
25
20
y (in millimeter)
-20
-15
-10
-5
0
5
10
15
20
x (in millimeter)
0.0005
0
-0.0005

Railroad Car Wheel No. 3 2nd Side Interferometry Results
Shear Strain Field After Cut No. 1

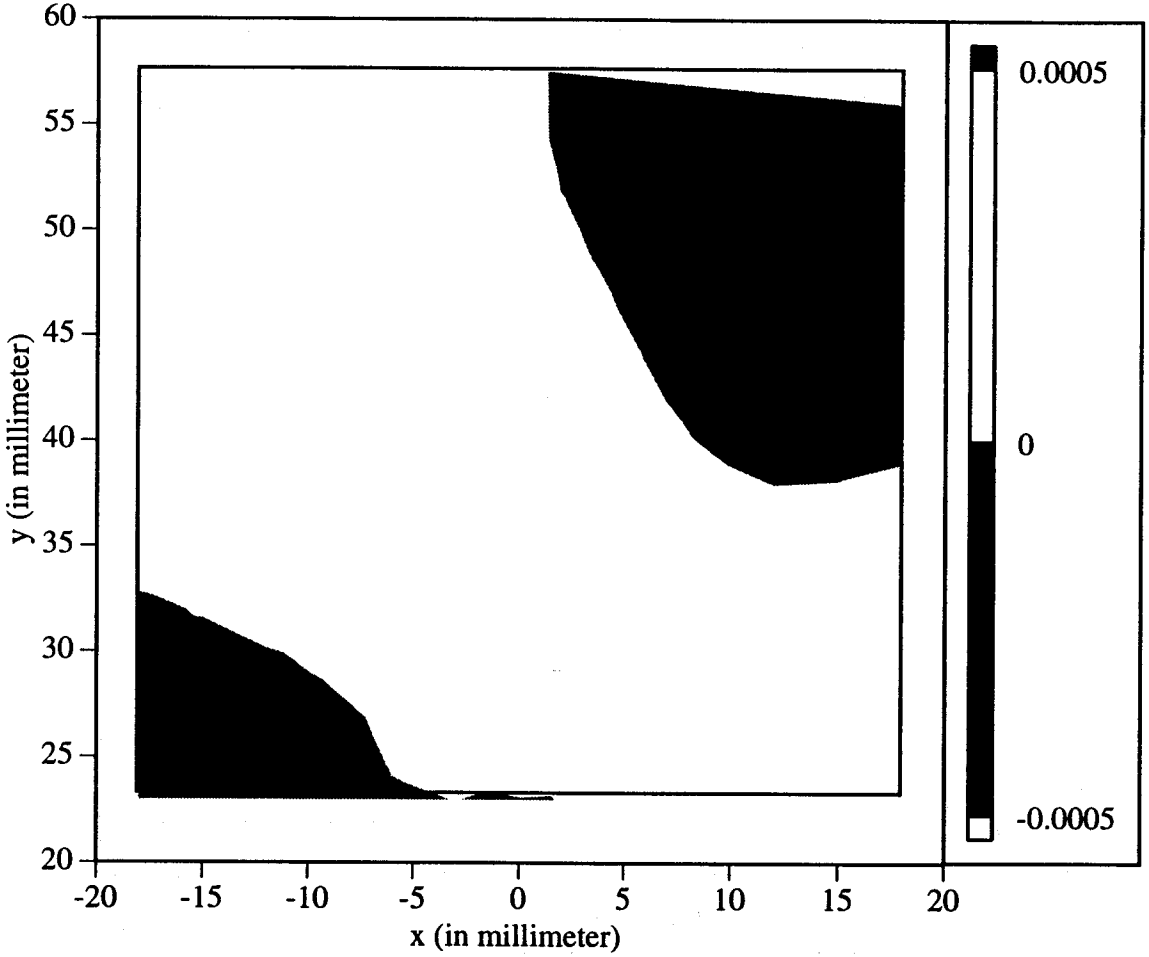

Railroad Car Wheel No. 3 2nd Side Interferometry Results
Horizontal Displacement Field After Cut No. 2 (in mm)

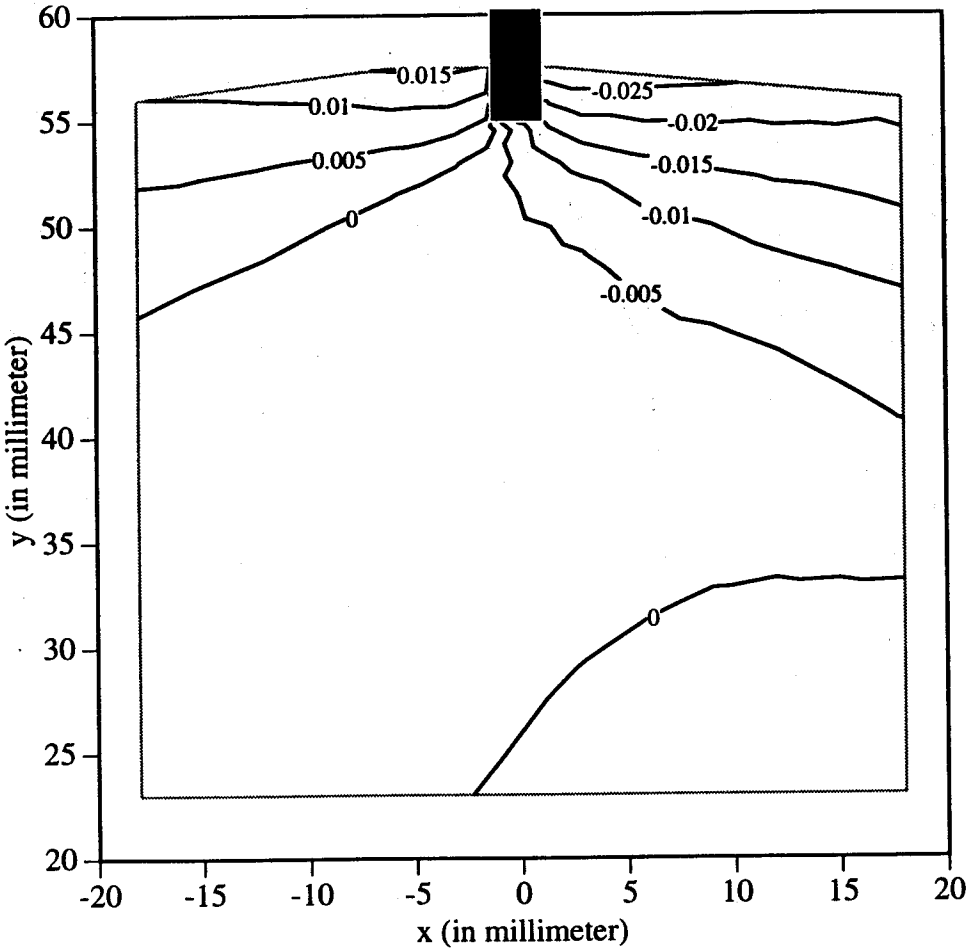

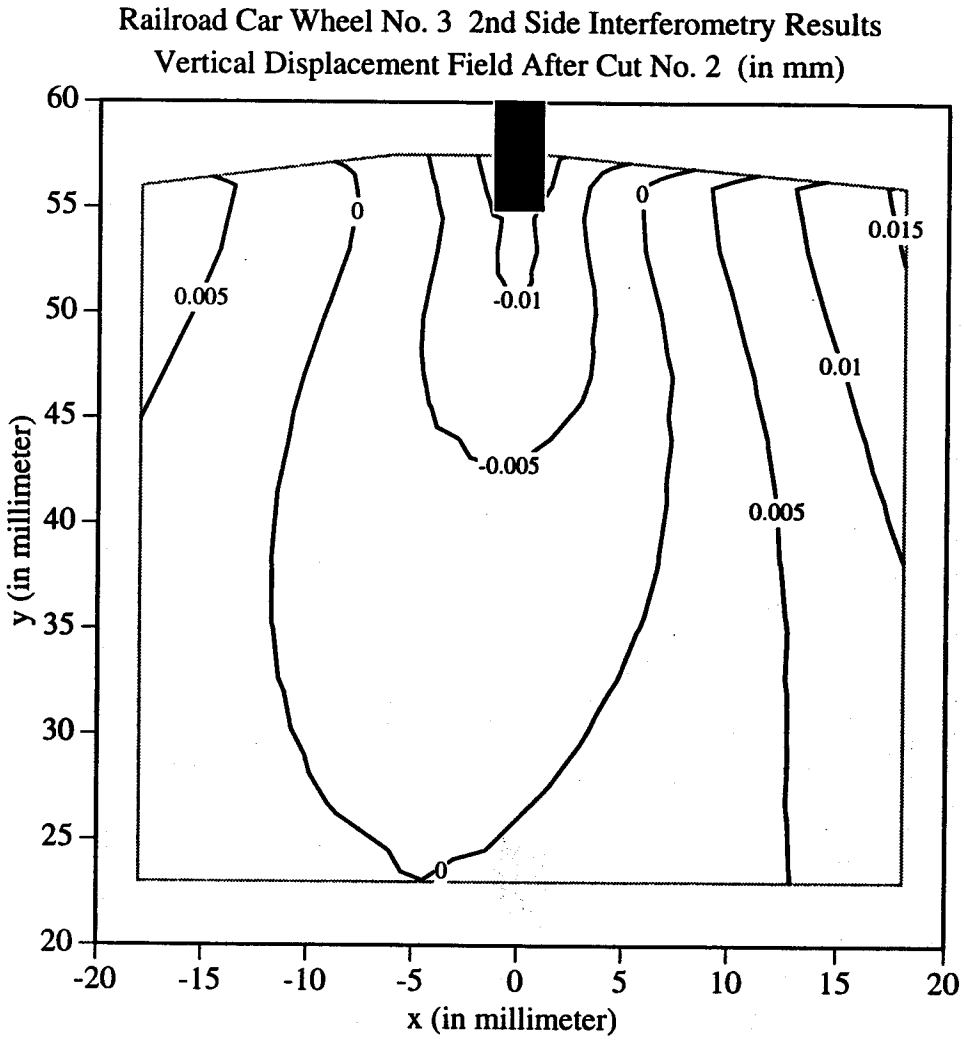
Railroad Car Wheel No. 3 2nd Side Interferometry Results
Vertical Displacement Field After Cut No. 2 (in mm)
60
55
50
45
40
35
30
25
20
y (in millimeter)
-20
-15
-10
-5
0
5
10
15
20
x (in millimeter)
0.005
0
-0.01
0
0.015
0.01
-0.005
0.005
0

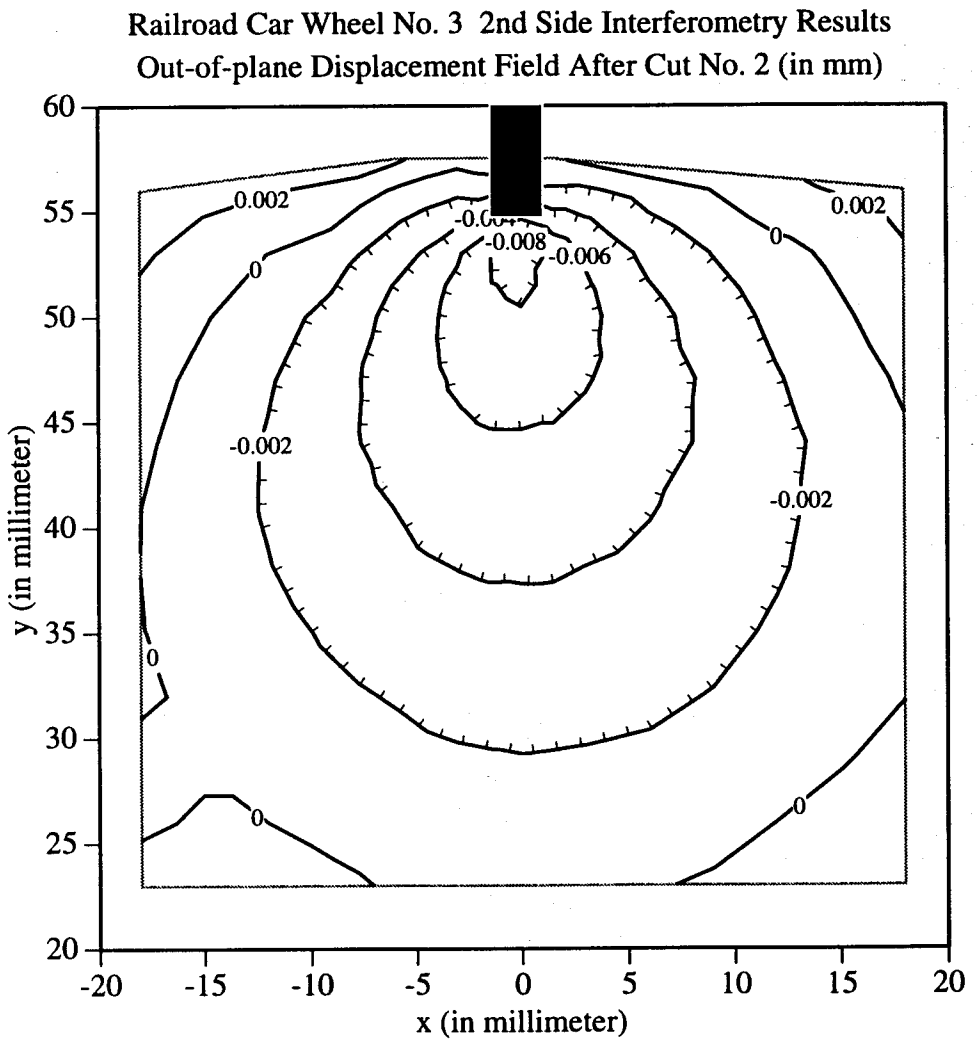
Railroad Car Wheel No. 3 2nd Side Interferometry Results
Out-of-plane Displacement Field After Cut No. 2 (in mm)
0.002
0
-0.008
-0.006
-0.002
y (in millimeter)
x (in millimeter)
60
55
50
45
40
35
30
25
20
-20
-15
-10
-5
0
5
10
15
20

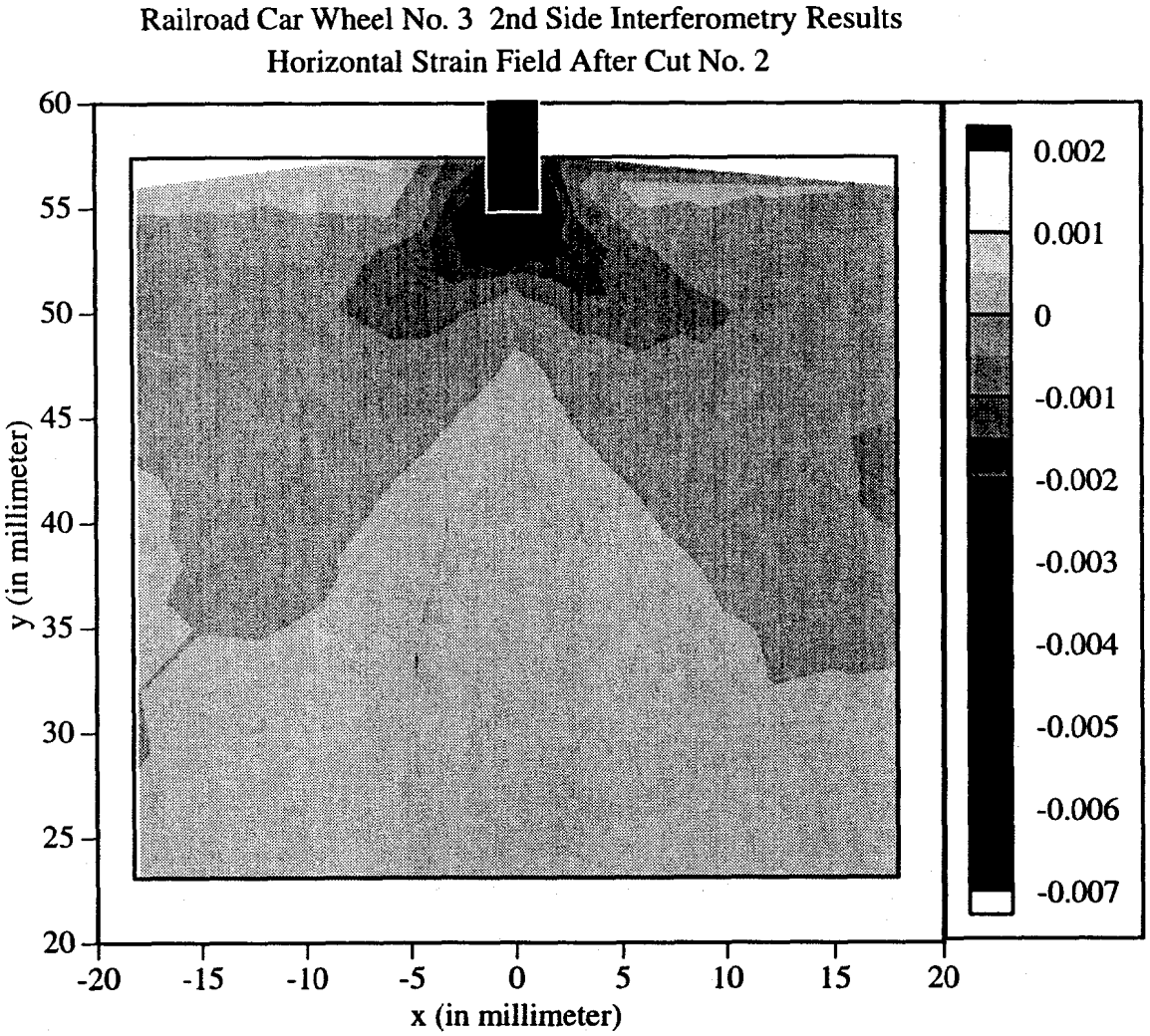
Railroad Car Wheel No. 3 2nd Side Interferometry Results
Horizontal Strain Field After Cut No. 2
60
55
50
45
40
35
30
25
20
y (in millimeter)
-20
-15
-10
-5
0
5
10
15
20
x (in millimeter)
0.002
0.001
0
-0.001
-0.002
-0.003
-0.004
-0.005
-0.006
-0.007

Railroad Car Wheel No. 3 2nd Side Interferometry Results
Vertical Strain Field After Cut No. 2

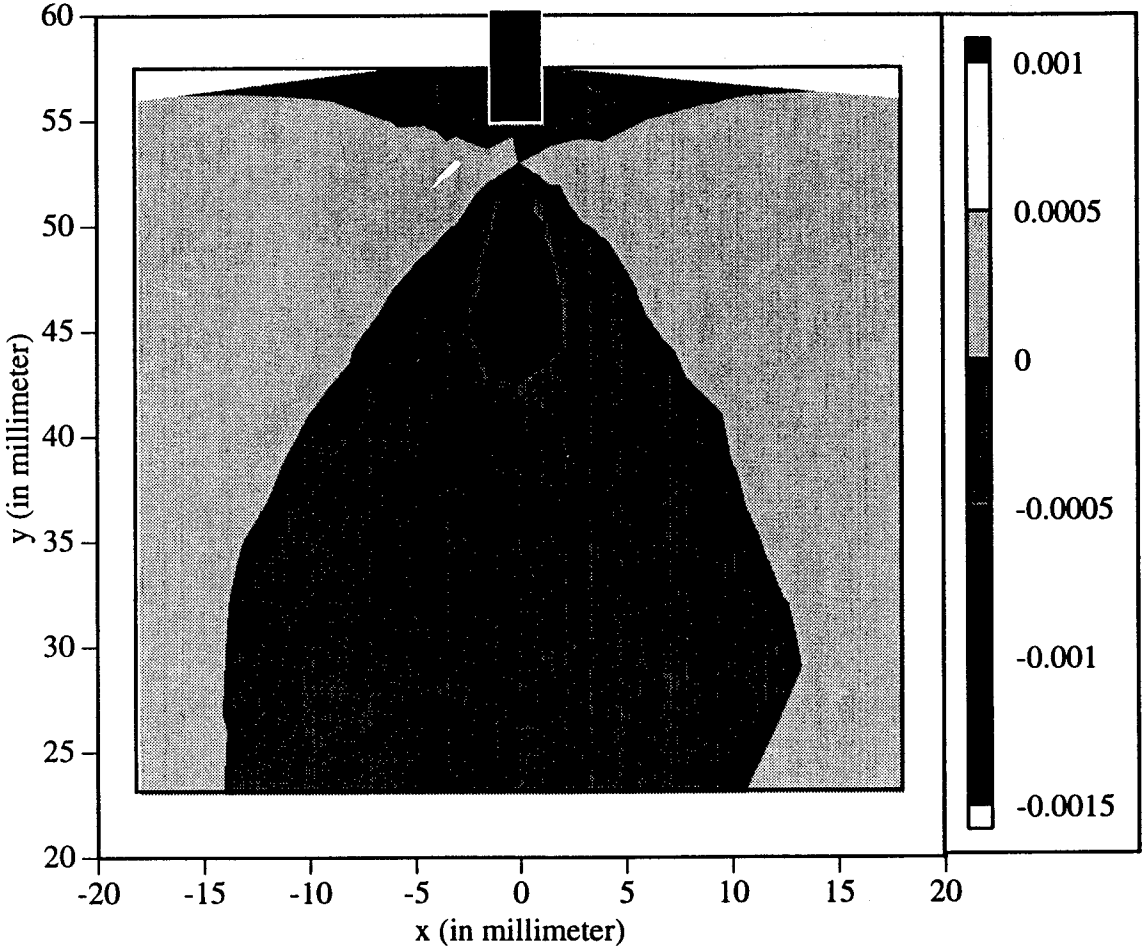

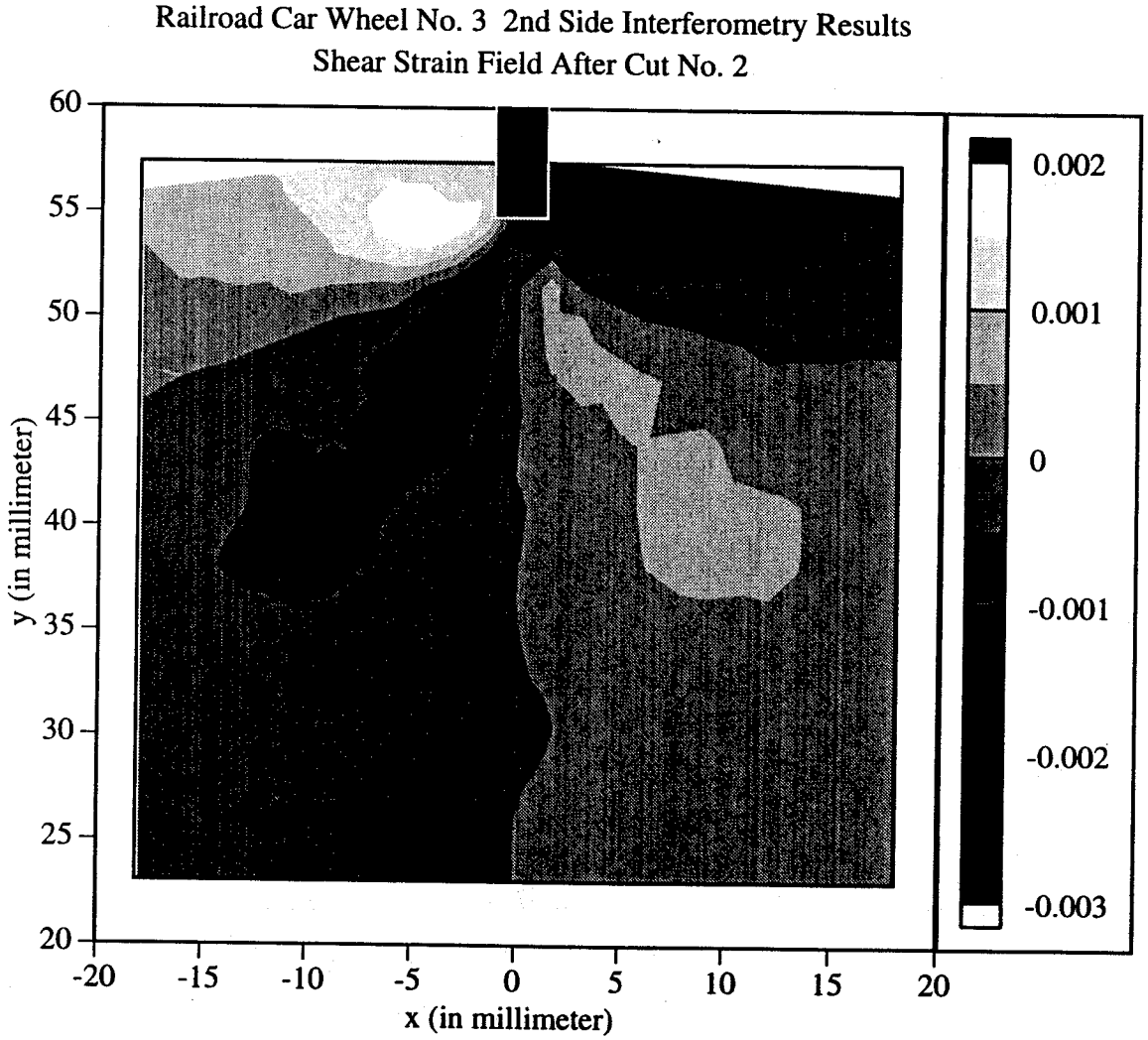
Railroad Car Wheel No. 3 2nd Side Interferometry Results
Shear Strain Field After Cut No. 2
60
55
50
45
40
35
30
25
20
y (in millimeter)
-20
-15
-10
-5
0
5
10
15
20
x (in millimeter)
0.002
0.001
0
-0.001
-0.002
-0.003

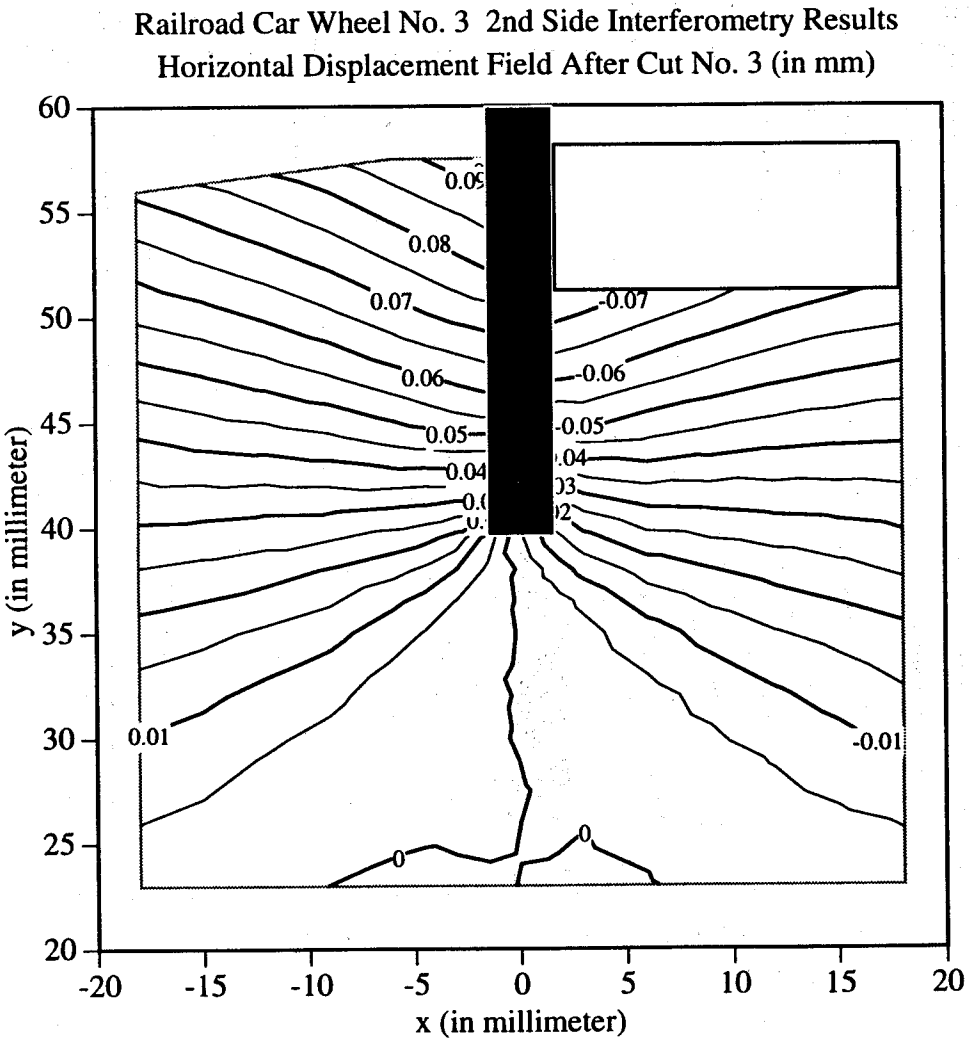
Railroad Car Wheel No. 3 2nd Side Interferometry Results
Horizontal Displacement Field After Cut No. 3 (in mm)
y (in millimeter)
x (in millimeter)
60
55
50
45
40
35
30
25
20
-20
-15
-10
-5
0
5
10
15
20
0.08
0.07
0.06
0.05
0.04
0.01
-0.07
-0.06
-0.05
-0.01
0

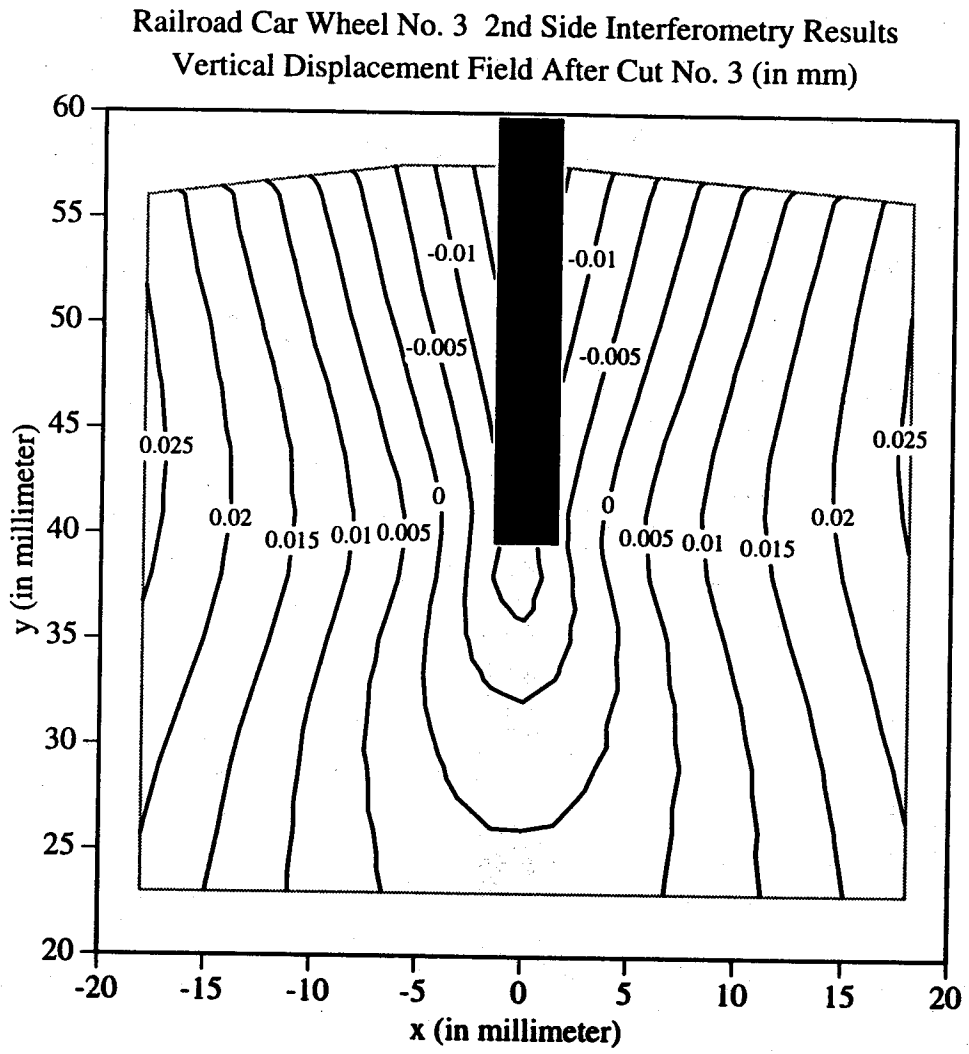
Railroad Car Wheel No. 3 2nd Side Interferometry Results
Vertical Displacement Field After Cut No. 3 (in mm)
y (in millimeter)
x (in millimeter)
60
55
50
45
40
35
30
25
20
-20
-15
-10
-5
0
5
10
15
20
-0.01
-0.01
-0.005
-0.005
0.025
0.025
0.02
0.02
0.015
0.015
0.01
0.01
0.005
0.005
0
0

Railroad Car Wheel No. 3 2nd Side Interferometry Results
Out-of-plane Displacement Field After Cut No. 3 (in mm)

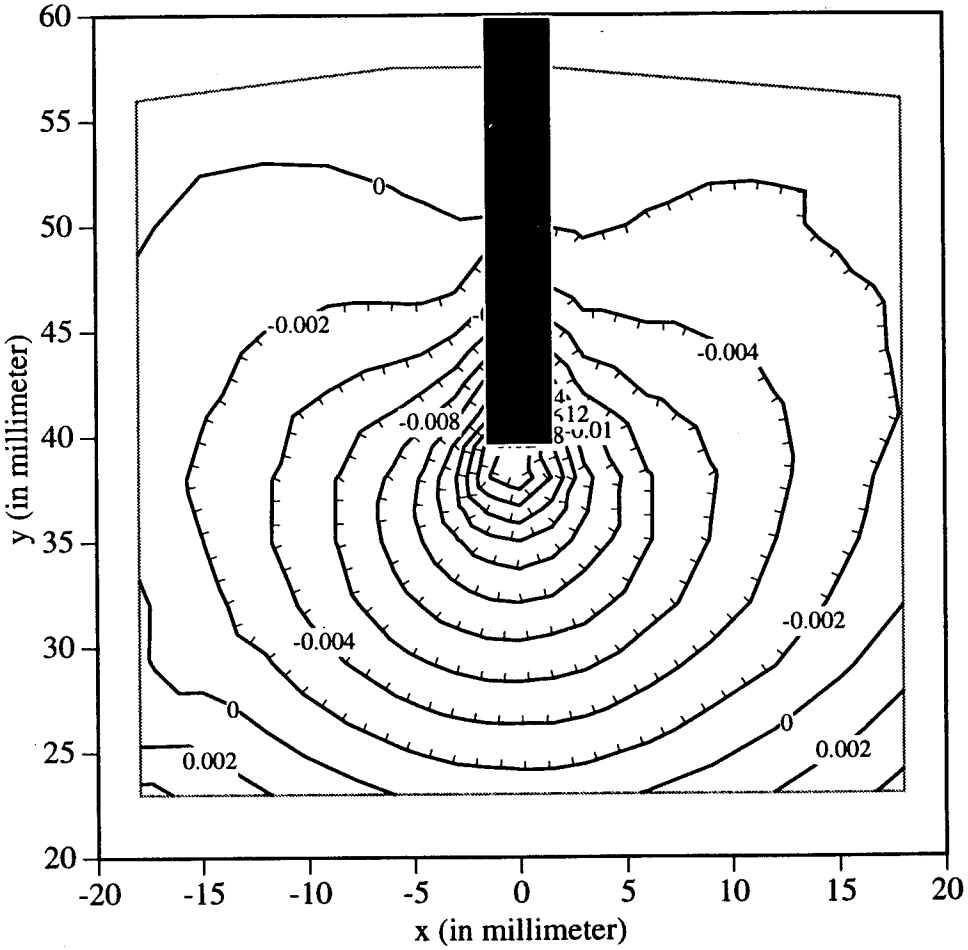

Railroad Car Wheel No. 3 2nd Side Interferometry Results
Horizontal Strain Field After Cut No. 3

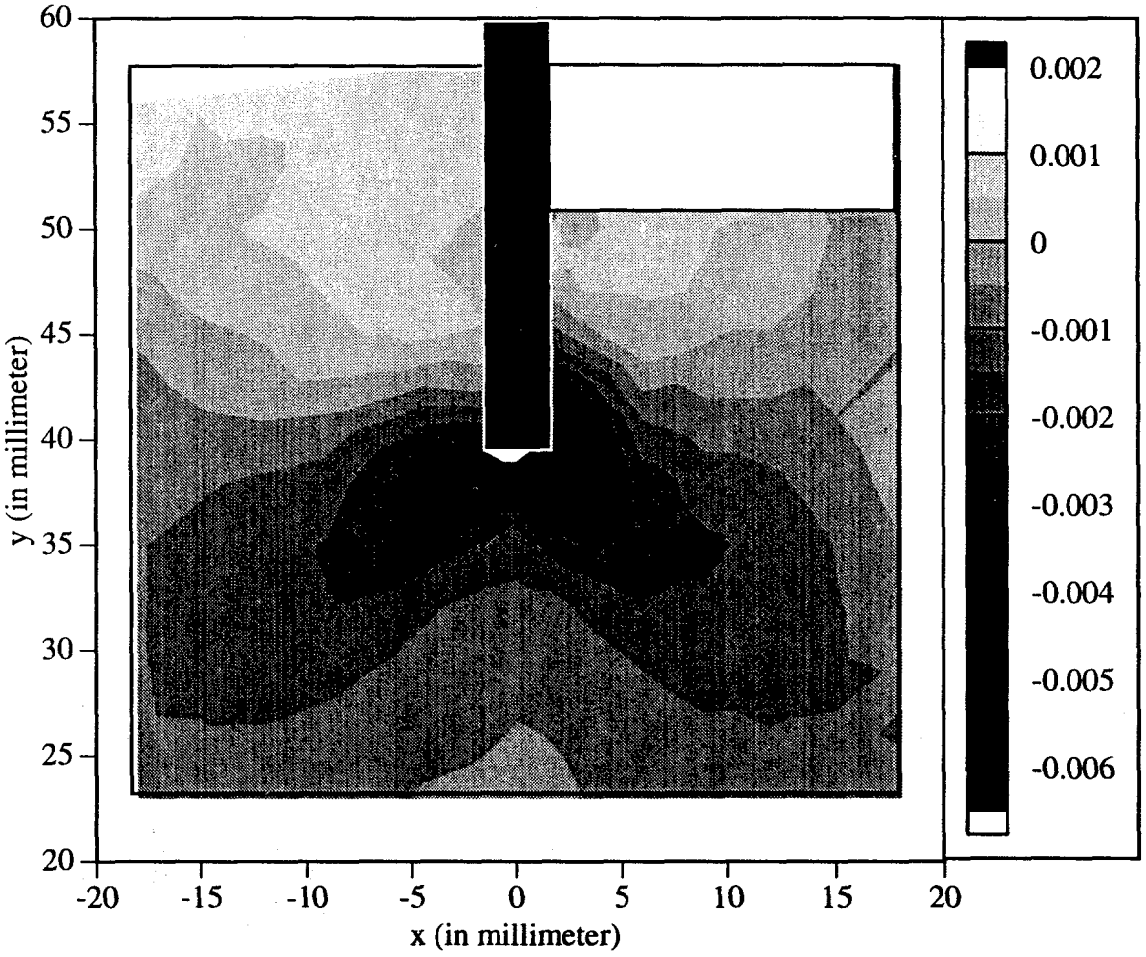

Railroad Car Wheel No. 3 2nd Side Interferometry Results
Vertical Strain Field After Cut No. 3

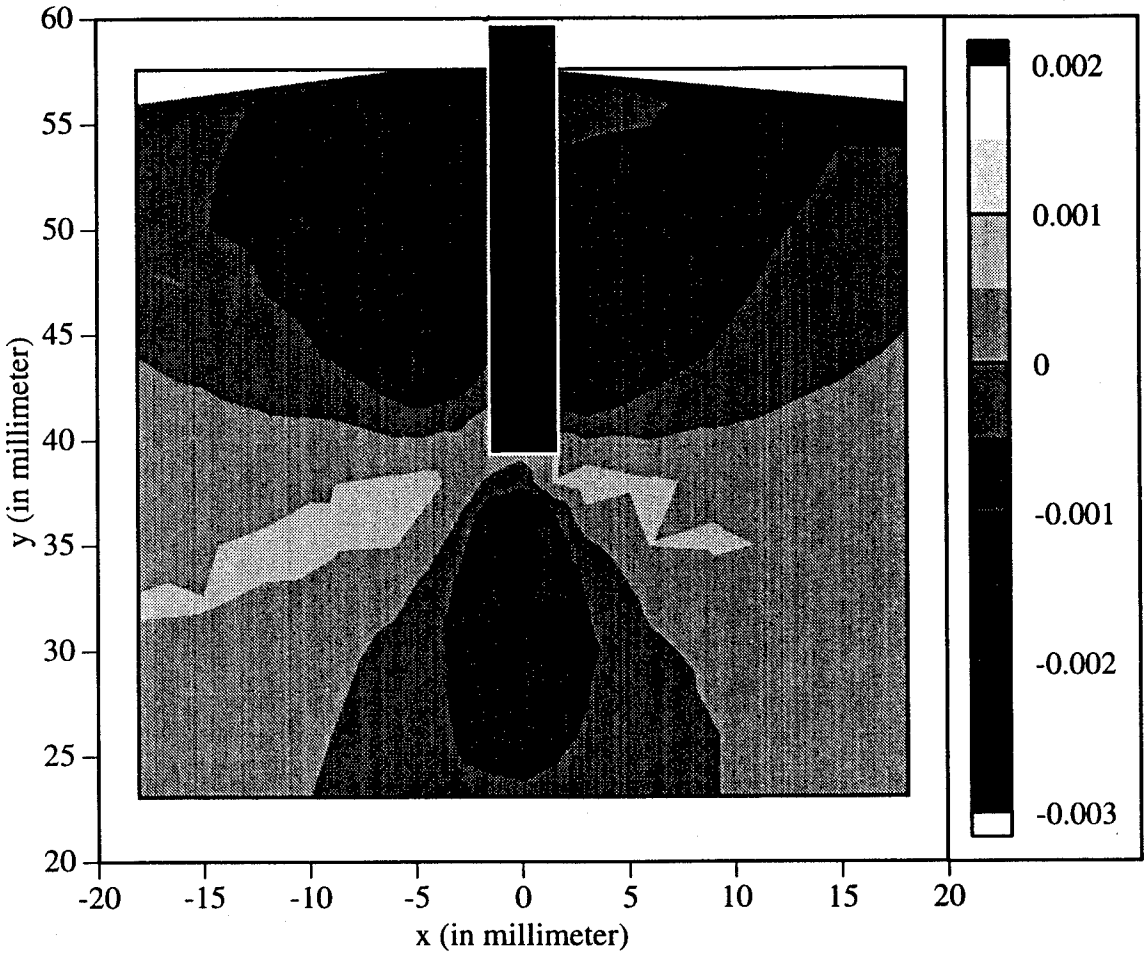

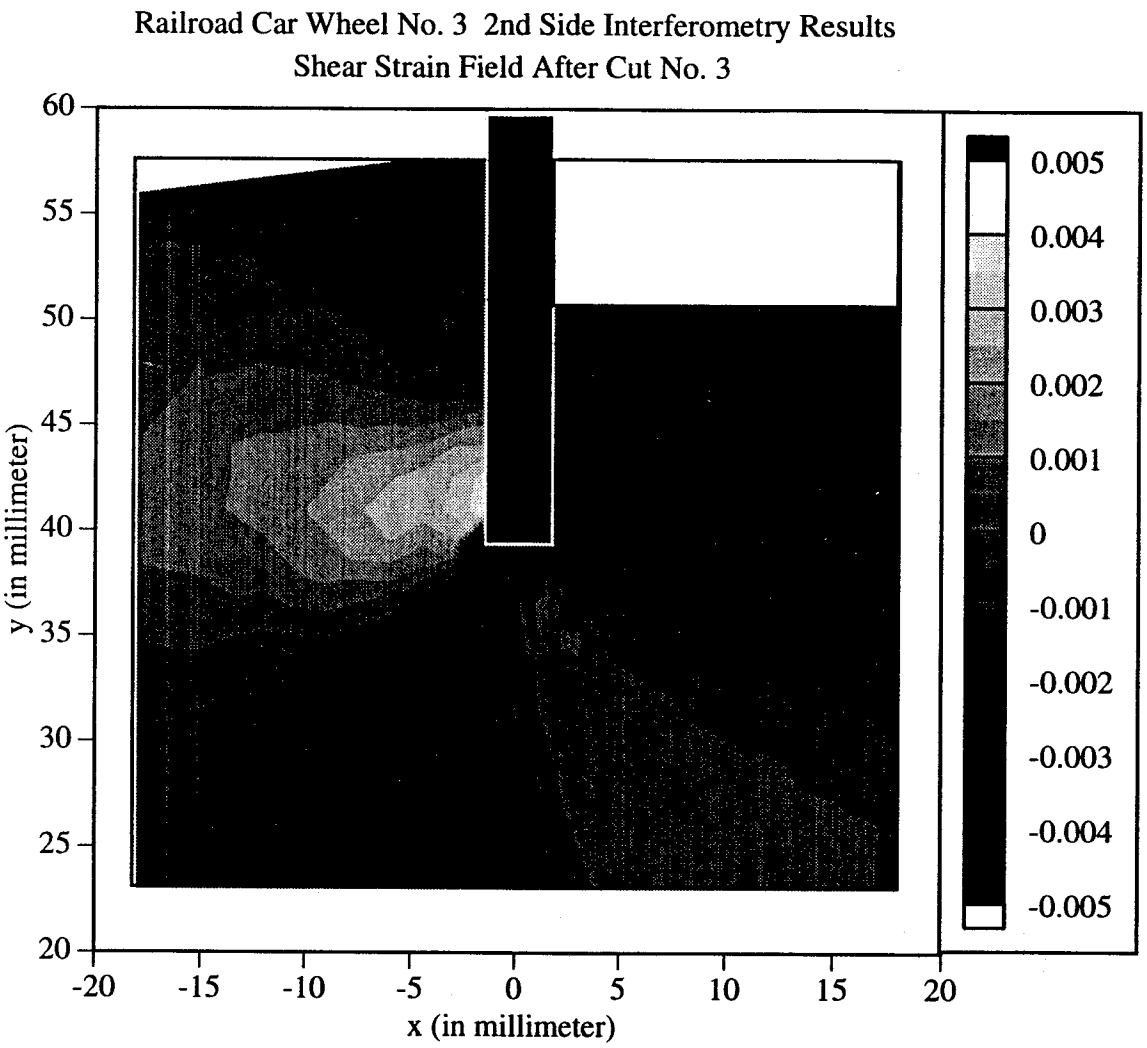
Railroad Car Wheel No. 3 2nd Side Interferometry Results
Shear Strain Field After Cut No. 3
y (in millimeter)
60
55
50
45
40
35
30
25
20
-20
-15
-10
-5
0
5
10
15
20
x (in millimeter)
0.005
0.004
0.003
0.002
0.001
0
-0.001
-0.002
-0.003
-0.004
-0.005

Page Intentionally Left Blank

Appendix 4. Wheel #4 Experimental Results

This appendix contains the results from the test on both sides (front and back rim faces) of the fourth wheel. All the data are in a local coordinate system that is located at the intersection of the inner edge of the rim and the cutting line; the vertical axis points away from the center of the wheel.

The attached figures show the location of all the sensors. At two points on the wheel, thermocouples (TC) measure the temperature difference (which never exceeded 1.7°C) immediately after each cut. The temperature at TC2, the one farther from the cut, was equal to the ambient temperature. The strain measurements were taken after the difference decreased to about 1°C or less at an ambient temperature in the range of 21°C to 23°C.

The extensometer, strain gage, and displacement sensor data are provided in tabular form. The interferometric data is provided in the form of contour maps and as data files in ASCII format for three specific cutting stages. The corresponding cut depths are 35 mm, 48 mm, and 63 mm.

The wheel was identified by the following markings:

44543-46
146

Location of strain gauges, thermocouples and gratings on wheel #4

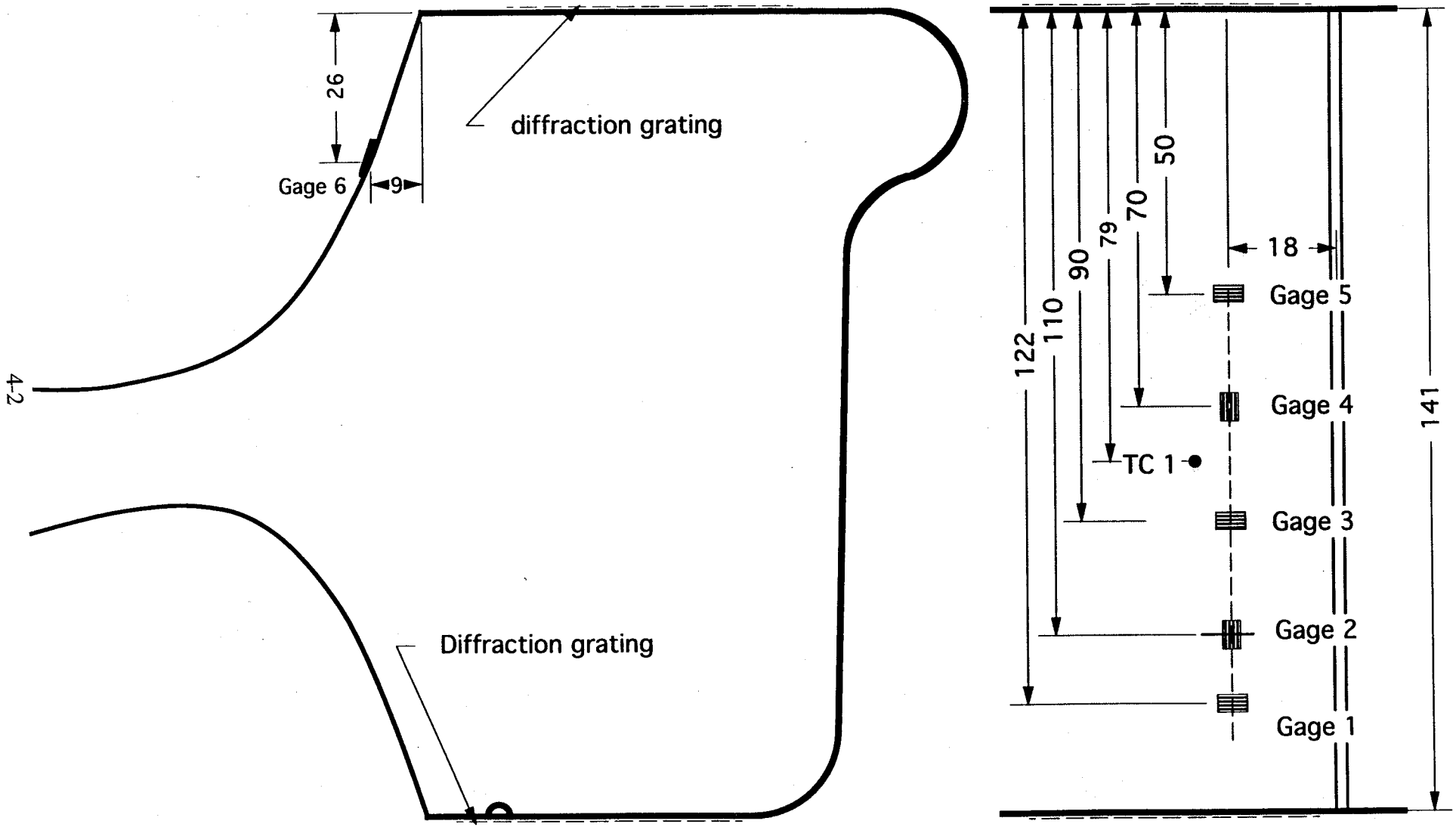

Gages 6 & 7 were located 20mm from the plane of the cut.

Location of displacement sensors thermocouples and gratings on wheel #4

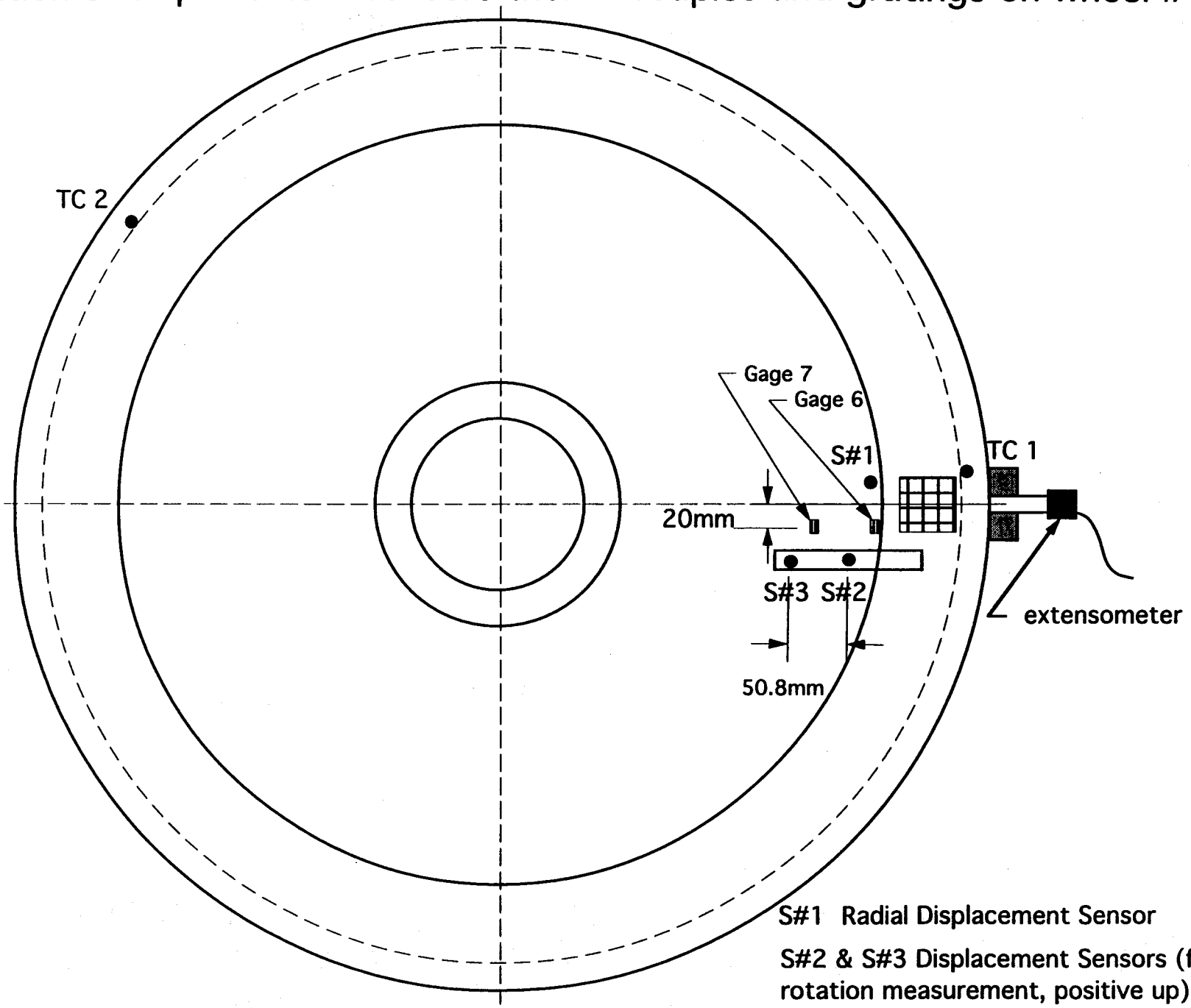

S#1 Radial Displacement Sensor

S#2 & S#3 Displacement Sensors (for rotation measurement, positive up)

WHEEL #4 TEST DATA

TESTING OF DOT RAILROAD CAR WHEEL #4							44543-46	146			
DATE:	17-May-95										
	mm/mm						mm	mm	rad	(°C)	(°C)
Cut Depth (mm)	Gage1	Gage2	Gage3	Gage4	Gage5	Gage6	Radial Displacement	Opening Displacement	Rotation	TC 1	TC 2
0	0	0	0	0	0	0	.000	.000	0.00E+00	22.9	22.9
28	-14	3	-37	22	-80	20	-.014	-.104	-2.36E-06	23.4	22.9
35	65	7	114	36	178	31	-.027	-.152	2.39E-05	23.7	22.9
48	654	-31	726	33	792	73	-.075	-.259	-7.10E-05	22.7	21.3
63	1122	-85	1085	1	1083	85	-.165	-.427	-1.19E-04	23.6	22.2
70	1185	-102	1132	-7	1119	29	-.213	-.505	-6.82E-05	23.5	22.9
80	1215	-135	1150	-33	1127	-162	-.283	-.615	-1.90E-04	NA	NA
90	1229	-161	1159	-57	1133	-501	-.350	-.723	-3.99E-04	24.4	22.9
100	1217	-191	1154	-99	1126	-739	-.428	-.826	-5.46E-04	24.4	23.0
110	1193	-187	1148	-131	1127	-722	-.542	-.920	-6.13E-04	24.7	23.0
120	1187	-180	1146	-134	1129	-776	-.621	-1.027	-9.28E-04	24.7	23.1
130	1187	-170	1147	-122	1135	-763	-.682	-1.136	-1.05E-03	24.5	23.1
140	1177	-172	1142	-125	1129	-759	-.733	-1.239	-1.28E-03	24.5	23.1
150	1172	-179	1132	-133	1121	-764	-.773	-1.319	-1.49E-03	24.5	23.1
wheel closed at bottom of the wheel (non-flange side)											
END											

Railroad Wheel No. 4 Test
Displacement vs. Cut Depth

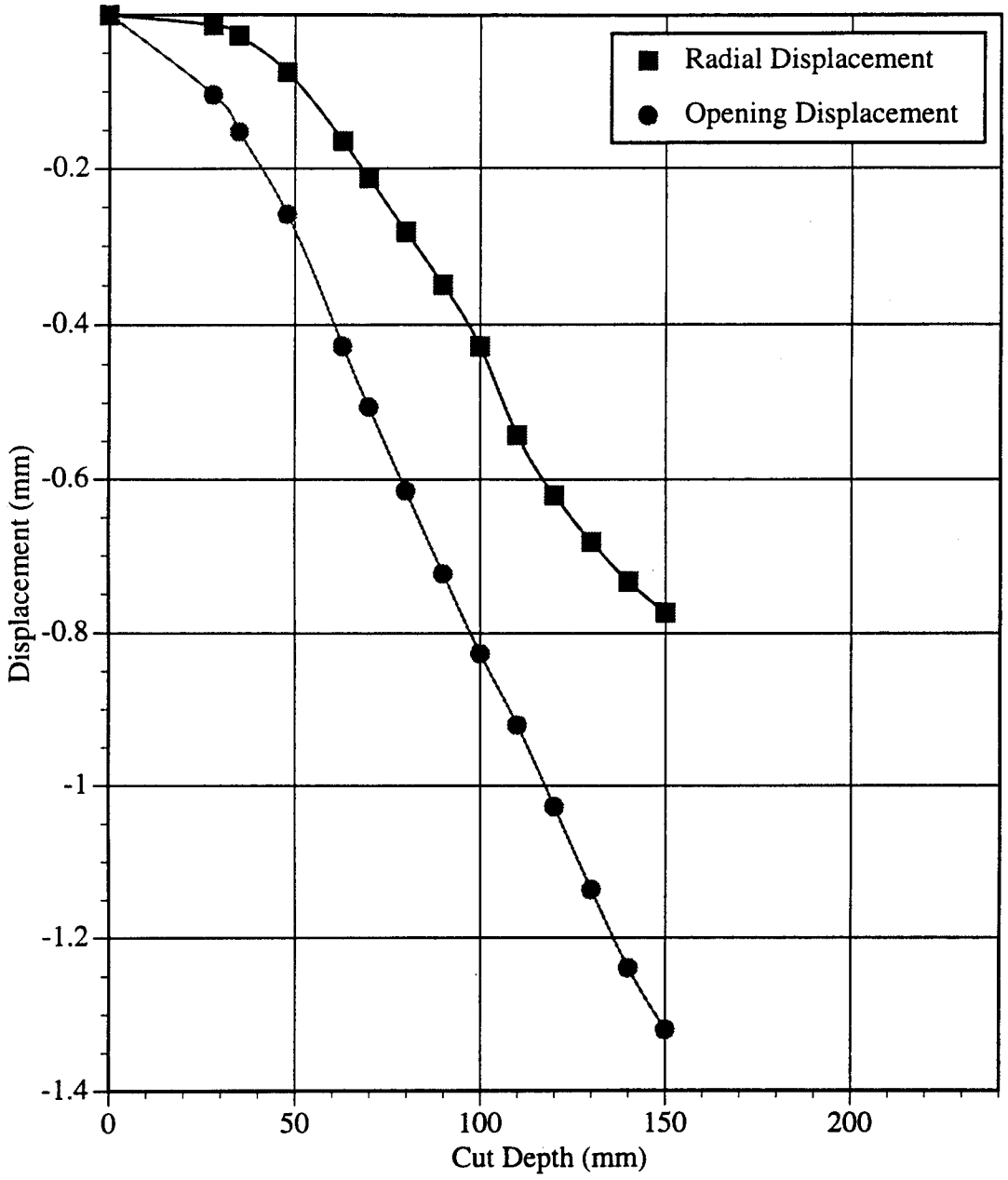

Railroad Wheel No. 4 Test
Strain Gage Readings vs. Cut Depth

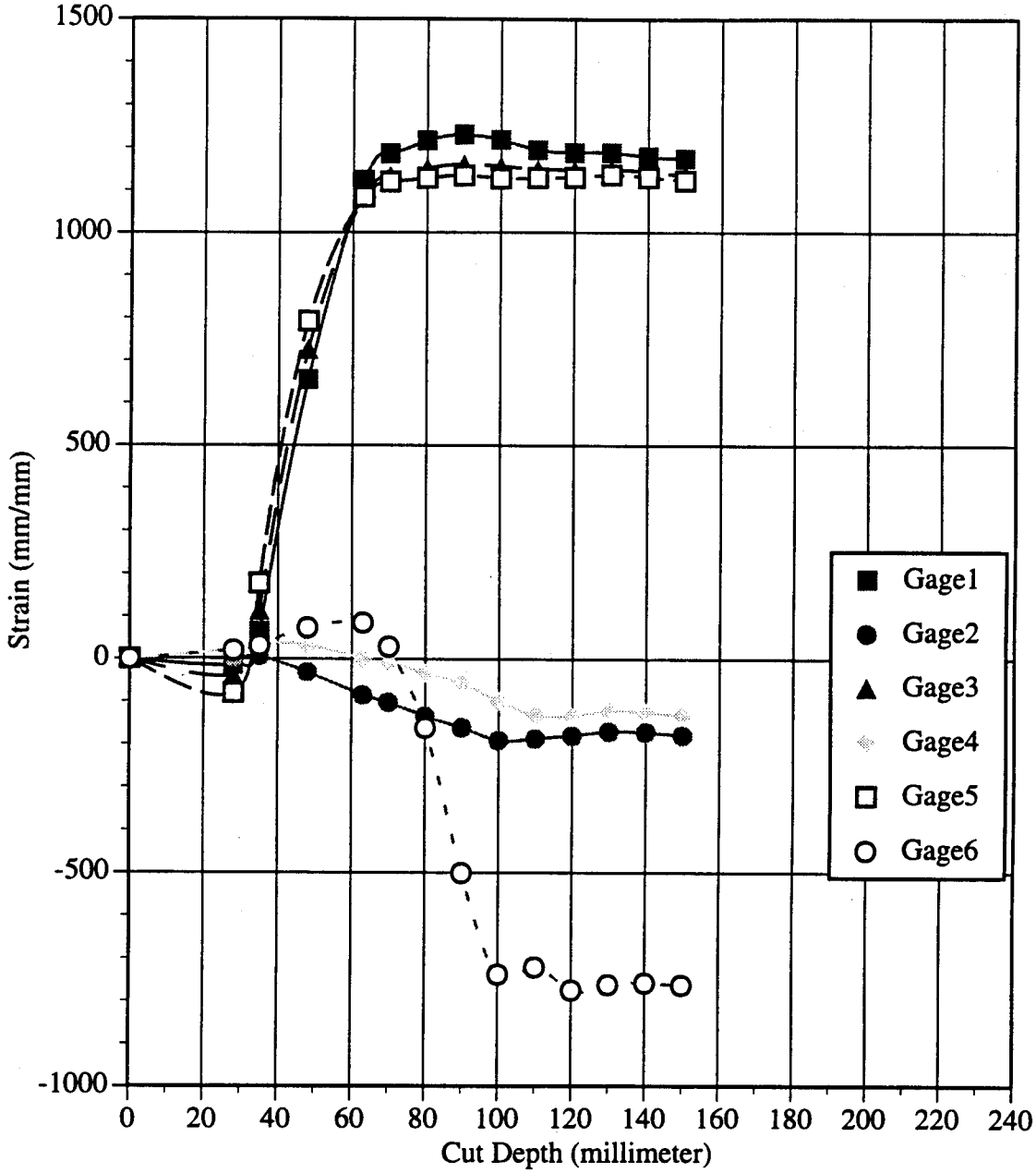

Railroad Wheel No. 4 Test
Wheel Rotation vs. Cut Depth

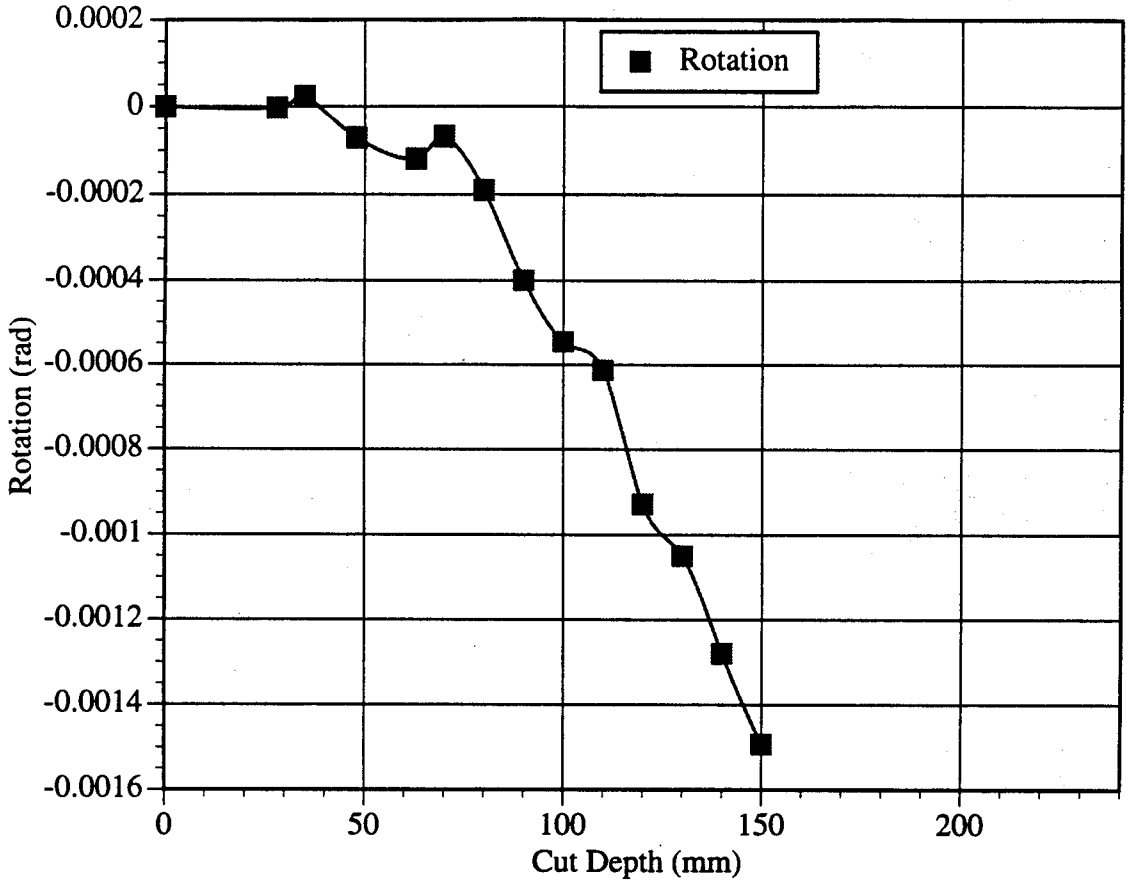

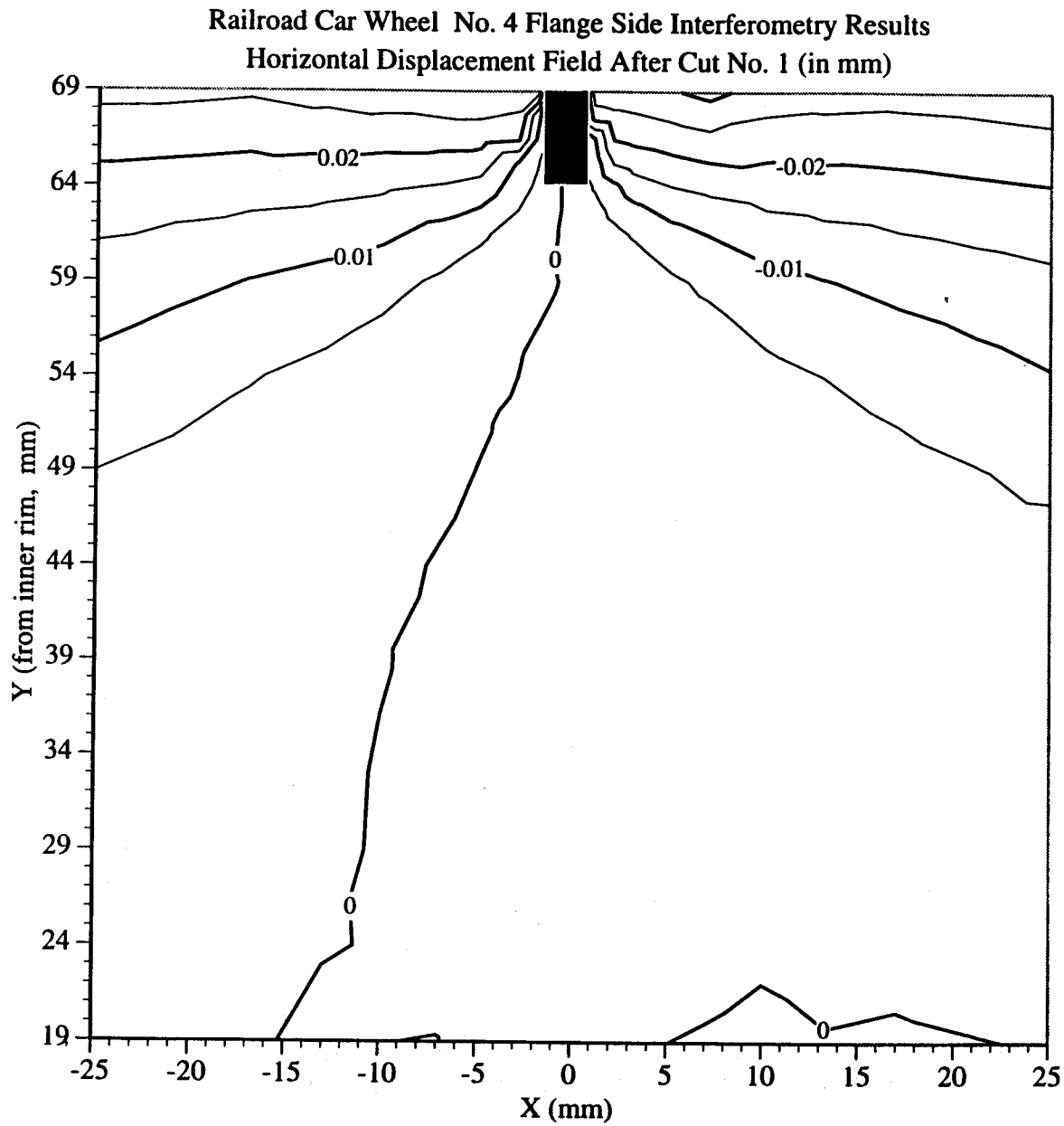
Railroad Car Wheel No. 4 Flange Side Interferometry Results
Horizontal Displacement Field After Cut No. 1 (in mm)
Y (from inner rim, mm)
X (mm)
69
64
59
54
49
44
39
34
29
24
19
-25
-20
-15
-10
-5
0
5
10
15
20
25
0.02
-0.02
0.01
-0.01
0
0
0
0

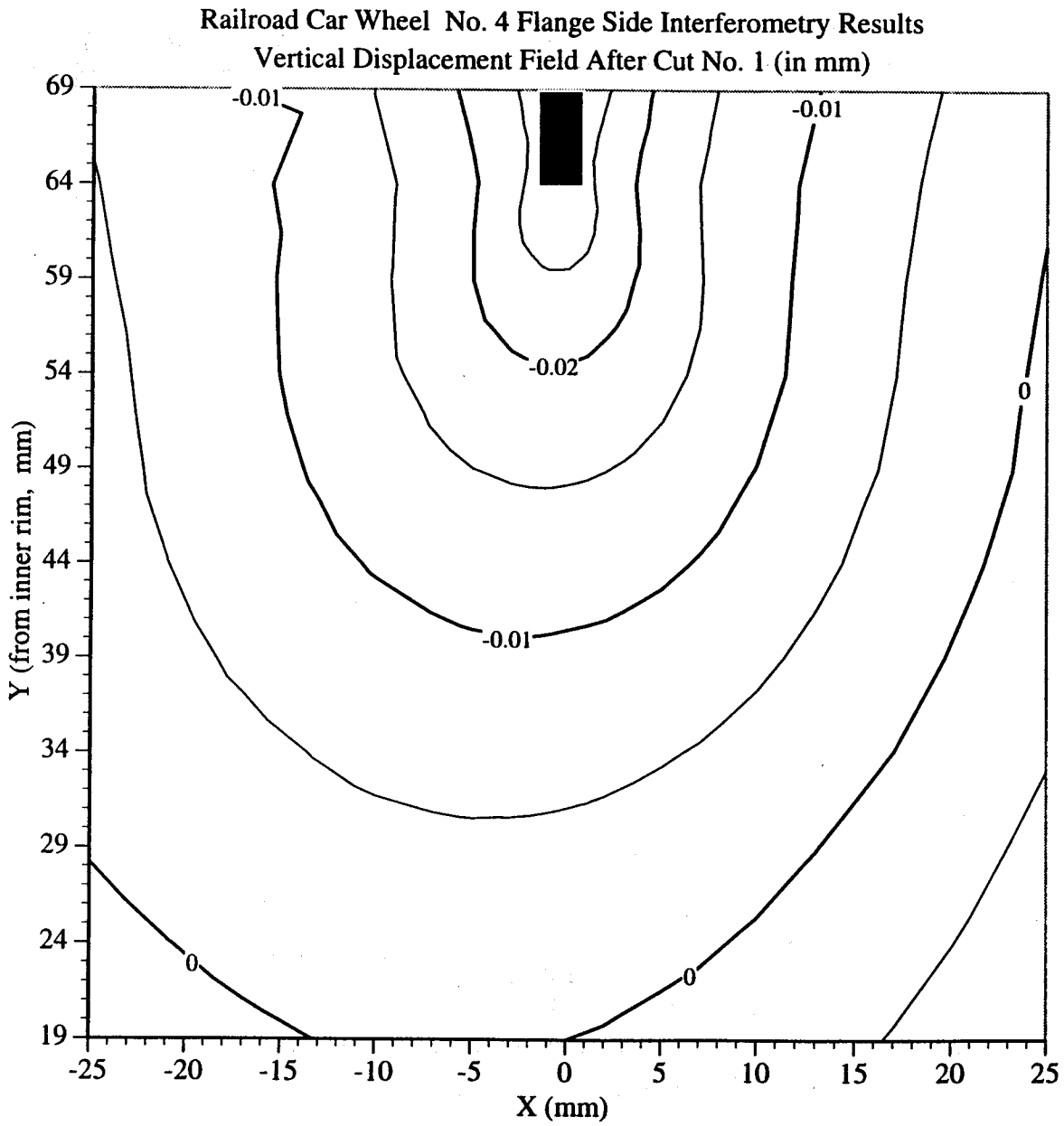
Railroad Car Wheel No. 4 Flange Side Interferometry Results
Vertical Displacement Field After Cut No. 1 (in mm)
Y (from inner rim, mm)
X (mm)
69
64
59
54
49
44
39
34
29
24
19
-25
-20
-15
-10
-5
0
5
10
15
20
25
-0.01
-0.01
-0.02
-0.01
0
0
0

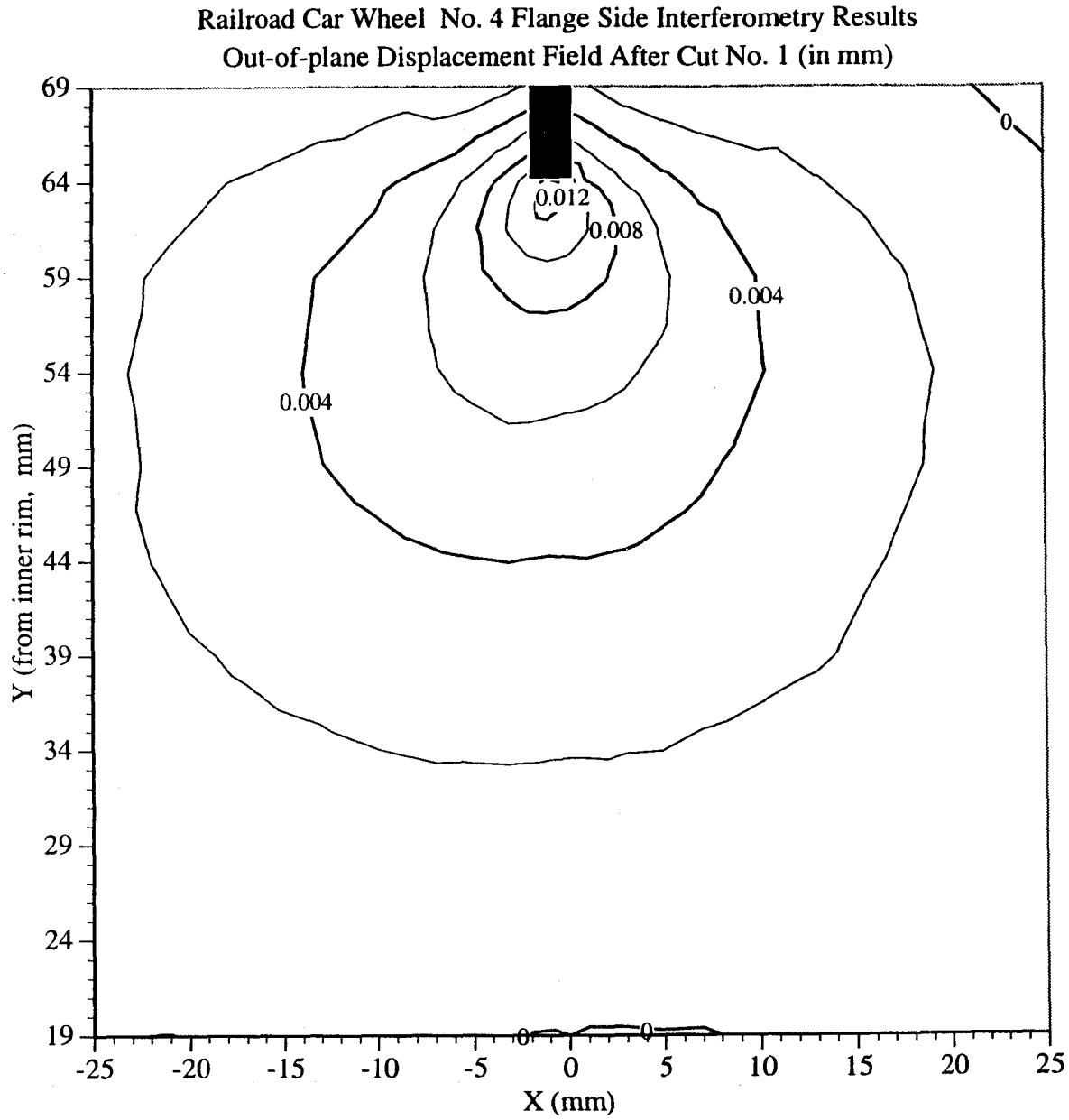
Railroad Car Wheel No. 4 Flange Side Interferometry Results
Out-of-plane Displacement Field After Cut No. 1 (in mm)
Y (from inner rim, mm)
X (mm)
69
64
59
54
49
44
39
34
29
24
19
-25
-20
-15
-10
-5
0
5
10
15
20
25
0.012
0.008
0.004
0.004
0
0
0

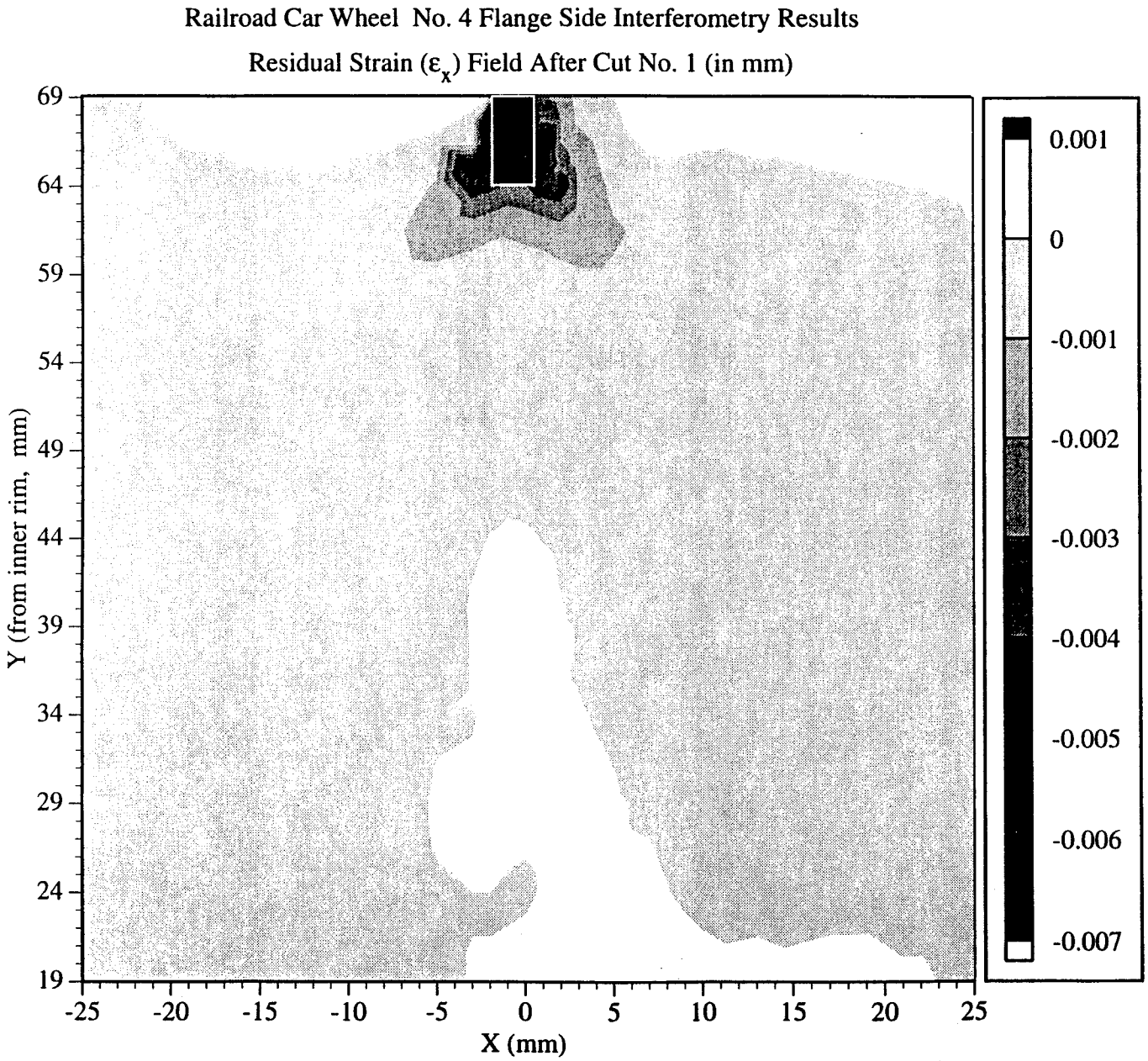
Railroad Car Wheel No. 4 Flange Side Interferometry Results
Residual Strain (ε_x) Field After Cut No. 1 (in mm)
Y (from inner rim, mm)
69
64
59
54
49
44
39
34
29
24
19
-25
-20
-15
-10
-5
0
5
10
15
20
25
X (mm)
0.001
0
-0.001
-0.002
-0.003
-0.004
-0.005
-0.006
-0.007

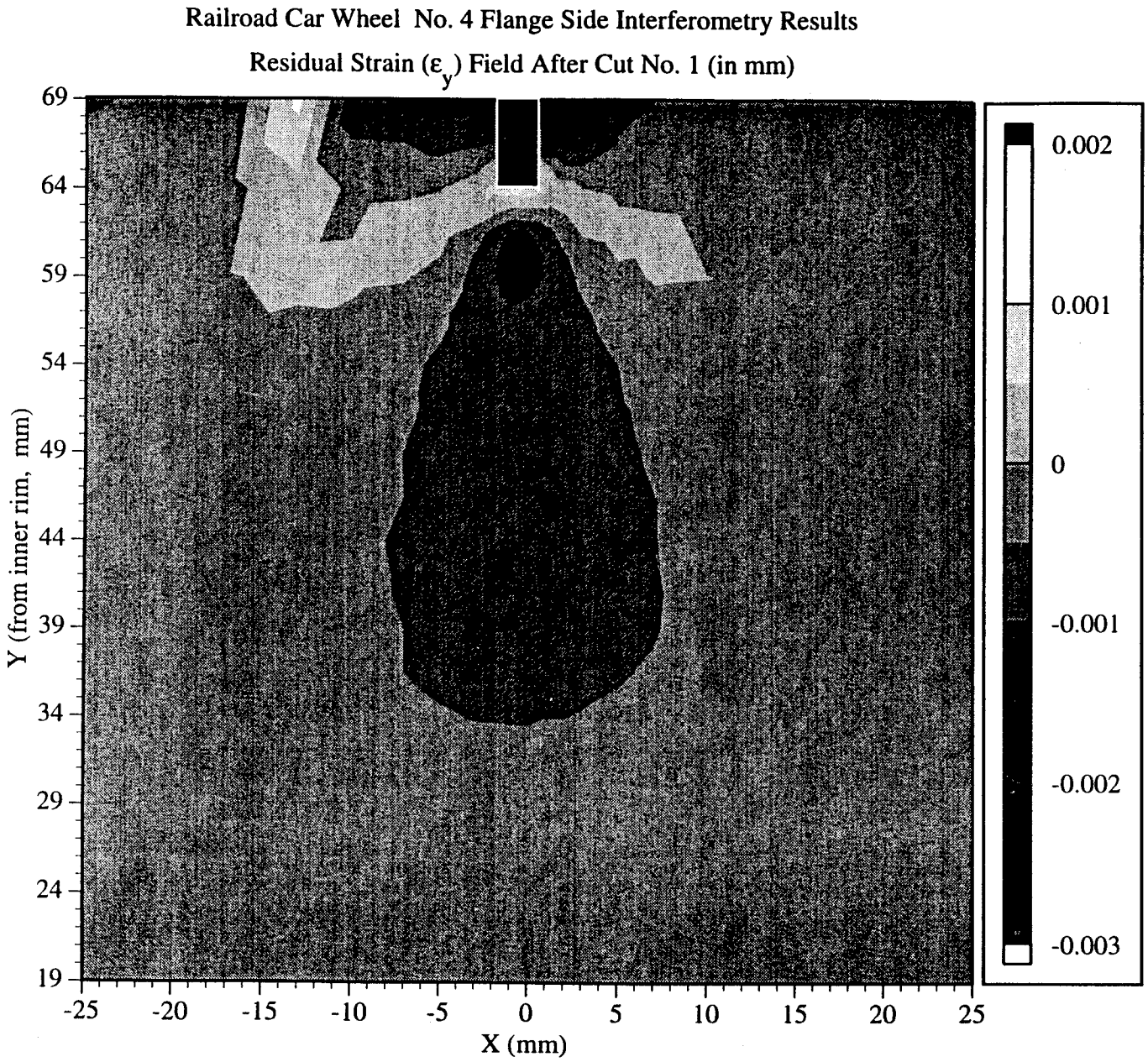
Railroad Car Wheel No. 4 Flange Side Interferometry Results
Residual Strain (ε_y) Field After Cut No. 1 (in mm)
Y (from inner rim, mm)
69
64
59
54
49
44
39
34
29
24
19
-25
-20
-15
-10
-5
0
5
10
15
20
25
X (mm)
0.002
0.001
0
-0.001
-0.002
-0.003

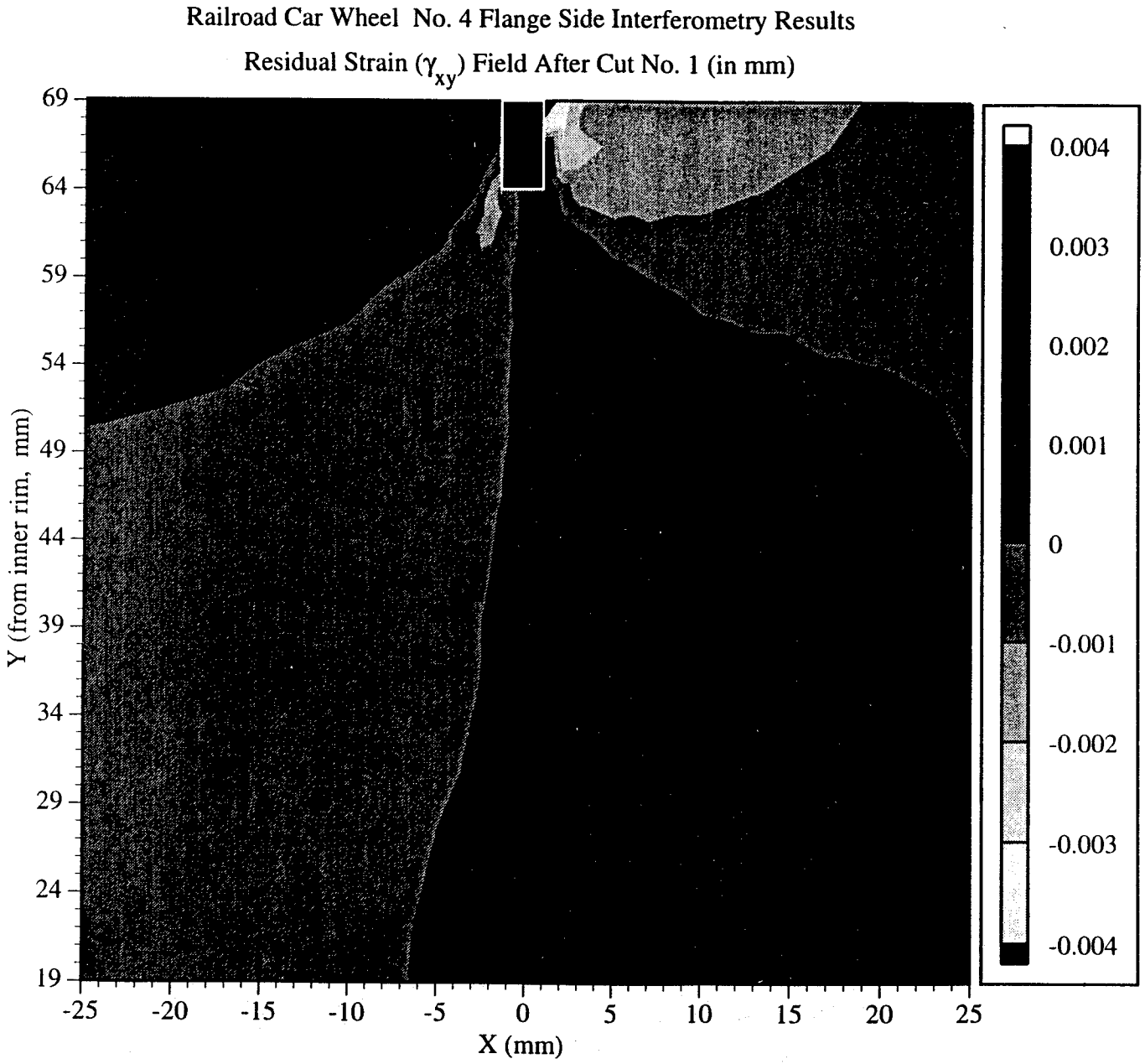
Railroad Car Wheel No. 4 Flange Side Interferometry Results
Residual Strain (γ_{xy}) Field After Cut No. 1 (in mm)
Y (from inner rim, mm)
69
64
59
54
49
44
39
34
29
24
19
-25
-20
-15
-10
-5
0
5
10
15
20
25
X (mm)
0.004
0.003
0.002
0.001
0
-0.001
-0.002
-0.003
-0.004

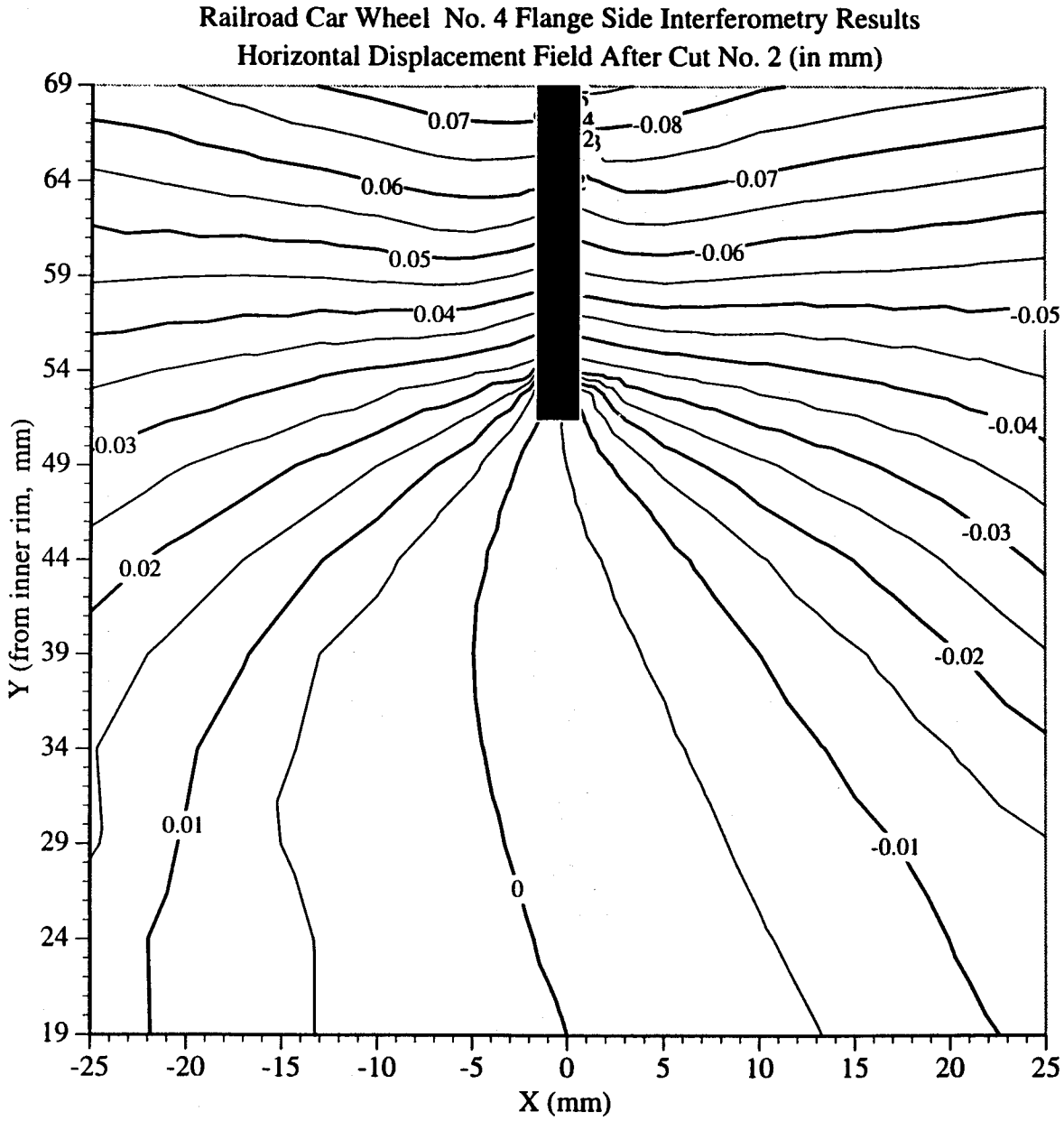
Railroad Car Wheel No. 4 Flange Side Interferometry Results
Horizontal Displacement Field After Cut No. 2 (in mm)
Y (from inner rim, mm)
X (mm)
69
64
59
54
49
44
39
34
29
24
19
-25
-20
-15
-10
-5
0
5
10
15
20
25
0.07
0.06
0.05
0.04
0.03
0.02
0.01
0
-0.08
-0.07
-0.06
-0.05
-0.04
-0.03
-0.02
-0.01

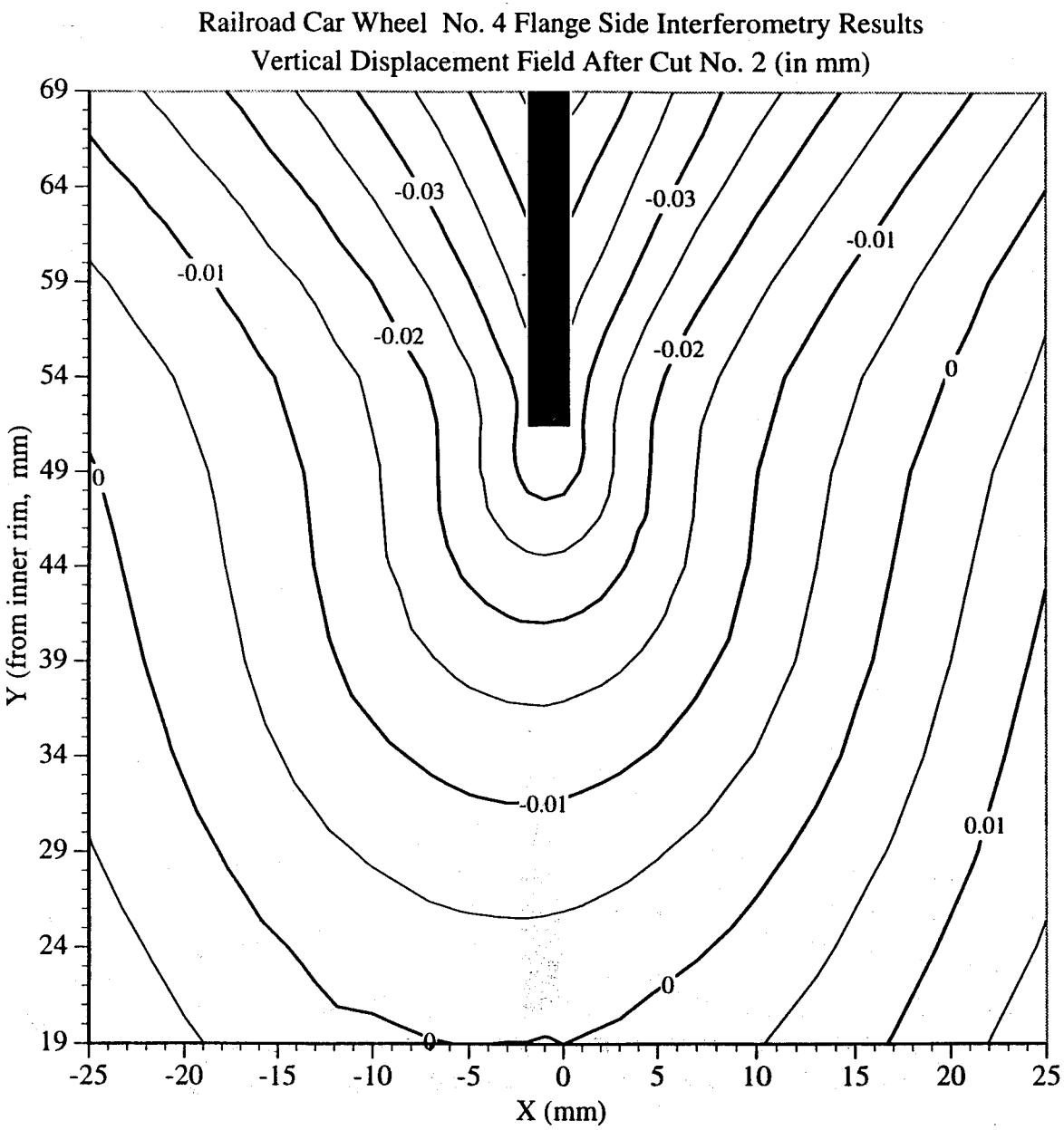
Railroad Car Wheel No. 4 Flange Side Interferometry Results
Vertical Displacement Field After Cut No. 2 (in mm)
Y (from inner rim, mm)
X (mm)
69
64
59
54
49
44
39
34
29
24
19
-25
-20
-15
-10
-5
0
5
10
15
20
25
-0.03
-0.03
-0.01
-0.01
-0.02
-0.02
0
0
-0.01
0.01
0
0

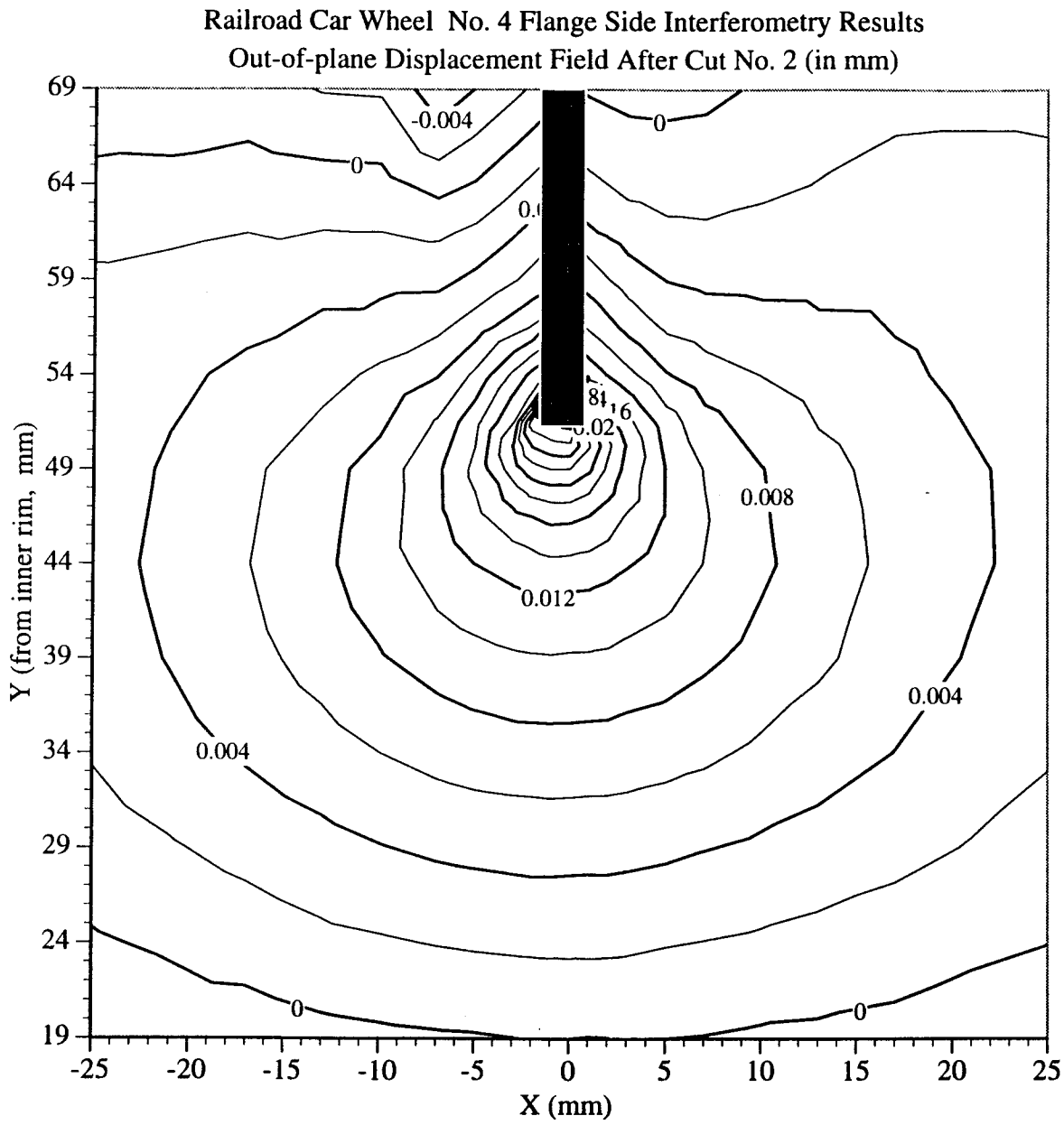
Railroad Car Wheel No. 4 Flange Side Interferometry Results
Out-of-plane Displacement Field After Cut No. 2 (in mm)
Y (from inner rim, mm)
X (mm)
69
64
59
54
49
44
39
34
29
24
19
-25
-20
-15
-10
-5
0
5
10
15
20
25
-0.004
0
0.008
0.012
0.004
0.004
0
0

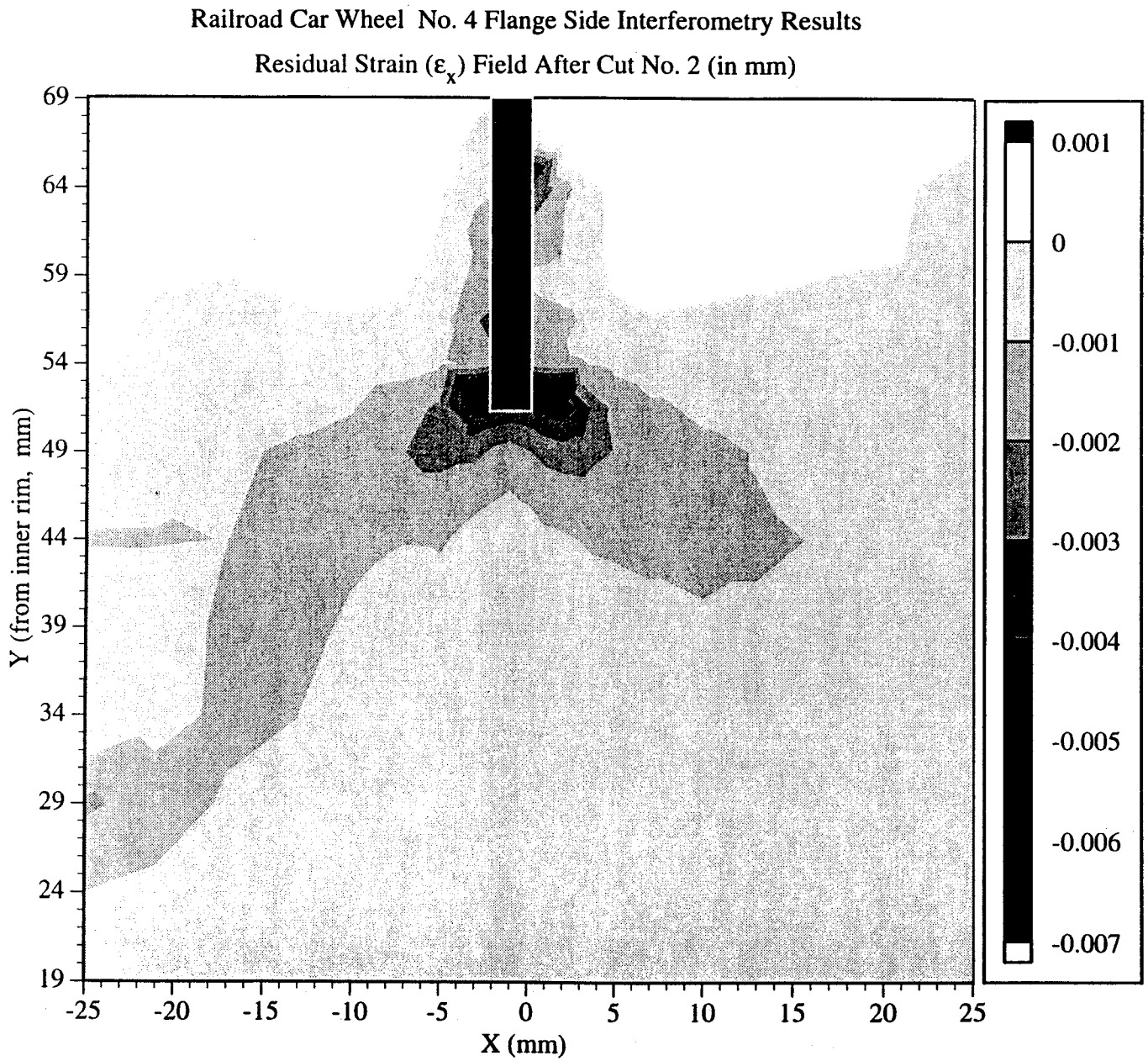
Railroad Car Wheel No. 4 Flange Side Interferometry Results
Residual Strain (ε_x) Field After Cut No. 2 (in mm)
Y (from inner rim, mm)
69
64
59
54
49
44
39
34
29
24
19
-25
-20
-15
-10
-5
0
5
10
15
20
25
X (mm)
0.001
0
-0.001
-0.002
-0.003
-0.004
-0.005
-0.006
-0.007

Railroad Car Wheel No. 4 Flange Side Interferometry Results

Residual Strain (ε_y) Field After Cut No. 2 (in mm)

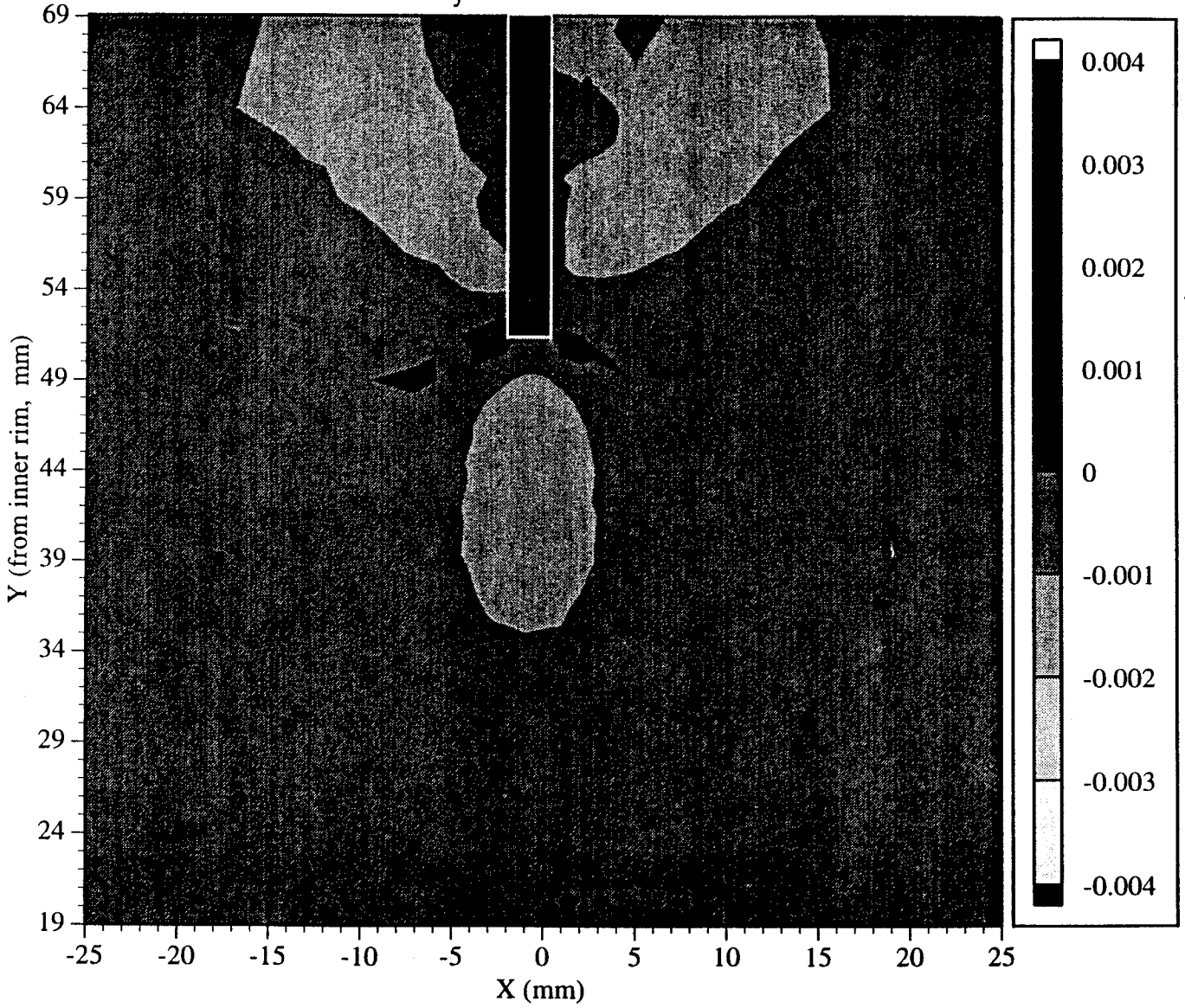

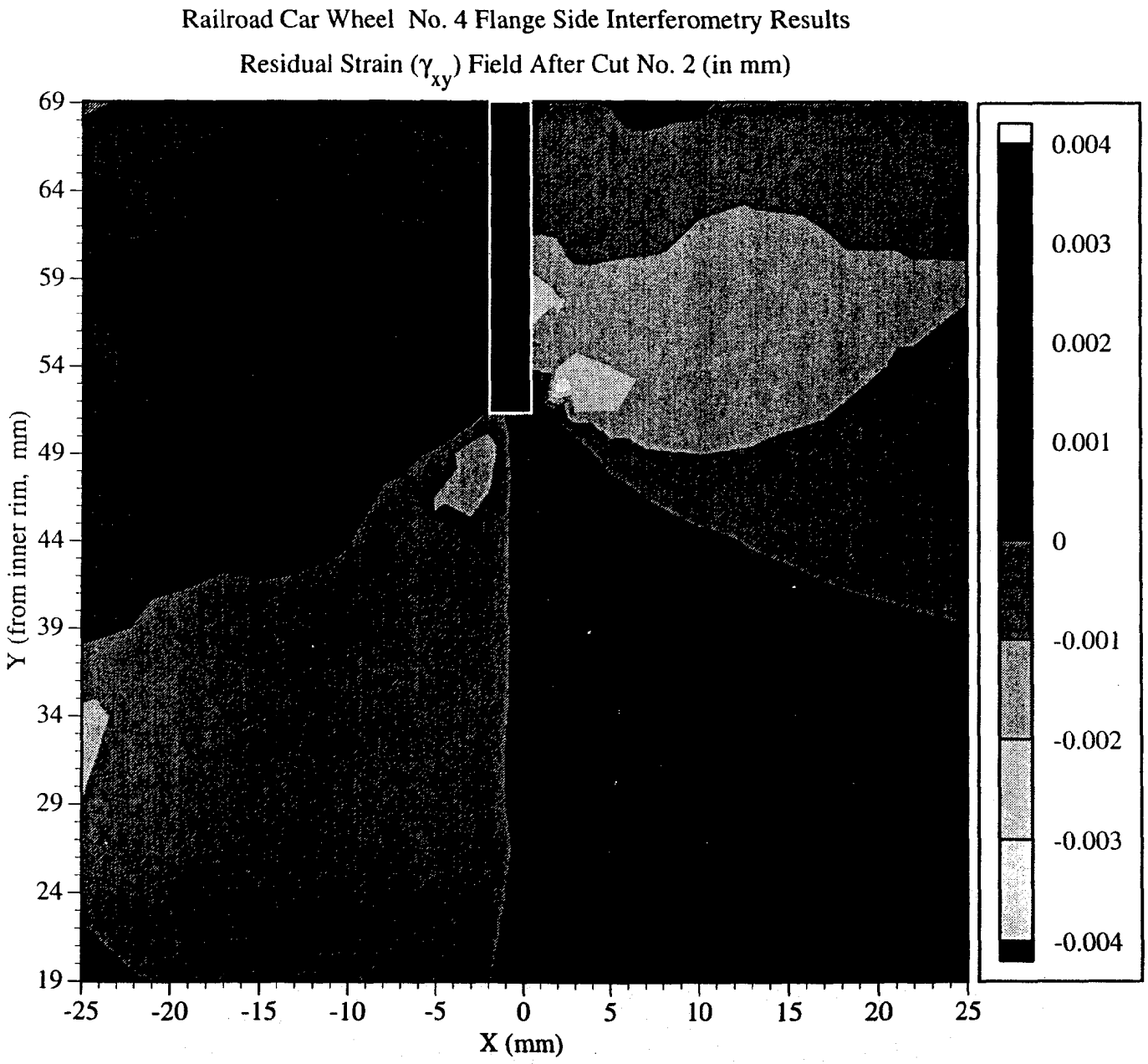
Railroad Car Wheel No. 4 Flange Side Interferometry Results
Residual Strain (γ_{xy}) Field After Cut No. 2 (in mm)
Y (from inner rim, mm)
69
64
59
54
49
44
39
34
29
24
19
-25
-20
-15
-10
-5
0
5
10
15
20
25
X (mm)
0.004
0.003
0.002
0.001
0
-0.001
-0.002
-0.003
-0.004

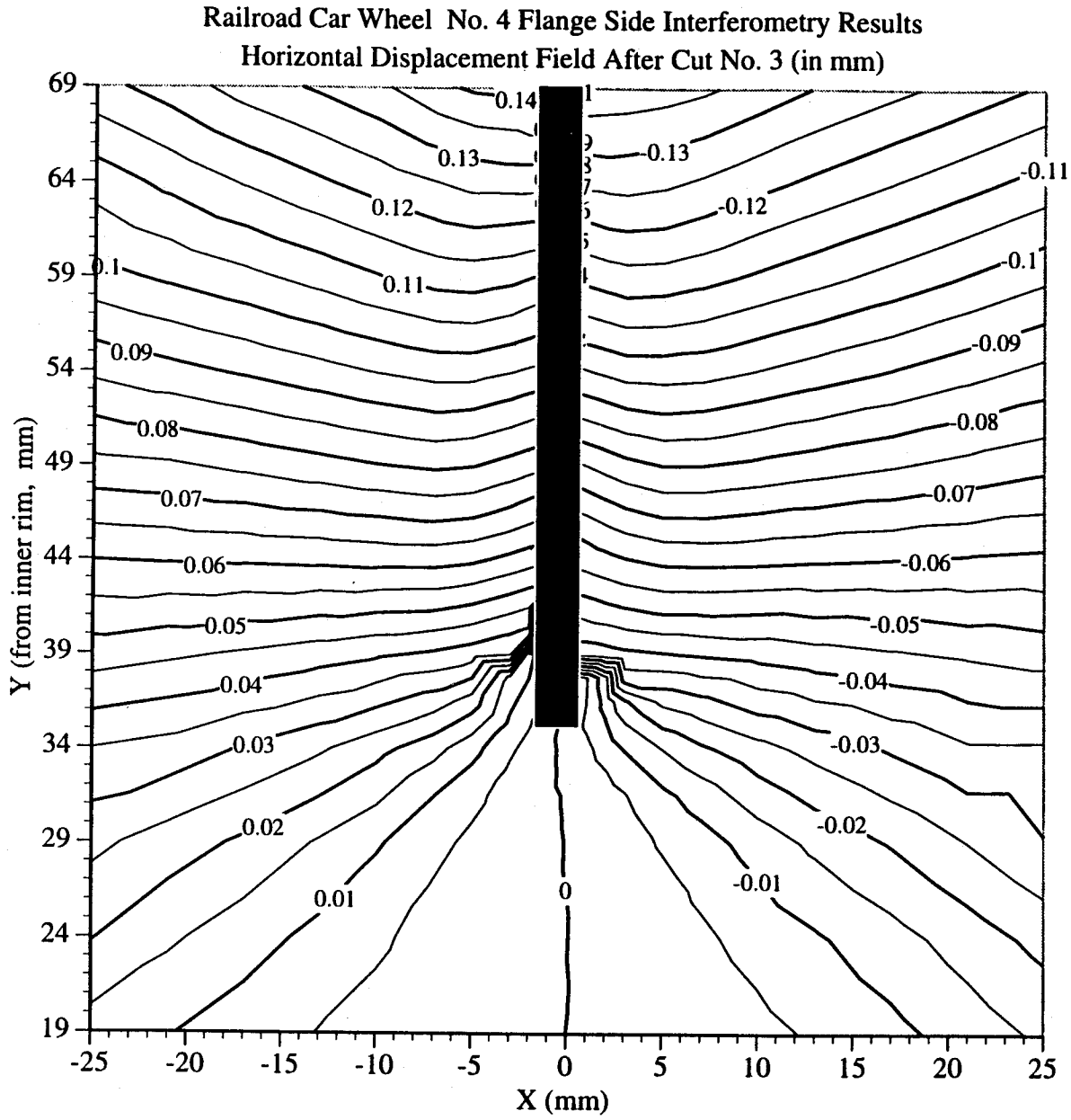
Railroad Car Wheel No. 4 Flange Side Interferometry Results
Horizontal Displacement Field After Cut No. 3 (in mm)
Y (from inner rim, mm)
X (mm)
69
64
59
54
49
44
39
34
29
24
19
-25
-20
-15
-10
-5
0
5
10
15
20
25
0.14
0.13
0.12
0.11
0.1
0.09
0.08
0.07
0.06
0.05
0.04
0.03
0.02
0.01
0
-0.13
-0.12
-0.11
-0.1
-0.09
-0.08
-0.07
-0.06
-0.05
-0.04
-0.03
-0.02
-0.01

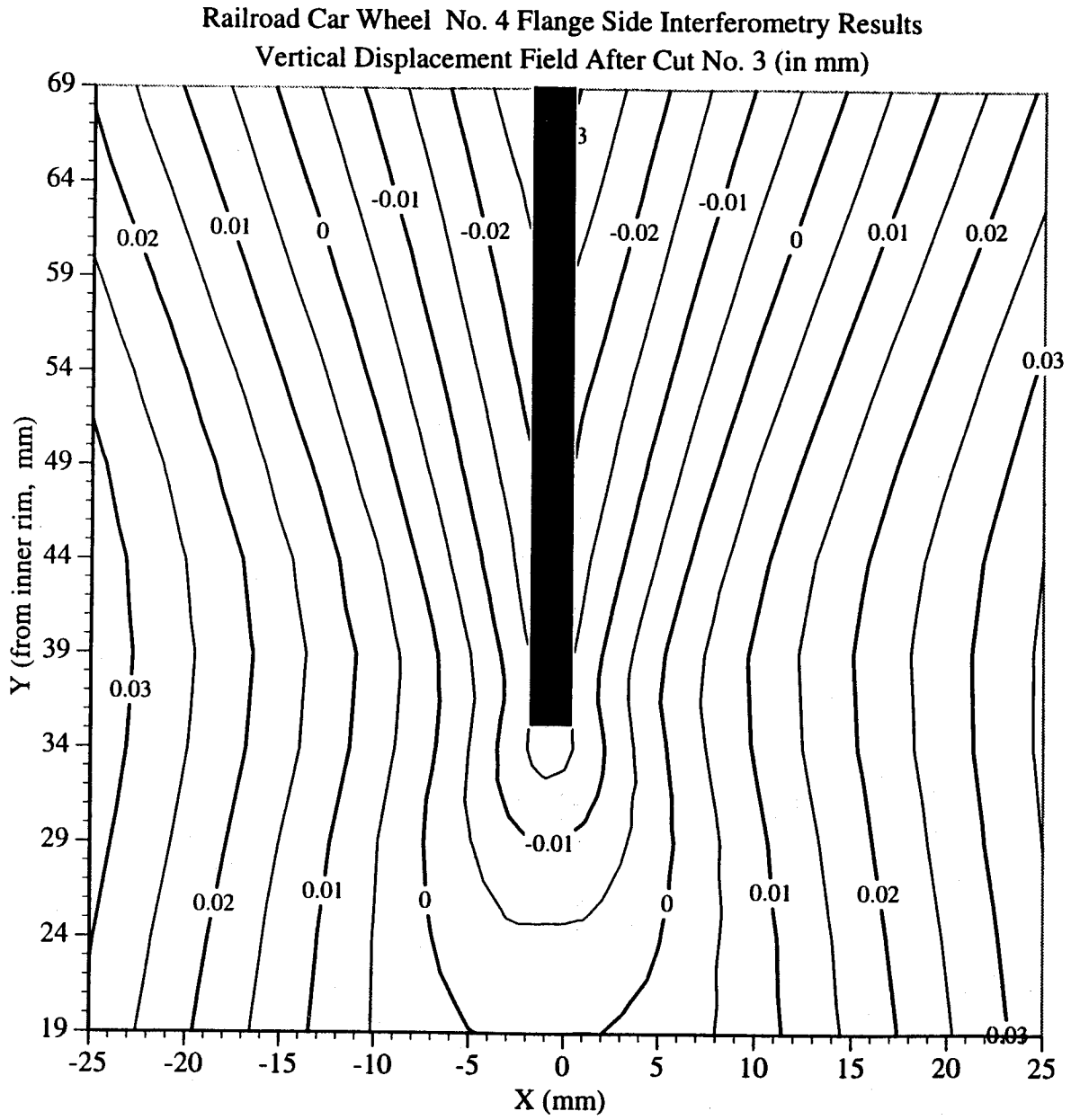
Railroad Car Wheel No. 4 Flange Side Interferometry Results
Vertical Displacement Field After Cut No. 3 (in mm)
Y (from inner rim, mm)
X (mm)
69
64
59
54
49
44
39
34
29
24
19
-25
-20
-15
-10
-5
0
5
10
15
20
25
0.02
0.01
0
-0.01
-0.02
0.03

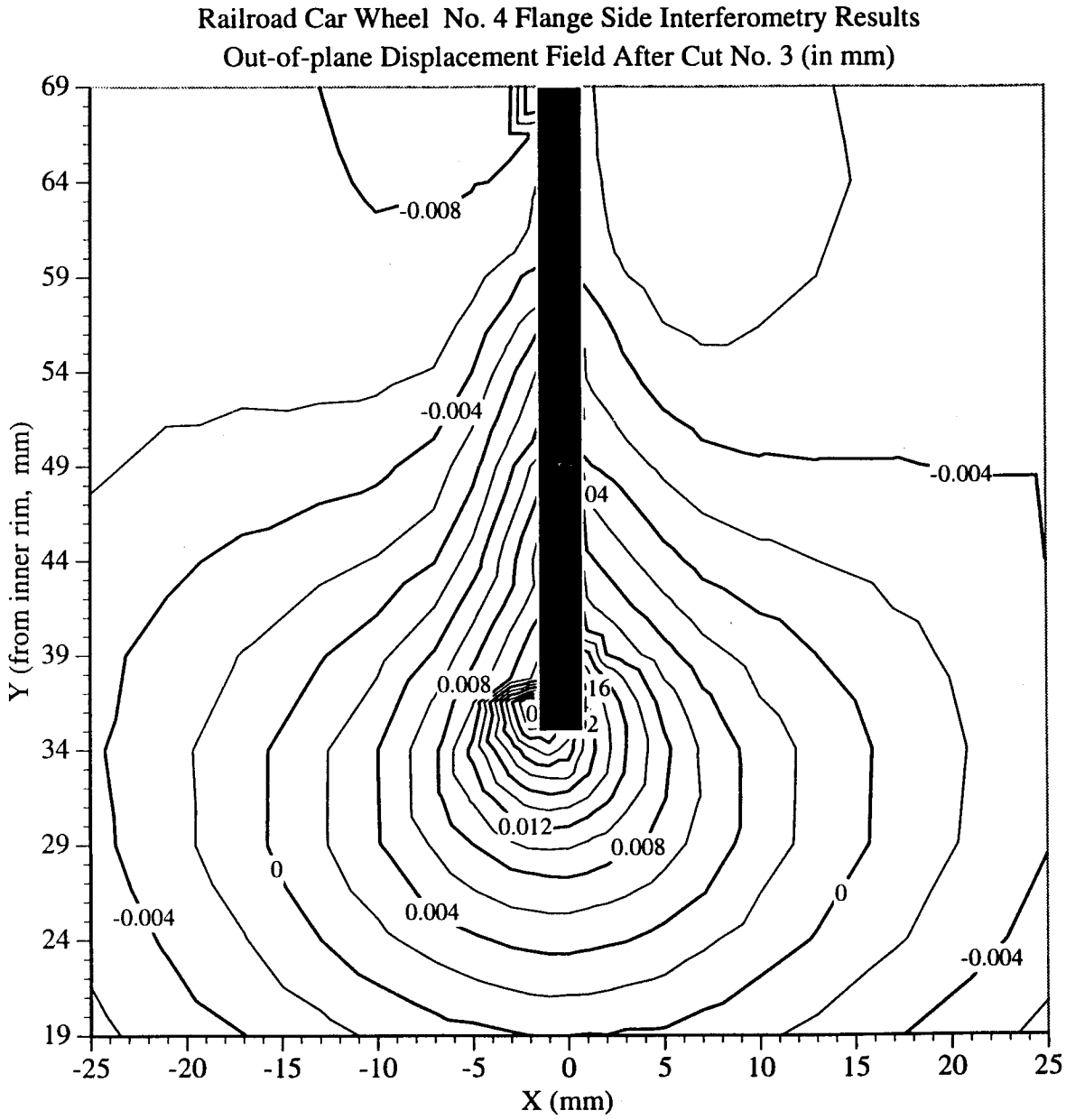
Railroad Car Wheel No. 4 Flange Side Interferometry Results
Out-of-plane Displacement Field After Cut No. 3 (in mm)
Y (from inner rim, mm)
X (mm)
69
64
59
54
49
44
39
34
29
24
19
-25
-20
-15
-10
-5
0
5
10
15
20
25
-0.008
-0.004
-0.004
04
0.008
16
2
0.012
0.008
0
0.004
0
-0.004
-0.004

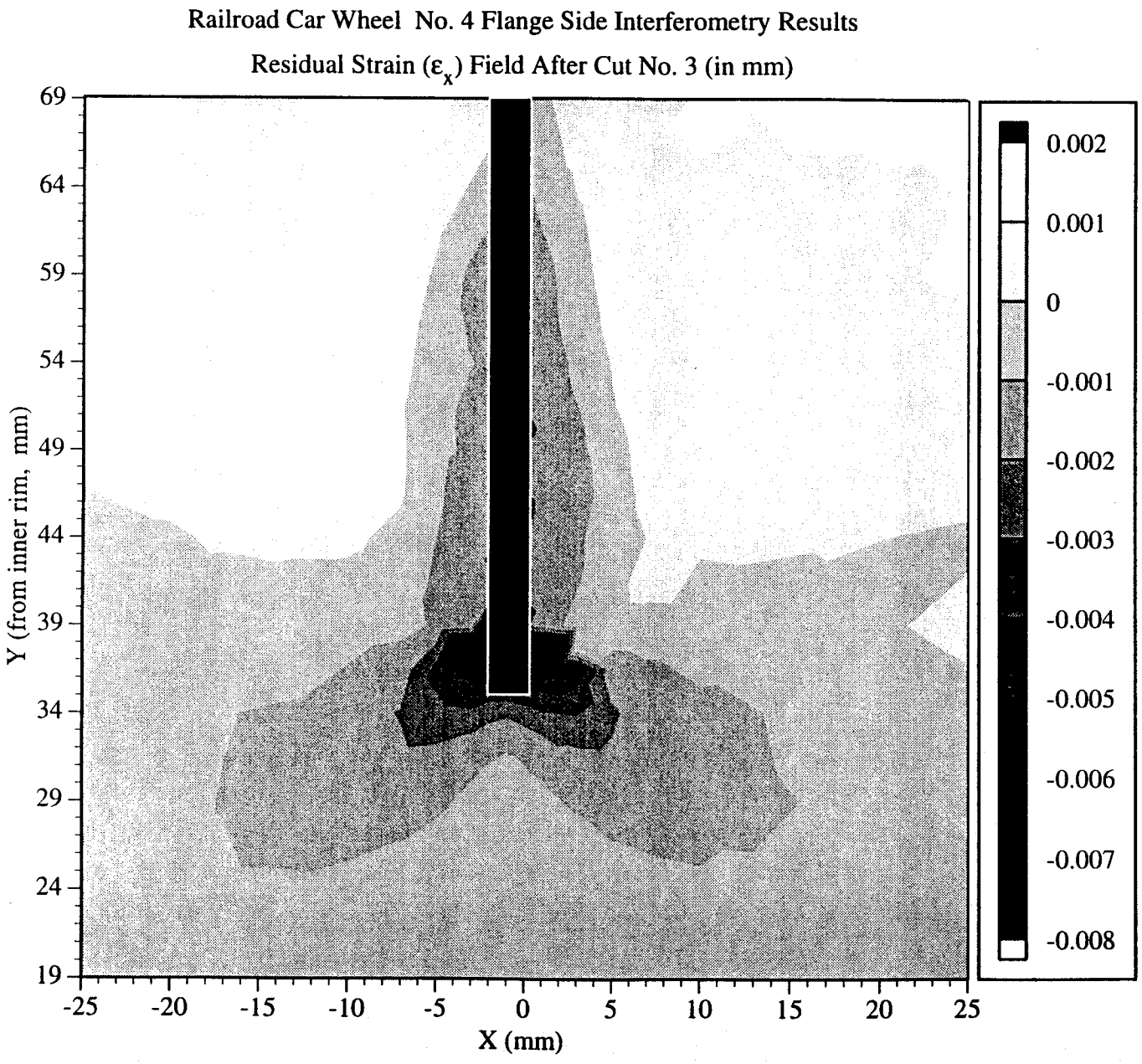
Railroad Car Wheel No. 4 Flange Side Interferometry Results
Residual Strain (ε_x) Field After Cut No. 3 (in mm)
Y (from inner rim, mm)
69
64
59
54
49
44
39
34
29
24
19
-25
-20
-15
-10
-5
0
5
10
15
20
25
X (mm)
0.002
0.001
0
-0.001
-0.002
-0.003
-0.004
-0.005
-0.006
-0.007
-0.008

Railroad Car Wheel No. 4 Flange Side Interferometry Results

Residual Strain (ε_y) Field After Cut No. 3 (in mm)

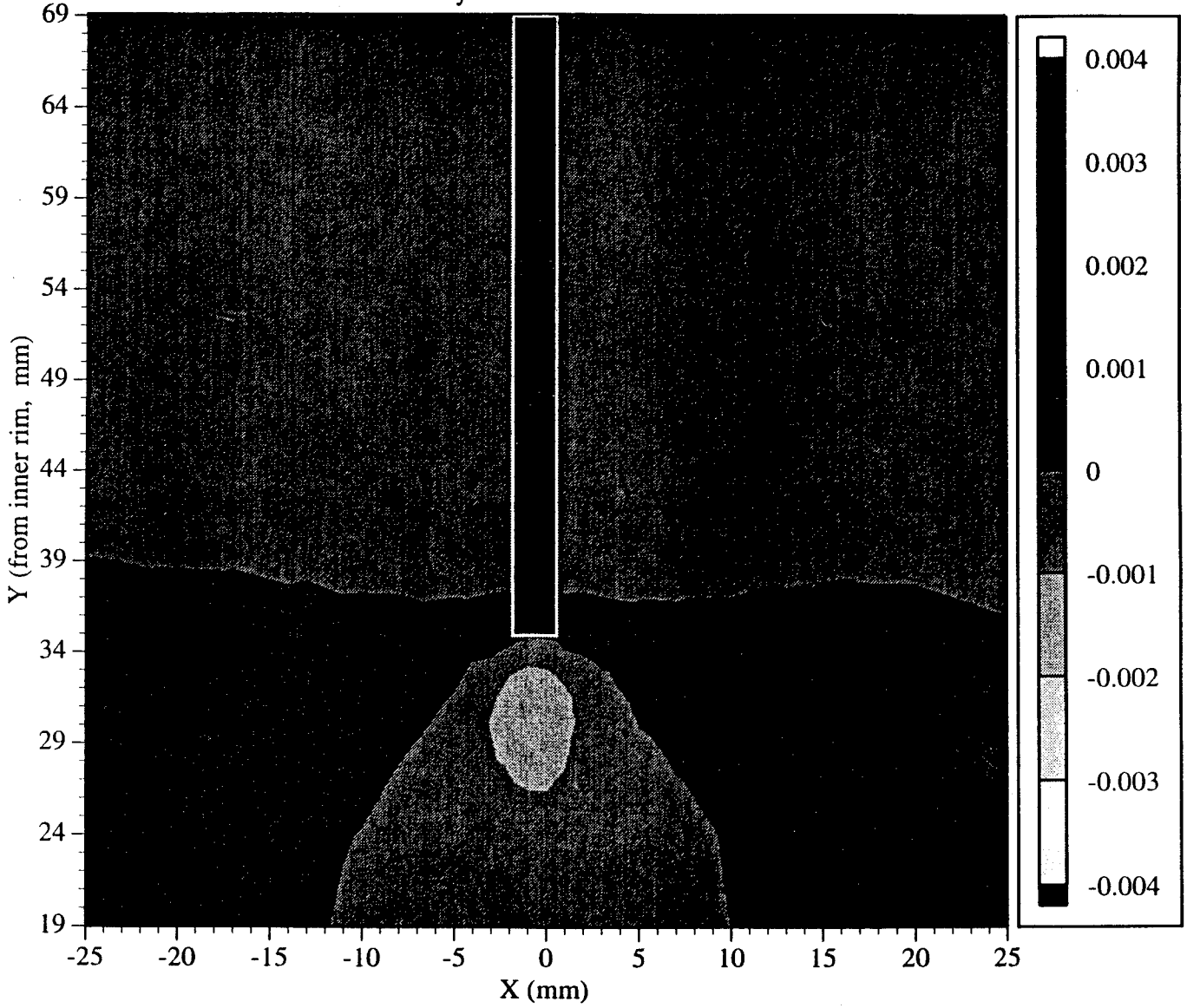

Railroad Car Wheel No. 4 Flange Side Interferometry Results

Residual Strain (γ_{xy}) Field After Cut No. 3 (in mm)

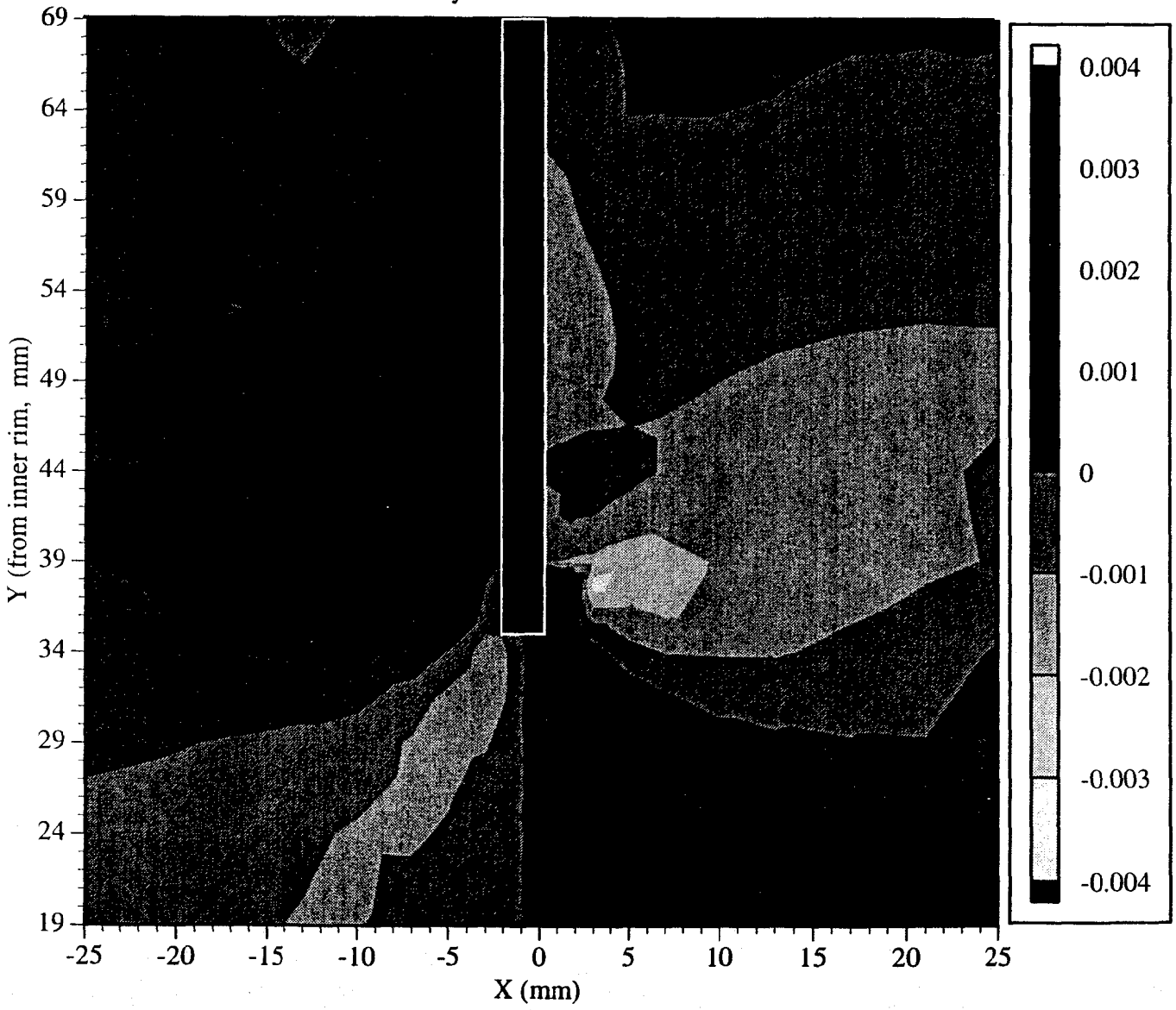

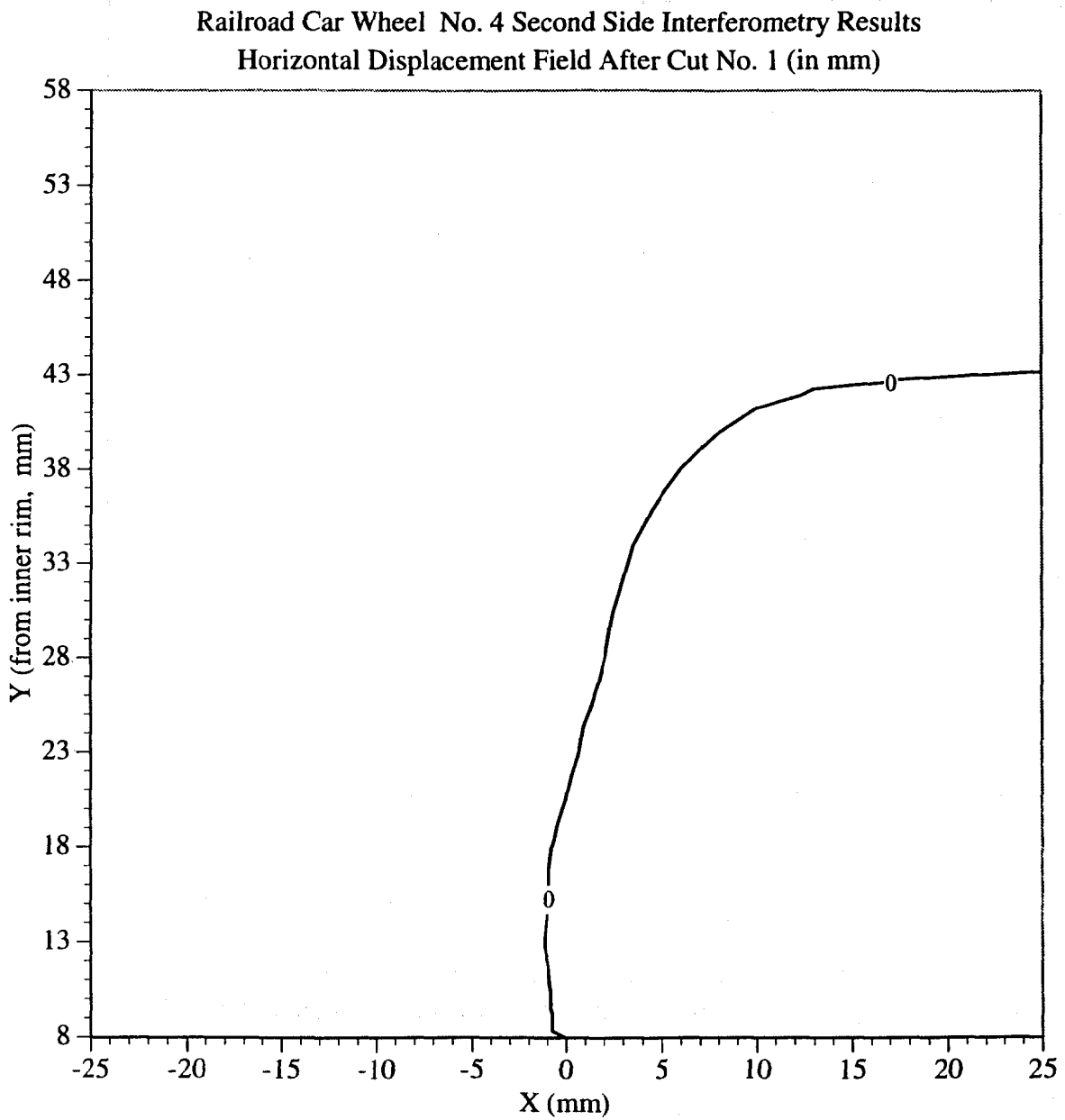
Railroad Car Wheel No. 4 Second Side Interferometry Results
Horizontal Displacement Field After Cut No. 1 (in mm)
Y (from inner rim, mm)
58
53
48
43
38
33
28
23
18
13
8
-25
-20
-15
-10
-5
0
5
10
15
20
25
X (mm)
0
0

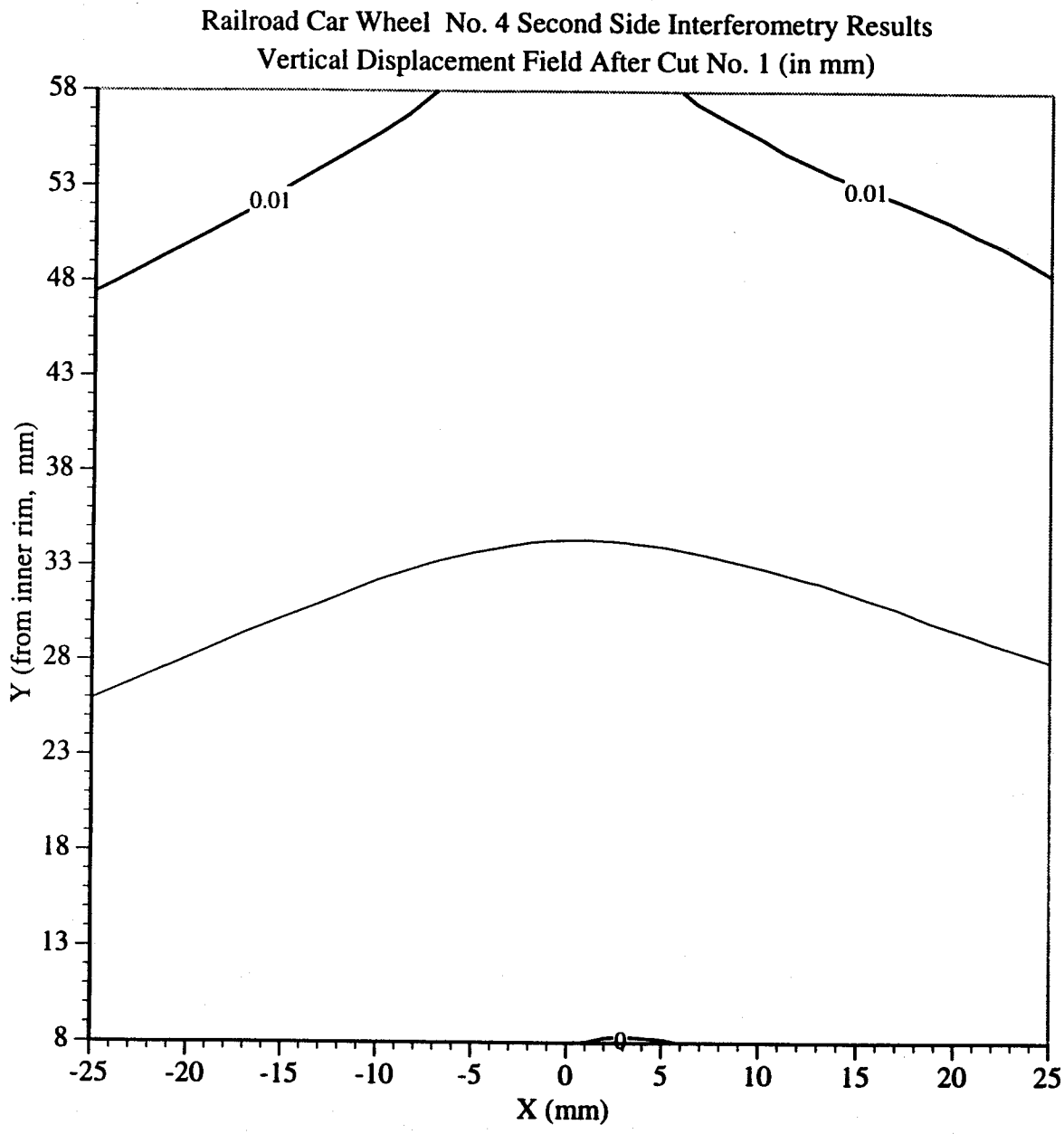
Railroad Car Wheel No. 4 Second Side Interferometry Results
Vertical Displacement Field After Cut No. 1 (in mm)
Y (from inner rim, mm)
58
53
48
43
38
33
28
23
18
13
8
0.01
0.01
0
-25
-20
-15
-10
-5
0
5
10
15
20
25
X (mm)

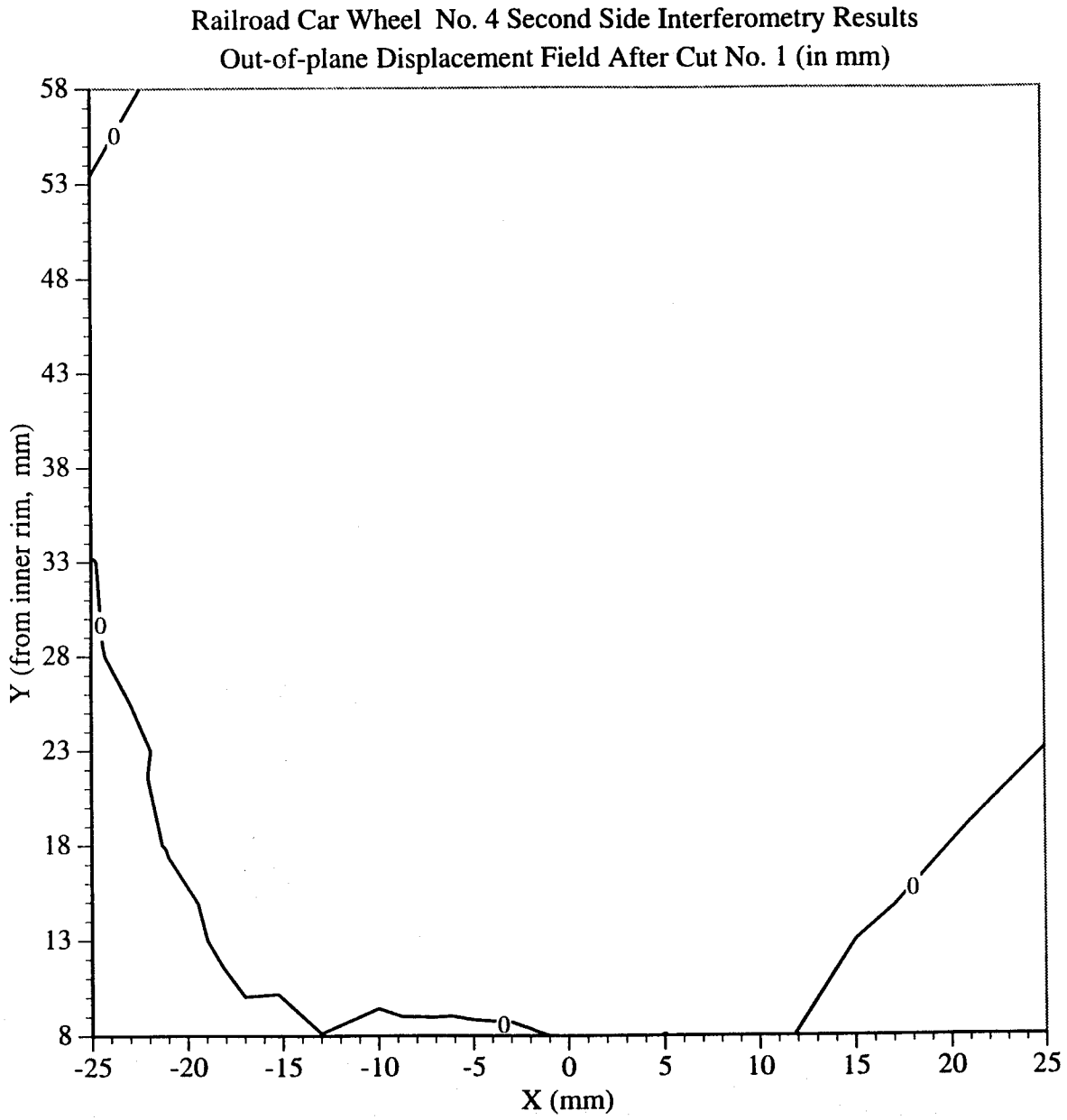
Railroad Car Wheel No. 4 Second Side Interferometry Results
Out-of-plane Displacement Field After Cut No. 1 (in mm)
Y (from inner rim, mm)
X (mm)
58
53
48
43
38
33
28
23
18
13
8
-25
-20
-15
-10
-5
0
5
10
15
20
25
0
0
0
0

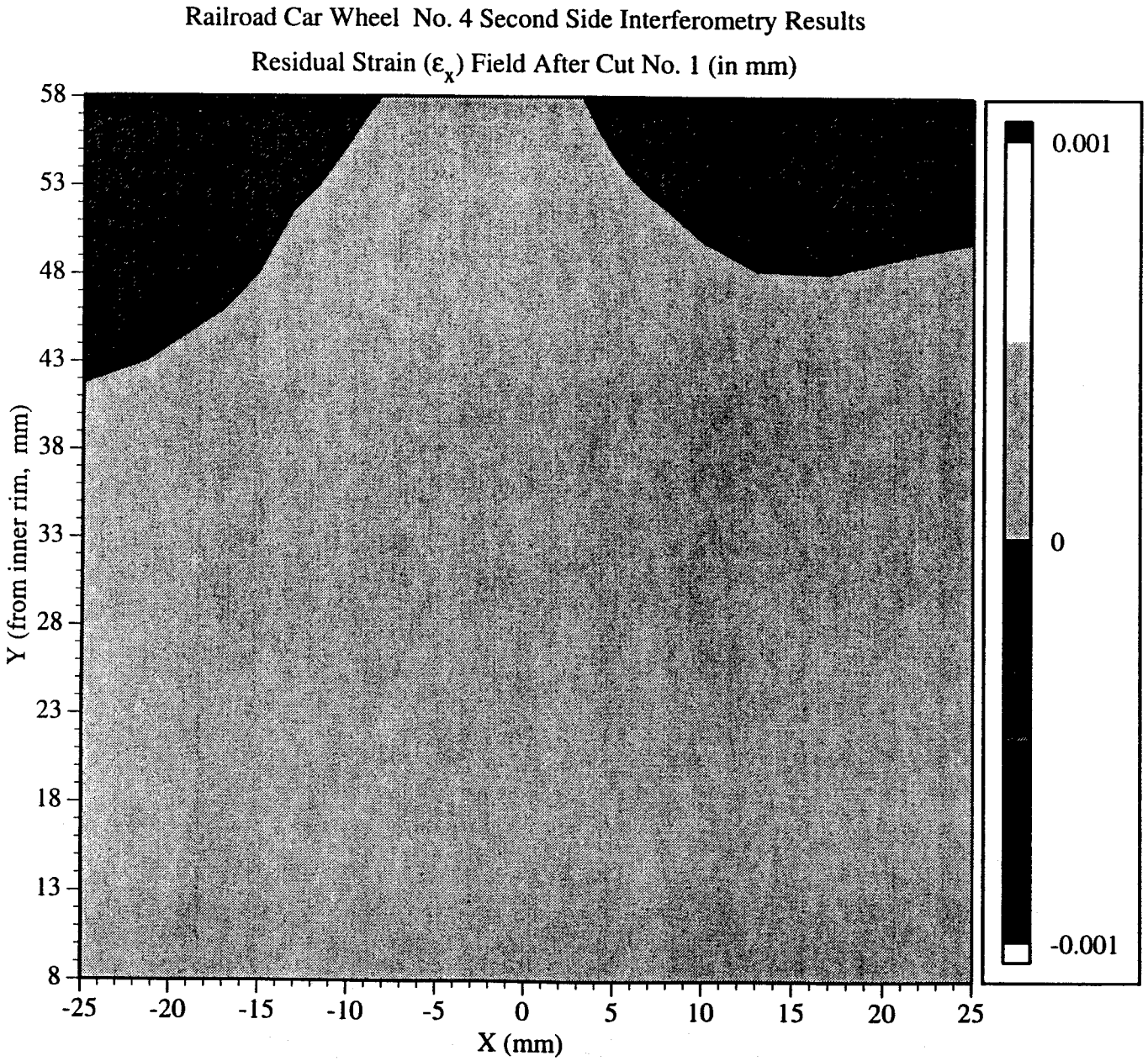
Railroad Car Wheel No. 4 Second Side Interferometry Results
Residual Strain (ε_x) Field After Cut No. 1 (in mm)
Y (from inner rim, mm)
58
53
48
43
38
33
28
23
18
13
8
-25
-20
-15
-10
-5
0
5
10
15
20
25
X (mm)
0.001
0
-0.001

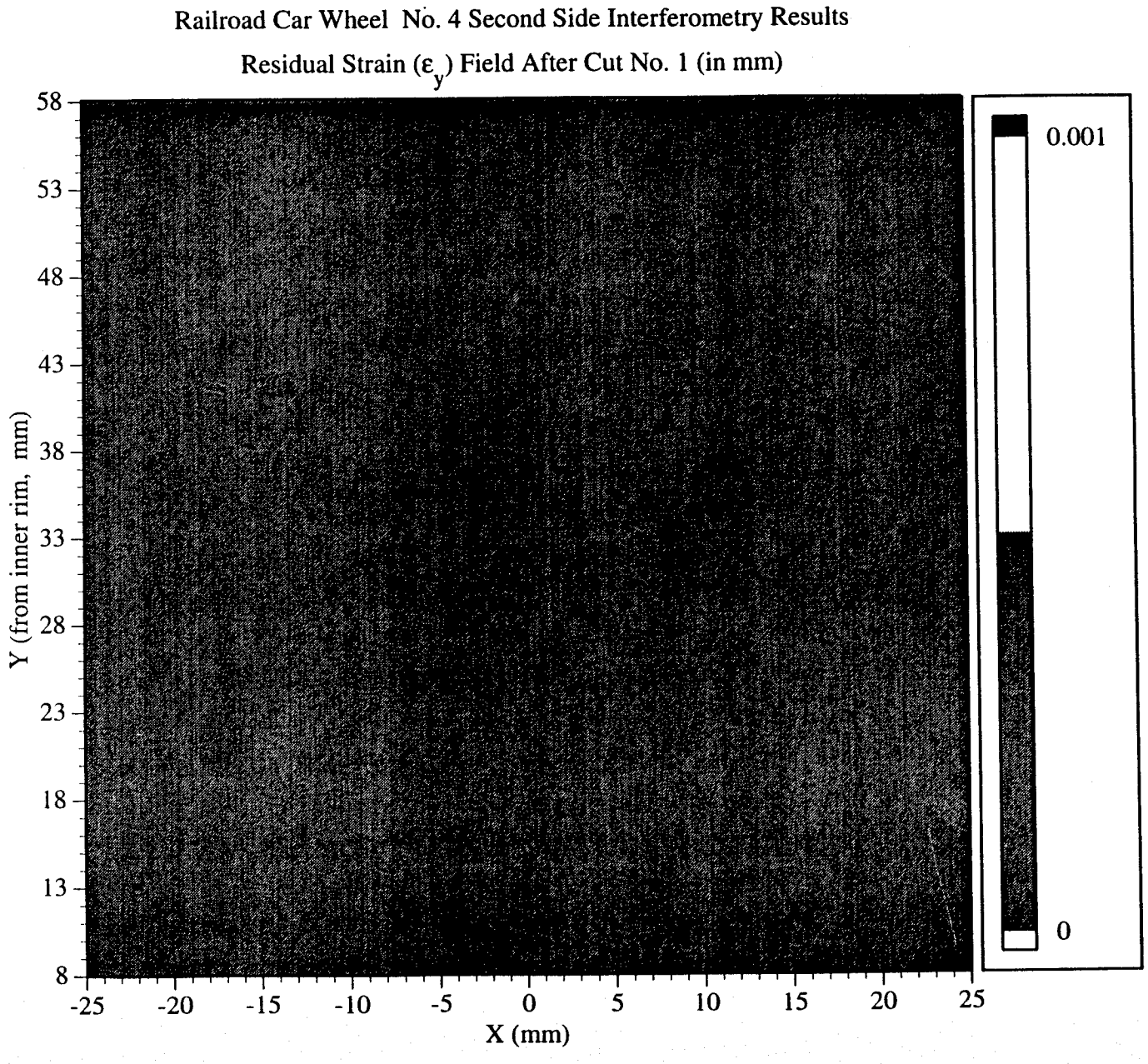
Railroad Car Wheel No. 4 Second Side Interferometry Results
Residual Strain (ε_y) Field After Cut No. 1 (in mm)
Y (from inner rim, mm)
58
53
48
43
38
33
28
23
18
13
8
-25
-20
-15
-10
-5
0
5
10
15
20
25
X (mm)
0.001
0

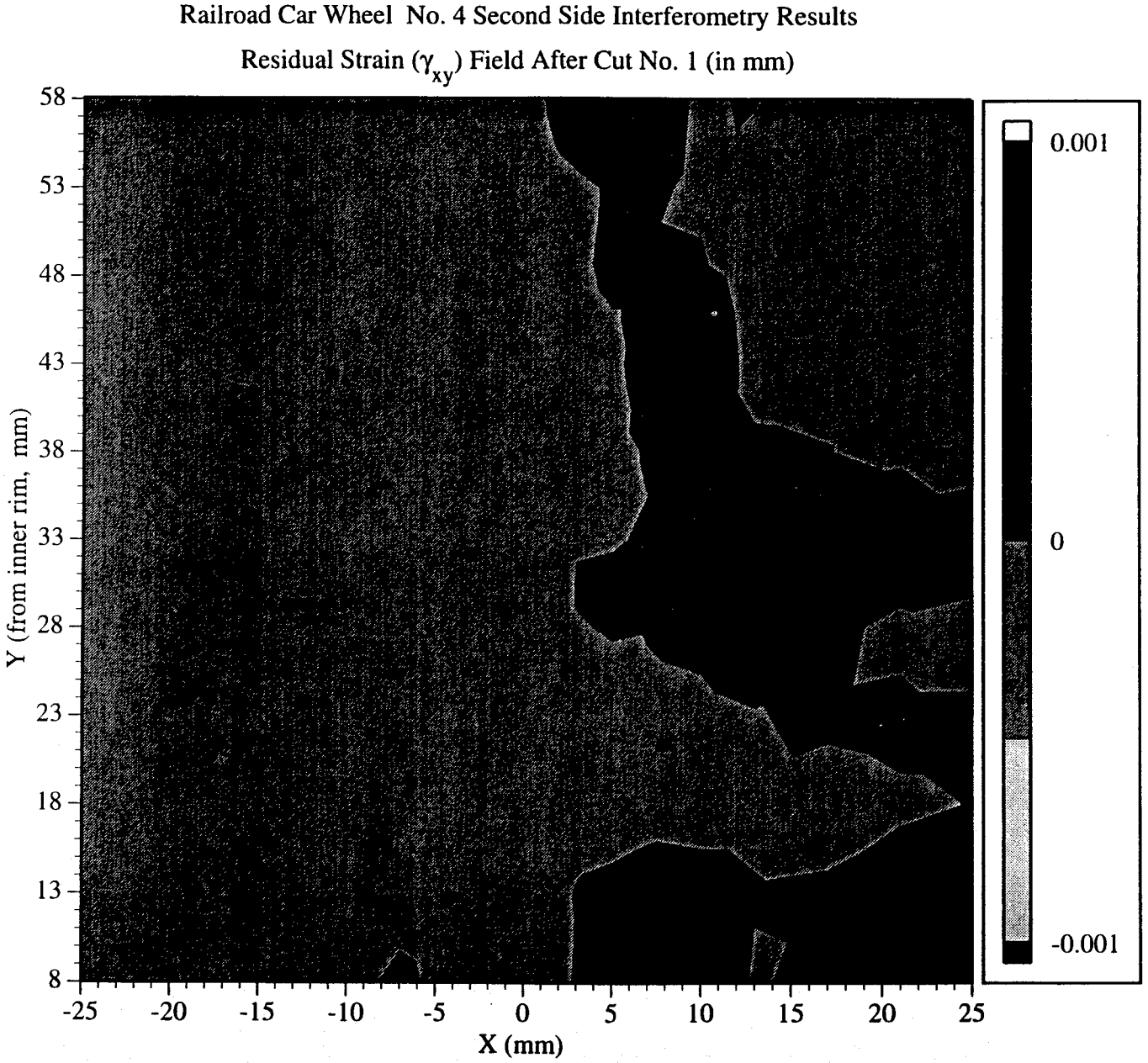
Railroad Car Wheel No. 4 Second Side Interferometry Results
Residual Strain (γ_{xy}) Field After Cut No. 1 (in mm)
Y (from inner rim, mm)
58
53
48
43
38
33
28
23
18
13
8
-25
-20
-15
-10
-5
0
5
10
15
20
25
X (mm)
0.001
0
-0.001

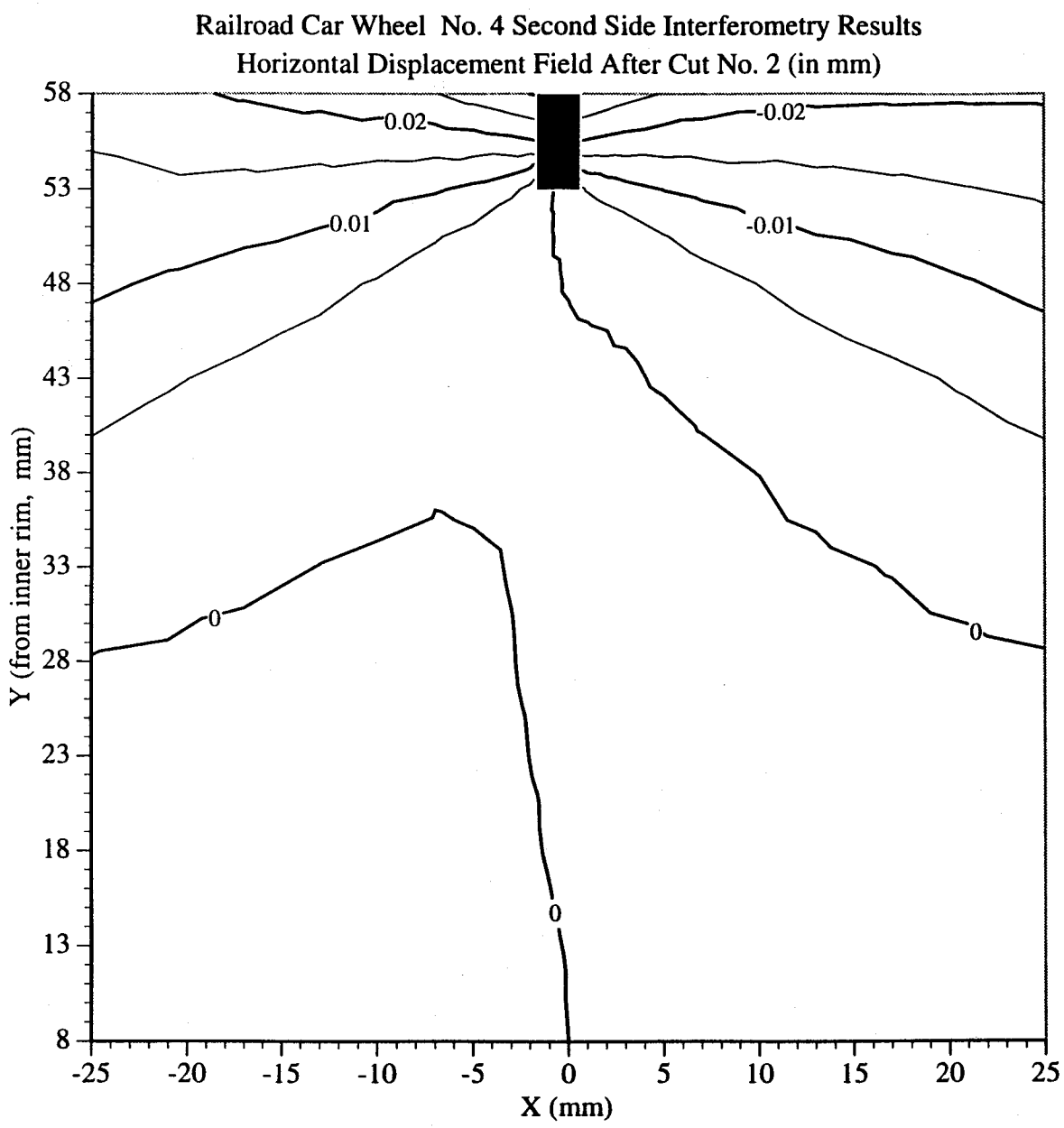
Railroad Car Wheel No. 4 Second Side Interferometry Results
Horizontal Displacement Field After Cut No. 2 (in mm)
Y (from inner rim, mm)
X (mm)
58
53
48
43
38
33
28
23
18
13
8
-25
-20
-15
-10
-5
0
5
10
15
20
25
0.02
-0.02
0.01
-0.01
0
0
0

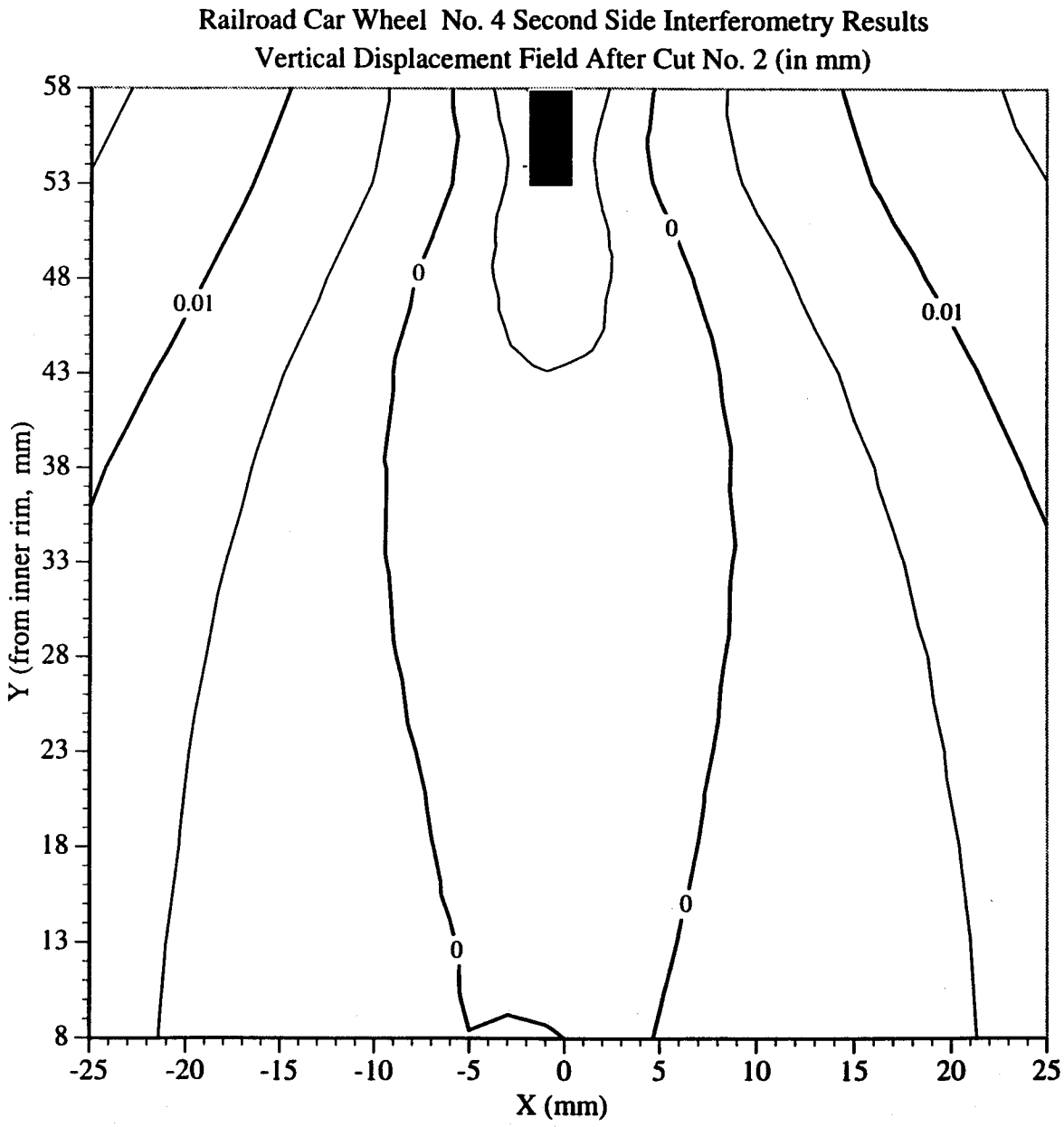
Railroad Car Wheel No. 4 Second Side Interferometry Results
Vertical Displacement Field After Cut No. 2 (in mm)
Y (from inner rim, mm)
X (mm)
58
53
48
43
38
33
28
23
18
13
8
-25
-20
-15
-10
-5
0
5
10
15
20
25
0.01
0
0
0
0
0.01

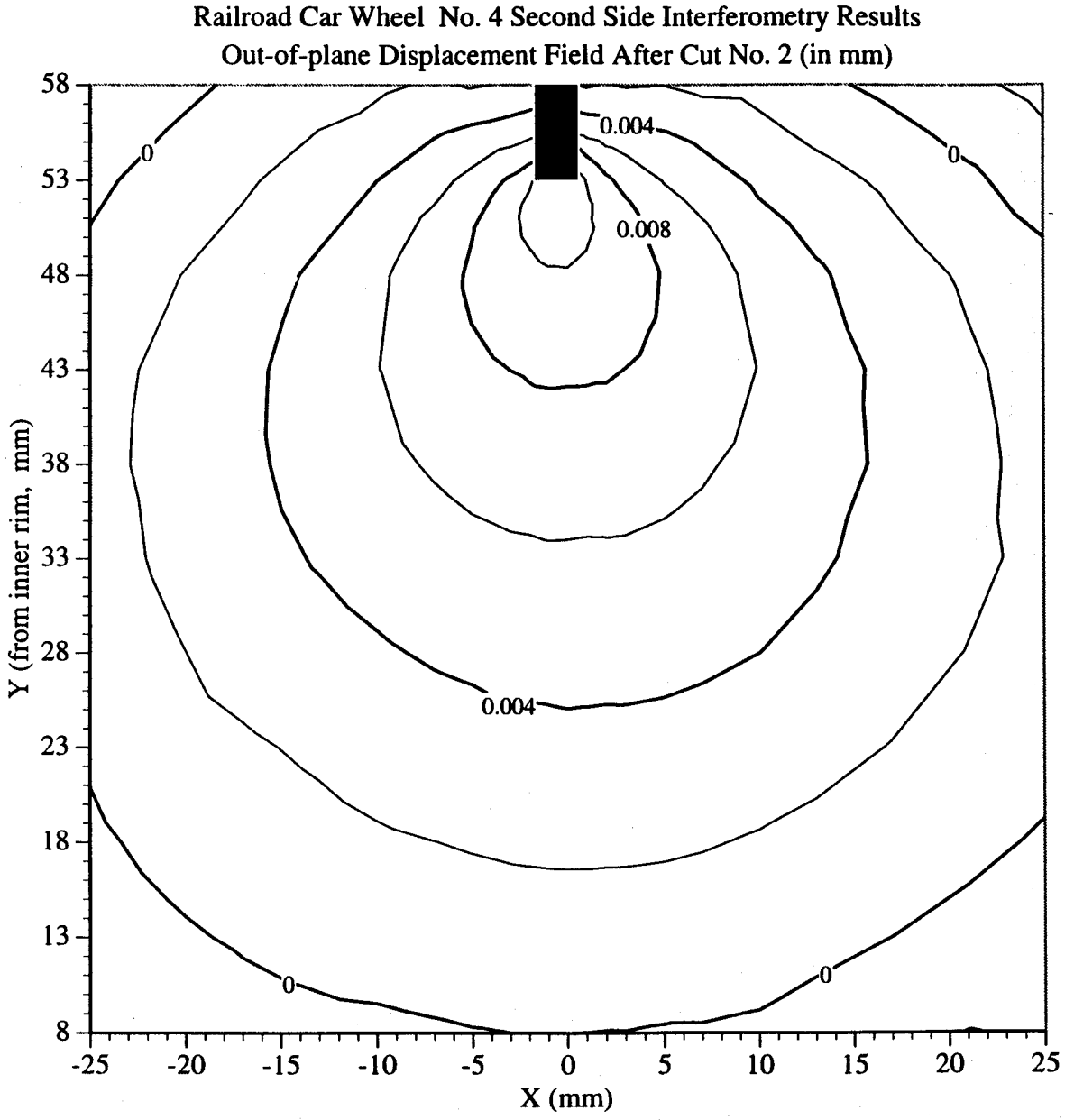
Railroad Car Wheel No. 4 Second Side Interferometry Results
Out-of-plane Displacement Field After Cut No. 2 (in mm)
Y (from inner rim, mm)
X (mm)
58
53
48
43
38
33
28
23
18
13
8
-25
-20
-15
-10
-5
0
5
10
15
20
25
0
0.004
0.008
0.004
0
0
0

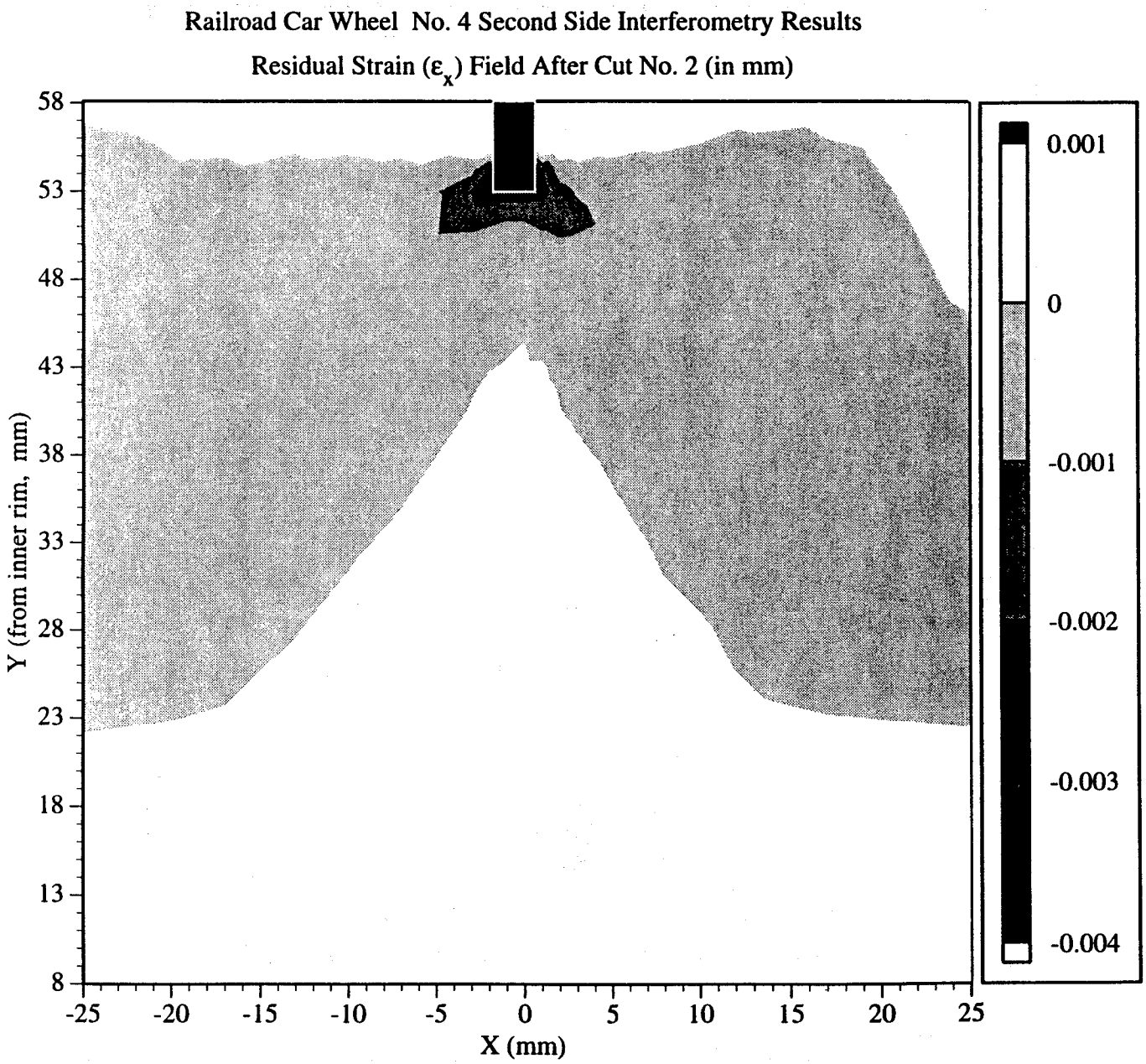
Railroad Car Wheel No. 4 Second Side Interferometry Results
Residual Strain (ε_x) Field After Cut No. 2 (in mm)
Y (from inner rim, mm)
58
53
48
43
38
33
28
23
18
13
8
-25
-20
-15
-10
-5
0
5
10
15
20
25
X (mm)
0.001
0
-0.001
-0.002
-0.003
-0.004

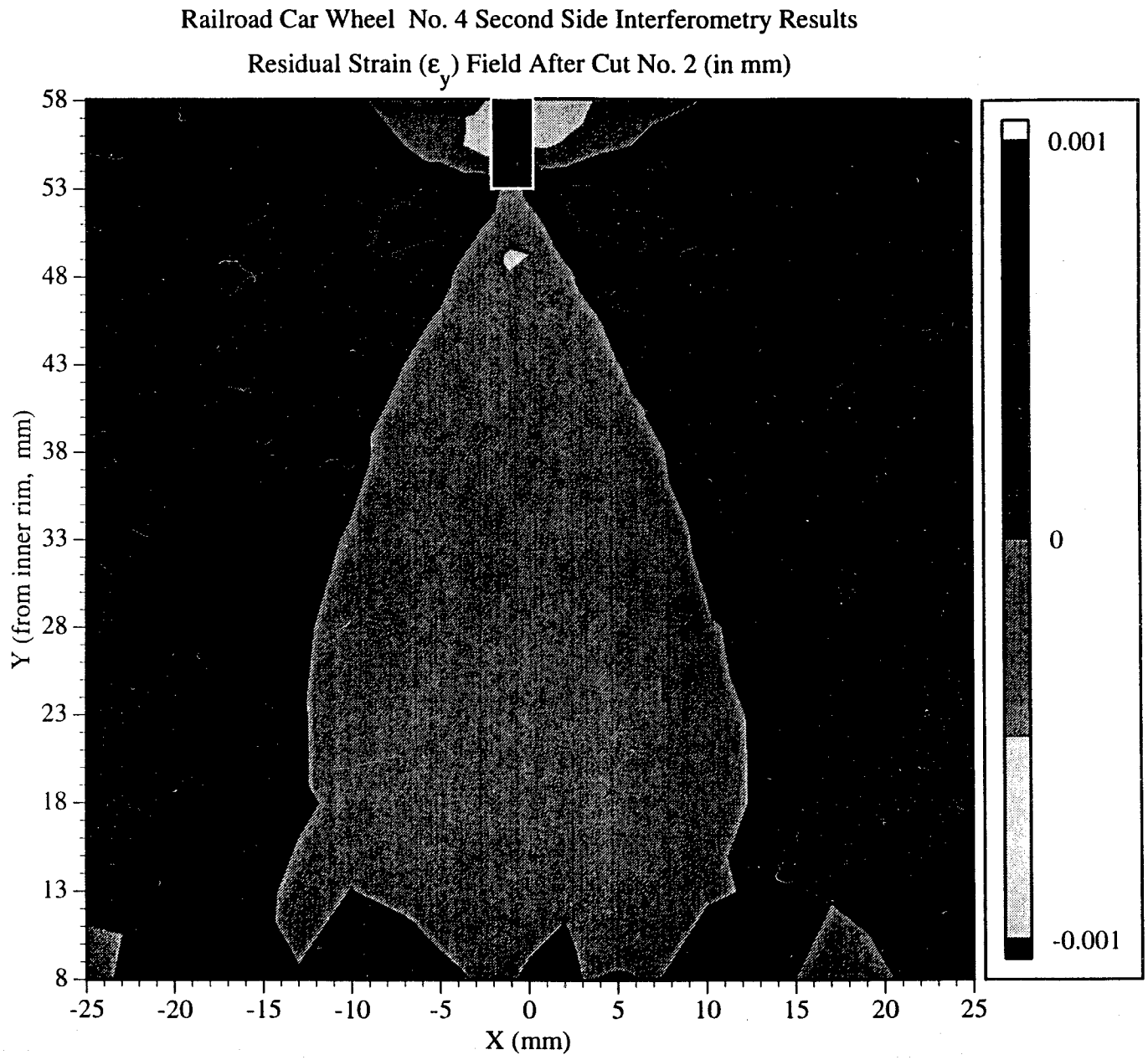
Railroad Car Wheel No. 4 Second Side Interferometry Results
Residual Strain (ε_y) Field After Cut No. 2 (in mm)
Y (from inner rim, mm)
58
53
48
43
38
33
28
23
18
13
8
-25
-20
-15
-10
-5
0
5
10
15
20
25
X (mm)
0.001
0
-0.001

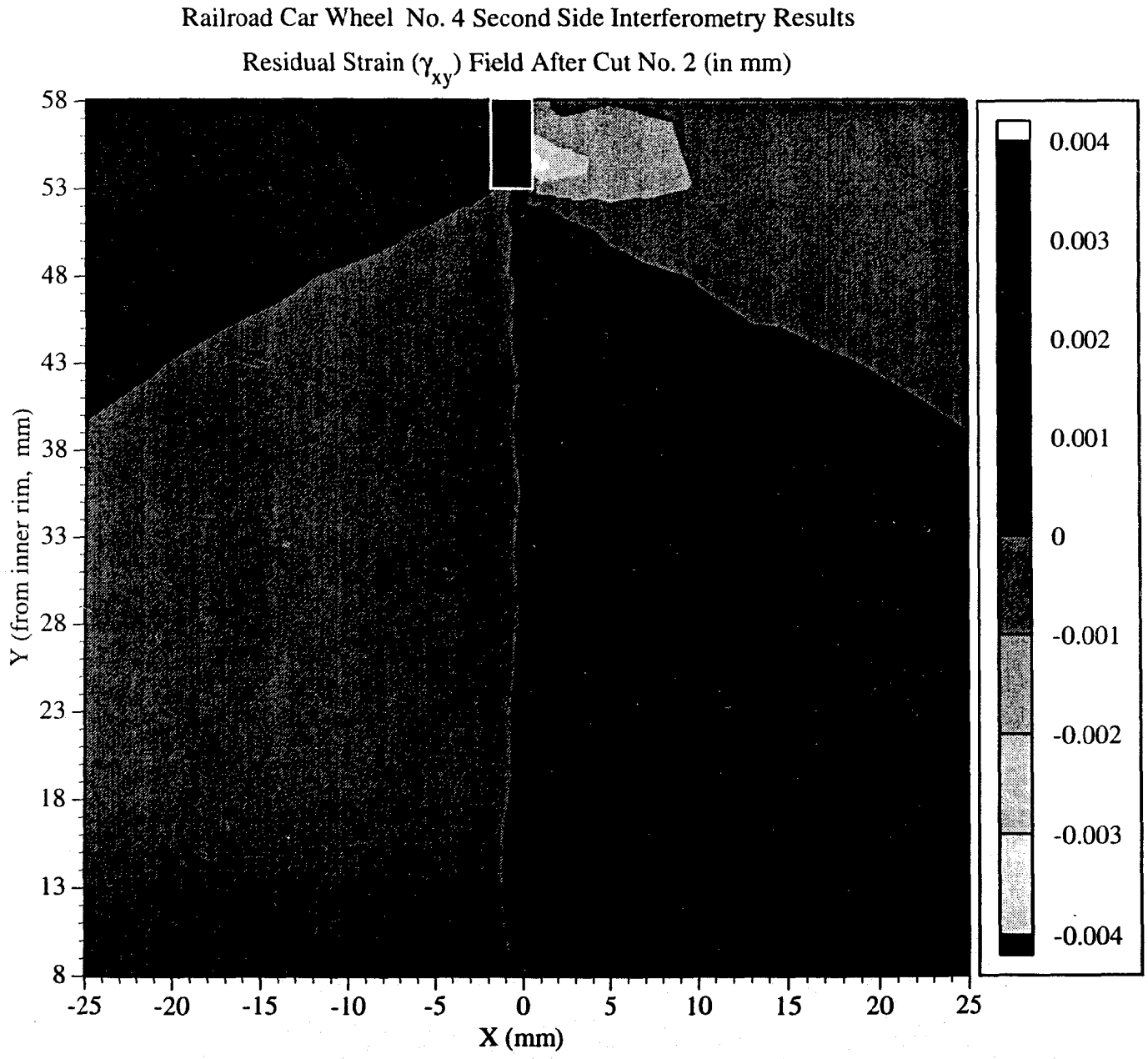
Railroad Car Wheel No. 4 Second Side Interferometry Results
Residual Strain (γ_{xy}) Field After Cut No. 2 (in mm)
Y (from inner rim, mm)
58
53
48
43
38
33
28
23
18
13
8
-25
-20
-15
-10
-5
0
5
10
15
20
25
X (mm)
0.004
0.003
0.002
0.001
0
-0.001
-0.002
-0.003
-0.004

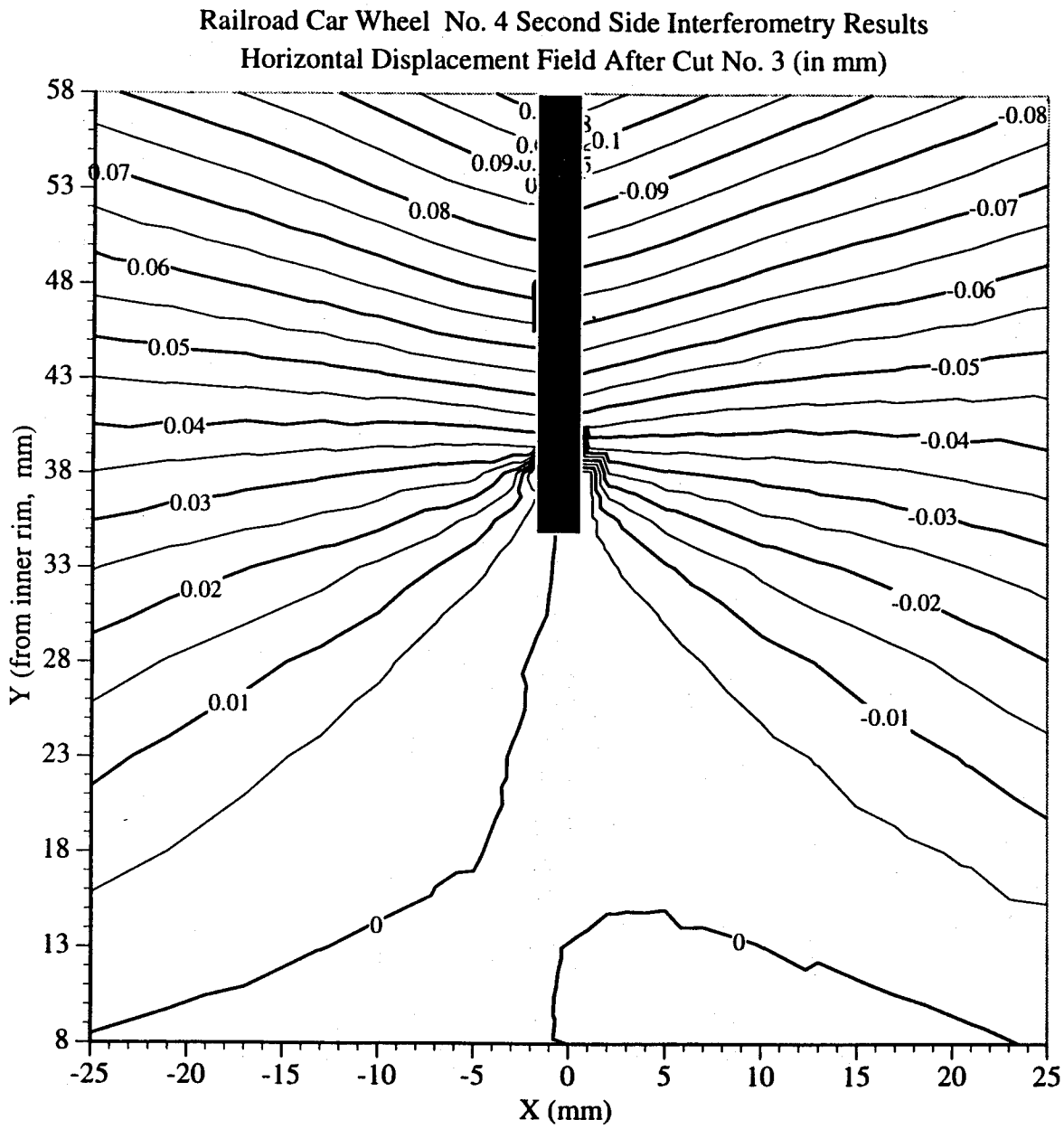
Railroad Car Wheel No. 4 Second Side Interferometry Results
Horizontal Displacement Field After Cut No. 3 (in mm)
Y (from inner rim, mm)
X (mm)
58
53
48
43
38
33
28
23
18
13
8
-25
-20
-15
-10
-5
0
5
10
15
20
25
0.07
0.08
0.06
0.05
0.04
0.03
0.02
0.01
0
-0.09
-0.08
-0.07
-0.06
-0.05
-0.04
-0.03
-0.02
-0.01
0

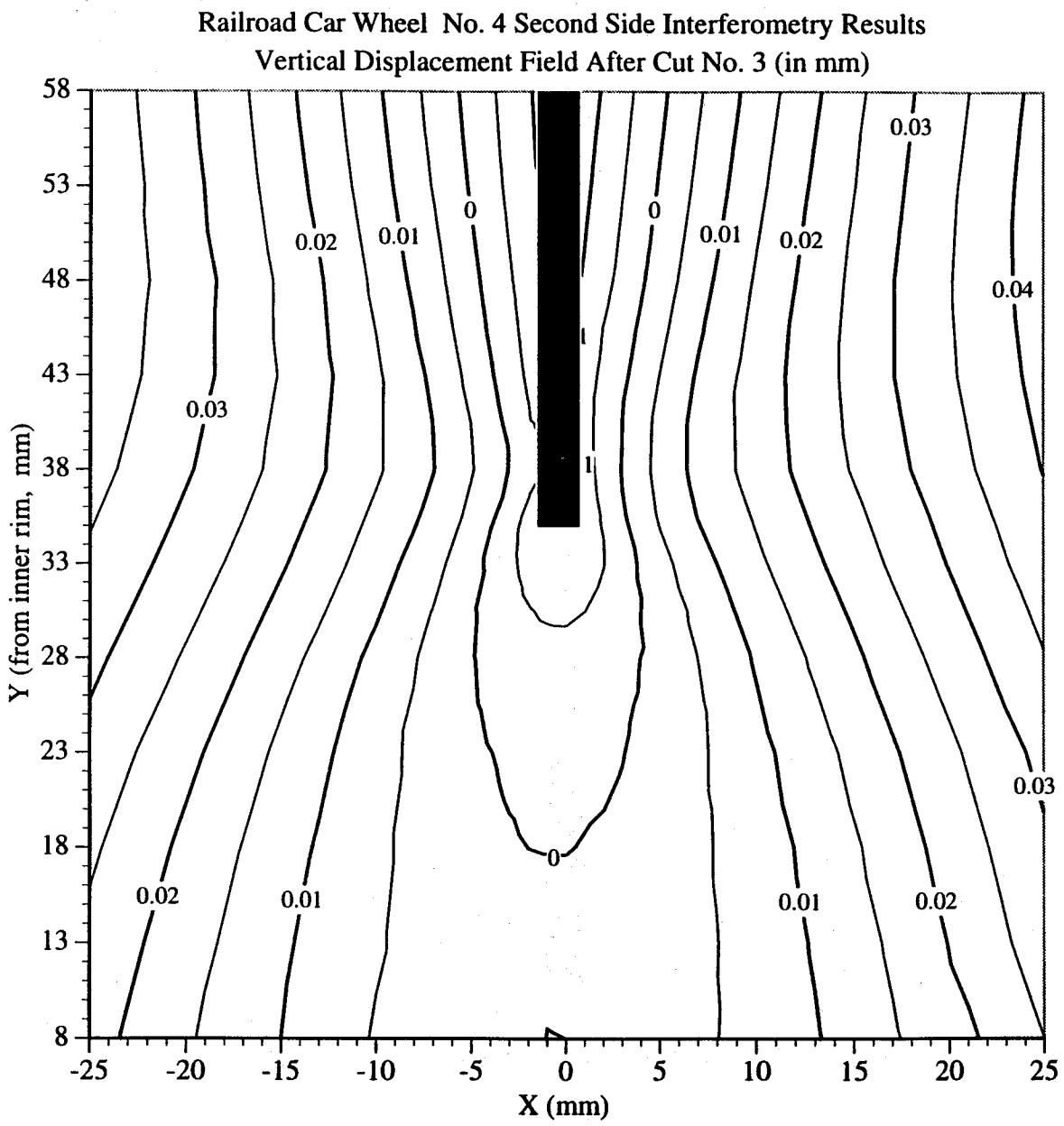
Railroad Car Wheel No. 4 Second Side Interferometry Results
Vertical Displacement Field After Cut No. 3 (in mm)
Y (from inner rim, mm)
X (mm)
58
53
48
43
38
33
28
23
18
13
8
-25
-20
-15
-10
-5
0
5
10
15
20
25
0.03
0.02
0.01
0
0
0.01
0.02
0.03
0.04
0.03
0.02
0.01
0
0.01
0.02
0.03

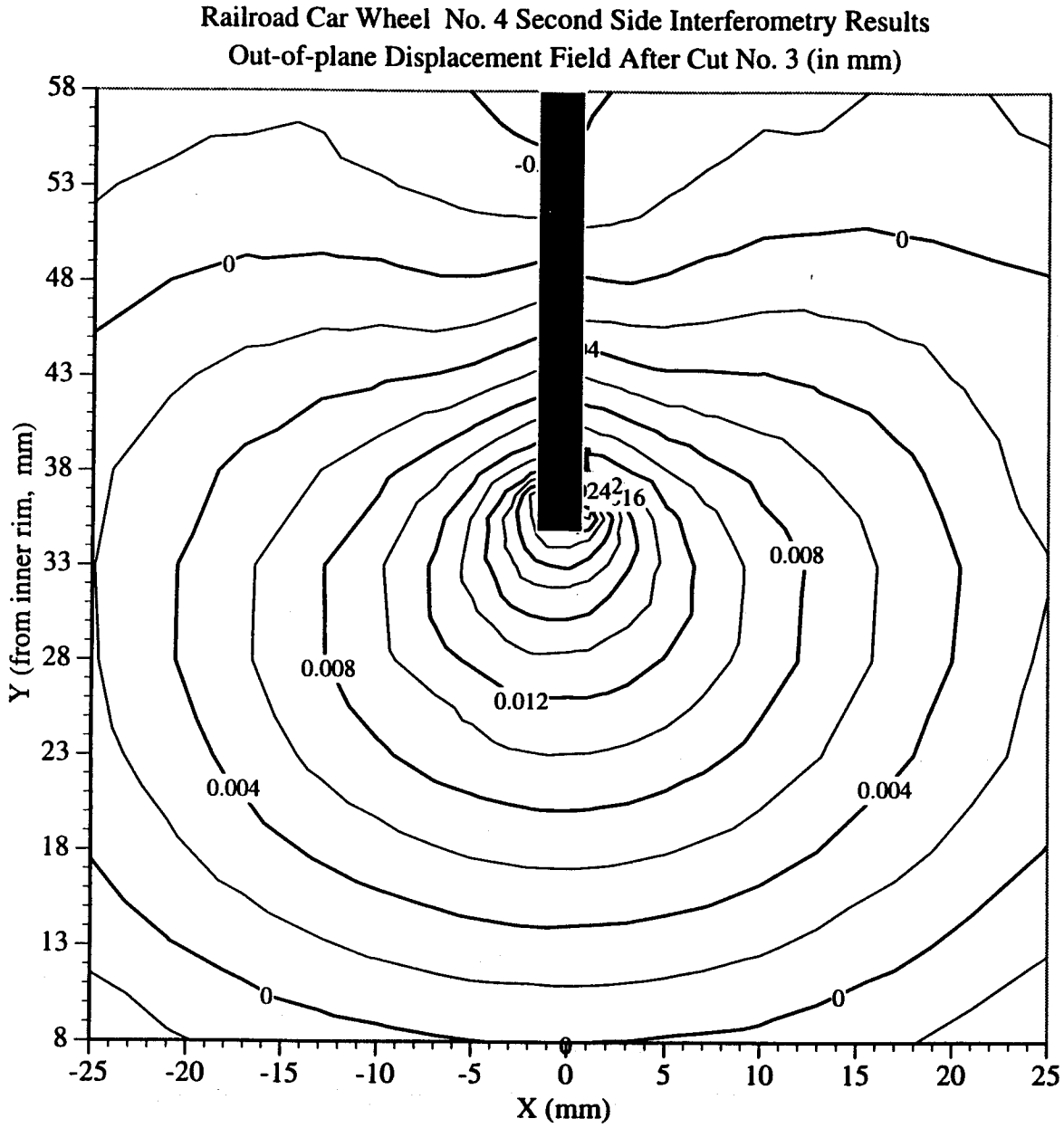
Railroad Car Wheel No. 4 Second Side Interferometry Results
Out-of-plane Displacement Field After Cut No. 3 (in mm)
Y (from inner rim, mm)
X (mm)
58
53
48
43
38
33
28
23
18
13
8
-25
-20
-15
-10
-5
0
5
10
15
20
25
0.008
0.008
0.012
0.004
0.004

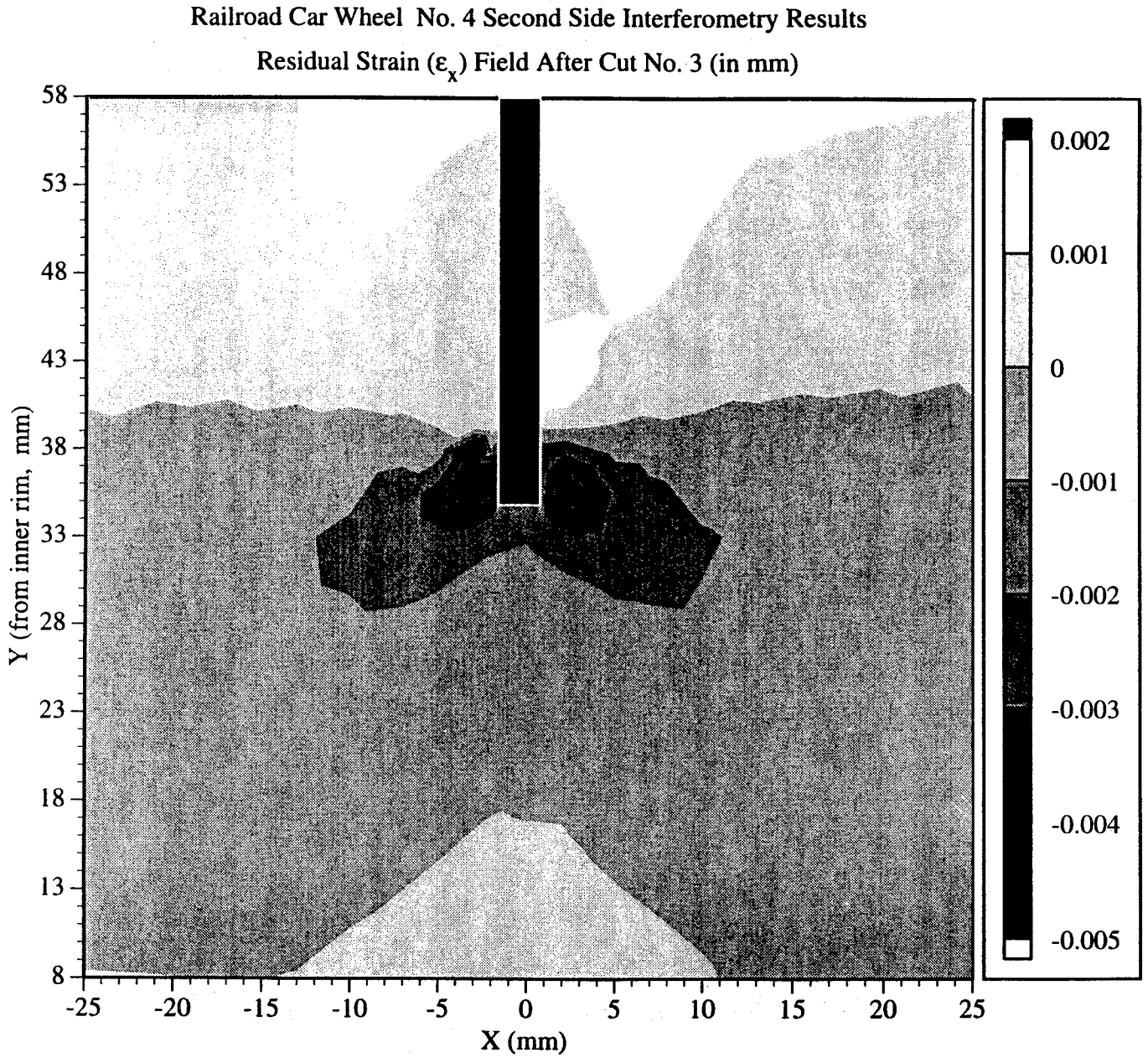
Railroad Car Wheel No. 4 Second Side Interferometry Results
Residual Strain (ε_x) Field After Cut No. 3 (in mm)
Y (from inner rim, mm)
58
53
48
43
38
33
28
23
18
13
8
-25
-20
-15
-10
-5
0
5
10
15
20
25
X (mm)
0.002
0.001
0
-0.001
-0.002
-0.003
-0.004
-0.005

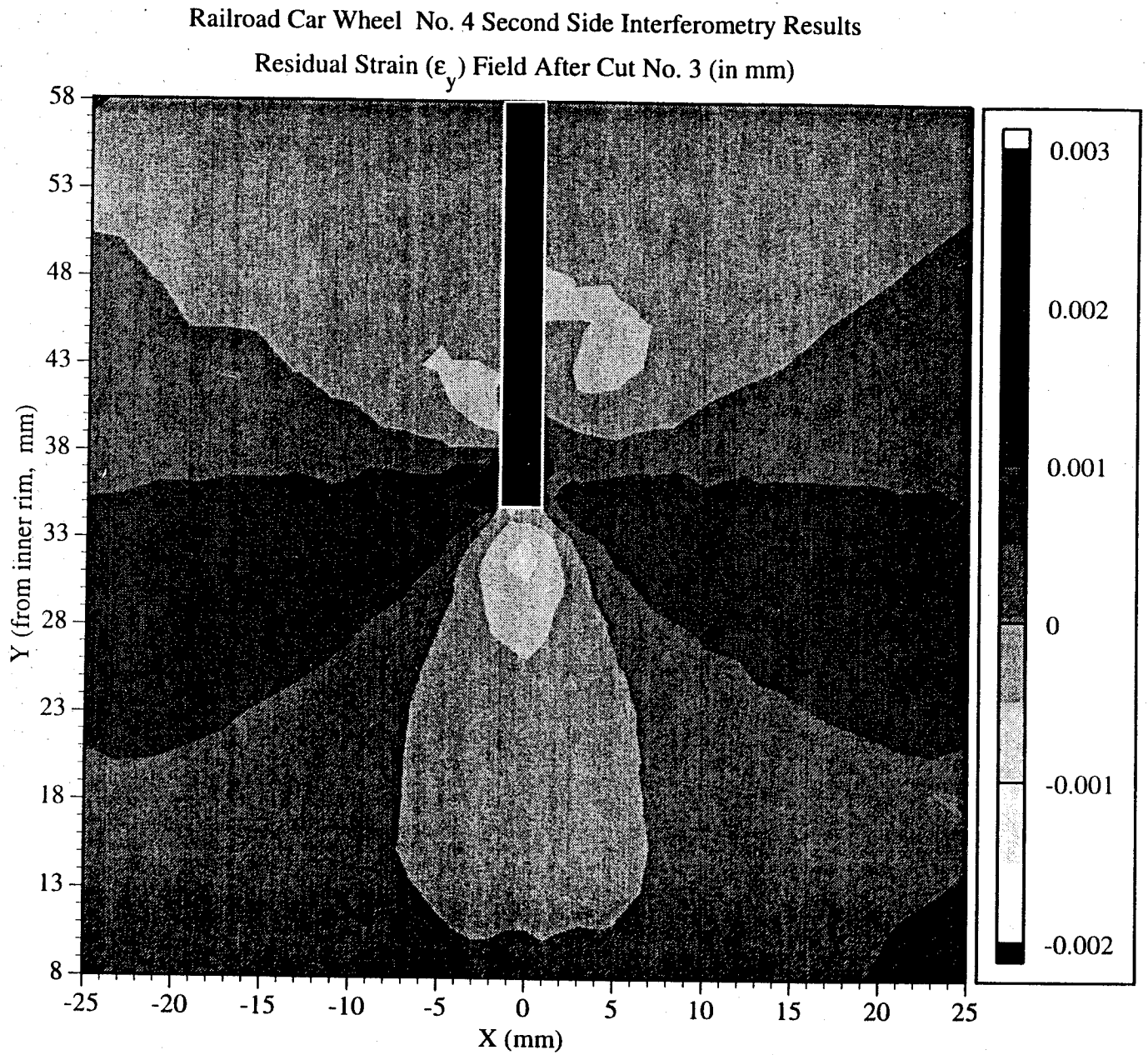
Railroad Car Wheel No. 4 Second Side Interferometry Results
Residual Strain (ε_y) Field After Cut No. 3 (in mm)
Y (from inner rim, mm)
58
53
48
43
38
33
28
23
18
13
8
-25
-20
-15
-10
-5
0
5
10
15
20
25
X (mm)
0.003
0.002
0.001
0
-0.001
-0.002

Railroad Car Wheel No. 4 Second Side Interferometry Results

Residual Strain (γ_{xy}) Field After Cut No. 3 (in mm)

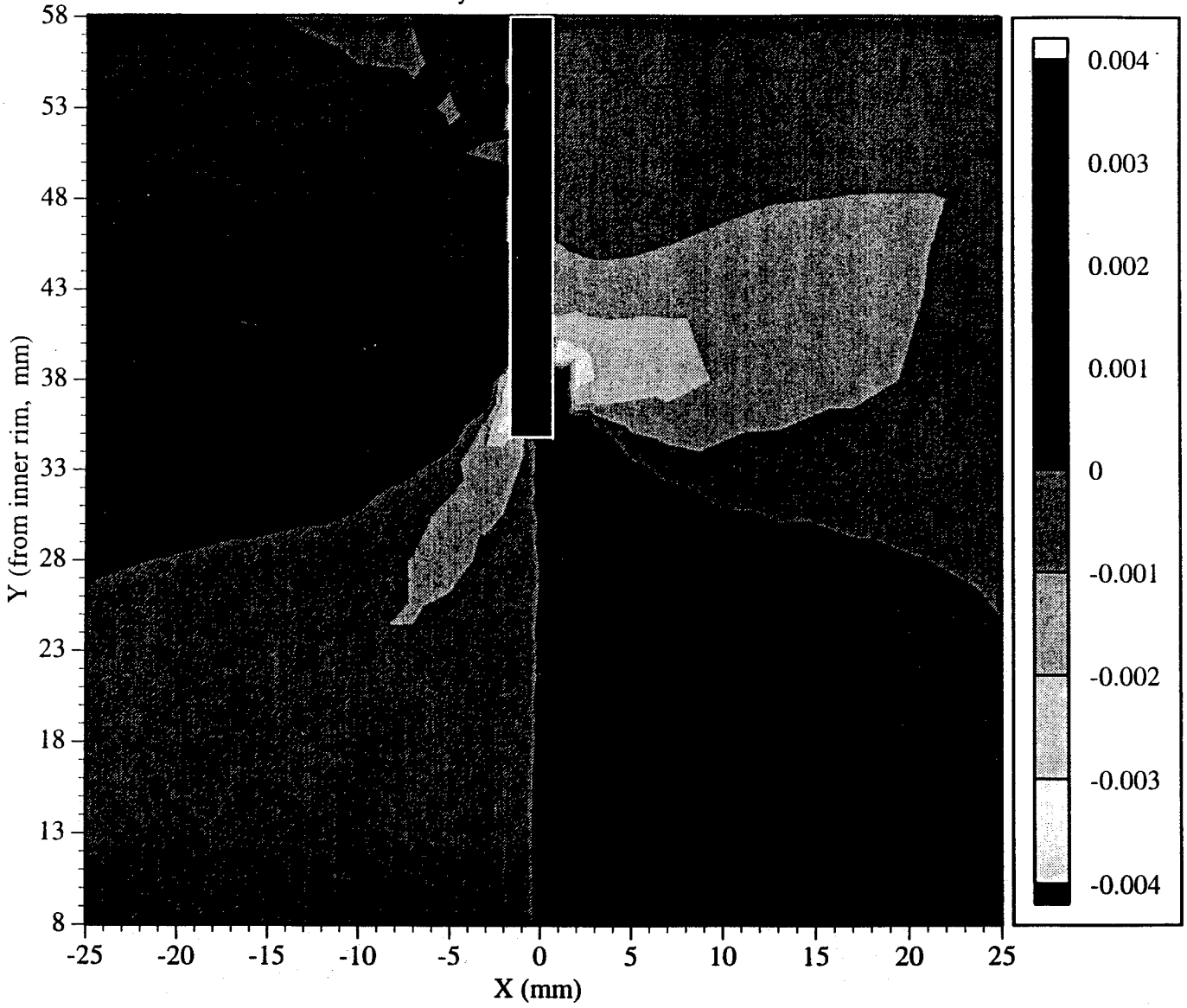

Page Intentionally Left Blank

Appendix 5. Wheel #5 Experimental Results

This appendix contains the results from the test on both sides (front and back rim faces) of the fifth wheel. All the data are in a local coordinate system that is located at the intersection of the inner edge of the rim and the cutting line; the vertical axis points away from the center of the wheel.

The attached figures show the location of all the sensors. At two points on the wheel, thermocouples (TC) measure the temperature difference (which never exceeded 1.5°C) immediately after each cut. The temperature at TC2, the one farther from the cut, was equal to the ambient temperature. The strain measurements were taken after the difference decreased to about 1°C or less at an ambient temperature in the range of 19°C to 22°C.

The extensometer, strain gage, and displacement sensor data are provided in tabular form. The interferometric data is provided in the form of contour maps and as data files in ASCII format for three specific cutting stages. The corresponding cut depths are 34 mm, 48 mm, and 60 mm.

The wheel was identified by the following markings:

26526
242

Location of strain gauges, thermocouples and gratings on wheel #5,6,7&8

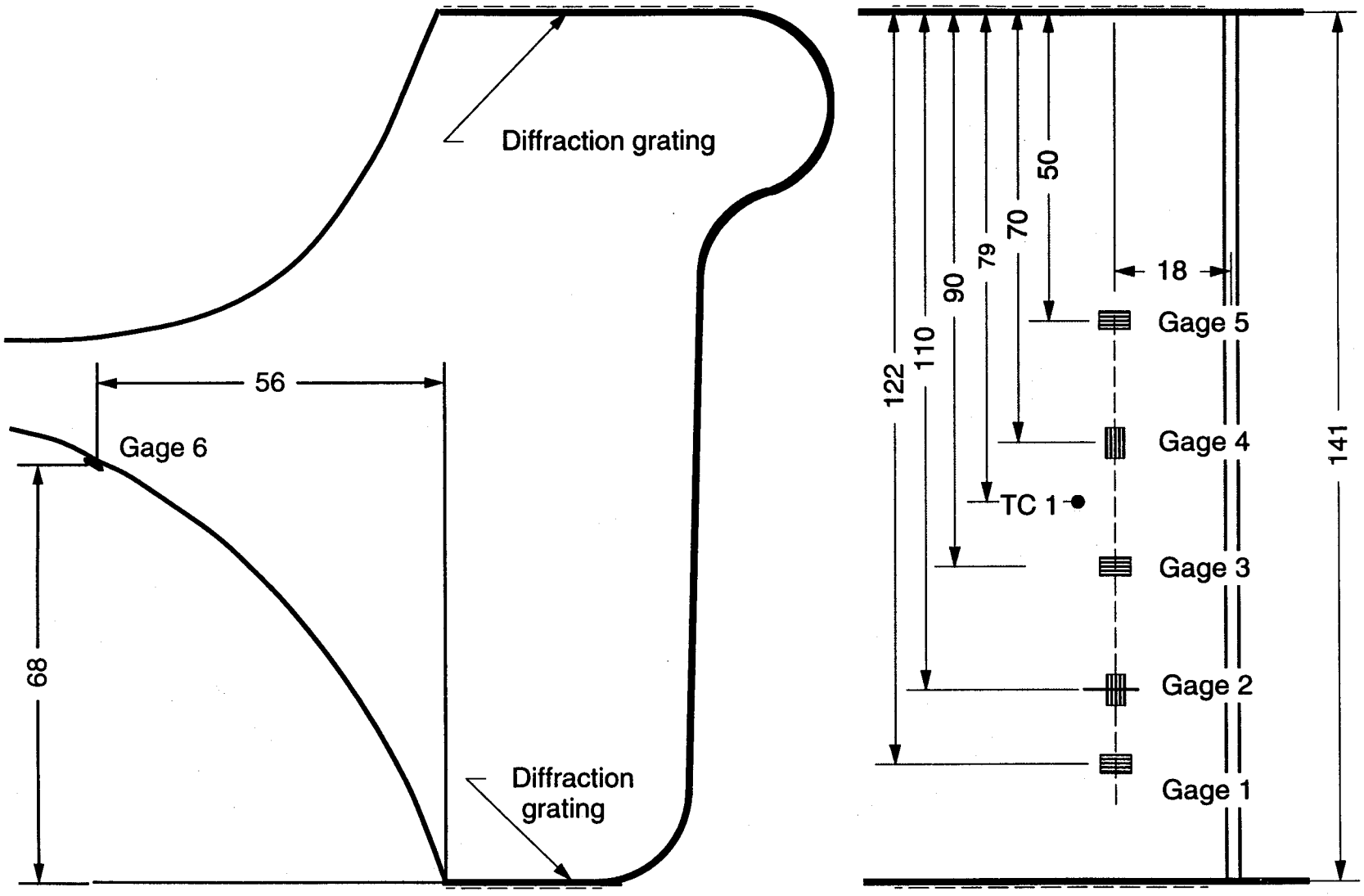

Gage 6 was located 20mm from the plane of the cut.

Location of displacement sensors thermocouples and gratings on wheel #5,6,7&8

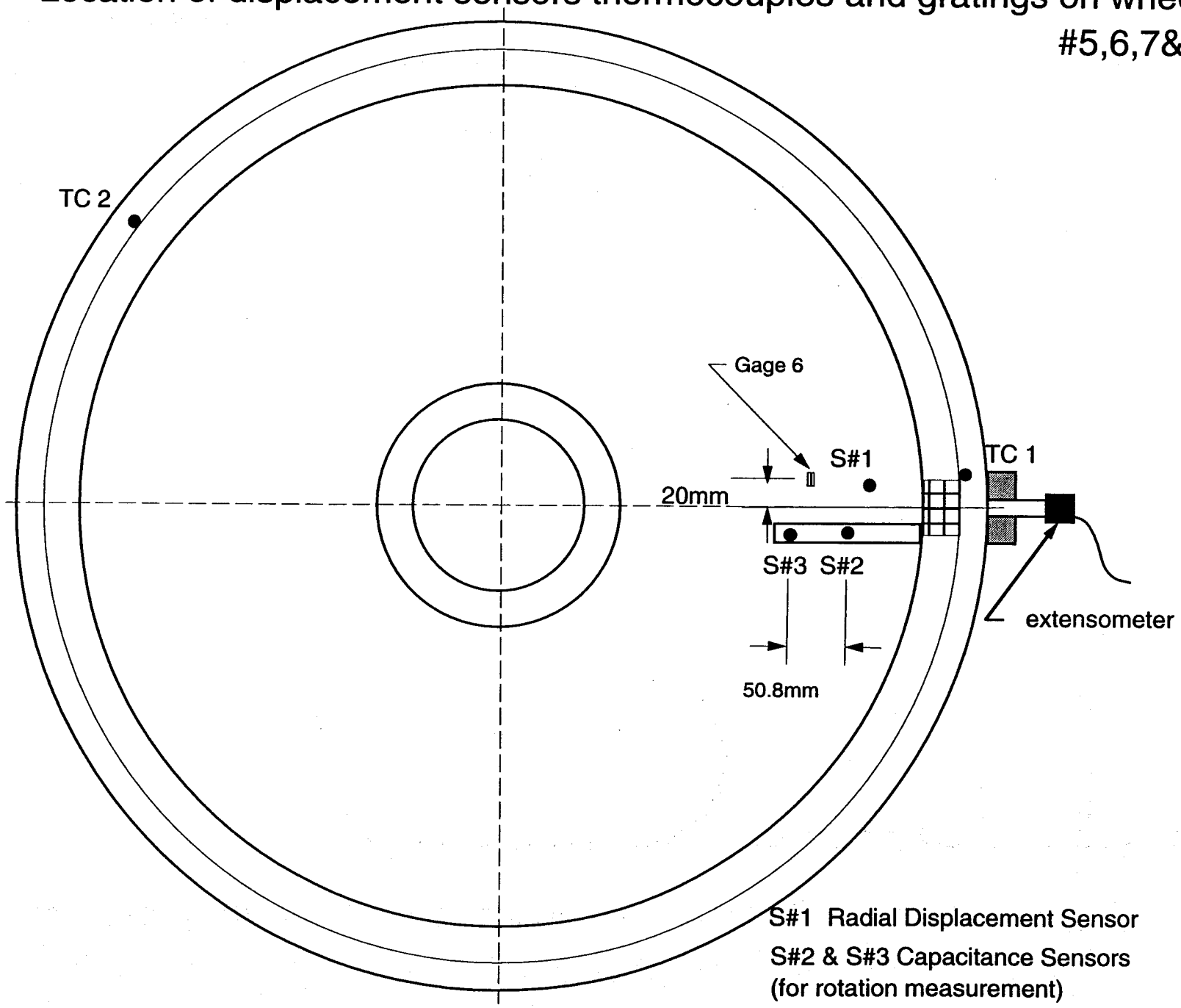

TESTING OF DOT RAILROAD CAR WHEEL #5							#26526				
DATE:	JUNE 12 1995										
	mm/mm						mm	mm	rad	(°C)	(°C)
Cut Depth (mm)	Gage1	Gage2	Gage3	Gage4	Gage5	Gage6	Radial Displacement	Opening Displacement	Rotation	TC 1	TC 2
0	0	0	0	0	0	0	0.000	0.000	0.00E+00	20.1	20.6
28	209	193	251	179	269	229	0.205	0.106	-1.39E-04	20.3	20.7
34	180	278	234	243	165	221	0.245	0.142	-2.38E-04	20.6	20.8
48	150	293	3	263	-100	188	0.362	0.214	-2.38E-04	21.6	21.4
60	160	323	-124	266	-243	172	0.513	0.294	-1.98E-04	19.1	18.9
70	162	346	-165	302	-291	142	0.697	0.388	-9.92E-05	21.6	21.2
80	133	373	-182	332	-297	58	0.920	0.523	-1.19E-04	22.1	21.3
90	110	396	-191	356	-285	5	1.339	0.680	-2.78E-04	22.5	21.3
100	102	414	-197	368	-275	67	1.759	0.833	-3.57E-04	22.7	22.5
110	103	423	-198	373	-270	264	2.074	0.947	-3.57E-04	22.9	21.4
120	104	424	-196	375	-267	445	2.381	1.041	-2.18E-04	23.0	21.5
130	108	424	-193	373	-264	457	2.660	1.116	2.20E-18	22.9	21.5
140	111	424	-189	372	-261	446	2.997	1.187	2.98E-04	22.8	21.5
150	114	423	-185	371	-259	441	3.349	1.264	6.55E-04	22.9	21.6
160	116	422	-183	370	-257	441	3.674	1.333	9.52E-04	22.8	21.5
170	118	421	-182	368	-257	439	4.009	1.409	1.21E-03	22.9	21.6
180	119	420	-179	366	-255	435	4.302	1.482	1.47E-03	22.9	21.6
190	120	420	-179	366	-254	436	4.628	1.559	1.77E-03	22.8	21.6
200	121	419	-178	363	-253	433	4.933	1.638	2.06E-03	22.8	21.6
END											

Railroad Wheel No. 5 Test
Displacement vs. Cut Depth

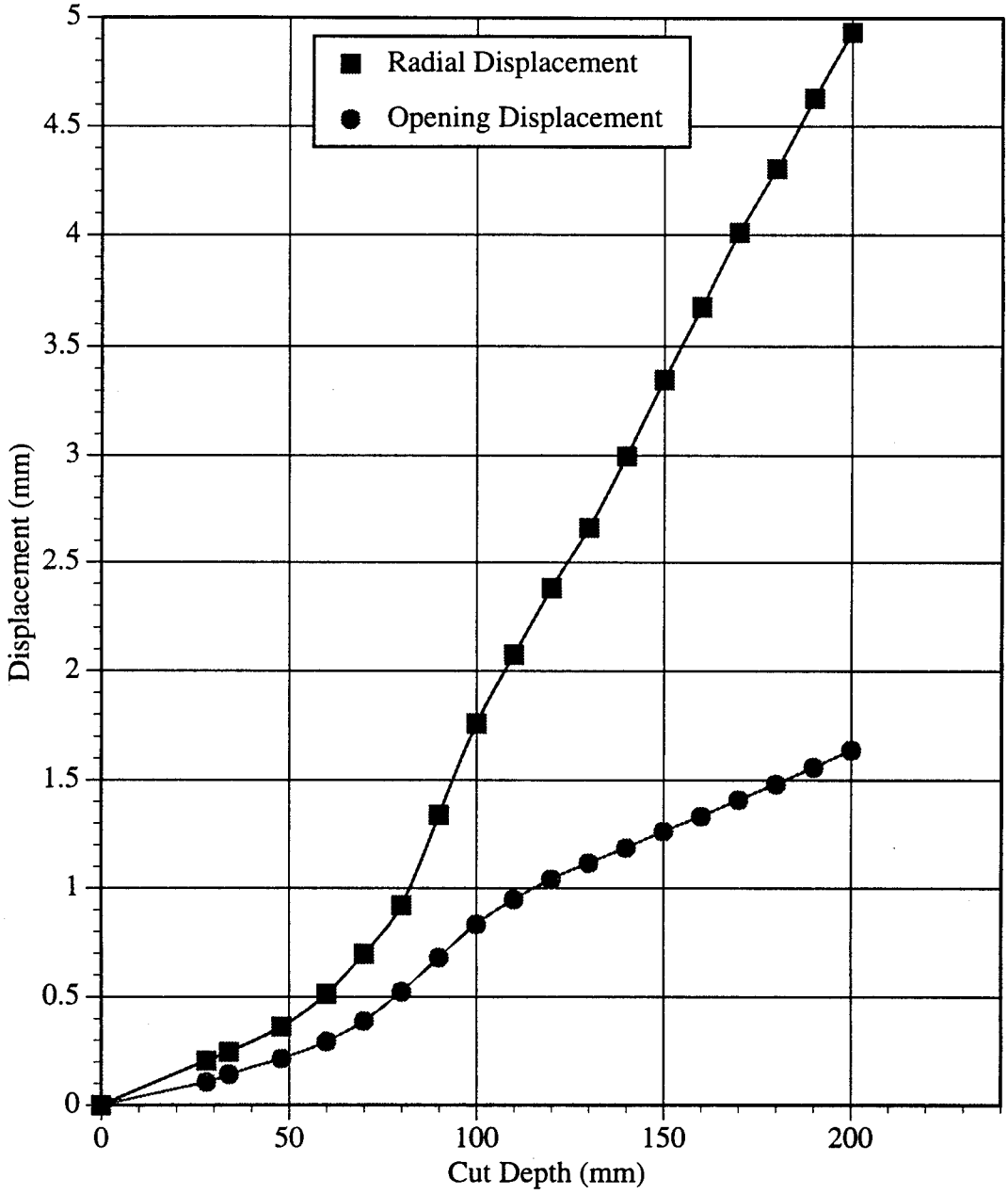

Railroad Wheel No. 5 Test
Strain Gage Readings vs. Cut Depth

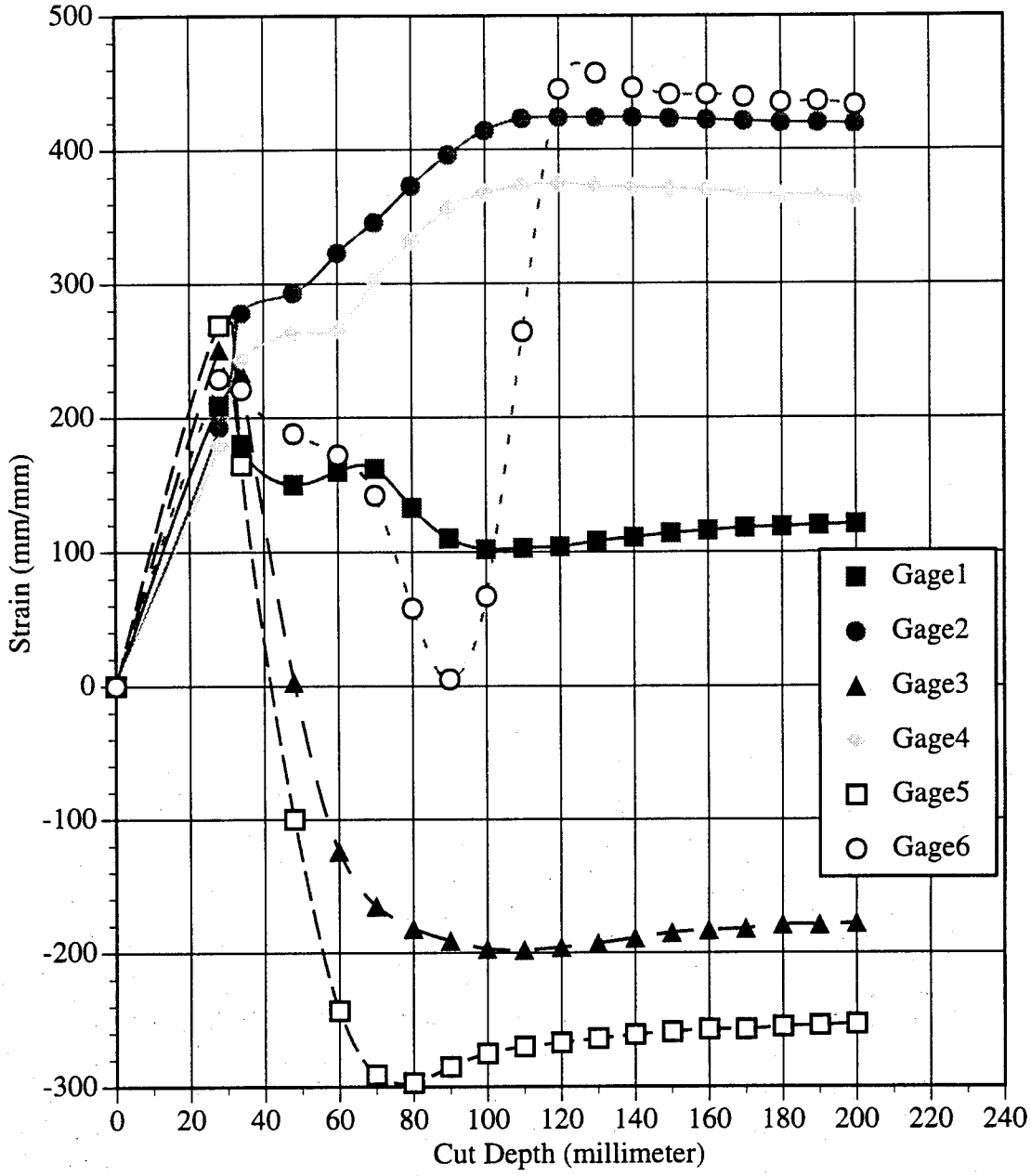

Railroad Wheel No. 5 Test
Wheel Rotation vs. Cut Depth

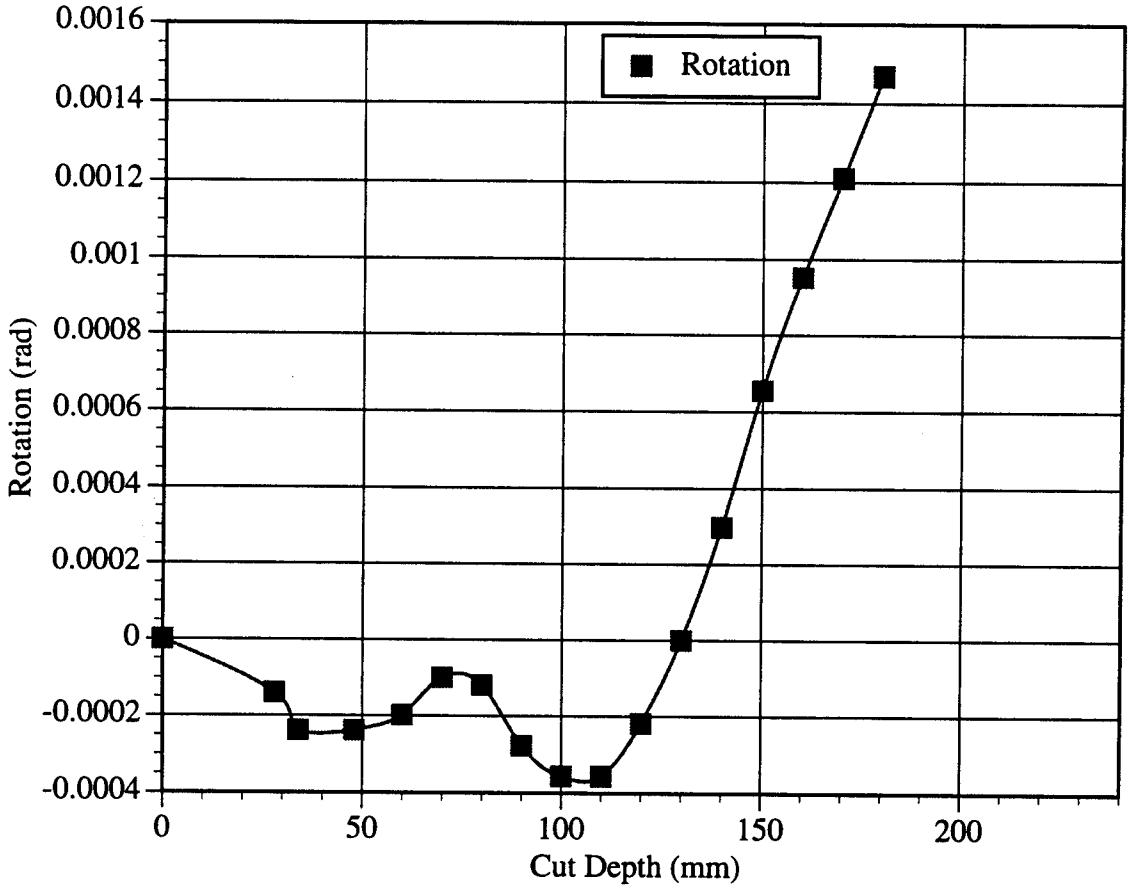

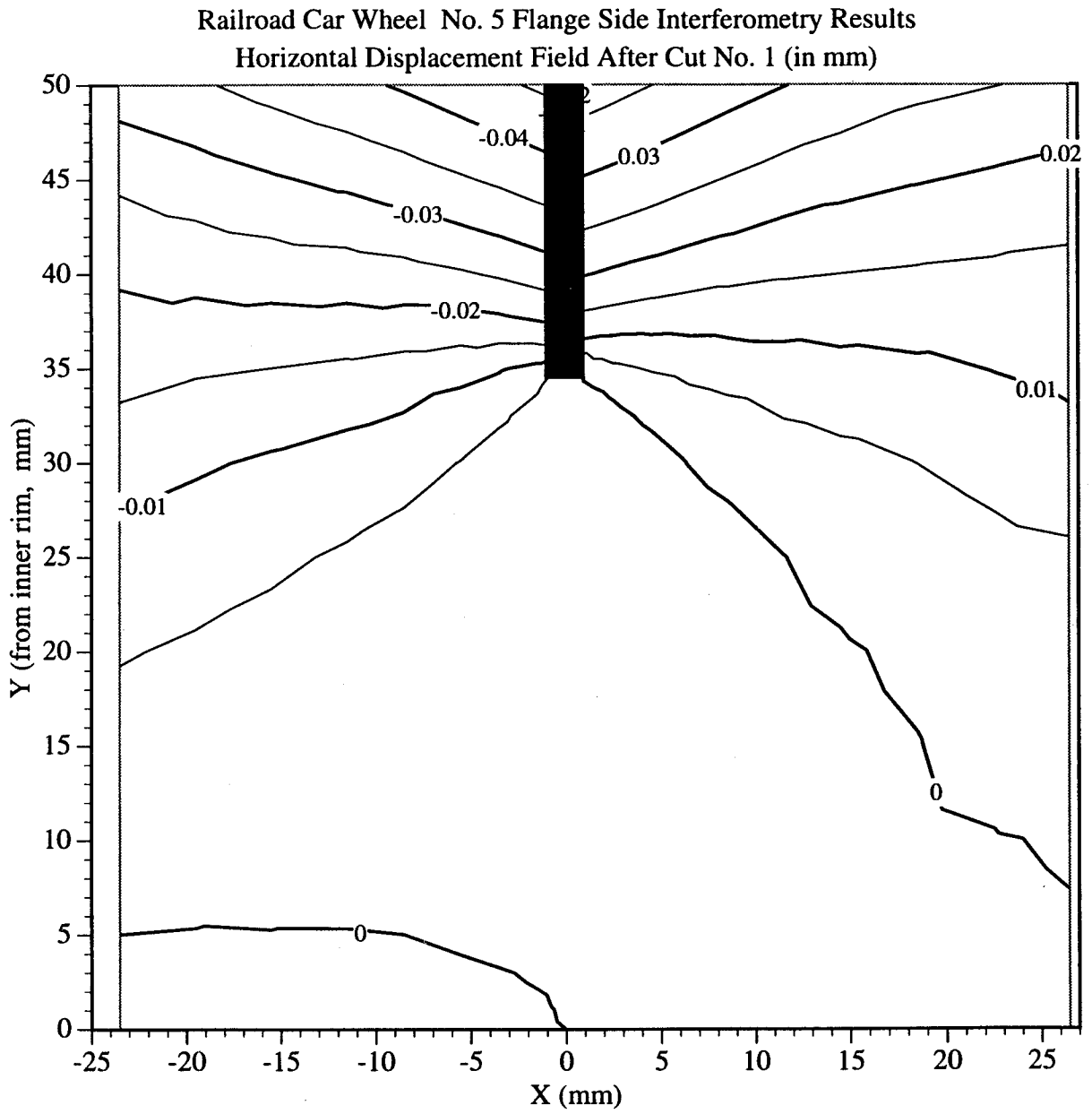
Railroad Car Wheel No. 5 Flange Side Interferometry Results
Horizontal Displacement Field After Cut No. 1 (in mm)
-0.04
0.03
0.02
-0.03
-0.02
0.01
-0.01
0
0
Y (from inner rim, mm)
X (mm)
50
45
40
35
30
25
20
15
10
5
0
-25
-20
-15
-10
-5
0
5
10
15
20
25

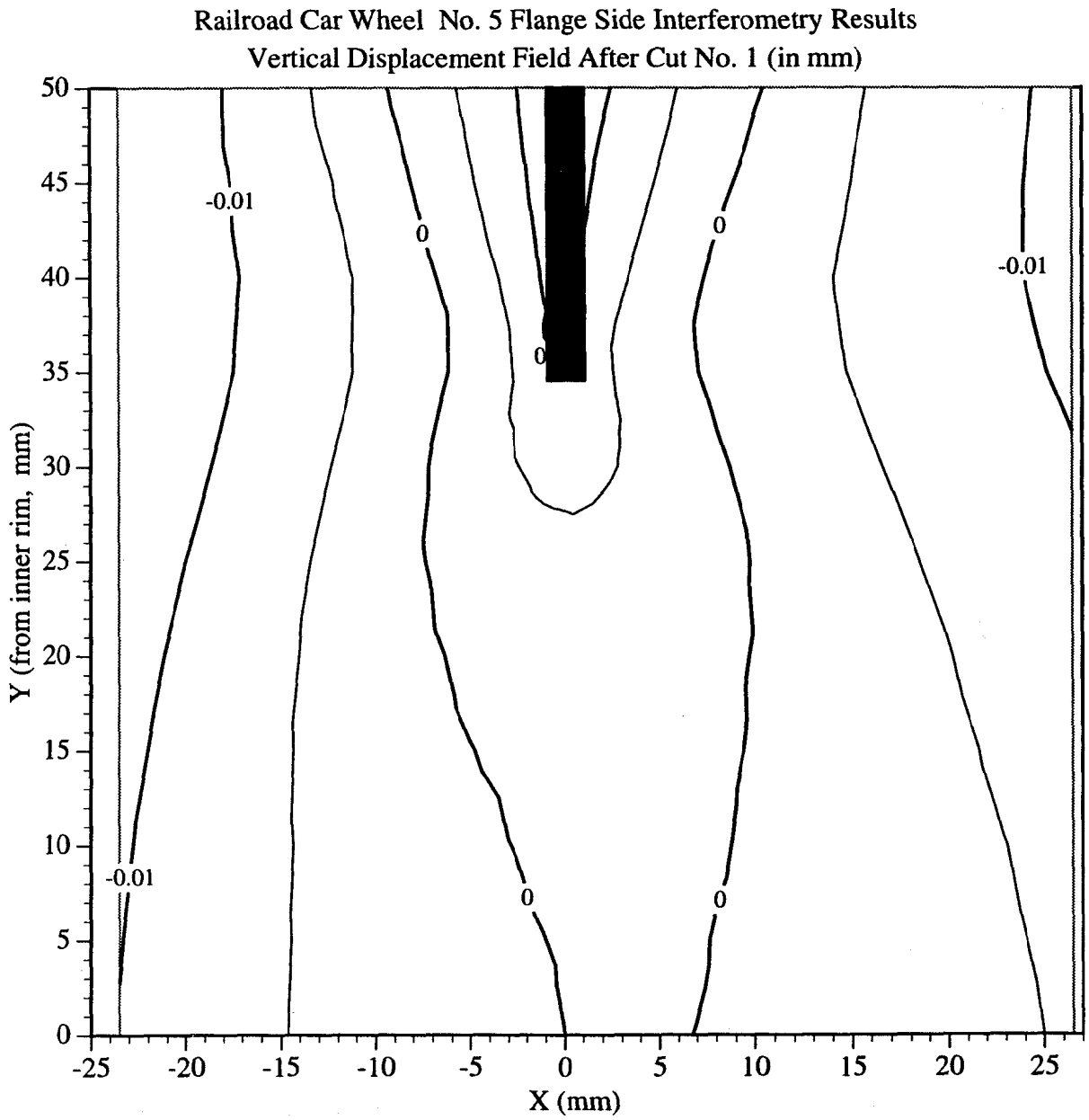
Railroad Car Wheel No. 5 Flange Side Interferometry Results
Vertical Displacement Field After Cut No. 1 (in mm)
Y (from inner rim, mm)
X (mm)
-0.01
0
0
0
-0.01
-0.01
0
0
50
45
40
35
30
25
20
15
10
5
0
-25
-20
-15
-10
-5
0
5
10
15
20
25

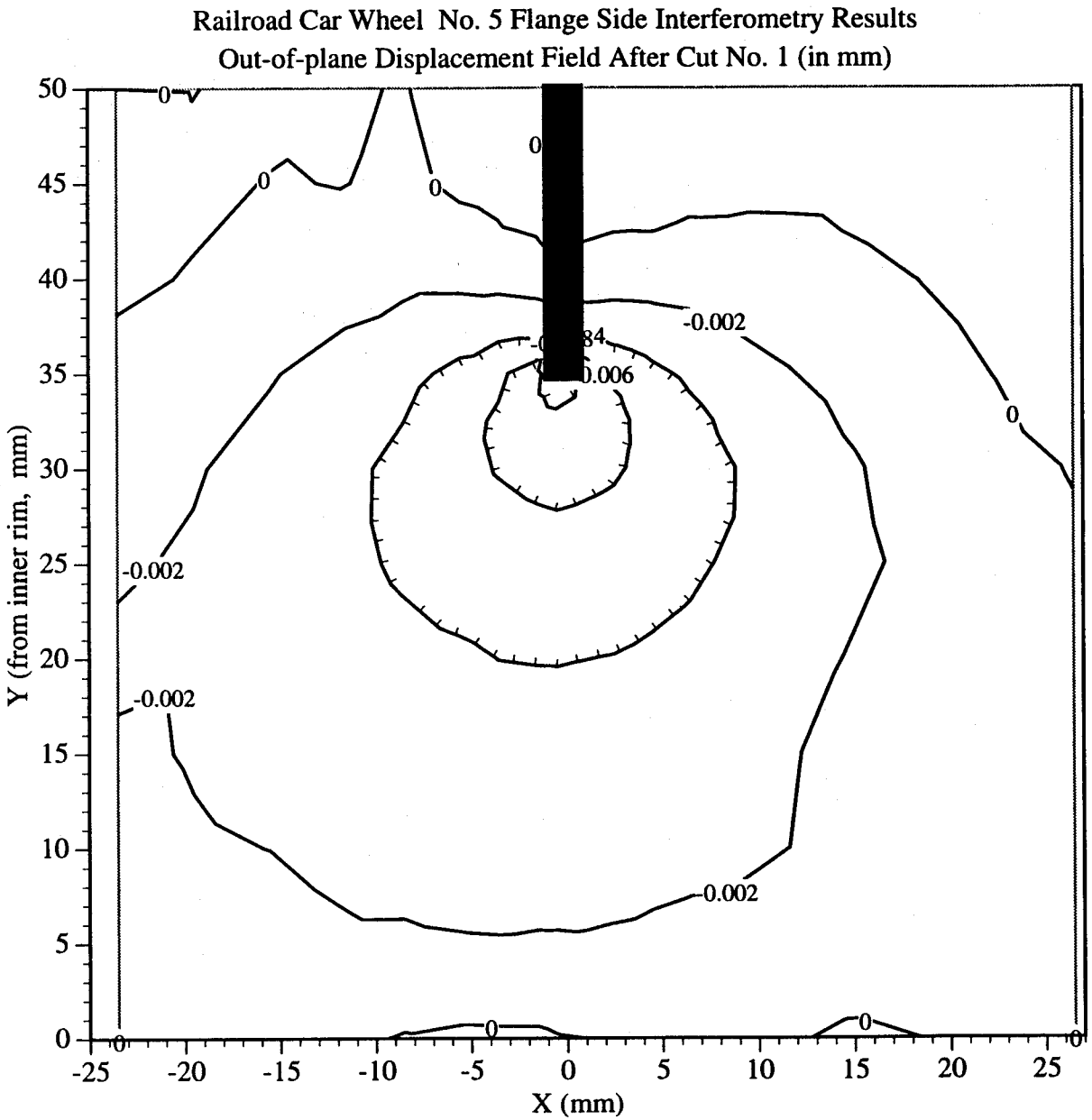
Railroad Car Wheel No. 5 Flange Side Interferometry Results
Out-of-plane Displacement Field After Cut No. 1 (in mm)
Y (from inner rim, mm)
X (mm)
50
45
40
35
30
25
20
15
10
5
0
-25
-20
-15
-10
-5
0
5
10
15
20
25
0
-0.002
0.006

Railroad Car Wheel No. 5 Flange Side Interferometry Results

Residual Strain (ε_x) Field After Cut No. 1 (in mm)

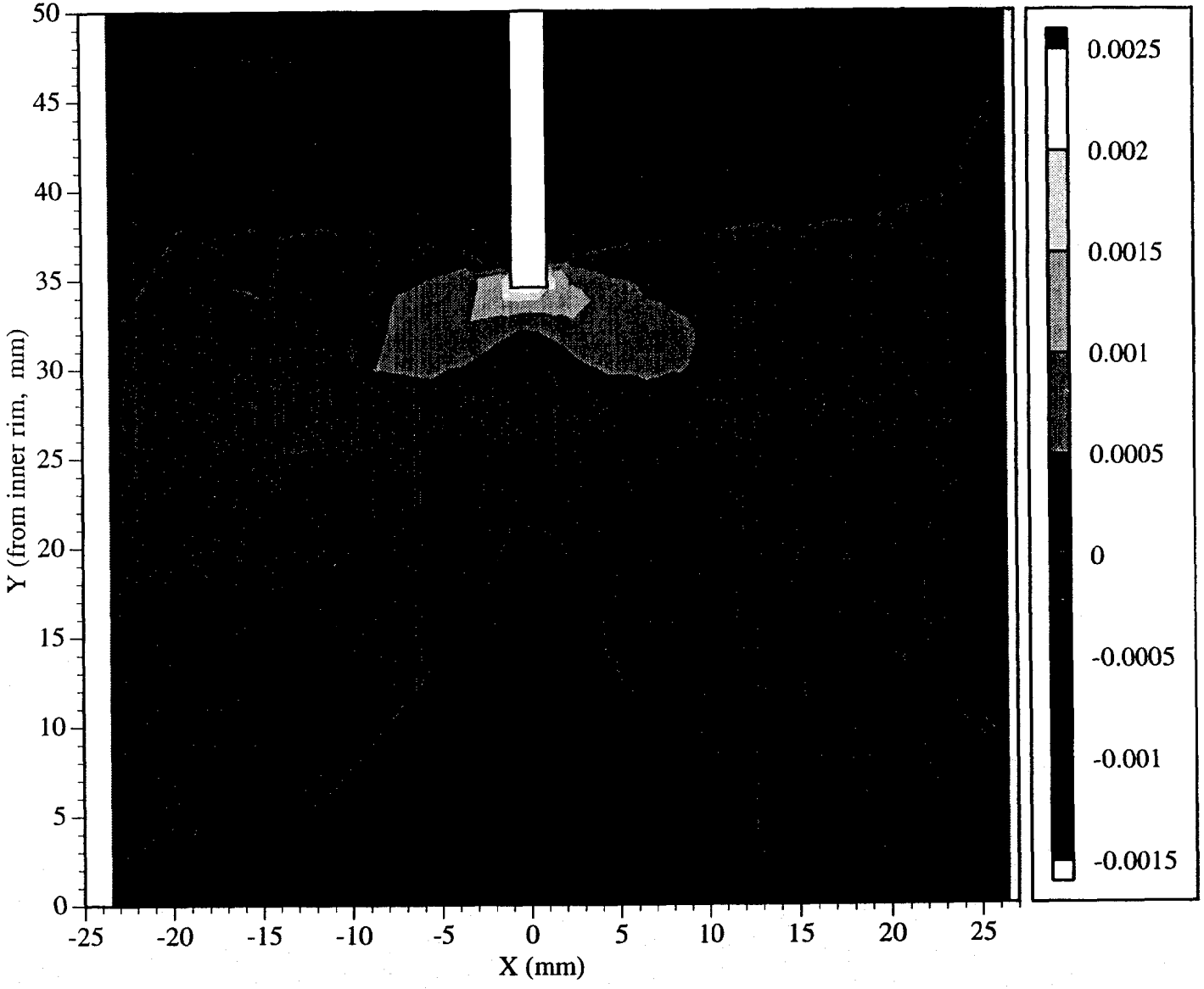

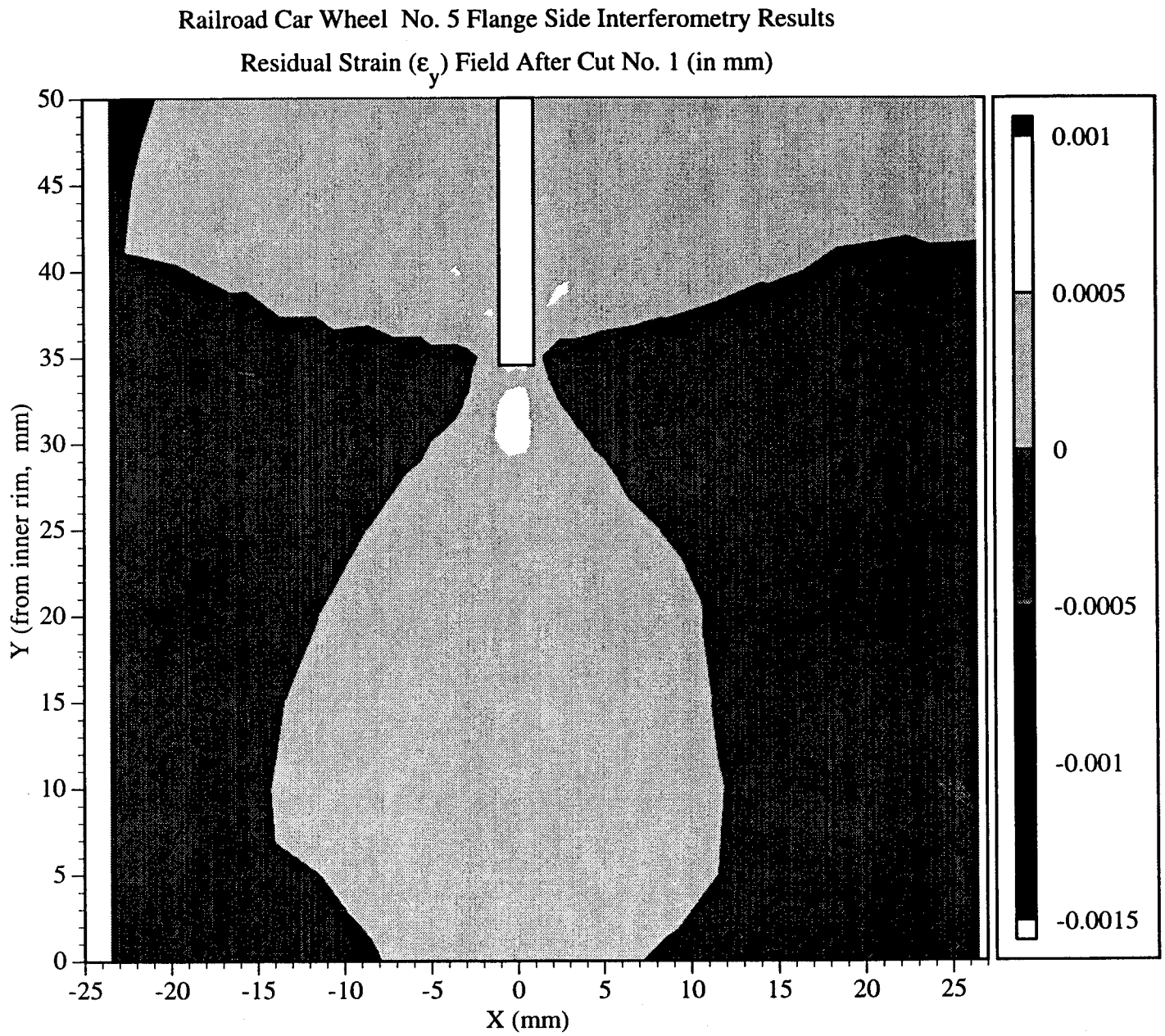
Railroad Car Wheel No. 5 Flange Side Interferometry Results
Residual Strain (ε_y) Field After Cut No. 1 (in mm)
Y (from inner rim, mm)
X (mm)
50
45
40
35
30
25
20
15
10
5
0
-25
-20
-15
-10
-5
0
5
10
15
20
25
0.001
0.0005
0
-0.0005
-0.001
-0.0015

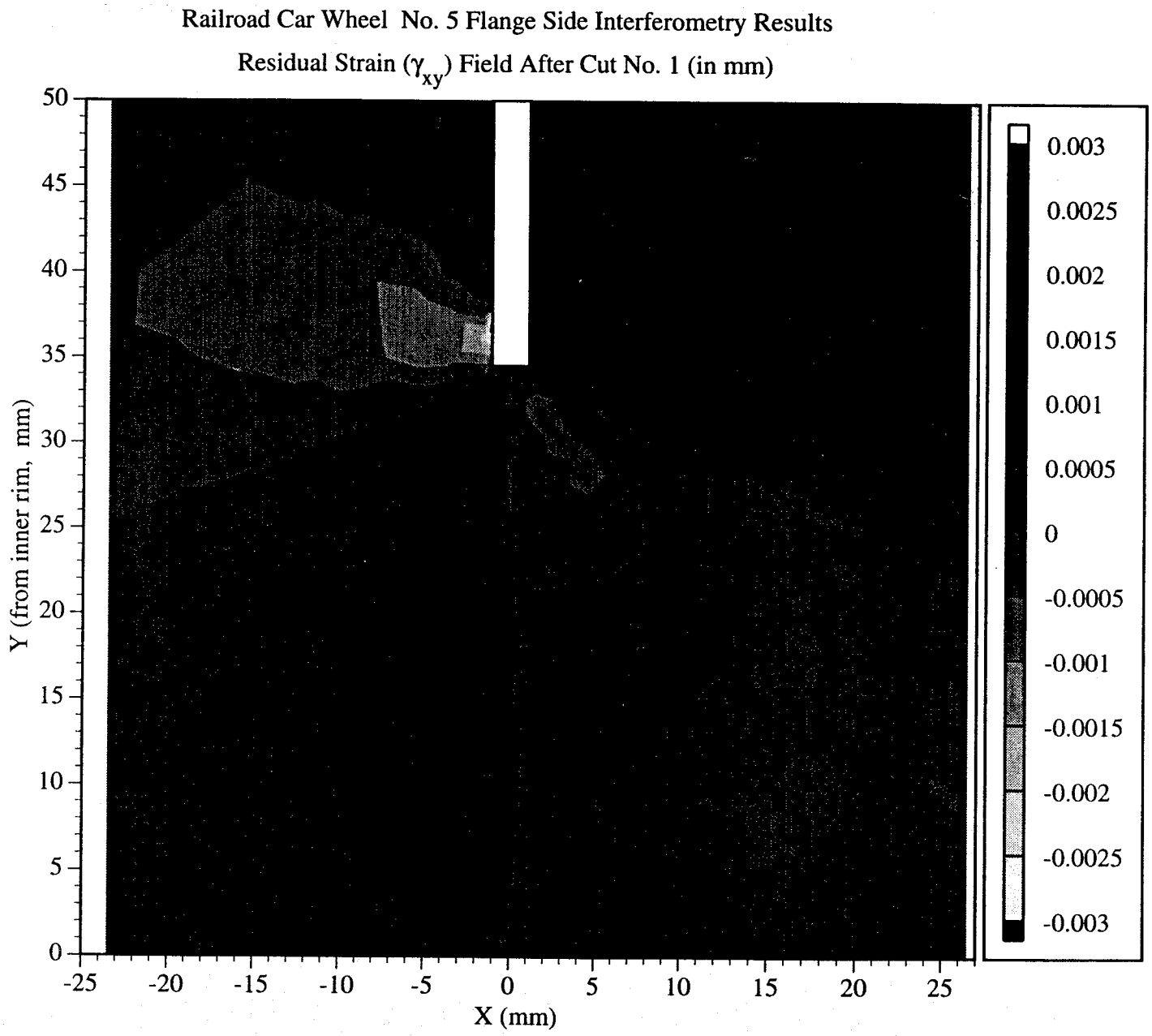
Railroad Car Wheel No. 5 Flange Side Interferometry Results
Residual Strain (γ_{xy}) Field After Cut No. 1 (in mm)
Y (from inner rim, mm)
X (mm)
50
45
40
35
30
25
20
15
10
5
0
-25
-20
-15
-10
-5
0
5
10
15
20
25
0.003
0.0025
0.002
0.0015
0.001
0.0005
0
-0.0005
-0.001
-0.0015
-0.002
-0.0025
-0.003

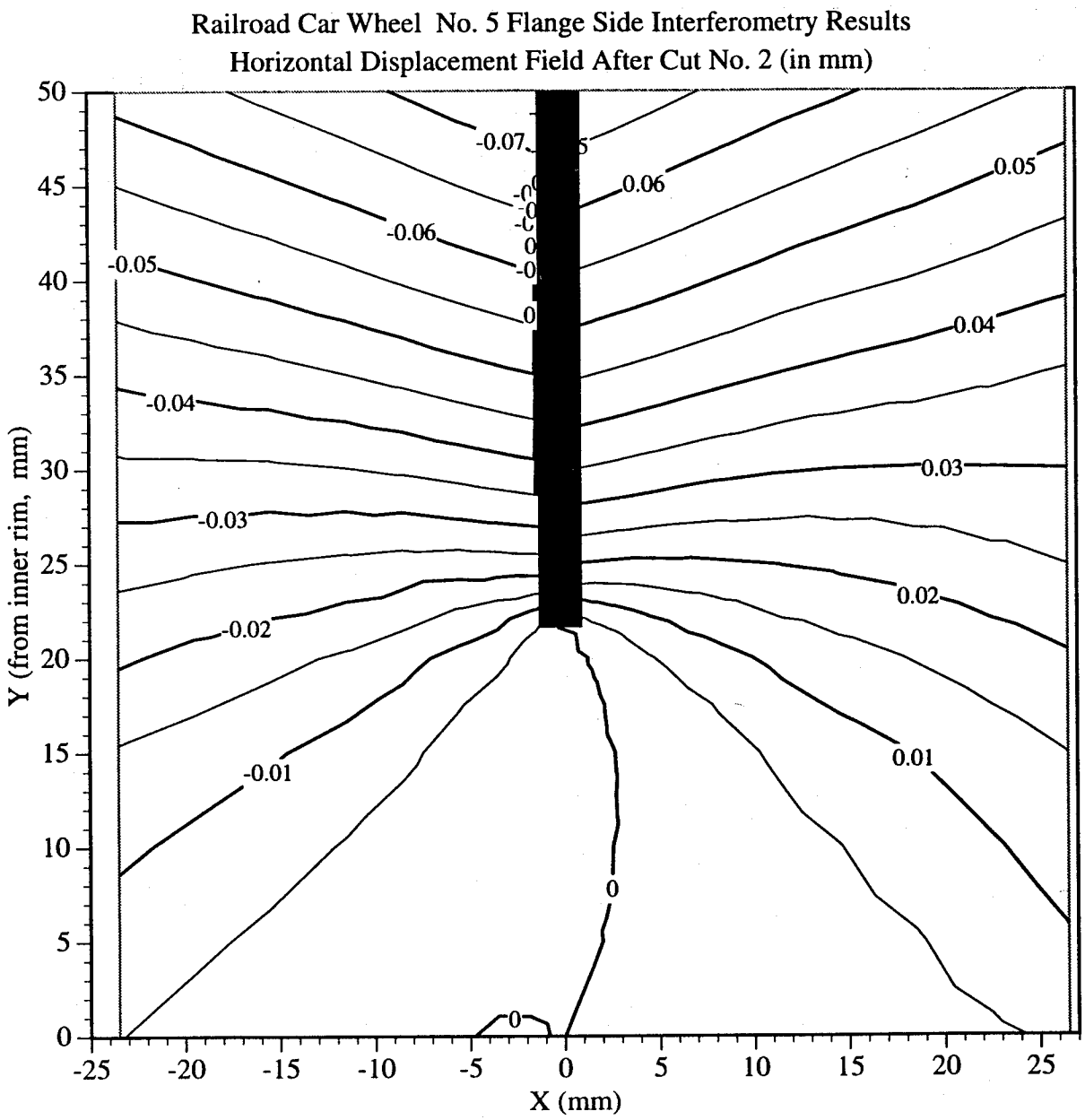
Railroad Car Wheel No. 5 Flange Side Interferometry Results
Horizontal Displacement Field After Cut No. 2 (in mm)
Y (from inner rim, mm)
X (mm)
-0.07
-0.06
-0.05
-0.04
-0.03
-0.02
-0.01
0
0.01
0.02
0.03
0.04
0.05
0.06

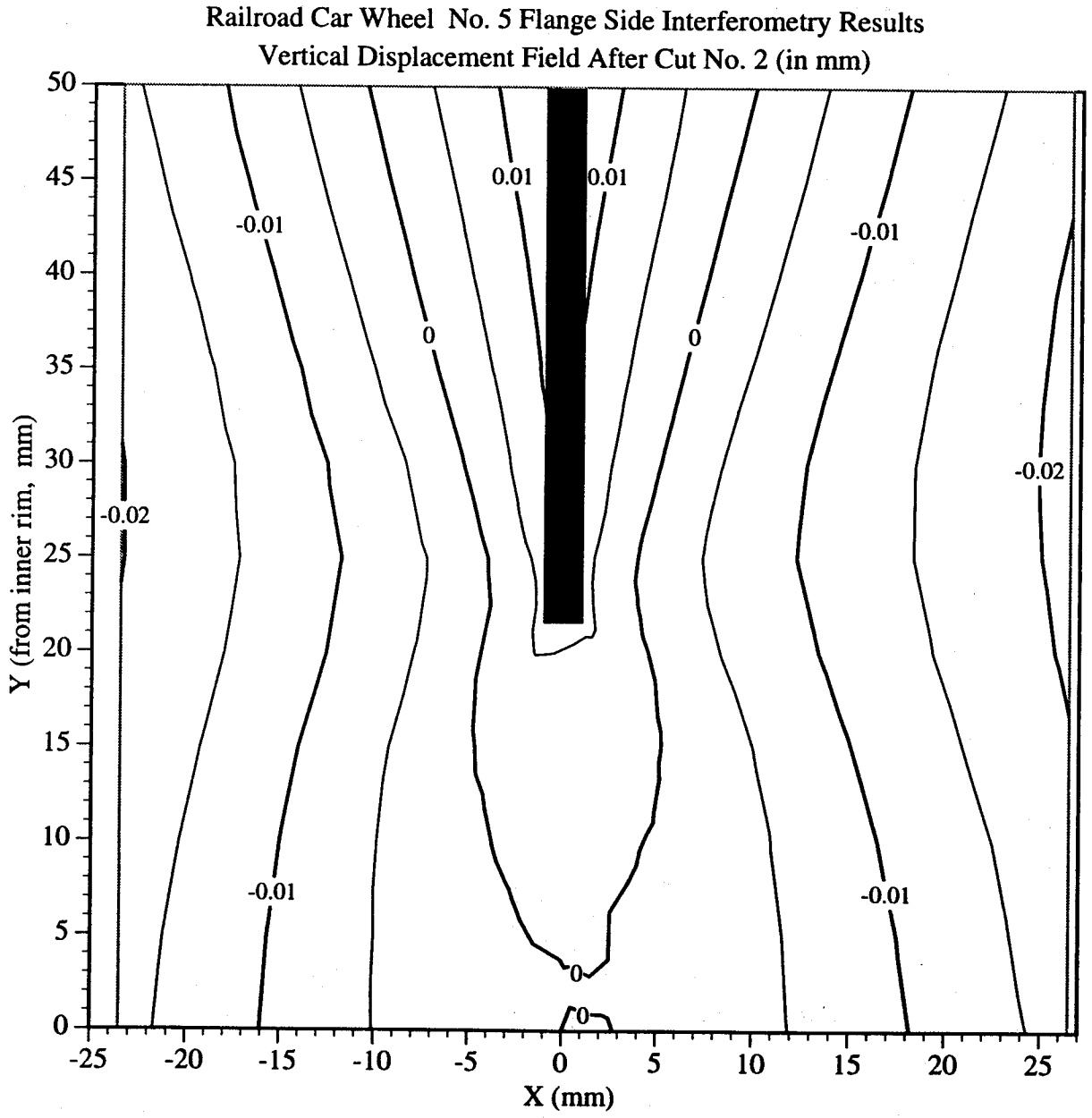
Railroad Car Wheel No. 5 Flange Side Interferometry Results
Vertical Displacement Field After Cut No. 2 (in mm)
Y (from inner rim, mm)
X (mm)
50
45
40
35
30
25
20
15
10
5
0
-25
-20
-15
-10
-5
0
5
10
15
20
25
-0.02
-0.01
0
0.01
0.01
0
-0.01
-0.02
-0.01
-0.01
0
0

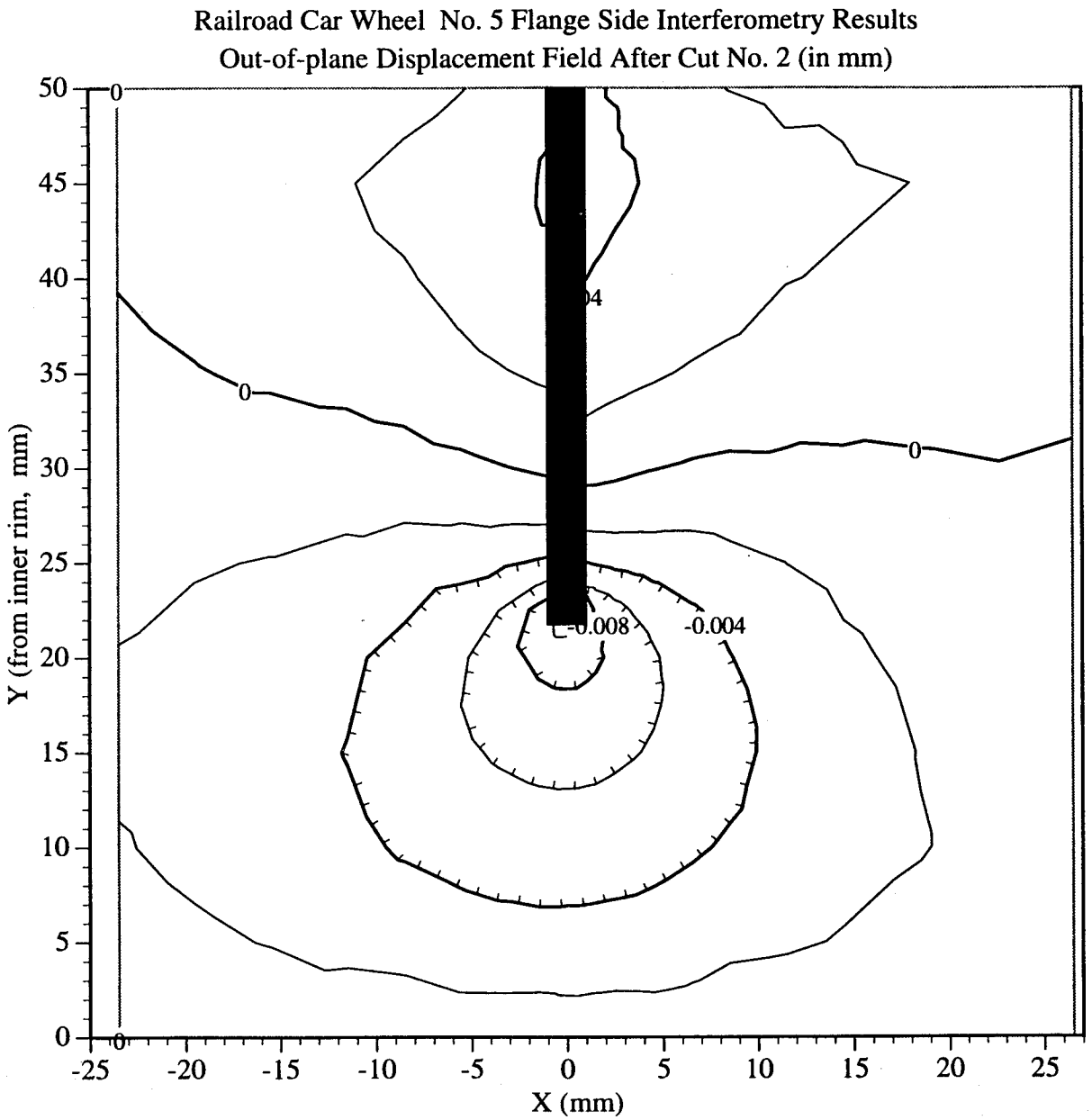
Railroad Car Wheel No. 5 Flange Side Interferometry Results
Out-of-plane Displacement Field After Cut No. 2 (in mm)
Y (from inner rim, mm)
X (mm)
0
-0.004
-0.008
50
45
40
35
30
25
20
15
10
5
0
-25
-20
-15
-10
-5
0
5
10
15
20
25

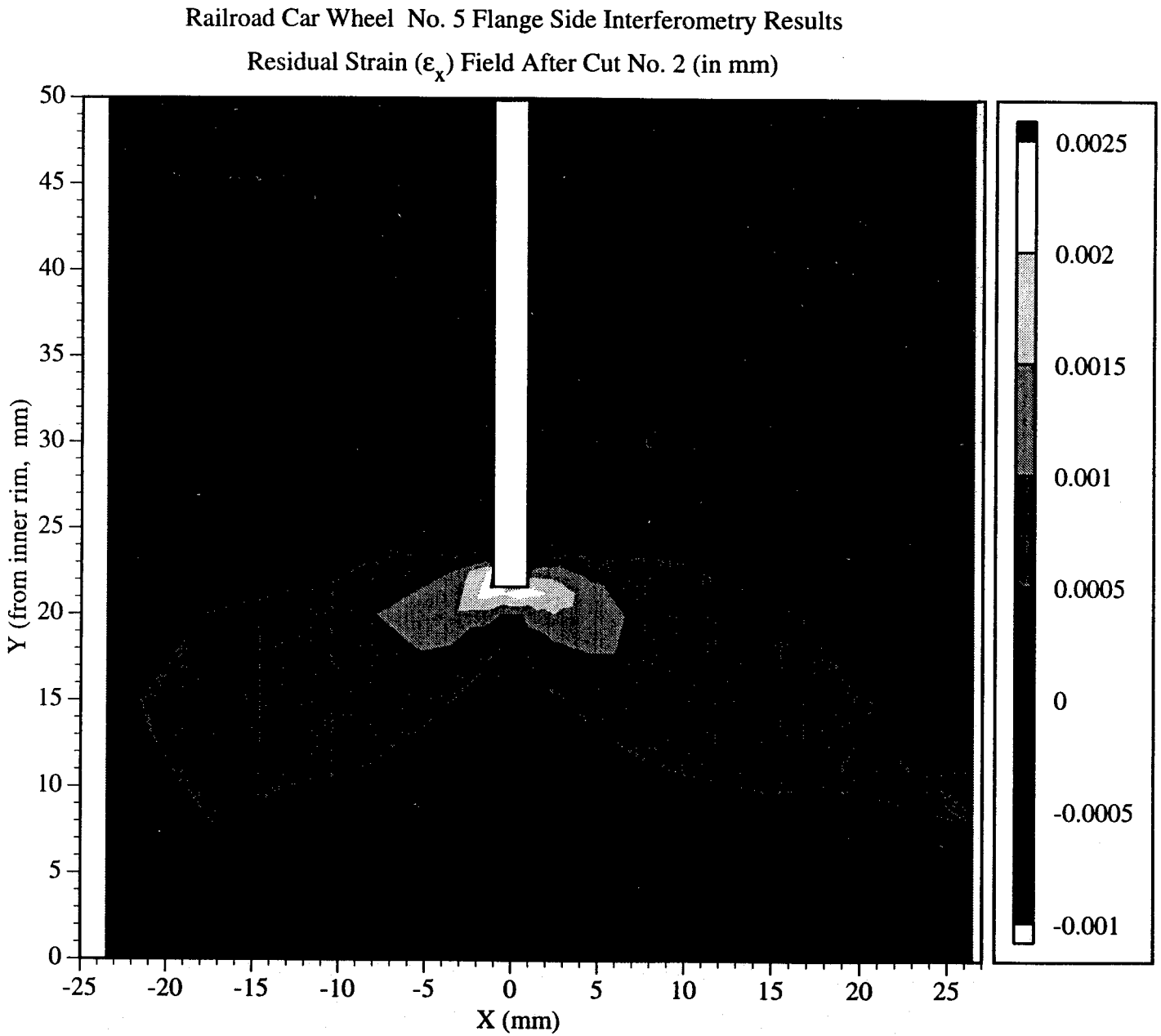
Railroad Car Wheel No. 5 Flange Side Interferometry Results
Residual Strain (ε_x) Field After Cut No. 2 (in mm)
Y (from inner rim, mm)
X (mm)
50
45
40
35
30
25
20
15
10
5
0
-25
-20
-15
-10
-5
0
5
10
15
20
25
0.0025
0.002
0.0015
0.001
0.0005
0
-0.0005
-0.001

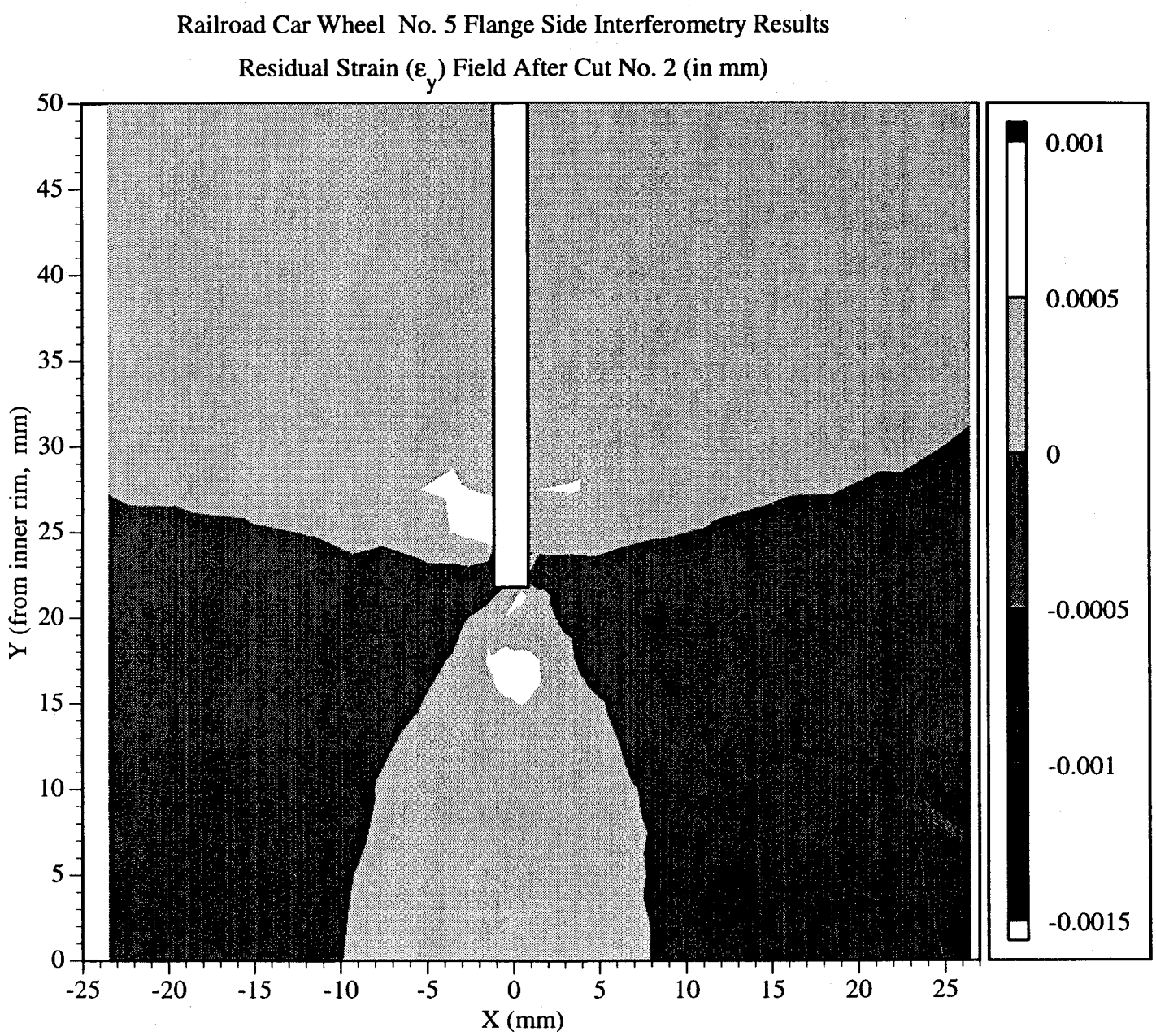
Railroad Car Wheel No. 5 Flange Side Interferometry Results
Residual Strain (ε_y) Field After Cut No. 2 (in mm)
Y (from inner rim, mm)
X (mm)
50
45
40
35
30
25
20
15
10
5
0
-25
-20
-15
-10
-5
0
5
10
15
20
25
0.001
0.0005
0
-0.0005
-0.001
-0.0015

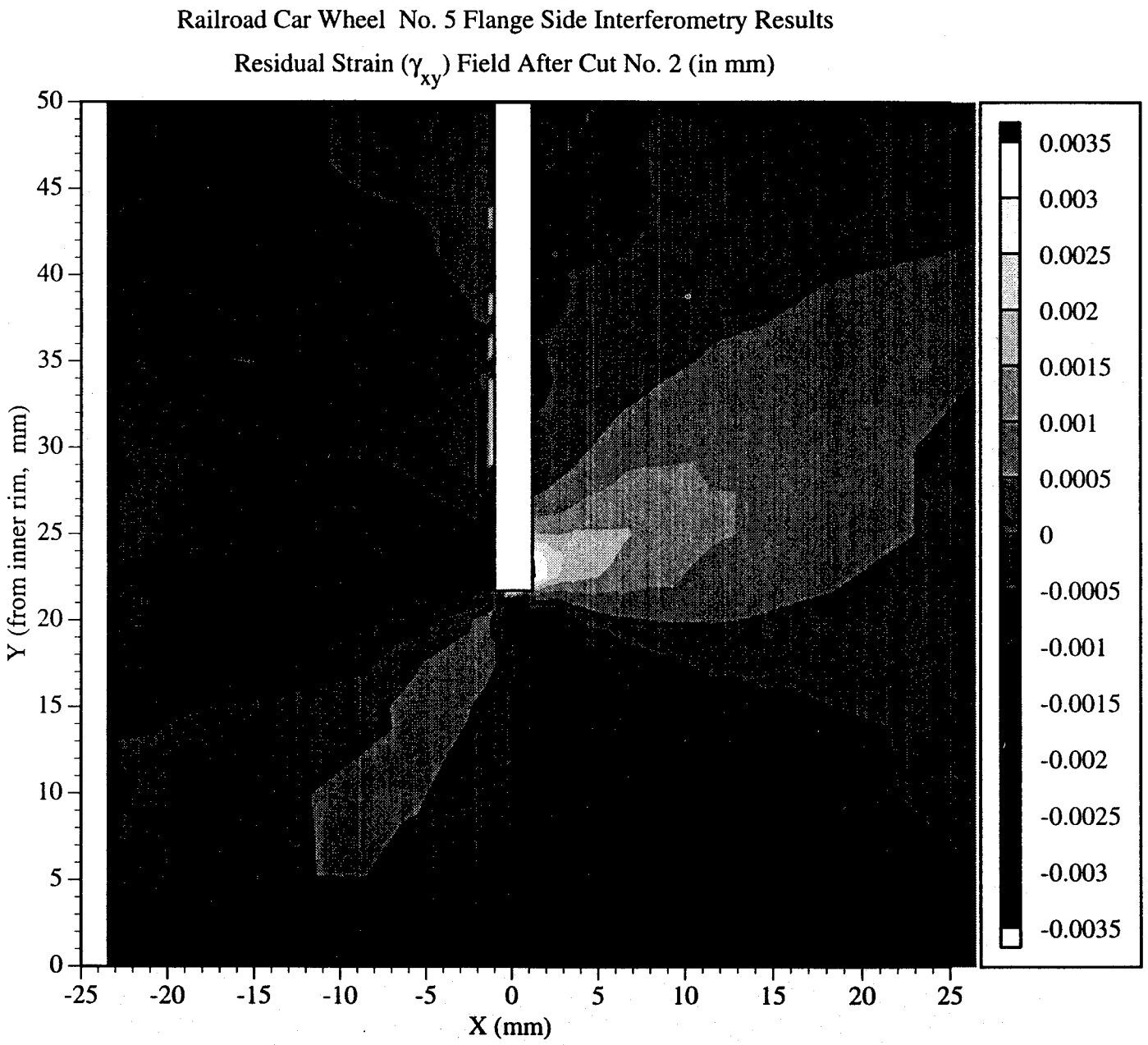
Railroad Car Wheel No. 5 Flange Side Interferometry Results
Residual Strain (γ_{xy}) Field After Cut No. 2 (in mm)
Y (from inner rim, mm)
X (mm)
50
45
40
35
30
25
20
15
10
5
0
-25
-20
-15
-10
-5
0
5
10
15
20
25
0.0035
0.003
0.0025
0.002
0.0015
0.001
0.0005
0
-0.0005
-0.001
-0.0015
-0.002
-0.0025
-0.003
-0.0035

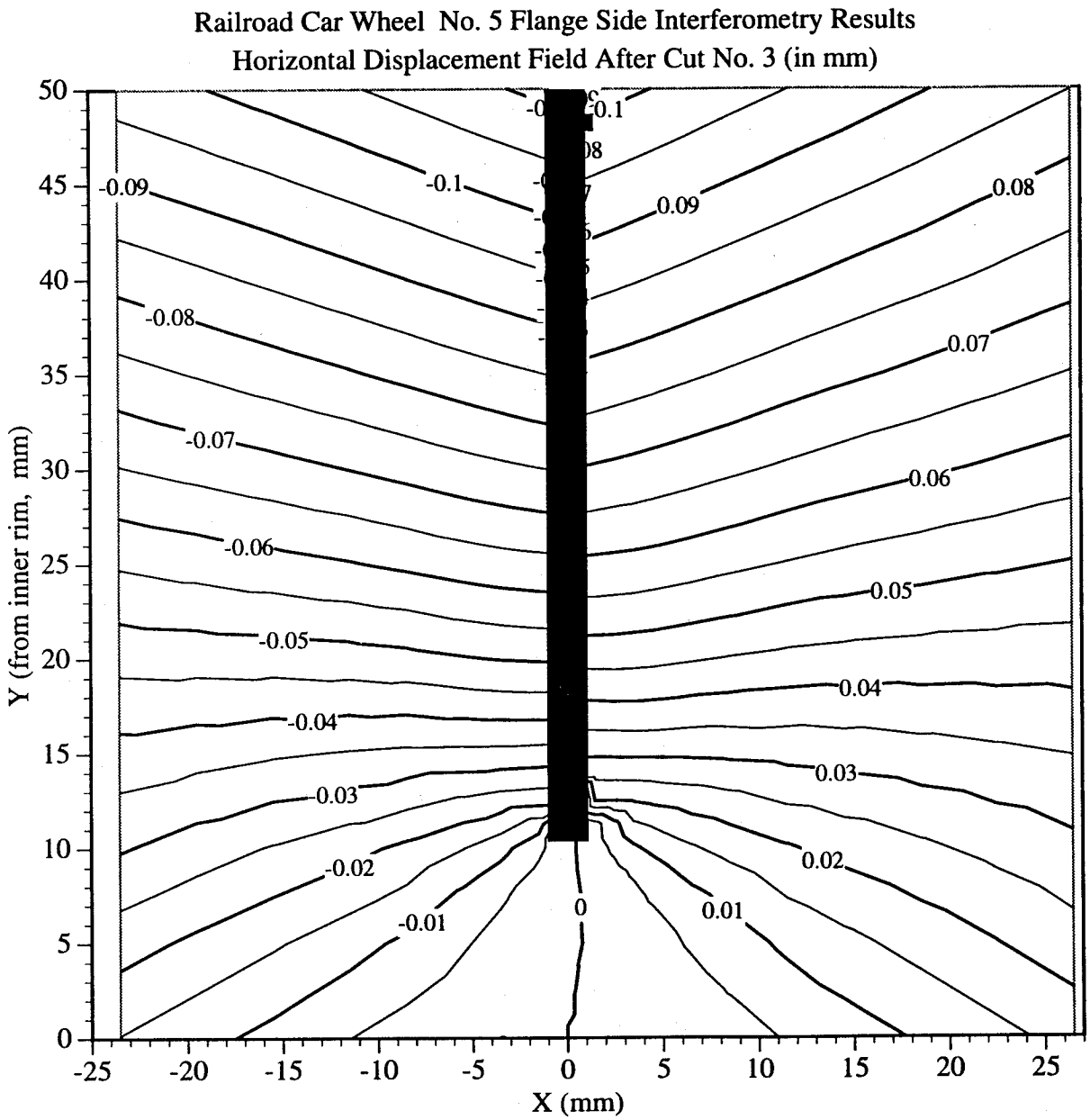
Railroad Car Wheel No. 5 Flange Side Interferometry Results
Horizontal Displacement Field After Cut No. 3 (in mm)
Y (from inner rim, mm)
X (mm)
50
45
40
35
30
25
20
15
10
5
0
-25
-20
-15
-10
-5
0
5
10
15
20
25
-0.09
-0.08
-0.07
-0.06
-0.05
-0.04
-0.03
-0.02
-0.01
0
0.01
0.02
0.03
0.04
0.05
0.06
0.07
0.08
0.09
-0.1
0.1

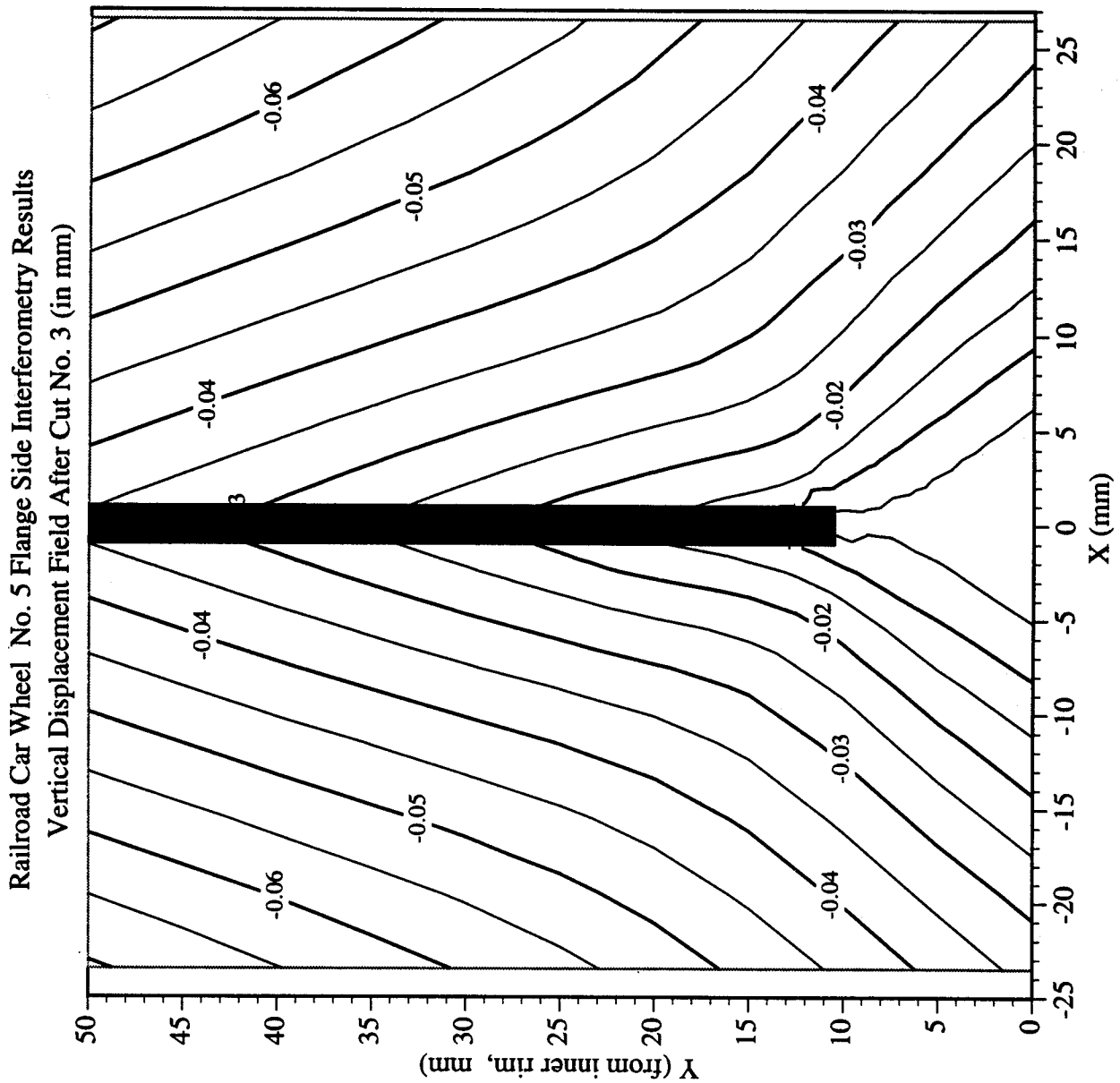
Railroad Car Wheel No. 5 Flange Side Interferometry Results
Vertical Displacement Field After Cut No. 3 (in mm)
-0.06
-0.05
-0.04
-0.03
-0.02
3
Y (from inner rim, mm)
X (mm)
50
45
40
35
30
25
20
15
10
5
0
-25
-20
-15
-10
-5
0
5
10
15
20
25

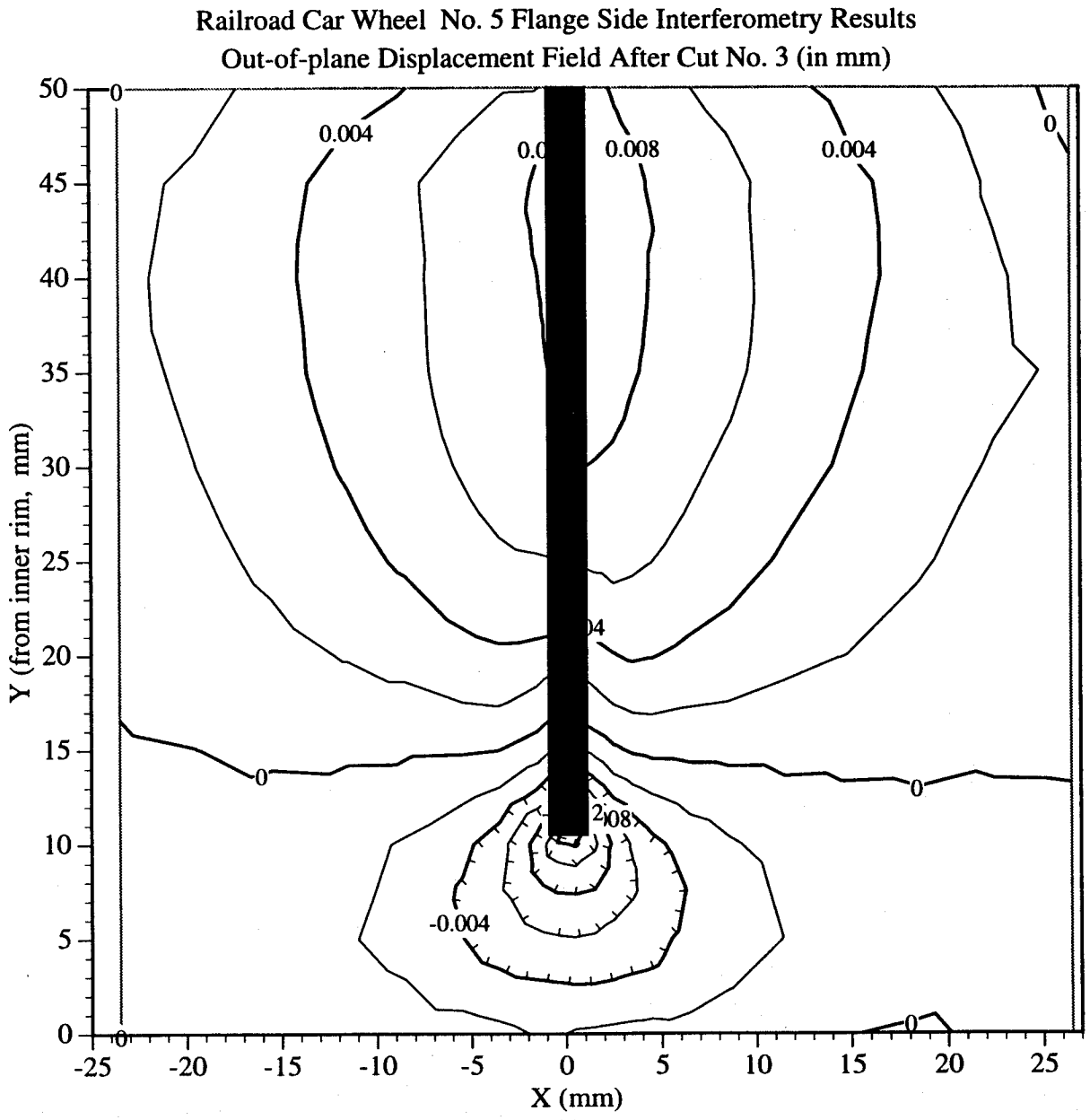
Railroad Car Wheel No. 5 Flange Side Interferometry Results
Out-of-plane Displacement Field After Cut No. 3 (in mm)
Y (from inner rim, mm)
X (mm)
0.004
0.008
-0.004

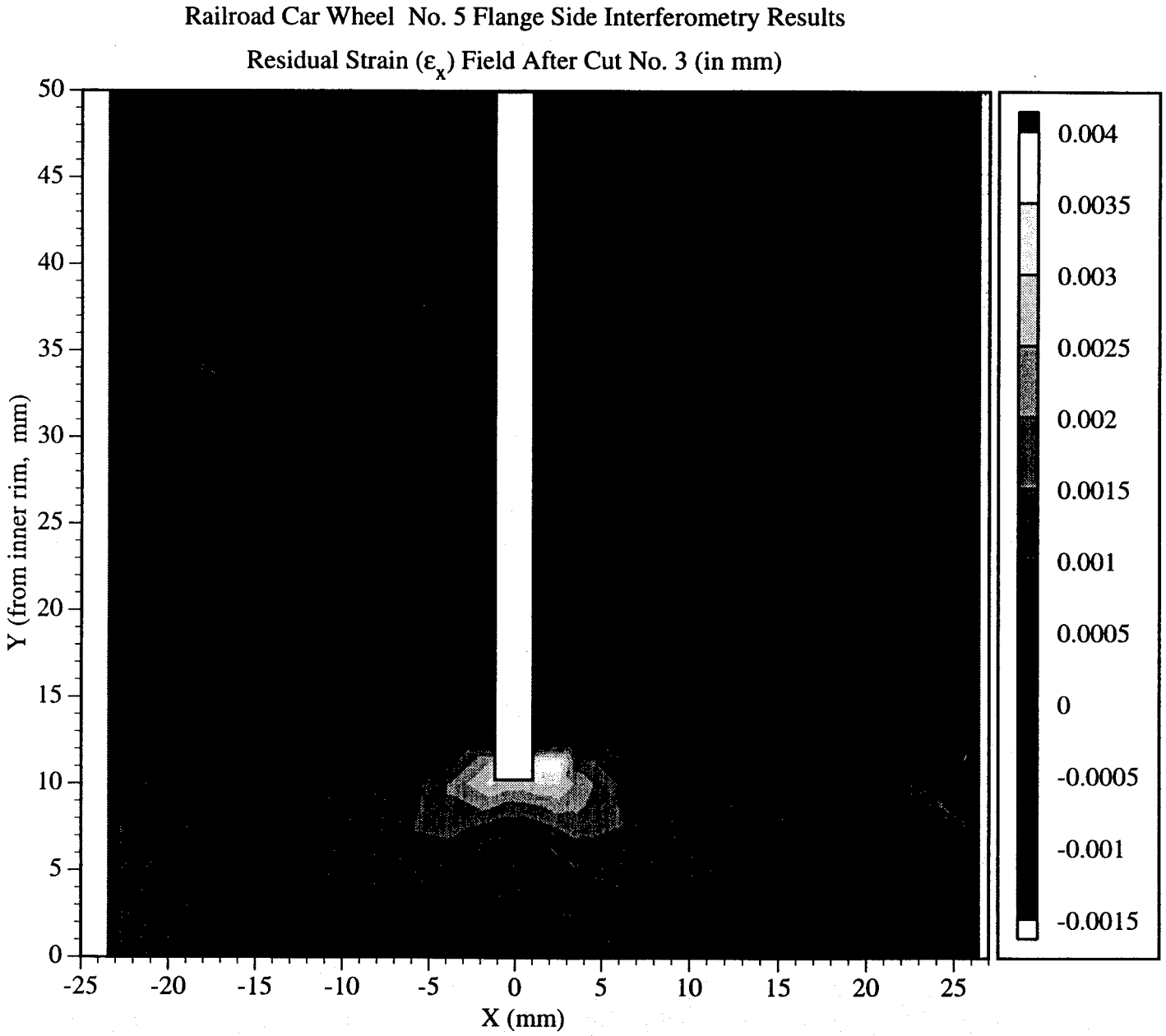
Railroad Car Wheel No. 5 Flange Side Interferometry Results
Residual Strain (ε_x) Field After Cut No. 3 (in mm)
Y (from inner rim, mm)
X (mm)
50
45
40
35
30
25
20
15
10
5
0
-25
-20
-15
-10
-5
0
5
10
15
20
25
0.004
0.0035
0.003
0.0025
0.002
0.0015
0.001
0.0005
0
-0.0005
-0.001
-0.0015

Railroad Car Wheel No. 5 Flange Side Interferometry Results

Residual Strain (ε_y) Field After Cut No. 3 (in mm)

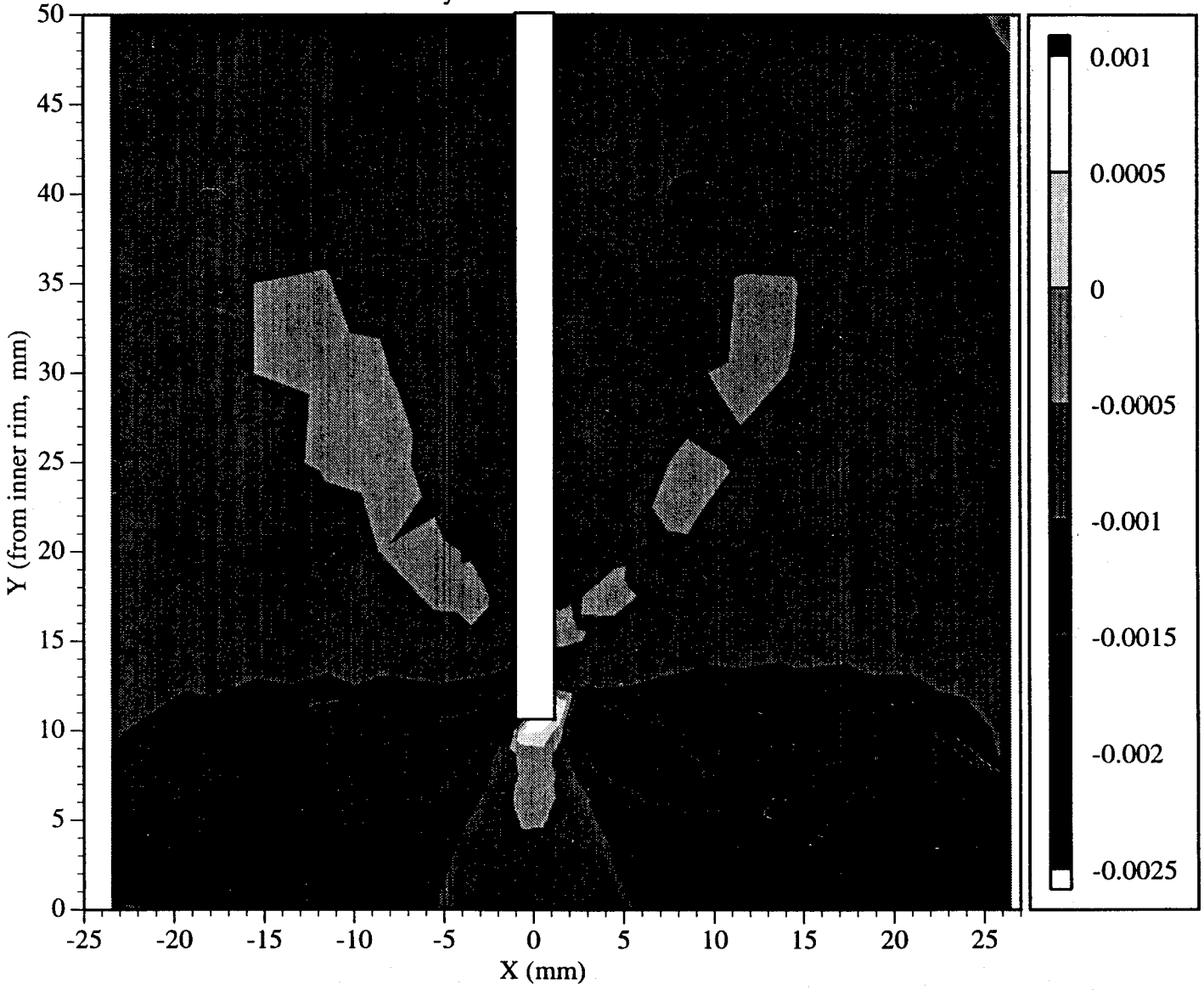

Railroad Car Wheel No. 5 Flange Side Interferometry Results

Residual Strain (γ_{xy}) Field After Cut No. 3 (in mm)

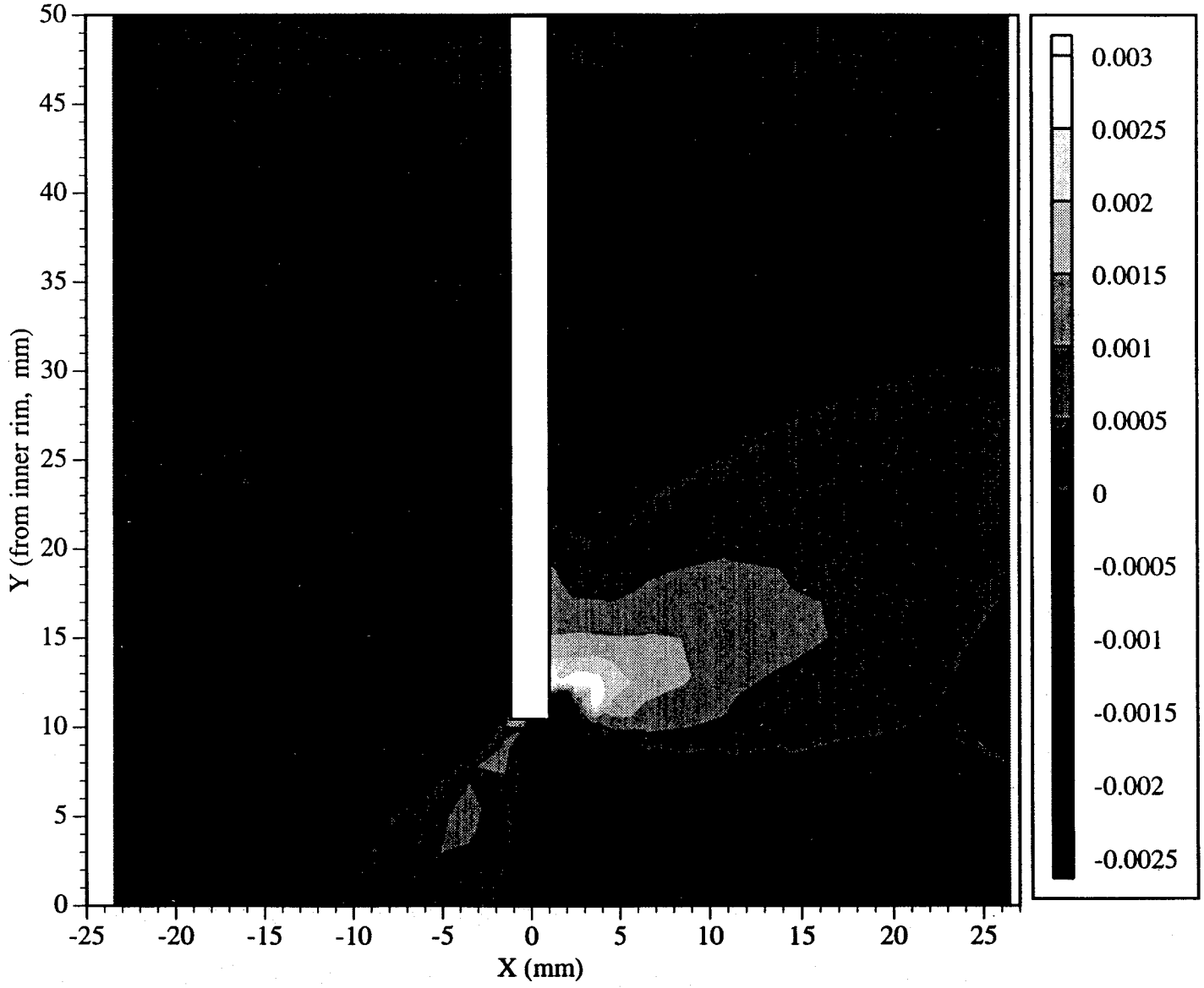

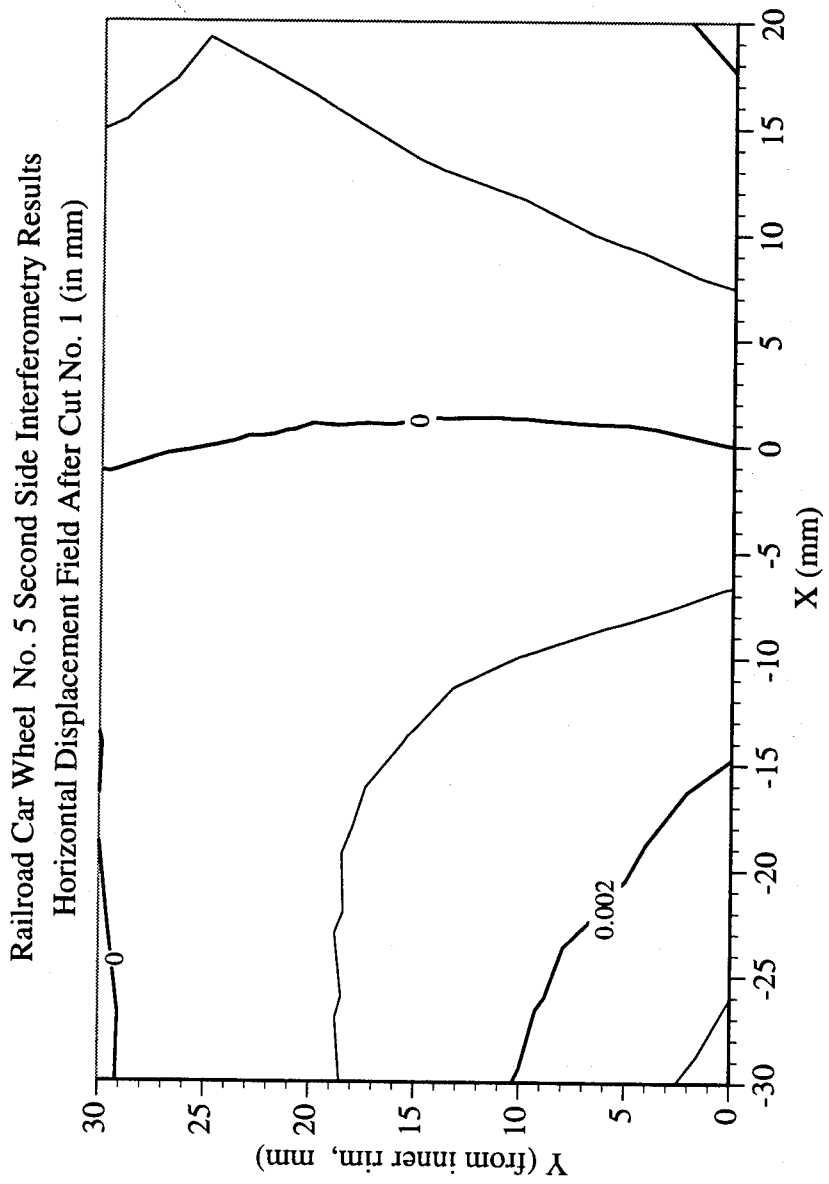
Railroad Car Wheel No. 5 Second Side Interferometry Results
Horizontal Displacement Field After Cut No. 1 (in mm)
0
0
0.002
Y (from inner rim, mm)
X (mm)
30
25
20
15
10
5
0
-30
-25
-20
-15
-10
-5
0
5
10
15
20

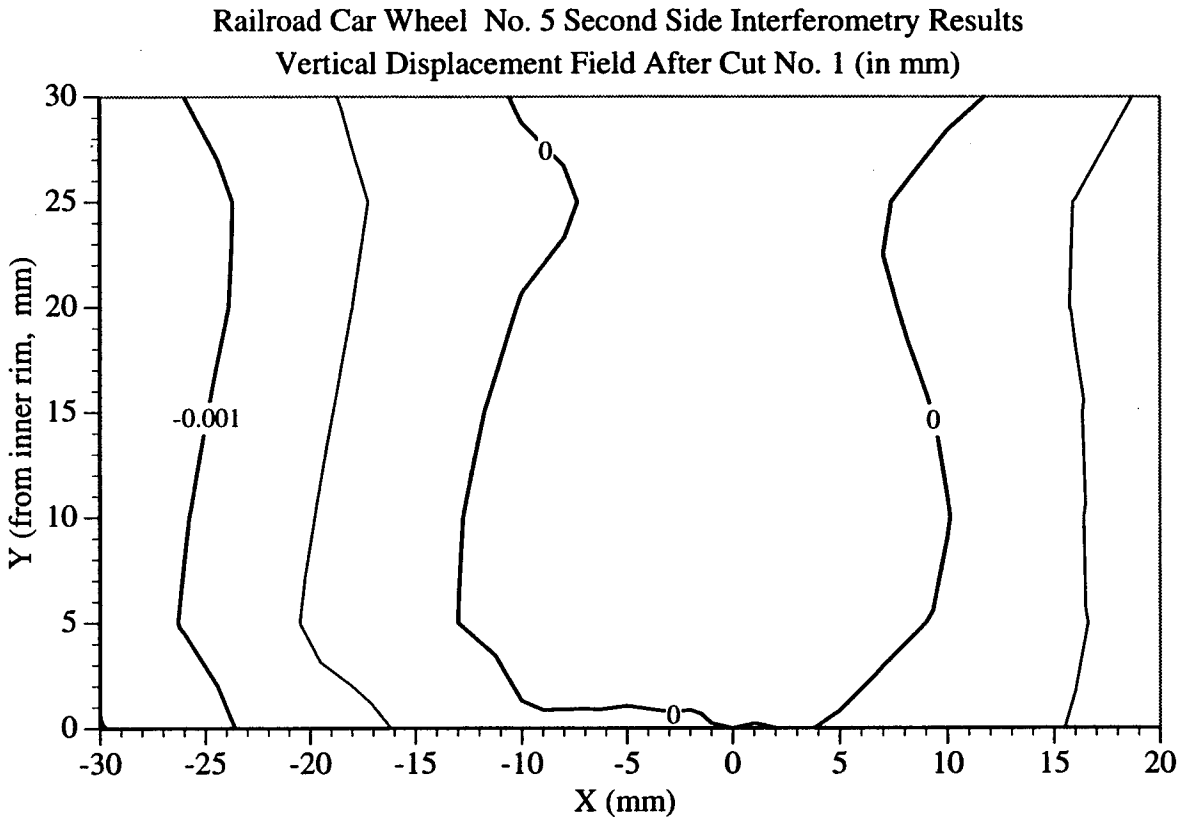
Railroad Car Wheel No. 5 Second Side Interferometry Results
Vertical Displacement Field After Cut No. 1 (in mm)
Y (from inner rim, mm)
X (mm)
30
25
20
15
10
5
0
-30
-25
-20
-15
-10
-5
0
5
10
15
20
-0.001
0
0
0

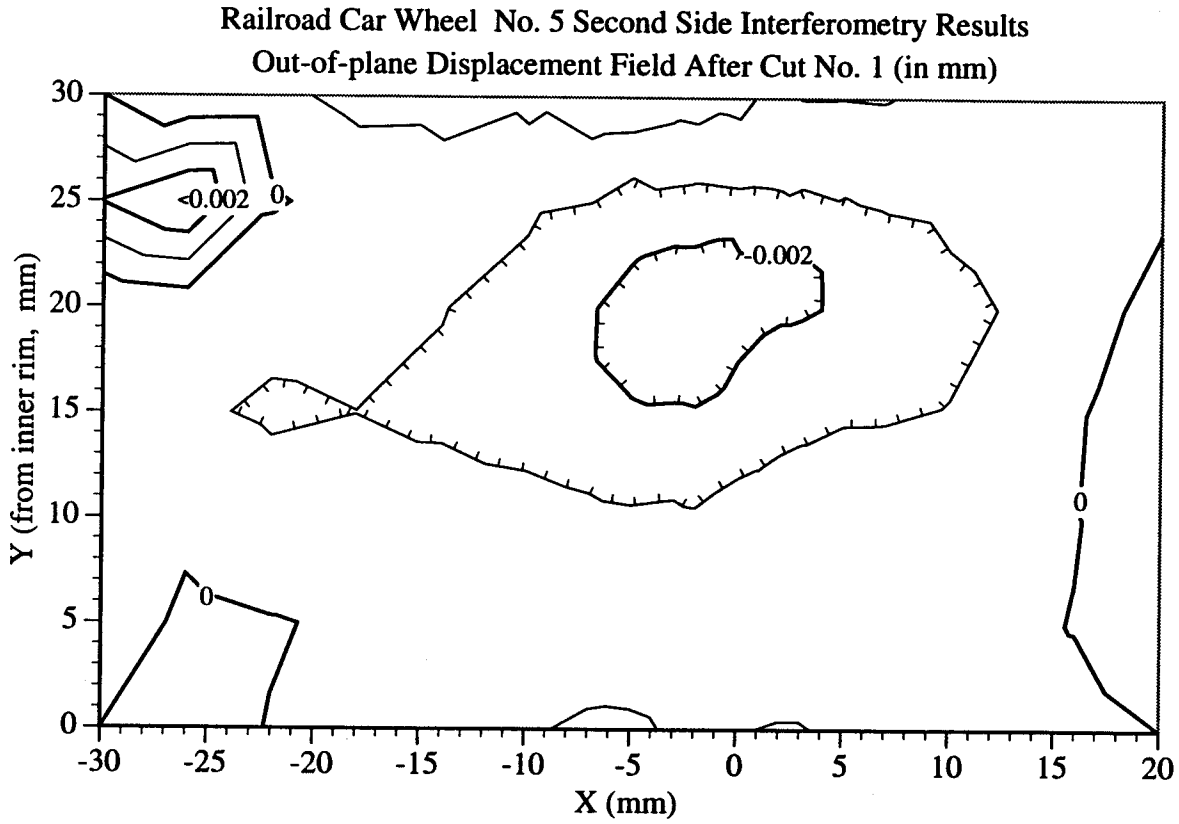
Railroad Car Wheel No. 5 Second Side Interferometry Results
Out-of-plane Displacement Field After Cut No. 1 (in mm)
Y (from inner rim, mm)
X (mm)
30
25
20
15
10
5
0
-30
-25
-20
-15
-10
-5
0
5
10
15
20
<-0.002
0
-0.002
0
0

Railroad Car Wheel No. 5 Second Side Interferometry Results

Residual Strain (ε_x) Field After Cut No. 1 (in mm)

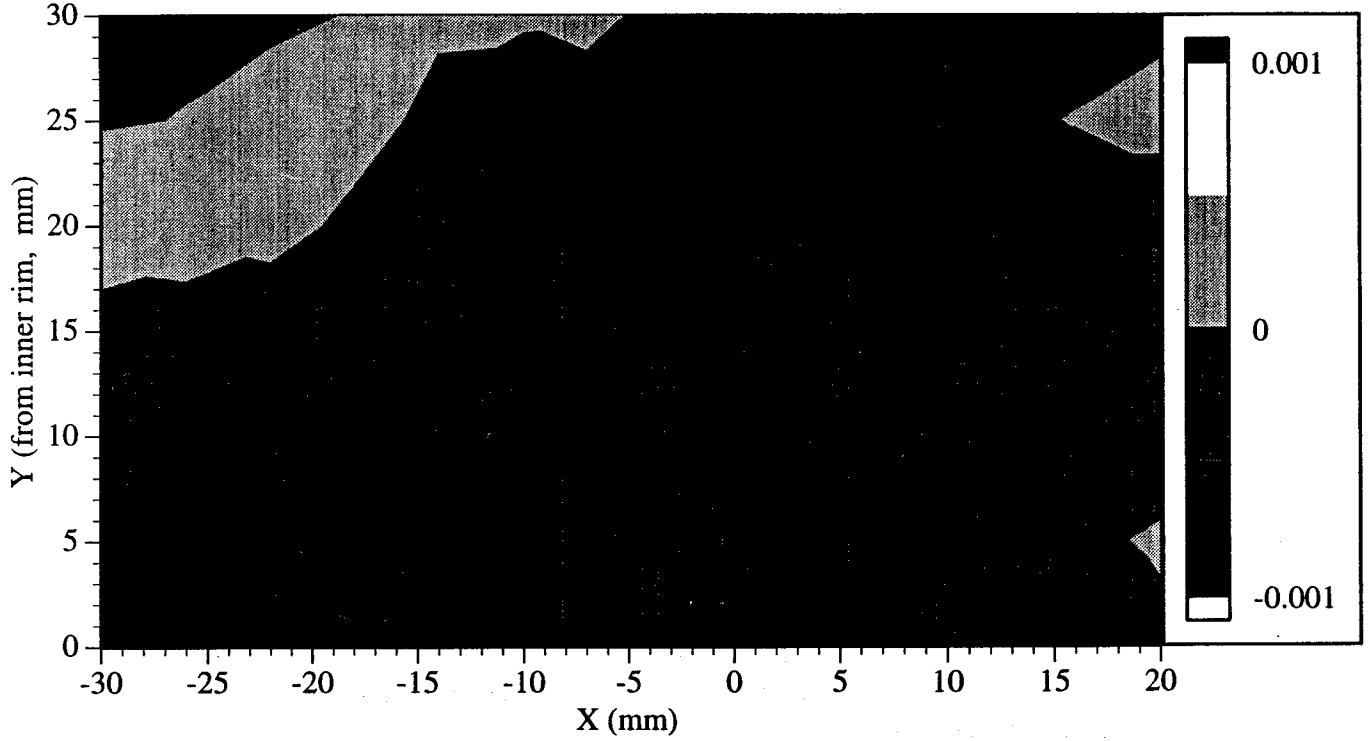

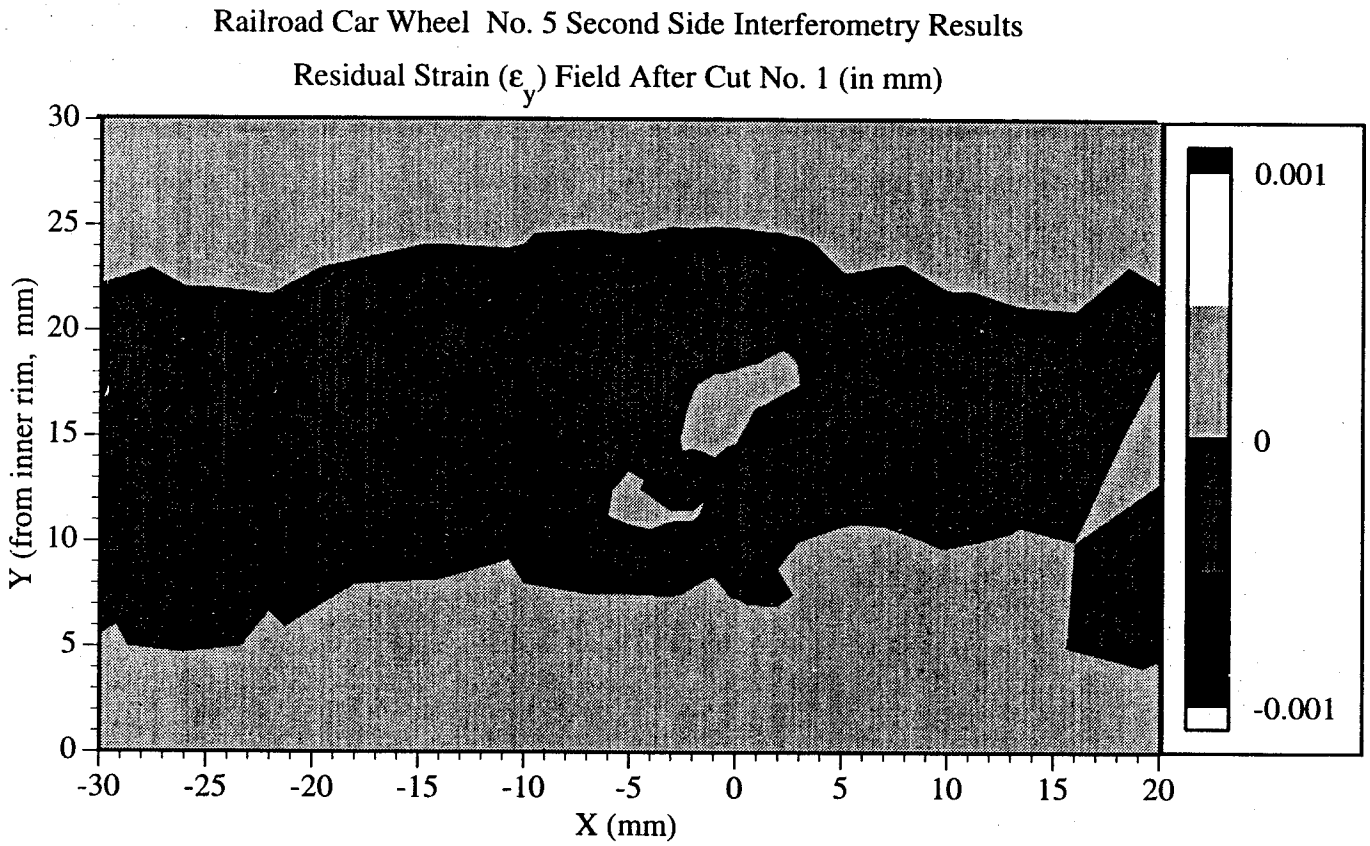
Railroad Car Wheel No. 5 Second Side Interferometry Results
Residual Strain (ε_y) Field After Cut No. 1 (in mm)
Y (from inner rim, mm)
30
25
20
15
10
5
0
-30
-25
-20
-15
-10
-5
0
5
10
15
20
X (mm)
0.001
0
-0.001

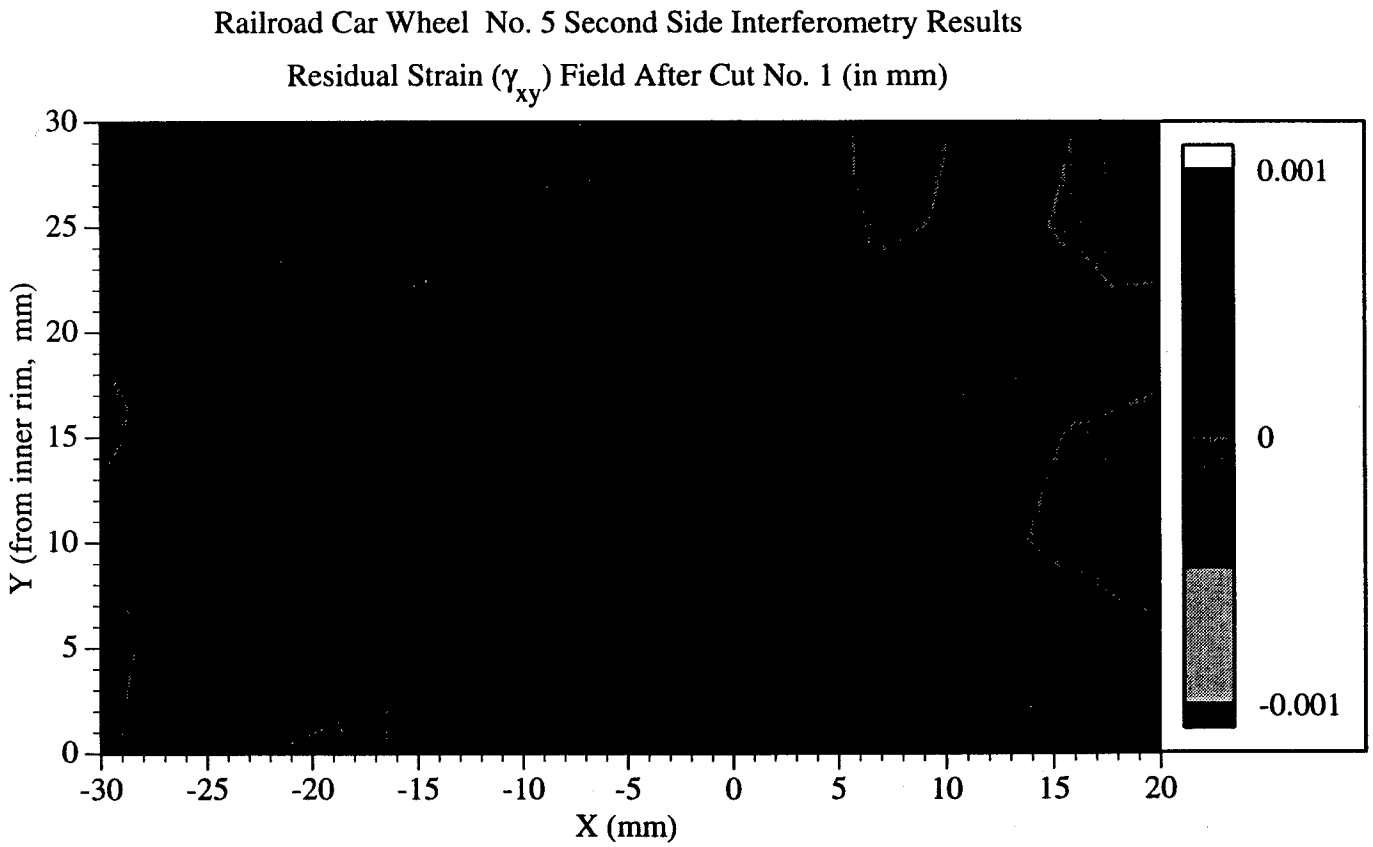
Railroad Car Wheel No. 5 Second Side Interferometry Results
Residual Strain (γ_{xy}) Field After Cut No. 1 (in mm)
Y (from inner rim, mm)
30
25
20
15
10
5
0
-30
-25
-20
-15
-10
-5
0
5
10
15
20
X (mm)
0.001
0
-0.001

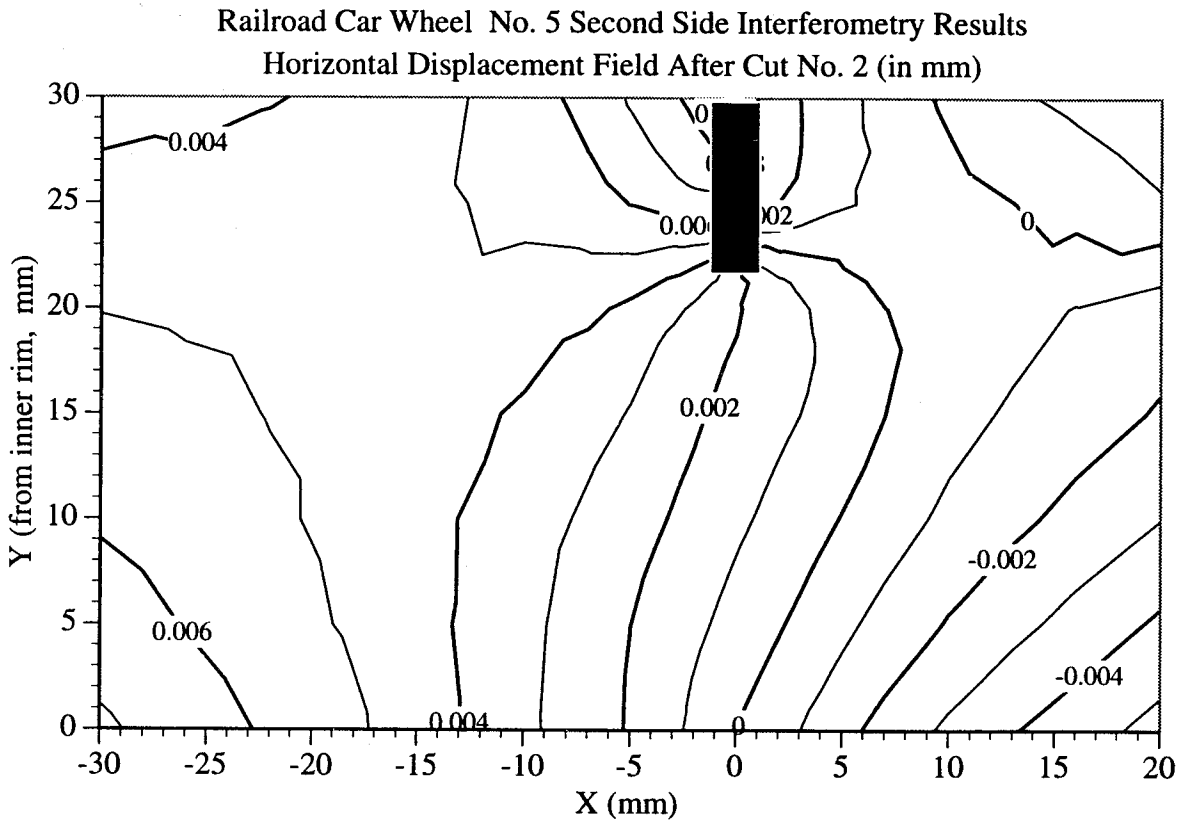
Railroad Car Wheel No. 5 Second Side Interferometry Results
Horizontal Displacement Field After Cut No. 2 (in mm)
Y (from inner rim, mm)
X (mm)
30
25
20
15
10
5
0
-30
-25
-20
-15
-10
-5
0
5
10
15
20
0.004
0.002
0
0.006
0.004
-0.002
-0.004

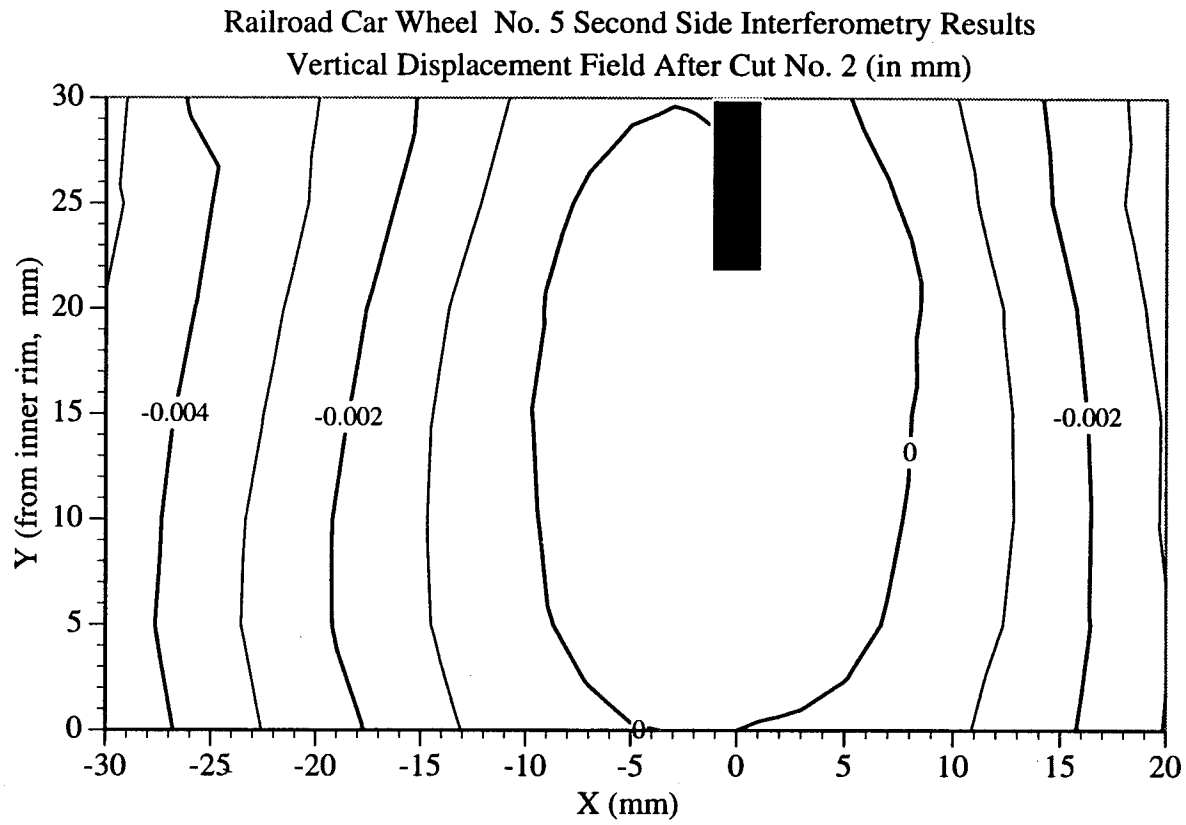
Railroad Car Wheel No. 5 Second Side Interferometry Results
Vertical Displacement Field After Cut No. 2 (in mm)
Y (from inner rim, mm)
X (mm)
-0.004
-0.002
0
-0.002
0
30
25
20
15
10
5
0
-30
-25
-20
-15
-10
-5
0
5
10
15
20

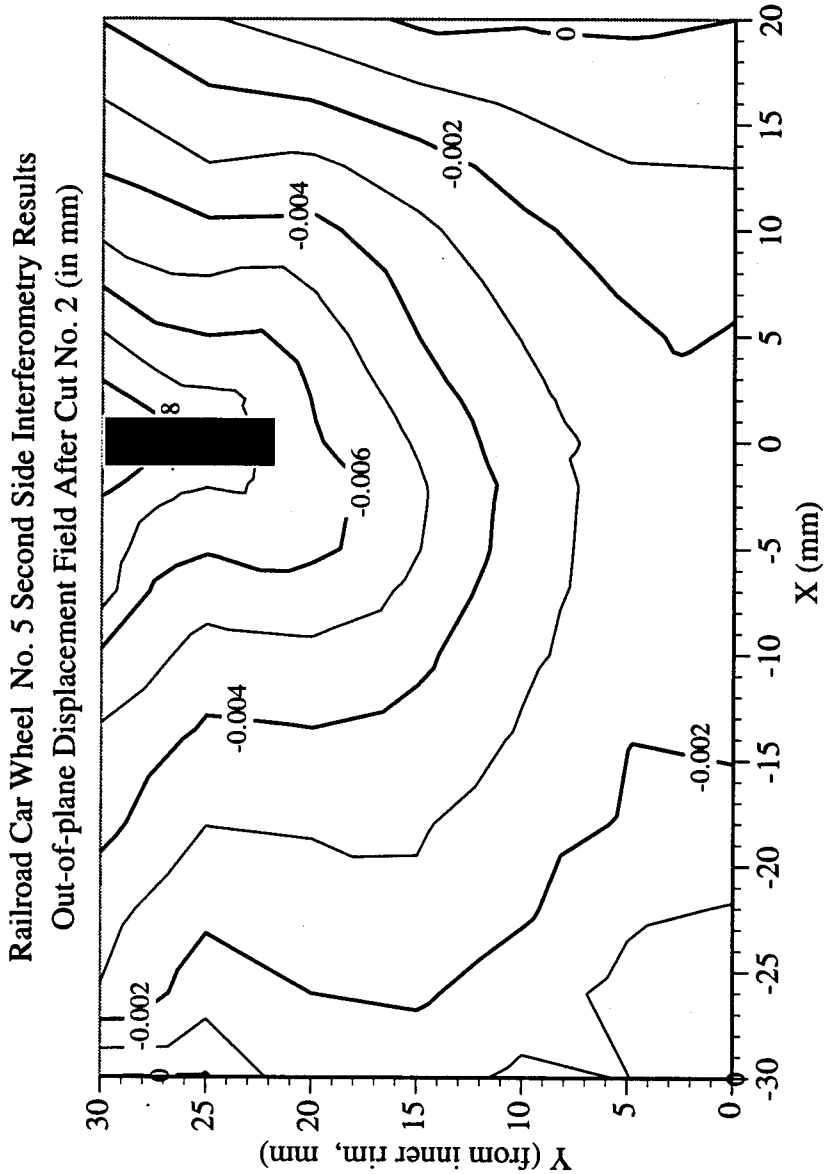
Railroad Car Wheel No. 5 Second Side Interferometry Results
Out-of-plane Displacement Field After Cut No. 2 (in mm)
Y (from inner rim, mm)
X (mm)
-0.002
-0.004
-0.006
0

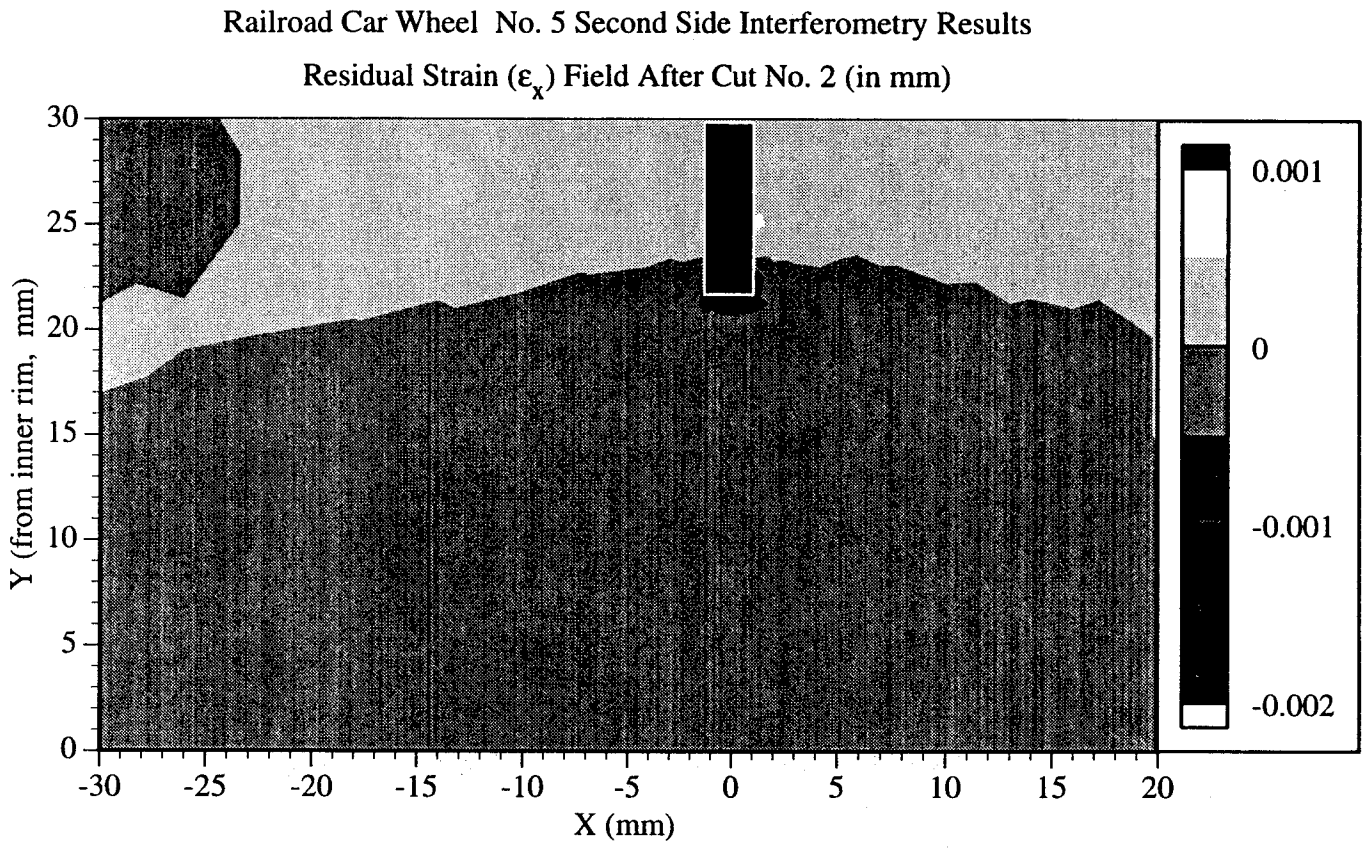
Railroad Car Wheel No. 5 Second Side Interferometry Results
Residual Strain (ε_x) Field After Cut No. 2 (in mm)
Y (from inner rim, mm)
30
25
20
15
10
5
0
-30
-25
-20
-15
-10
-5
0
5
10
15
20
X (mm)
0.001
0
-0.001
-0.002

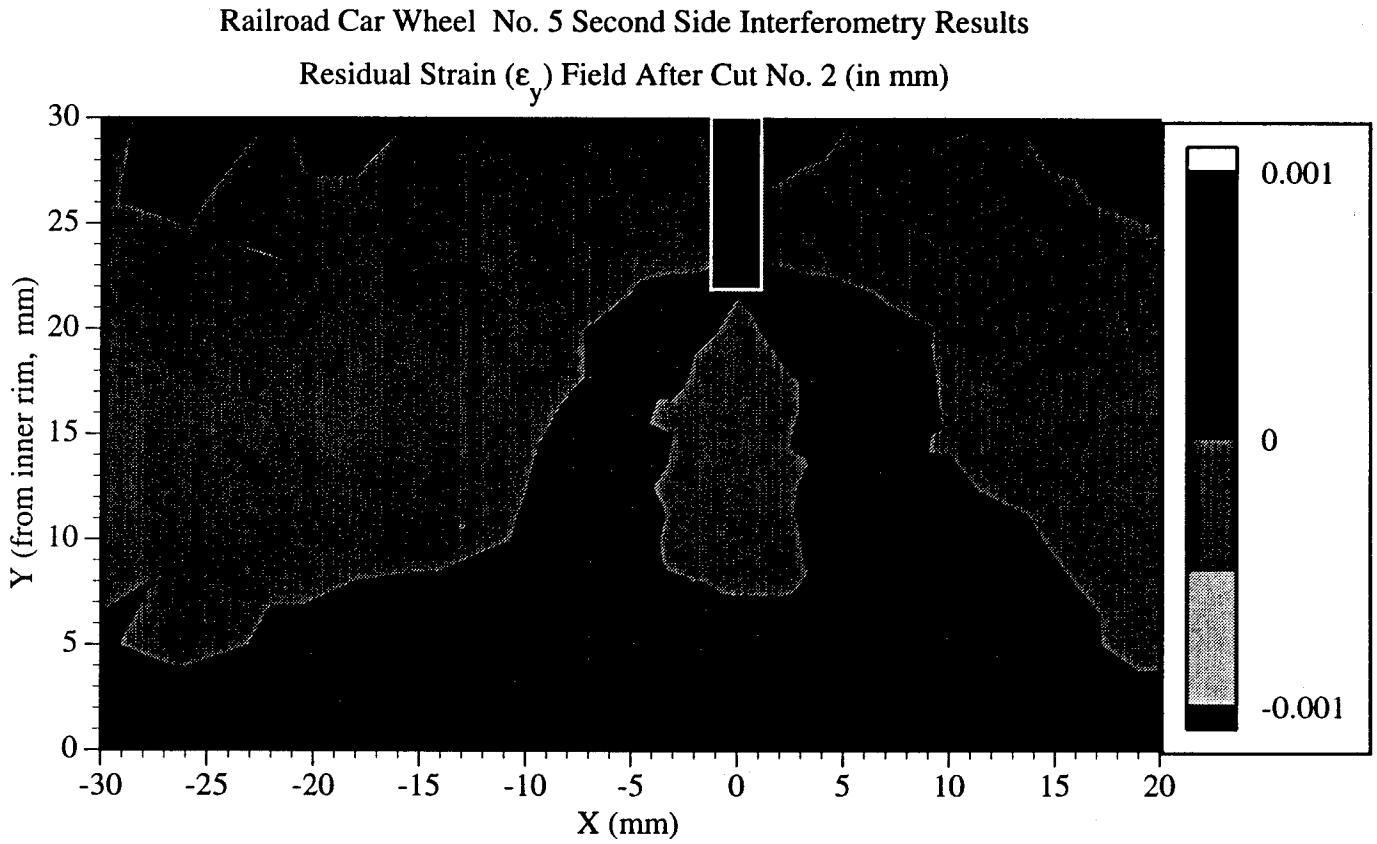
Railroad Car Wheel No. 5 Second Side Interferometry Results
Residual Strain (ε_y) Field After Cut No. 2 (in mm)
Y (from inner rim, mm)
30
25
20
15
10
5
0
-30
-25
-20
-15
-10
-5
0
5
10
15
20
X (mm)
0.001
0
-0.001

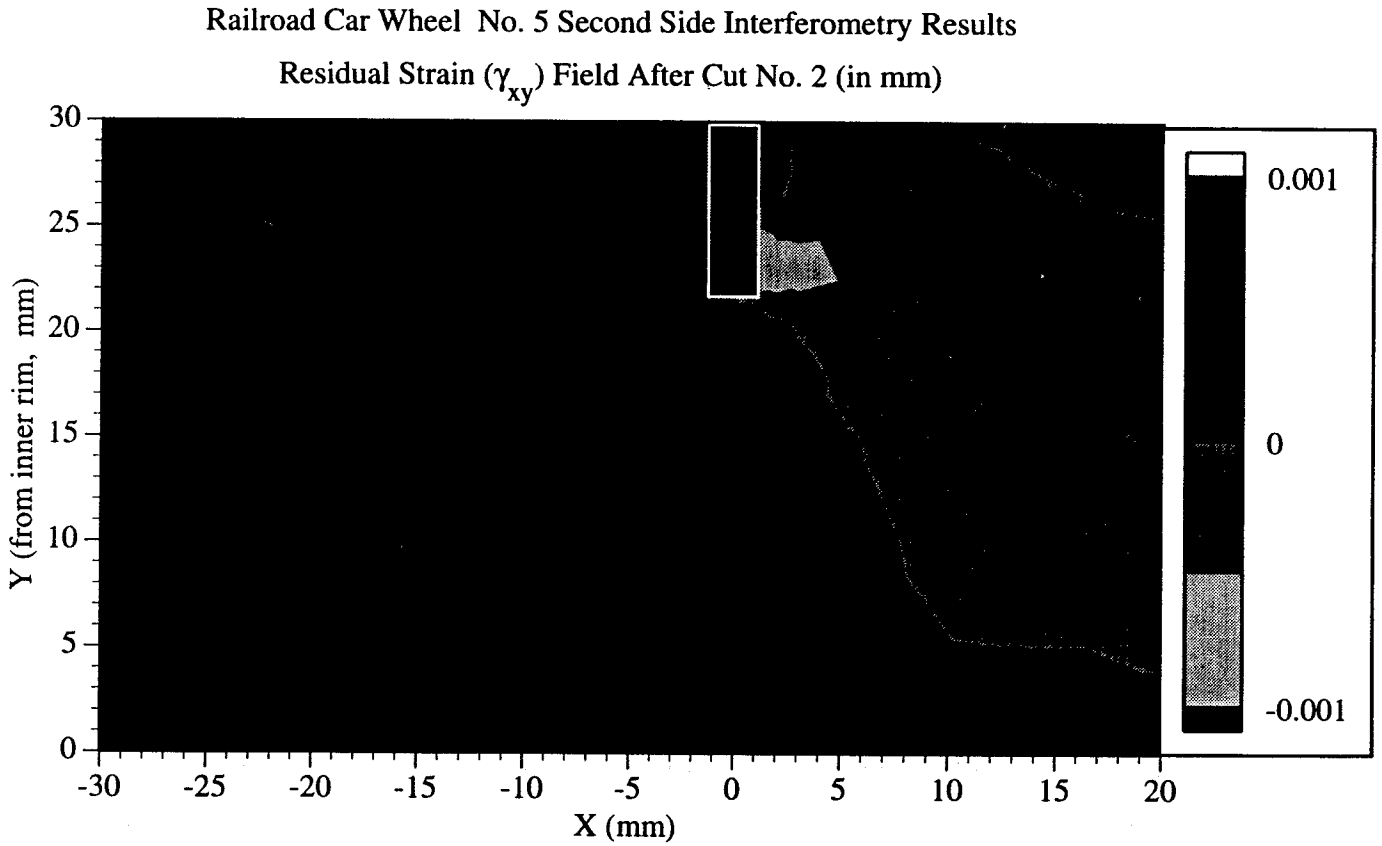
Railroad Car Wheel No. 5 Second Side Interferometry Results
Residual Strain (γ_{xy}) Field After Cut No. 2 (in mm)
Y (from inner rim, mm)
30
25
20
15
10
5
0
-30
-25
-20
-15
-10
-5
0
5
10
15
20
X (mm)
0.001
0
-0.001

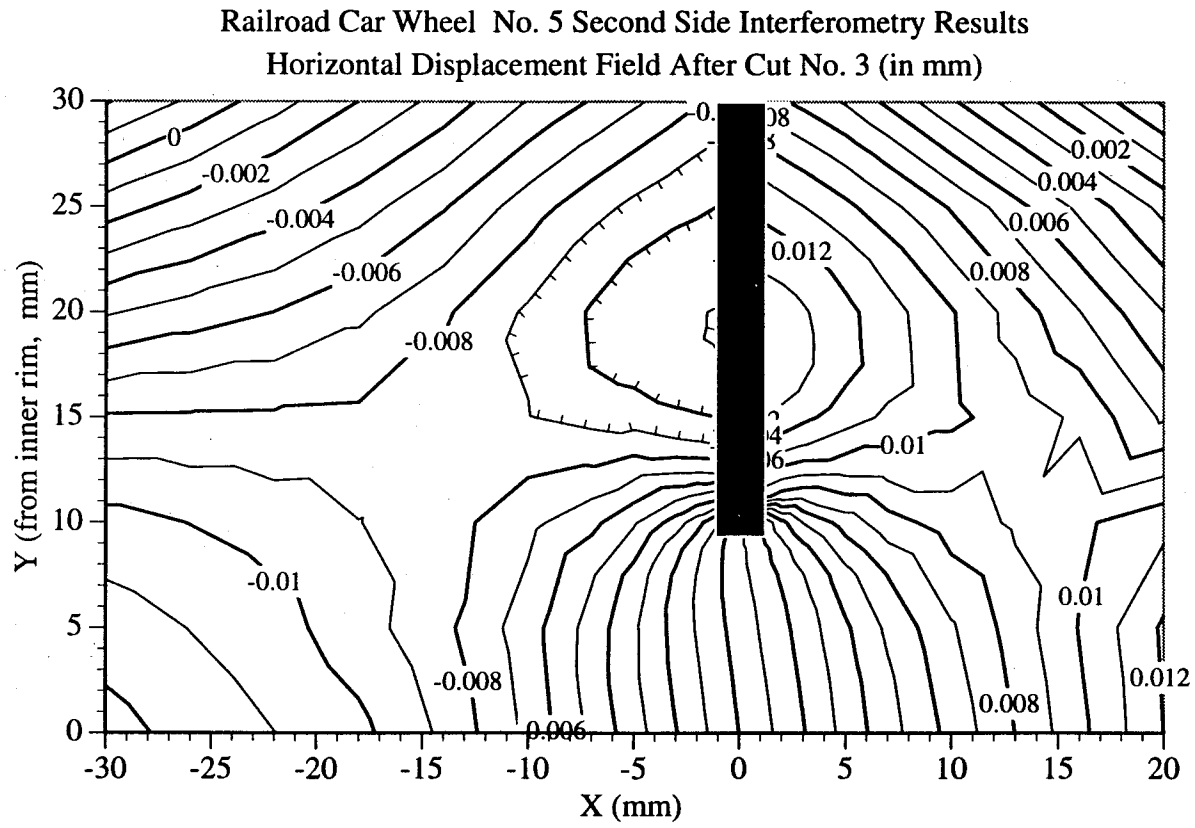
Railroad Car Wheel No. 5 Second Side Interferometry Results
Horizontal Displacement Field After Cut No. 3 (in mm)
Y (from inner rim, mm)
X (mm)
30
25
20
15
10
5
0
-30
-25
-20
-15
-10
-5
0
5
10
15
20
0
-0.002
-0.004
-0.006
-0.008
-0.01
0.002
0.004
0.006
0.008
0.01
0.012

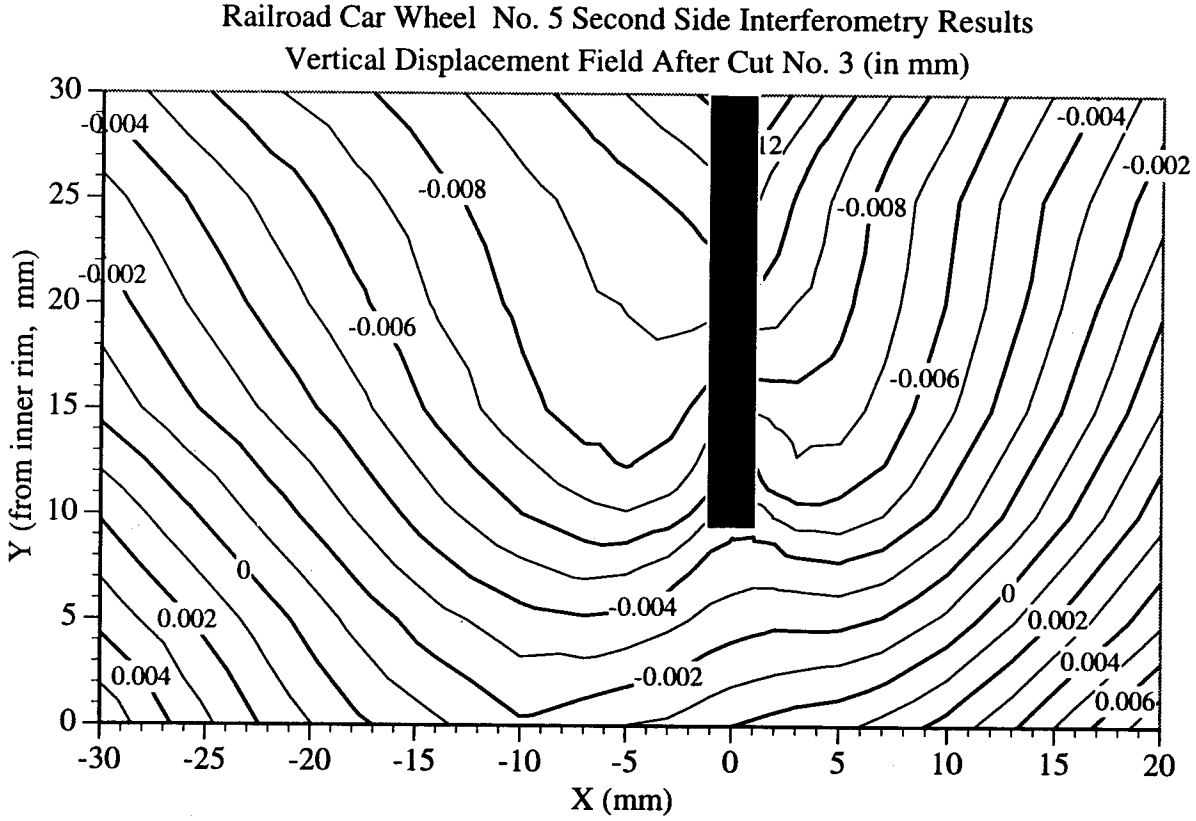
Railroad Car Wheel No. 5 Second Side Interferometry Results
Vertical Displacement Field After Cut No. 3 (in mm)
Y (from inner rim, mm)
X (mm)
-0.004
-0.008
-0.002
-0.006
0
0.002
0.004
0.006
12
30
25
20
15
10
5
0
-30
-25
-20
-15
-10
-5
0
5
10
15
20

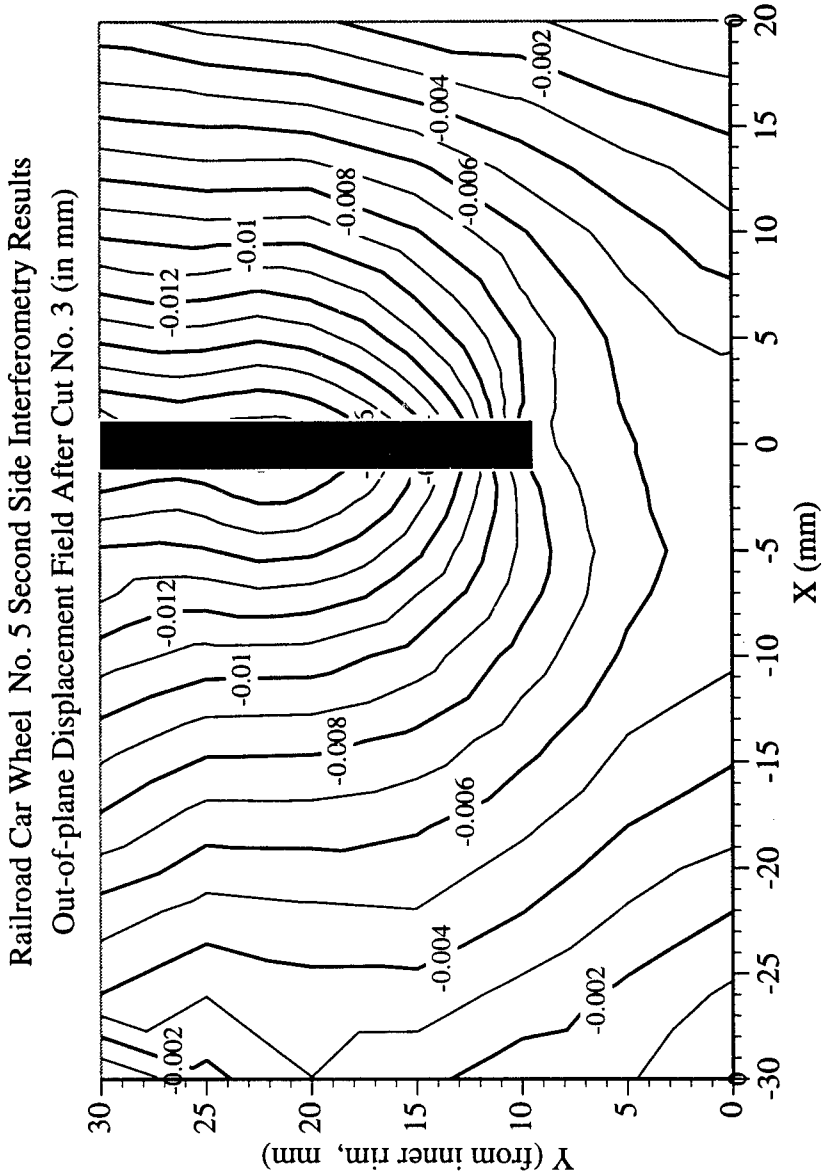
Railroad Car Wheel No. 5 Second Side Interferometry Results
Out-of-plane Displacement Field After Cut No. 3 (in mm)
Y (from inner rim, mm)
X (mm)
-0.002
-0.004
-0.006
-0.008
-0.01
-0.012

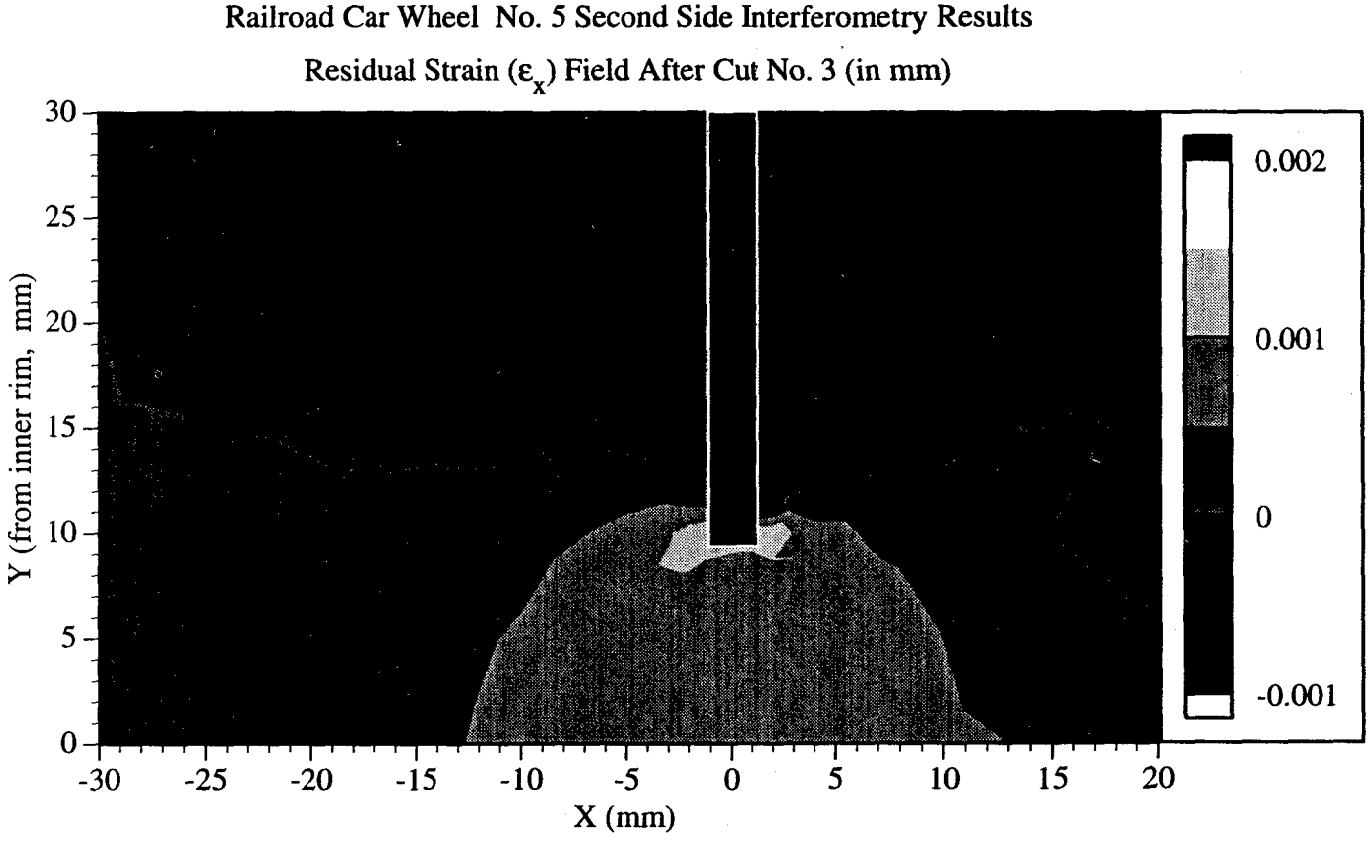
Railroad Car Wheel No. 5 Second Side Interferometry Results
Residual Strain (ε_x) Field After Cut No. 3 (in mm)
Y (from inner rim, mm)
30
25
20
15
10
5
0
-30
-25
-20
-15
-10
-5
0
5
10
15
20
X (mm)
0.002
0.001
0
-0.001

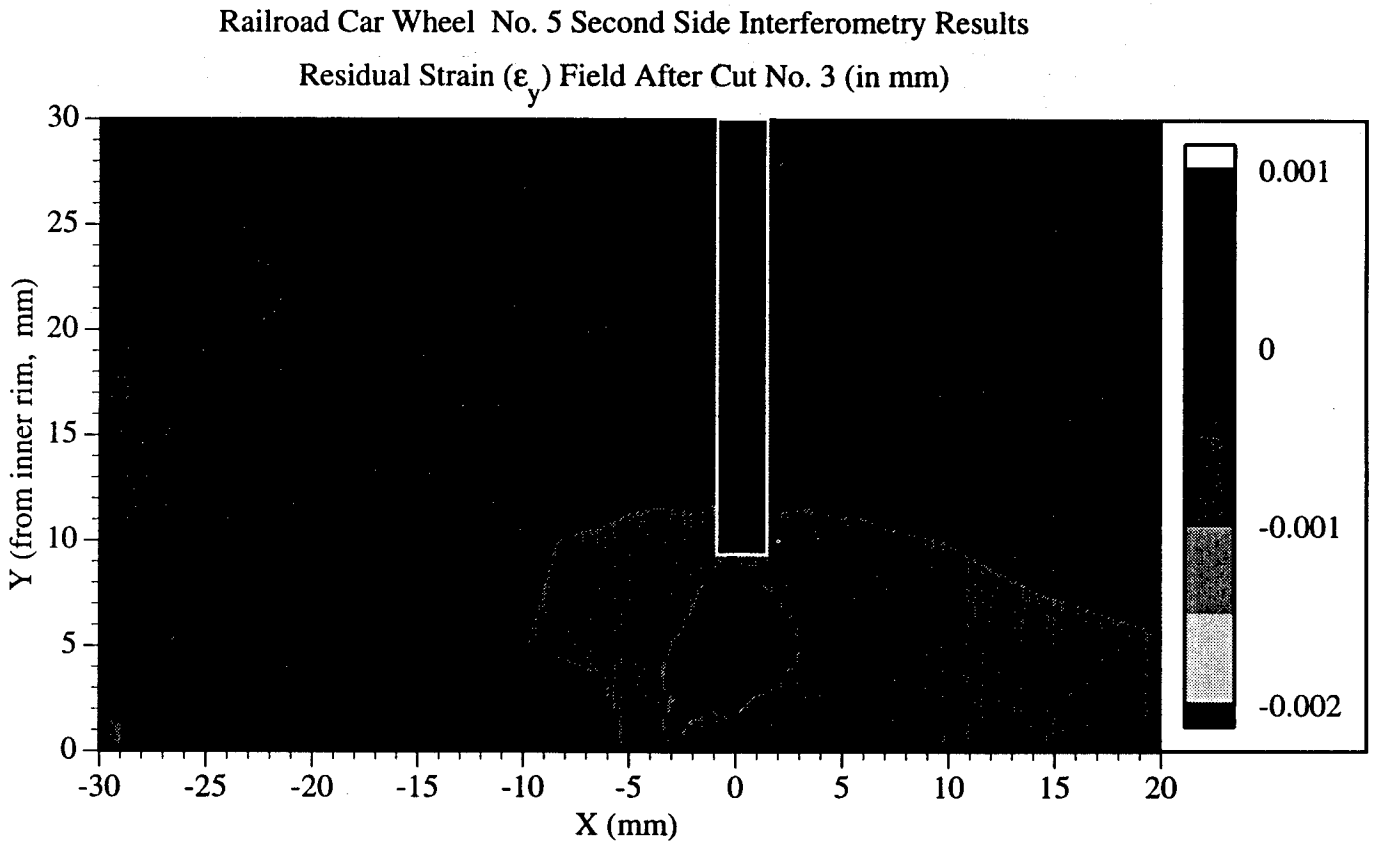
Railroad Car Wheel No. 5 Second Side Interferometry Results
Residual Strain (ε_y) Field After Cut No. 3 (in mm)
Y (from inner rim, mm)
30
25
20
15
10
5
0
-30
-25
-20
-15
-10
-5
0
5
10
15
20
X (mm)
0.001
0
-0.001
-0.002

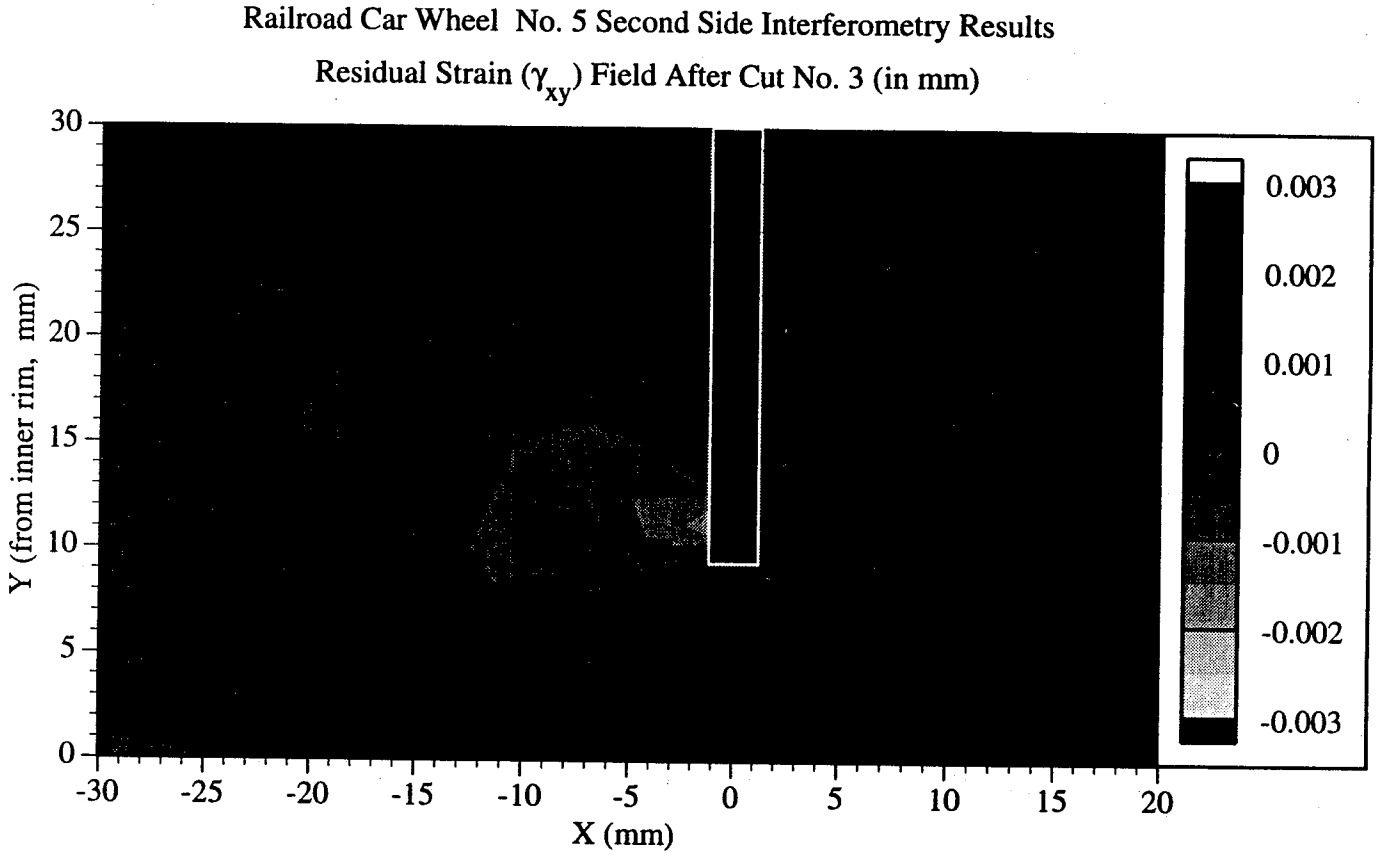
Railroad Car Wheel No. 5 Second Side Interferometry Results
Residual Strain (γ_{xy}) Field After Cut No. 3 (in mm)
Y (from inner rim, mm)
30
25
20
15
10
5
0
-30
-25
-20
-15
-10
-5
0
5
10
15
20
X (mm)
0.003
0.002
0.001
0
-0.001
-0.002
-0.003

Page Intentionally Left Blank

Appendix 6. Wheel #6 Experimental Results

This appendix contains the results from the test on both sides (front and back rim faces) of the sixth wheel. All the data are in a local coordinate system that is located at the intersection of the inner edge of the rim and the cutting line; the vertical axis points away from the center of the wheel.

The attached figures show the location of all the sensors. At two points on the wheel, thermocouples (TC) measure the temperature difference (which never exceeded 4.8°C) immediately after each cut. The temperature at TC2, the one farther from the cut, was equal to the ambient temperature. The strain measurements were taken after the difference decreased to about 1°C or less at an ambient temperature in the range of 22°C to 27°C.

The extensometer, strain gage, and displacement sensor data are provided in tabular form. The interferometric data is provided in the form of contour maps and as data files in ASCII format for three specific cutting stages. The corresponding cut depths are 35 mm, 45 mm, and 60 mm.

The wheel was identified by the following markings:

26508
242

Location of strain gauges, thermocouples and gratings on wheel #5,6,7&8

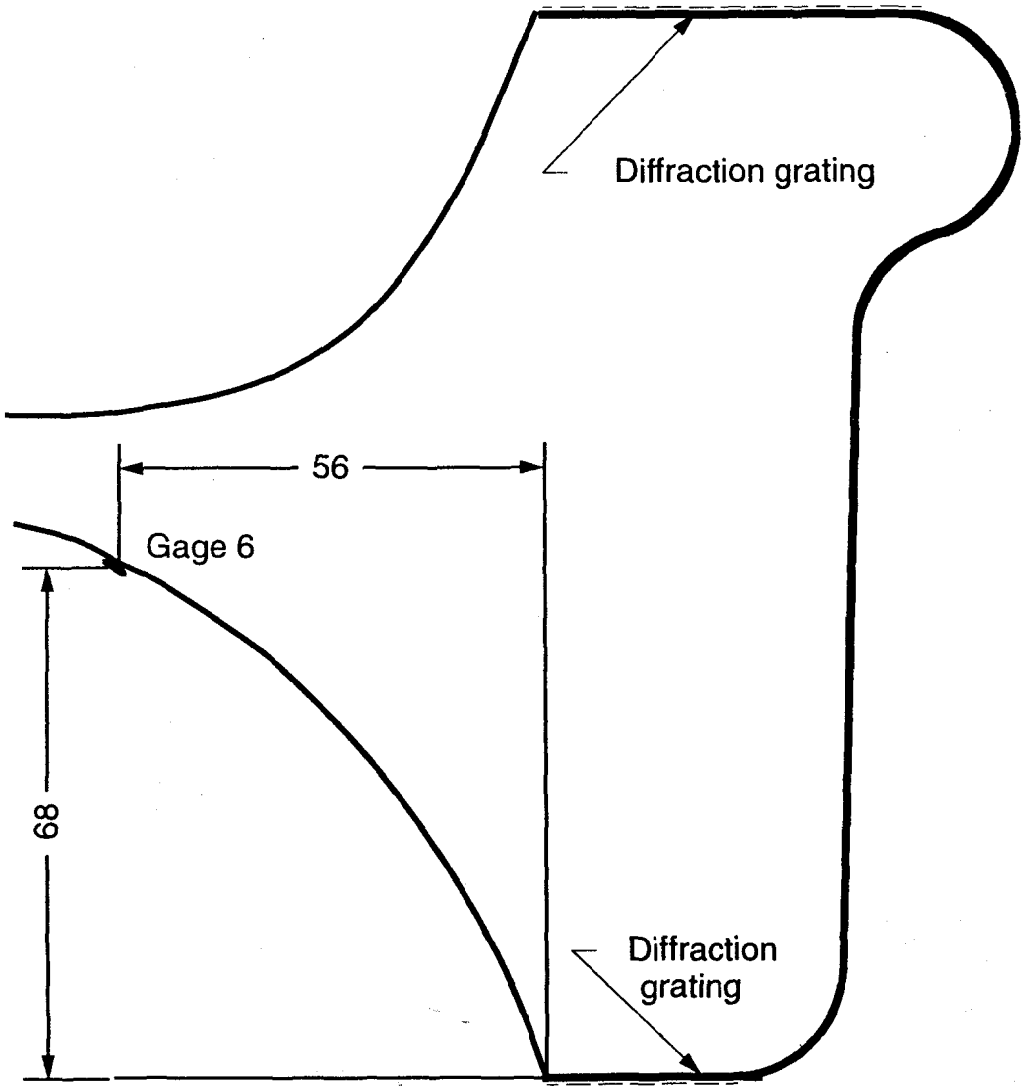

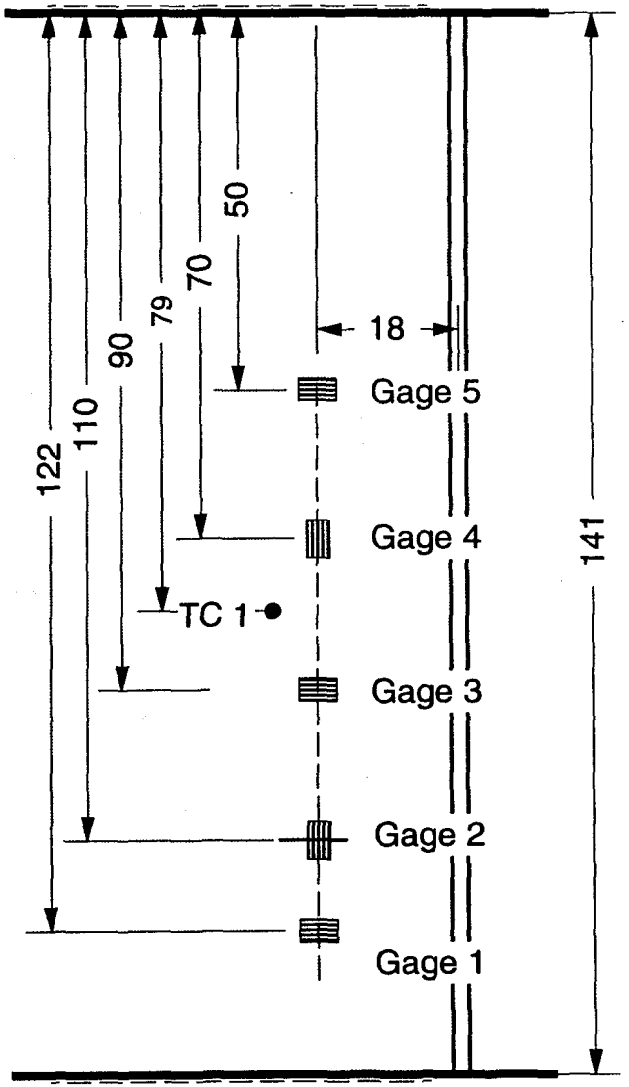

Gage 6 was located 20mm from the plane of the cut.

Location of displacement sensors thermocouples and gratings on wheel #5,6,7&8

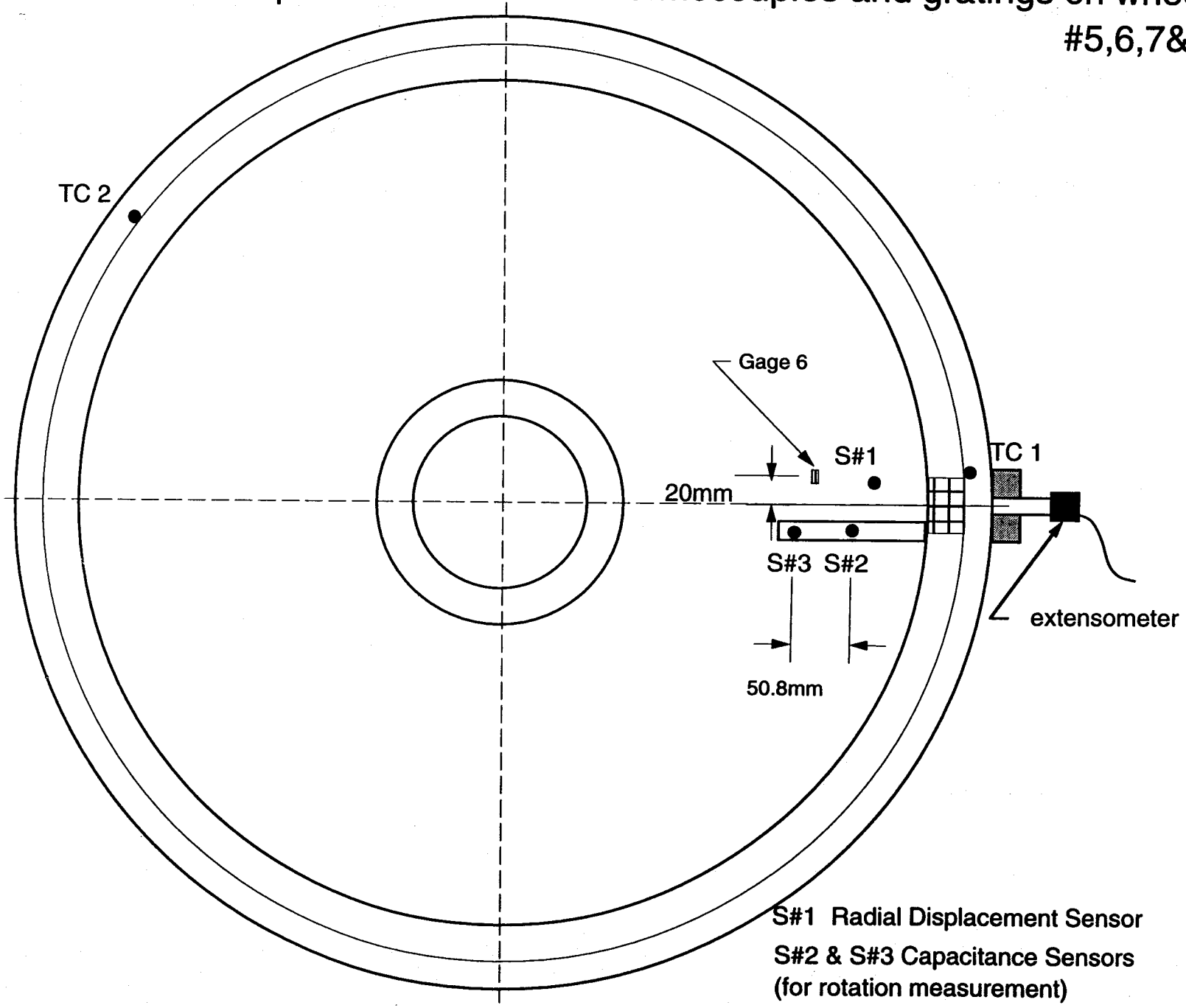

S#1 Radial Displacement Sensor

S#2 & S#3 Capacitance Sensors
(for rotation measurement)

TESTING OF DOT RAILROAD CAR WHEEL #6								#26508 as man., 6HB 242			
DATE:		JUNE 23 1995									
	mm/mm						mm	mm	rad	(°C)	(°C)
Cut Depth (mm)	Gage1	Gage2	Gage3	Gage4	Gage5	Gage6	Radial Displacement	Opening Displacement	Rotation	TC 1	TC 2
0	0	0	0	0	0	0	0.000	0.000	0.00E+00	22.3	22.8
27	7	-1	-16	9	-27	11	0.000	-0.077	1.79E-04	26.9	23.4
35	38	8	37	15	100	28	-0.001	-0.099	3.57E-04	27.1	23.3
45	209	-1	237	15	308	48	-0.024	-0.136	5.75E-04	28.2	23.4
60	389	-25	394	6	429	71	-0.061	-0.210	7.54E-04	27.2	25.2
70	415	-40	419	-10	446	56	-0.096	-0.262	8.73E-04	26.8	26.1
80	405	-60	426	-41	444	-3	-0.132	-0.325	8.13E-04	27.6	26.1
90	397	-68	422	-56	434	-70	-0.160	-0.385	7.54E-04	27.9	26.1
100	395	-75	419	-58	431	-152	-0.189	-0.442	7.14E-04	28.1	26.1
110	397	-77	418	-60	430	-229	-0.212	-0.482	7.34E-04	28.2	26.2
120	393	-81	416	-59	427	-300	-0.227	-0.516	7.54E-04	28.2	26.2
130	394	-80	416	-59	426	-332	-0.240	-0.540	7.54E-04	28.2	26.2
140	393	-81	415	-58	426	-339	-0.249	-0.559	8.13E-04	28.1	26.2
150	394	-79	416	-58	426	-345	-0.247	-0.575	5.36E-04	28.1	26.2
160	393	-79	416	-57	426	-344	-0.255	-0.590	5.95E-04	28.0	26.3
170	394	-79	416	-57	427	-346	-0.263	-0.603	6.15E-04	28.0	26.3
180	392	-80	416	-59	426	-346	-0.272	-0.618	6.75E-04	27.9	26.4
190	392	-79	416	-56	428	-347	-0.281	-0.633	7.54E-04	27.9	26.4
200	393	-78	415	-56	426	-345	-0.291	-0.649	8.13E-04	27.9	26.4
210	394	-79	416	-56	426	-346	-0.300	-0.666	7.94E-04	27.8	26.3
END											

Railroad Wheel No. 6 Test
Displacement vs. Cut Depth

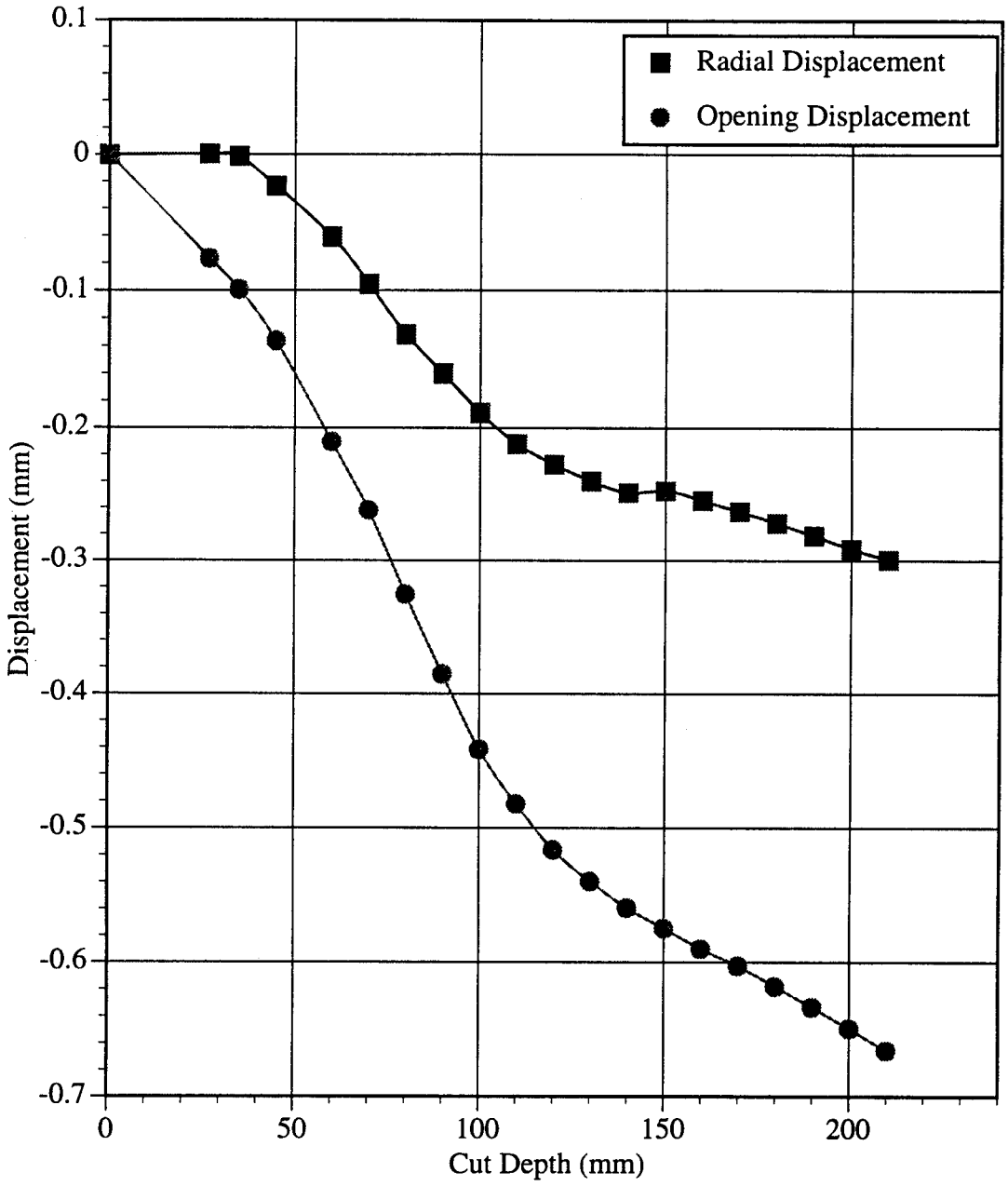

Railroad Wheel No. 6 Test
Strain Gage Readings vs. Cut Depth

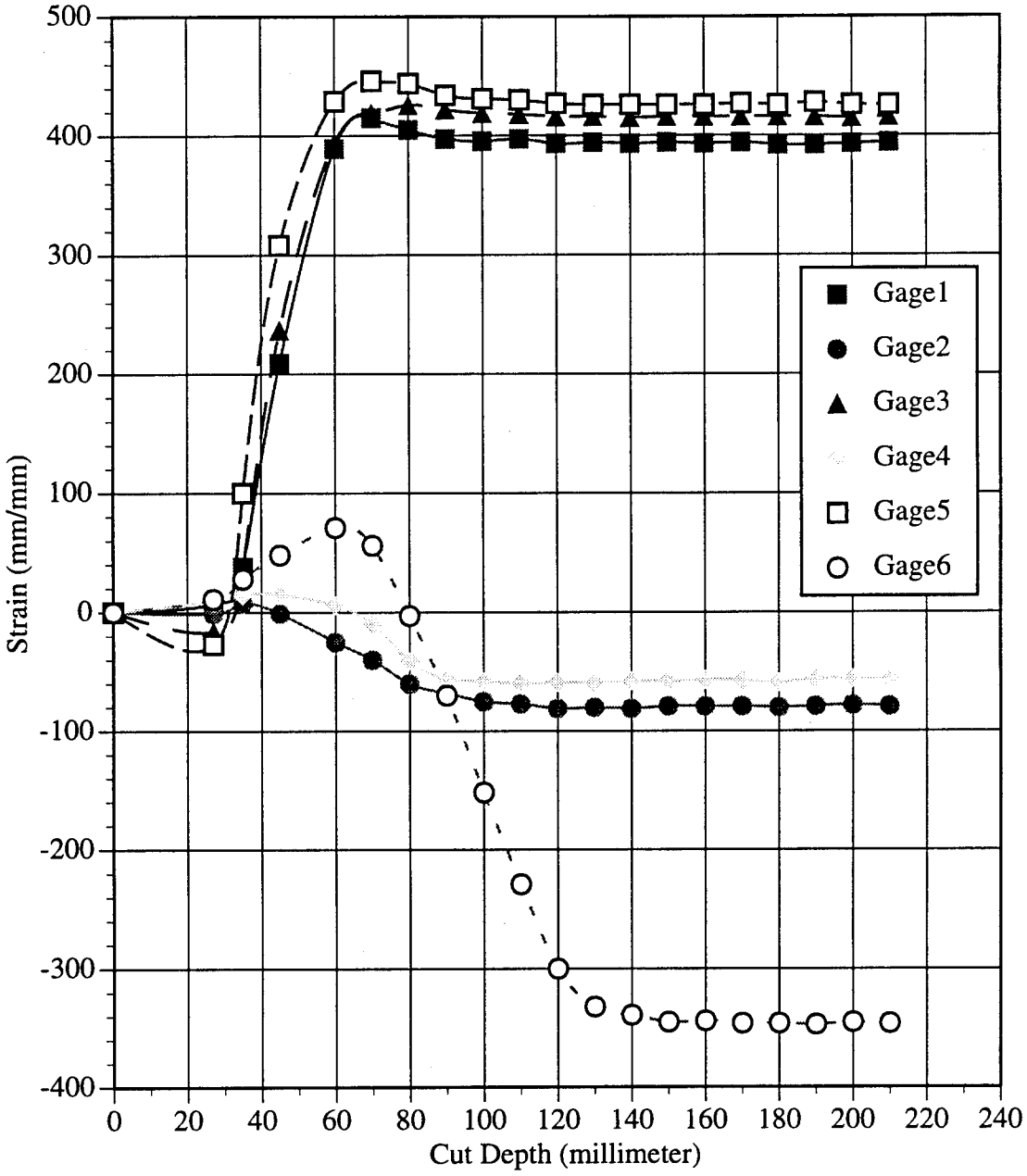

Railroad Wheel No. 6 Test
Wheel Rotation vs. Cut Depth

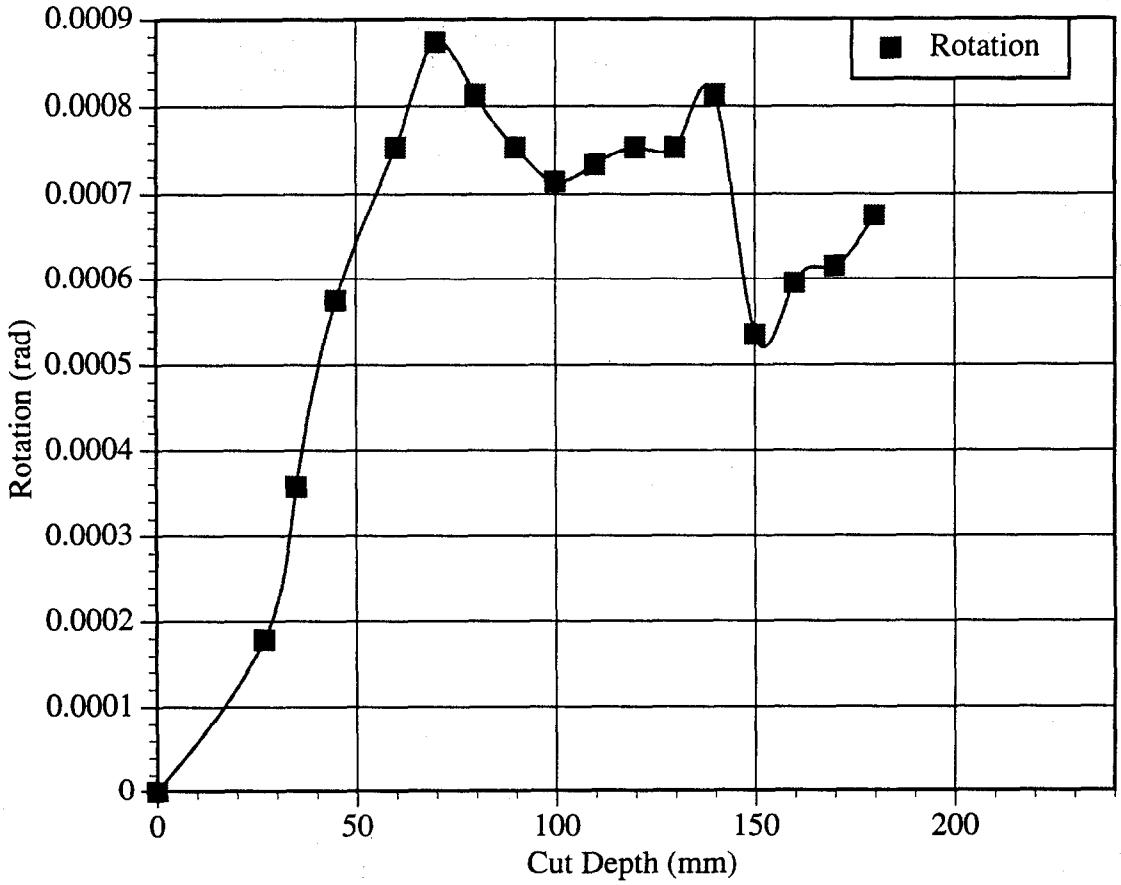

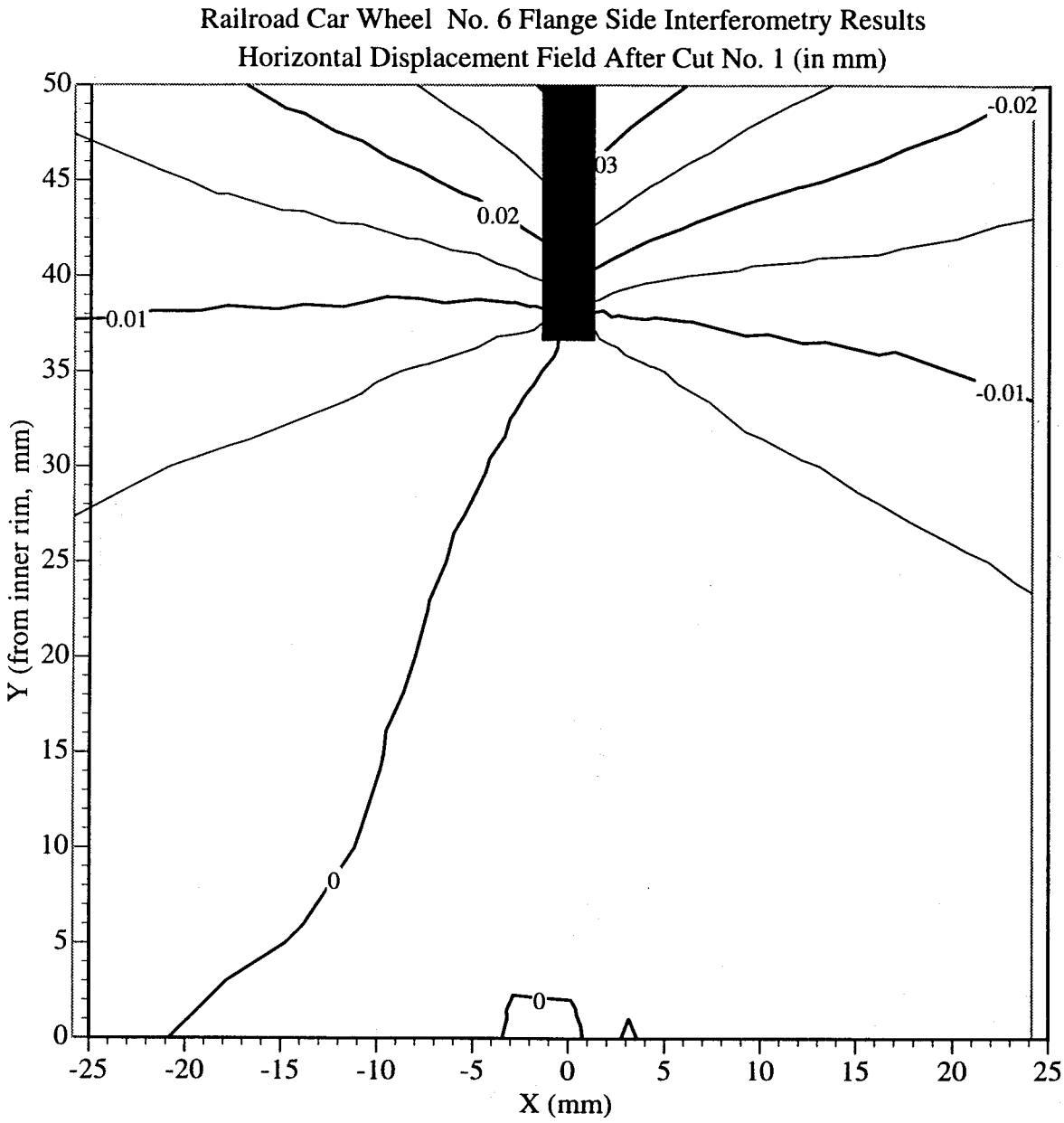
Railroad Car Wheel No. 6 Flange Side Interferometry Results
Horizontal Displacement Field After Cut No. 1 (in mm)
Y (from inner rim, mm)
X (mm)
50
45
40
35
30
25
20
15
10
5
0
-25
-20
-15
-10
-5
0
5
10
15
20
25
-0.02
03
0.02
-0.01
-0.01
0
0

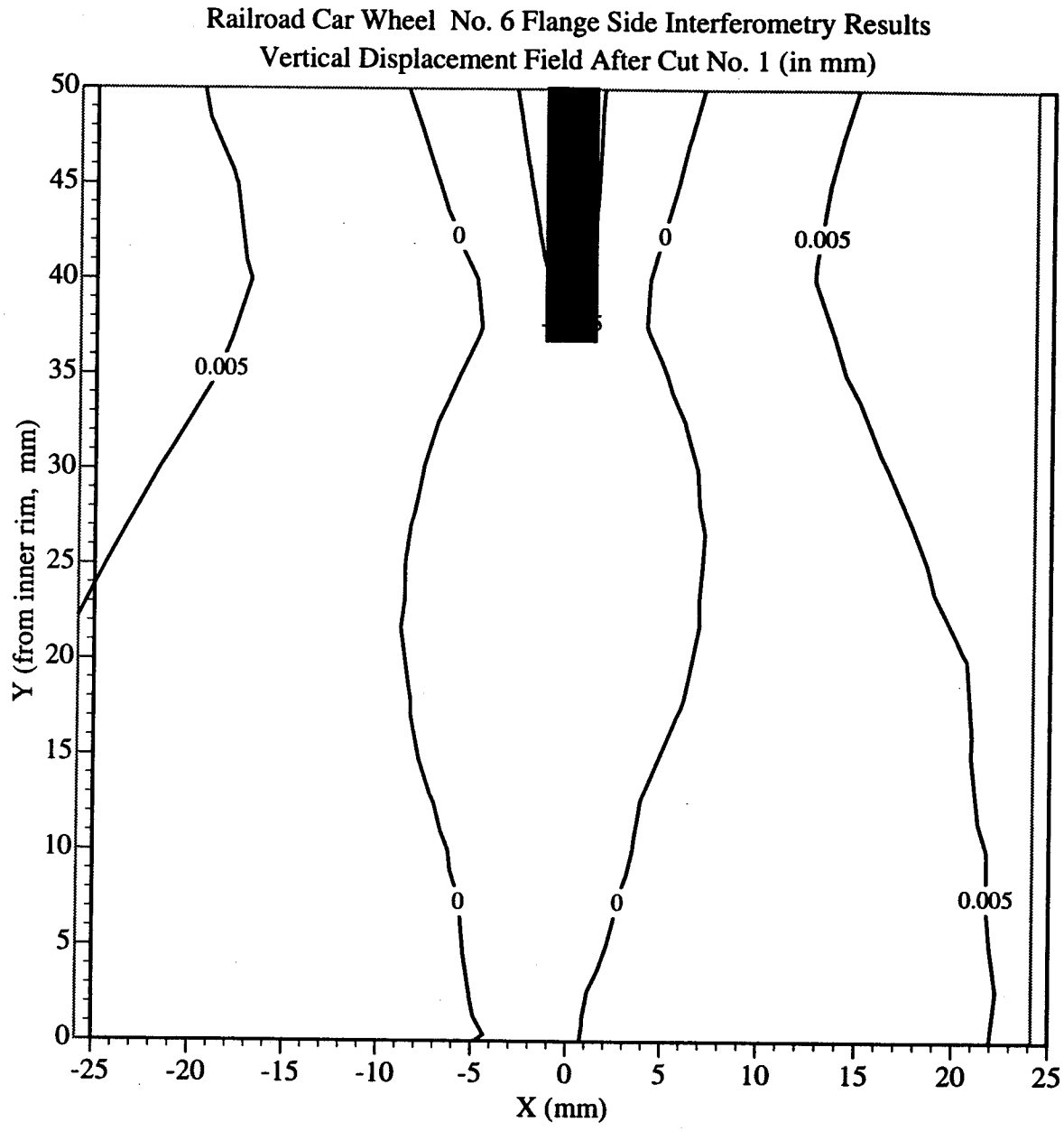
Railroad Car Wheel No. 6 Flange Side Interferometry Results
Vertical Displacement Field After Cut No. 1 (in mm)
Y (from inner rim, mm)
X (mm)
0.005
0
0
0.005
0
0
0.005
50
45
40
35
30
25
20
15
10
5
0
-25
-20
-15
-10
-5
0
5
10
15
20
25

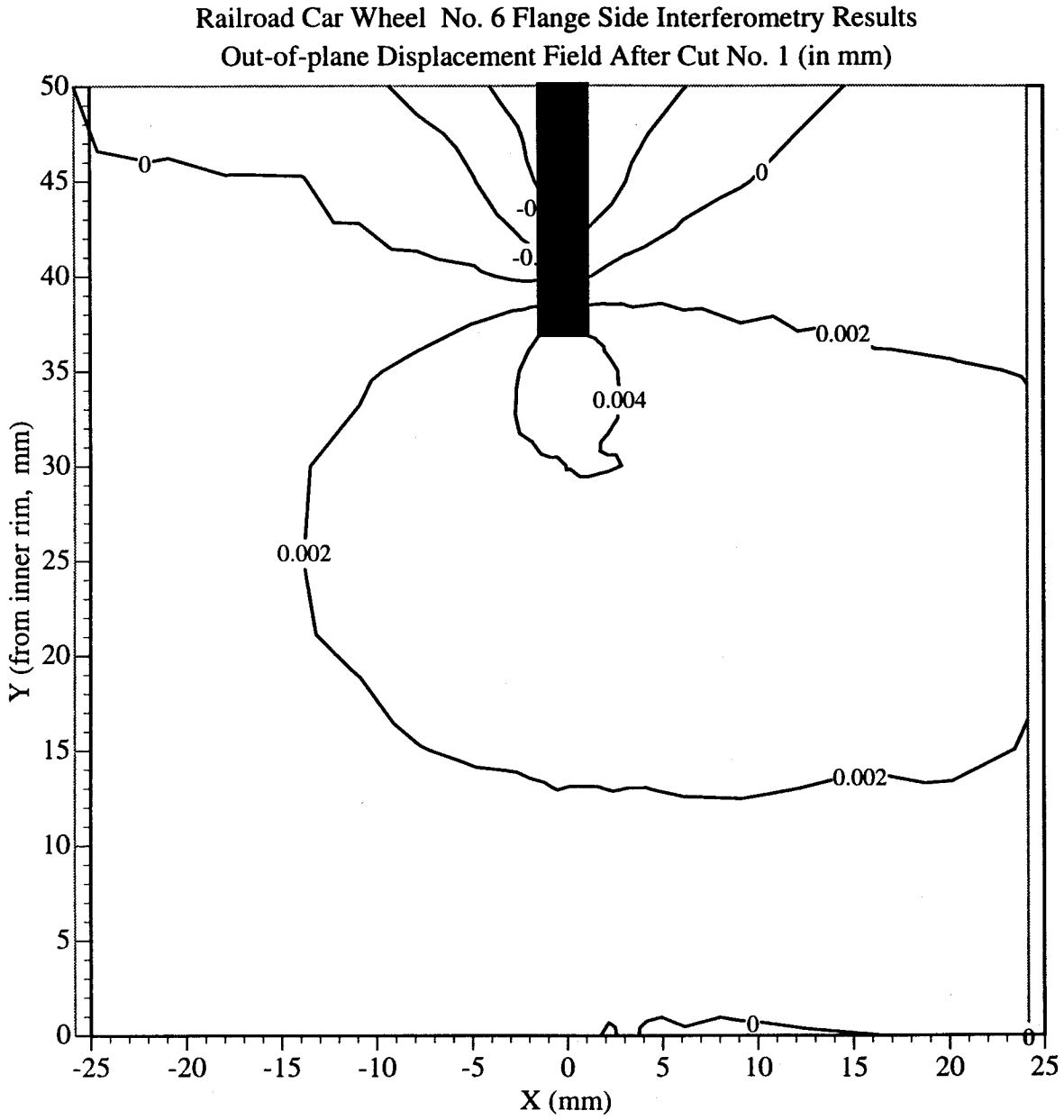
Railroad Car Wheel No. 6 Flange Side Interferometry Results
Out-of-plane Displacement Field After Cut No. 1 (in mm)
Y (from inner rim, mm)
X (mm)
50
45
40
35
30
25
20
15
10
5
0
-25
-20
-15
-10
-5
0
5
10
15
20
25
0
0
-0
-0
0
0.002
0.004
0.002
0.002
0
0

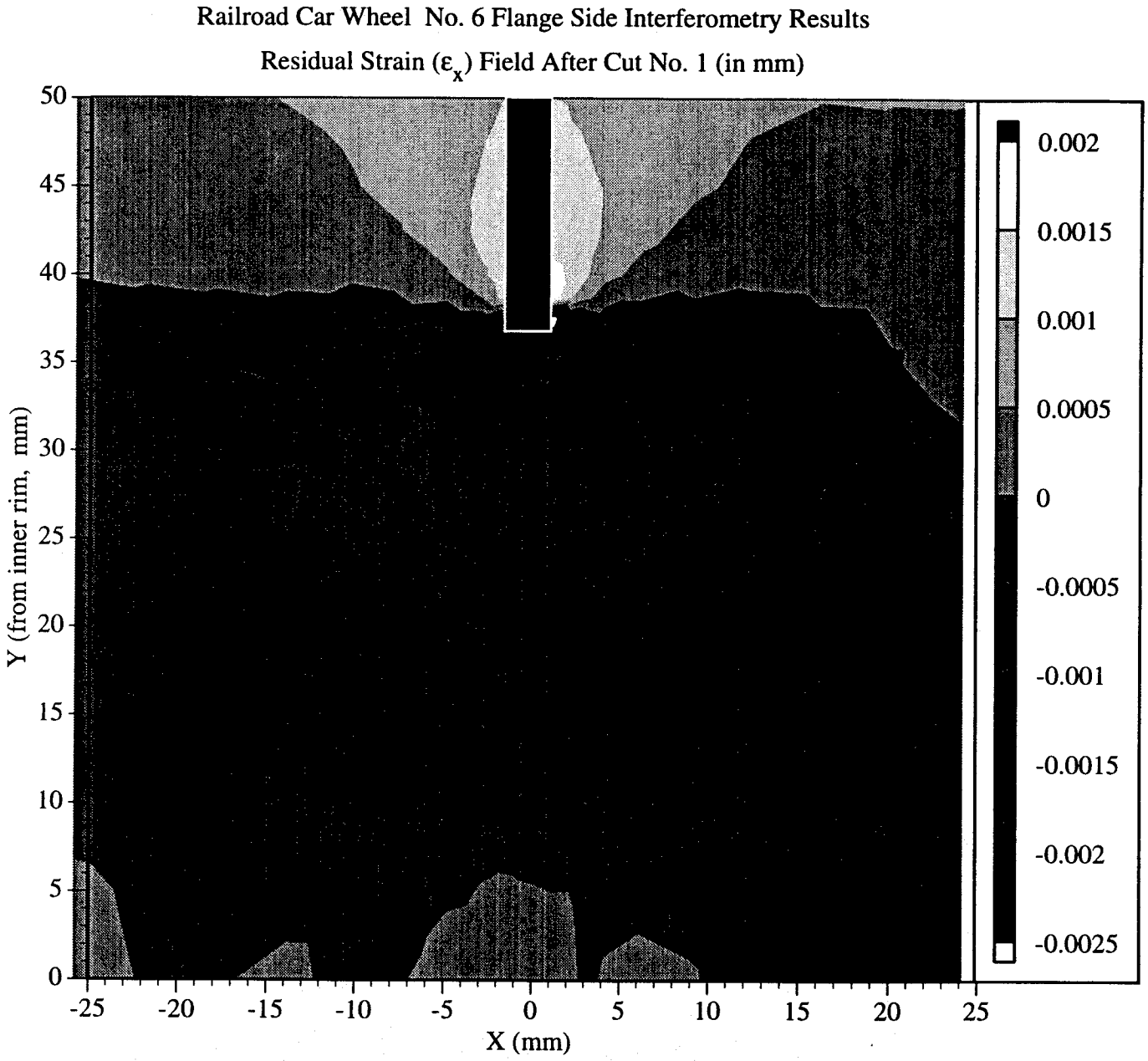
Railroad Car Wheel No. 6 Flange Side Interferometry Results
Residual Strain (ε_x) Field After Cut No. 1 (in mm)
Y (from inner rim, mm)
X (mm)
50
45
40
35
30
25
20
15
10
5
0
-25
-20
-15
-10
-5
0
5
10
15
20
25
0.002
0.0015
0.001
0.0005
0
-0.0005
-0.001
-0.0015
-0.002
-0.0025

Railroad Car Wheel No. 6 Flange Side Interferometry Results

Residual Strain (ε_y) Field After Cut No. 1 (in mm)

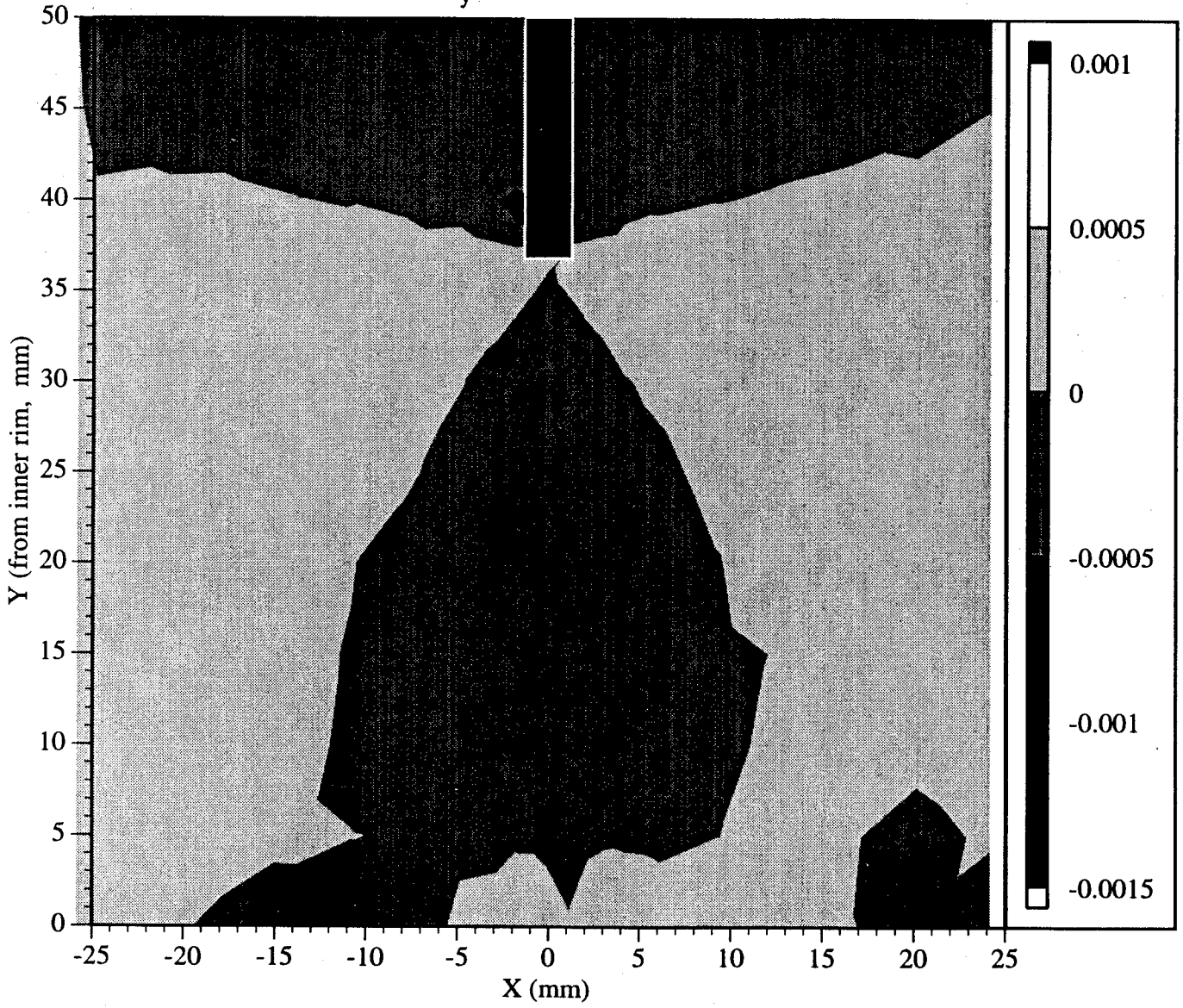

Railroad Car Wheel No. 6 Flange Side Interferometry Results

Residual Strain (γ_{xy}) Field After Cut No. 1 (in mm)

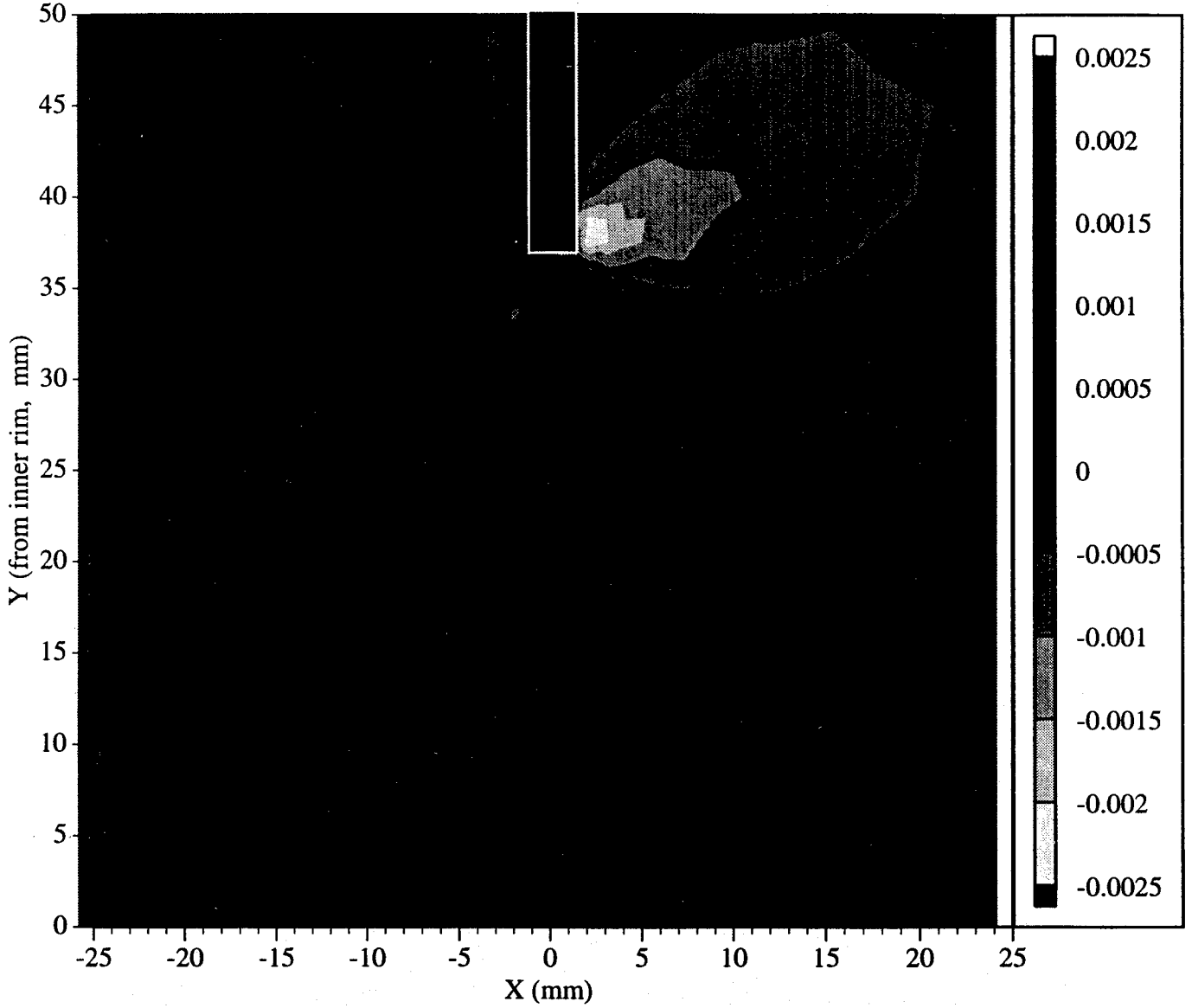

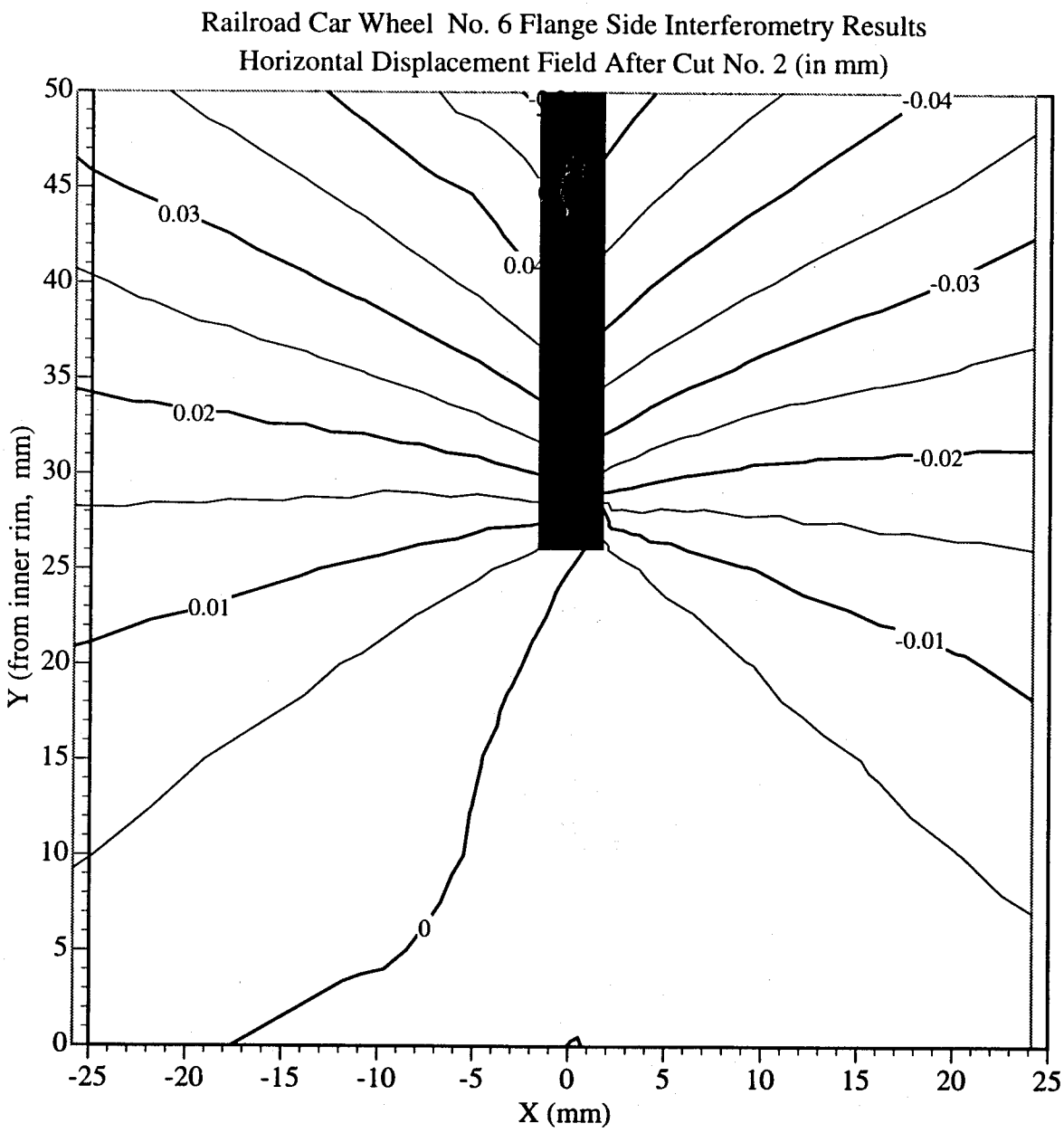
Railroad Car Wheel No. 6 Flange Side Interferometry Results
Horizontal Displacement Field After Cut No. 2 (in mm)
Y (from inner rim, mm)
X (mm)
0.03
0.02
0.01
0
-0.04
-0.03
-0.02
-0.01
50
45
40
35
30
25
20
15
10
5
0
-25
-20
-15
-10
-5
0
5
10
15
20
25

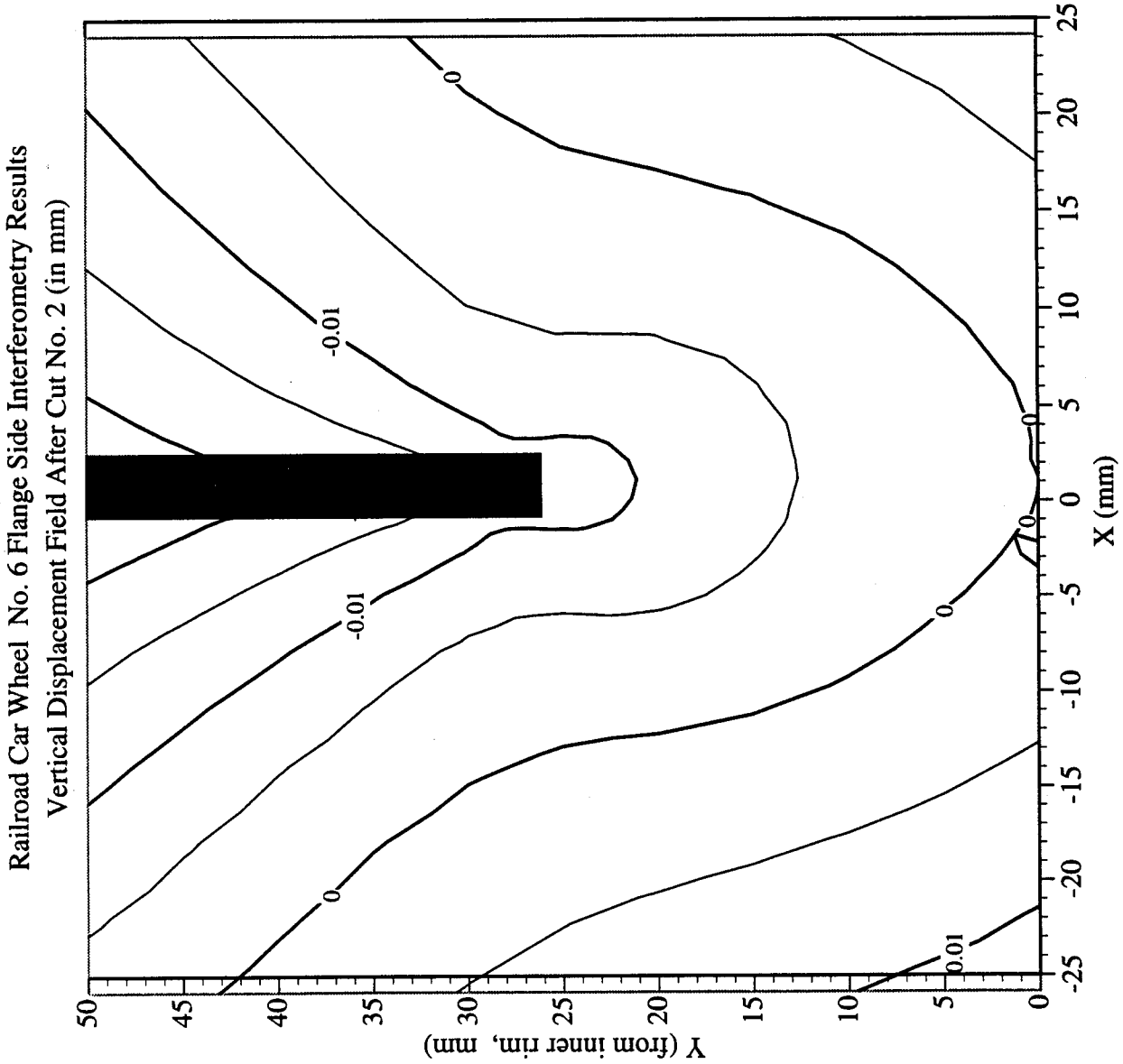
Railroad Car Wheel No. 6 Flange Side Interferometry Results
Vertical Displacement Field After Cut No. 2 (in mm)
Y (from inner rim, mm)
X (mm)
50
45
40
35
30
25
20
15
10
5
0
-25
-20
-15
-10
-5
0
5
10
15
20
25
-0.01
-0.01
0
0
0
0
0
0.01

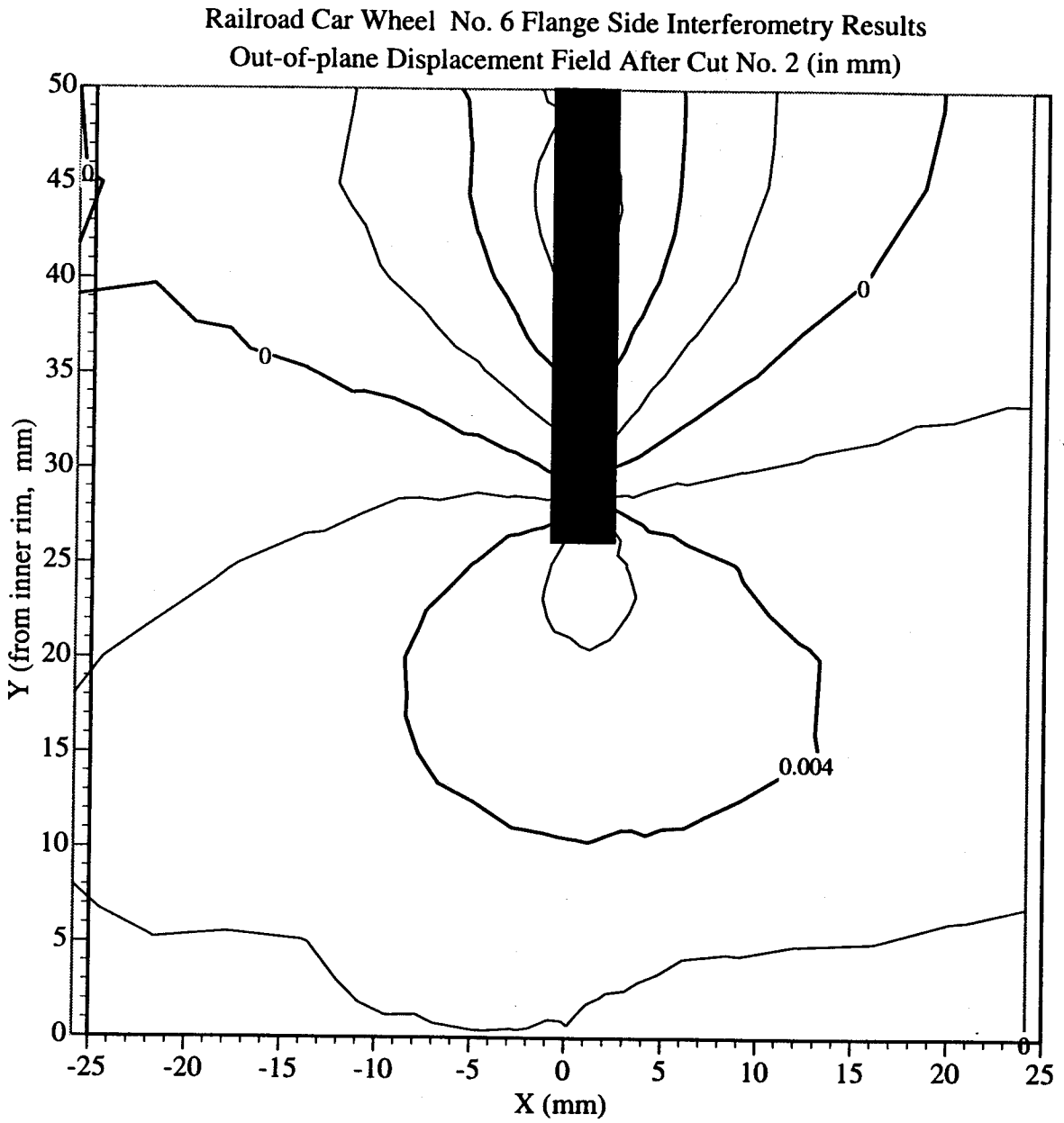
Railroad Car Wheel No. 6 Flange Side Interferometry Results
Out-of-plane Displacement Field After Cut No. 2 (in mm)
Y (from inner rim, mm)
X (mm)
50
45
40
35
30
25
20
15
10
5
0
-25
-20
-15
-10
-5
0
5
10
15
20
25
0
0
0
0.004
0

Railroad Car Wheel No. 6 Flange Side Interferometry Results

Residual Strain (ε_x) Field After Cut No. 2 (in mm)

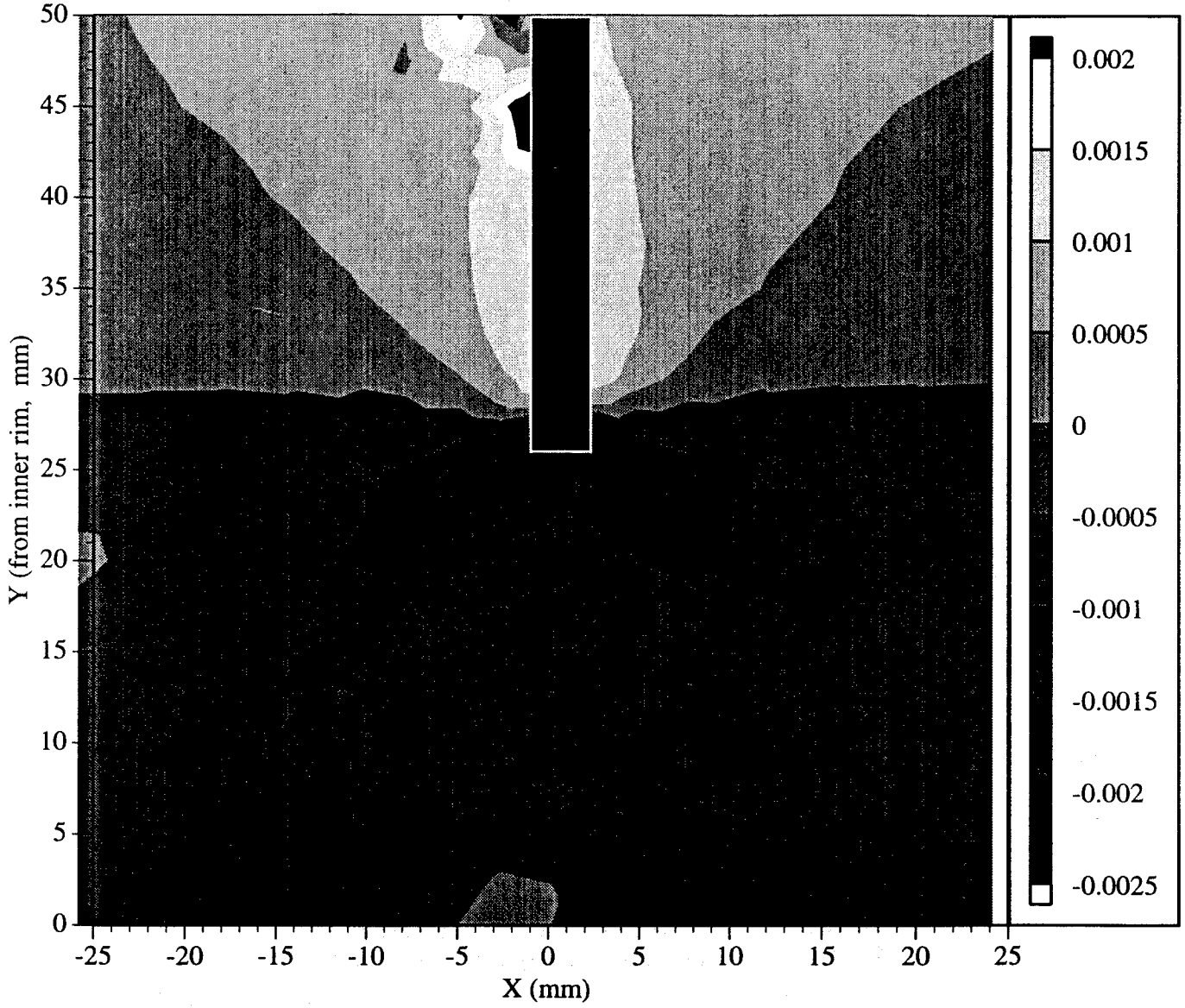

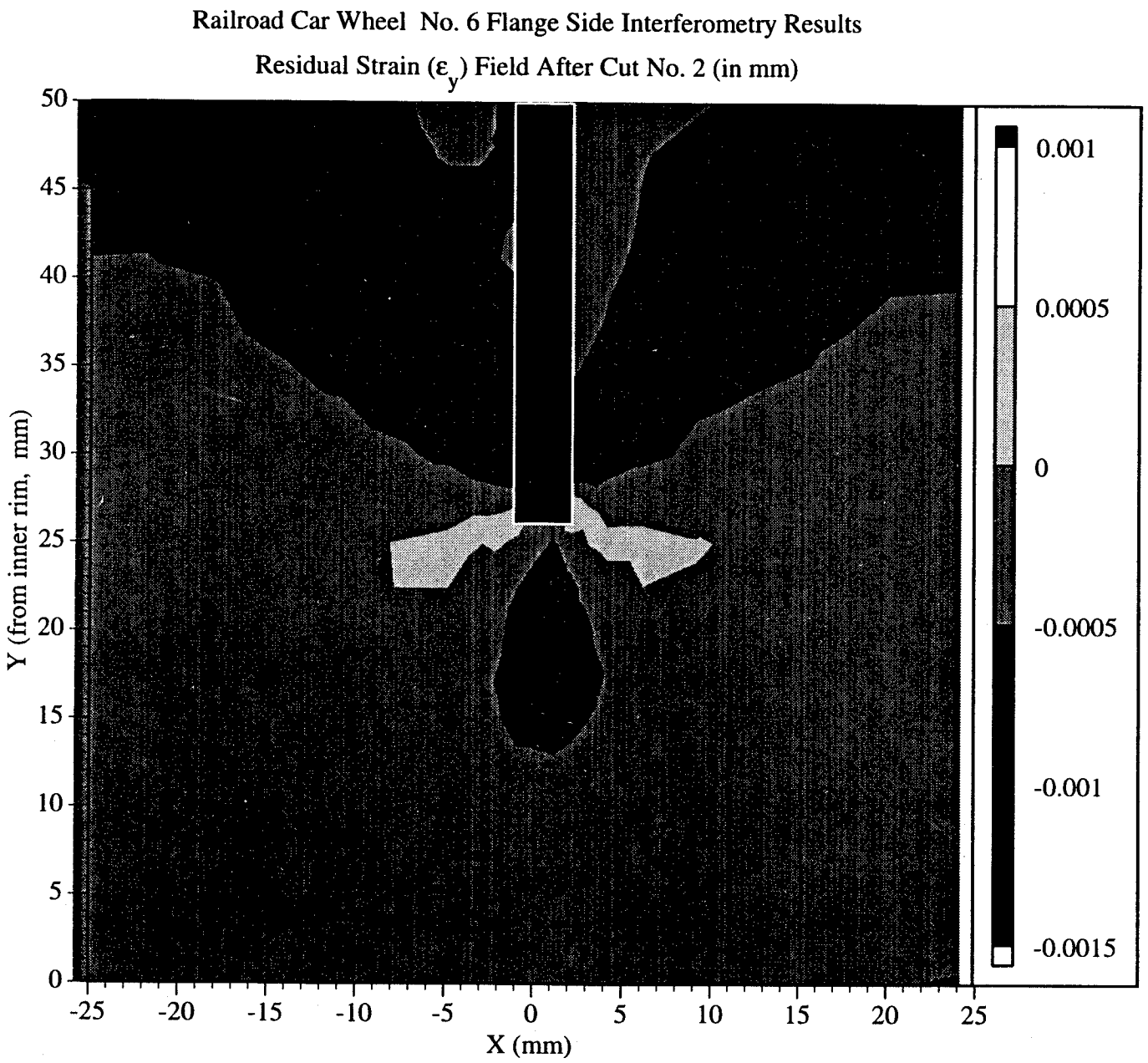
Railroad Car Wheel No. 6 Flange Side Interferometry Results
Residual Strain (ε_y) Field After Cut No. 2 (in mm)
Y (from inner rim, mm)
X (mm)
50
45
40
35
30
25
20
15
10
5
0
-25
-20
-15
-10
-5
0
5
10
15
20
25
0.001
0.0005
0
-0.0005
-0.001
-0.0015

Railroad Car Wheel No. 6 Flange Side Interferometry Results

Residual Strain (γ_{xy}) Field After Cut No. 2 (in mm)

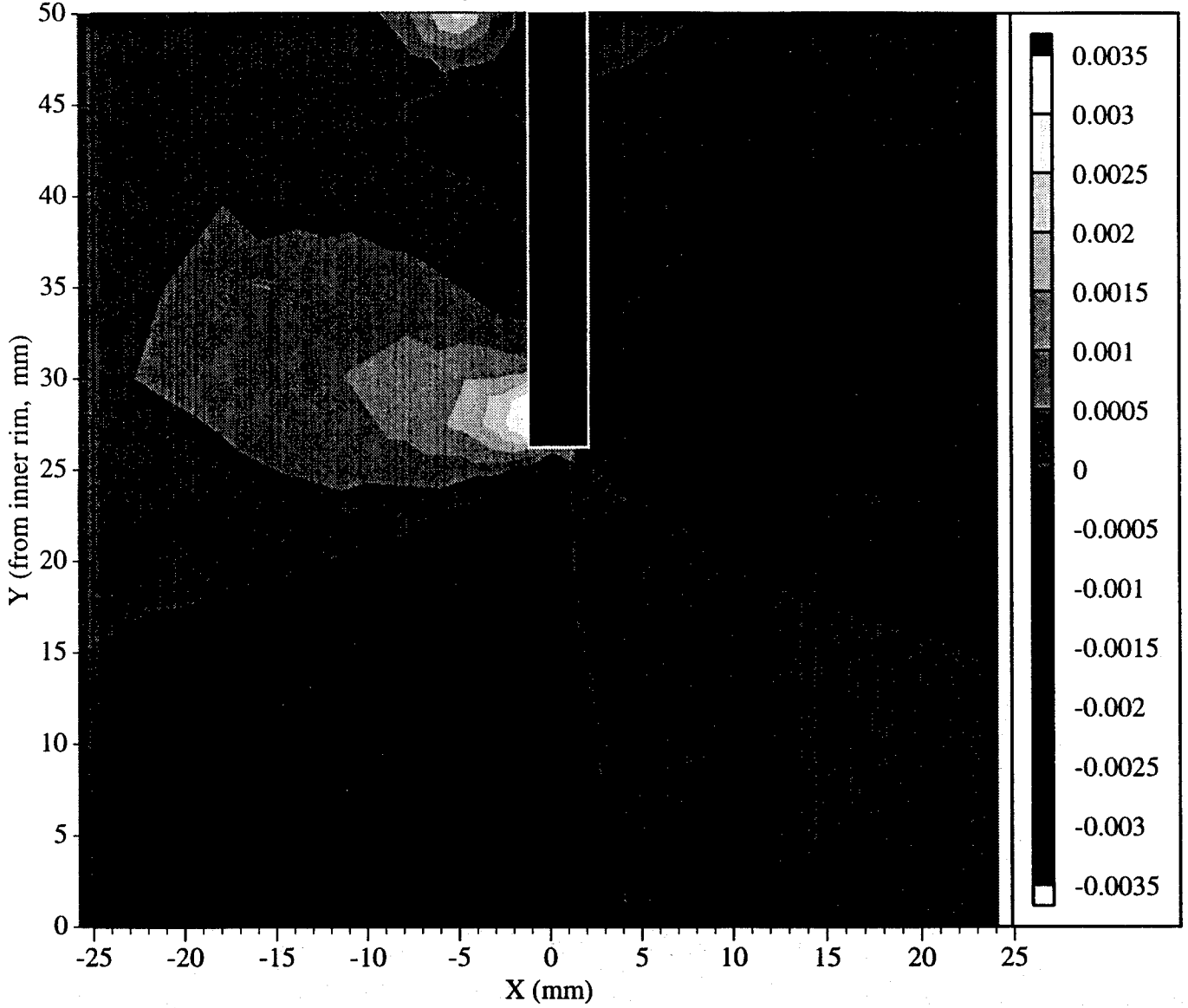

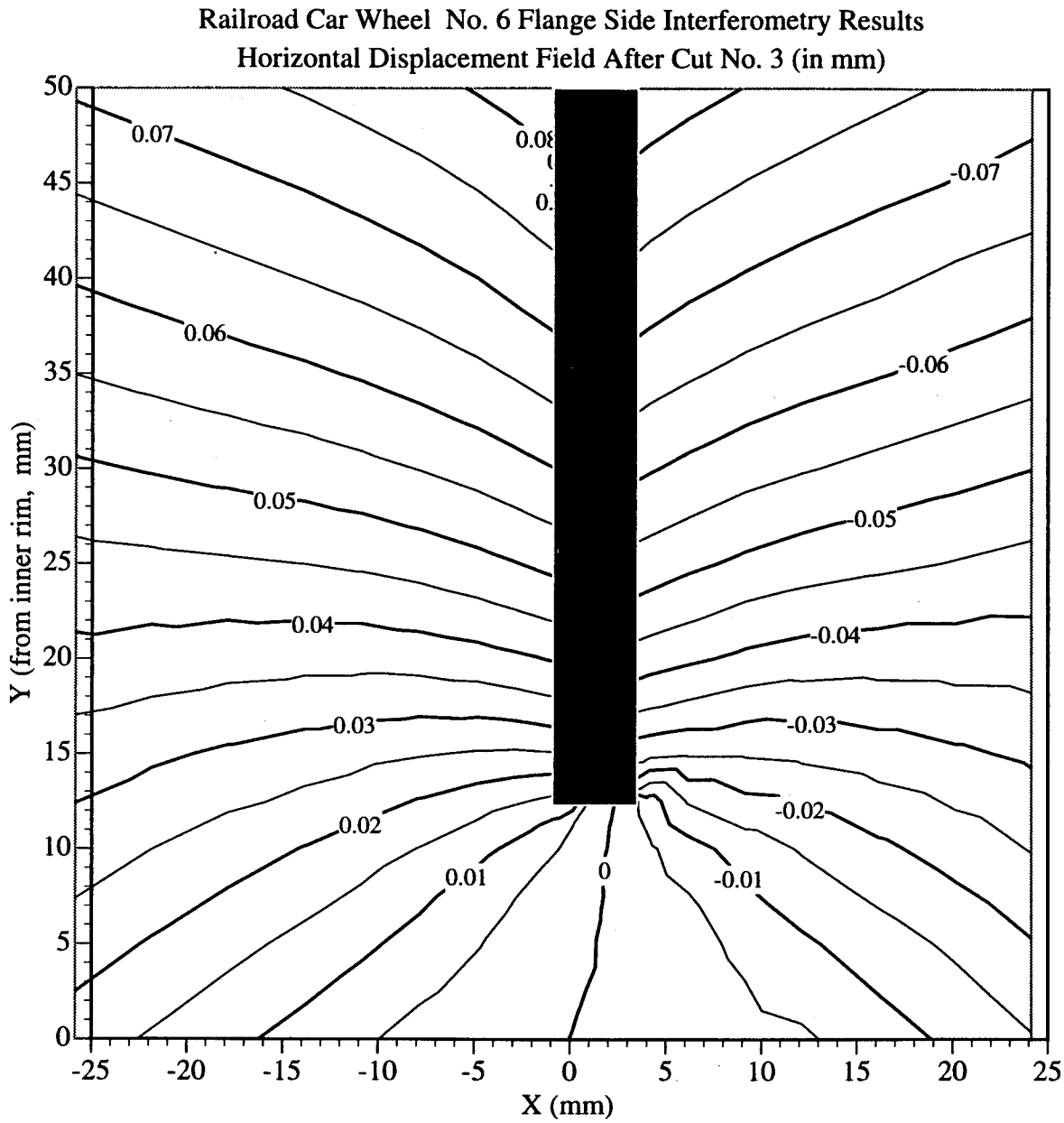
Railroad Car Wheel No. 6 Flange Side Interferometry Results
Horizontal Displacement Field After Cut No. 3 (in mm)
Y (from inner rim, mm)
X (mm)
0.07
0.06
0.05
0.04
0.03
0.02
0.01
0
-0.01
-0.02
-0.03
-0.04
-0.05
-0.06
-0.07
50
45
40
35
30
25
20
15
10
5
0
-25
-20
-15
-10
-5
0
5
10
15
20
25

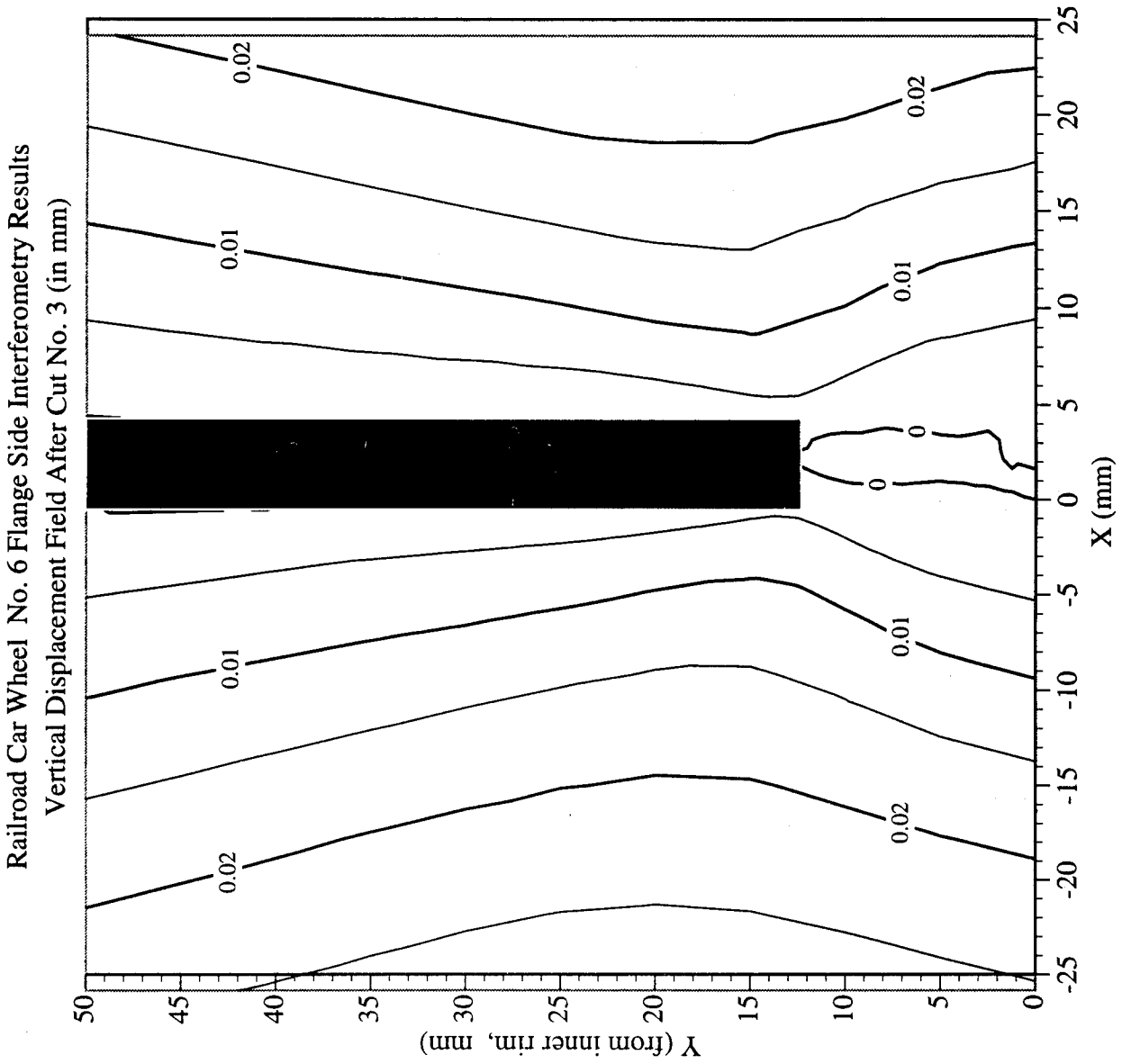
Railroad Car Wheel No. 6 Flange Side Interferometry Results
Vertical Displacement Field After Cut No. 3 (in mm)
Y (from inner rim, mm)
X (mm)
0.02
0.01
0
50
45
40
35
30
25
20
15
10
5
0
-25
-20
-15
-10
-5
0
5
10
15
20
25

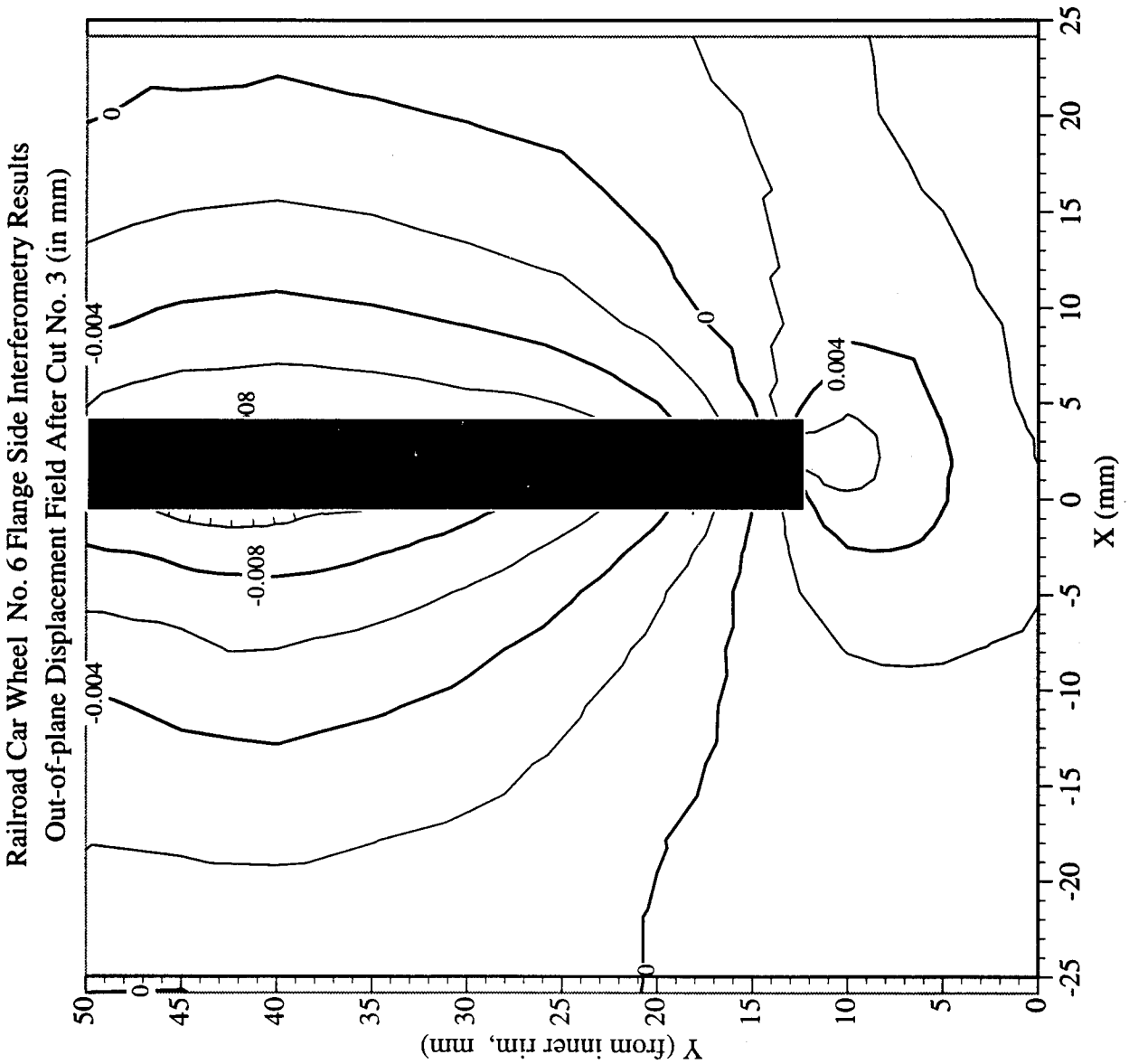
Railroad Car Wheel No. 6 Flange Side Interferometry Results
Out-of-plane Displacement Field After Cut No. 3 (in mm)
-0.004
-0.008
0
-0.004
0
0.004
Y (from inner rim, mm)
X (mm)
50
45
40
35
30
25
20
15
10
5
0
-25
-20
-15
-10
-5
0
5
10
15
20
25

Railroad Car Wheel No. 6 Flange Side Interferometry Results

Residual Strain (ε_x) Field After Cut No. 3 (in mm)

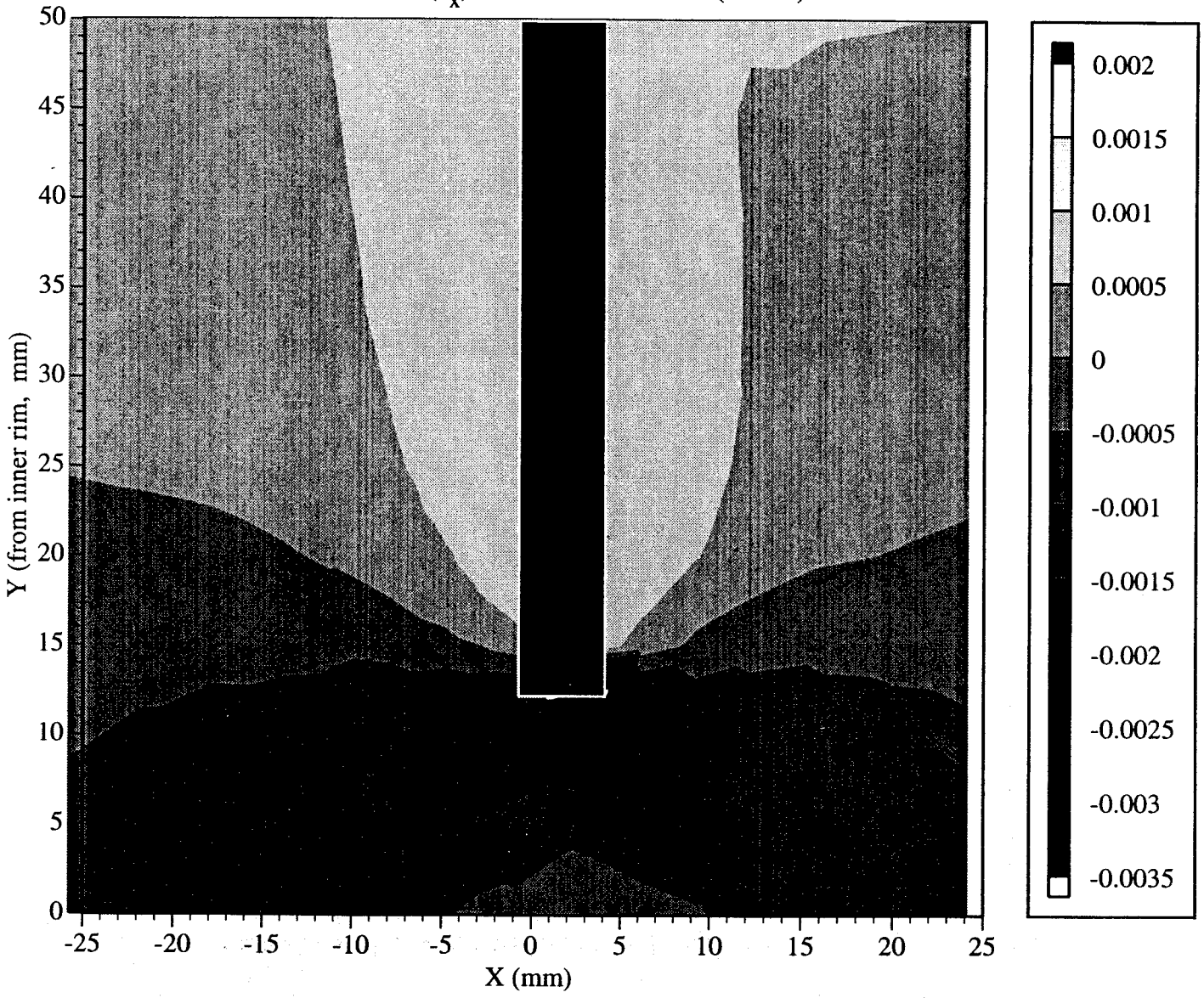

Railroad Car Wheel No. 6 Flange Side Interferometry Results

Residual Strain (ε_y) Field After Cut No. 3 (in mm)

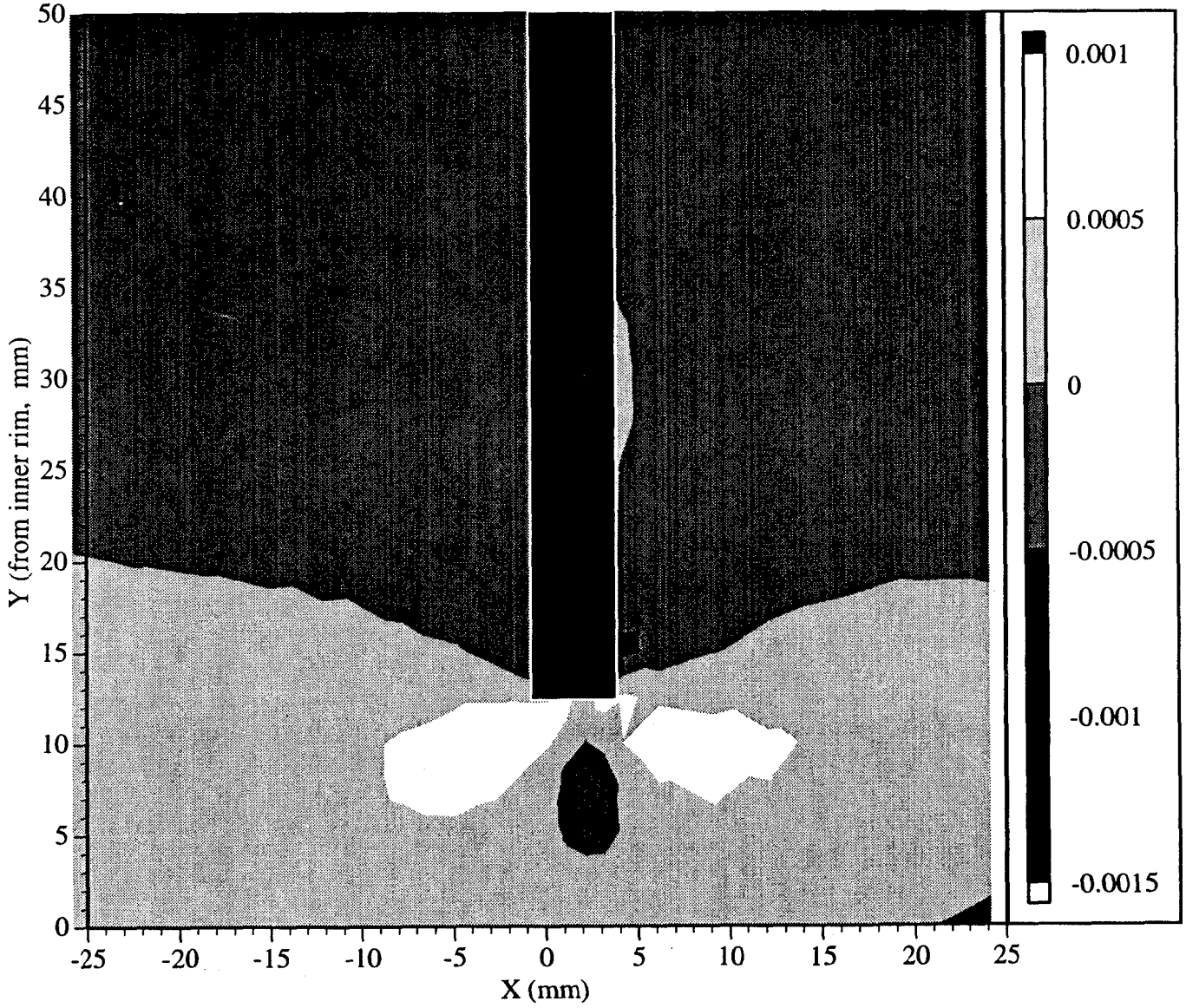

Railroad Car Wheel No. 6 Flange Side Interferometry Results

Residual Strain (γ_{xy}) Field After Cut No. 3 (in mm)

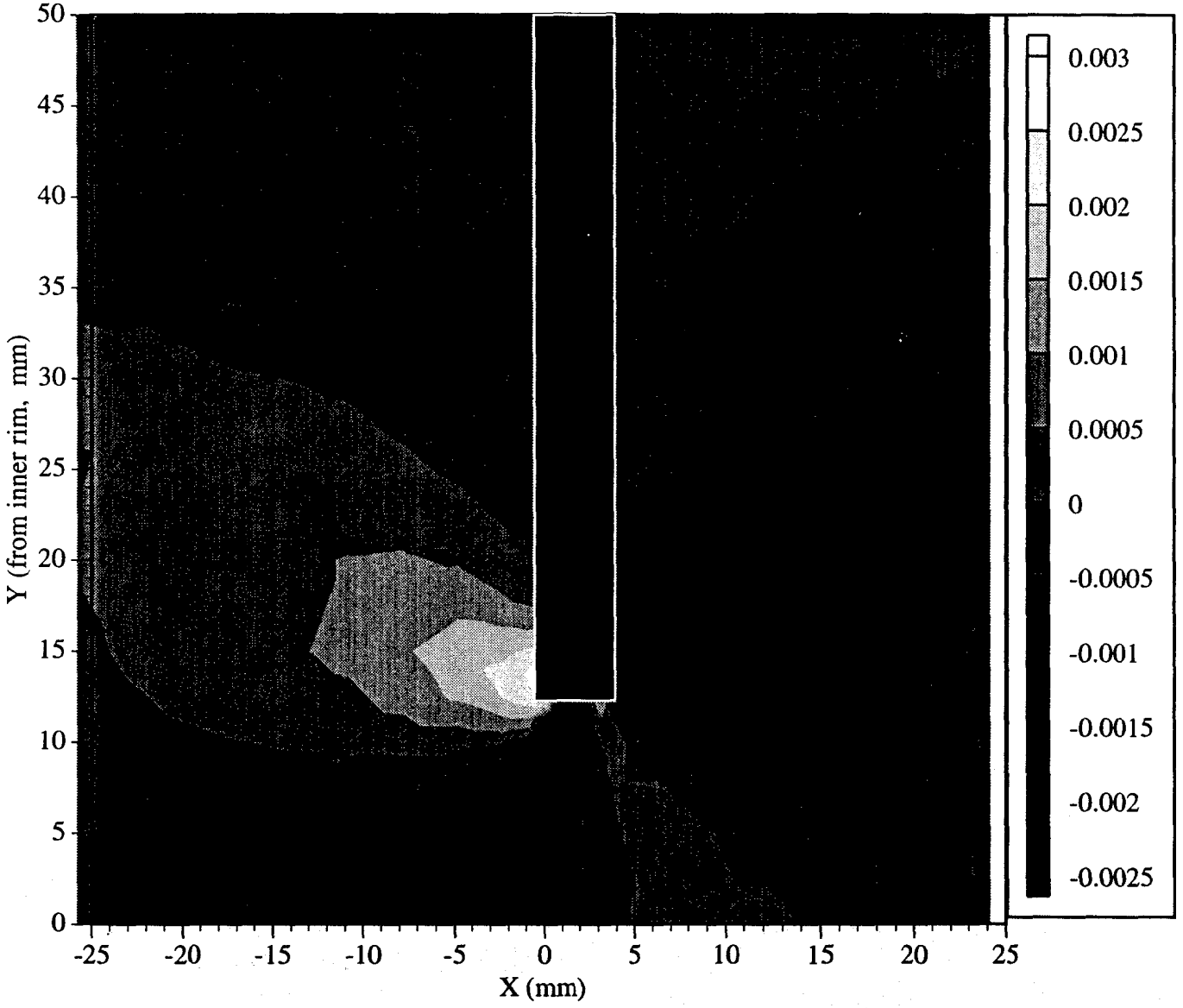

Railroad Car Wheel No. 6 Second Side Interferometry Results
Horizontal Displacement Field After Cut No. 1 (in mm)

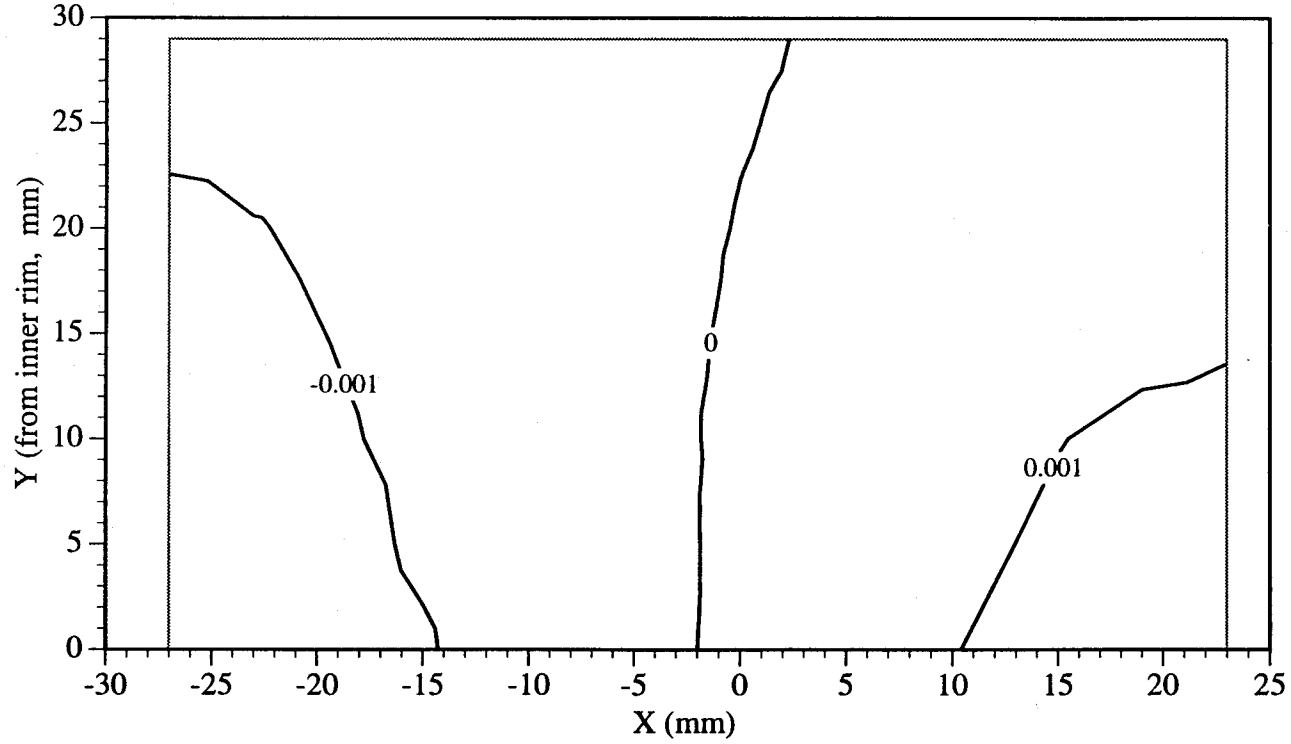

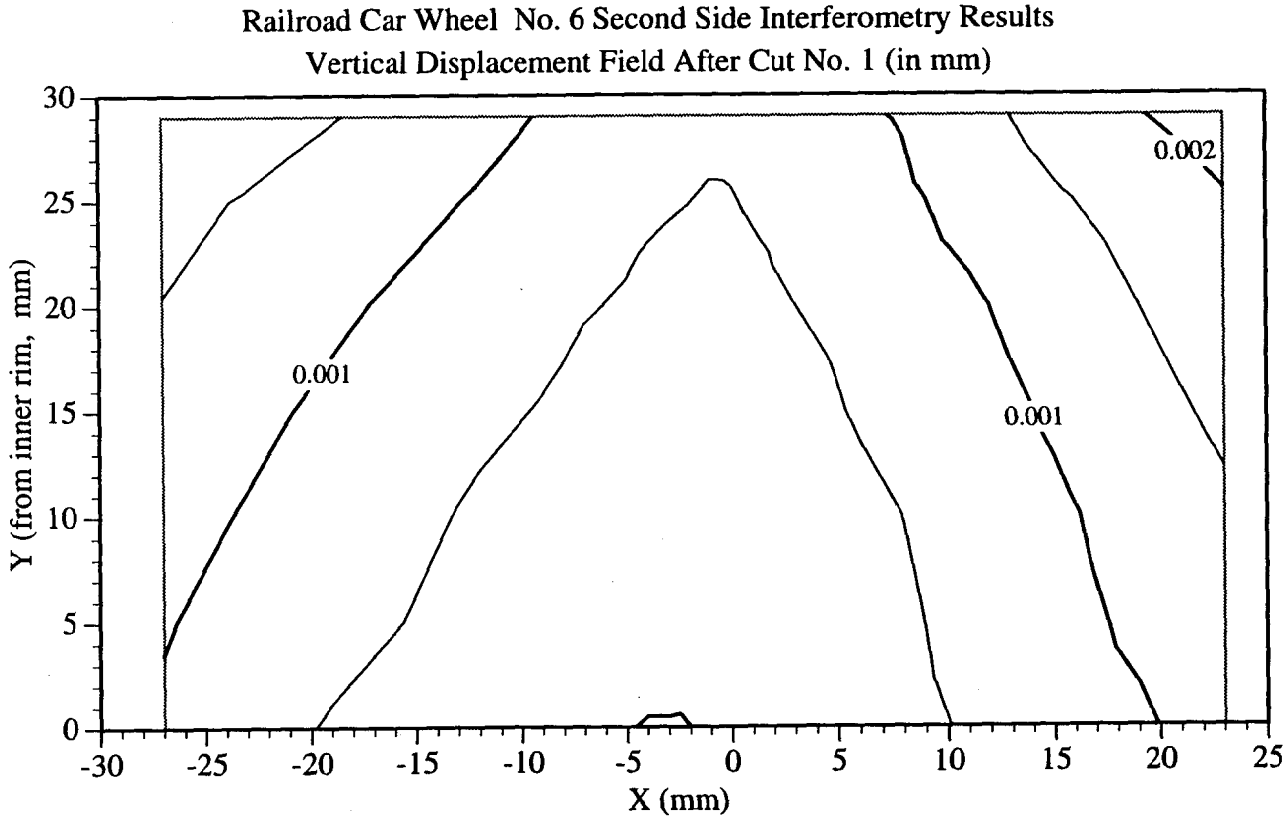
Railroad Car Wheel No. 6 Second Side Interferometry Results
Vertical Displacement Field After Cut No. 1 (in mm)
Y (from inner rim, mm)
X (mm)
0.001
0.001
0.002
30
25
20
15
10
5
0
-30
-25
-20
-15
-10
-5
0
5
10
15
20
25

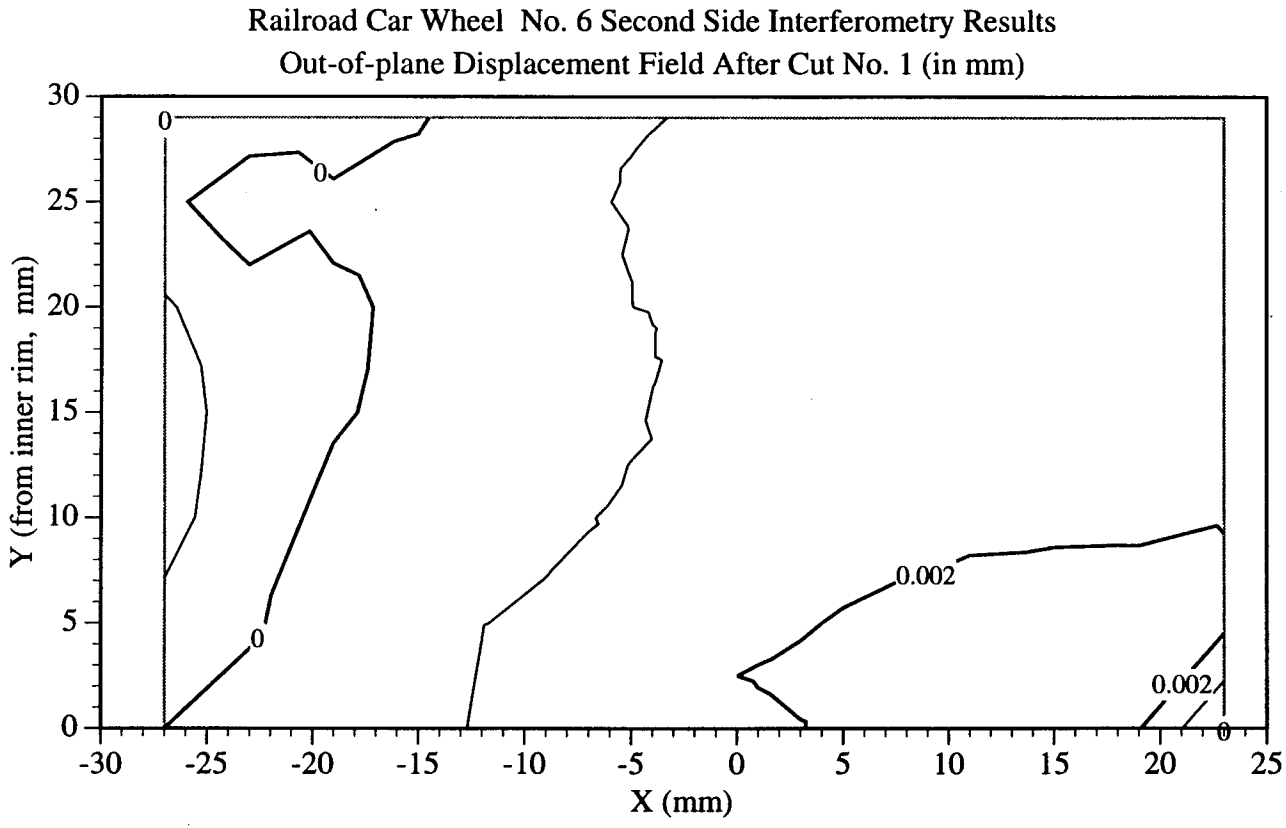
Railroad Car Wheel No. 6 Second Side Interferometry Results
Out-of-plane Displacement Field After Cut No. 1 (in mm)
Y (from inner rim, mm)
X (mm)
30
25
20
15
10
5
0
-30
-25
-20
-15
-10
-5
0
5
10
15
20
25
0
0
0
0.002
0.002
0

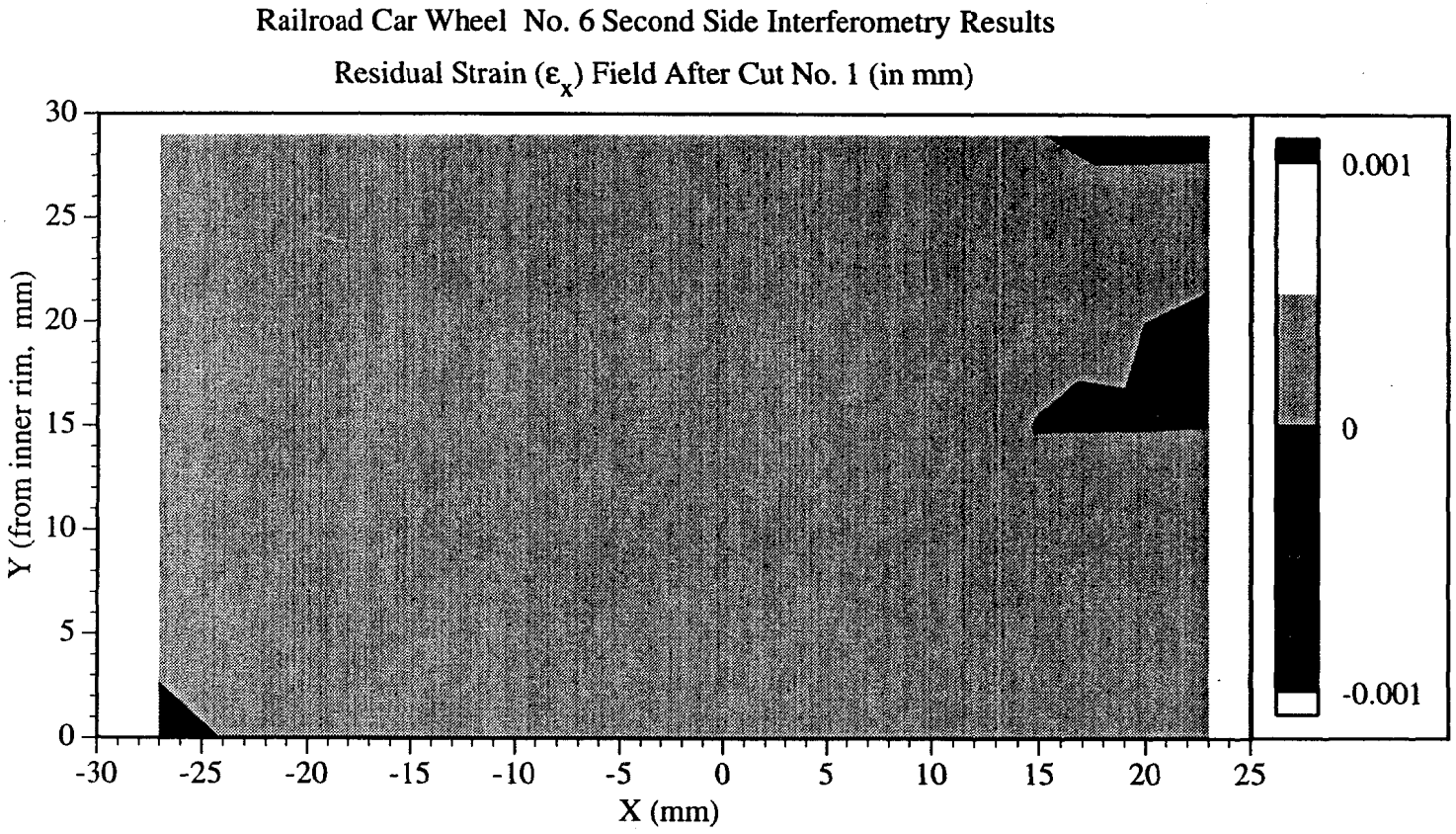
Railroad Car Wheel No. 6 Second Side Interferometry Results
Residual Strain (ε_x) Field After Cut No. 1 (in mm)
Y (from inner rim, mm)
30
25
20
15
10
5
0
-30
-25
-20
-15
-10
-5
0
5
10
15
20
25
X (mm)
0.001
0
-0.001

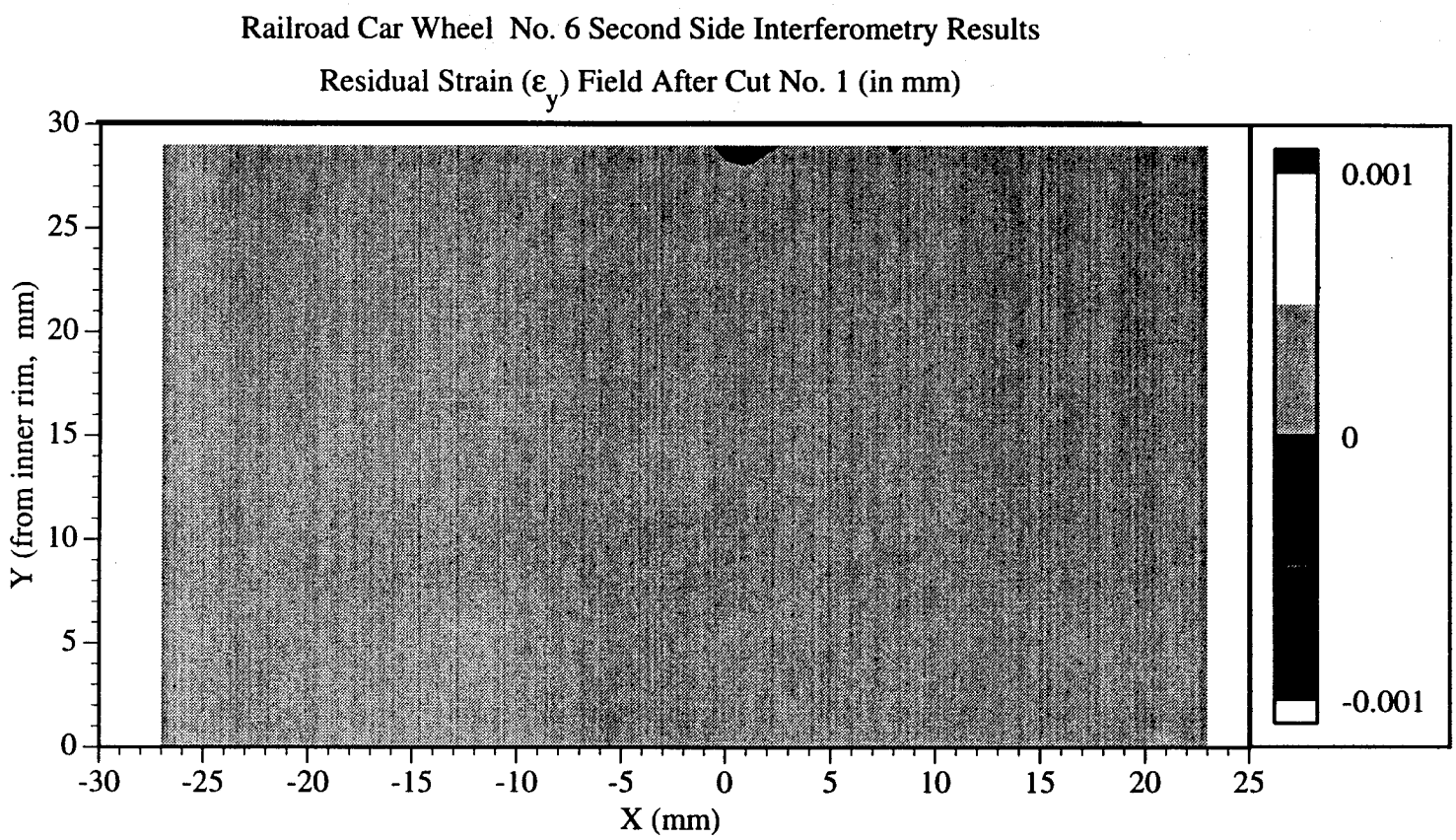
Railroad Car Wheel No. 6 Second Side Interferometry Results
Residual Strain (ε_y) Field After Cut No. 1 (in mm)
Y (from inner rim, mm)
30
25
20
15
10
5
0
-30
-25
-20
-15
-10
-5
0
5
10
15
20
25
X (mm)
0.001
0
-0.001

Railroad Car Wheel No. 6 Second Side Interferometry Results

Residual Strain (γ_{xy}) Field After Cut No. 1 (in mm)

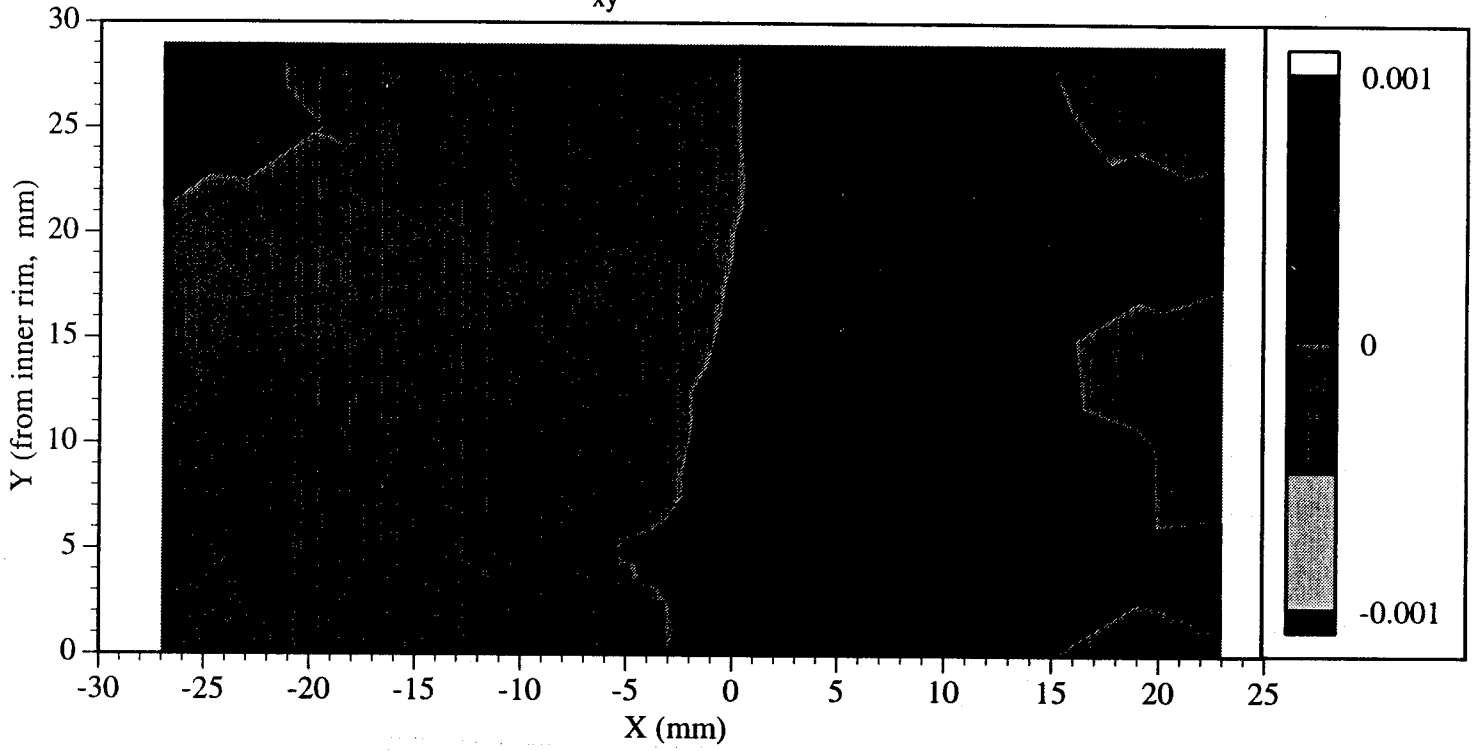

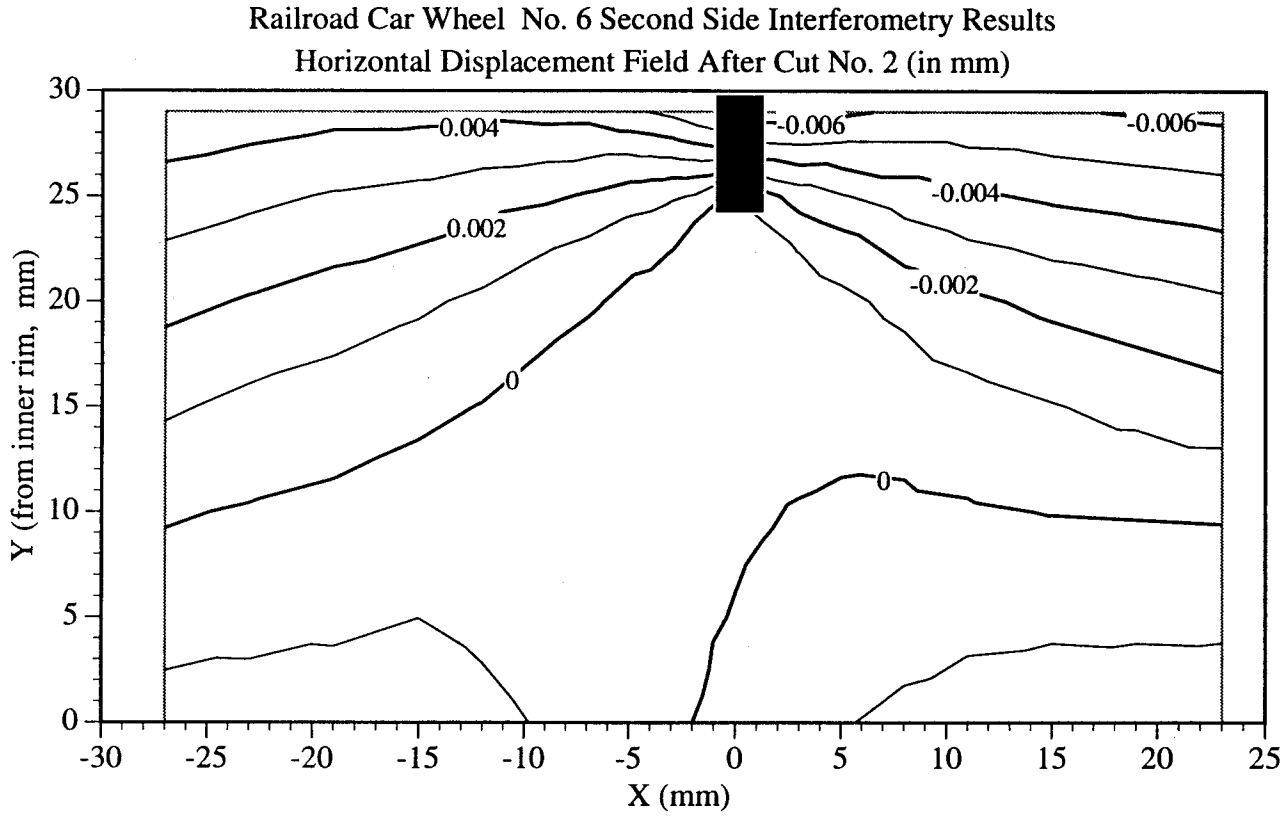
Railroad Car Wheel No. 6 Second Side Interferometry Results
Horizontal Displacement Field After Cut No. 2 (in mm)
0.004
0.002
0
-0.006
-0.006
-0.004
-0.002
0
Y (from inner rim, mm)
X (mm)
30
25
20
15
10
5
0
-30
-25
-20
-15
-10
-5
0
5
10
15
20
25

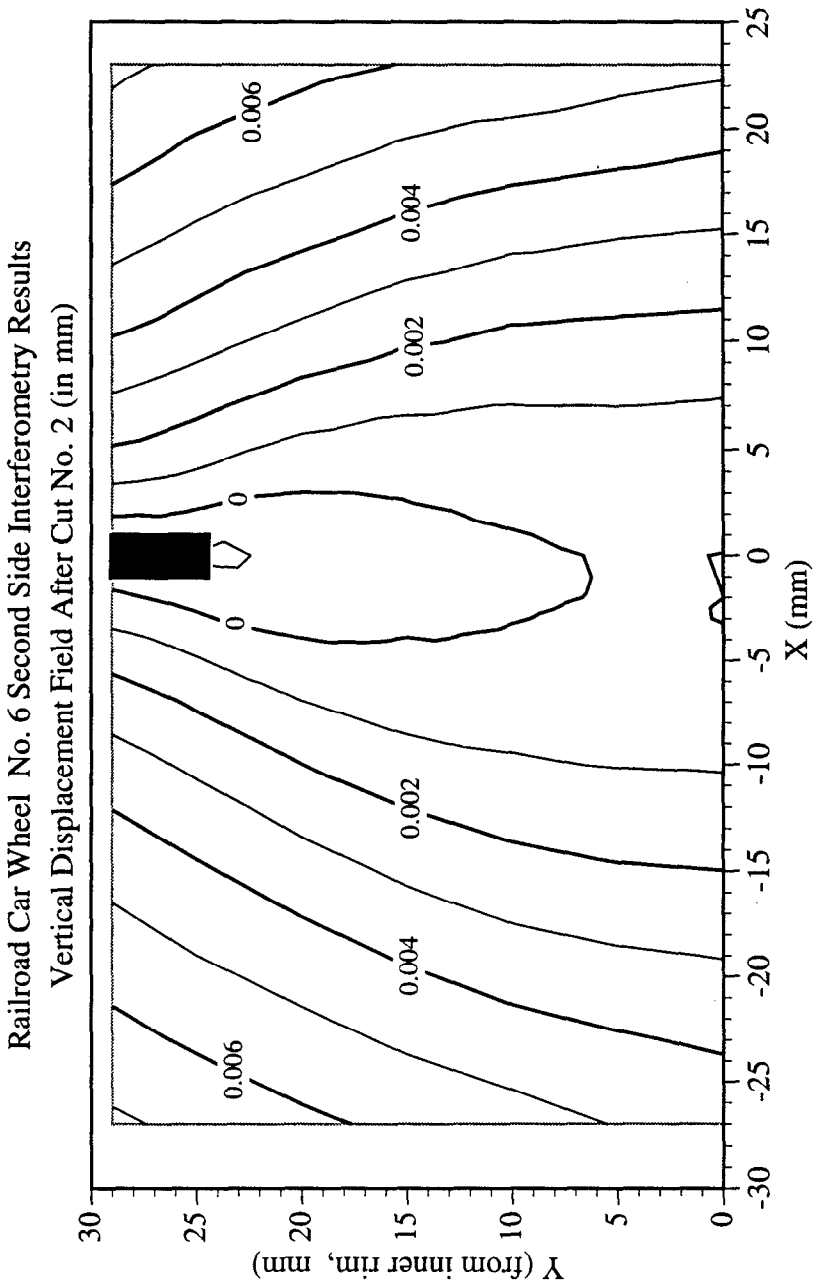
Railroad Car Wheel No. 6 Second Side Interferometry Results
Vertical Displacement Field After Cut No. 2 (in mm)
0.006
0.004
0.002
0
0
0.002
0.004
0.006
Y (from inner rim, mm)
X (mm)
30
25
20
15
10
5
0
-30
-25
-20
-15
-10
-5
0
5
10
15
20
25

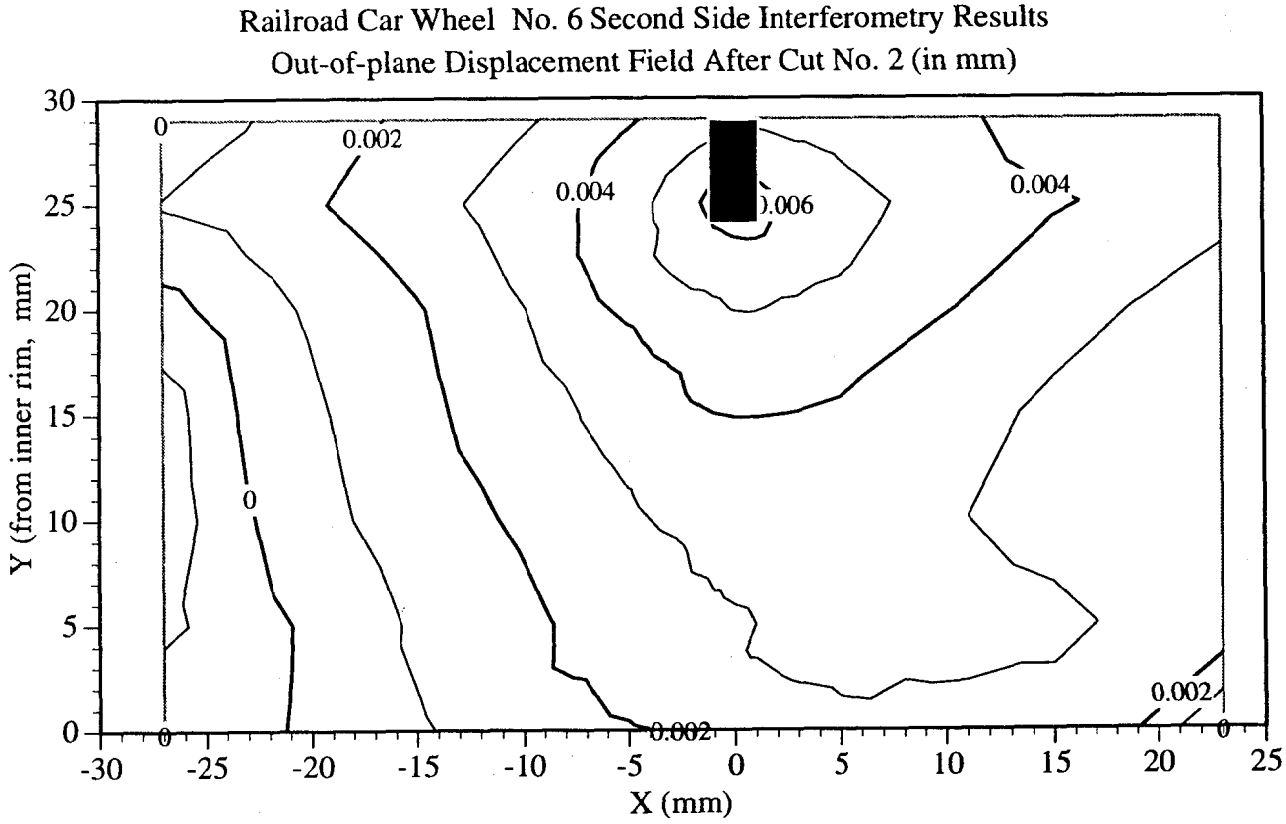
Railroad Car Wheel No. 6 Second Side Interferometry Results
Out-of-plane Displacement Field After Cut No. 2 (in mm)
Y (from inner rim, mm)
X (mm)
30
25
20
15
10
5
0
-30
-25
-20
-15
-10
-5
0
5
10
15
20
25
0
0.002
0.004
0.006
0.004
0
0.002
0.002
0
0

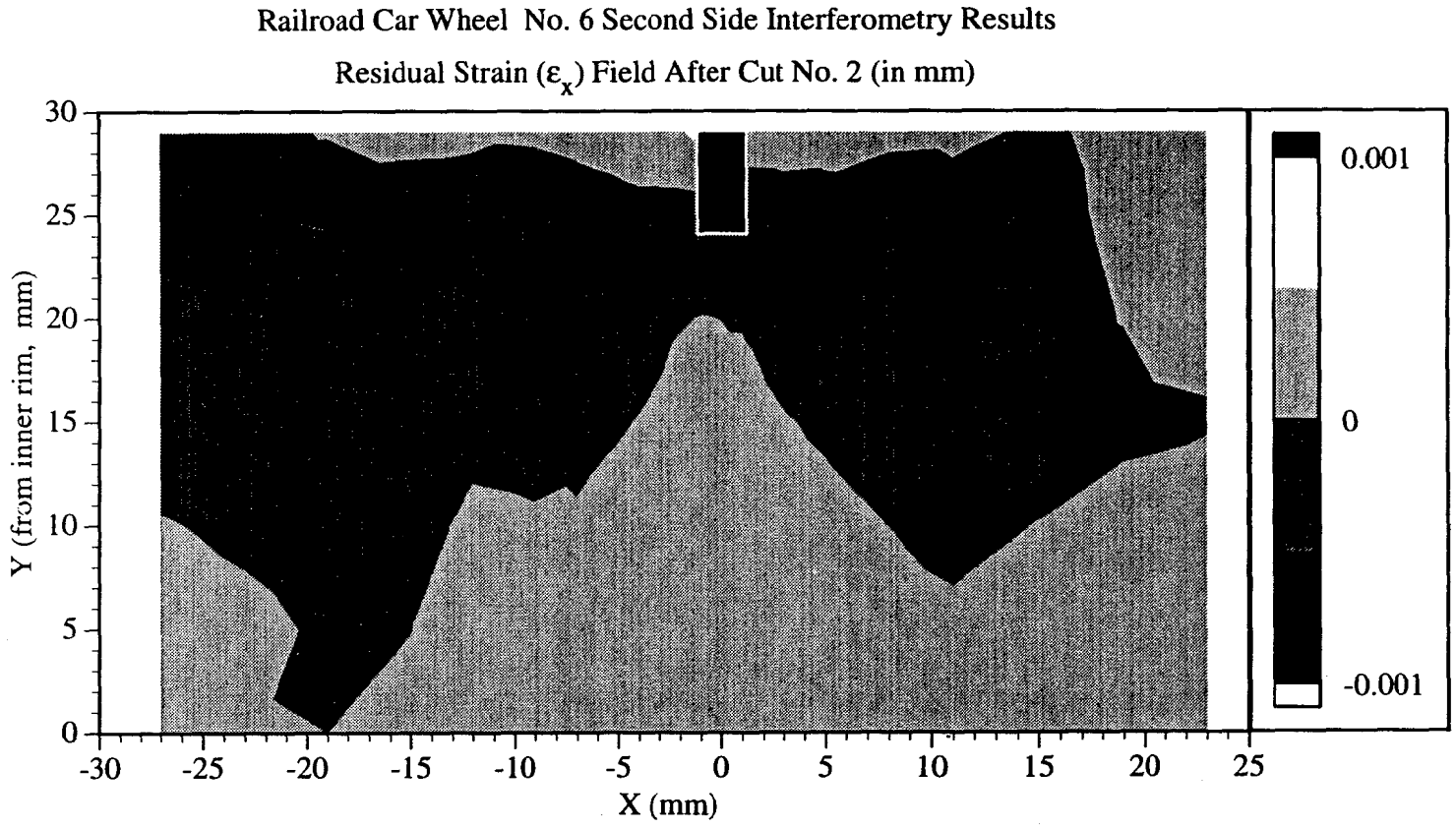
Railroad Car Wheel No. 6 Second Side Interferometry Results
Residual Strain (ε_x) Field After Cut No. 2 (in mm)
Y (from inner rim, mm)
30
25
20
15
10
5
0
-30
-25
-20
-15
-10
-5
0
5
10
15
20
25
X (mm)
0.001
0
-0.001

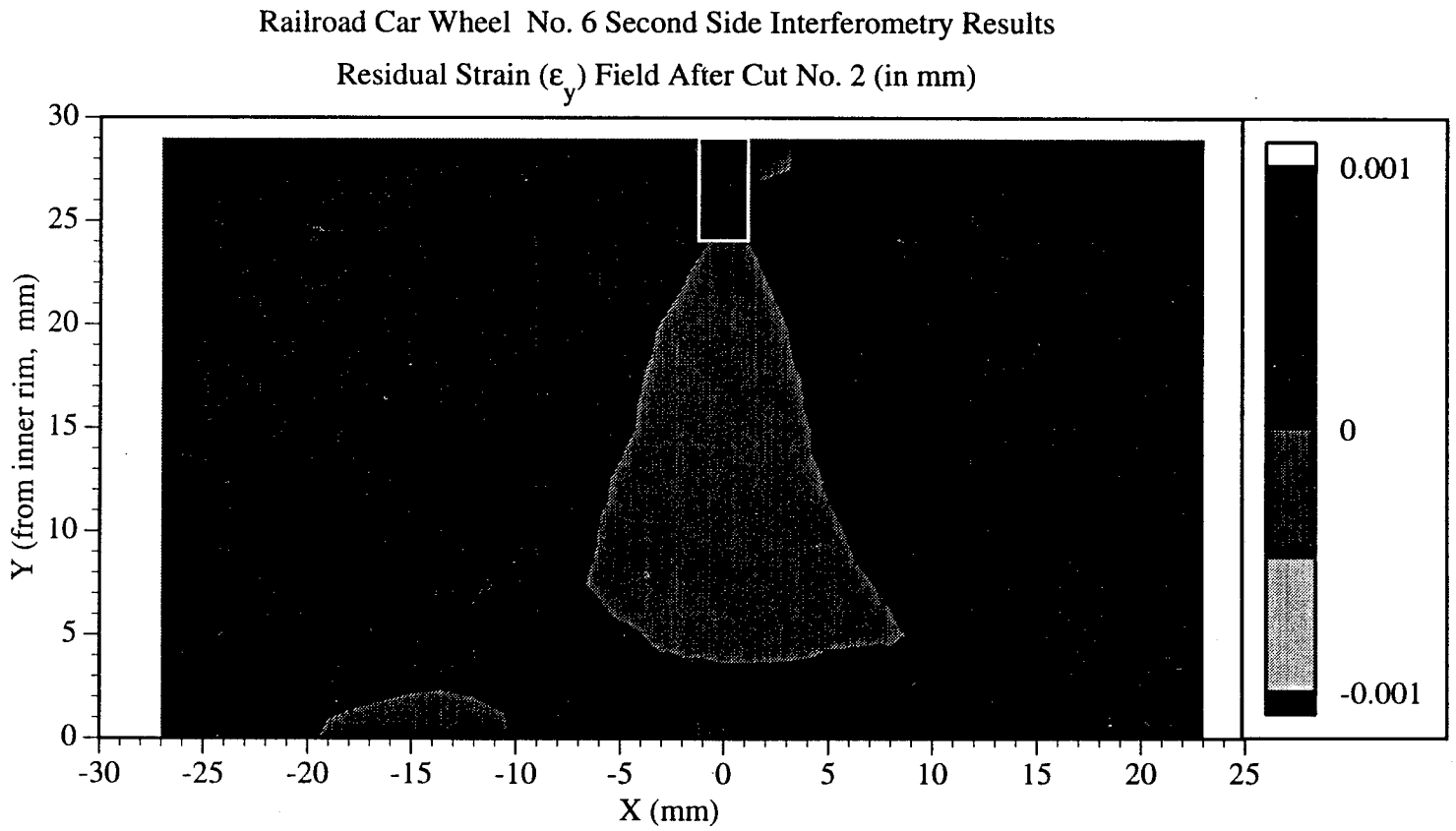
Railroad Car Wheel No. 6 Second Side Interferometry Results
Residual Strain (ε_y) Field After Cut No. 2 (in mm)
Y (from inner rim, mm)
X (mm)
30
25
20
15
10
5
0
-30
-25
-20
-15
-10
-5
0
5
10
15
20
25
0.001
0
-0.001

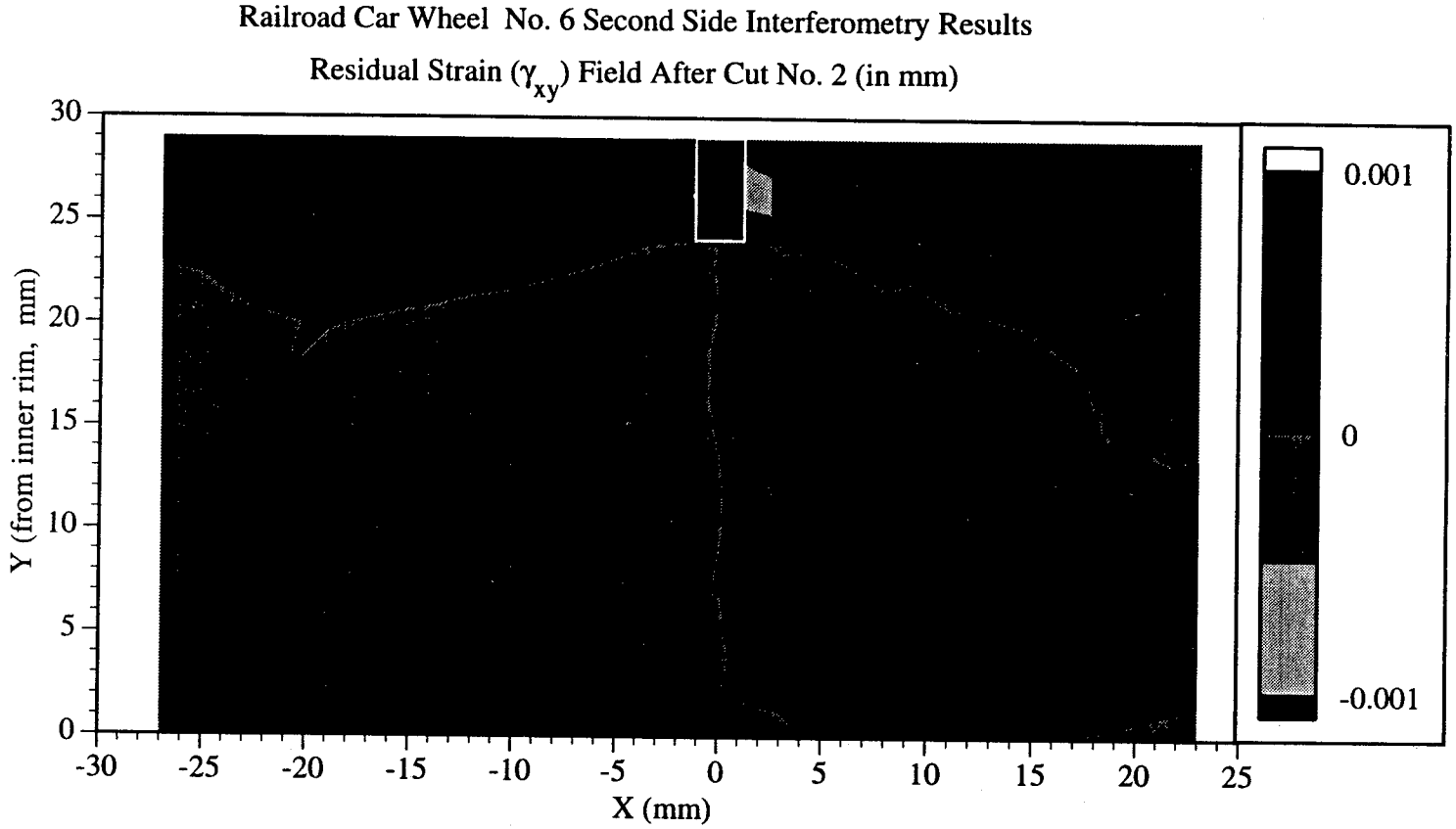
Railroad Car Wheel No. 6 Second Side Interferometry Results
Residual Strain (γ_{xy}) Field After Cut No. 2 (in mm)
Y (from inner rim, mm)
30
25
20
15
10
5
0
-30
-25
-20
-15
-10
-5
0
5
10
15
20
25
X (mm)
0.001
0
-0.001

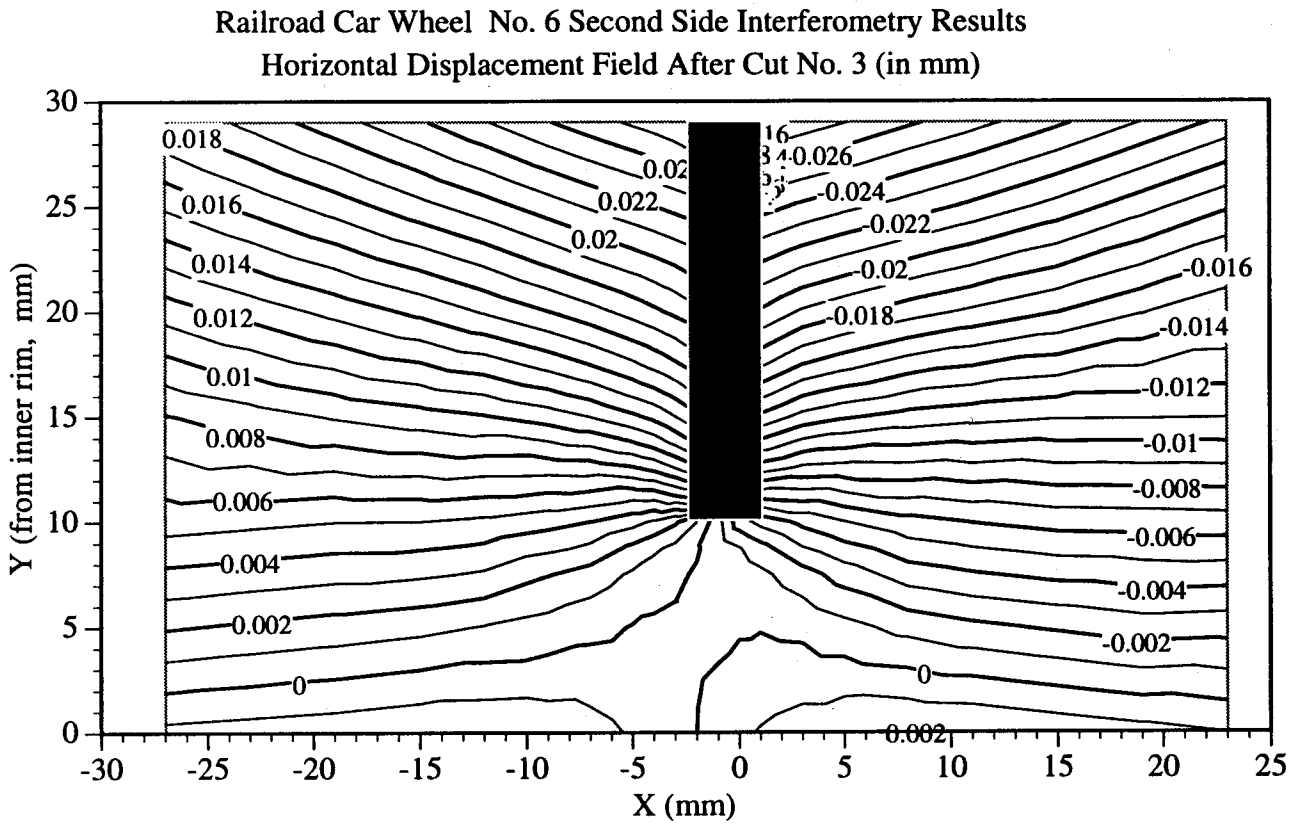
Railroad Car Wheel No. 6 Second Side Interferometry Results
Horizontal Displacement Field After Cut No. 3 (in mm)
Y (from inner rim, mm)
X (mm)
0.018
0.016
0.014
0.012
0.01
0.008
0.006
0.004
0.002
0
-0.002
-0.004
-0.006
-0.008
-0.01
-0.012
-0.014
-0.016
-0.018
-0.02
-0.022
-0.024
-0.026
0.022
0.02
0.002

U

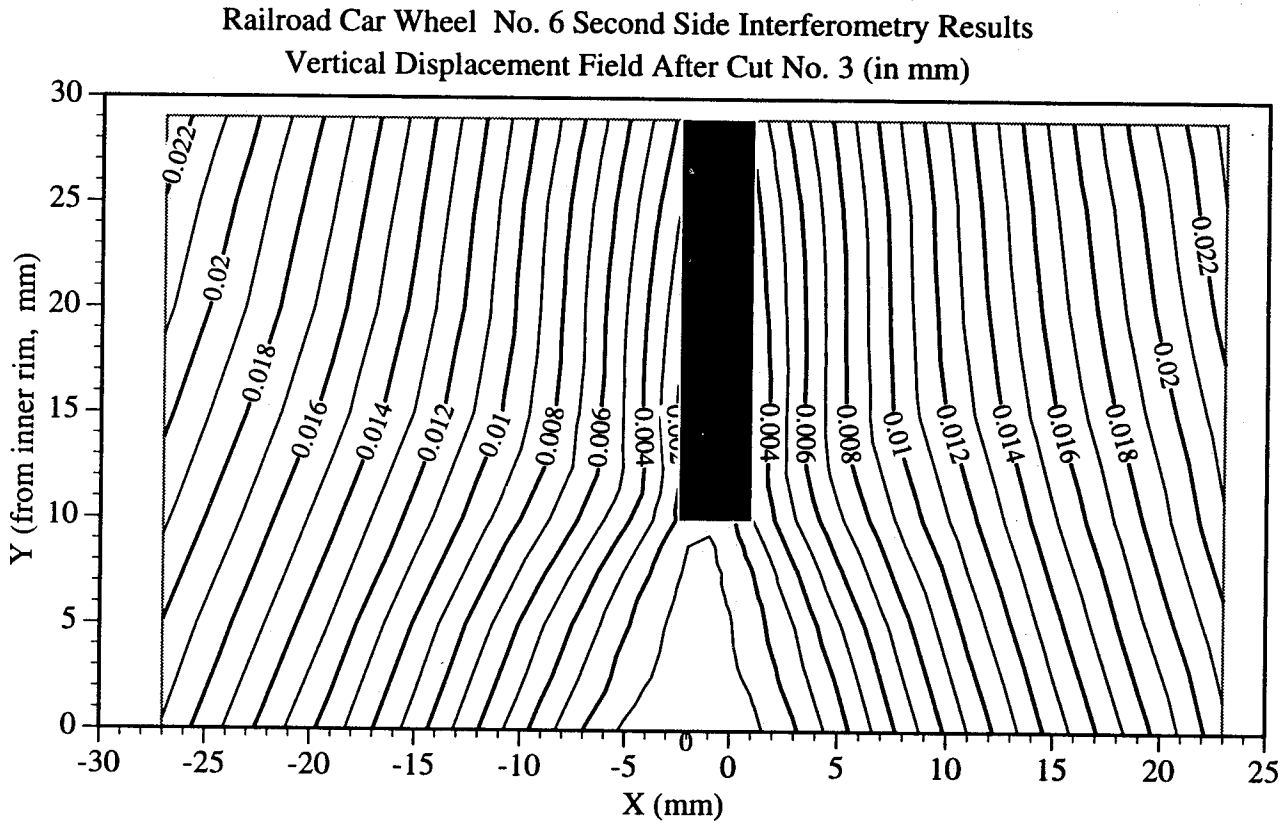
Railroad Car Wheel No. 6 Second Side Interferometry Results
Vertical Displacement Field After Cut No. 3 (in mm)
Y (from inner rim, mm)
X (mm)
30
25
20
15
10
5
0
-30
-25
-20
-15
-10
-5
0
5
10
15
20
25
0.022
0.02
0.018
0.016
0.014
0.012
0.01
0.008
0.006
0.004
0.002
0
0.004
0.006
0.008
0.01
0.012
0.014
0.016
0.018
0.02
0.022

V

Railroad Car Wheel No. 6 Second Side Interferometry Results
Out-of-plane Displacement Field After Cut No. 3 (in mm)

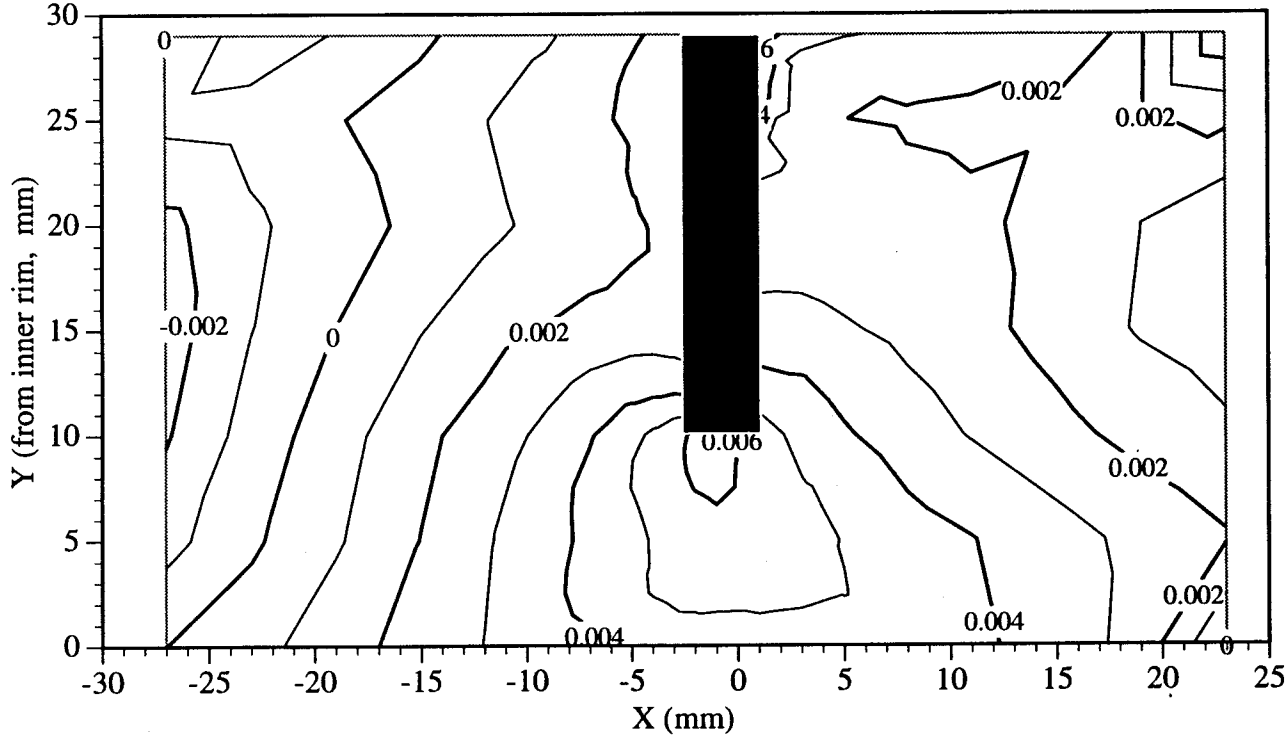

W

Railroad Car Wheel No. 6 Second Side Interferometry Results

Residual Strain (ε_x) Field After Cut No. 3 (in mm)

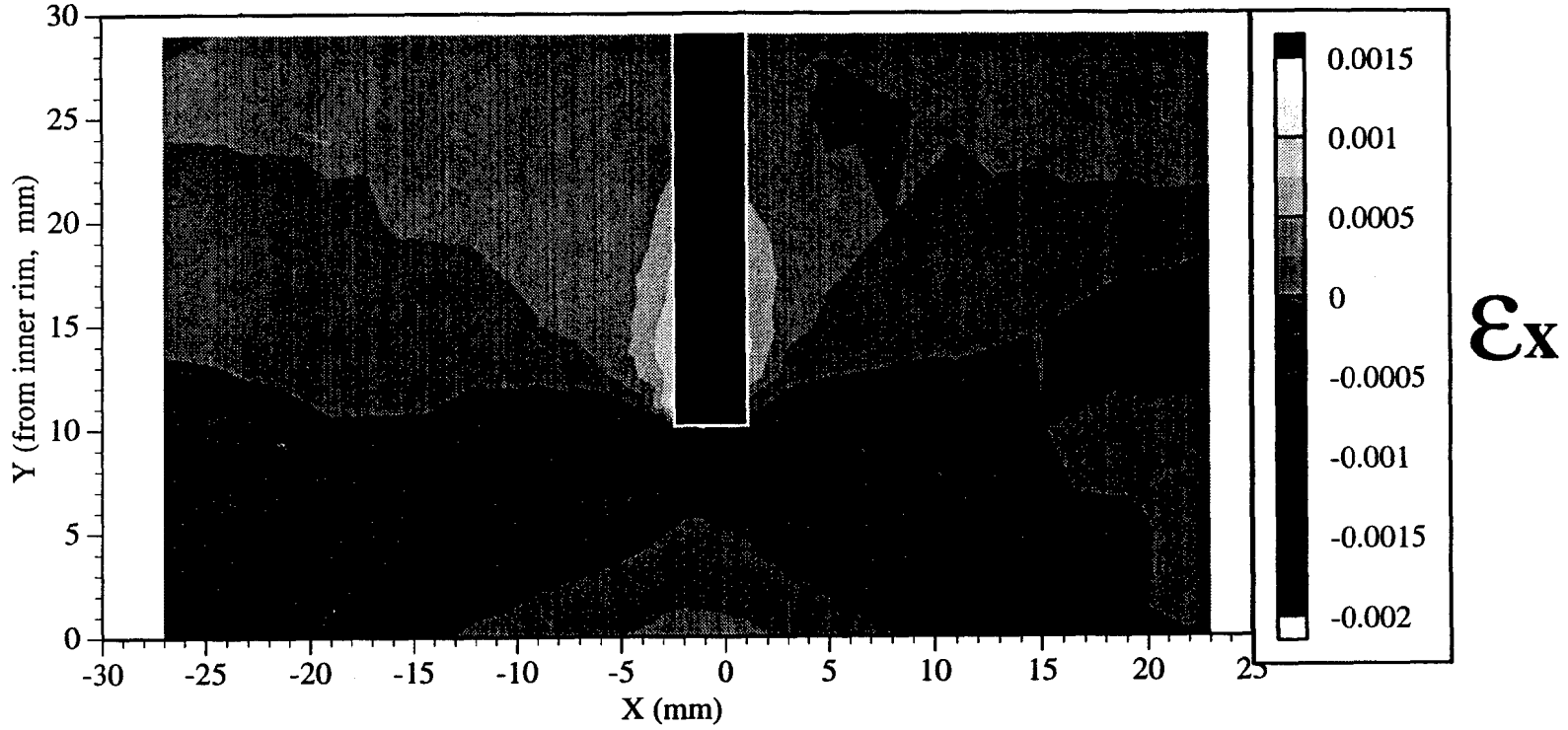

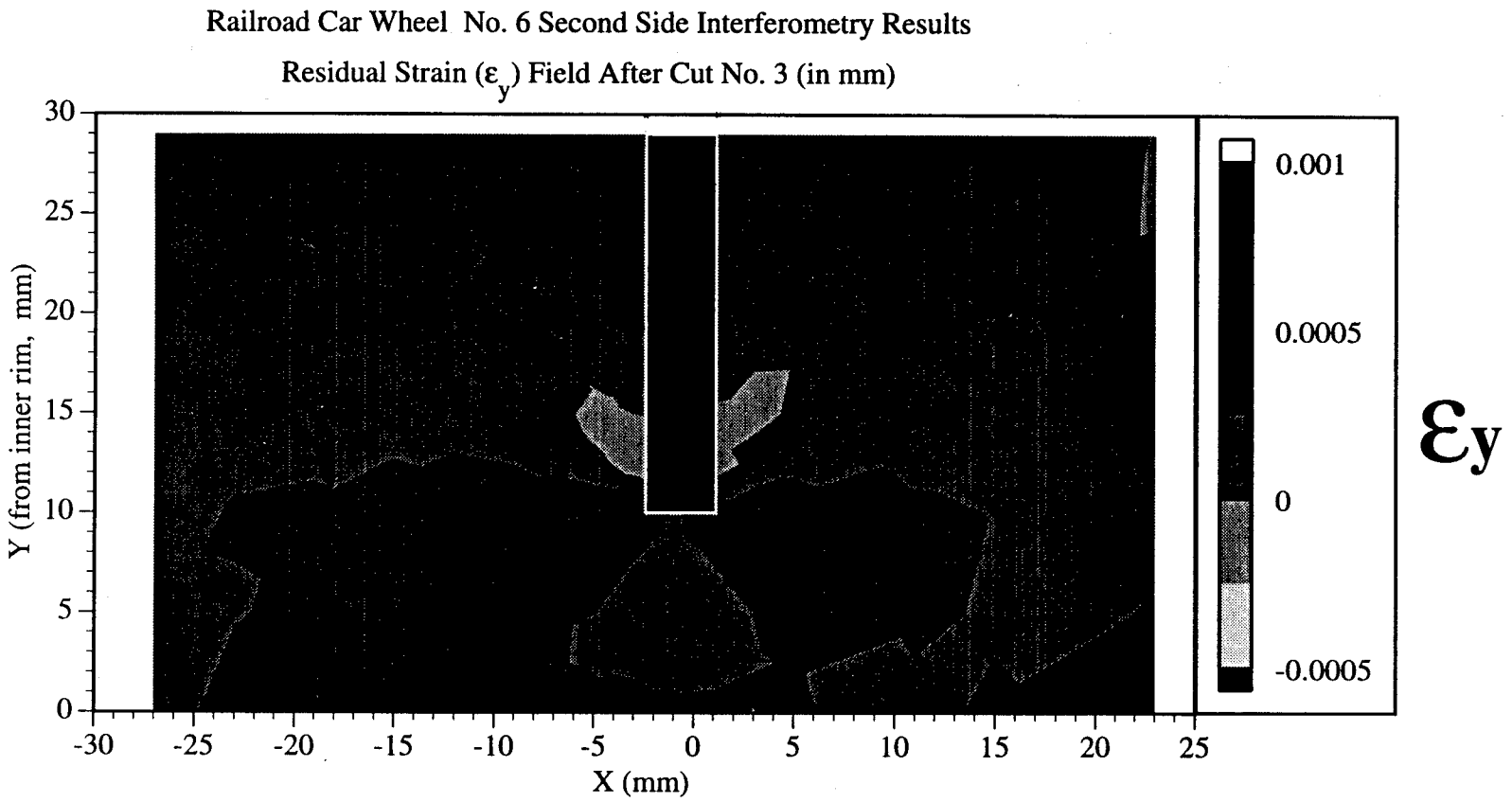
Railroad Car Wheel No. 6 Second Side Interferometry Results
Residual Strain (εy) Field After Cut No. 3 (in mm)
Y (from inner rim, mm)
X (mm)
30
25
20
15
10
5
0
-30
-25
-20
-15
-10
-5
0
5
10
15
20
25
0.001
0.0005
0
-0.0005
εy

Railroad Car Wheel No. 6 Second Side Interferometry Results

Residual Strain (γ_{xy}) Field After Cut No. 3 (in mm)

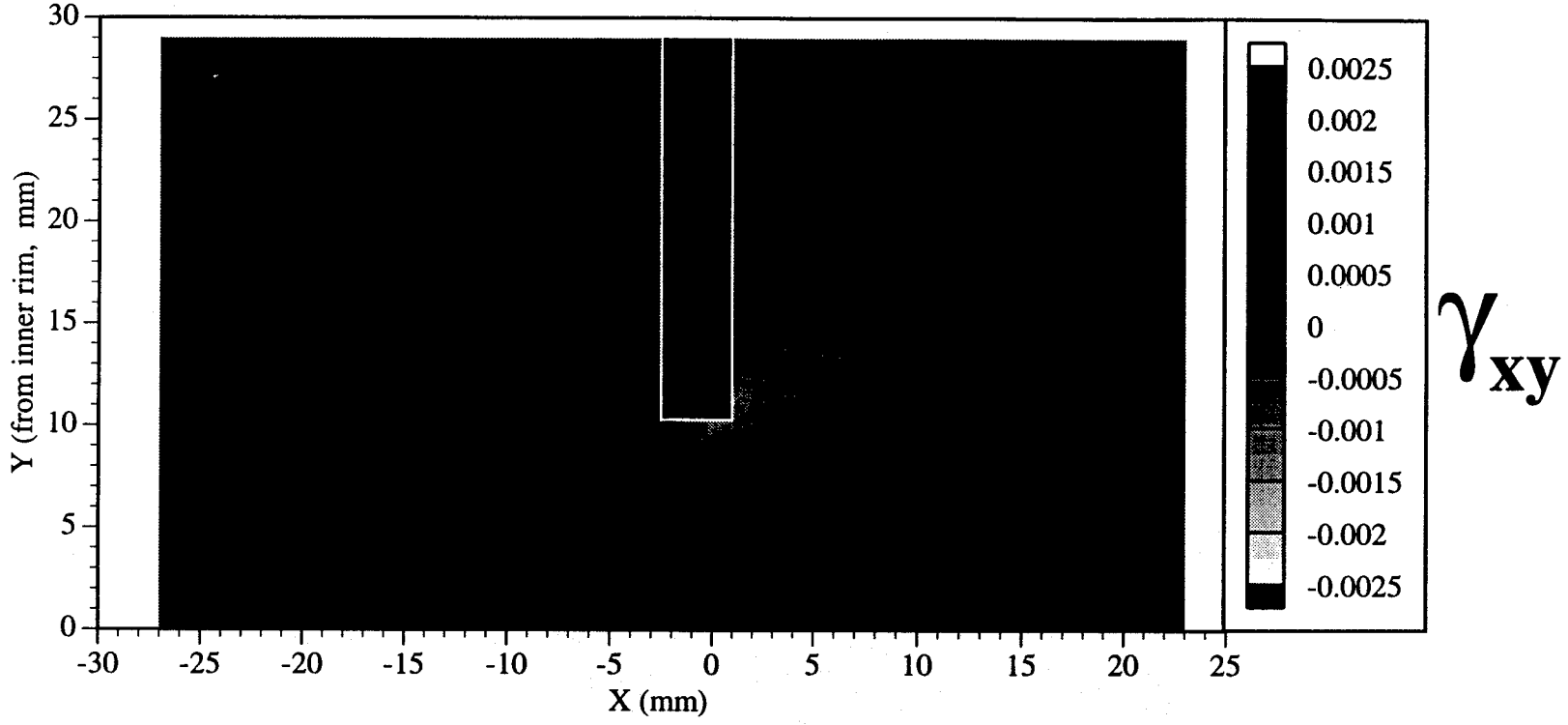

Page Intentionally Left Blank

Appendix 7. Wheel #7 Experimental Results

This appendix contains the results from the test on both sides (front and back rim faces) of the seventh wheel. All the data are in a local coordinate system that is located at the intersection of the inner edge of the rim and the cutting line; the vertical axis points away from the center of the wheel.

The attached figures show the location of all the sensors. At two points on the wheel, thermocouples (TC) measure the temperature difference (which never exceeded 5.4°C) immediately after each cut. The temperature at TC2, the one farther from the cut, was equal to the ambient temperature. The strain measurements were taken after the difference decreased to about 1°C or less at an ambient temperature in the range of 28°C to 30°C.

The extensometer, strain gage, and displacement sensor data are provided in tabular form. The interferometric data is provided in the form of contour maps and as data files in ASCII format for three specific cutting stages. The corresponding cut depths are 35 mm, 44 mm, and 60 mm.

The wheel was identified by the following markings:

26524

Location of strain gauges, thermocouples and gratings on wheel #5,6,7&8

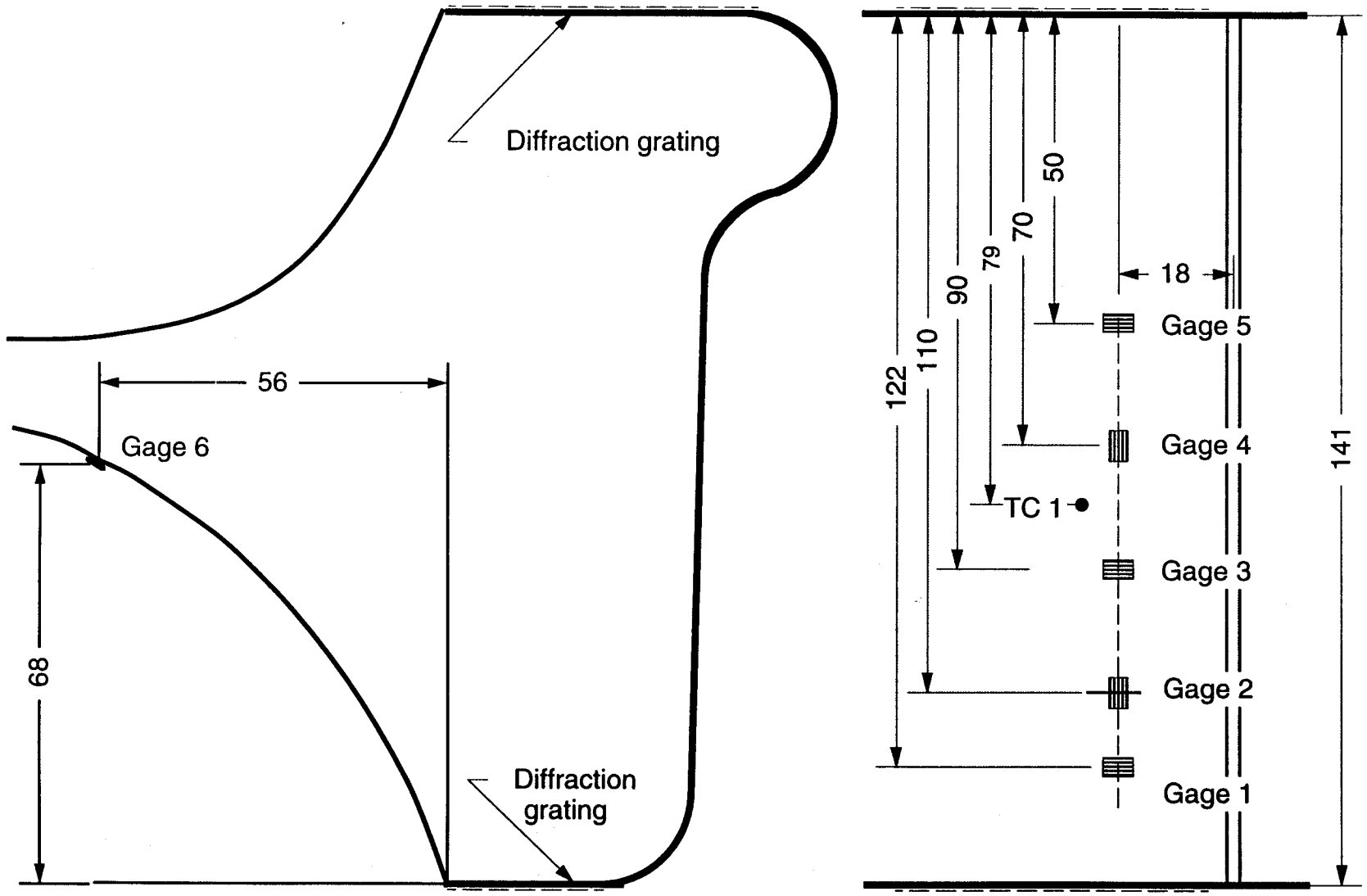

Gage 6 was located 20mm from the plane of the cut.

Location of displacement sensors thermocouples and gratings on wheel #5,6,7&8

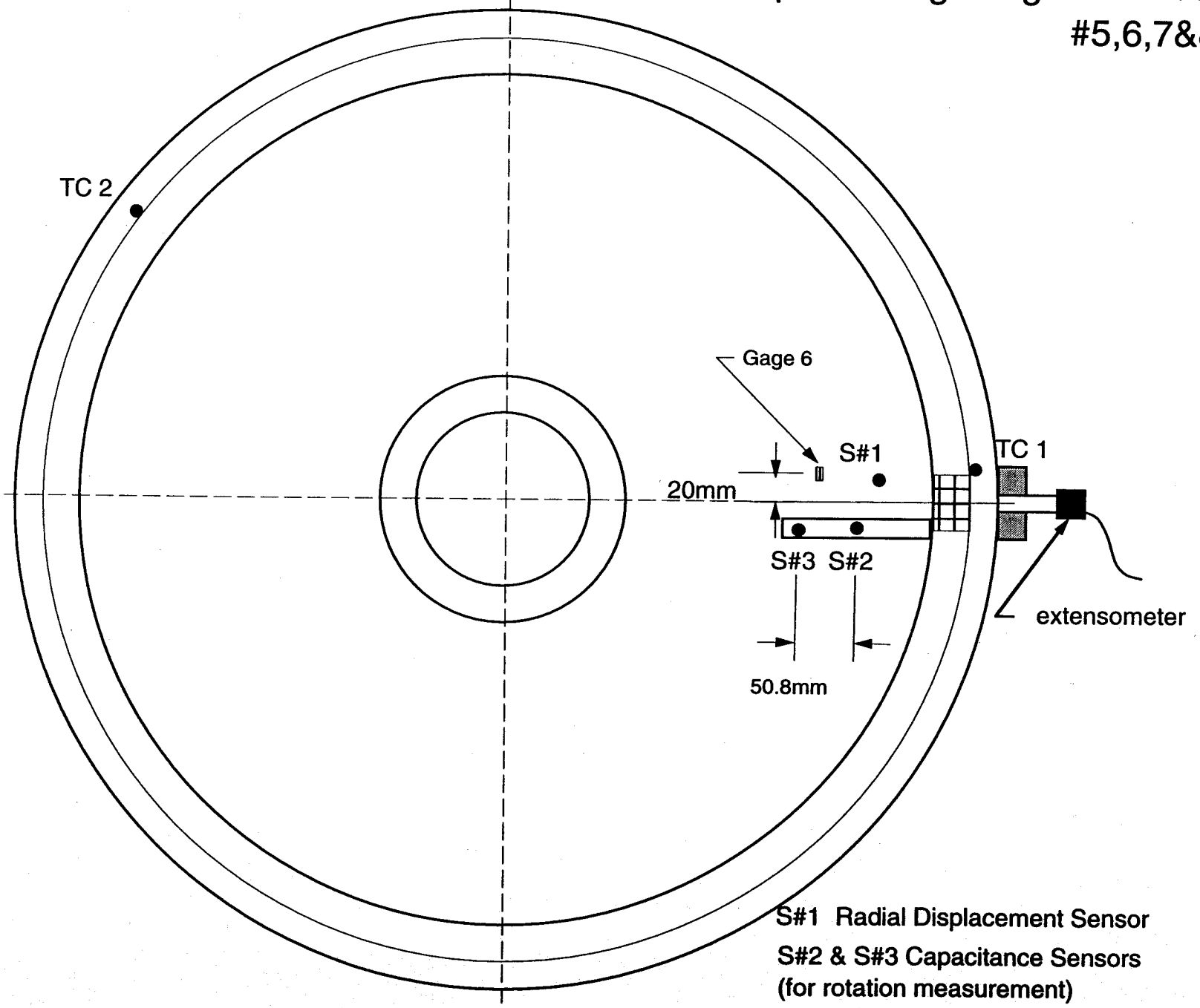

S#1 Radial Displacement Sensor
S#2 & S#3 Capacitance Sensors
(for rotation measurement)

WHEEL #7 TEST DATA

TESTING OF DOT RAILROAD CAR WHEEL #7							26524				
DATE:	August 9 1995										
	mm/mm						mm	mm	rad	(°C)	(°C)
Cut Depth (mm)	Gage1	Gage2	Gage3	Gage4	Gage5	Gage6	Radial Displacement	Opening Displacement	Rotation	TC 1	TC 2
0	0	0	0	0	0	0	0.000	0.000	0.00E+00	29.2	29.2
28	19	-11	48	-37	39	-44	0.037	0.133	-1.18E-04	32.2	29.2
35	13	-19	79	-40	-180	-68	0.045	0.172	-5.91E-05	34.8	29.4
44	-11	-16	-164	-34	-440	-104	0.061	0.226	3.94E-05	30.3	26.9
54	-27	-2	-318	-19	-593	-153	0.082	0.291	2.36E-04	33.1	30.1
60	-31	7	-356	-5	-634	-188	0.096	0.329	3.35E-04	33.9	30.2
70	-35	24	-384	24	-665	-260	0.125	0.419	6.50E-04	30.1	28.2
80	-61	39	-389	57	-660	-406	0.169	0.551	8.27E-04	31.0	28.3
90	-81	62	-386	81	-640	-560	0.244	0.726	-3.94E-04	31.5	28.4
100	-89	86	-388	88	-624	-576	0.309	0.892	2.17E-03	31.6	28.4
110	-90	98	-387	90	-616	-367	0.358	1.015	1.81E-03	31.7	28.5
120	-89	102	-385	89	-611	41	0.402	1.112	2.11E-03	31.7	28.6
130	-88	102	-382	87	-607	295	0.447	1.192	2.91E-03	31.5	28.7
140	-87	100	-380	84	-606	301	0.488	1.264	4.04E-03	31.6	28.8
150	-84	100	-378	82	-603	298	0.530	1.332	5.04E-03	31.5	28.7
160	-83	98	-376	80	-602	298	0.576	1.399	5.98E-03	31.6	28.8
170	-82	97	-375	80	-601	297	0.629	1.467	6.81E-03	31.5	28.8
180	-81	97	-374	78	-600	297	0.672	1.538	7.70E-03	31.5	28.8
190	-80	97	-373	76	-602	295	0.718	1.615	8.64E-03	31.4	28.9
200	-81	96	-372	76	-599	294	0.750	1.679	9.31E-03	31.4	29.0
END											

Railroad Wheel No. 7 Test
Displacement vs. Cut Depth

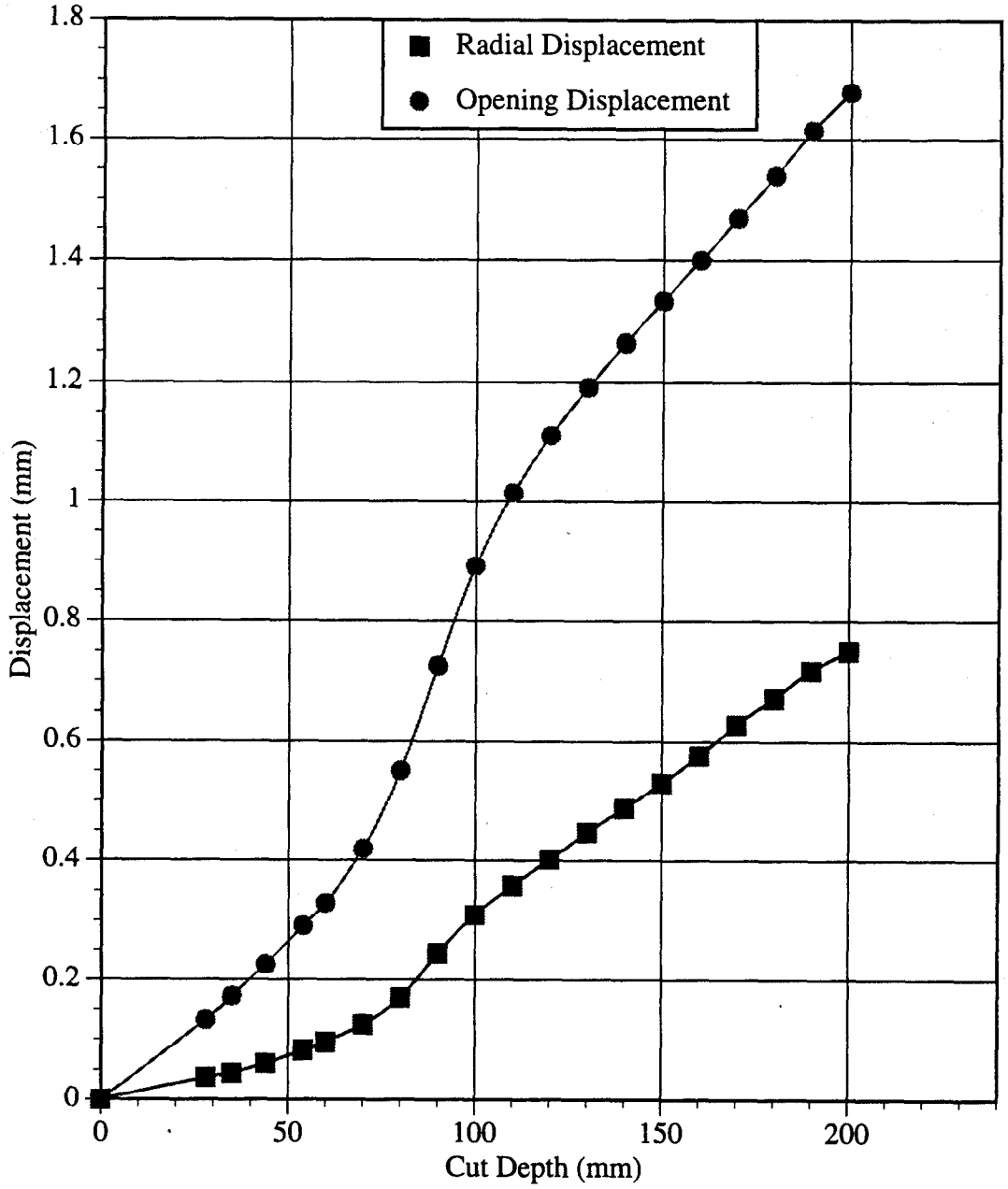

Railroad Wheel No. 7 Test
Strain Gage Readings vs. Cut Depth

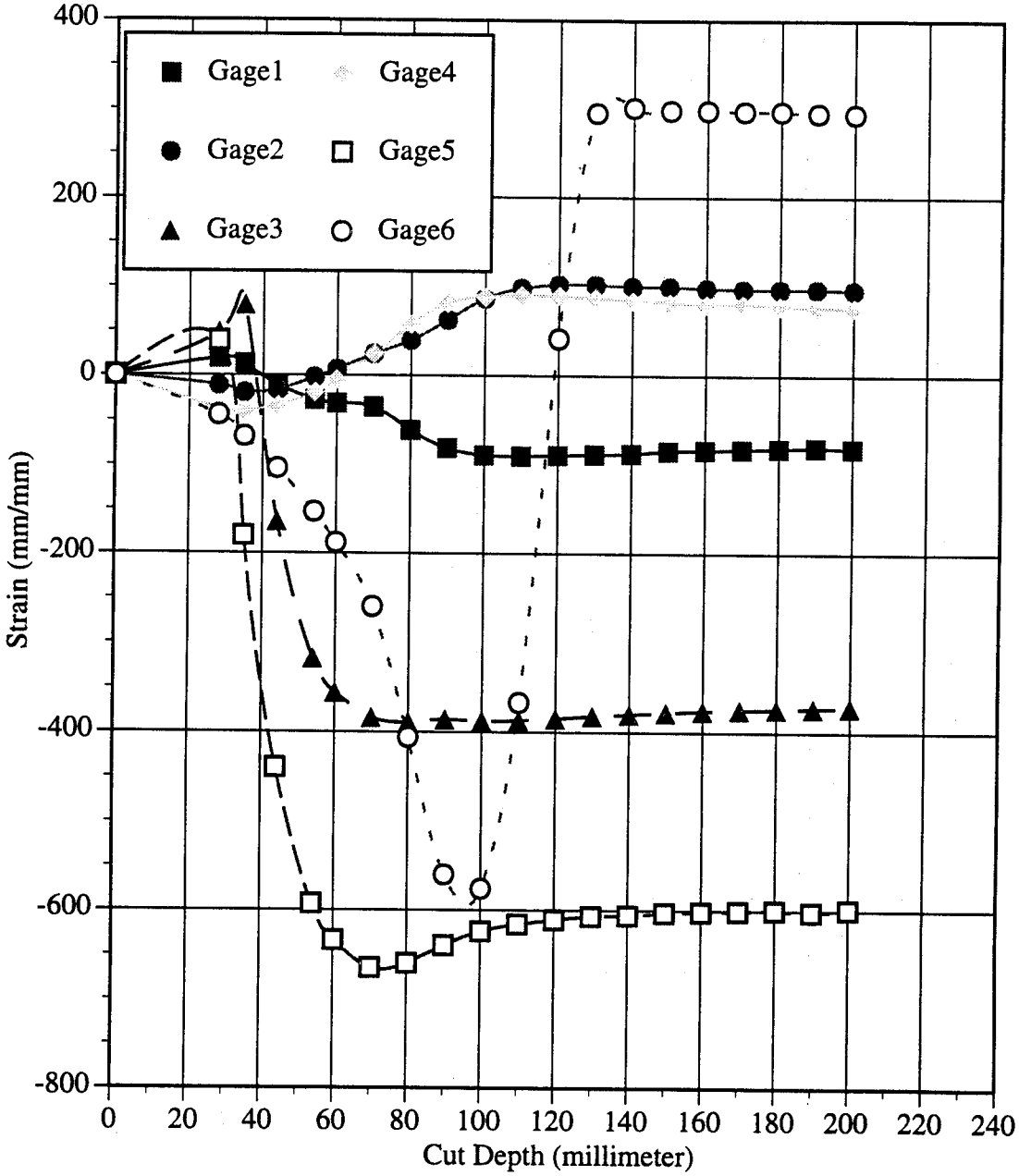

Railroad Wheel No. 7 Test
Wheel Rotation vs. Cut Depth

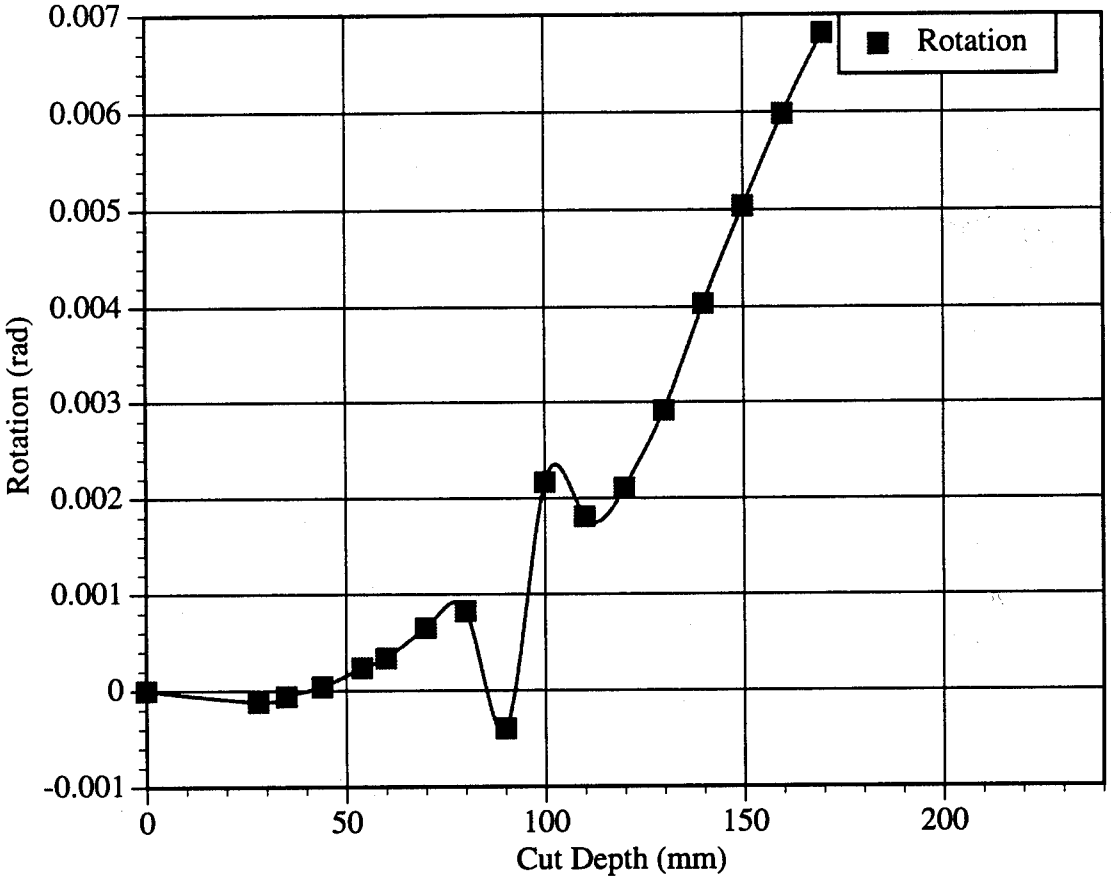

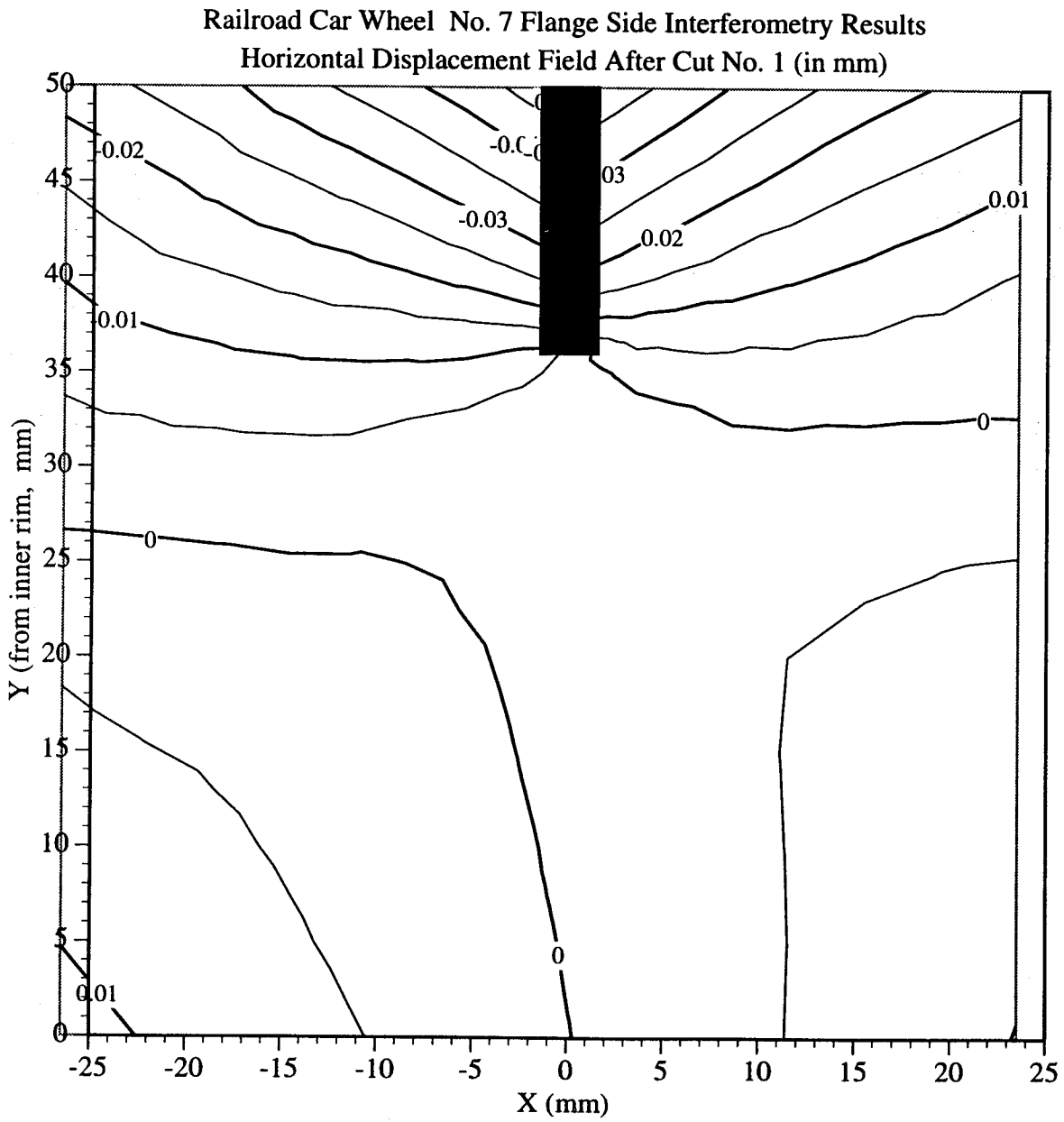
Railroad Car Wheel No. 7 Flange Side Interferometry Results
Horizontal Displacement Field After Cut No. 1 (in mm)
Y (from inner rim, mm)
X (mm)
50
45
40
35
30
25
20
15
10
5
0
-25
-20
-15
-10
-5
0
5
10
15
20
25
-0.02
-0.03
0.02
0.01
0
0.01

Railroad Car Wheel No. 7 Flange Side Interferometry Results
Vertical Displacement Field After Cut No. 1 (in mm)

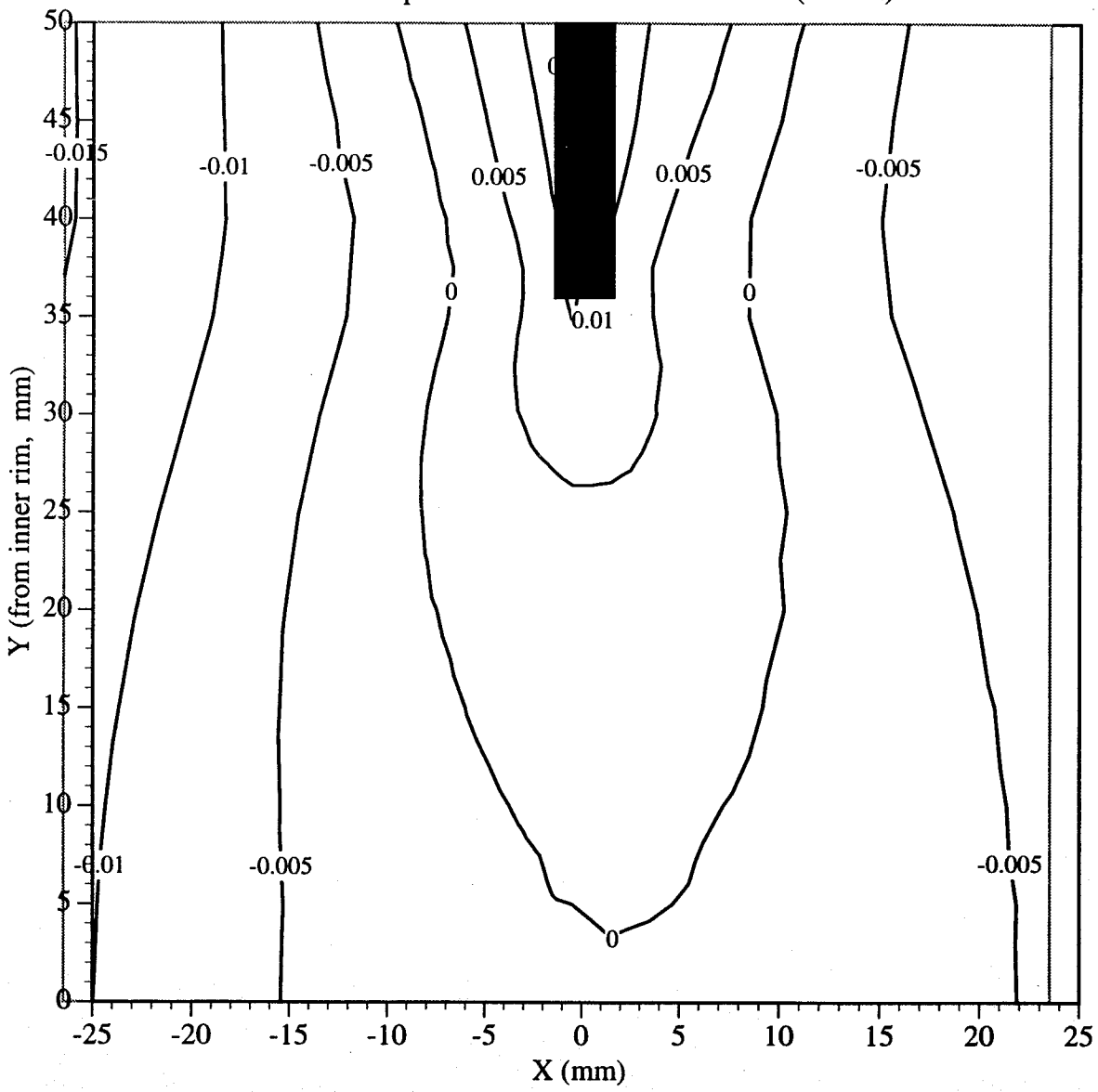

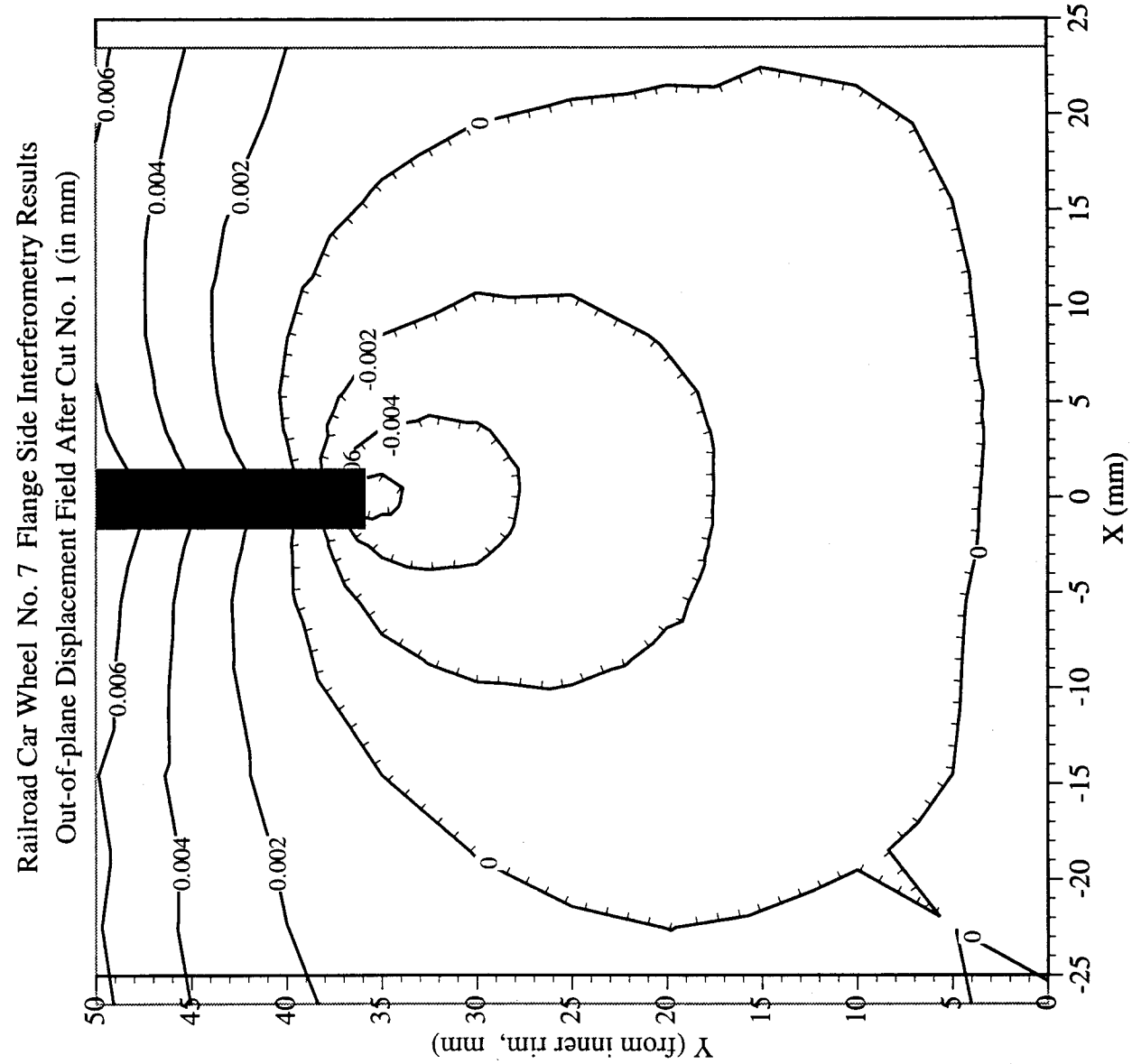
Railroad Car Wheel No. 7 Flange Side Interferometry Results
Out-of-plane Displacement Field After Cut No. 1 (in mm)
Y (from inner rim, mm)
X (mm)
0.006
0.004
0.002
0
-0.002
-0.004
50
45
40
35
30
25
20
15
10
5
0
-25
-20
-15
-10
-5
0
5
10
15
20
25

Railroad Car Wheel No. 7 Flange Side Interferometry Results

Residual Strain (ε_x) Field After Cut No. 1 (in mm)

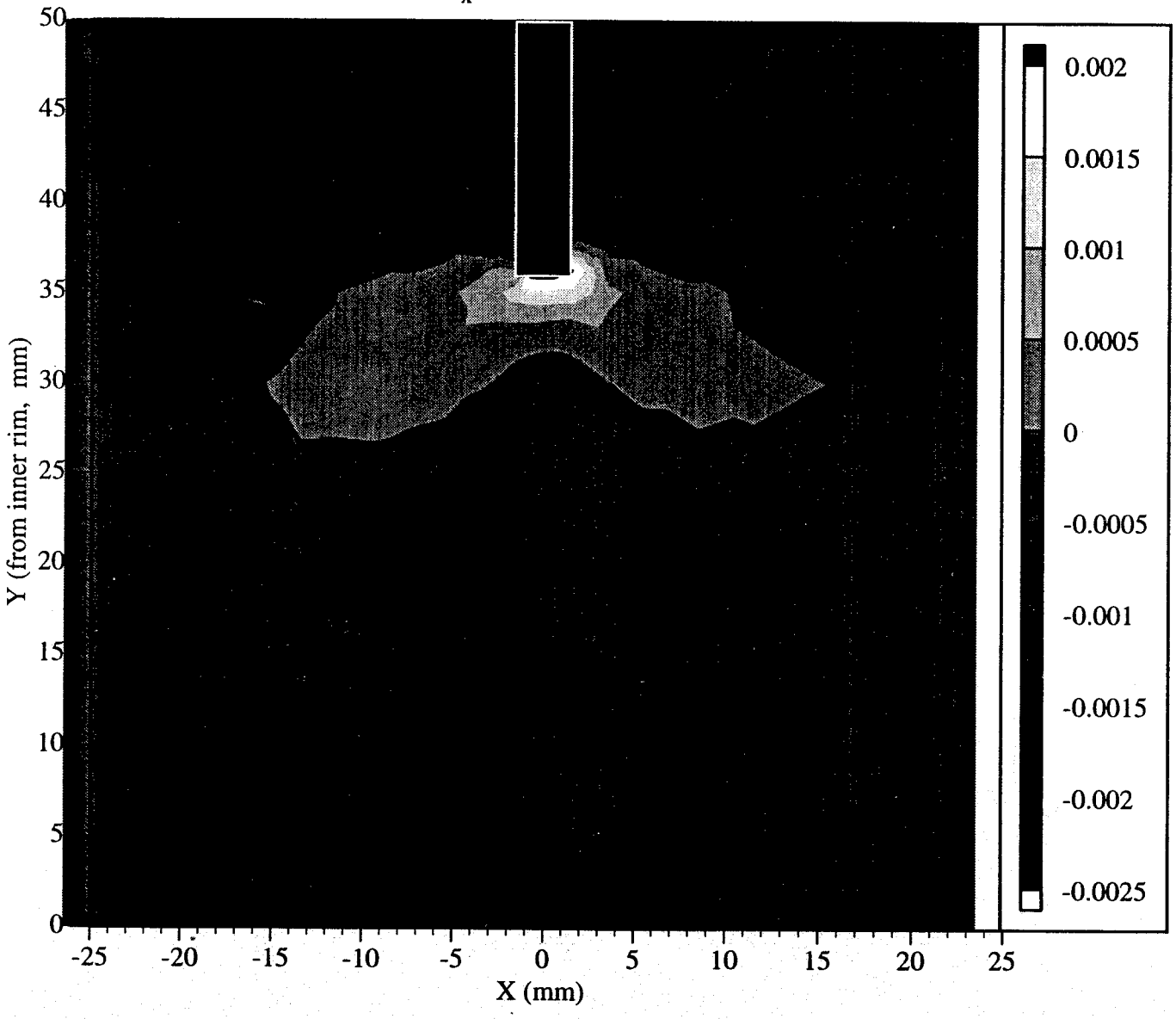

Railroad Car Wheel No. 7 Flange Side Interferometry Results

Residual Strain (ε_y) Field After Cut No. 1 (in mm)

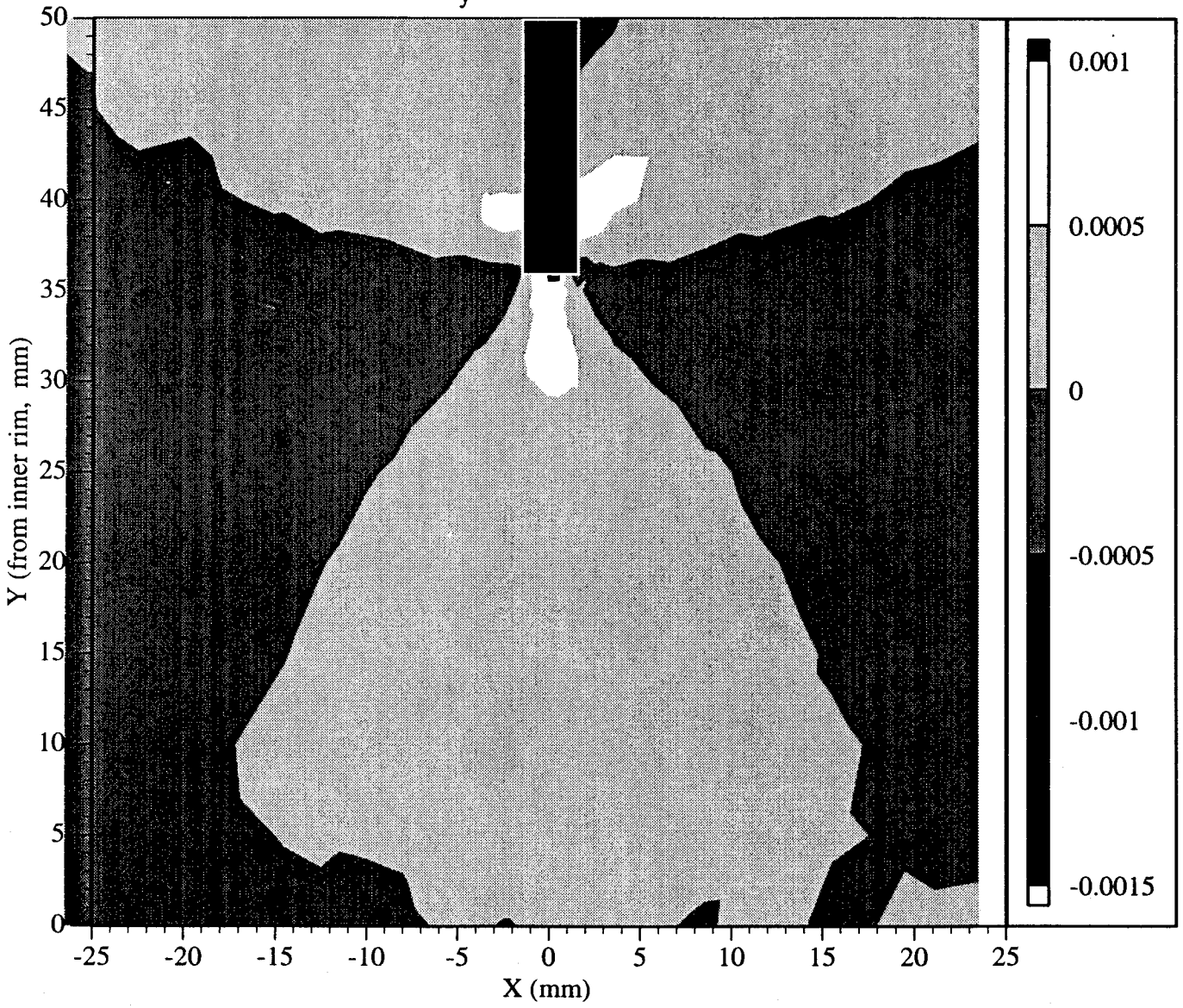

Railroad Car Wheel No. 7 Flange Side Interferometry Results

Residual Strain (γ_{xy}) Field After Cut No. 1 (in mm)

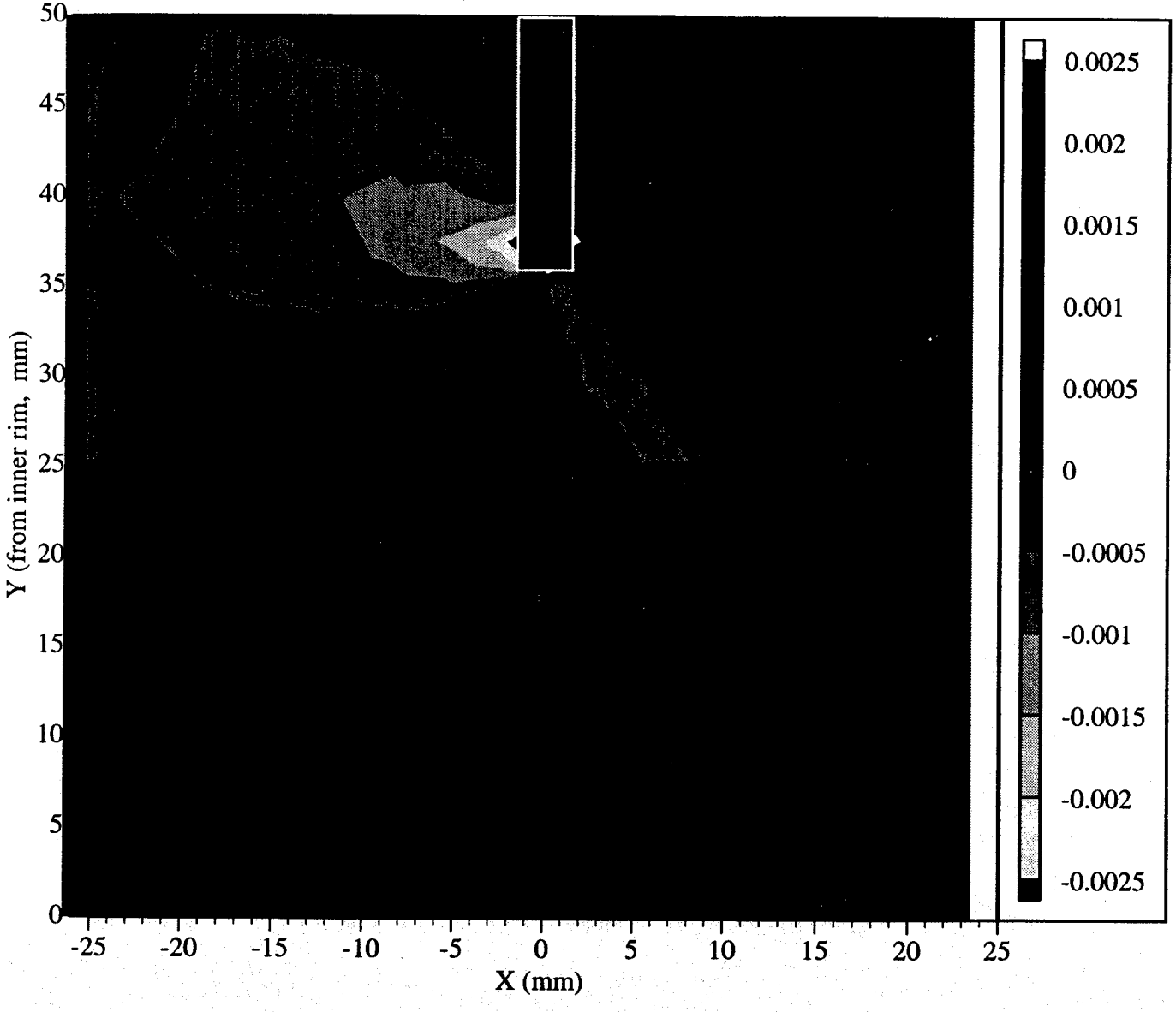

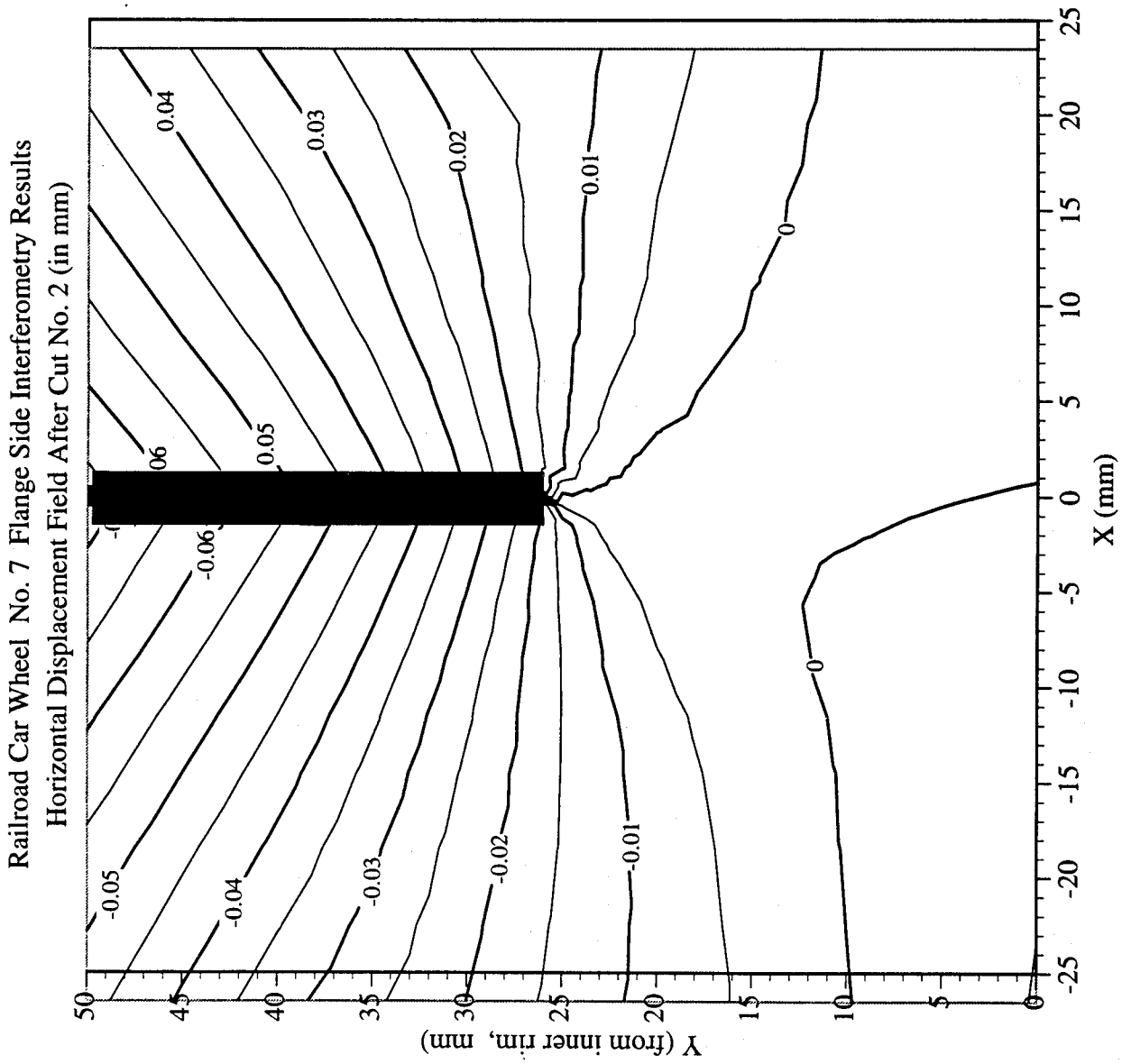
Railroad Car Wheel No. 7 Flange Side Interferometry Results
Horizontal Displacement Field After Cut No. 2 (in mm)
Y (from inner rim, mm)
X (mm)
0.04
0.03
0.02
0.01
0
-0.01
-0.02
-0.03
-0.04
-0.05
-0.06
0.05
50
45
40
35
30
25
20
15
10
5
0
-25
-20
-15
-10
-5
0
5
10
15
20
25

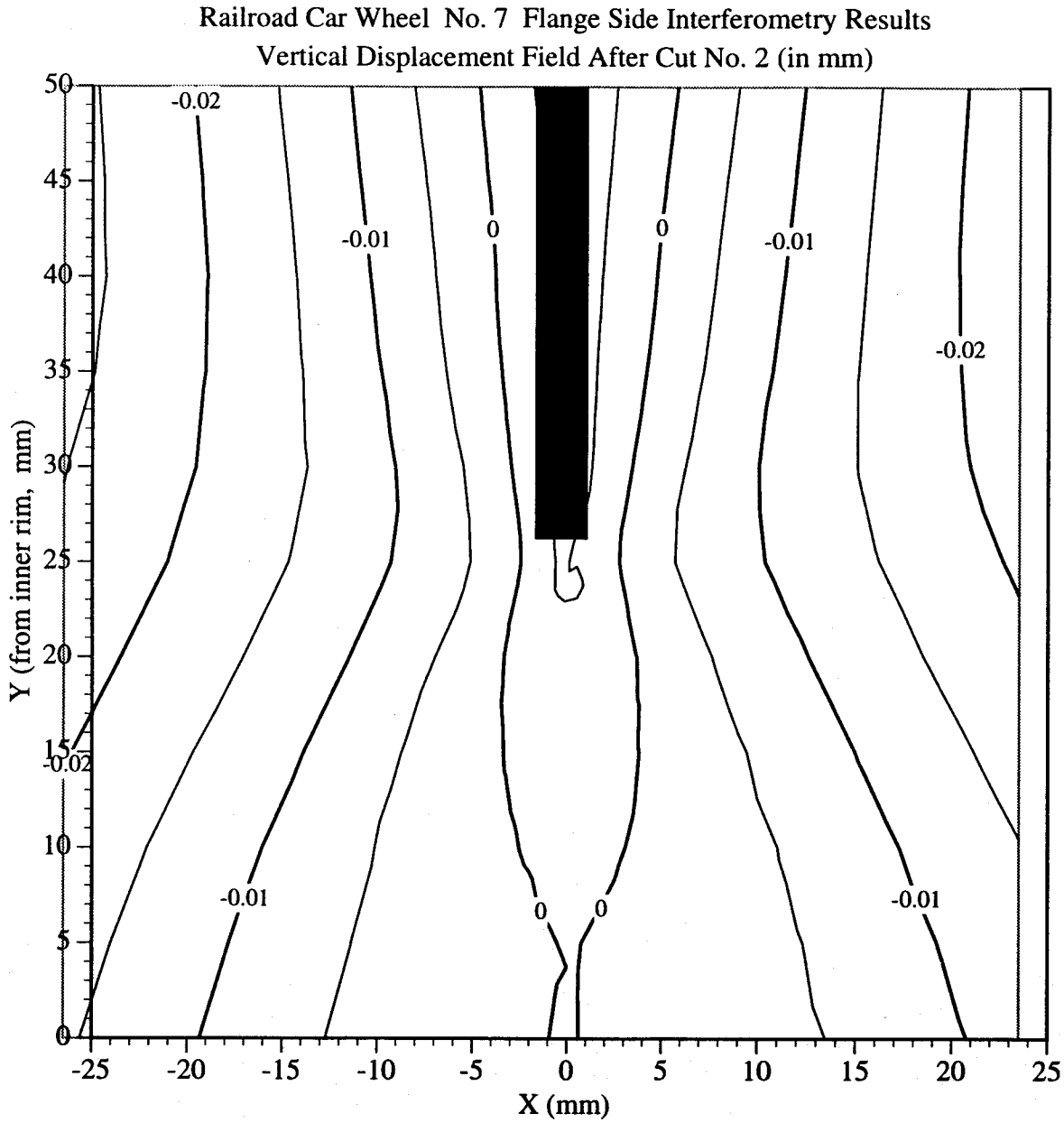
Railroad Car Wheel No. 7 Flange Side Interferometry Results
Vertical Displacement Field After Cut No. 2 (in mm)
Y (from inner rim, mm)
X (mm)
-0.02
-0.01
0
0
-0.01
-0.02
-0.02
-0.01
0
0
-0.01
50
45
40
35
30
25
20
15
10
5
0
-25
-20
-15
-10
-5
0
5
10
15
20
25

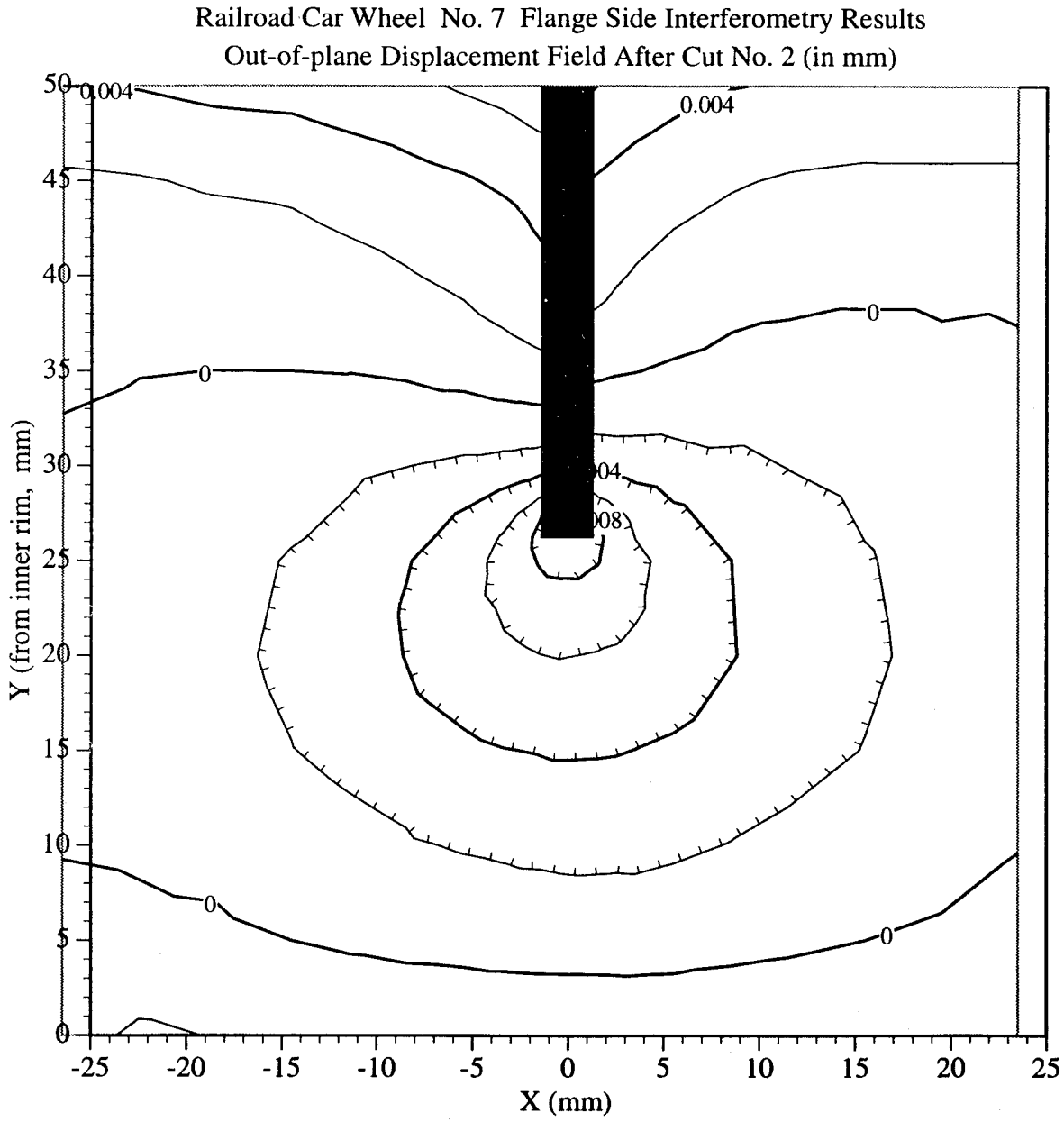
Railroad Car Wheel No. 7 Flange Side Interferometry Results
Out-of-plane Displacement Field After Cut No. 2 (in mm)
0.004
0.004
0
0
0
0
0
Y (from inner rim, mm)
X (mm)
50
45
40
35
30
25
20
15
10
5
0
-25
-20
-15
-10
-5
0
5
10
15
20
25

Railroad Car Wheel No. 7 Flange Side Interferometry Results

Residual Strain (ε_x) Field After Cut No. 2 (in mm)

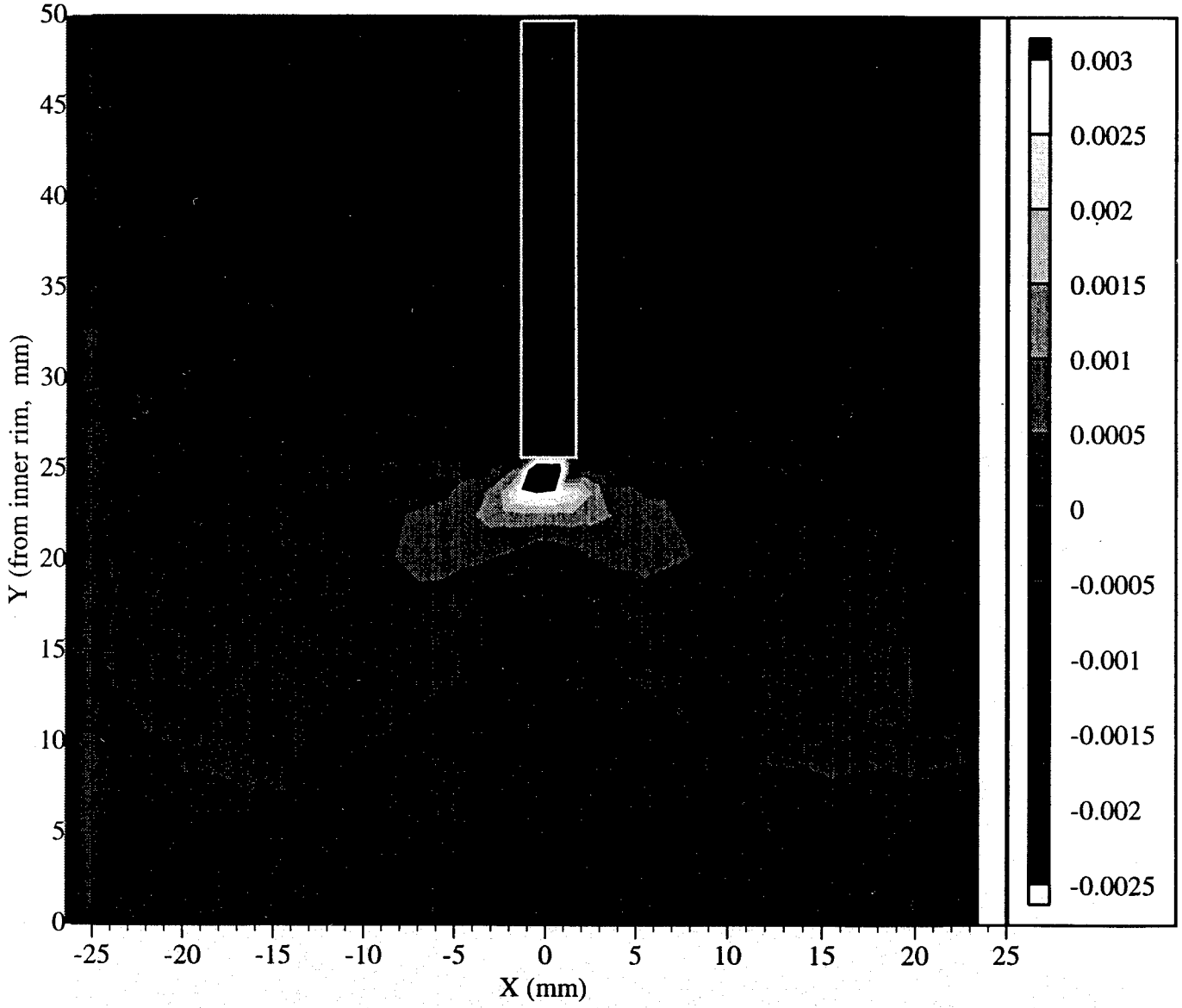

Railroad Car Wheel No. 7 Flange Side Interferometry Results

Residual Strain (ε_y) Field After Cut No. 2 (in mm)

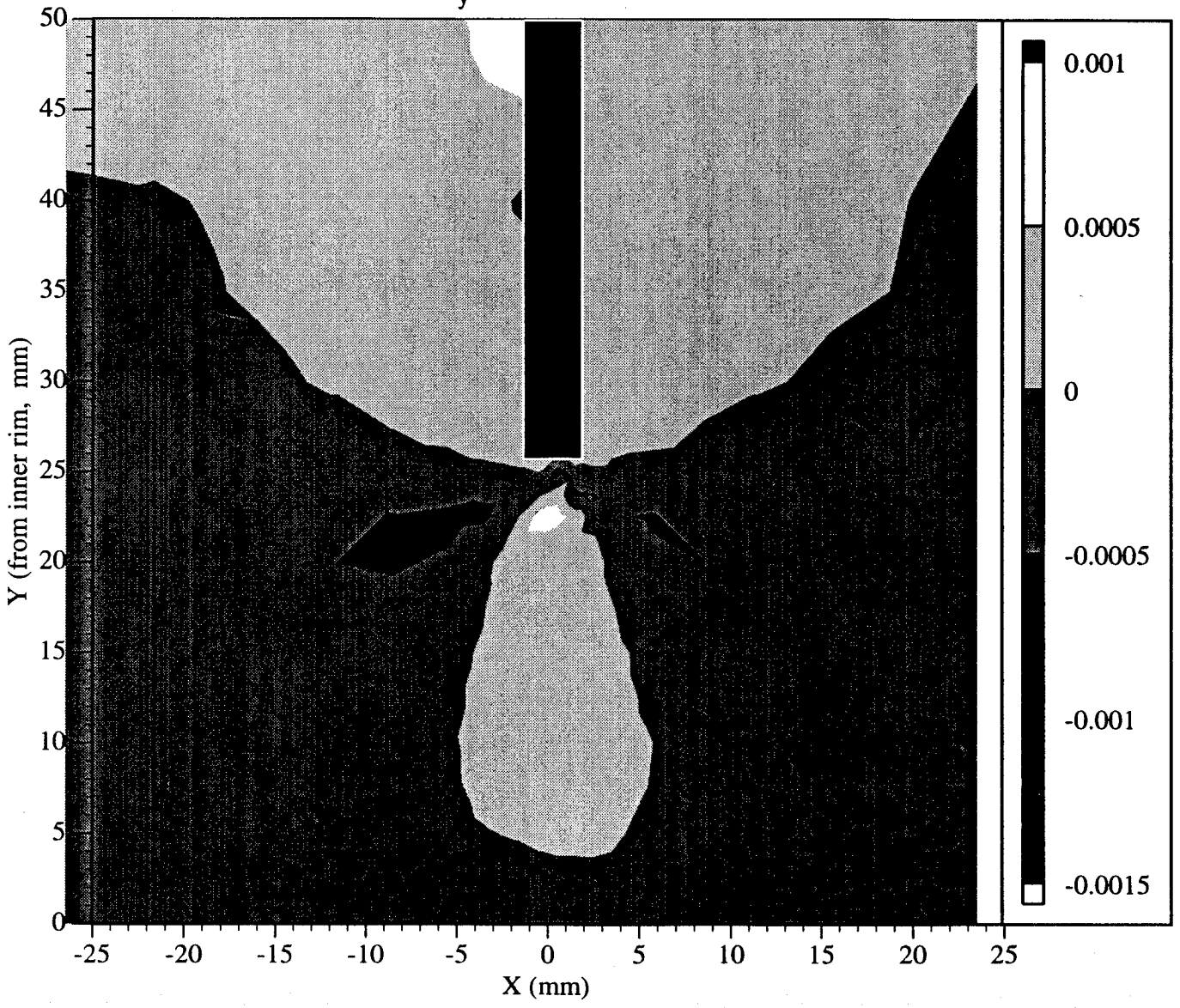

Railroad Car Wheel No. 7 Flange Side Interferometry Results

Residual Strain (γ_{xy}) Field After Cut No. 2 (in mm)

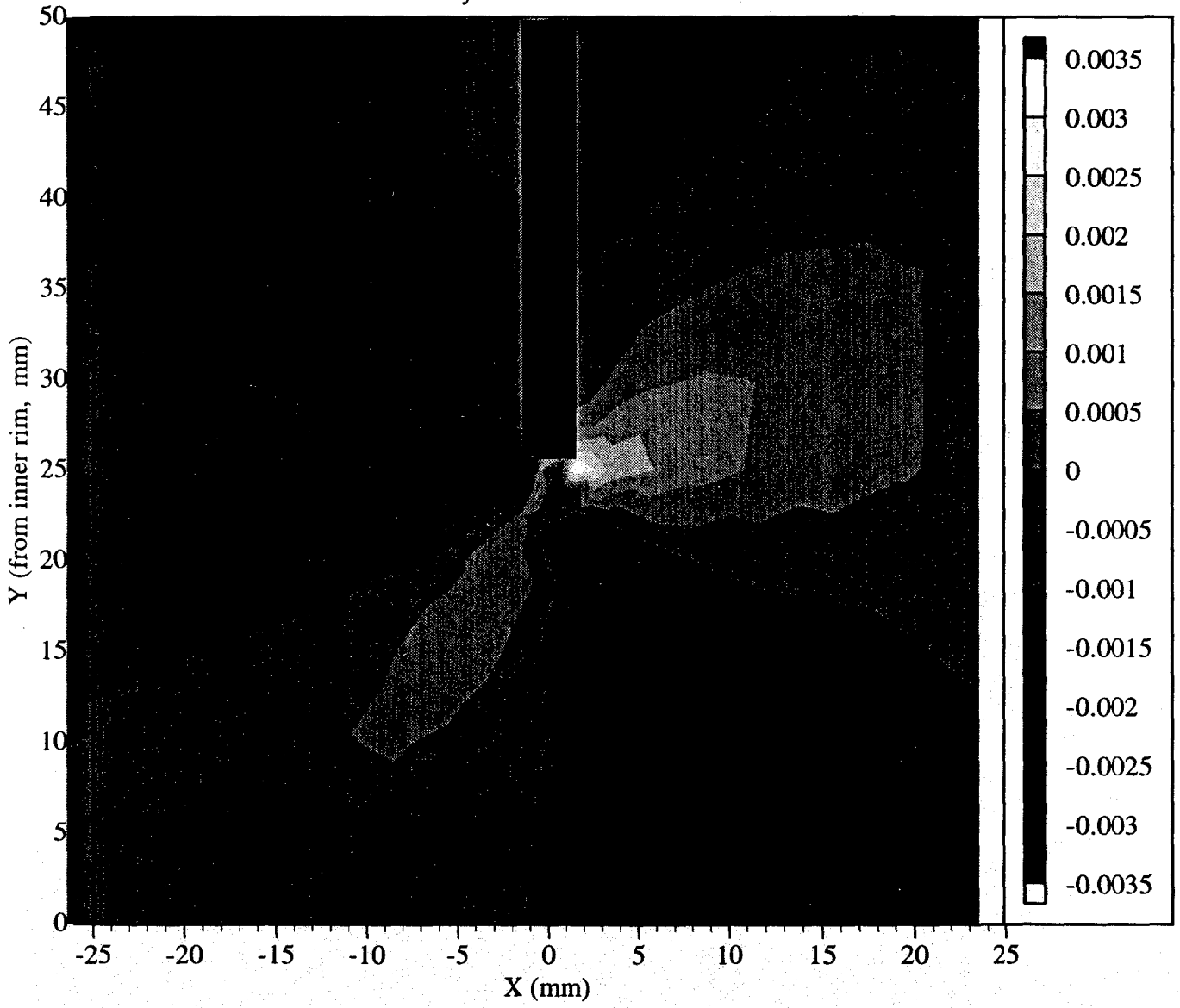

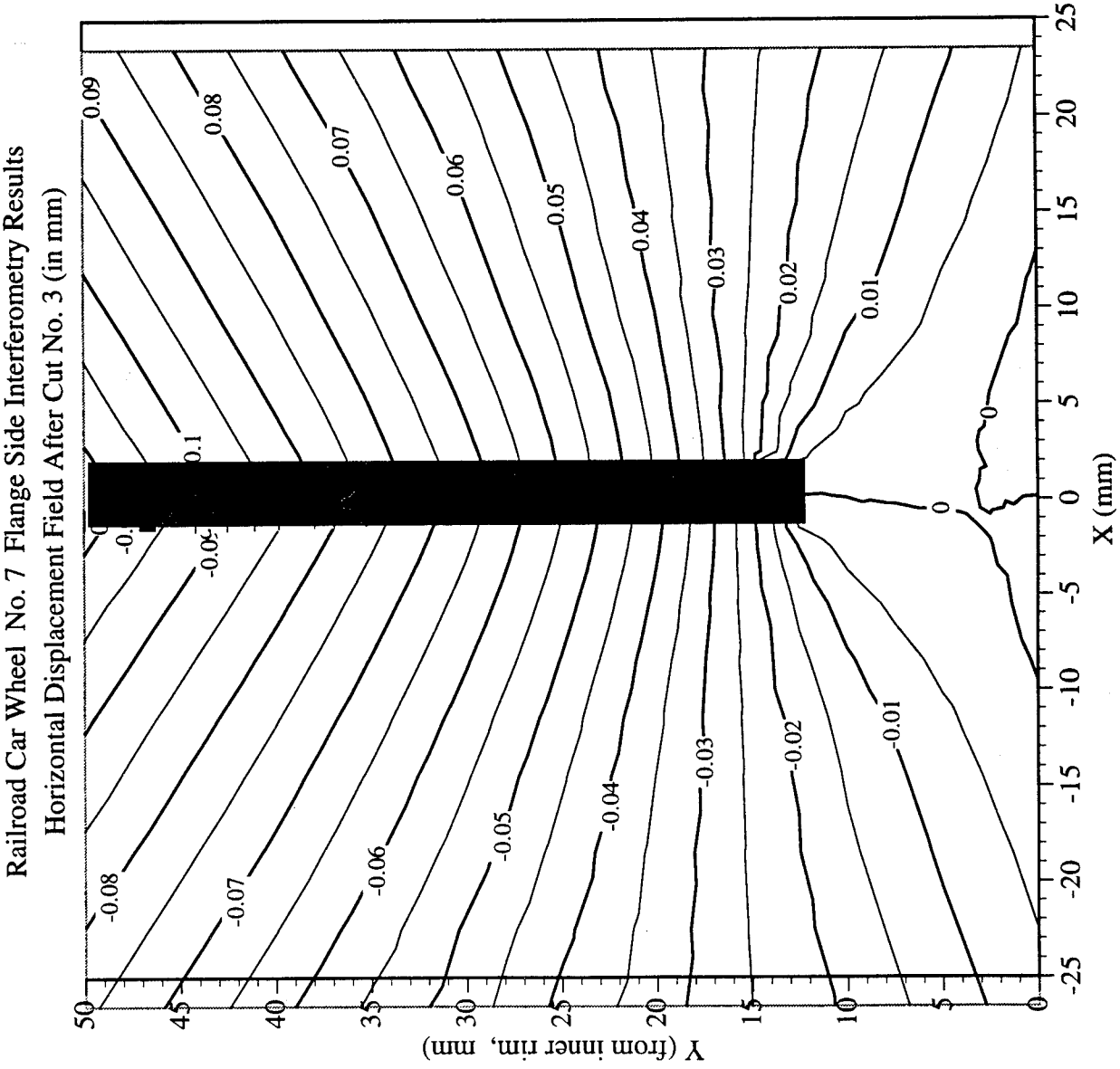
Railroad Car Wheel No. 7 Flange Side Interferometry Results
Horizontal Displacement Field After Cut No. 3 (in mm)
Y (from inner rim, mm)
X (mm)
0.09
0.08
0.07
0.06
0.05
0.04
0.03
0.02
0.01
0
-0.01
-0.02
-0.03
-0.04
-0.05
-0.06
-0.07
-0.08

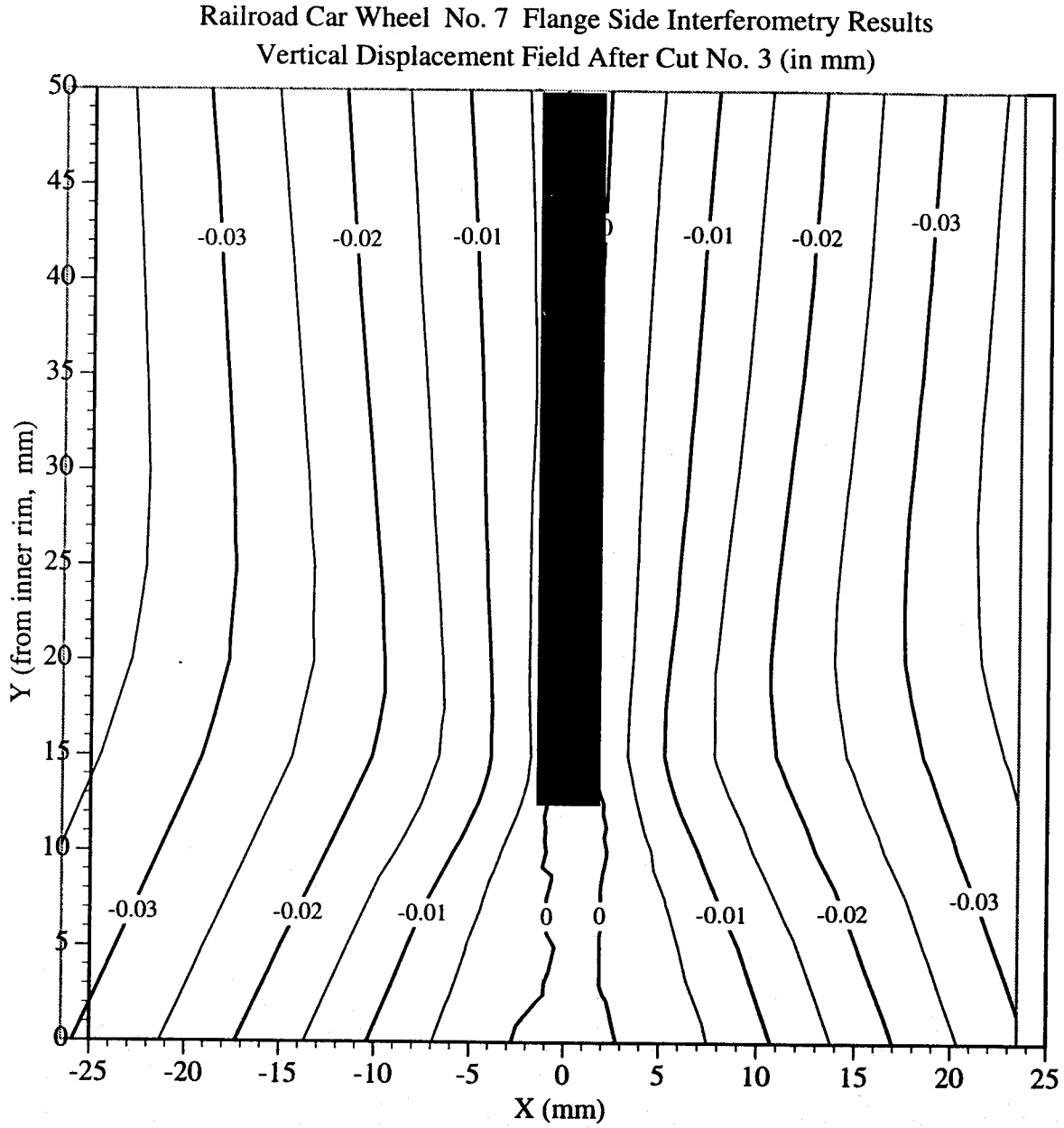
Railroad Car Wheel No. 7 Flange Side Interferometry Results
Vertical Displacement Field After Cut No. 3 (in mm)
Y (from inner rim, mm)
X (mm)
-0.03
-0.02
-0.01
0
-0.01
-0.02
-0.03

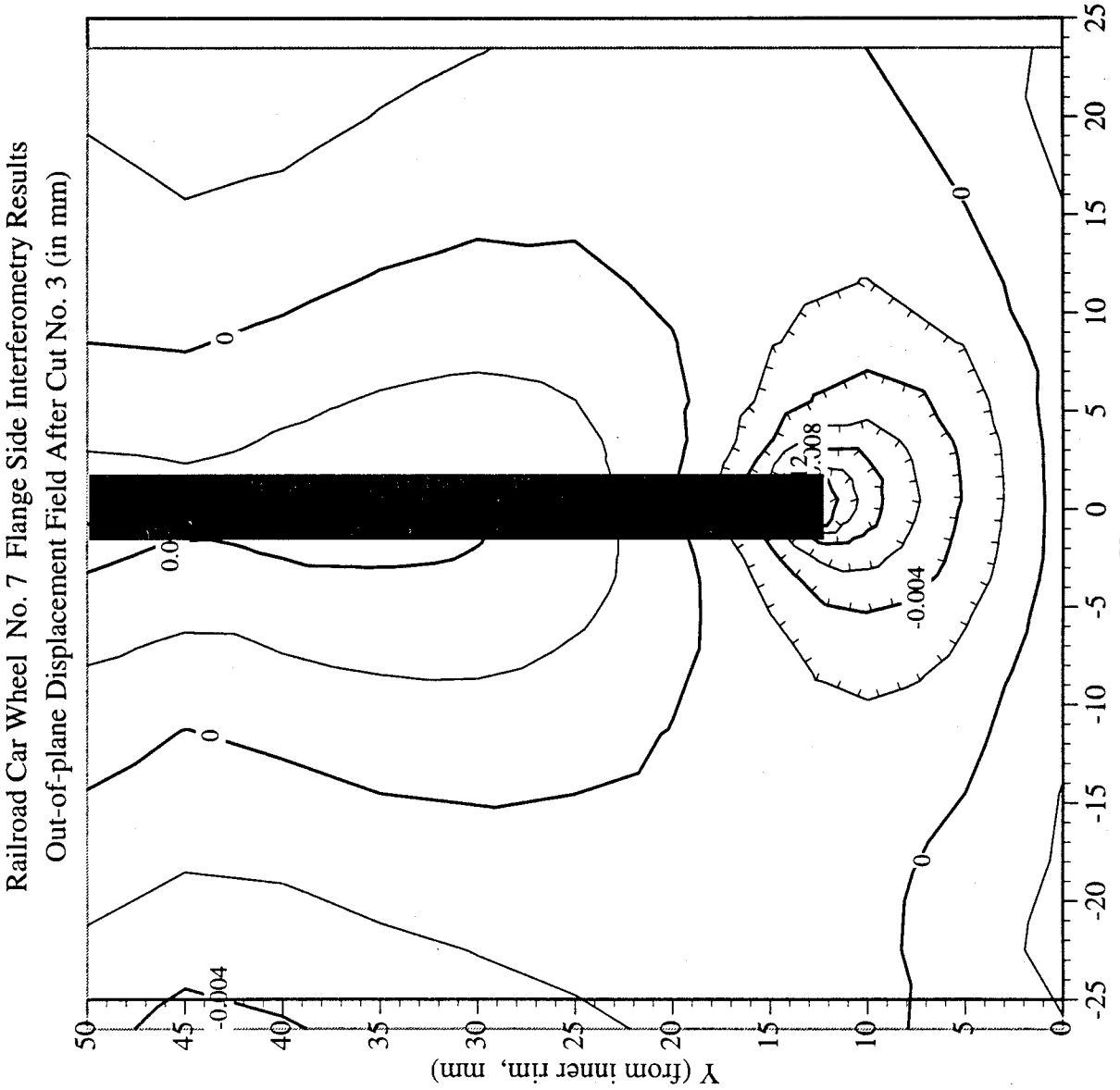
Railroad Car Wheel No. 7 Flange Side Interferometry Results
Out-of-plane Displacement Field After Cut No. 3 (in mm)
Y (from inner rim, mm)
X (mm)
0.0
0
-0.004
-0.008

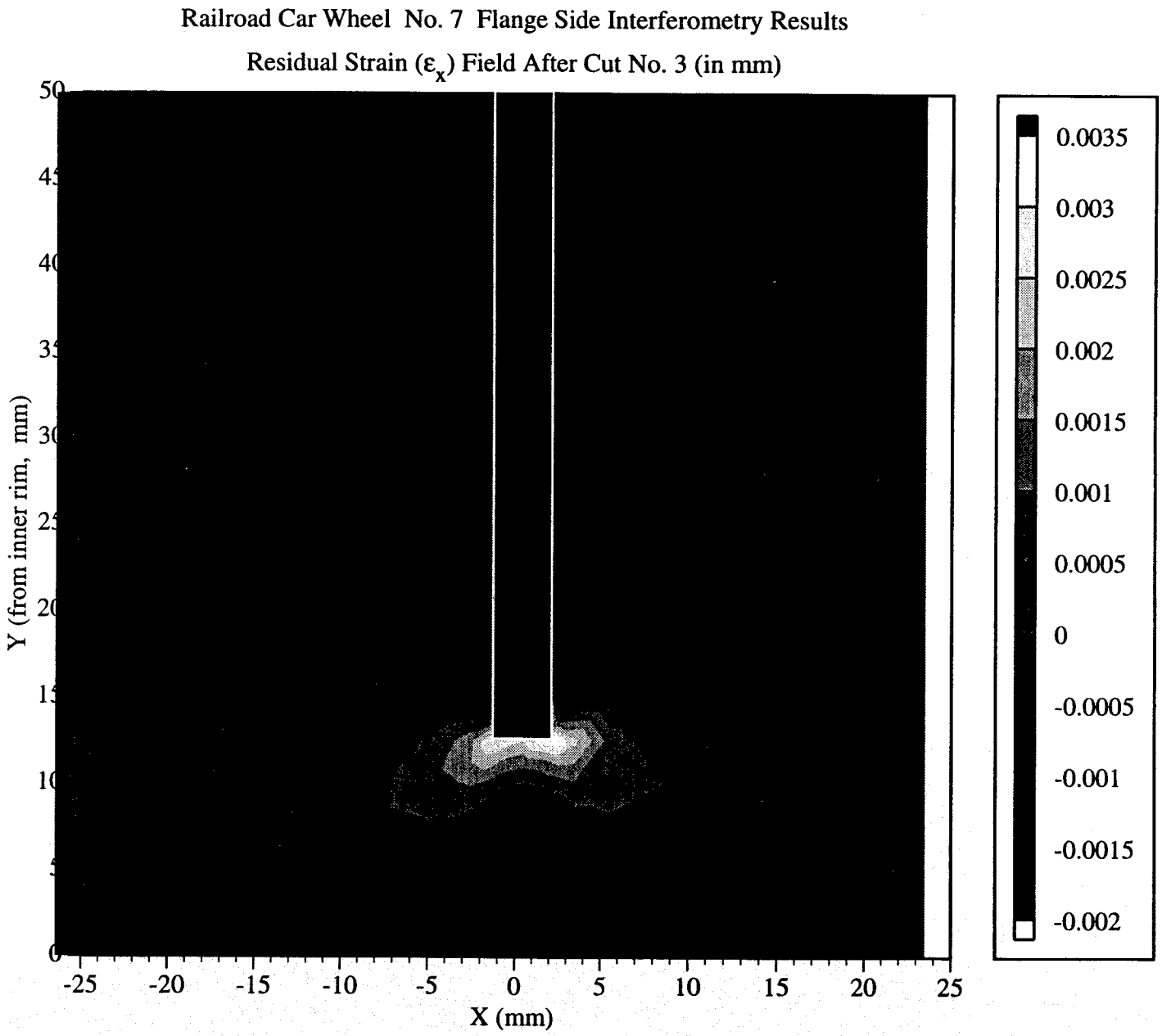
Railroad Car Wheel No. 7 Flange Side Interferometry Results
Residual Strain (ε_x) Field After Cut No. 3 (in mm)
Y (from inner rim, mm)
X (mm)
-25
-20
-15
-10
-5
0
5
10
15
20
25
0.0035
0.003
0.0025
0.002
0.0015
0.001
0.0005
0
-0.0005
-0.001
-0.0015
-0.002

Railroad Car Wheel No. 7 Flange Side Interferometry Results

Residual Strain (ε_y) Field After Cut No. 3 (in mm)

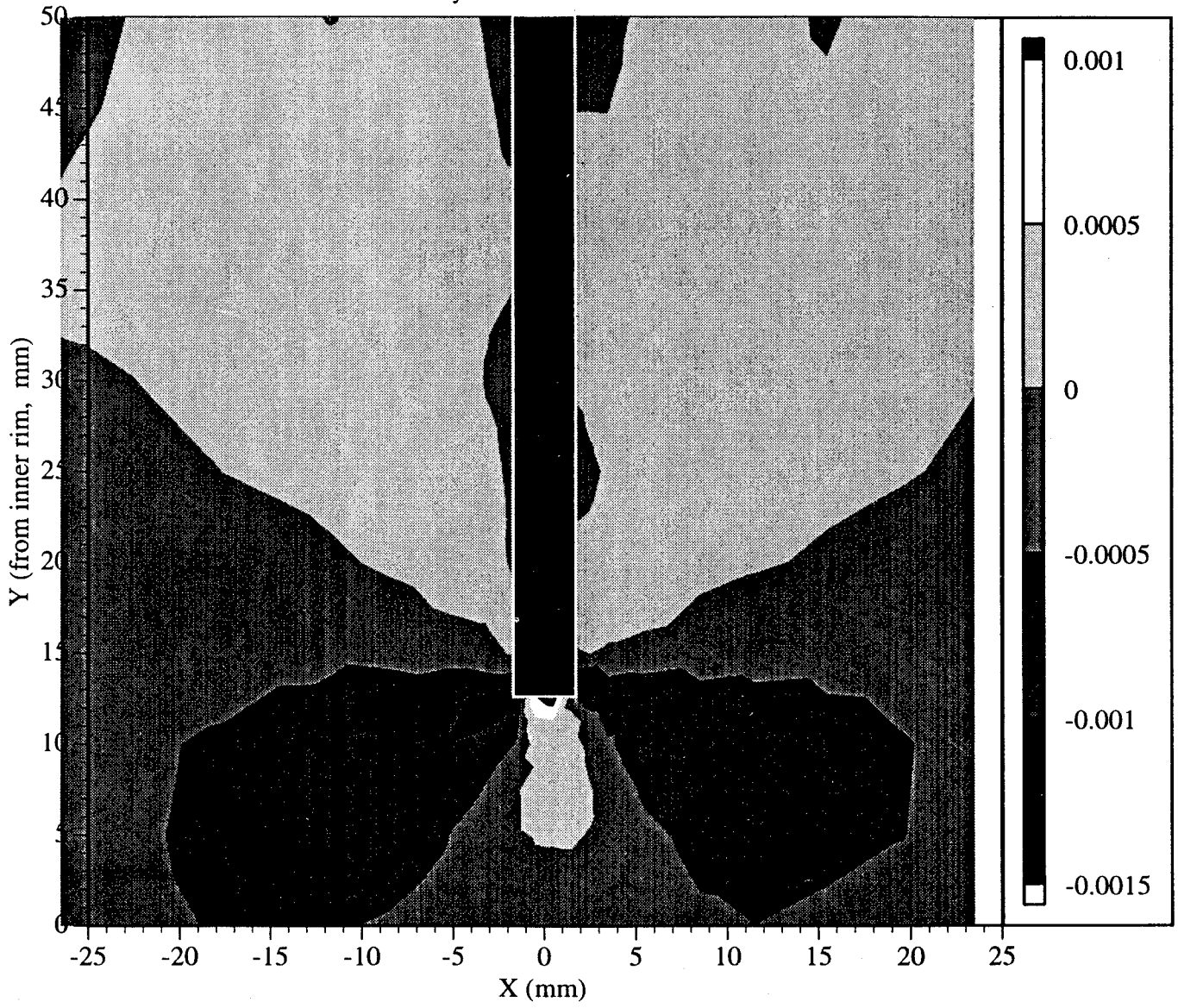

Railroad Car Wheel No. 7 Flange Side Interferometry Results

Residual Strain (γ_{xy}) Field After Cut No. 3 (in mm)

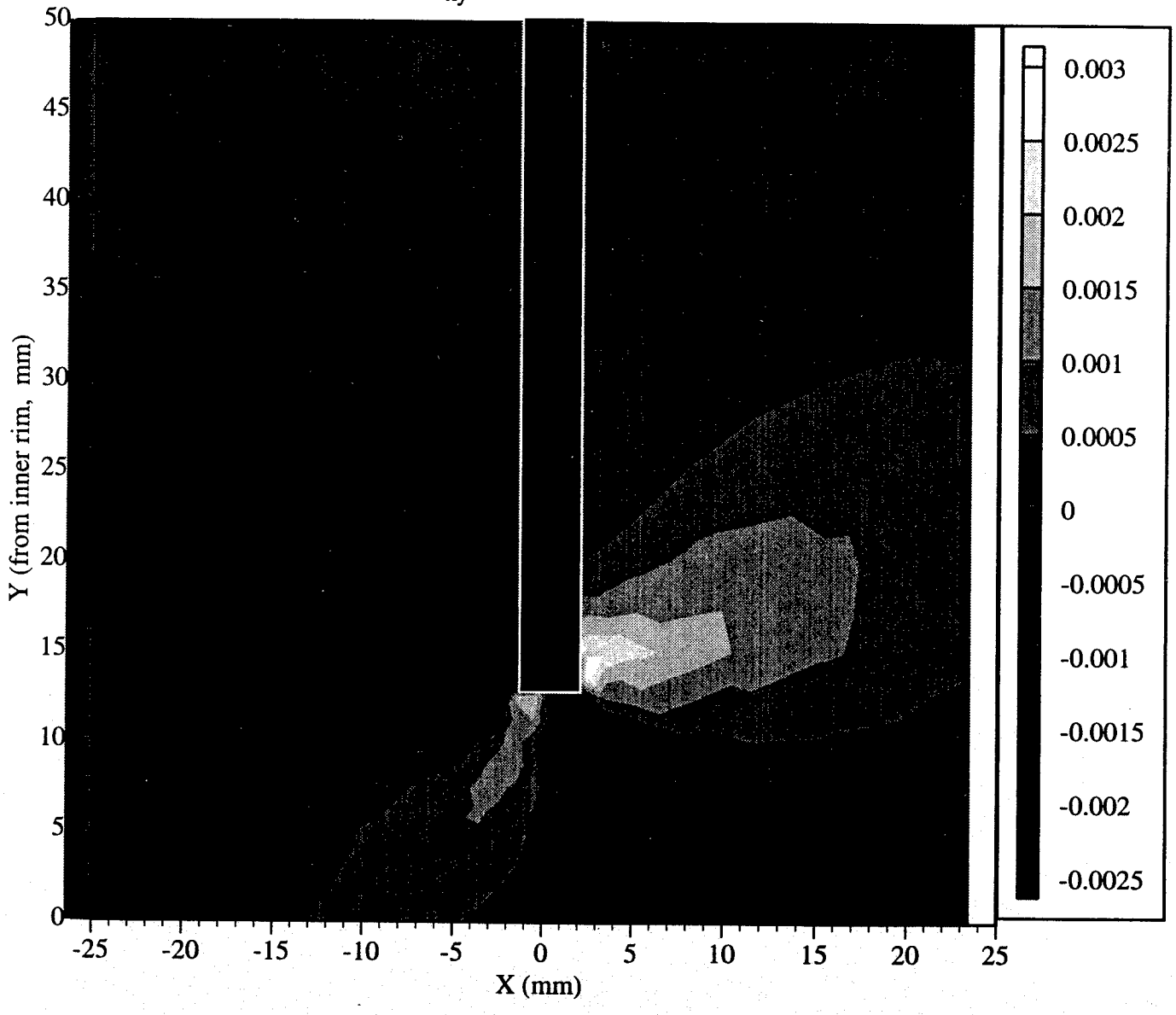

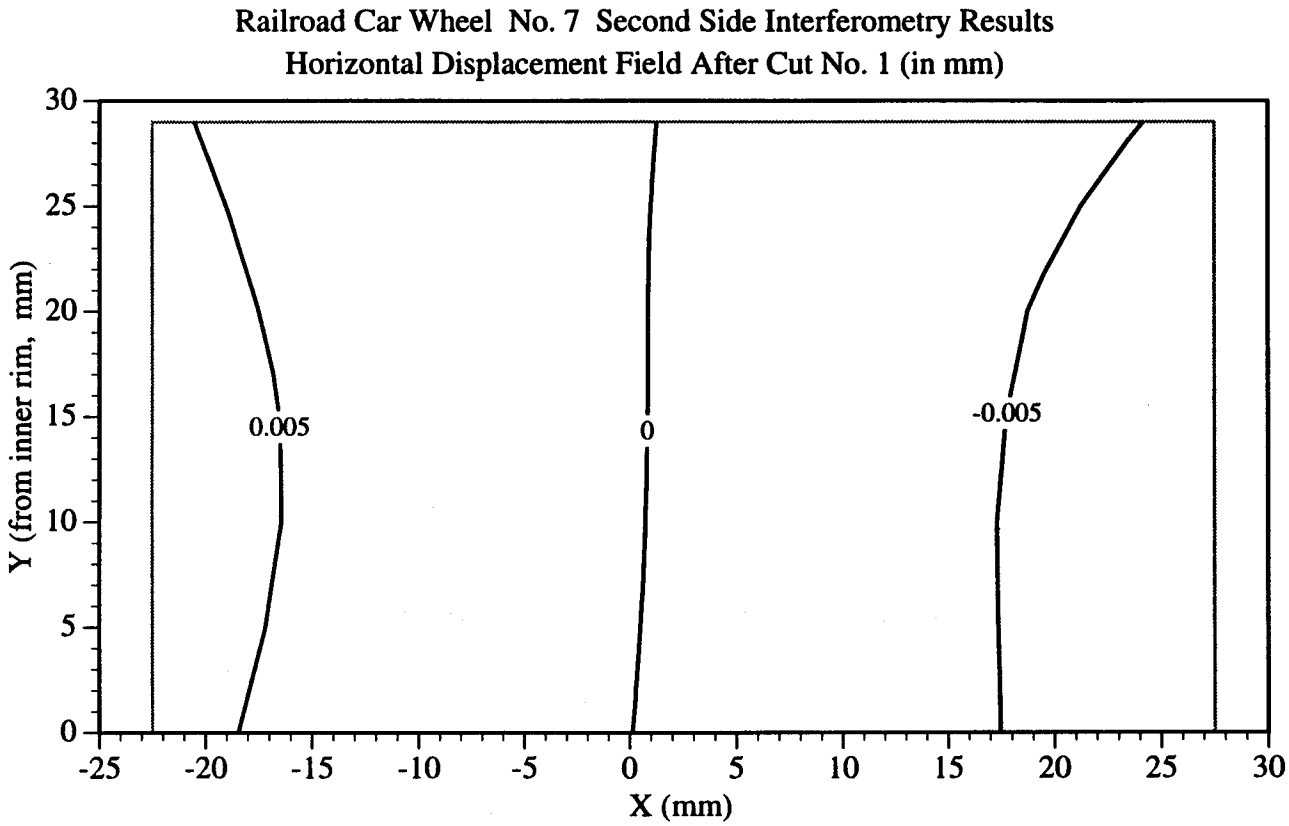
Railroad Car Wheel No. 7 Second Side Interferometry Results
Horizontal Displacement Field After Cut No. 1 (in mm)
Y (from inner rim, mm)
X (mm)
0.005
0
-0.005
30
25
20
15
10
5
0
-25
-20
-15
-10
-5
0
5
10
15
20
25
30

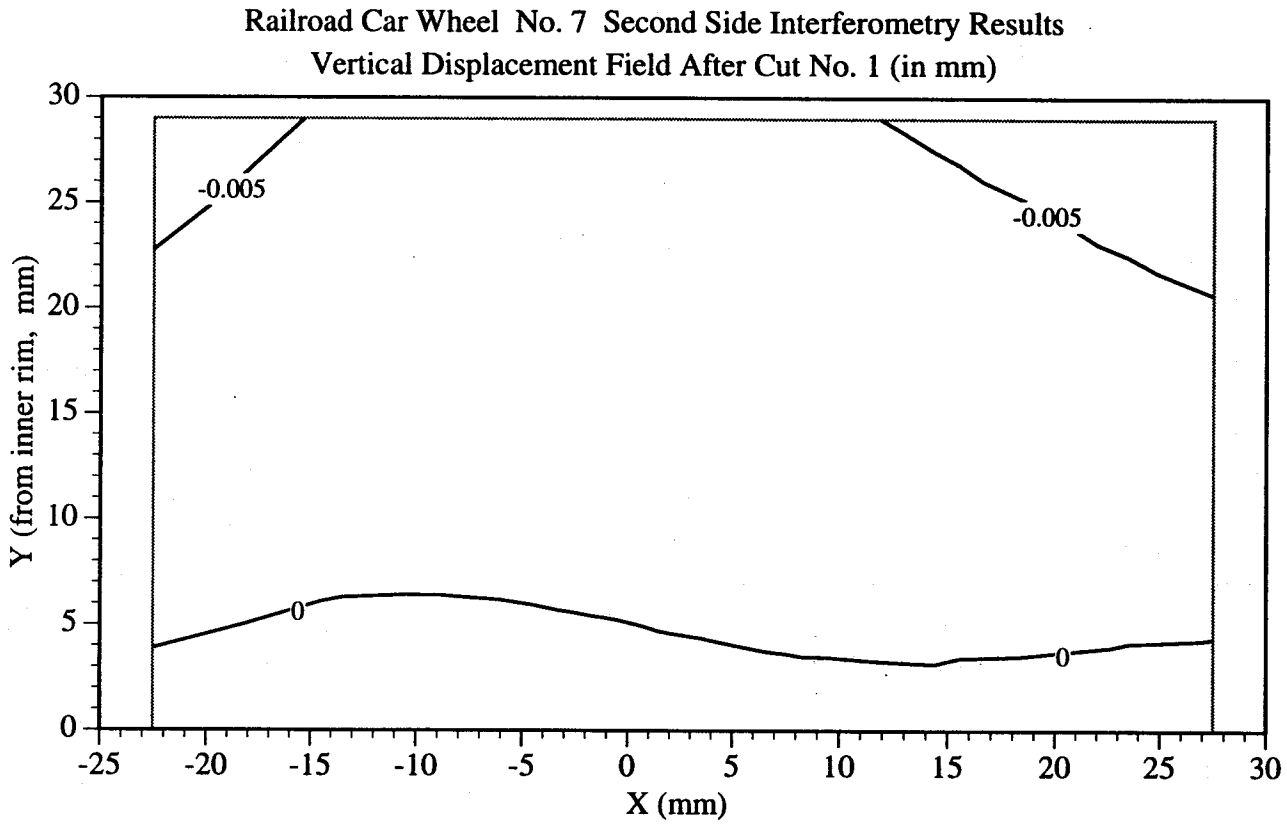
Railroad Car Wheel No. 7 Second Side Interferometry Results
Vertical Displacement Field After Cut No. 1 (in mm)
Y (from inner rim, mm)
X (mm)
-0.005
-0.005
0
0
30
25
20
15
10
5
0
-25
-20
-15
-10
-5
0
5
10
15
20
25
30

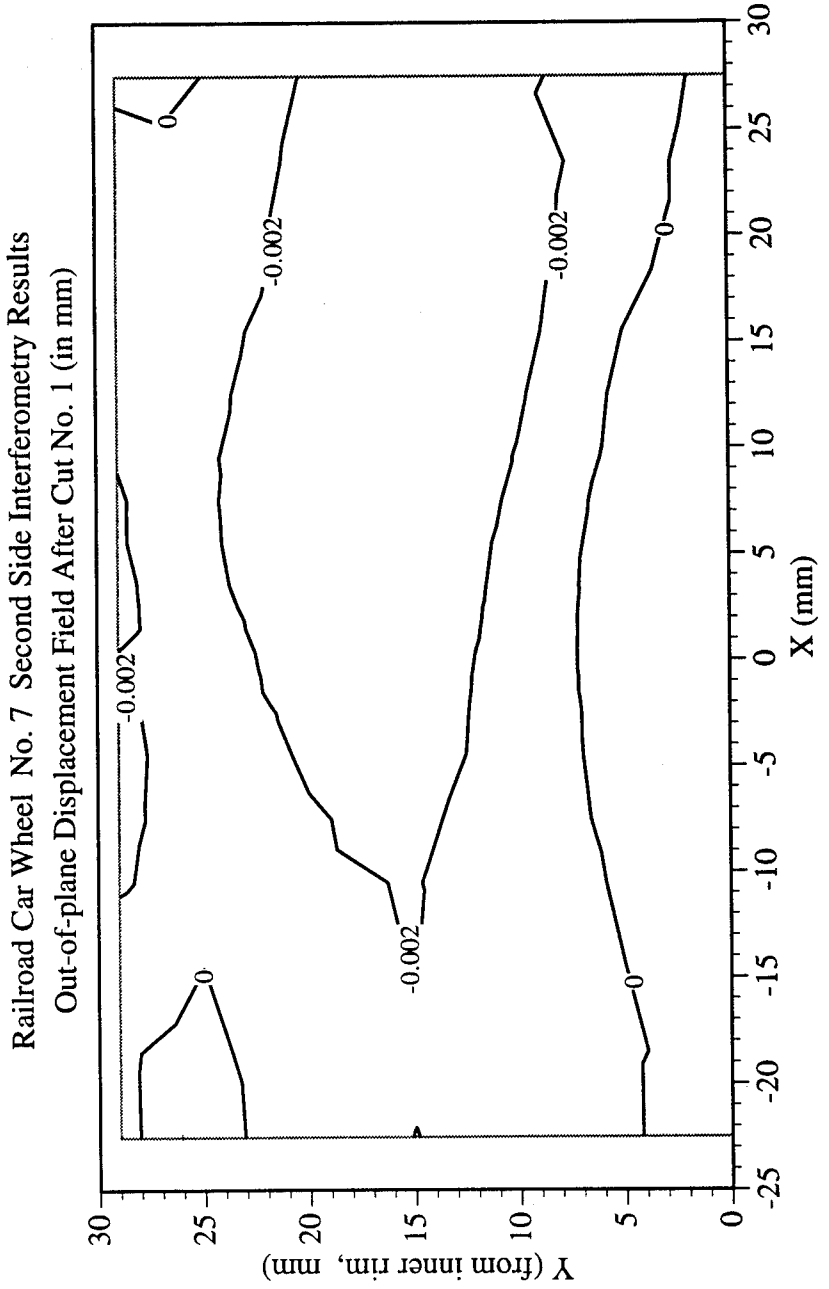
Railroad Car Wheel No. 7 Second Side Interferometry Results
Out-of-plane Displacement Field After Cut No. 1 (in mm)
Y (from inner rim, mm)
X (mm)
0
-0.002
-0.002
-0.002
0
0
0
30
25
20
15
10
5
0
-25
-20
-15
-10
-5
0
5
10
15
20
25
30

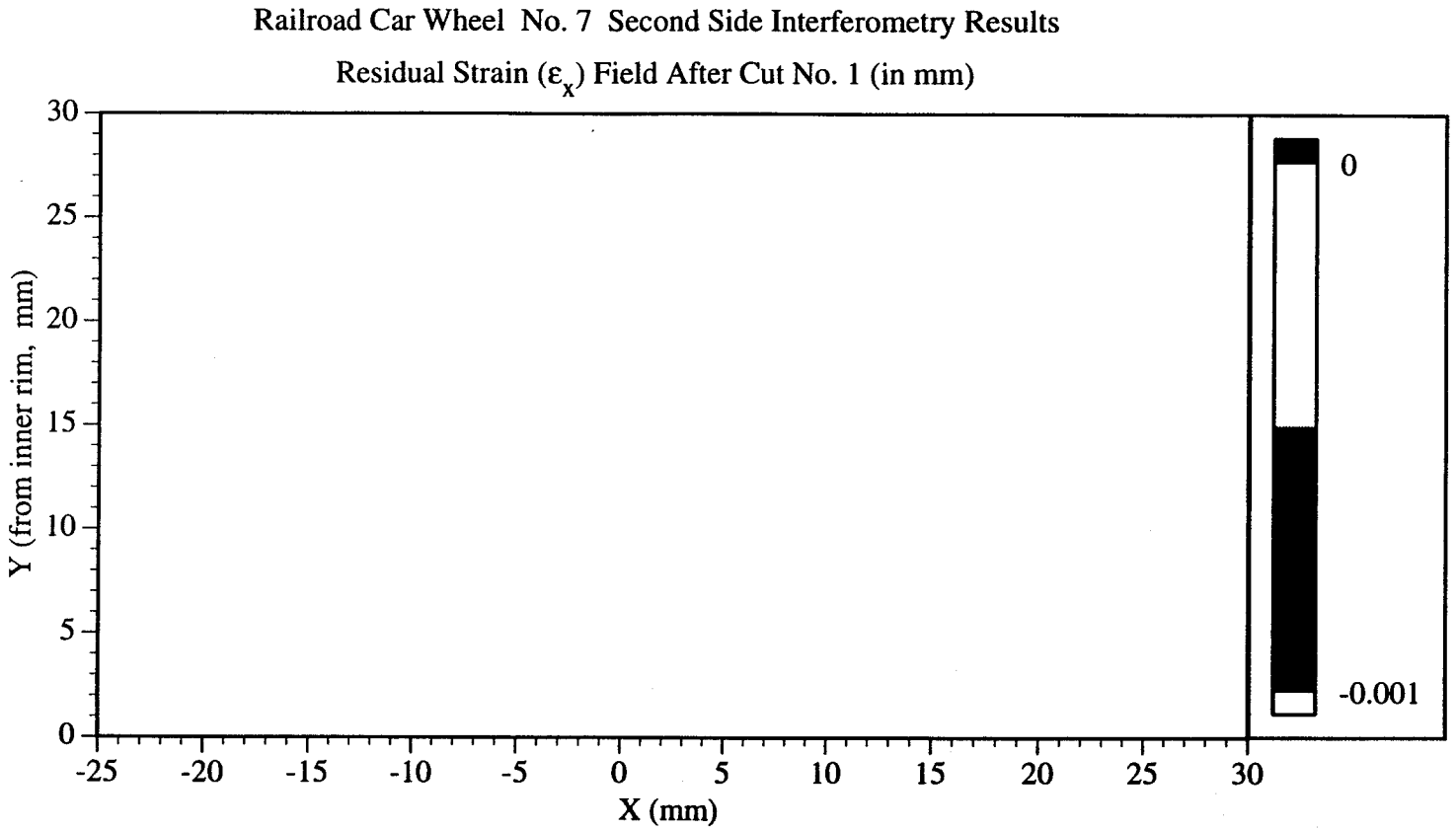
Railroad Car Wheel No. 7 Second Side Interferometry Results
Residual Strain (ε_x) Field After Cut No. 1 (in mm)
Y (from inner rim, mm)
30
25
20
15
10
5
0
-25
-20
-15
-10
-5
0
5
10
15
20
25
30
X (mm)
0
-0.001

Railroad Car Wheel No. 7 Second Side Interferometry Results

Residual Strain (ε_y) Field After Cut No. 1 (in mm)

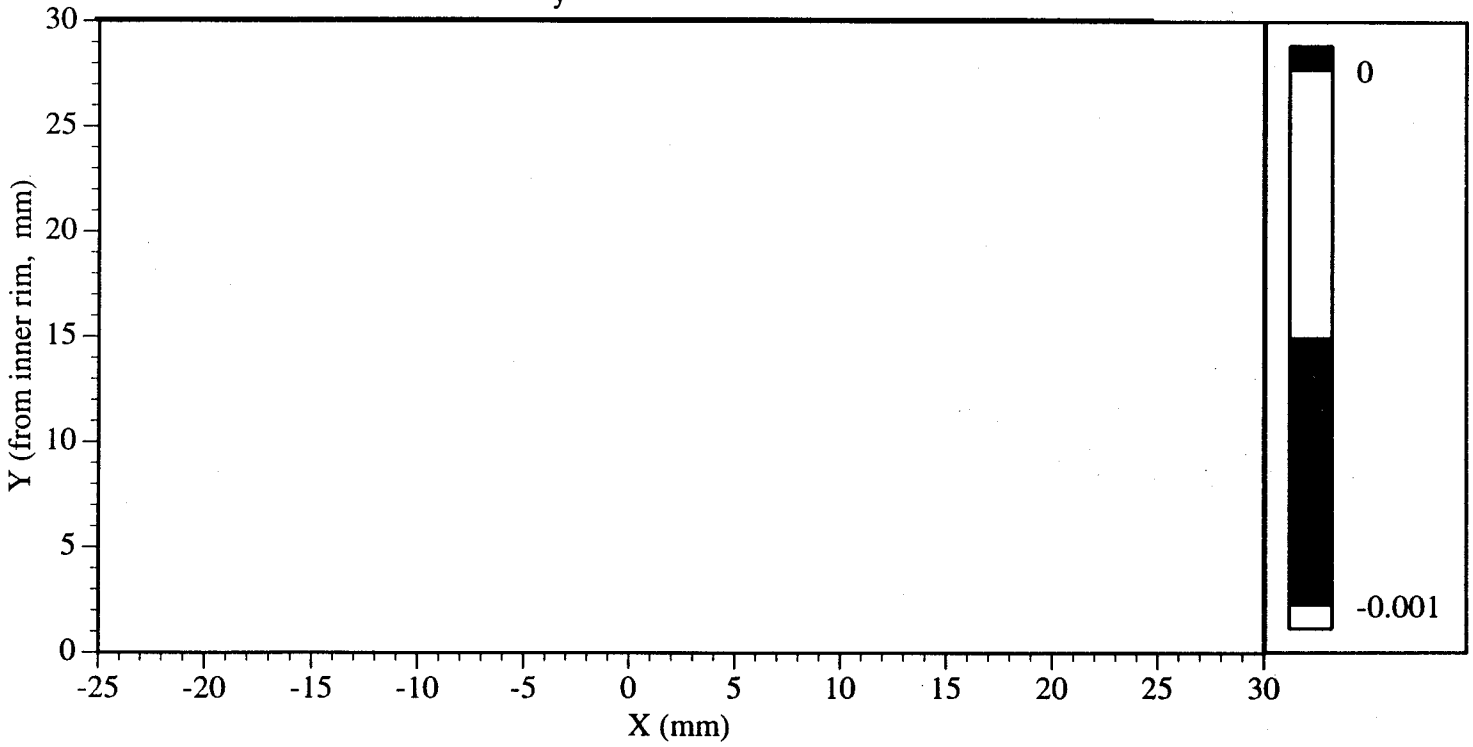

Railroad Car Wheel No. 7 Second Side Interferometry Results

Residual Strain (γ_{xy}) Field After Cut No. 1 (in mm)

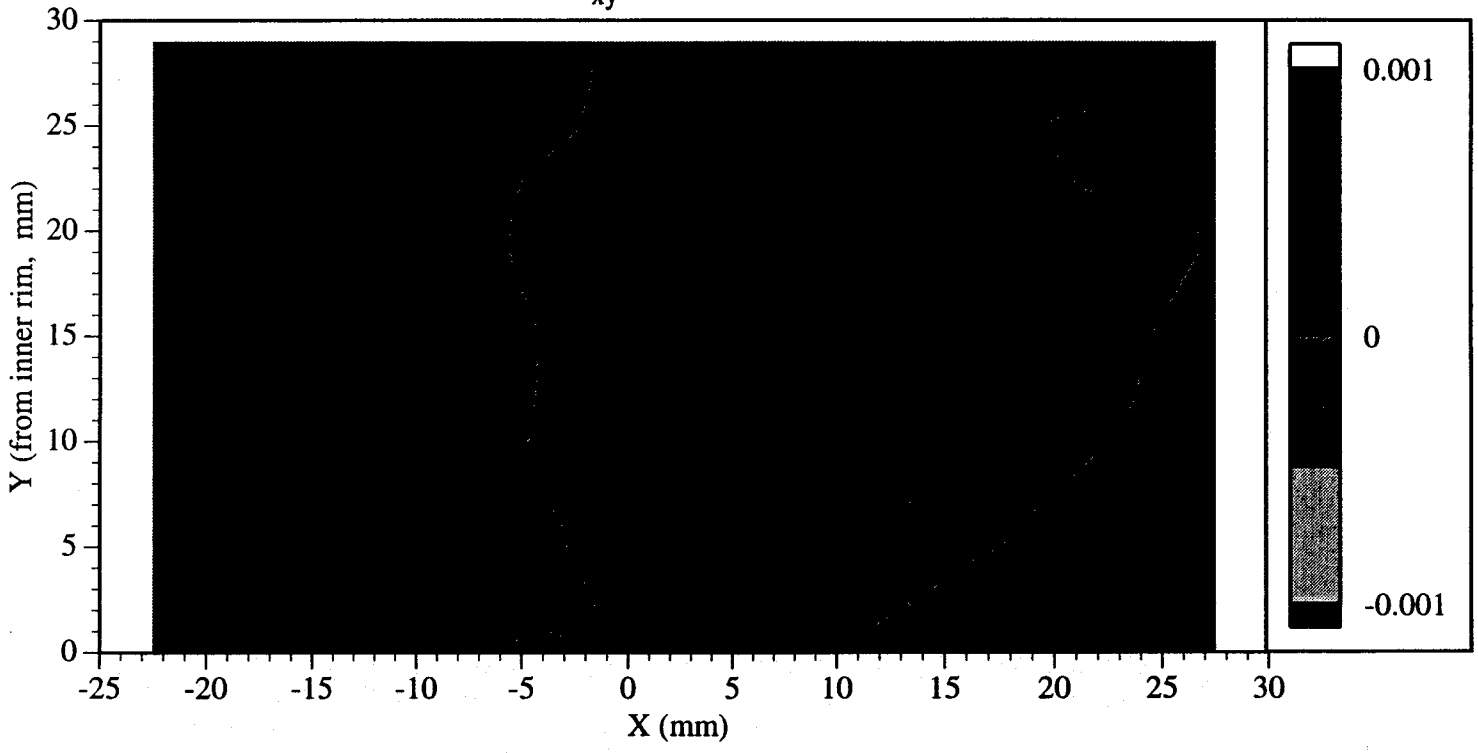

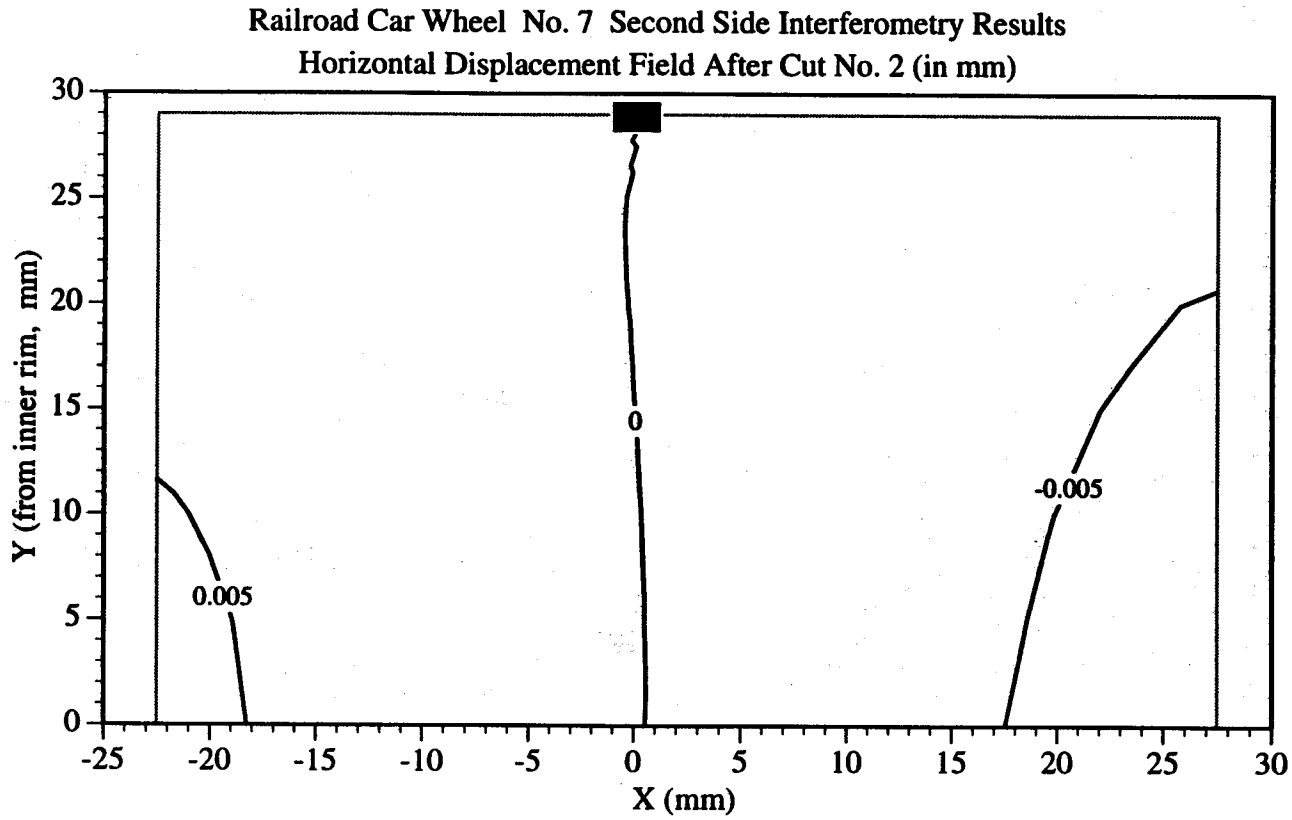
Railroad Car Wheel No. 7 Second Side Interferometry Results
Horizontal Displacement Field After Cut No. 2 (in mm)
Y (from inner rim, mm)
X (mm)
0.005
0
-0.005
30
25
20
15
10
5
0
-25
-20
-15
-10
-5
0
5
10
15
20
25
30

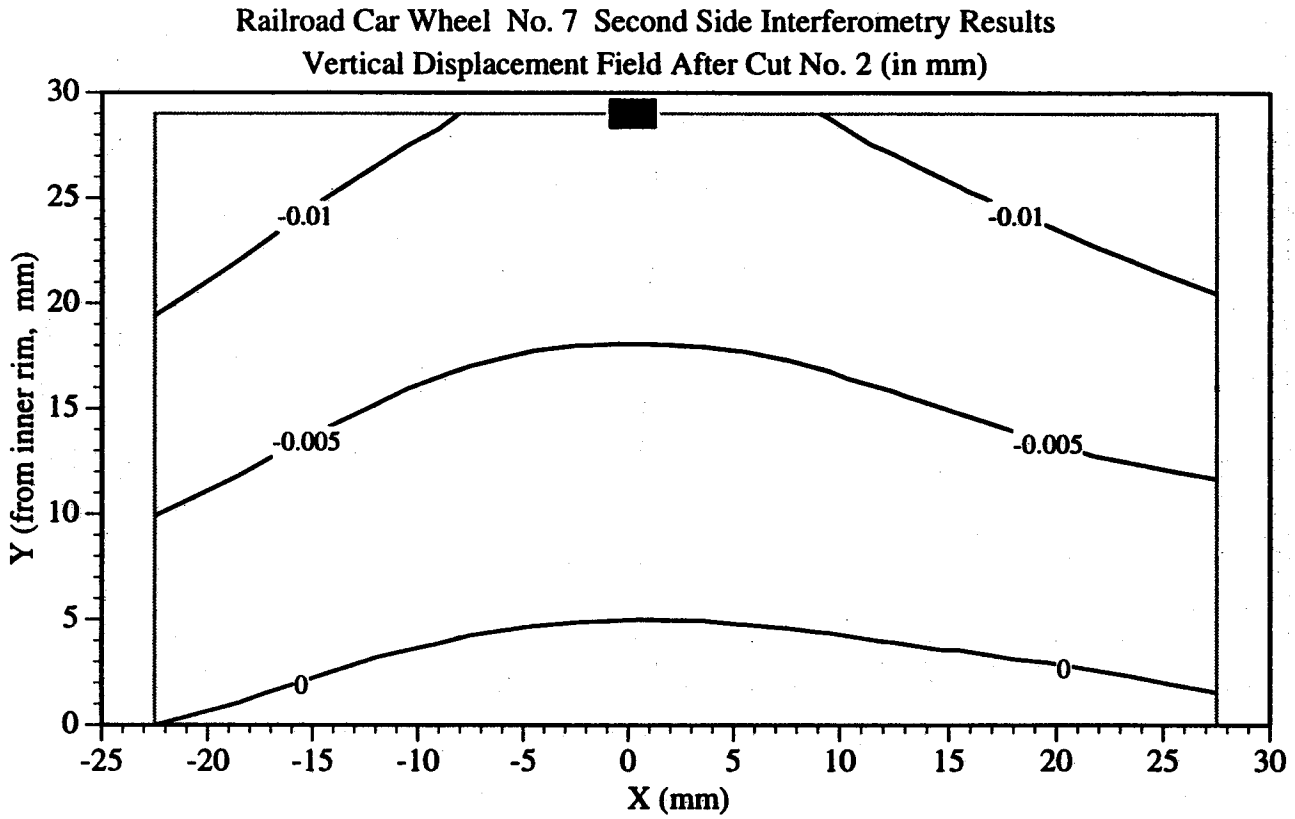
Railroad Car Wheel No. 7 Second Side Interferometry Results
Vertical Displacement Field After Cut No. 2 (in mm)
Y (from inner rim, mm)
X (mm)
-0.01
-0.01
-0.005
-0.005
0
0
30
25
20
15
10
5
0
-25
-20
-15
-10
-5
0
5
10
15
20
25
30

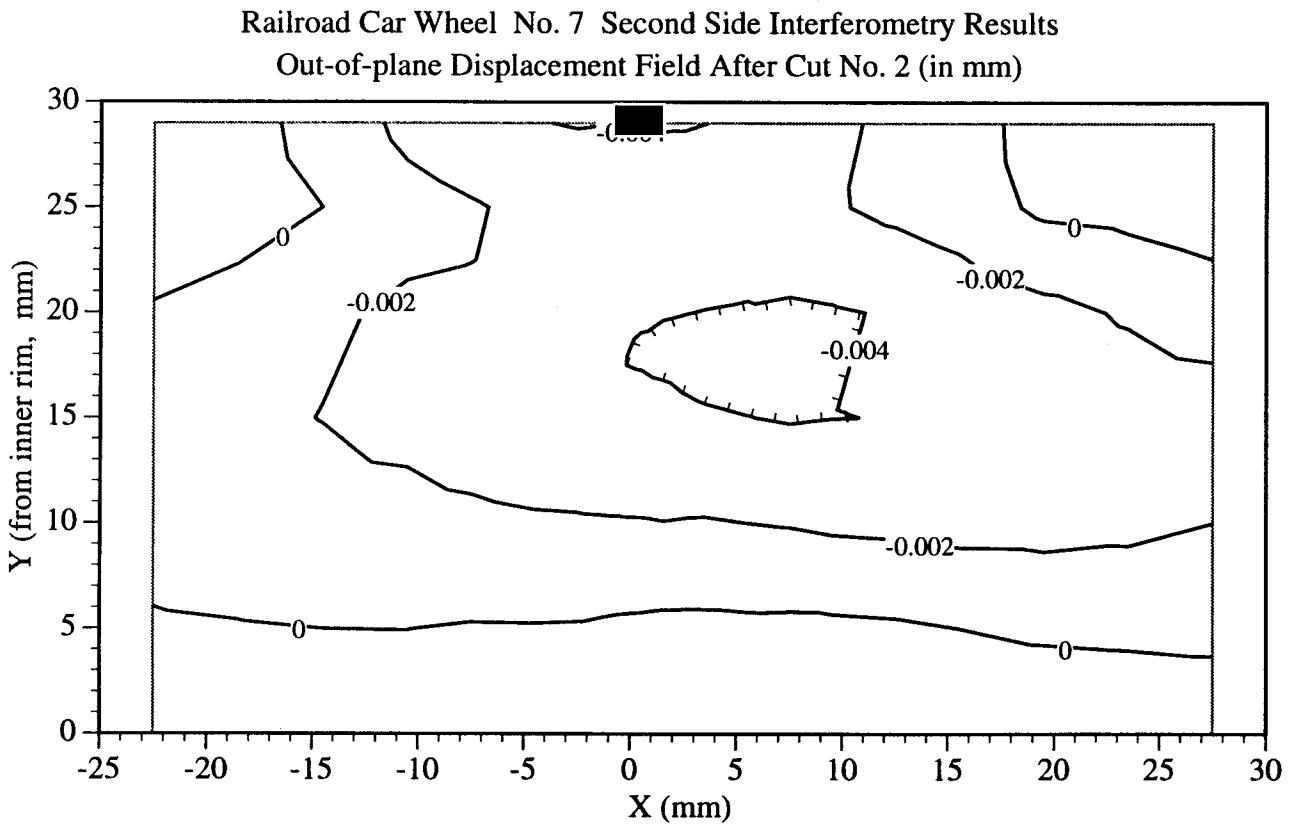
Railroad Car Wheel No. 7 Second Side Interferometry Results
Out-of-plane Displacement Field After Cut No. 2 (in mm)
Y (from inner rim, mm)
X (mm)
30
25
20
15
10
5
0
-25
-20
-15
-10
-5
0
5
10
15
20
25
30
0
-0.002
-0.004
-0.002
0
-0.002
0
0

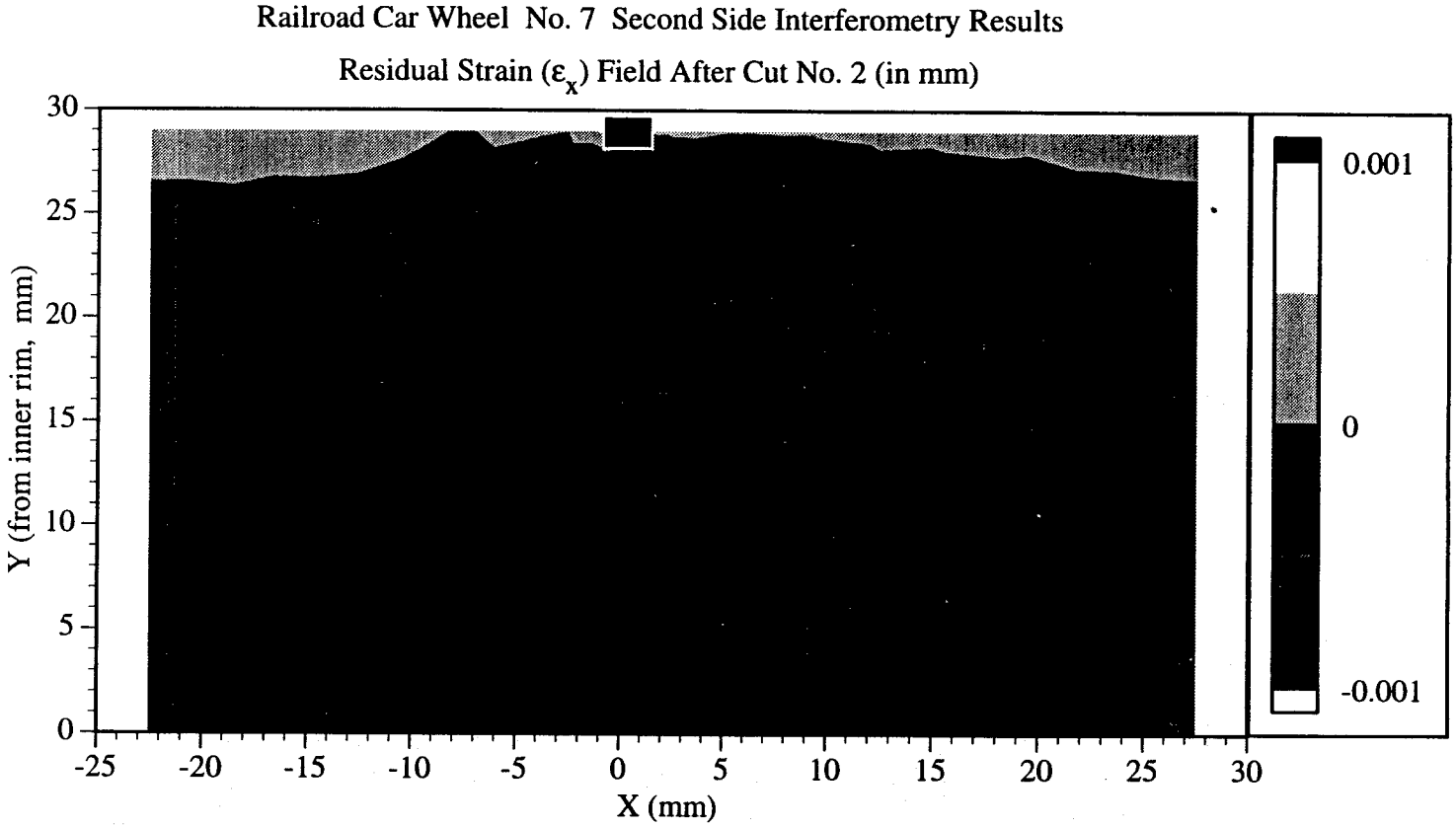
Railroad Car Wheel No. 7 Second Side Interferometry Results
Residual Strain (ε_x) Field After Cut No. 2 (in mm)
Y (from inner rim, mm)
30
25
20
15
10
5
0
-25
-20
-15
-10
-5
0
5
10
15
20
25
30
X (mm)
0.001
0
-0.001

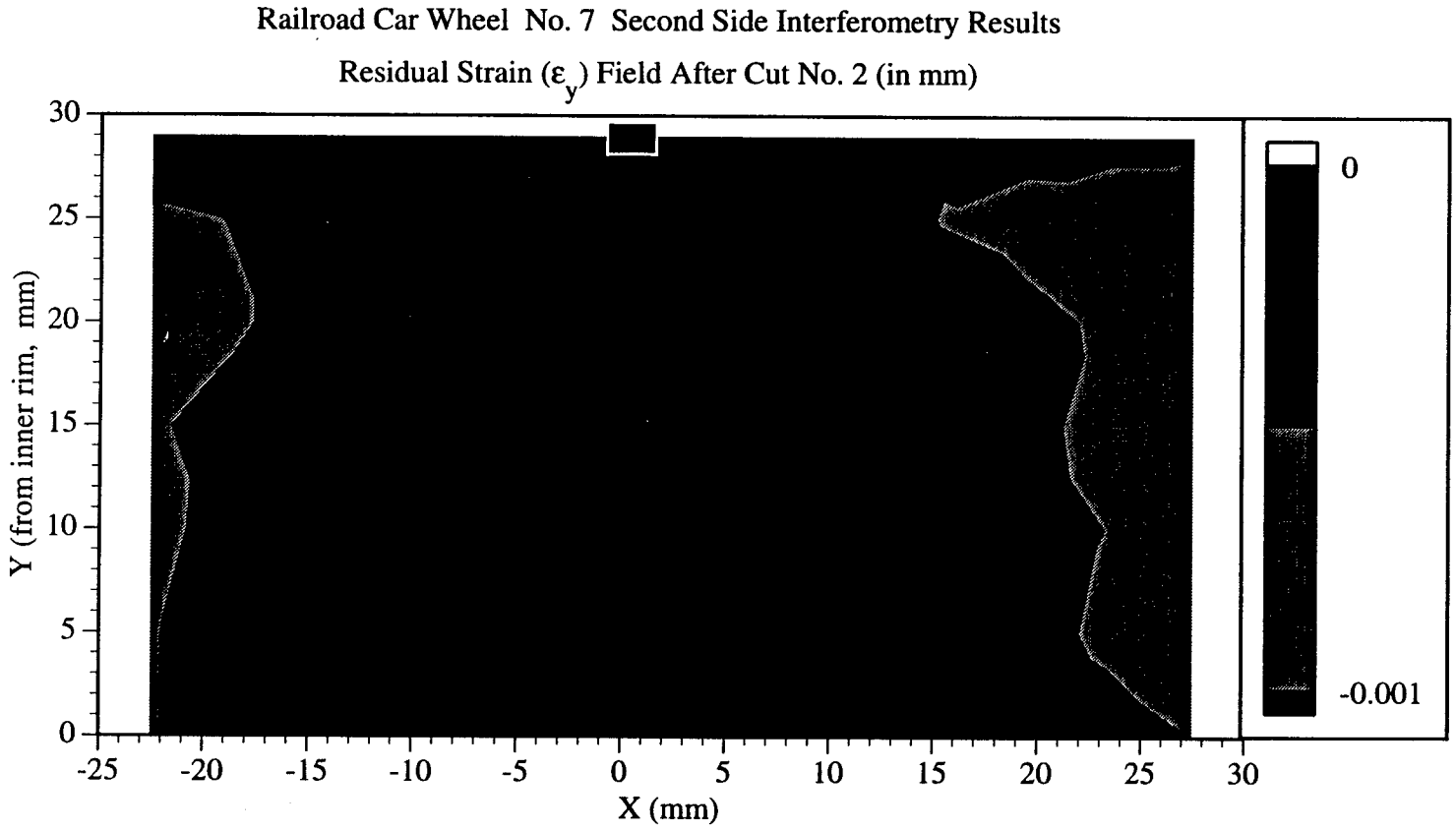
Railroad Car Wheel No. 7 Second Side Interferometry Results
Residual Strain (ε_y) Field After Cut No. 2 (in mm)
Y (from inner rim, mm)
30
25
20
15
10
5
0
-25
-20
-15
-10
-5
0
5
10
15
20
25
30
X (mm)
0
-0.001

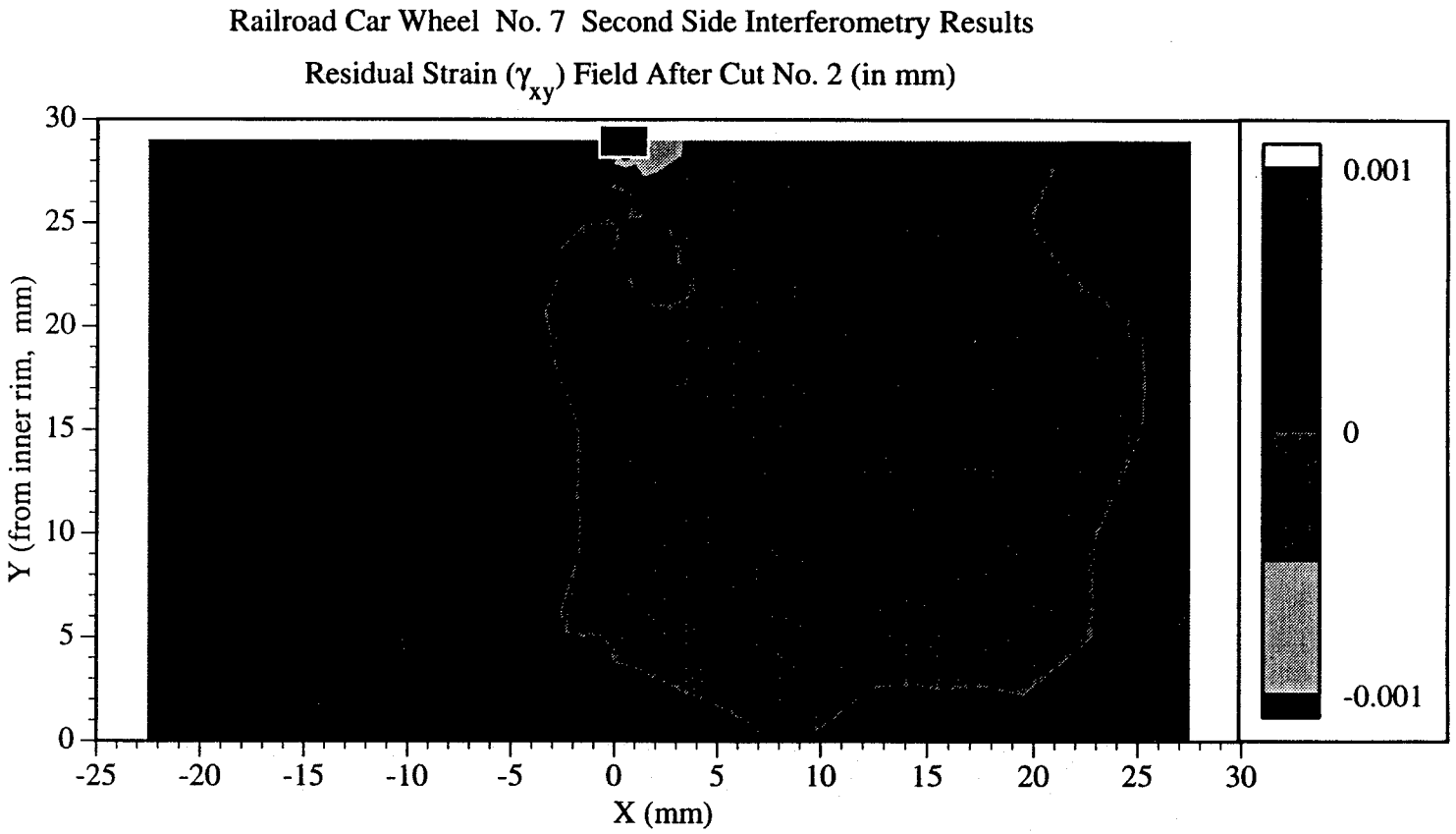
Railroad Car Wheel No. 7 Second Side Interferometry Results
Residual Strain (γ_{xy}) Field After Cut No. 2 (in mm)
Y (from inner rim, mm)
X (mm)
30
25
20
15
10
5
0
-25
-20
-15
-10
-5
0
5
10
15
20
25
30
0.001
0
-0.001

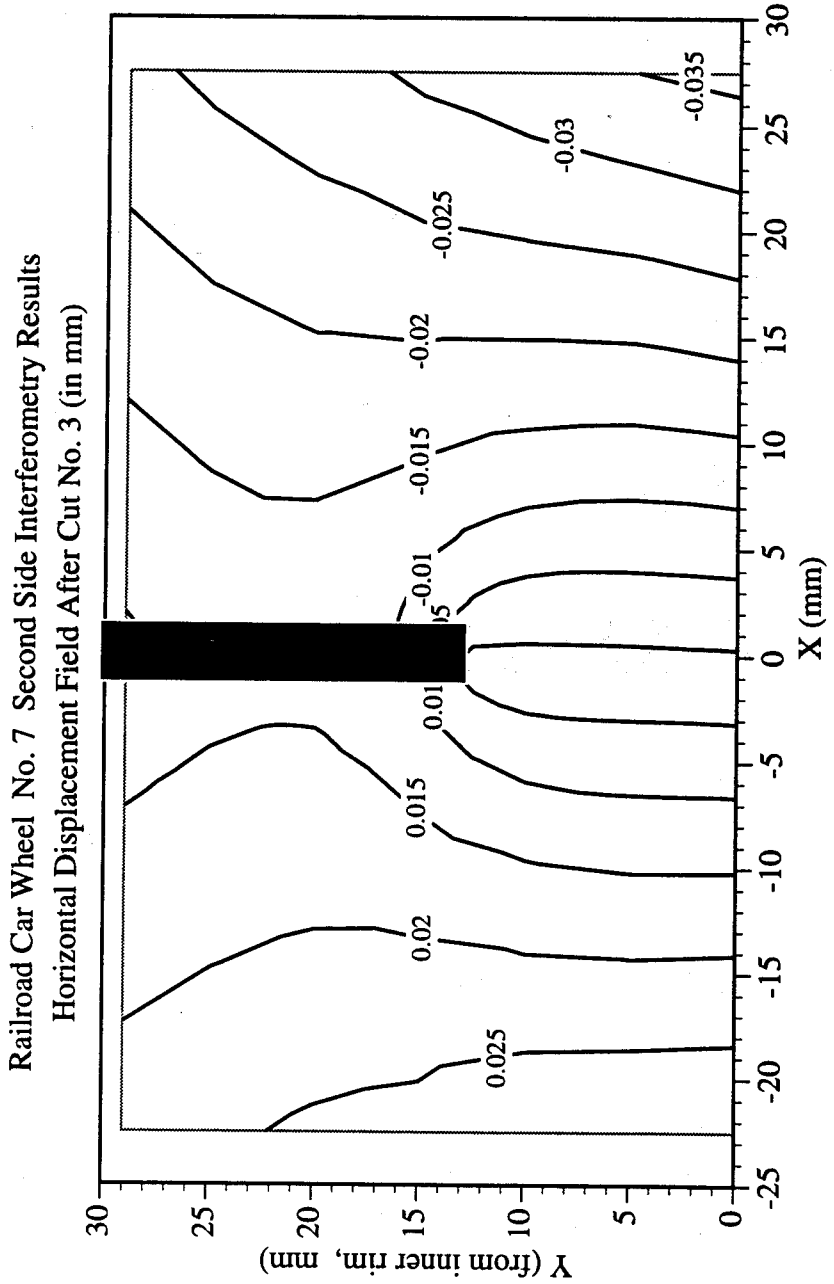
Railroad Car Wheel No. 7 Second Side Interferometry Results
Horizontal Displacement Field After Cut No. 3 (in mm)
Y (from inner rim, mm)
X (mm)
0.025
0.02
0.015
0.01
-0.01
-0.015
-0.02
-0.025
-0.03
-0.035

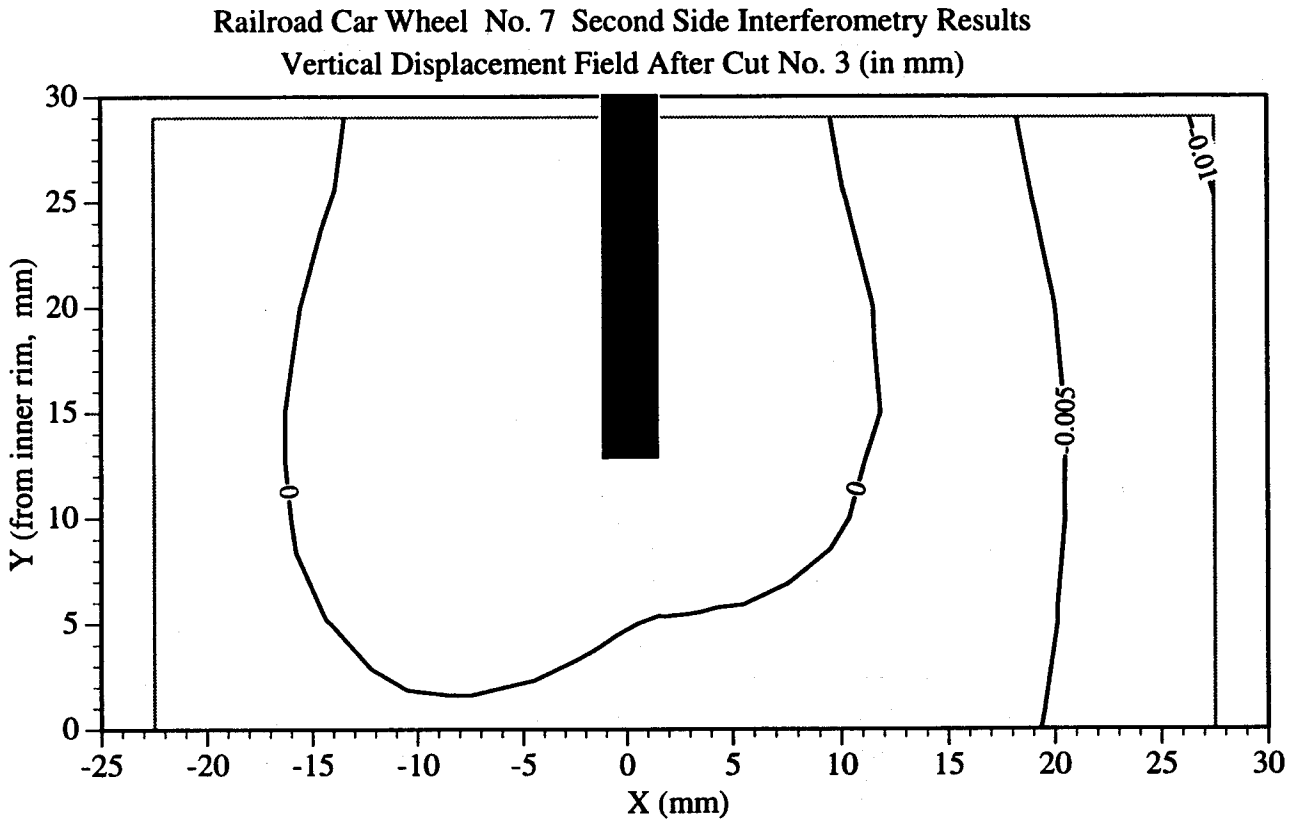
Railroad Car Wheel No. 7 Second Side Interferometry Results
Vertical Displacement Field After Cut No. 3 (in mm)
Y (from inner rim, mm)
X (mm)
30
25
20
15
10
5
0
-25
-20
-15
-10
-5
0
5
10
15
20
25
30
0
0
-0.005
-0.010

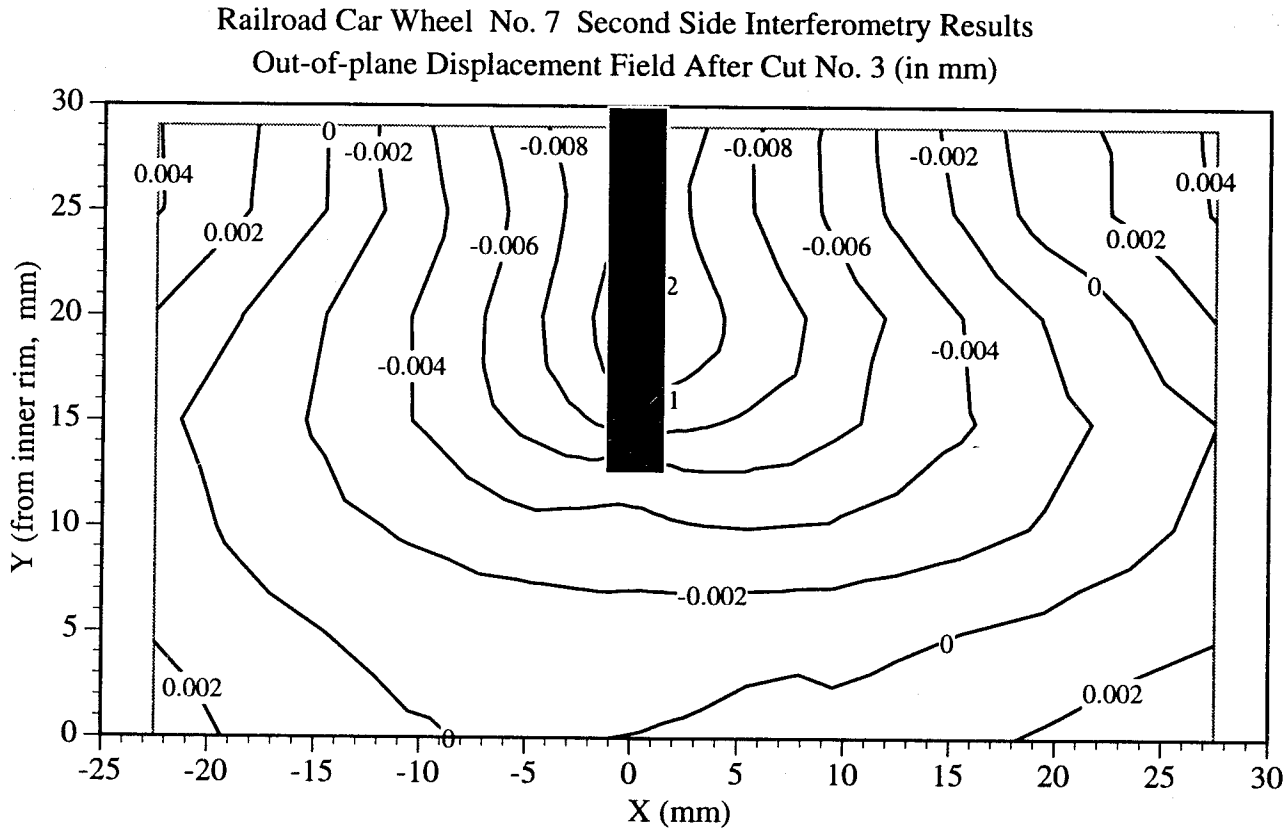
Railroad Car Wheel No. 7 Second Side Interferometry Results
Out-of-plane Displacement Field After Cut No. 3 (in mm)
Y (from inner rim, mm)
X (mm)
0.004
0.002
0
-0.002
-0.004
-0.006
-0.008
2
1

Railroad Car Wheel No. 7 Second Side Interferometry Results

Residual Strain (ε_x) Field After Cut No. 3 (in mm)

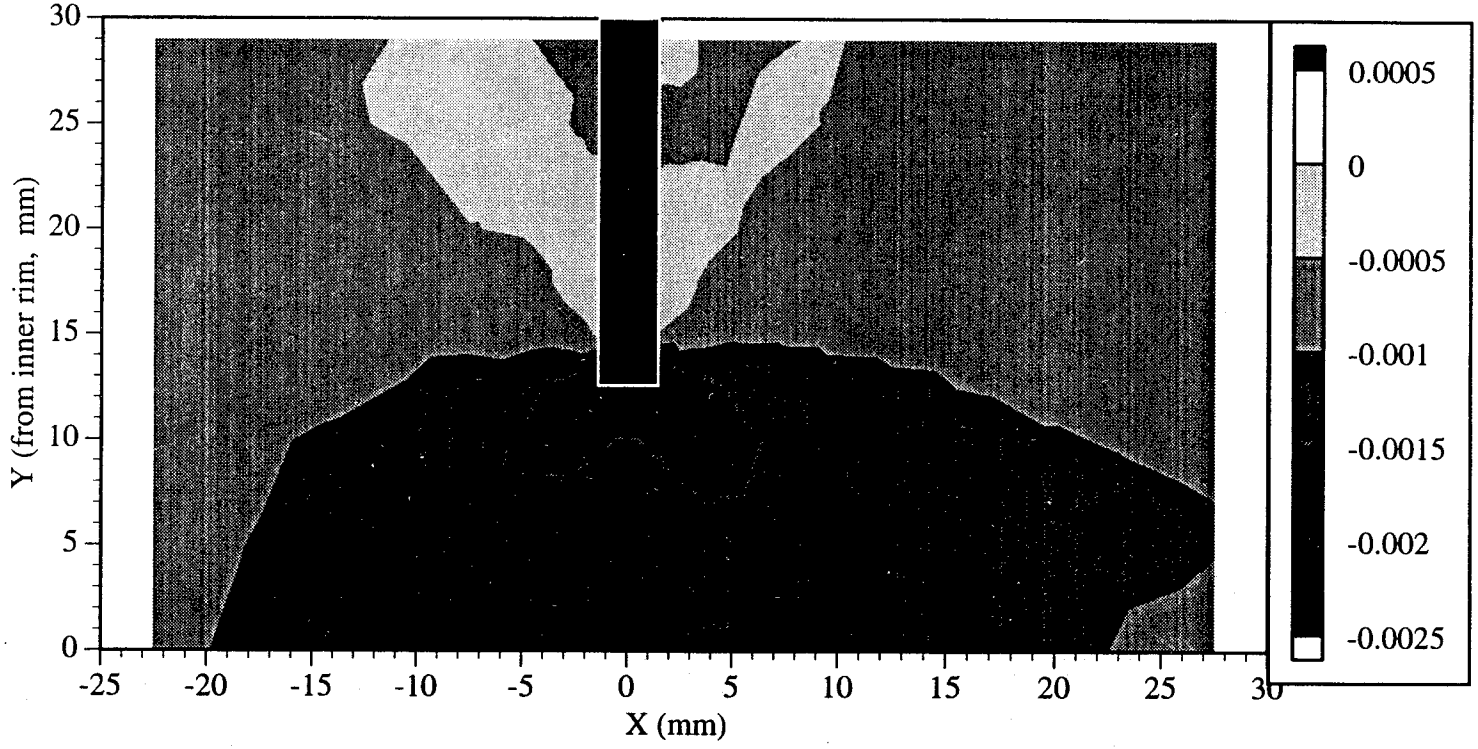

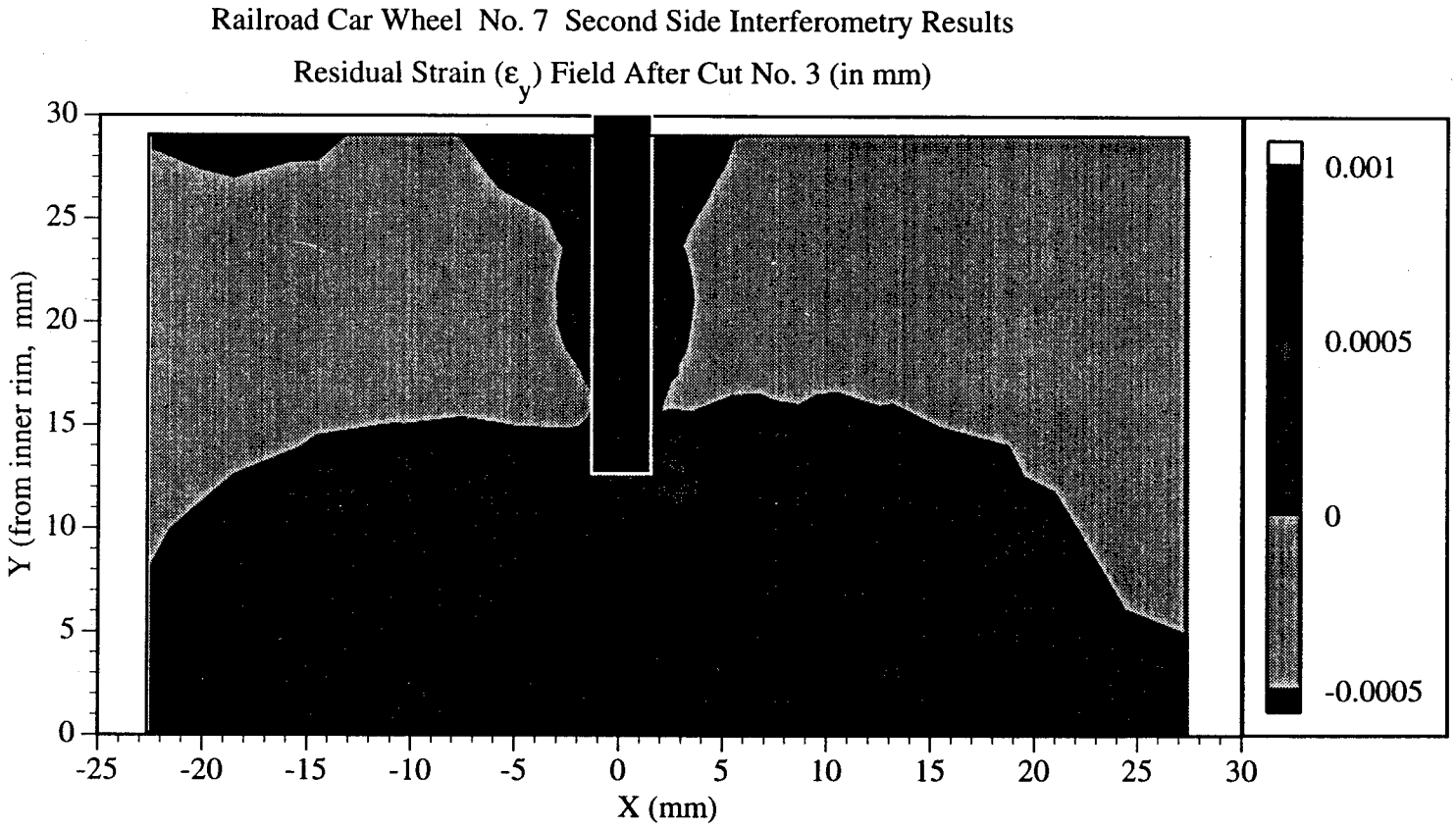
Railroad Car Wheel No. 7 Second Side Interferometry Results
Residual Strain (ε_y) Field After Cut No. 3 (in mm)
Y (from inner rim, mm)
30
25
20
15
10
5
0
-25
-20
-15
-10
-5
0
5
10
15
20
25
30
X (mm)
0.001
0.0005
0
-0.0005

Railroad Car Wheel No. 7 Second Side Interferometry Results

Residual Strain (γ_{xy}) Field After Cut No. 3 (in mm)

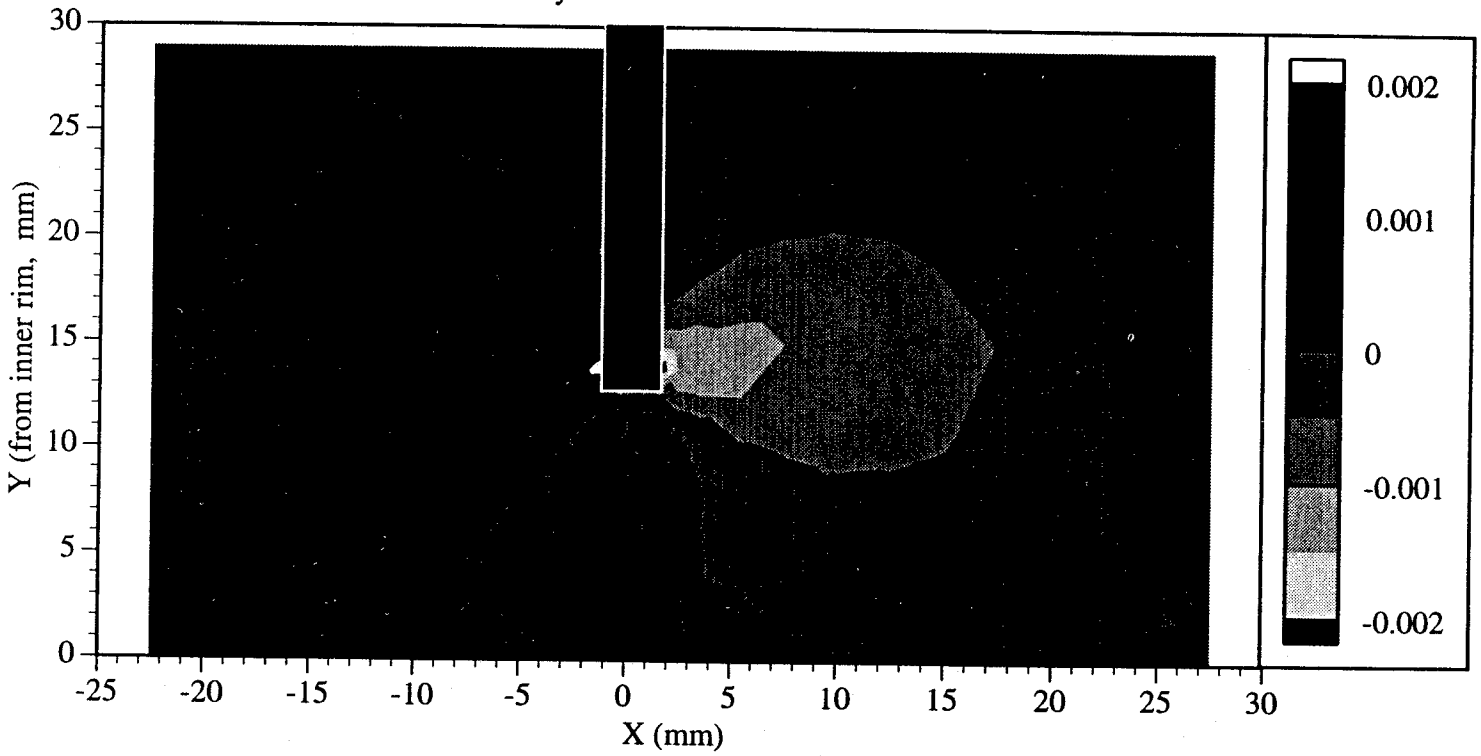

Page Intentionally Left Blank

Appendix 8. Wheel #8 Experimental Results

This appendix contains the results from the test on both sides (front and back rim faces) of the eighth wheel. Each side has a local coordinate system that is located at the intersection of the inner edge of the rim and the cutting line; the vertical axis points away from the center of the wheel. Due to the hardened outer rim, the cutting had to start with a carbide blade and then continue with a regular blade.

The attached figures show the location of all the sensors. At two points on the wheel, thermocouples (TC) measure the temperature difference (which never exceeded 10.8°C) immediately after each cut. The temperature at TC2, the one farther from the cut, was equal to the ambient temperature. The strain measurements were taken after the difference decreased to about 1°C or less at an ambient temperature in the range of 20°C to 25°C.

The extensometer, strain gage, and displacement sensor data are provided in tabular form. The interferometric data is provided in the form of contour maps and as data files in ASCII format for three specific cutting stages. The corresponding cut depths are 35 mm, 45 mm, and 60 mm.

The wheel was identified by the following markings:

26512

Location of strain gauges, thermocouples and gratings on wheel #5,6,7&8

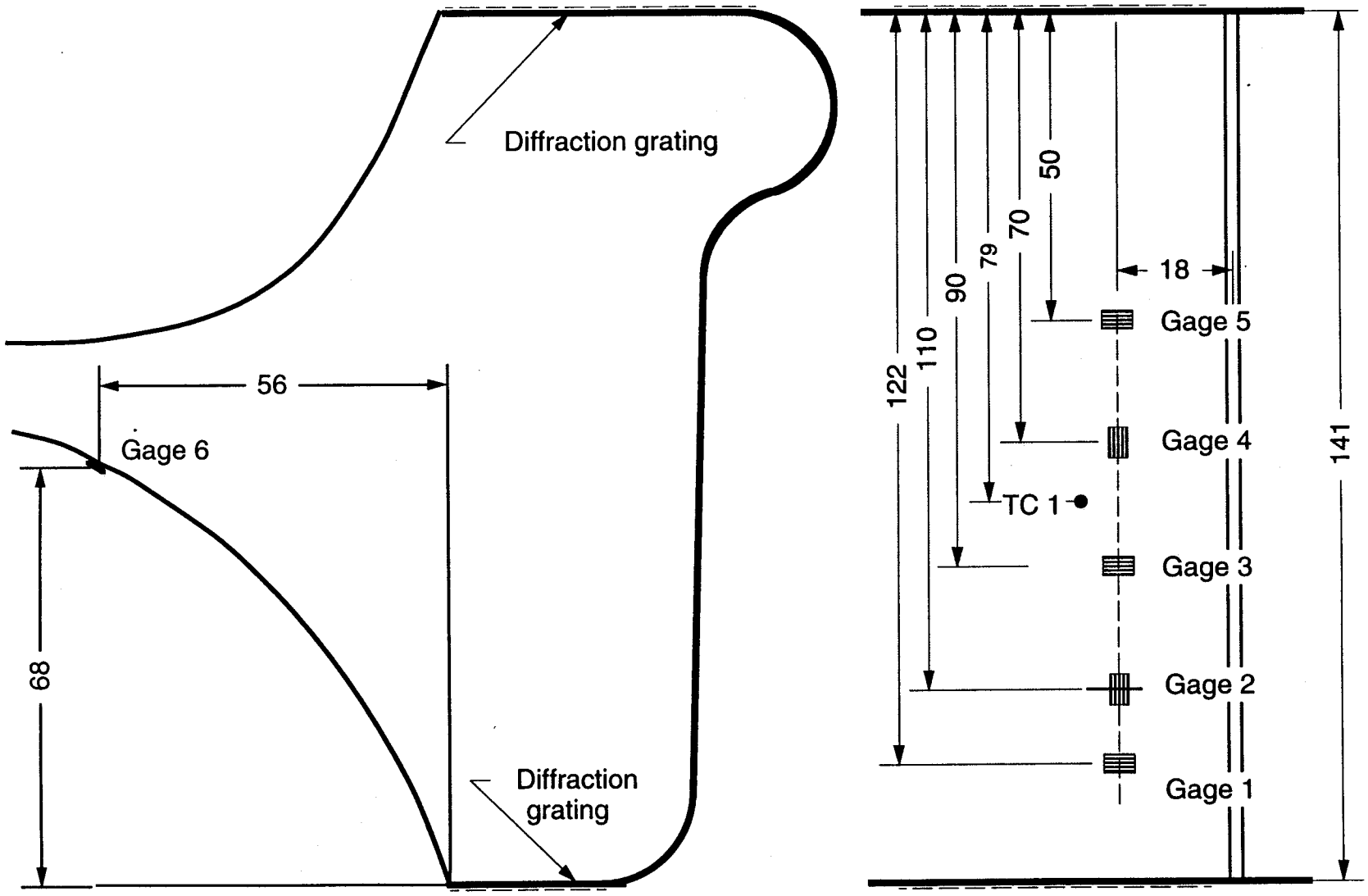

Gage 6 was located 20mm from the plane of the cut.

Location of displacement sensors thermocouples and gratings on wheel #5,6,7&8

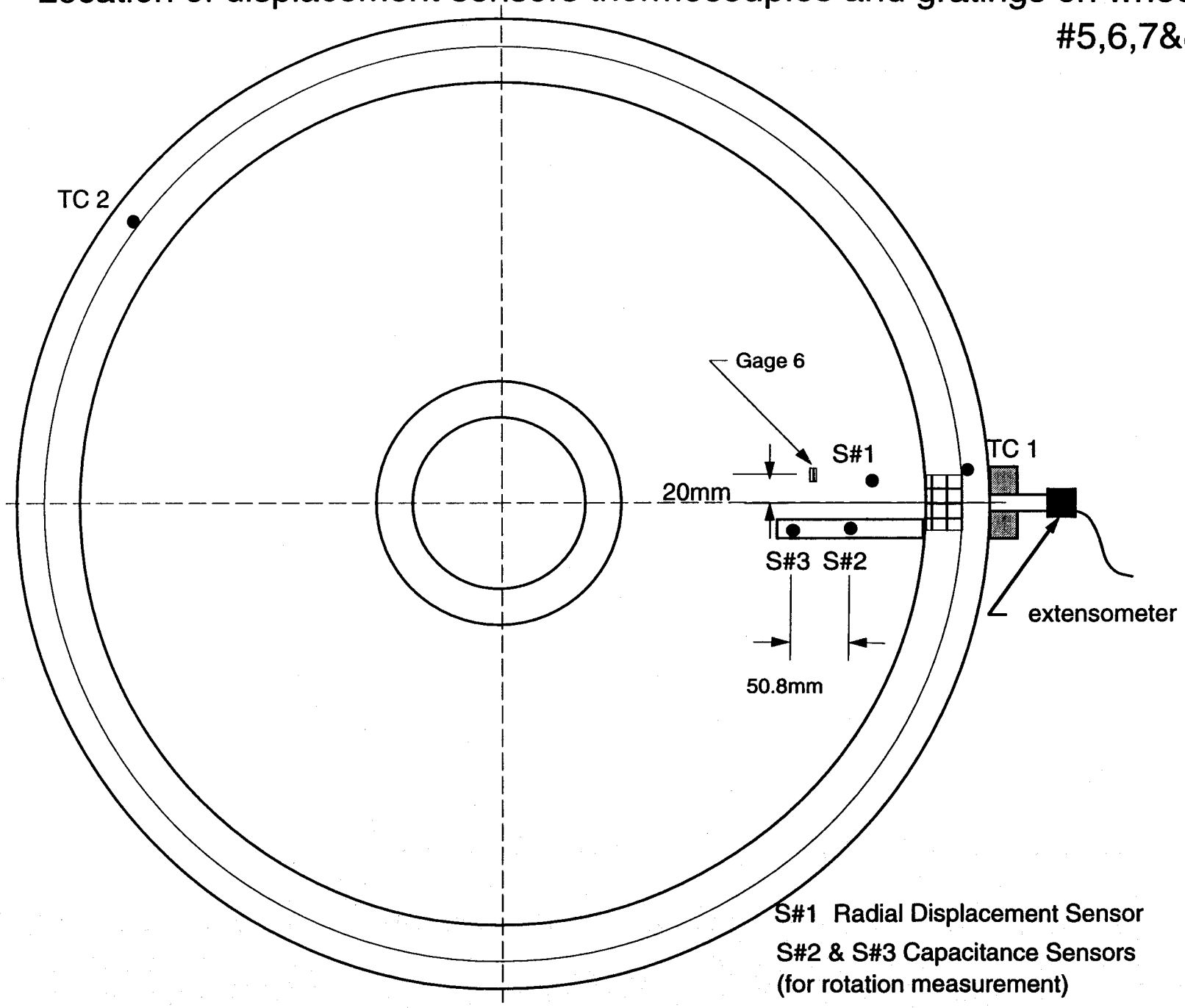

S#1 Radial Displacement Sensor

S#2 & S#3 Capacitance Sensors
(for rotation measurement)

WHEEL #8 TEST DATA

TESTING OF DOT RAILROAD CAR WHEEL #8							26512				
DATE:	September 13 1995										
	mm/mm						mm	mm	rad	(°C)	(°C)
Cut Depth (mm)	Gage1	Gage2	Gage3	Gage4	Gage5	Gage6	Radial Displacement	Opening Displacement	Rotation	TC 1	TC 2
0	0	0	0	0	0	0	0	0	0.00E+00	24.0	24.1
28	13	-7	-32	8	-38	15	.0073	-.0411	0.00E+00	30.8	24.3
35	23	-8	-24	17	41	21	.0131	-.0542	2.71E-05	35.2	24.4
45	167	-16	190	15	278	44	-.0002	-.0942	9.80E-05	25.3	24.0
55	279	-32	293	8	361	70	-.0191	-.1332	7.69E-05	25.9	24.8
60	309	-41	318	5	378	79	-.0331	-.1611	5.19E-05	26.2	24.8
70	335	-59	339	-10	389	89	-.0556	-.1819	3.09E-05	21.0	20.8
80	325	-80	345	-36	388	80	-.0809	-.2553	3.58E-05	21.7	20.7
90	317	-91	346	-55	380	55	-.1049	-.3090	4.55E-05	22.3	20.8
100	312	-96	342	-61	374	14	-.1273	-.3644	-6.14E-05	22.6	20.8
110	312	-100	341	-61	368	-47	-.1440	-.4066	-1.39E-04	22.7	20.8
120	310	-101	340	-61	366	-133	-.1578	-.4411	-1.88E-04	22.8	20.8
130	311	-101	339	-60	364	-233	-.1676	-.4647	-2.32E-04	22.7	20.8
140	310	-102	339	-60	364	-298	-.1771	-.4844	-2.80E-04	22.8	20.8
151	310	-102	339	-60	363	-307	-.1784	-.5008	-2.85E-04	22.7	20.8
160	309	-101	338	-59	363	-302	-.1880	-.5140	-3.63E-04	22.7	20.9
170	309	-101	338	-58	363	-299	-.1978	-.5282	-4.02E-04	22.6	20.9
180	310	-100	338	-59	362	-299	-.2069	-.5403	-4.45E-04	22.5	20.9
190	309	-100	338	-59	363	-300	-.2164	-.5573	NA	22.2	20.9
200	309	-100	337	-59	363	-299	-.2242	-.5715	NA	22.1	20.8
210	309	-99	338	-58	363	-299	-.2329	-.5879	NA	22.1	20.9
220	309	-99	336	-58	363	-299	-.2409	-.6542	NA	22.0	20.9
End											

Railroad Wheel No. 8 Test
Displacement vs. Cut Depth

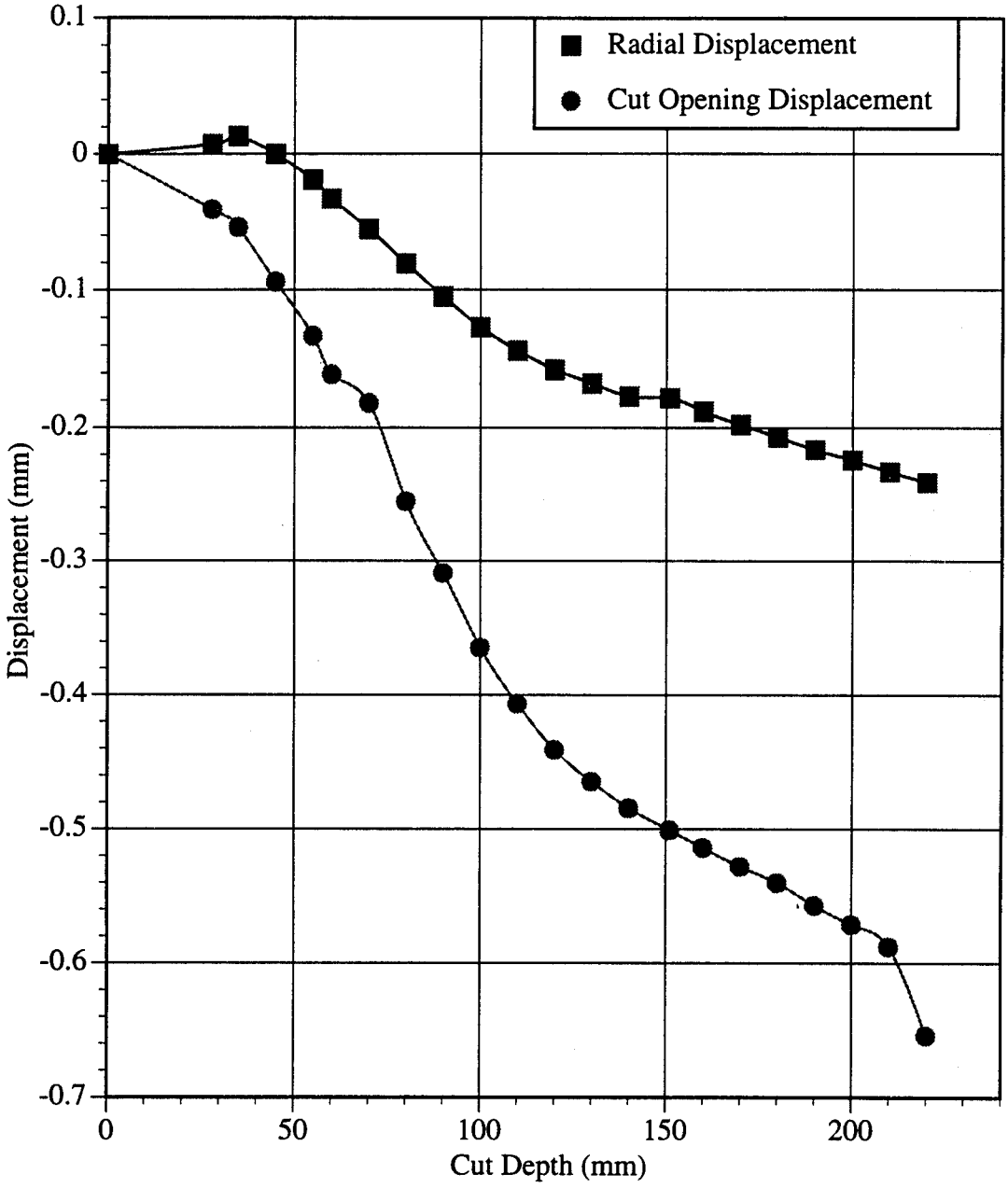

Railroad Wheel No. 8 Test
Strain Gage Readings vs. Cut Depth

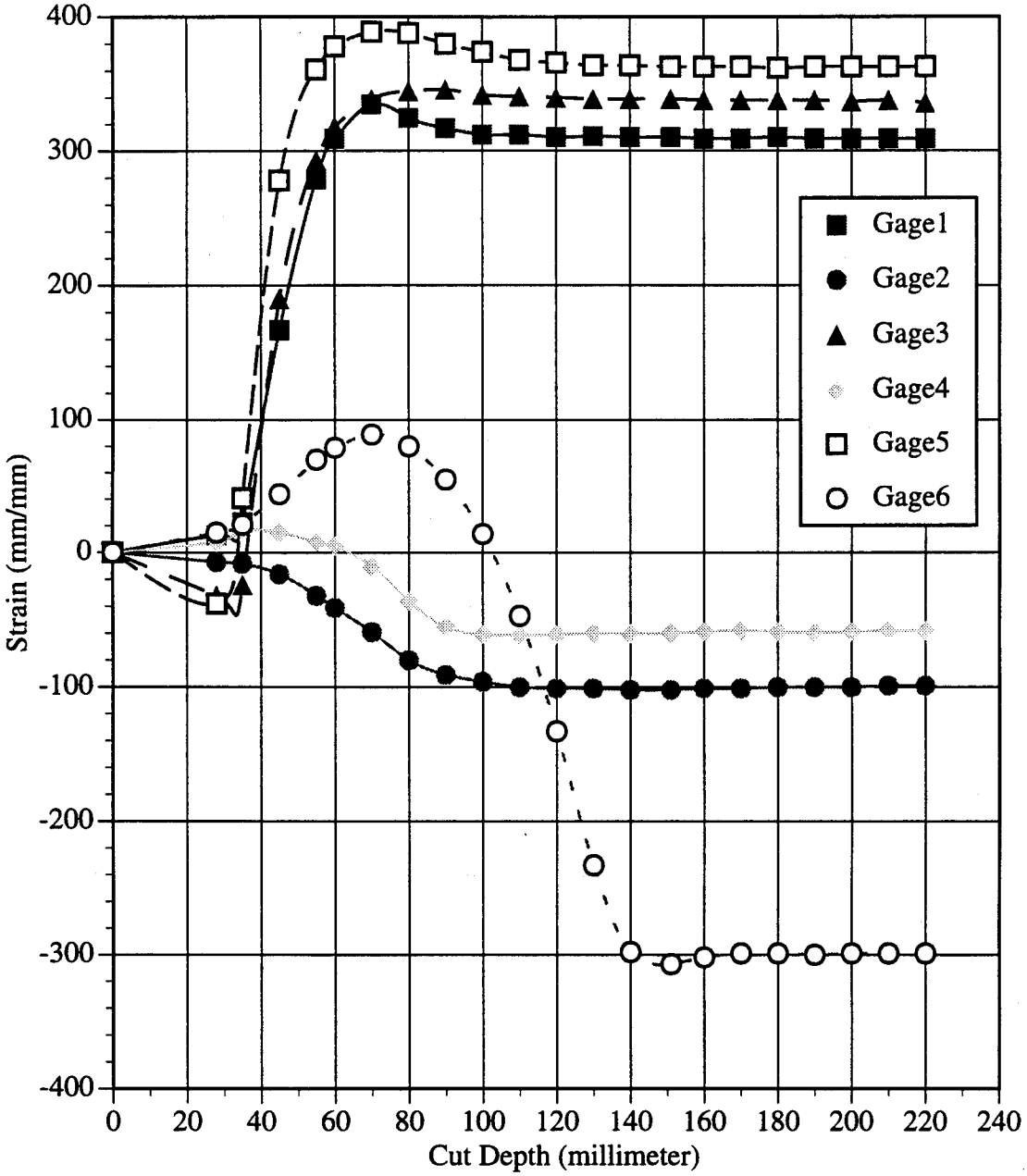

Railroad Wheel No. 8 Test
Wheel Rotation vs. Cut Depth

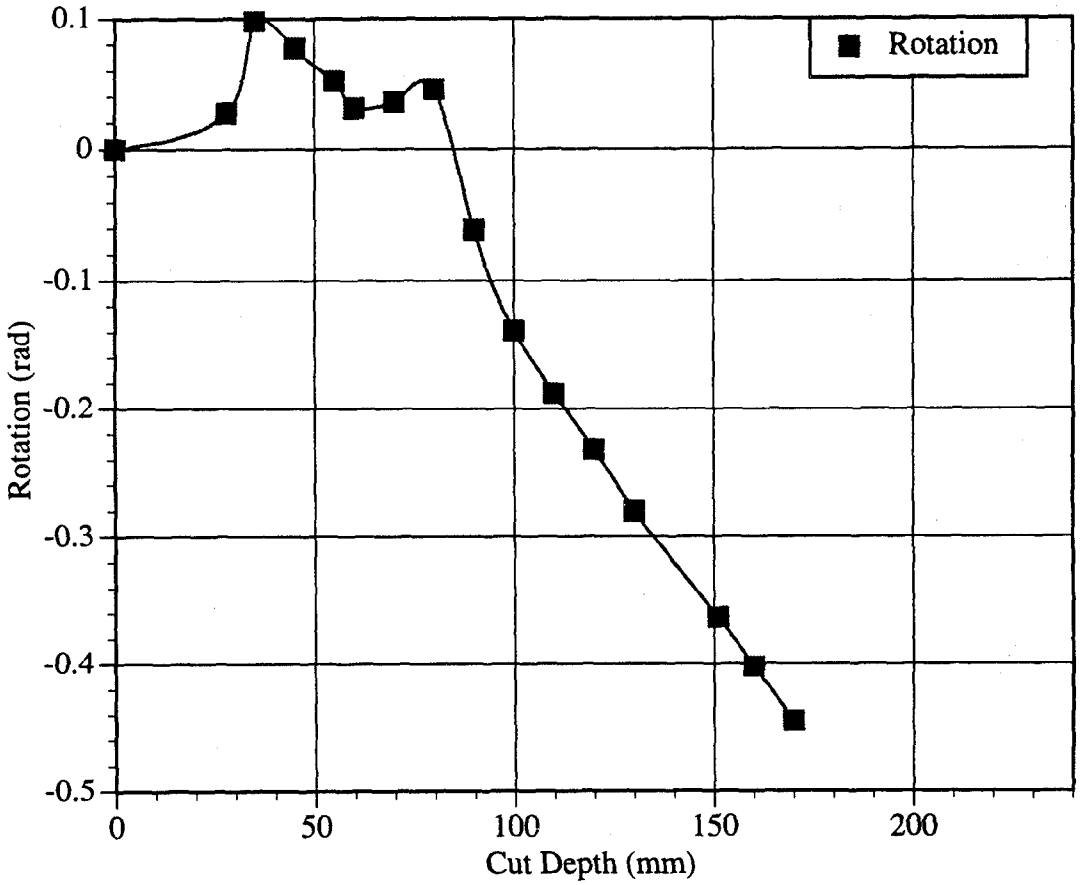

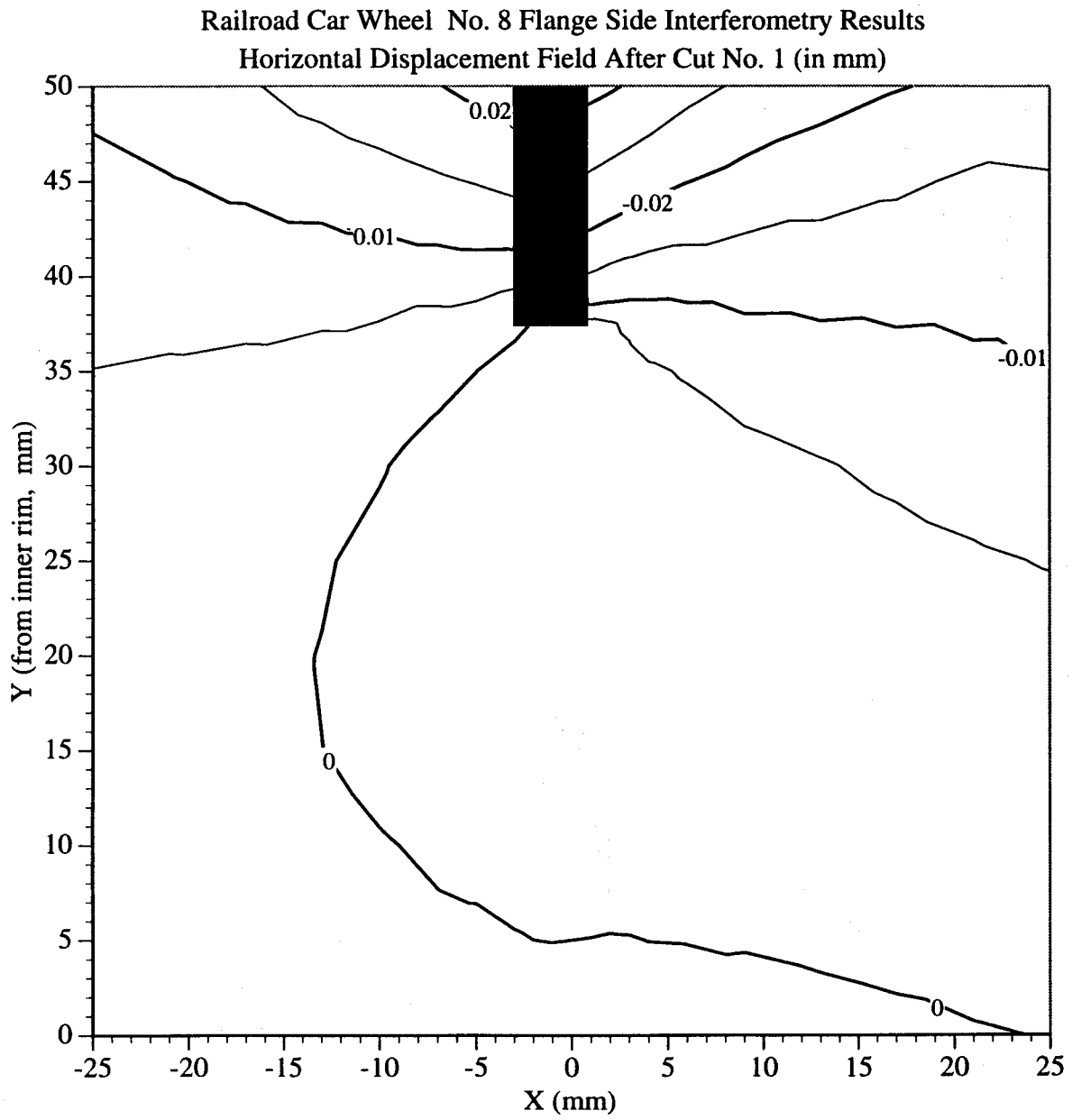
Railroad Car Wheel No. 8 Flange Side Interferometry Results
Horizontal Displacement Field After Cut No. 1 (in mm)
0.02
-0.02
-0.01
-0.01
0
0
Y (from inner rim, mm)
X (mm)
50
45
40
35
30
25
20
15
10
5
0
-25
-20
-15
-10
-5
0
5
10
15
20
25

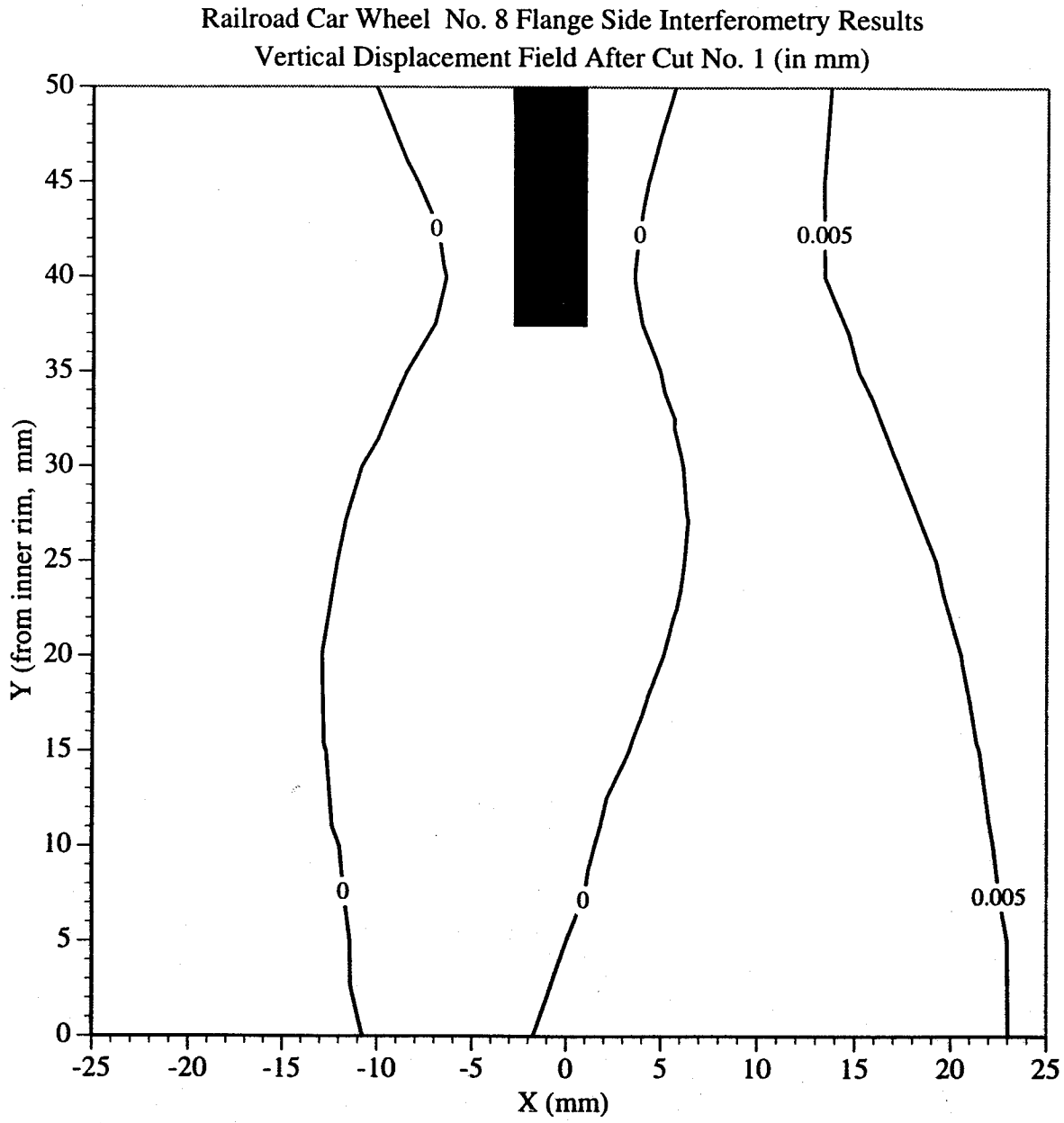
Railroad Car Wheel No. 8 Flange Side Interferometry Results
Vertical Displacement Field After Cut No. 1 (in mm)
Y (from inner rim, mm)
X (mm)
50
45
40
35
30
25
20
15
10
5
0
-25
-20
-15
-10
-5
0
5
10
15
20
25
0
0
0
0
0.005
0.005

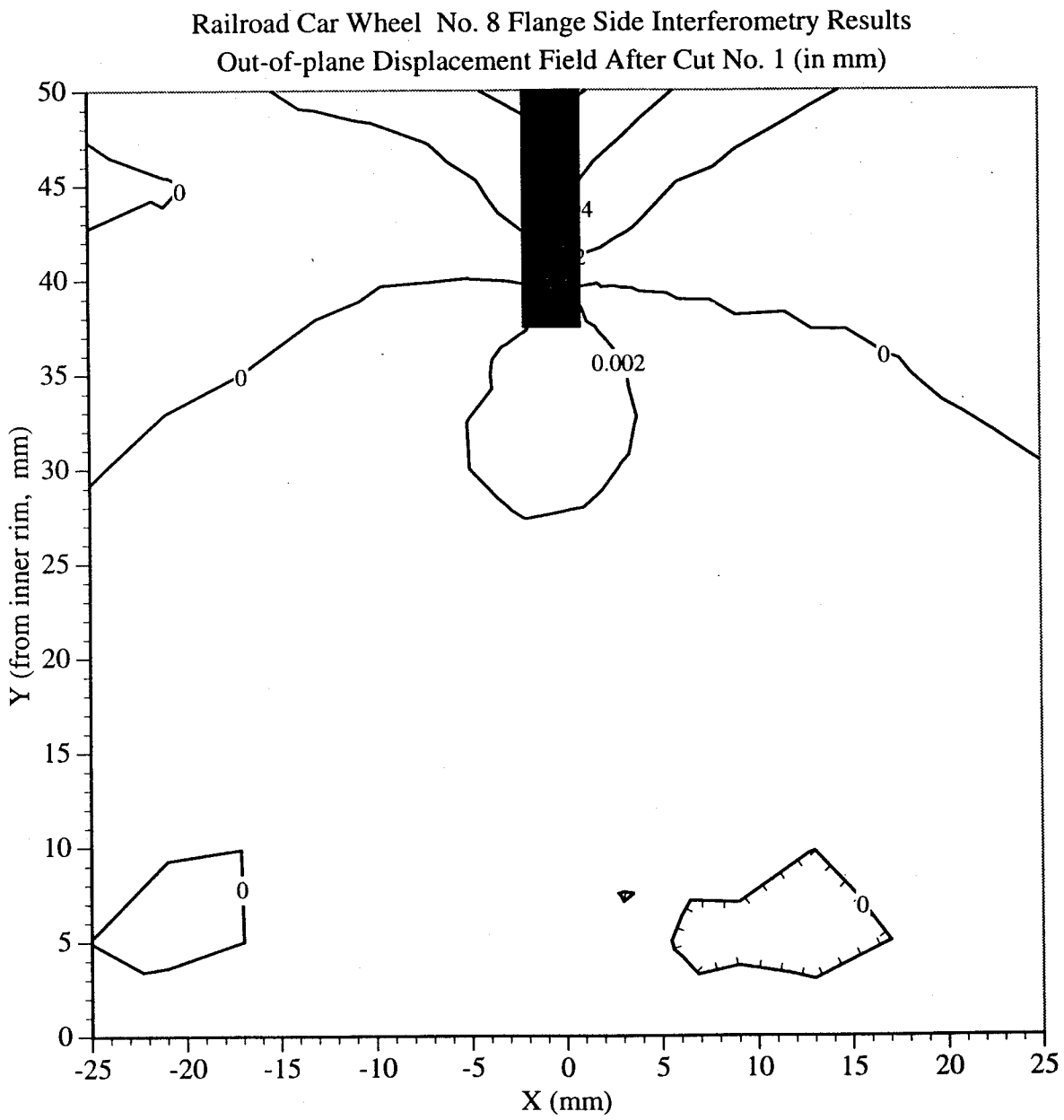
Railroad Car Wheel No. 8 Flange Side Interferometry Results
Out-of-plane Displacement Field After Cut No. 1 (in mm)
Y (from inner rim, mm)
X (mm)
50
45
40
35
30
25
20
15
10
5
0
-25
-20
-15
-10
-5
0
5
10
15
20
25
0
0
0.002
0
0
0

Railroad Car Wheel No. 8 Flange Side Interferometry Results

Residual Strain (ε_x) Field After Cut No. 1 (in mm)

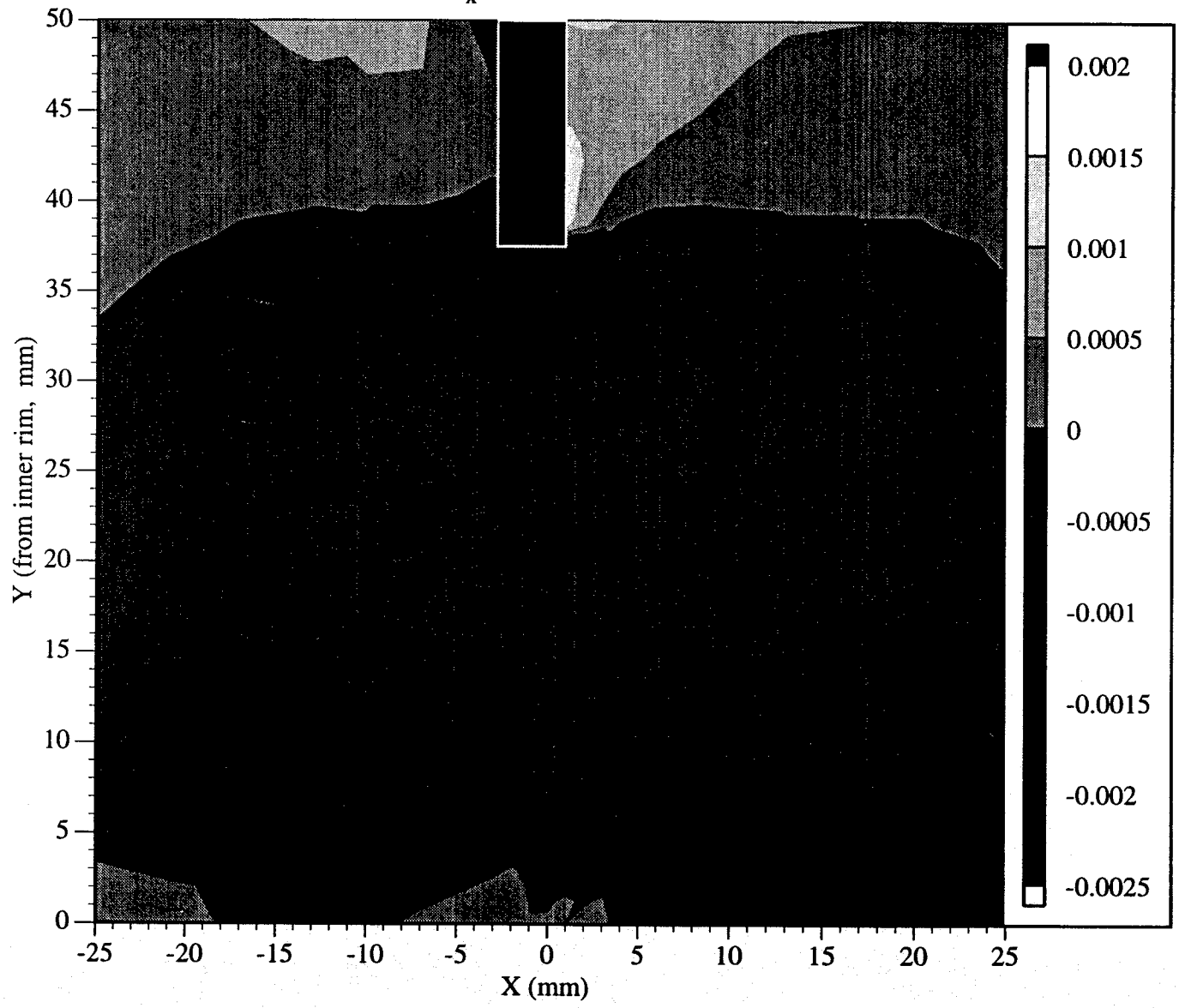

Railroad Car Wheel No. 8 Flange Side Interferometry Results

Residual Strain (ε_y) Field After Cut No. 1 (in mm)

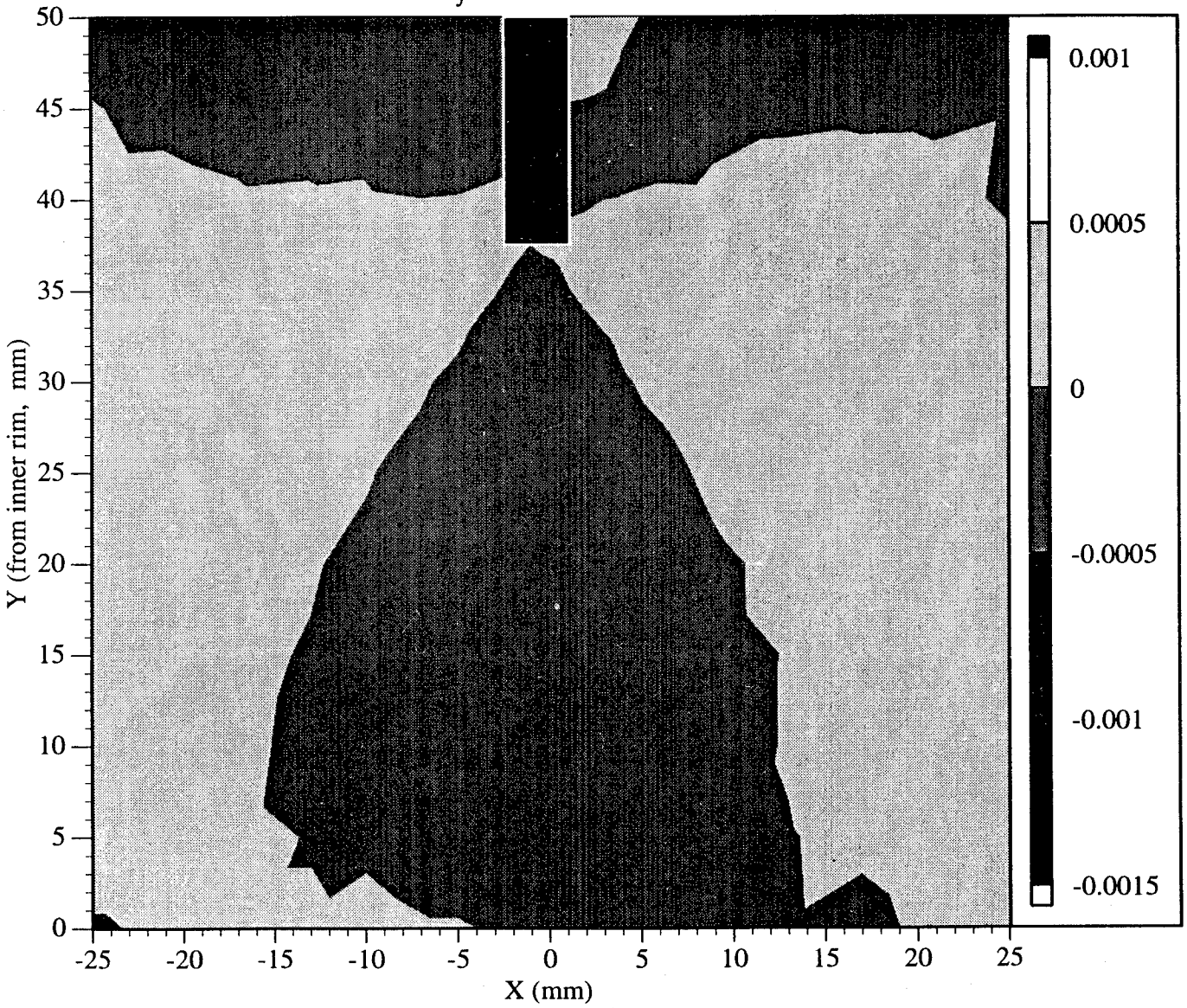

Railroad Car Wheel No. 8 Flange Side Interferometry Results

Residual Strain (γ_{xy}) Field After Cut No. 1 (in mm)

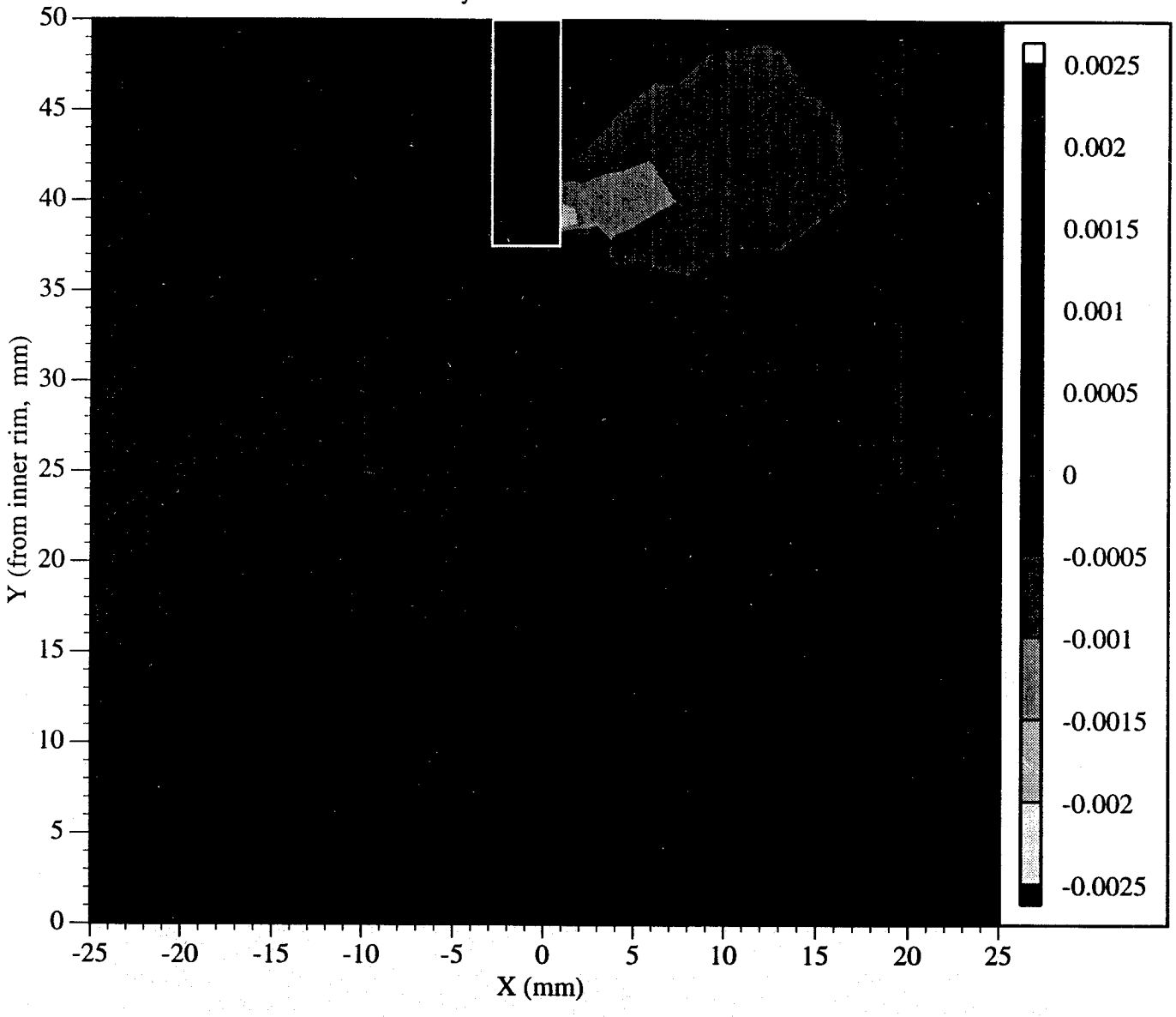

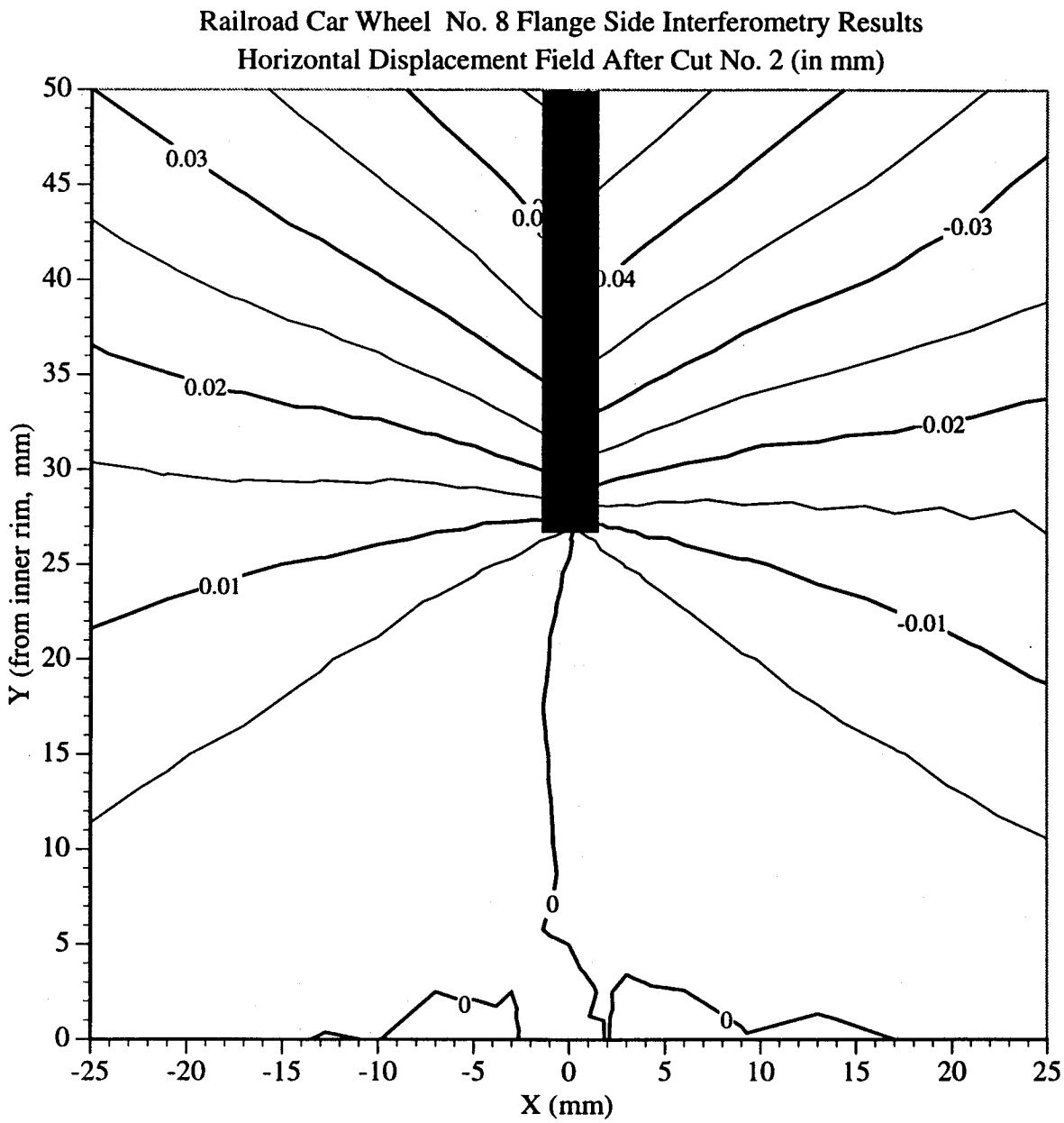
Railroad Car Wheel No. 8 Flange Side Interferometry Results
Horizontal Displacement Field After Cut No. 2 (in mm)
Y (from inner rim, mm)
X (mm)
0.03
0.04
-0.03
0.02
0.02
0.01
-0.01
0
0
0
50
45
40
35
30
25
20
15
10
5
0
-25
-20
-15
-10
-5
0
5
10
15
20
25

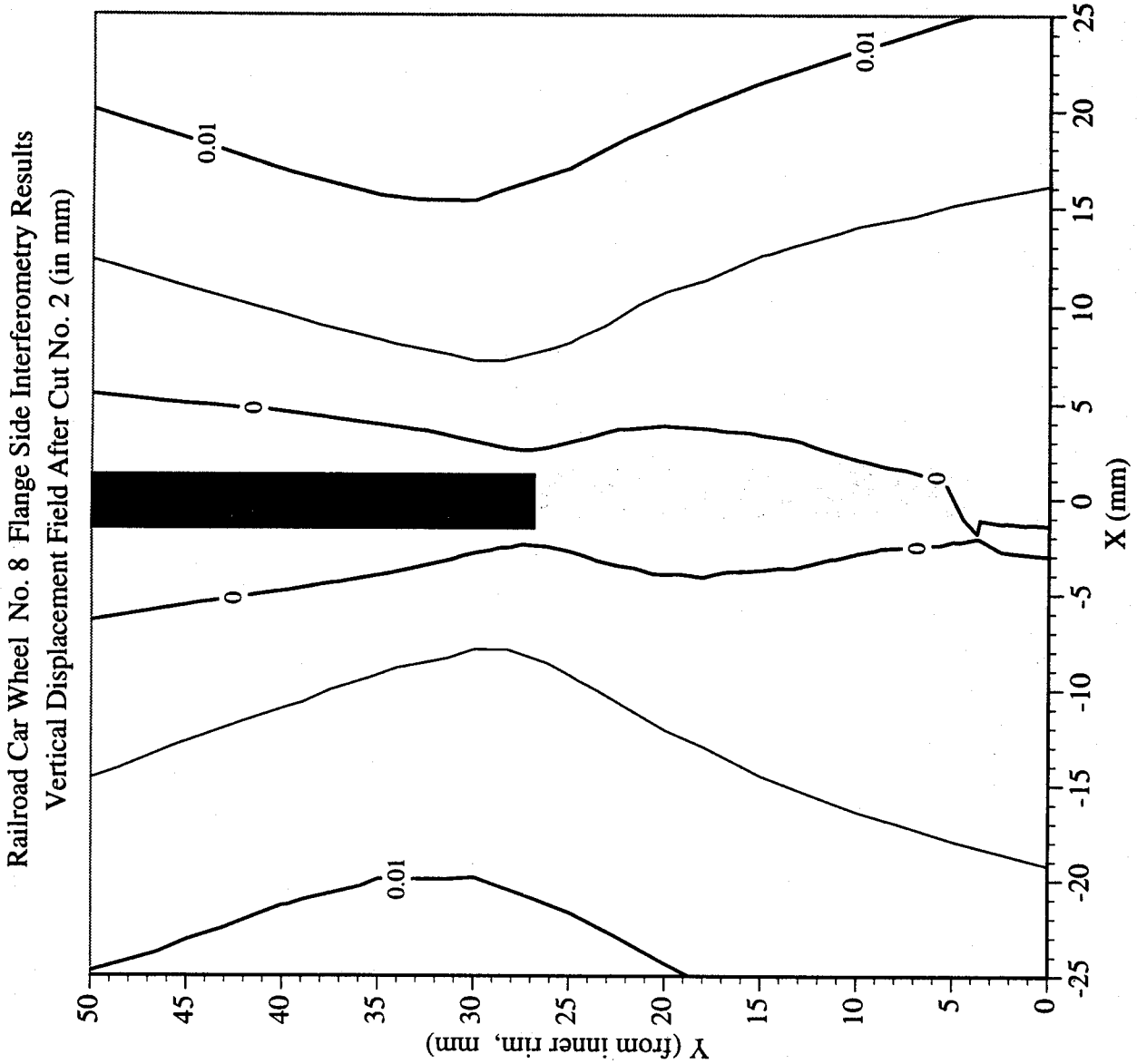
Railroad Car Wheel No. 8 Flange Side Interferometry Results
Vertical Displacement Field After Cut No. 2 (in mm)
0.01
0
0
0
0
0.01
0.01
Y (from inner rim, mm)
X (mm)
50
45
40
35
30
25
20
15
10
5
0
-25
-20
-15
-10
-5
0
5
10
15
20
25

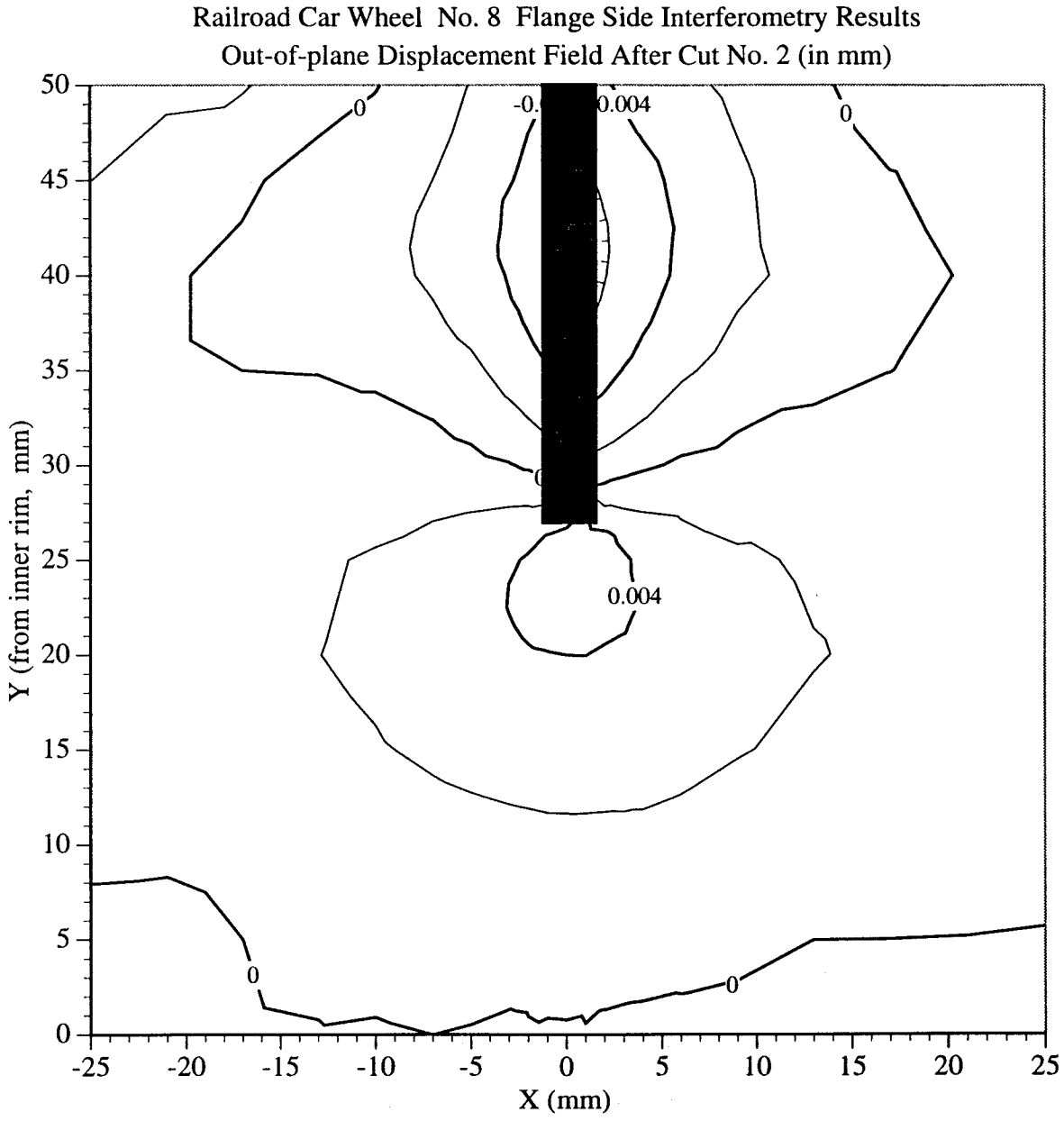
Railroad Car Wheel No. 8 Flange Side Interferometry Results
Out-of-plane Displacement Field After Cut No. 2 (in mm)
Y (from inner rim, mm)
X (mm)
0
0.004
0.004
0
0
0
50
45
40
35
30
25
20
15
10
5
0
-25
-20
-15
-10
-5
0
5
10
15
20
25

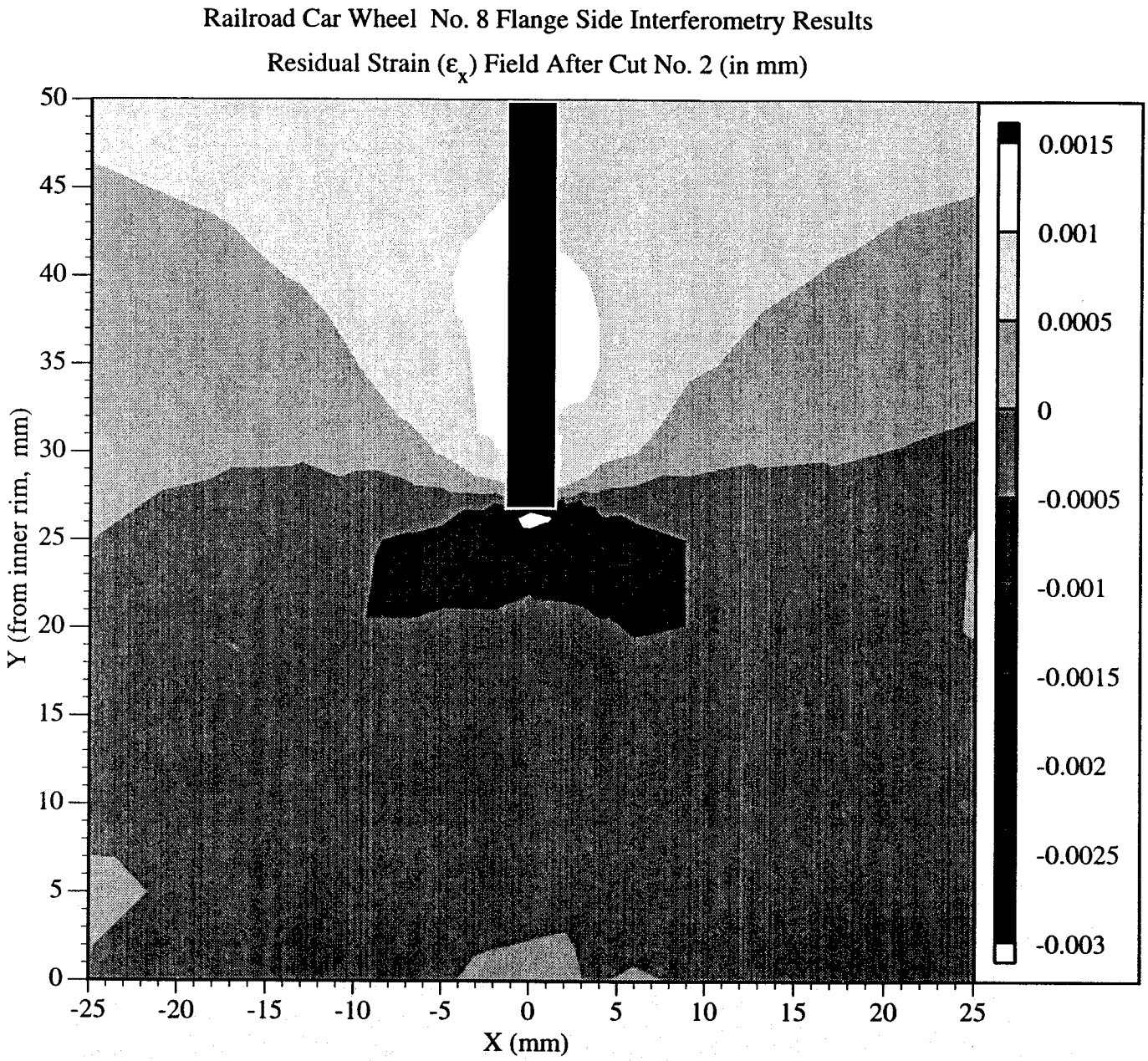
Railroad Car Wheel No. 8 Flange Side Interferometry Results
Residual Strain (ε_x) Field After Cut No. 2 (in mm)
Y (from inner rim, mm)
X (mm)
50
45
40
35
30
25
20
15
10
5
0
-25
-20
-15
-10
-5
0
5
10
15
20
25
0.0015
0.001
0.0005
0
-0.0005
-0.001
-0.0015
-0.002
-0.0025
-0.003

Railroad Car Wheel No. 8 Flange Side Interferometry Results

Residual Strain (ε_y) Field After Cut No. 2 (in mm)

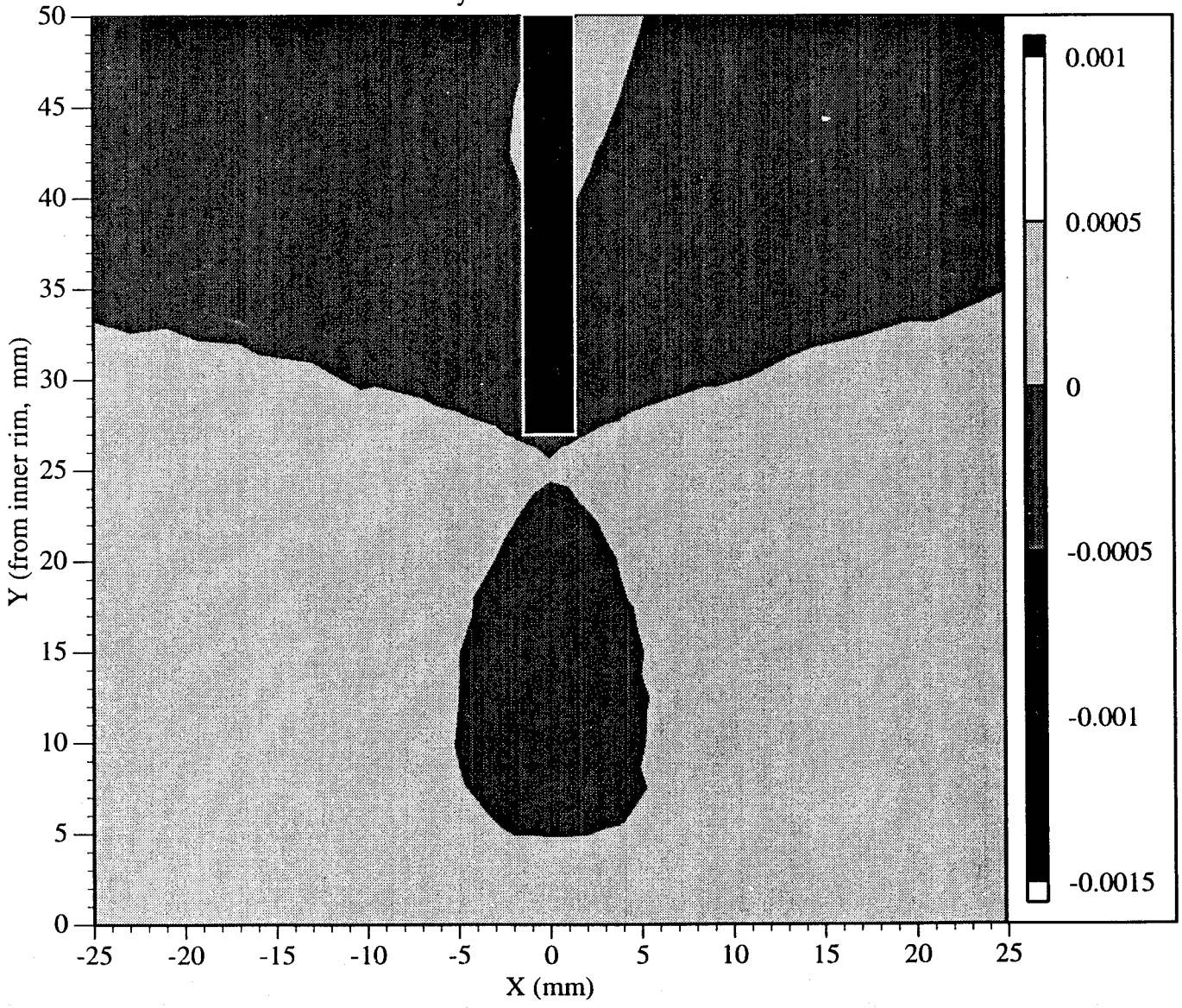

Railroad Car Wheel No. 8 Flange Side Interferometry Results

Residual Strain (γ_{xy}) Field After Cut No. 2 (in mm)

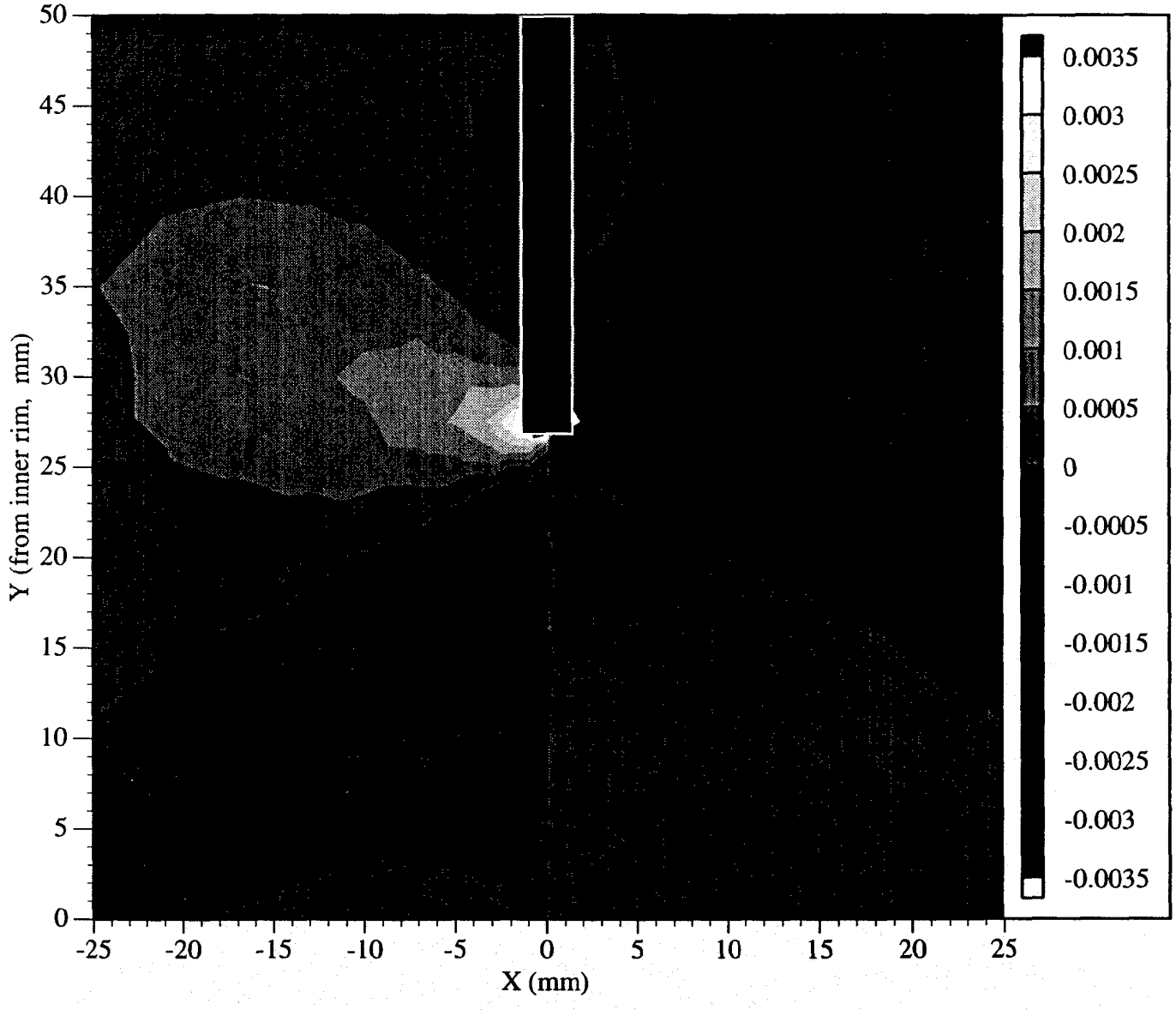

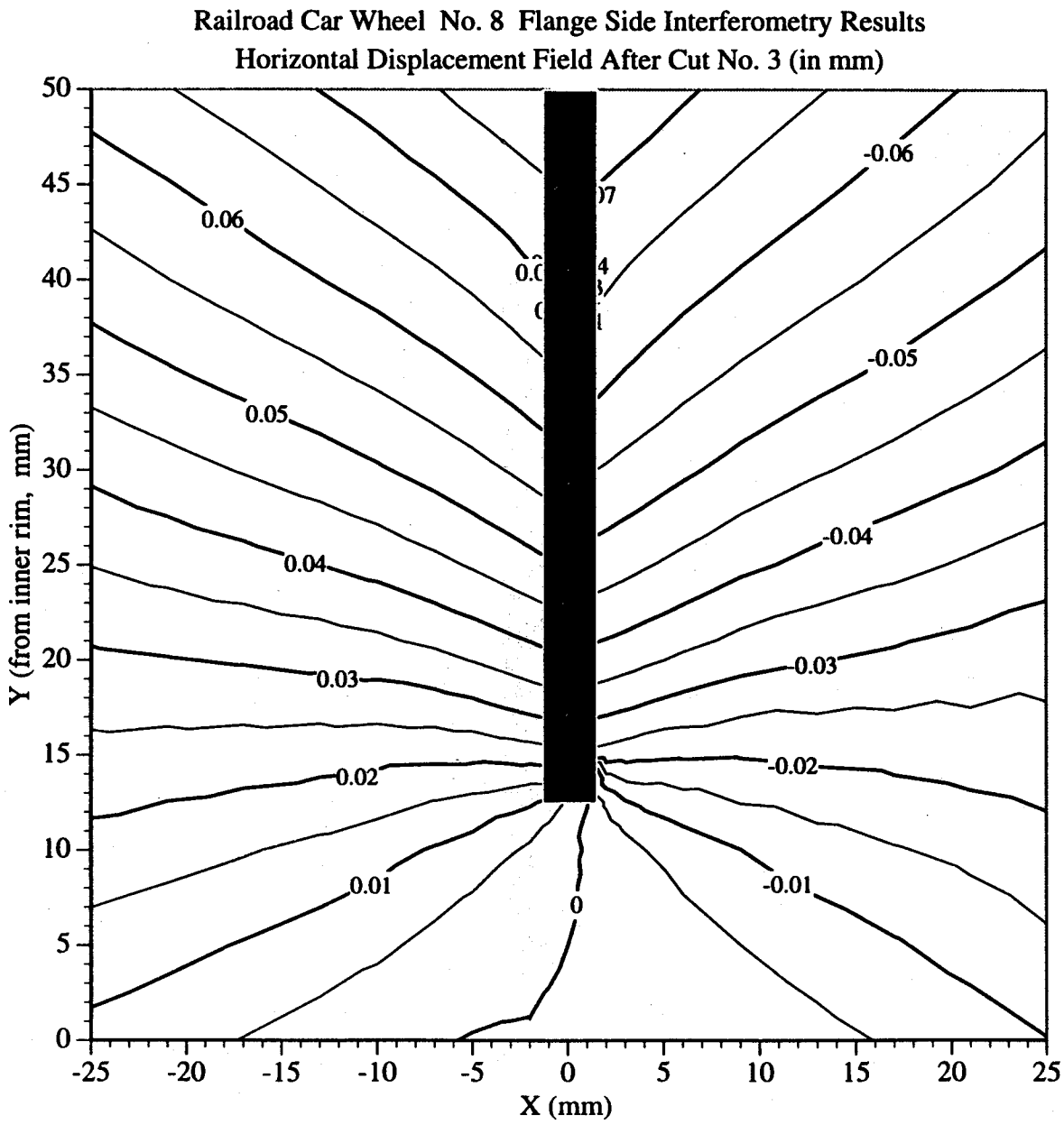
Railroad Car Wheel No. 8 Flange Side Interferometry Results
Horizontal Displacement Field After Cut No. 3 (in mm)
Y (from inner rim, mm)
X (mm)
0.06
0.05
0.04
0.03
0.02
0.01
0
-0.06
-0.05
-0.04
-0.03
-0.02
-0.01
50
45
40
35
30
25
20
15
10
5
0
-25
-20
-15
-10
-5
0
5
10
15
20
25

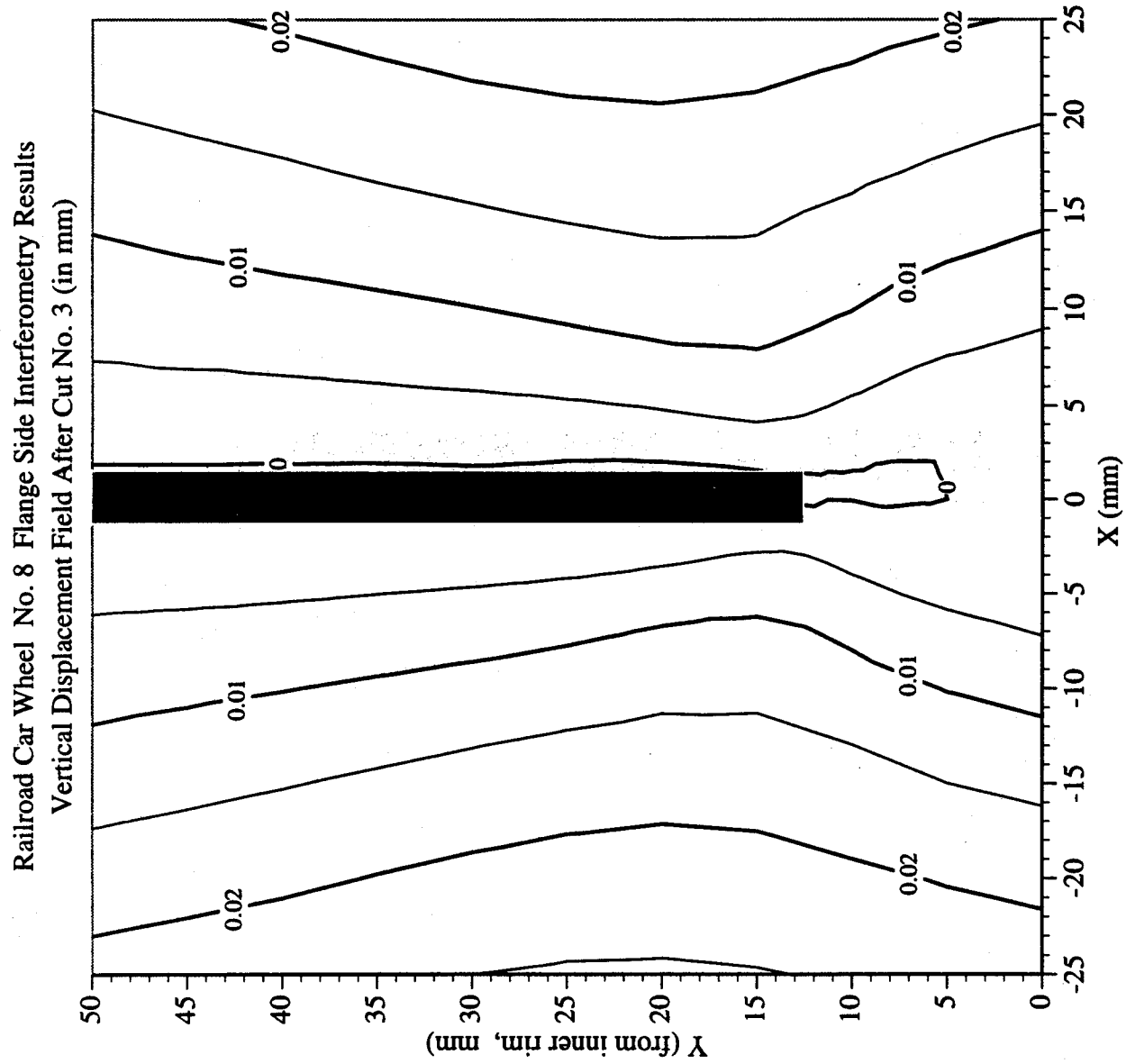
Railroad Car Wheel No. 8 Flange Side Interferometry Results
Vertical Displacement Field After Cut No. 3 (in mm)
Y (from inner rim, mm)
X (mm)
0.02
0.01
0
0.01
0.02
0.02
0.01
0
0.01
0.02
50
45
40
35
30
25
20
15
10
5
0
-25
-20
-15
-10
-5
0
5
10
15
20
25

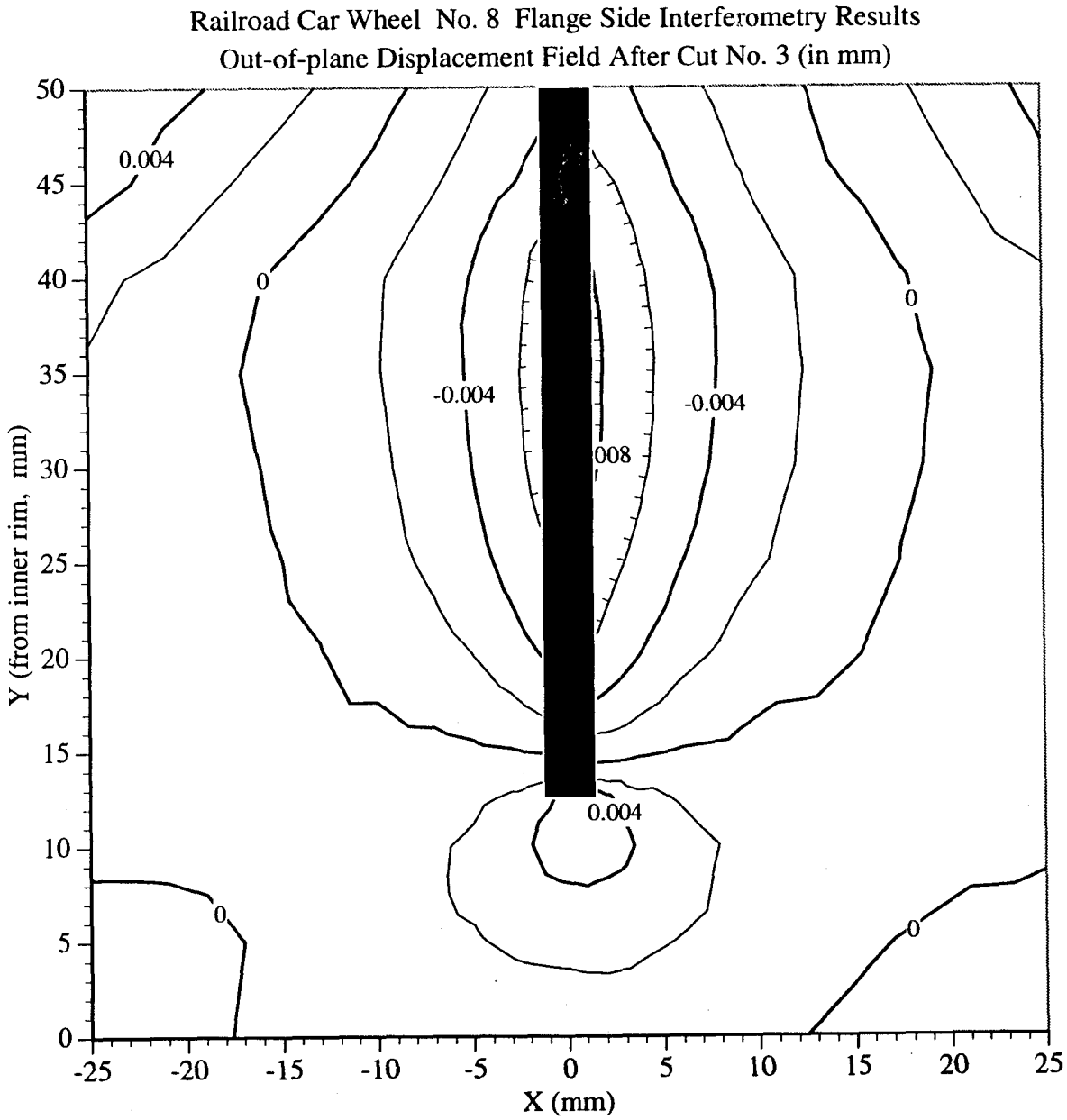
Railroad Car Wheel No. 8 Flange Side Interferometry Results
Out-of-plane Displacement Field After Cut No. 3 (in mm)
Y (from inner rim, mm)
X (mm)
0.004
0
-0.004
-0.004
008
0.004
0
0
0
50
45
40
35
30
25
20
15
10
5
0
-25
-20
-15
-10
-5
0
5
10
15
20
25

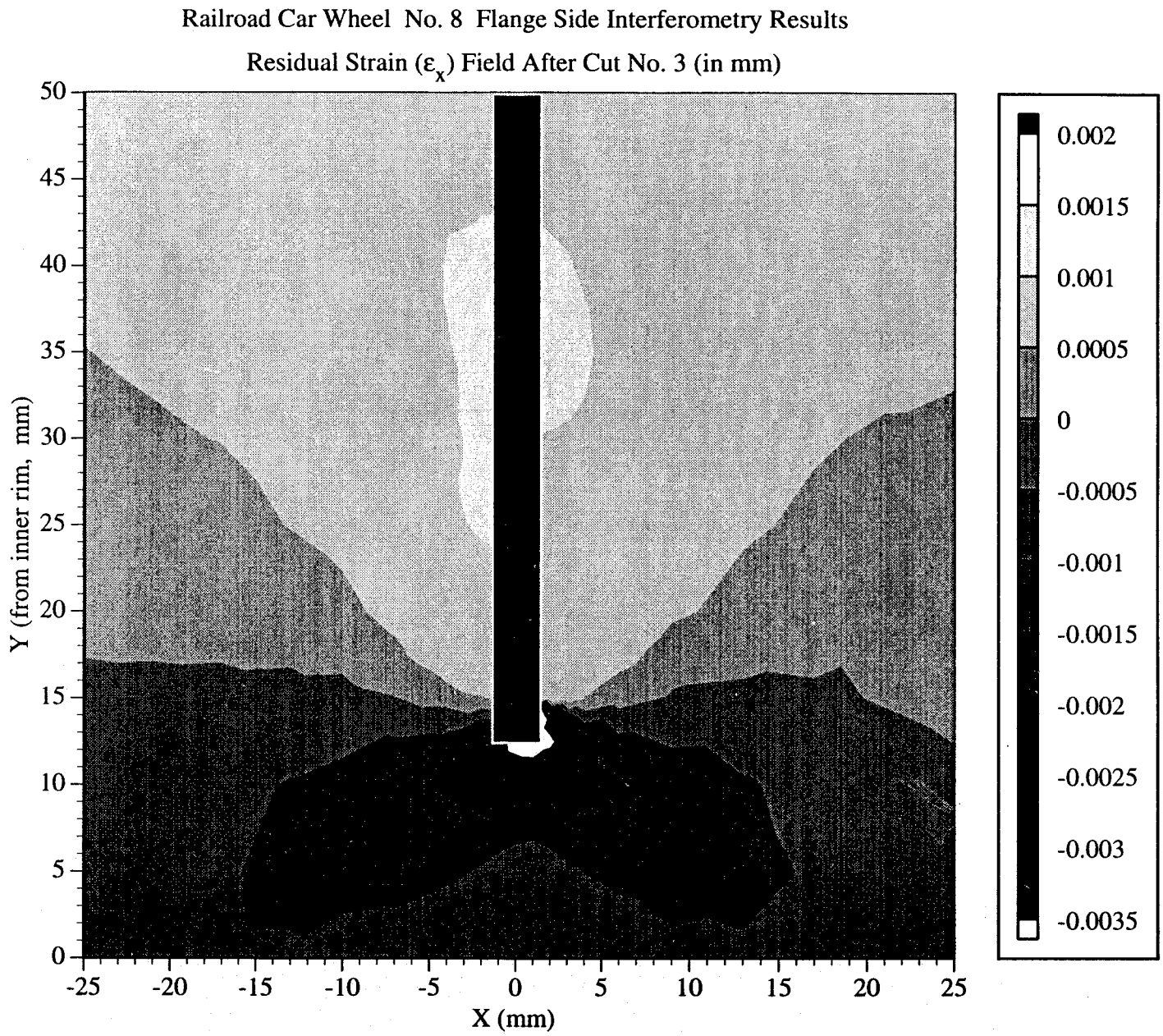
Railroad Car Wheel No. 8 Flange Side Interferometry Results
Residual Strain (ε_x) Field After Cut No. 3 (in mm)
Y (from inner rim, mm)
X (mm)
50
45
40
35
30
25
20
15
10
5
0
-25
-20
-15
-10
-5
0
5
10
15
20
25
0.002
0.0015
0.001
0.0005
0
-0.0005
-0.001
-0.0015
-0.002
-0.0025
-0.003
-0.0035

Railroad Car Wheel No. 8 Flange Side Interferometry Results

Residual Strain (ε_y) Field After Cut No. 3 (in mm)

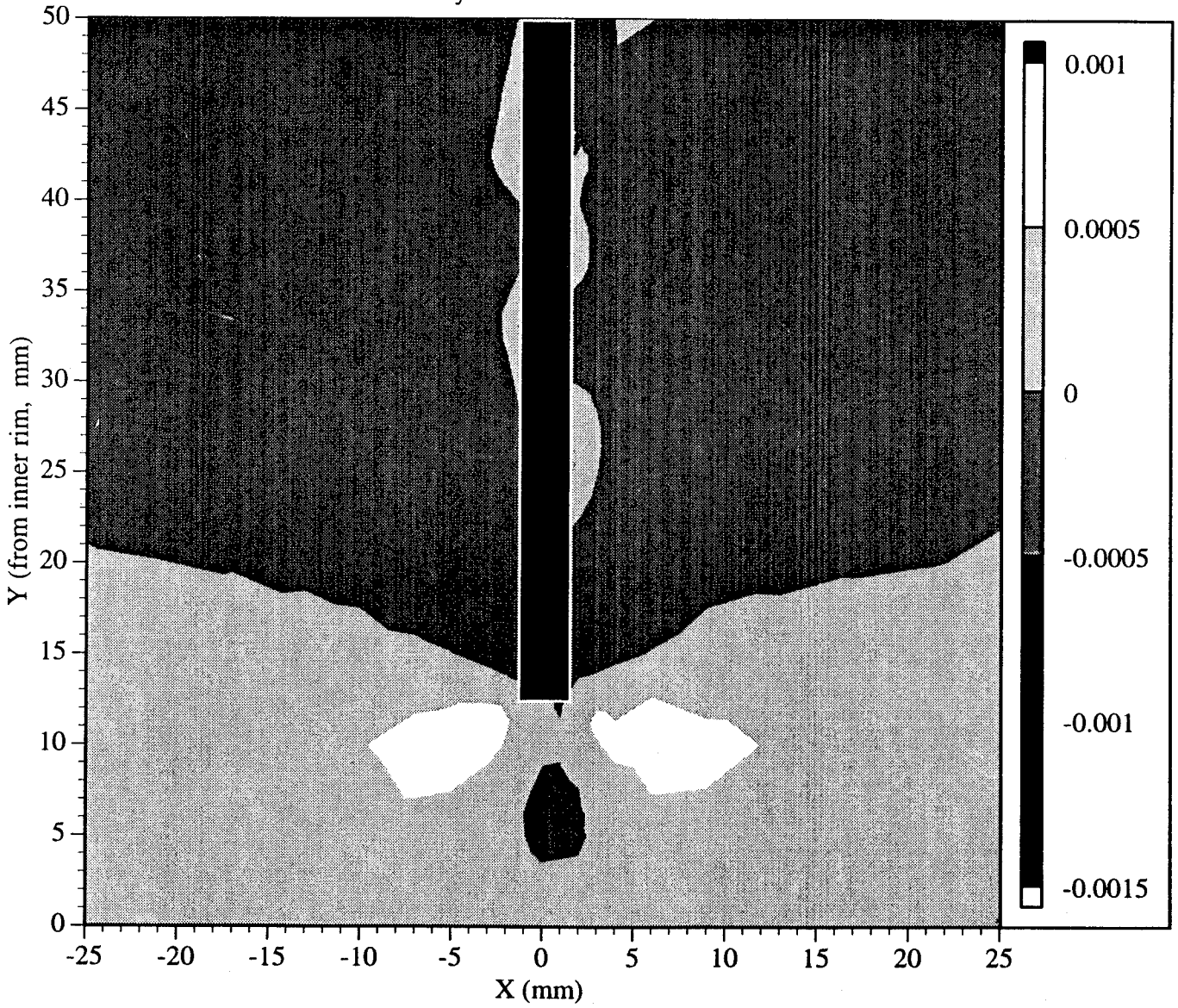

Railroad Car Wheel No. 8 Flange Side Interferometry Results

Residual Strain (γ_{xy}) Field After Cut No. 3 (in mm)

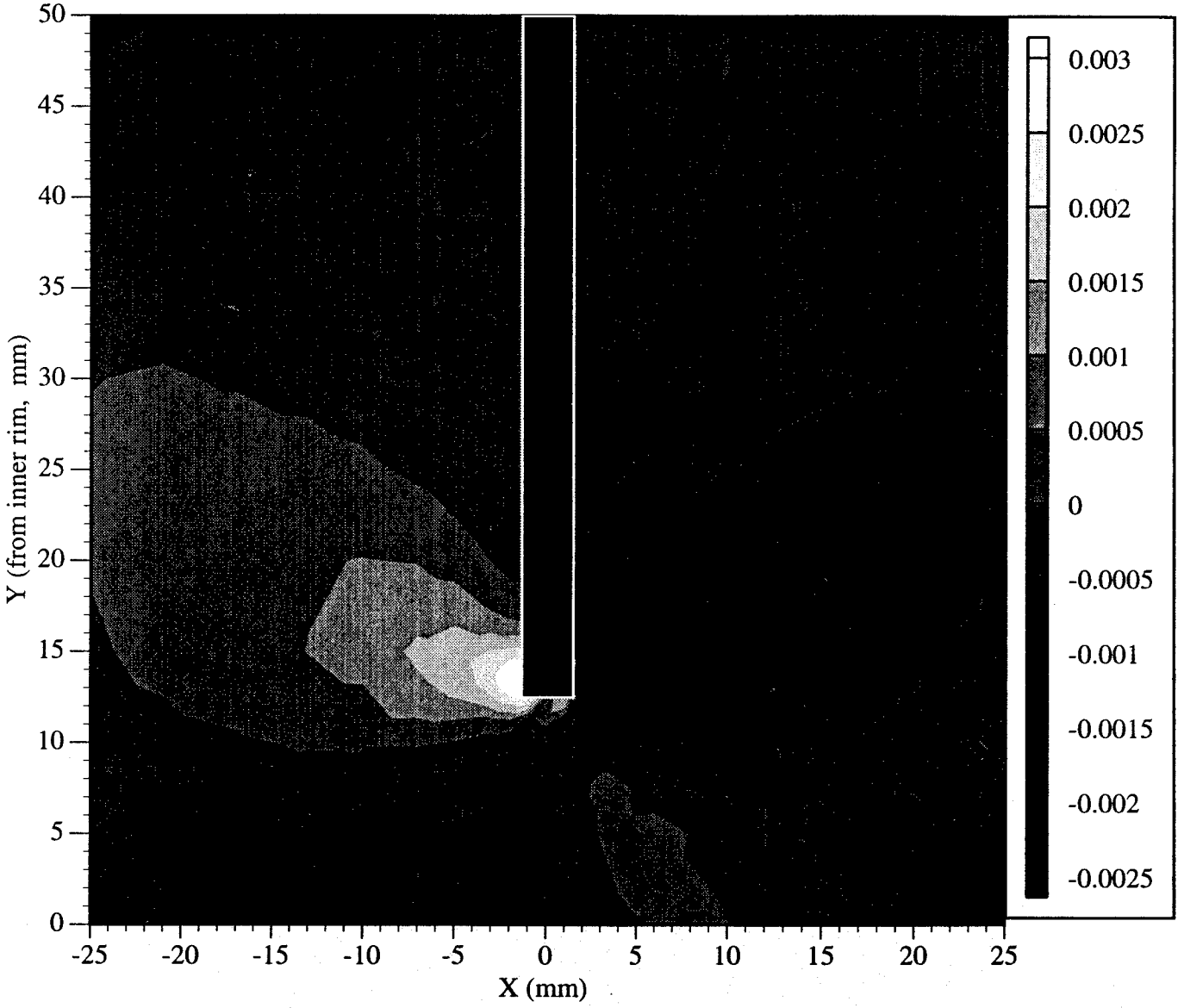

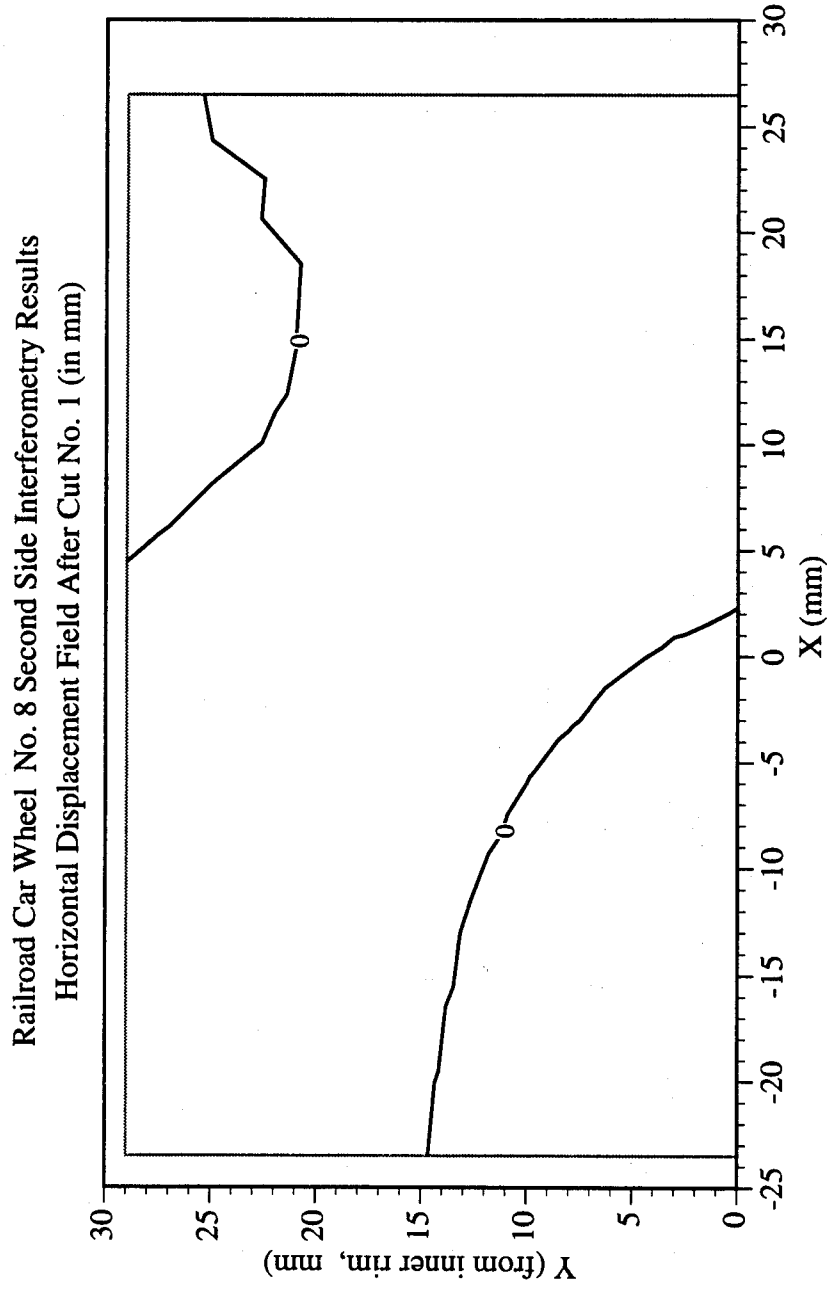
Railroad Car Wheel No. 8 Second Side Interferometry Results
Horizontal Displacement Field After Cut No. 1 (in mm)
Y (from inner rim, mm)
X (mm)
0
0
30
25
20
15
10
5
0
-25
-20
-15
-10
-5
0
5
10
15
20
25
30

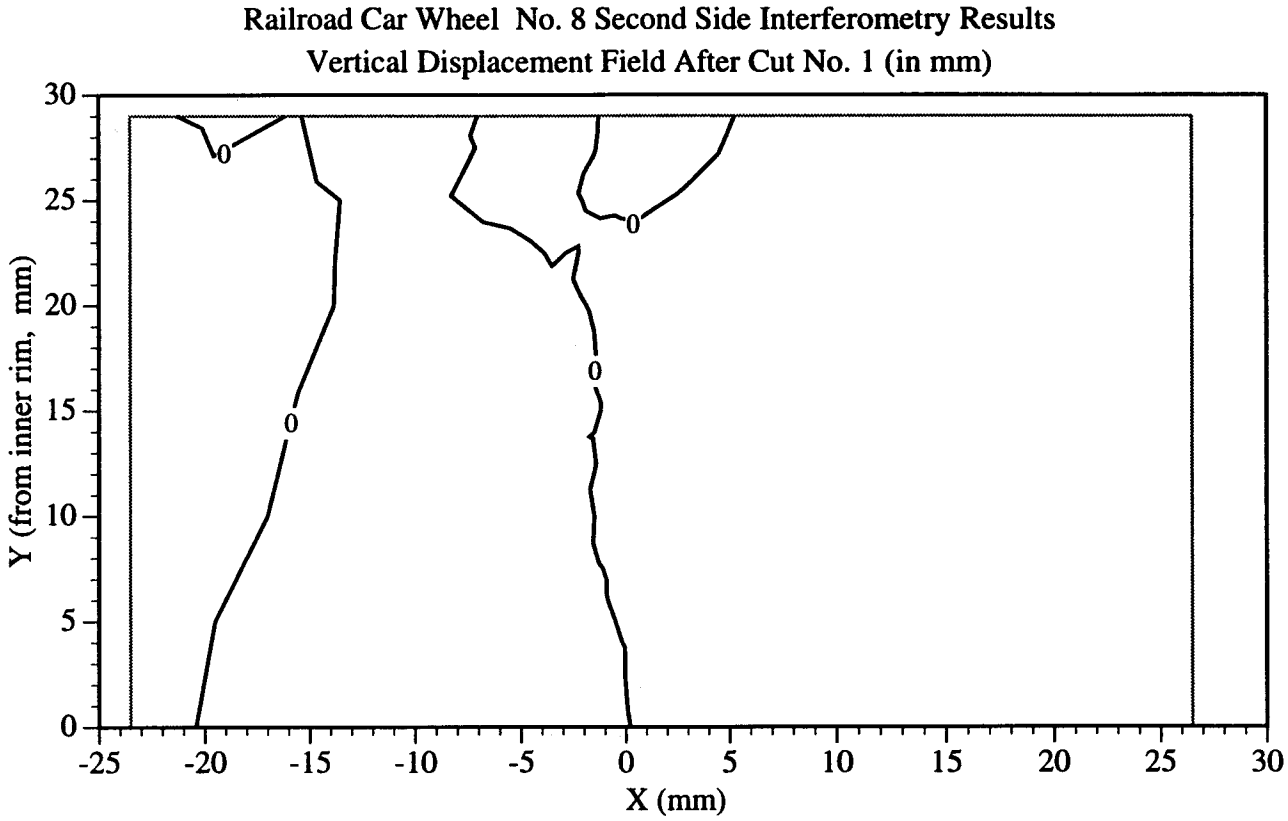
Railroad Car Wheel No. 8 Second Side Interferometry Results
Vertical Displacement Field After Cut No. 1 (in mm)
Y (from inner rim, mm)
X (mm)
30
25
20
15
10
5
0
-25
-20
-15
-10
-5
0
5
10
15
20
25
30
0
0
0
0

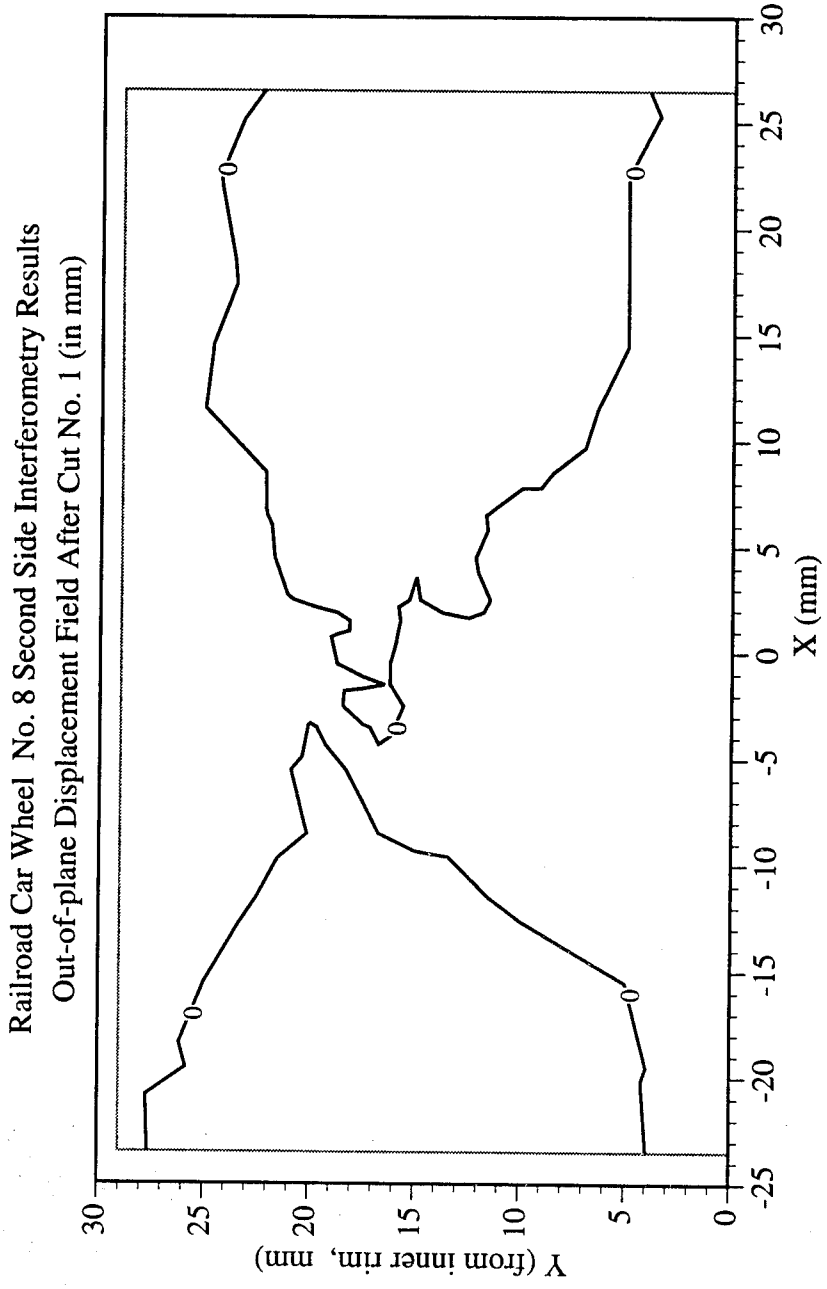
Railroad Car Wheel No. 8 Second Side Interferometry Results
Out-of-plane Displacement Field After Cut No. 1 (in mm)
Y (from inner rim, mm)
X (mm)
30
25
20
15
10
5
0
-25
-20
-15
-10
-5
0
5
10
15
20
25
30
0
0
0
0
0

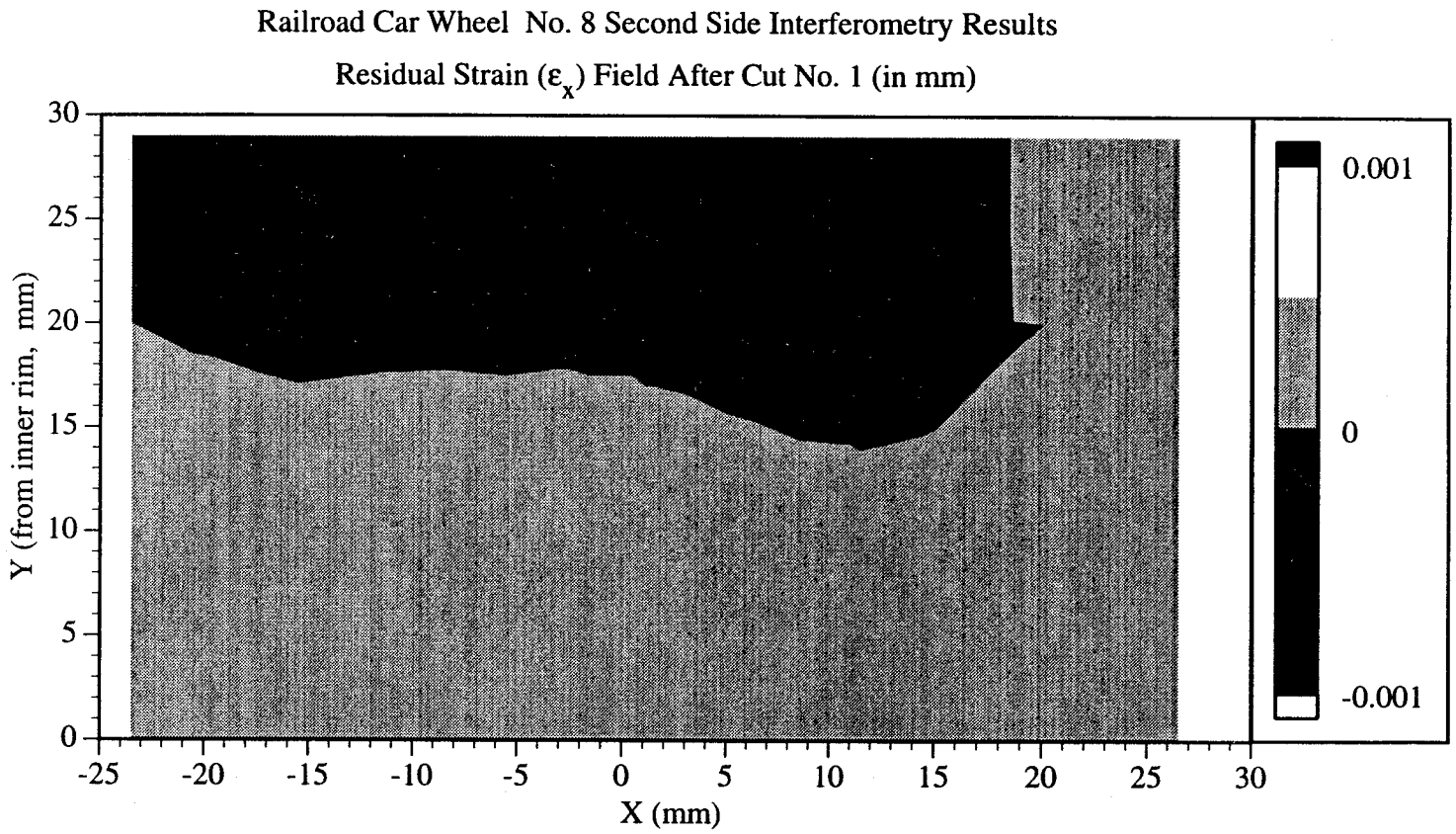
Railroad Car Wheel No. 8 Second Side Interferometry Results
Residual Strain (ε_x) Field After Cut No. 1 (in mm)
Y (from inner rim, mm)
30
25
20
15
10
5
0
-25
-20
-15
-10
-5
0
5
10
15
20
25
30
X (mm)
0.001
0
-0.001

Railroad Car Wheel No. 8 Second Side Interferometry Results

Residual Strain (ε_y) Field After Cut No. 1 (in mm)

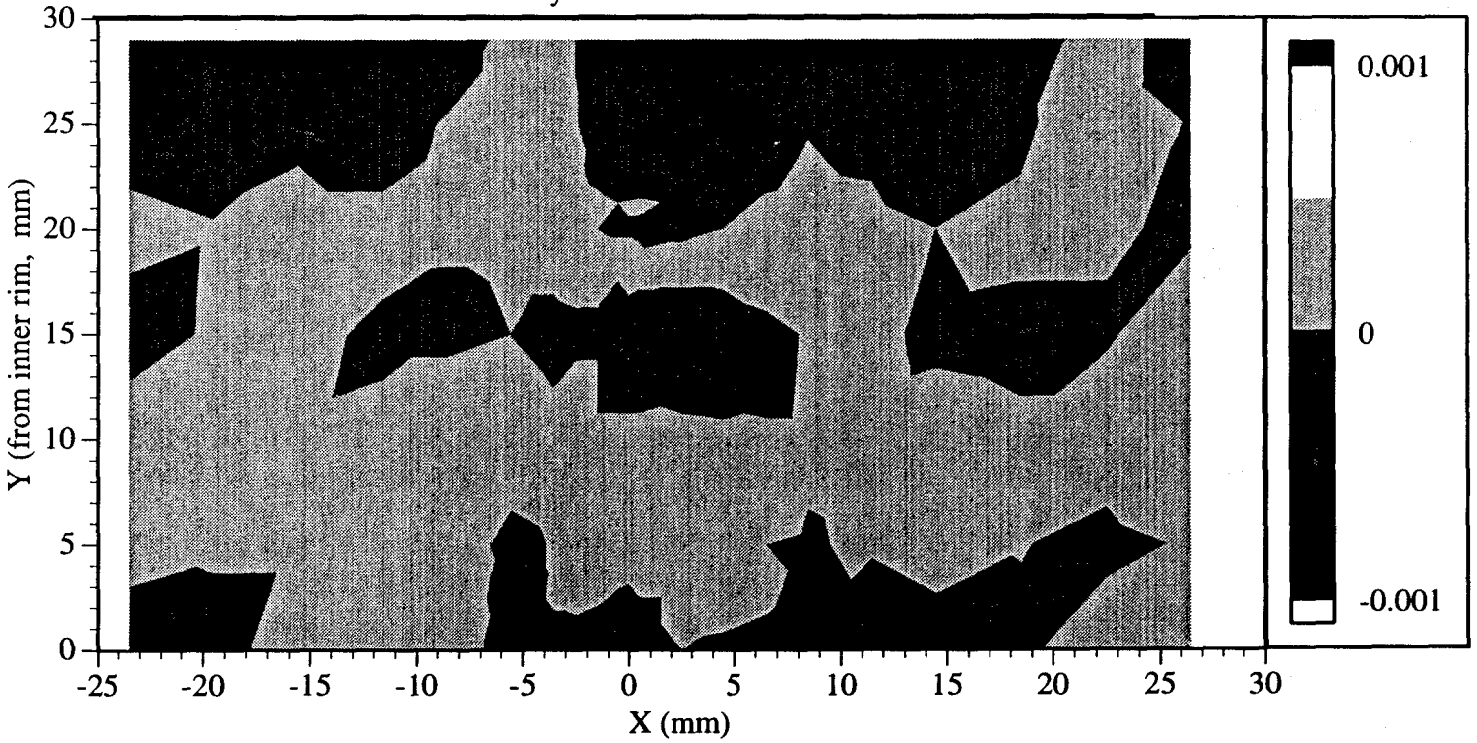

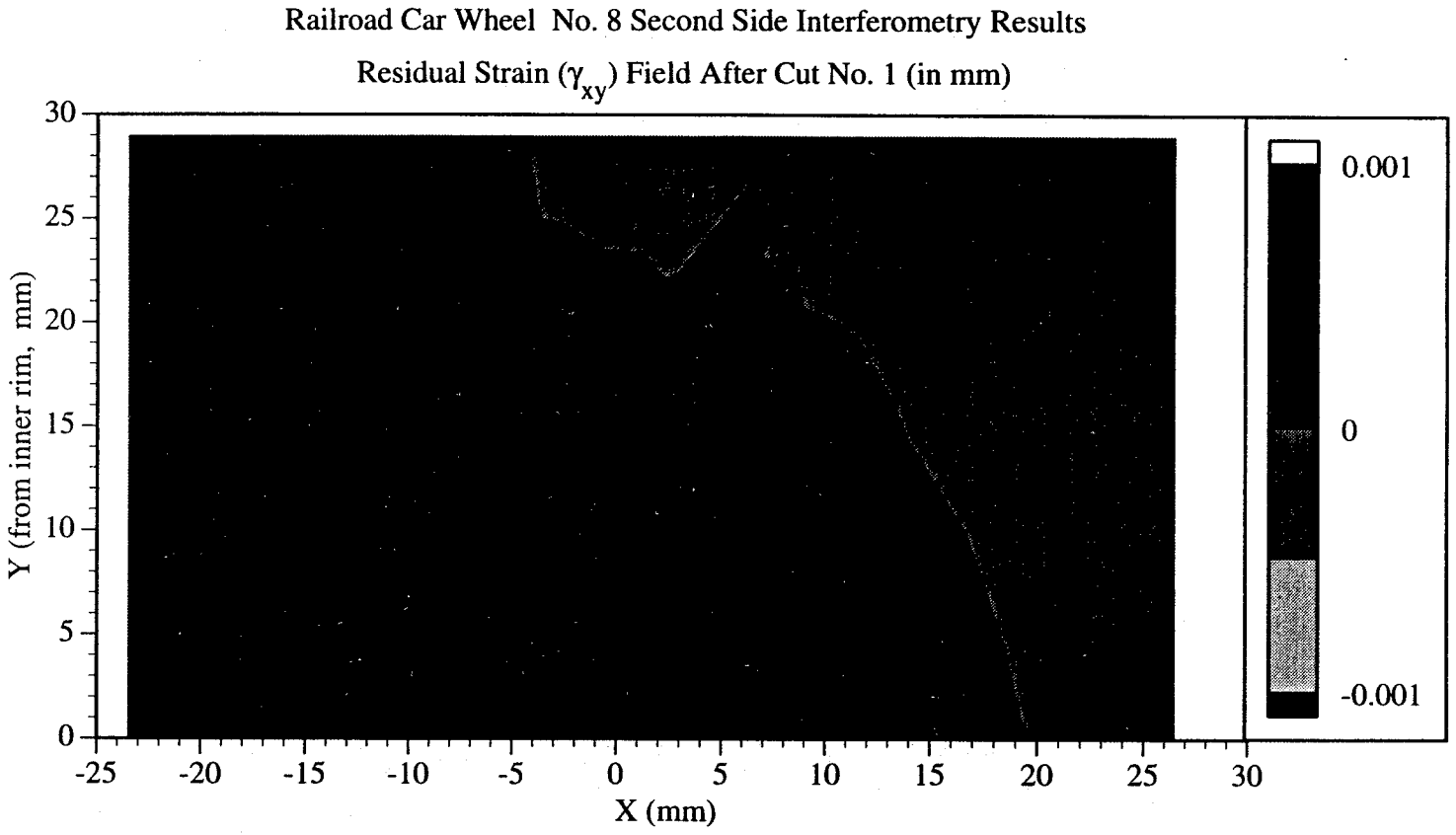
Railroad Car Wheel No. 8 Second Side Interferometry Results
Residual Strain (γ_{xy}) Field After Cut No. 1 (in mm)
Y (from inner rim, mm)
X (mm)
0.001
0
-0.001

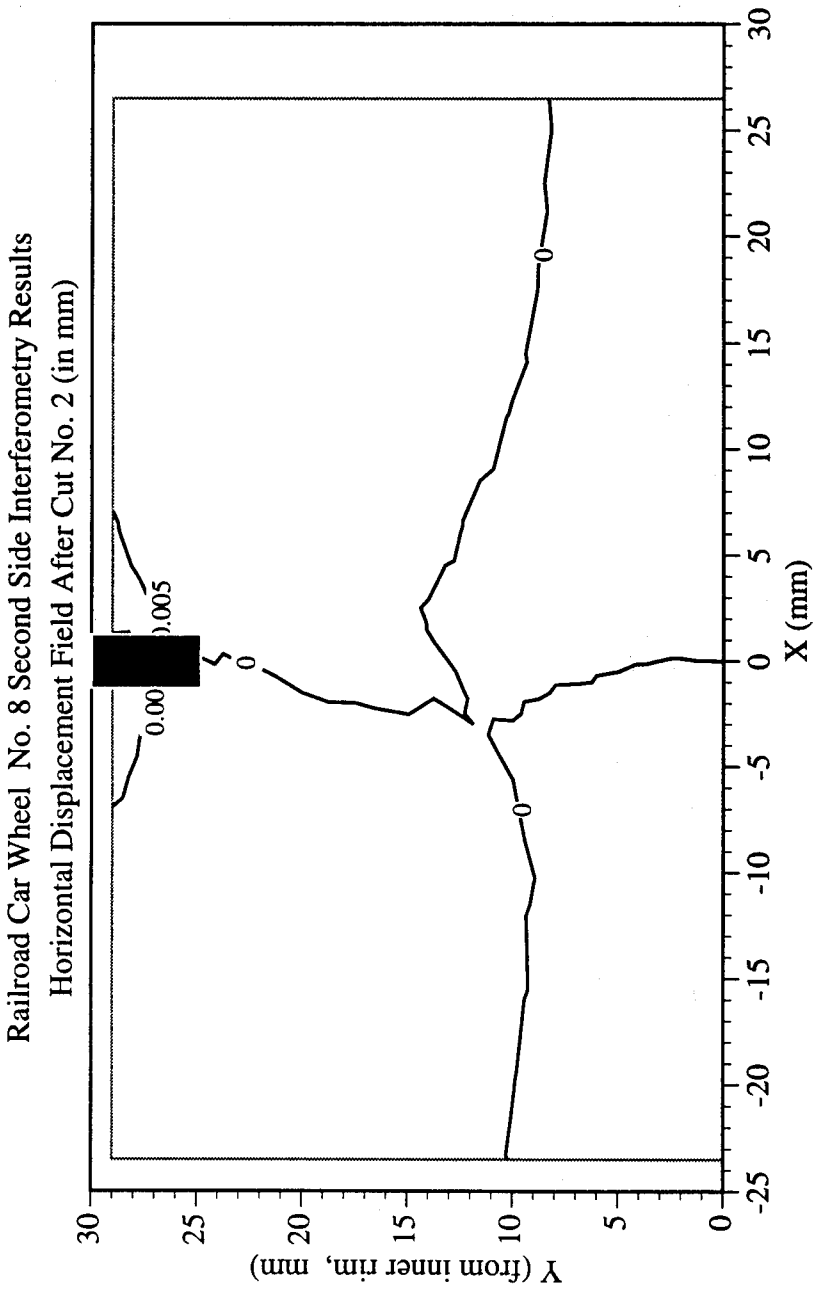
Railroad Car Wheel No. 8 Second Side Interferometry Results
Horizontal Displacement Field After Cut No. 2 (in mm)
0.00
0.005
0
0
0
Y (from inner rim, mm)
X (mm)
30
25
20
15
10
5
0
-25
-20
-15
-10
-5
0
5
10
15
20
25
30

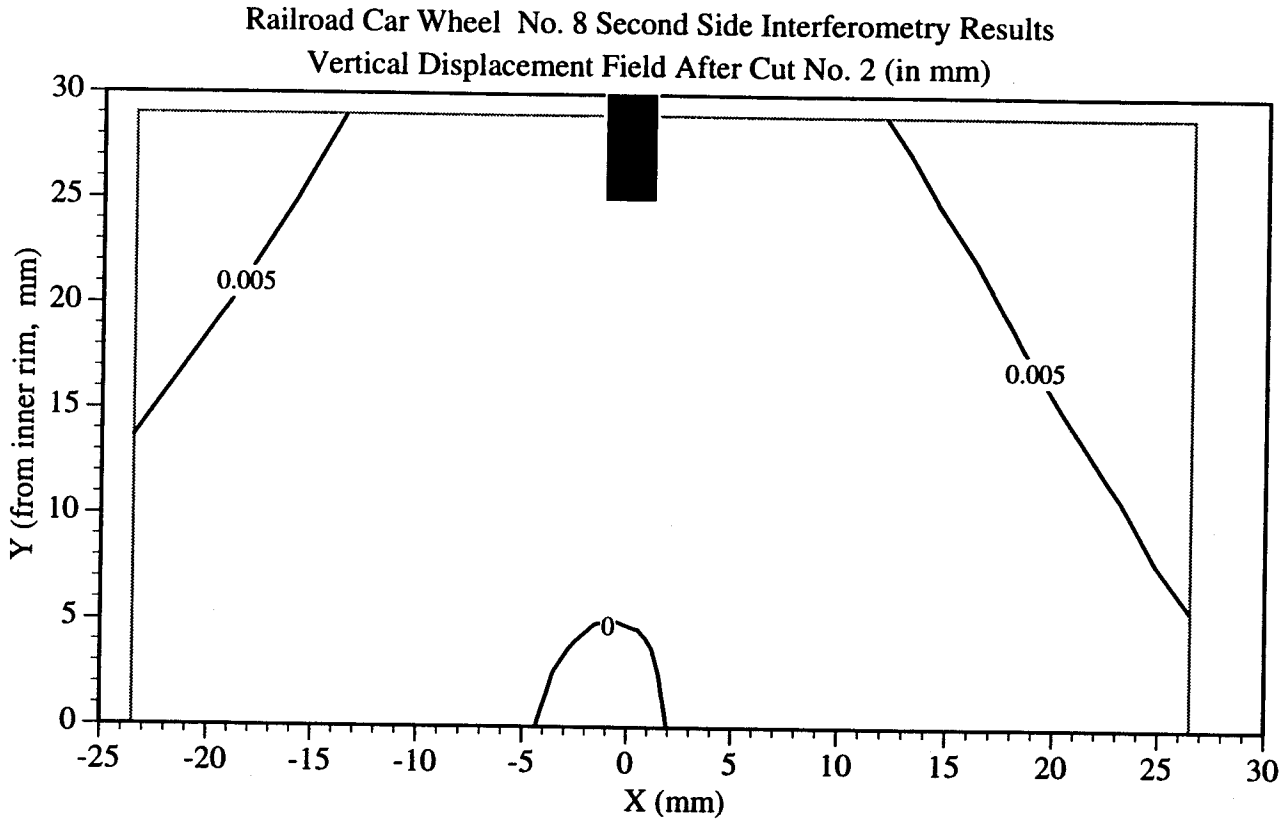
Railroad Car Wheel No. 8 Second Side Interferometry Results
Vertical Displacement Field After Cut No. 2 (in mm)
Y (from inner rim, mm)
X (mm)
0.005
0.005
0
30
25
20
15
10
5
0
-25
-20
-15
-10
-5
0
5
10
15
20
25
30

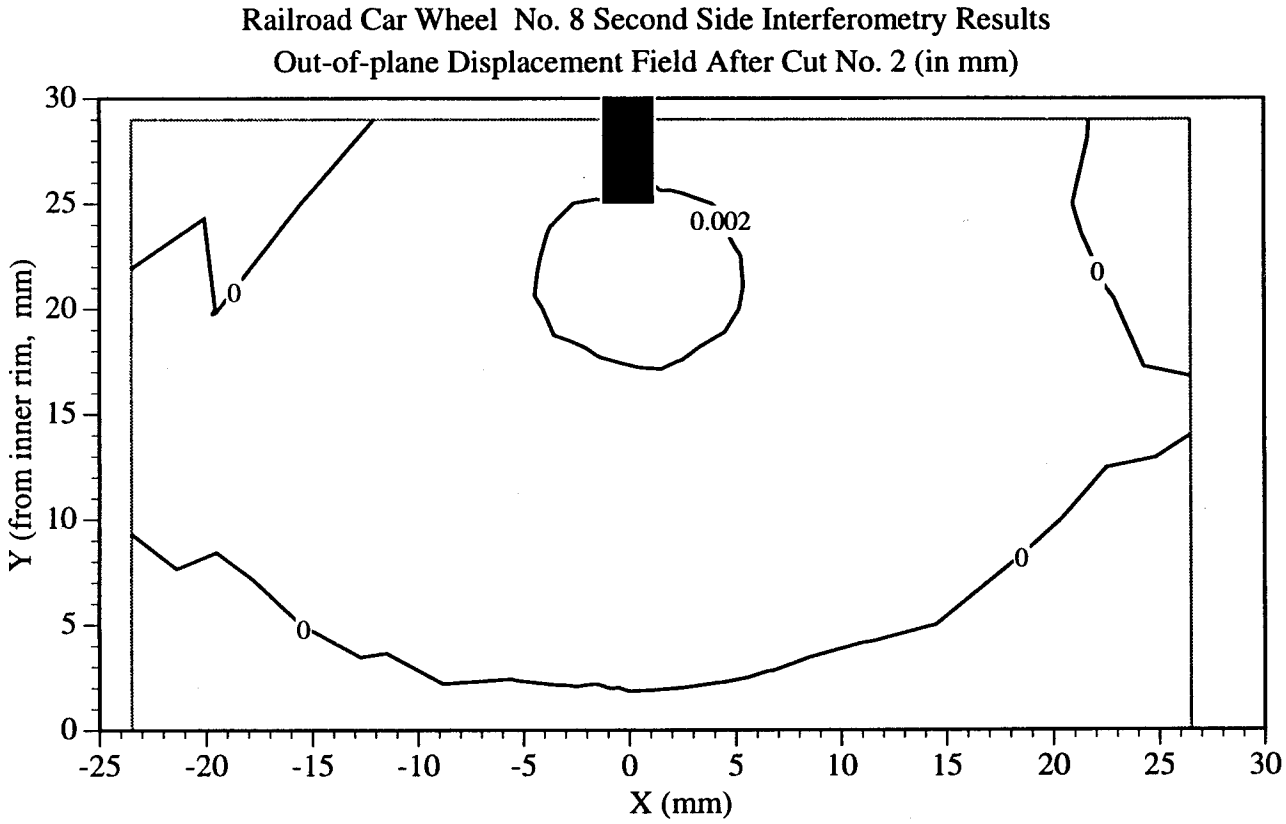
Railroad Car Wheel No. 8 Second Side Interferometry Results
Out-of-plane Displacement Field After Cut No. 2 (in mm)
Y (from inner rim, mm)
X (mm)
0.002
0
0
0
0
30
25
20
15
10
5
0
-25
-20
-15
-10
-5
0
5
10
15
20
25
30

Railroad Car Wheel No. 8 Second Side Interferometry Results

Residual Strain (ε_x) Field After Cut No. 2 (in mm)

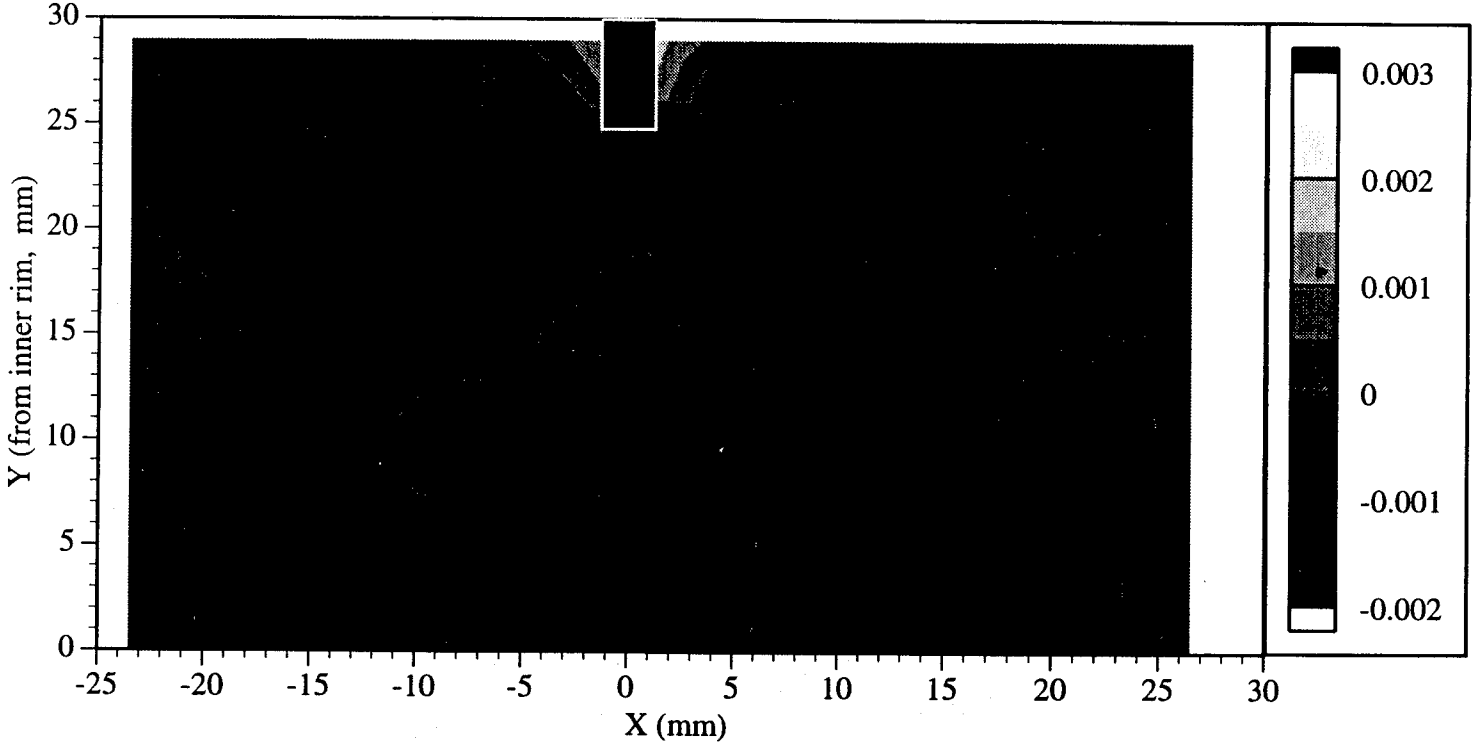

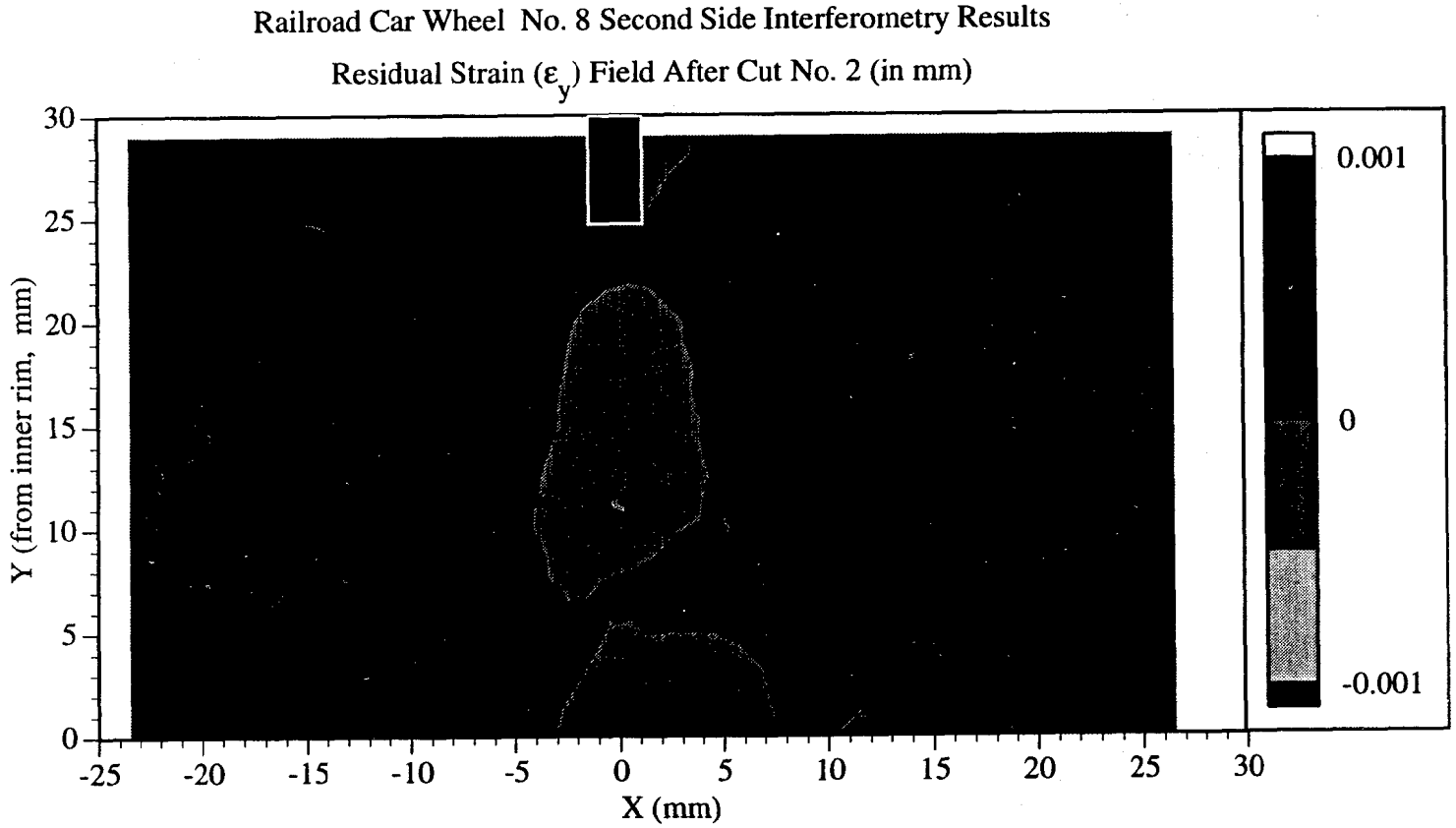
Railroad Car Wheel No. 8 Second Side Interferometry Results
Residual Strain (ε_y) Field After Cut No. 2 (in mm)
Y (from inner rim, mm)
30
25
20
15
10
5
0
-25
-20
-15
-10
-5
0
5
10
15
20
25
30
X (mm)
0.001
0
-0.001

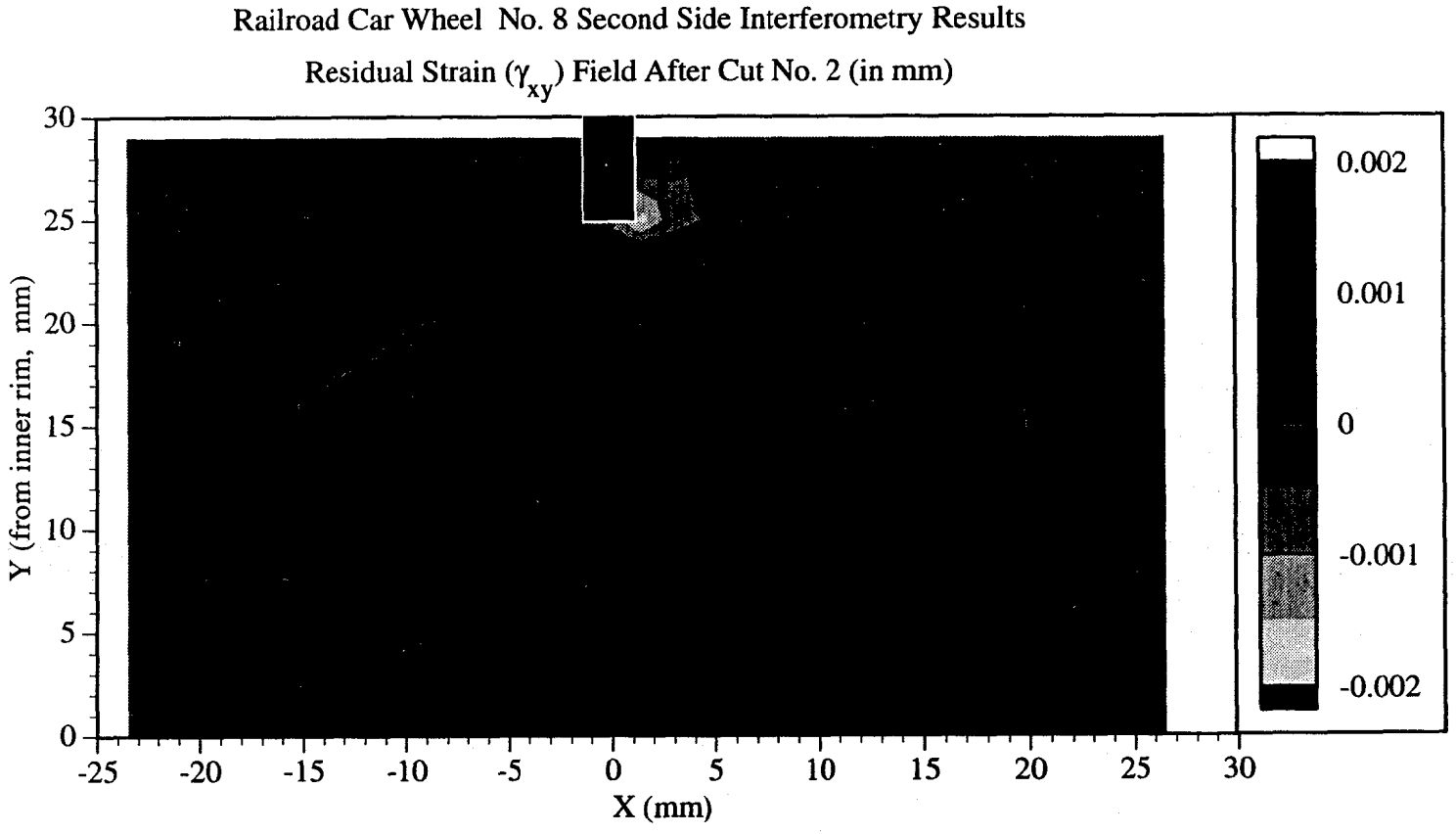
Railroad Car Wheel No. 8 Second Side Interferometry Results
Residual Strain (γ_{xy}) Field After Cut No. 2 (in mm)
Y (from inner rim, mm)
X (mm)
30
25
20
15
10
5
0
-25
-20
-15
-10
-5
0
5
10
15
20
25
30
0.002
0.001
0
-0.001
-0.002

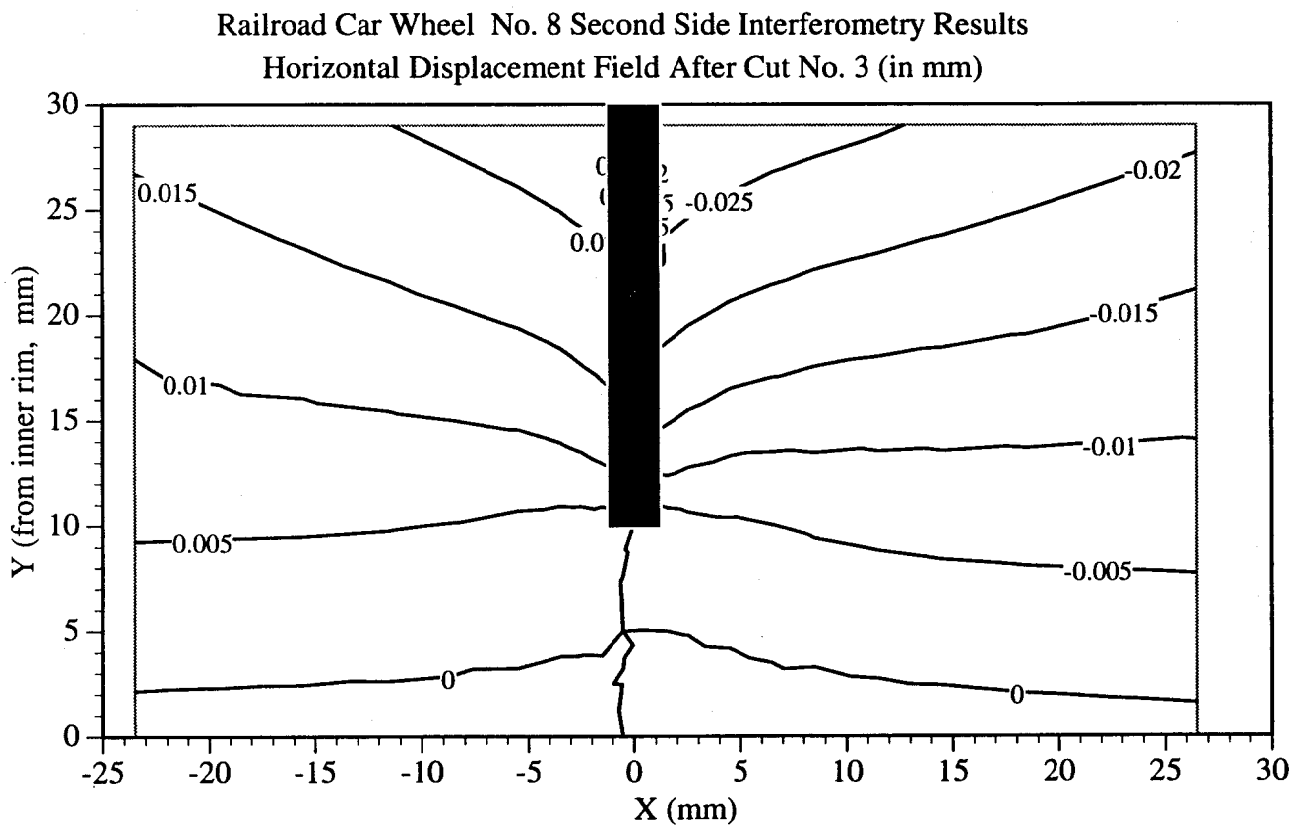
Railroad Car Wheel No. 8 Second Side Interferometry Results
Horizontal Displacement Field After Cut No. 3 (in mm)
Y (from inner rim, mm)
X (mm)
0.015
0.01
0.005
0
-0.02
-0.015
-0.01
-0.005
0
-0.025

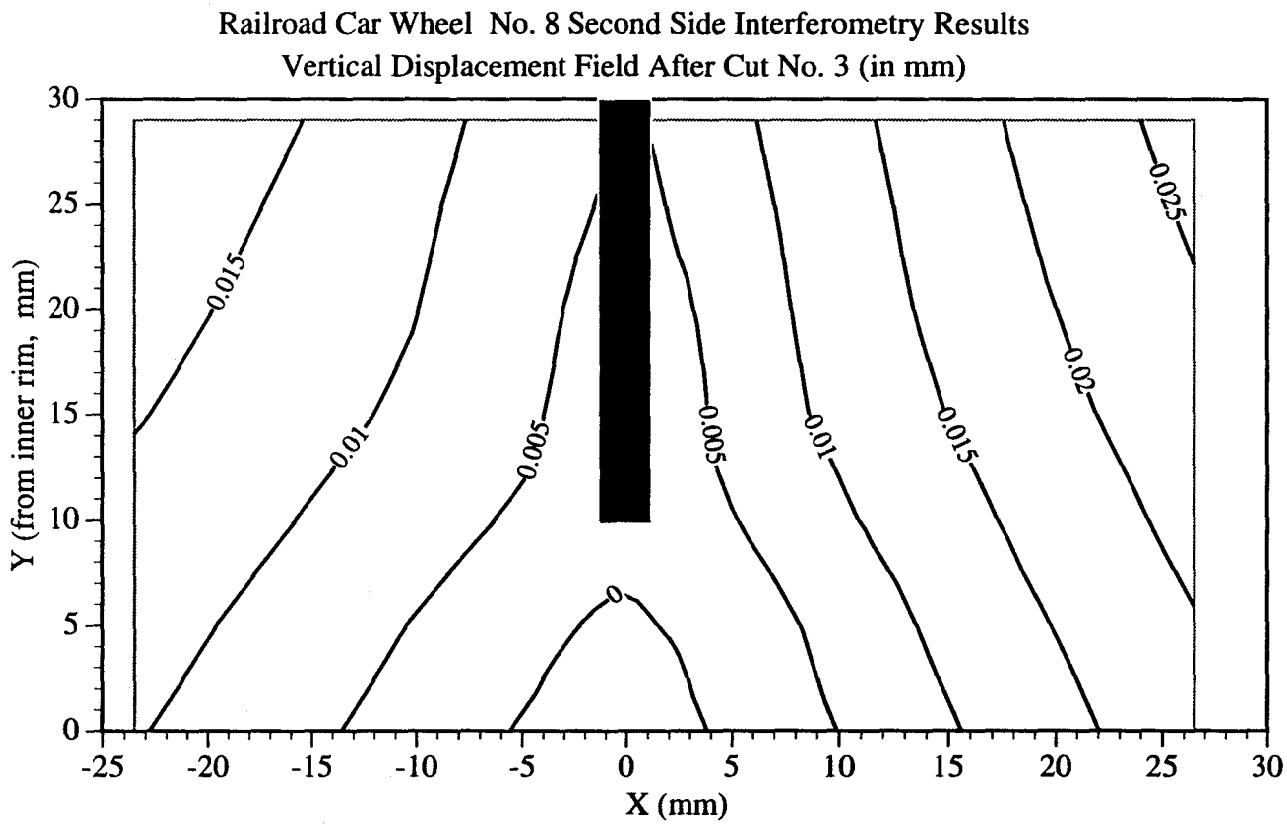
Railroad Car Wheel No. 8 Second Side Interferometry Results
Vertical Displacement Field After Cut No. 3 (in mm)
Y (from inner rim, mm)
X (mm)
0.015
0.01
0.005
0
0.005
0.01
0.015
0.02
0.025

Railroad Car Wheel No. 8 Second Side Interferometry Results
Out-of-plane Displacement Field After Cut No. 3 (in mm)

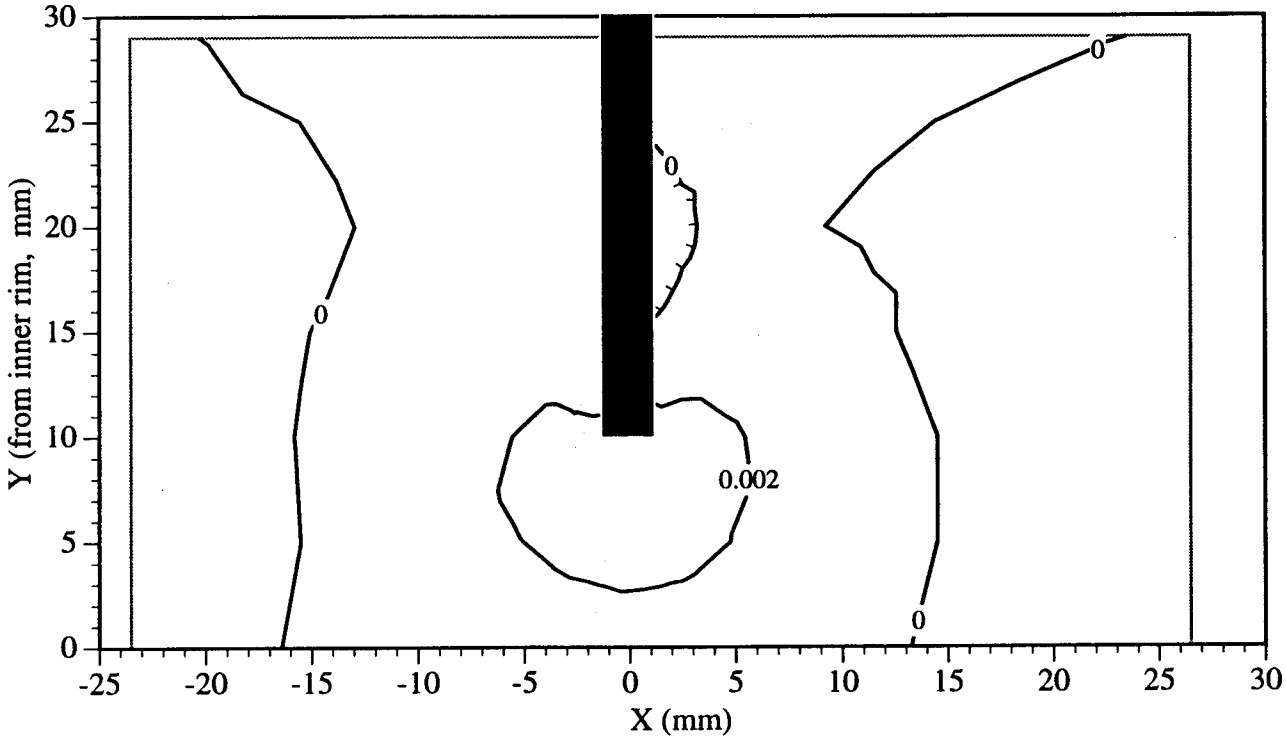

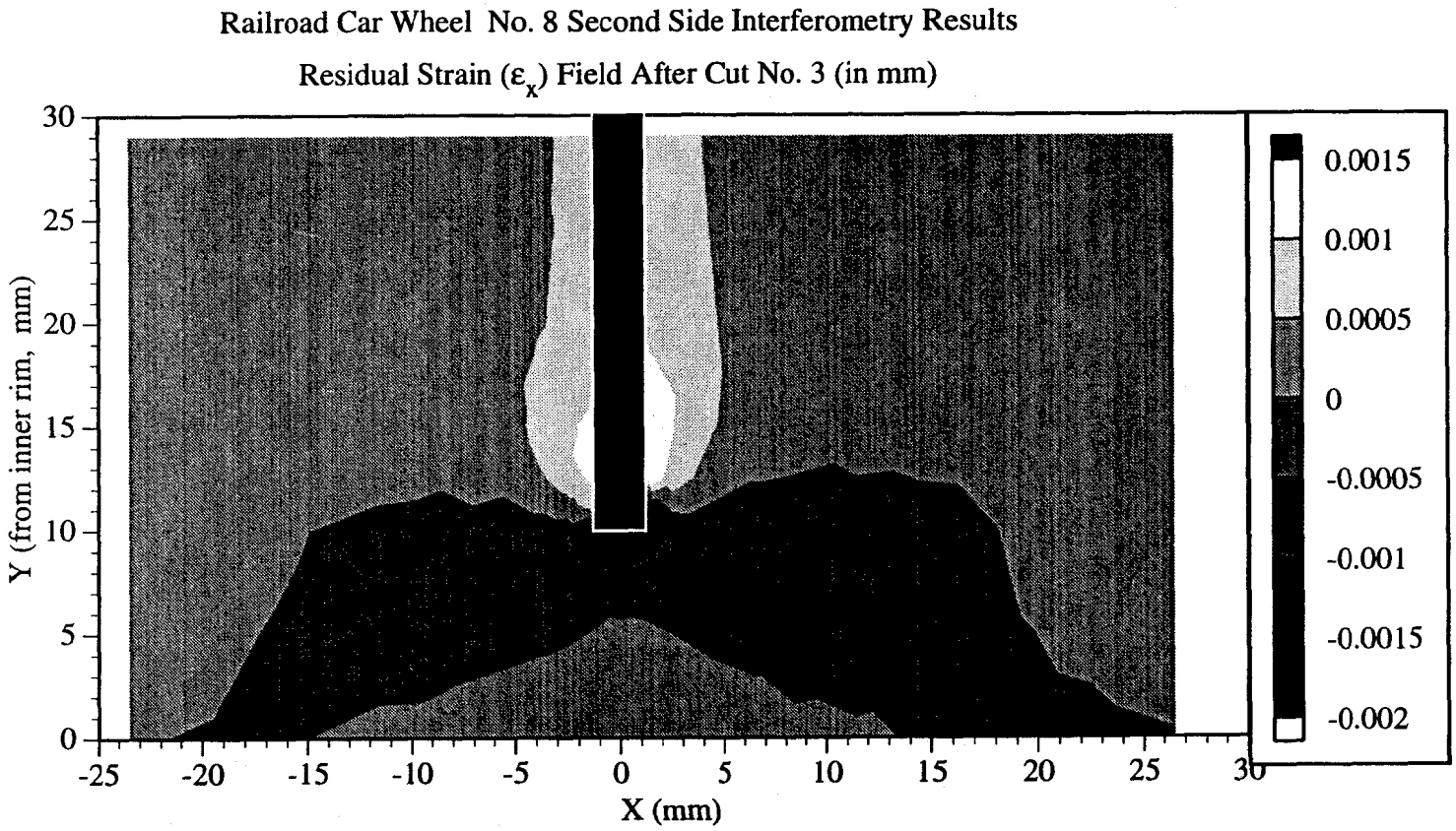
Railroad Car Wheel No. 8 Second Side Interferometry Results
Residual Strain (ε_x) Field After Cut No. 3 (in mm)
Y (from inner rim, mm)
X (mm)
30
25
20
15
10
5
0
-25
-20
-15
-10
-5
0
5
10
15
20
25
0.0015
0.001
0.0005
0
-0.0005
-0.001
-0.0015
-0.002

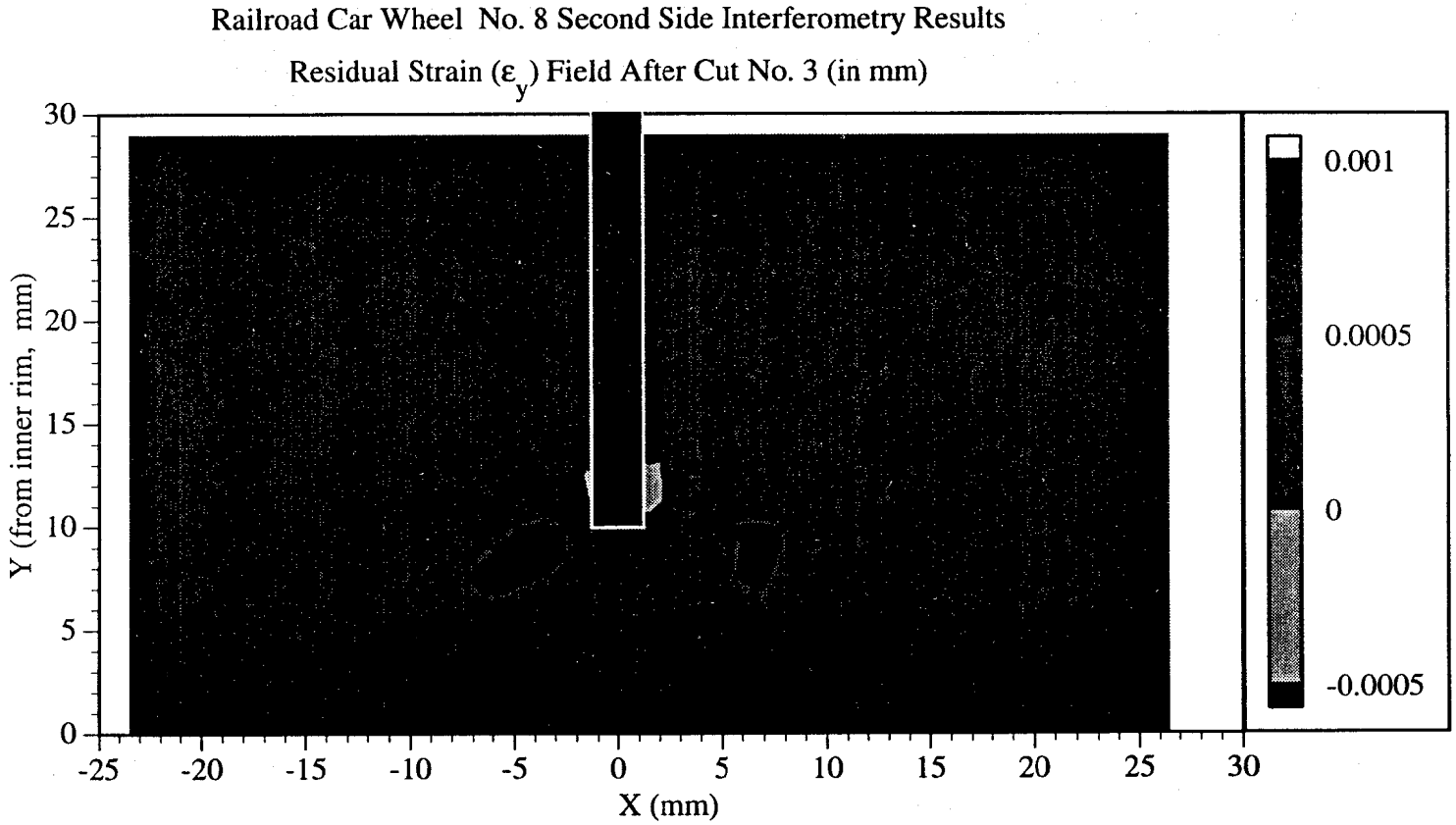
Railroad Car Wheel No. 8 Second Side Interferometry Results
Residual Strain (ε_y) Field After Cut No. 3 (in mm)
Y (from inner rim, mm)
30
25
20
15
10
5
0
-25
-20
-15
-10
-5
0
5
10
15
20
25
30
X (mm)
0.001
0.0005
0
-0.0005

★U.S. GOVERNMENT PRINTING OFFICE:1999-455-129/16564

Railroad Car Wheel No. 8 Second Side Interferometry Results

Residual Strain (γ_{xy}) Field After Cut No. 3 (in mm)

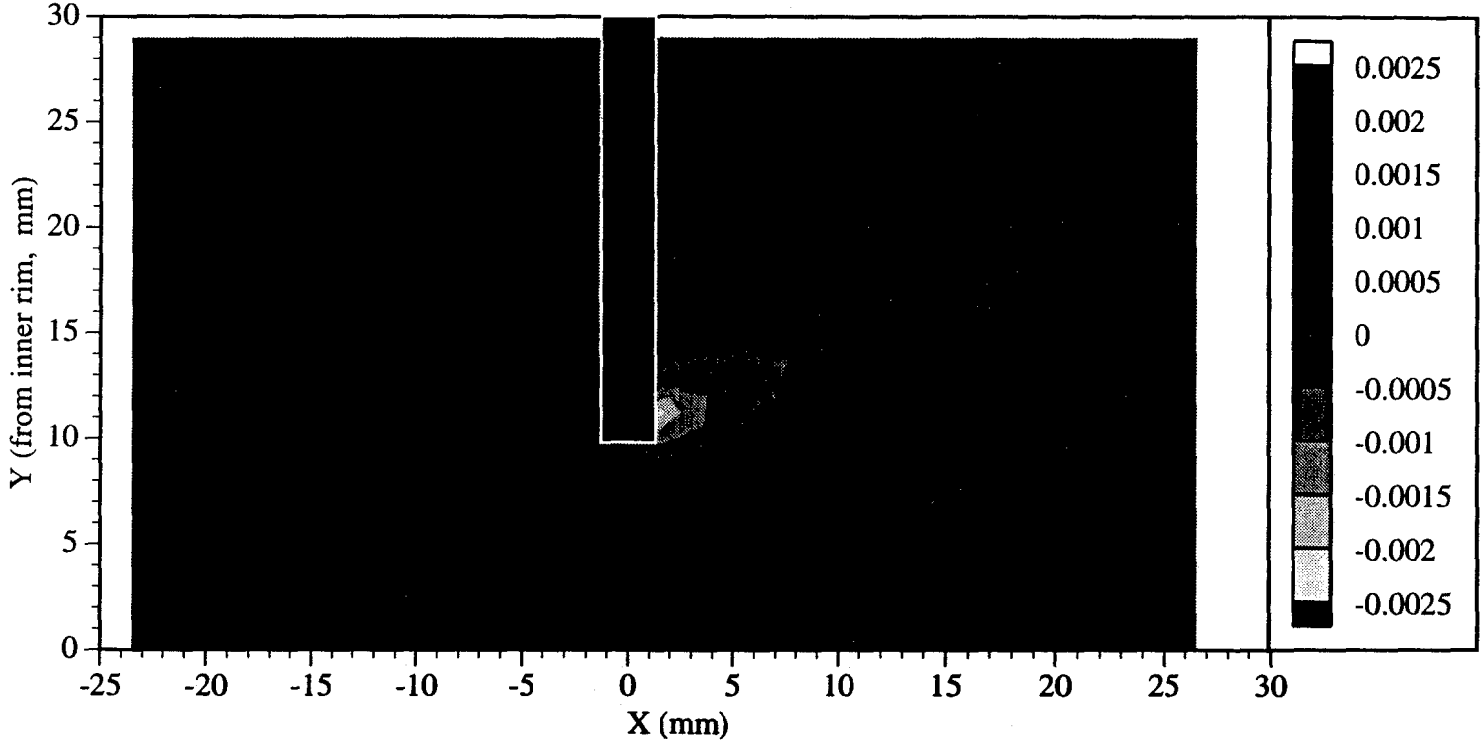

Page Intentionally Left Blank